August 2015

Revision 44

NAC-LWT

Legal Weight Truck Cask System

SAFETY ANALYSIS REPORT

Volume 2 of 3

NON-PROPRIETARY VERSION

Docket No. 71-9225

NAC INTERNATIONAL

Atlanta Corporate Headquarters: 3930 East Jones Bridge Road, Norcross, Georgia 30092 USA
Phone 770-447-1144, Fax 770-447-1797, www.nacintl.com

LIST OF EFFECTIVE PAGES

LIST OF EFFECTIVE PAGES (Continued)

LIST OF EFFECTIVE PAGES (Continued)

Table of Contents

Table of Contents (continued)

Table of Contents (continued)

Table of Contents (continued)

Table of Contents (continued)

Table of Contents (continued)

List of Figures

List of Figures (continued)

List of Figures (continued)

List of Figures (continued)

List of Figures (continued)

List of Figures (continued)

List of Tables

List of Tables (continued)

List of Tables (continued)

List of Tables (continued)

List of Tables (continued)

List of Tables (continued)

List of Tables (continued)

List of Tables (continued)

List of Tables (continued)

List of Tables (continued)

List of Tables (continued)

List of Tables (continued)

List of Tables (continued)

2 STRUCTURAL EVALUATION

The structural analysis of the NAC-LWT spent-fuel transportation cask demonstrates that the package satisfies the requirements of Part 71 of Title 10, Chapter 1 of the Code of Federal Regulations, specifically, Subpart E, "Package Approval Standards" and Subpart F, "Package and Special Form Tests." It is shown that containment is not breached under any of the normal operations or hypothetical accident conditions.

Analysis techniques that utilize the current state-of-the-art methods for the calculation of stresses in large structures subject to both steady state and transient loadings are used throughout these analyses. The evaluation of the structural characteristics of the containment boundary is based upon a conservative interpretation of the requirements of the American Society of Mechanical Engineers (ASME) Boiler and Pressure Vessel Code.

This section of the Safety Analysis Report demonstrates that the NAC-LWT cask design is capable of meeting the rigors of transport while carrying nuclear fuel; it documents the results of the analyses that are performed to provide assurance that the design also satisfies the statutory requirements for licensing.

2.1 Structural Design

2.1.1 Discussion

The NAC-LWT cask consists of six major components: (1) the cask body; (2) the closure lid and bolts; (3) the neutron shield/expansion tanks; (4) the trunnions; (5) the fuel basket; and (6) the energy absorbing impact limiters, which are located over the ends of the cask. The bottom plate, the inner shell, the upper ring and the closure lid, including seals and bolts, form the primary containment boundary.

The NAC-LWT cask body is constructed of Type 304 stainless steel with Type XM-19 stainless steel inner and outer shells and with lead shielding in the side wall and bottom end (Section 1.4, License Drawings). The cask bottom consists of a 3.5-inch thick, 20.75-inch diameter Type 304 stainless steel forging on the outside; a 3.0-inch thick, 20.75-inch diameter lead plate; and a 4.0-inch thick, 17.80-inch diameter Type 304 stainless steel forging on the inside; these components are enclosed by a 10.5-inch thick, 28.63-inch outside diameter, 17.80-inch inside diameter, Type 304 stainless steel forging. The cask bottom is welded directly to the Type XM-19 stainless steel inner shell (0.75-inch thick with 1.26-inch thick transition regions at each end; 13.375-inch inside diameter, 14.88-inch outside diameter) and the Type XM-19 stainless steel outer shell (1.20-inch thick with 1.87-inch thick transition regions at each end; 26.38-inch inside diameter, 28.78-inch outside diameter); the shells are 175.05 inches long. The annulus between the shells (26.38-inch outside diameter, 14.88-inch inside diameter) is filled with lead for gamma shielding. The Type 304 stainless steel top forging is welded directly to the inner and outer shells and has three stepped regions to accommodate the closure lid, the seals and the lid bolts. The total height of the top forging is 14.25 inches with an outside diameter of 28.63 inches and stepped inside diameters of 13.375 inches × 6.25 inches long, 20.6 inches × 4.9 inches long, and 22.63 inches × 3.1 inches long.

The stainless steel closure lid is 11.3 inches thick with stepped regions of length and diameters to match those of the top forging so that the closure lid is recessed in the top forging and flush with its top surface. The twelve 1-8 UNC closure lid bolts are SA-453, Grade 660 high alloy bolting material. The inner and outer seals on the closure lid are metallic and tetrafloroetheylene (TFE) O-rings, respectively.

There are three penetrations into the NAC-LWT cask cavity – the closure lid, a vent port and a drain port. There also is a penetration into the region between the two closure lid O-rings to test the containment seal. The vent and drain ports contain quick-disconnect valves and are located in the cask body upper ring region. There are two port cover designs—the alternate port cover and the Alternate B port cover.

The port cover designs are physically similar, but the O-ring designs and materials are different. The primary containment O-ring seal for the alternate port cover is provided by a Viton® O-ring located in a groove on the face (inner end) of the port barrel of the cover body. The secondary (test annulus) seal is a single Viton® O-ring located in a groove on the barrel of the port cover. The bolts for the alternate port cover are SA-193 (Type 410 stainless steel) socket-head cap screws.

The Alternate B port cover has the same basic geometry as the alternate port cover. With the exception of modifications made to the sealing surface and the material of construction, the Alternate B port cover is the same design as the alternate port cover. The Alternate B port cover has two face seals on the inner end of the port cover. The primary containment seal is provided by an inner metal face seal located in a groove on the inner end of the barrel of the port cover body. The metal face seal maintains the containment boundary meeting the leaktight definition of ANSI N14.5-1997. The secondary (test annulus) face seal is a Viton® O-ring located in a groove on the inner end towards the outer edge of the barrel of the port cover body. The Alternate B port cover is fabricated from Type XM-19 stainless steel to provide maximum thermal expansion compatibility with the Type 304 stainless steel cask body. The Alternate B port cover is fastened to the cask body using three high-strength SB-637 Grade N07718 bolts.

The neutron shield tank shell is 0.24-inch thick stainless steel, which is 164.0 inches long with an outside diameter of 39.28 inches and an inside diameter of 38.81 inches. The bottom plate of the neutron shield tank is 0.50-inch thick stainless steel. The expansion tank shell is 0.32-inch thick stainless steel, which is 46.0 inches long with an outside diameter of 44.24 inches and an inside diameter of 43.61 inches. The top end of the shield and expansion tanks is a single 0.50-inch thick stainless steel plate. A pressure relief valve is located in the neutron shield tank shell. The relief valve is selected to contain any shield/expansion tank pressure due to the 10 CFR 71 prescribed normal operations conditions, but will release at higher pressures (165 psig) before gross failure of either tank occurs.

Four stainless steel lifting trunnions, located at 90-degree intervals, are welded to the exterior of the upper ring. Two stainless steel socket pads are welded to the outer shell for support of the cask on a trailer or in a shipping container.

The fuel basket assembly locates and supports the fuel in the cask cavity.

The aluminum honeycomb impact limiters control the g loads acting on the cask during impact load conditions. The g loads acting upon the cask are controlled by the honeycomb material crush strength.

2.1.2 Basic Design Criteria

2.1.2.1 Containment Structures

Regulatory Guides 7.6 and 7.8 are used to establish the design criteria for analyses to evaluate the package containment boundaries for both the normal transport and the hypothetical accident conditions. Material data used in the evaluations correspond to the design stress values (S_m), yield strengths (S_y), and ultimate strengths (S_u) presented in Section 2.3. The containment cavity is described by the solid 4.0-inch thick bottom end forging, welded to a 13.375-inch inner diameter 0.75-inch thick stainless steel shell, which is welded at the upper end to the upper end ring. The 11.3-inch thick stainless steel lid and metal O-ring seal, when bolted in place to the upper ring, close the containment cavity at the top of the cask. The cavity shell has two penetrations located near the top of the cask body: 1) the vent port for venting and filling; and 2) the drain port for draining. These penetrations are closed by either alternate port covers or the Alternate B port covers with the respective O-ring seals. The containment boundary is further described in Section 4.1.

A summary of allowable stress criteria used for containment structures and bolting materials is presented in Table 2.1.2-1. This data is consistent with Regulatory Guide 7.6 and applicable parts of Subsection NB-3000 and Appendix F of the "ASME Boiler and Pressure Vessel Code."

2.1.2.2 Noncontainment Structures

Noncontainment structures include all structural members other than the primary containment boundary components, but excluding the impact limiters. Noncontainment structural members are shown to satisfy similar structural criteria as the containment structure, although Regulatory Guide 7.6 applies only to containment structures. Allowable stresses for the noncontainment structures and noncontainment bolting materials are presented in Table 2.1.2-2. In addition, noncontainment lifting and handling structures satisfy the requirements of NUREG-0612 for the lifting of heavy loads.

While performing their intended function during all free drop conditions, the impact limiters crush and absorb the energy of impact. Crushing of the impact limiter prevents any cask "peak load hard points" from occurring during the impact.

Table 2.1.2-1 Allowable Stress Limits for Containment Structures

	Allowable Stresses		Bolt Allowable Stresses*	
Stress Category	**Normal Conditions**	**Accident Conditions**	**Normal Conditions**	**Accident Conditions**
Primary Membrane	S_m	Lesser of: 2.4 S_m and: 0.7 S_u	S_y	S_y
Primary Membrane + Primary Bending	1.5 S_m	Lesser of: 3.6 S_m and: S_u	S_y	S_y
Range of Primary + Secondary	3.0 S_m	NA		
Bearing	S_y	S_y for containment boundary surfaces S_u elsewhere		
Pure Shear	0.5 S_y	0.5 S_u		
Peak	Per Section 2.6.5			
Buckling	Per Section 2.10.6			

* Not considering stress concentrations (Section 2.1.3-1).

Table 2.1.2-2 Allowable Stress Limits for Noncontainment Structures

	Allowable Stresses		Bolt Allowable Stresses*	
Stress Category	Normal Conditions	Accident Conditions	Normal Conditions	Accident Conditions
Primary Membrane	Greater of: S_m and: S_y	0.7 S_u	Greater of: 2.0 S_m and: S_y	Greater of: S_y and: 0.7 S_u
Primary Membrane + Primary Bending	Greater of: 1.5 S_m and: S_y	S_u	Greater of: 3.0 S_m and: S_y	S_u
Range of Primary + Secondary	Greater of: 3.0 S_m and: S_y	NA		
Bearing	S_y	S_u		
Pure Shear	Greater of: 0.6 S_m and: 0.6 S_y	0.5 S_u		
Peak	Per Section 2.6.5			
Buckling	Per Section 2.10.6			

* Not considering stress concentrations (Section 2.1.3.2).

2.1.3 Miscellaneous Structural Failure Modes

2.1.3.1 Brittle Fracture

The materials used to fabricate the NAC-LWT cask body meet all appropriate brittle fracture requirements. The cask structure consists of Type XM-19 stainless steel inner and outer shells with the remainder of the cask body being Type 304 stainless steel. The neutron shield/ expansion tank system is also fabricated of Type 304 stainless steel. The Type XM-19 and Type 304 austenitic stainless steels do not undergo a ductile to brittle transition in the temperature range of interest.

The closure lid bolts are SA-453, Grade 660 high alloy bolting material. The port covers are SA-705, Grade 630 stainless steel. The port cover bolts are SA-193, Grade B6 alloy steel bolting material. All of these materials meet the impact energy absorption requirements of ASTM A370 and A20-77 (Annual Book of ASTM Standards, 1986).

The impact limiters and the fuel basket are fabricated from aluminum. Since the aluminum does not undergo a ductile to brittle transition in the cask structure temperature range, brittle fracture is not a concern.

2.1.3.2 Fatigue - Normal Operating Cycles

2.1.3.2.1 Cask Structure

A normal operating cycle is defined as the sequence of loading an empty cask at ambient temperature with contents of maximum heat load, transporting the contents to a destination, unloading the contents and letting the cask return to ambient temperature. The expected number of operating cycles for the NAC-LWT cask is approximately 480 (24 cycles/year × 20 years). For the purpose of performing a fatigue stress evaluation, the LWT cask is assumed to be subjected to 2,000 cycles. From the "ASME Boiler and Pressure Vessel Code," Appendix I, Figure I-9.2.1, the fatigue allowable stress intensity amplitude (S_a) for austenitic stainless steels for 2,000 cycles is 98,000 psi (one-half of the alternating stress range). This value, when multiplied by the ratio of elastic moduli at 70°F to that at 300°F ($27.0 \times 10^6 / 28.3 \times 10^6$), and multiplied by two, gives a fatigue allowable alternating stress intensity range of 187,000 psi. However, the allowable primary plus secondary (S_n) stress intensity range, from "ASME Boiler and Pressure Vessel Code," Subsection NB-3222.2, is 60,000 psi (3.0 S_m) for Type 304 stainless steel. No stress concentration factor is greater than 3.0 for the Type 304 stainless steel cask body components. The fatigue allowable alternating stress intensity range, 187,000 psi, is greater than three times the maximum allowable S_n stress intensity range for Type 304 stainless steel.

Similarly, for Type XM-19 stainless steel, the allowable S_n stress intensity range is 100,000 psi (3.0 S_m). No stress concentration factor for the inner and outer shells is greater than 1.5; the fatigue allowable alternating stress intensity range, 187,000 psi, is greater than 1.5 times the maximum allowable S_n stress intensity range for Type XM-19 stainless steel. Therefore, the S_n allowable stress intensity governs.

2.1.3.2.2 Bolts – Closure Lid (Fatigue)

Lid closure bolts indirectly complete containment by holding the lid in place on the upper forging. The maximum cyclic stress in the lid bolts results from preloading the bolts to the 260 foot-pounds torque (3120 inch-pounds) specified for installation. The actual required bolt preload torque (T), is given by:

$$T = \left[\frac{d_m}{2d}\left(\frac{\tan\psi + \mu\sec\alpha}{1 - \mu\tan\psi\sec\alpha}\right) + 0.625\mu\right](F)(d)$$

$$= 2862 \text{ in-lb } (238.5 \text{ ft-lb})$$

where:

F = preload force, lb

d = 1.0 in (bolt diameter)

ψ = 2.494° (helix angle)

α = 30° (one-half the thread angle)

μ = 0.060 (coefficient of friction)

d_m = 0.9134 in (mean diameter of threads)

The required bolt preload force is calculated for the top corner drop as follows:

1. Inertial Weight of Lid

$$F_1 = \frac{W_t}{g}(a) = \frac{941}{32.2}(60 \text{ x } 32.2)$$

$$= 56{,}460 \text{ lbs}$$

where:

W_t = 941 lbs (Table 2.2.0-1)

a = 60 g (Table 2.6.7-34)

2. Inertial Weight of Cask Contents

$$F_2 = \frac{W_c}{g}(a) = \frac{4000}{32.2}(60 \times 32.2)$$

$$= 240{,}000 \text{ lbs}$$

where:

W_c = 4000 lbs (Table 2.2.0-1)

a = 60 g (Table 2.6.7-34)

3. Force Resulting From Internal Pressure

$F_{ip} = P_{ip}(A) = 30(171.36)$

$= 5141$ lbs

where:

$P_{ip} = 30$ psig

$$A = \frac{\pi}{4}(14.771^2)$$

$$= 171.36 \text{ in}^2$$

4. Force Resulting From Compression of TFE O-Ring

The TFE material used in the NAC-LWT cask lid O-ring (outer) (Shamban, Part No. S11214-460) has a nominal diameter of 0.275 inch and is compressed to a height of 0.242 inch, yielding a compression of 12 percent. The rated load on the O-ring using a shore hardness of 90 and 12 percent compression is 50 pounds per linear inch. The total compressive force on the O-ring is calculated as:

$F_{tr} = 50(\pi \times 15.75)$

$= 2{,}474$ lbs

5. Force Resulting From Compression of Metallic O-Ring

The rated load on the 14.75-inch diameter metal O-ring, Inconel X-750 material, with an 0.188-inch outside diameter and 0.032-inch wall thickness is 1.4(1225) pounds per linear inch. The compressive force on the O-ring is calculated as:

$F_{mr} = (1.4 \times 1225)(\pi \times 14.75)$

$= 79{,}470$ lbs

The total required bolt preload force (12 bolts) is:

$$F_T = F_1 + F_2 + F_{ip} + F_{tr} + F_{mr}$$

$$= 383{,}545 \text{ lbs}$$

For each of the twelve 1 - 8 UNC bolts in the lid, the required maximum bolt preload force is:

$$F = 383{,}545 / 12$$

$$= 31{,}962 \text{ lbs}$$

Conservatively, an installed bolt preload of 34,843 pounds is specified.

From Table 6-2, page 230, of Shigley, the tensile stress area (A_t) of each lid bolt is 0.606 square inches. Bolt stress resulting from the specified preload is:

$$S = F/At = 34{,}843 \text{ lb}/0.606 \text{ in}^2$$

$$= 57{,}497 \text{ psi}$$

According to Juvinall, page 251, it is assumed that the stress concentration factor is approximately 3.8 for unified and American standard threads. The modulus of elasticity of the bolting material at 300°F is 26.7 x 10^6 psi. The extreme temperature, normal transport condition, which the bolting material may experience, is actually calculated to be 230°F, adding a level of conservatism to this analysis. Figure 2.1.3-1 ("ASME Boiler and Pressure Vessel Code," Figure I-9.4, page 199) is based on a modulus of elasticity of 30.0 x 10^6 psi; therefore, by ratioing the moduli, the equivalent stress range is given by:

$$S_{range} = (57{,}497 \text{ psi})\ (3.8)\ [(30.0/26.7)]$$

$$= 245{,}492 \text{ psi}$$

The equivalent stress range defines the endpoints of the stress cycle; thus, the alternating component would be half the range or 122,746 psi. From Figure 2.1.3-1, using the 3.0 S_m curve, the allowable number of operating cycles is greater than 550. Conservatively assuming that the bolts are torqued twice each month, the bolts would be cycled 24 times in one year. Then, 550 cycles represent a minimum service life of 22.9 years. The lid bolts will be replaced after 20 years of operational service to ensure that the fatigue limit is satisfied.

2.1.3.2.3 Containment Vessel

Fatigue concerns associated with normal over-the-road vibration are addressed in Section 2.6.5.

2.1.3.3 Extreme Total Stress Intensity Range

Regulatory Guide 7.6, paragraph C.7 requires that the extreme total stress intensity range (including stress concentrations) between the initial state, the fabrication state, the normal operations condition, and the accident condition be less than twice the adjusted value (adjusted to account for the modulus of elasticity at the highest temperature) of S_a at 10 cycles given by the appropriate design fatigue curves. Table 2.1.3-1 (constructed from the finite element analysis results of the normal operations and accident conditions) shows a maximum total stress intensity range of 1311 ksi in component 7. This stress intensity range is based on an unrealistic finite element analysis calculated stress intensity value, which results from the applied boundary condition in the ANSYS program (refer to Section 2.7.1.3 for the explanation of this singularity condition). From the Type 304 stainless steel material property summary Table 2.3.1-1, the allowable stress for 10 cycles at 230°F is 686.0 ksi. The allowable stress range is then 1372 ksi (2 × 686.0 ksi). For Type 304 stainless steel, this allowable stress at 10 cycles (1372 ksi) is greater than the unrealistically high limiting stress range for low cycle fatigue (1311 ksi). Based on the significantly higher strength of Type XM-19 stainless steel, when compared to Type 304 stainless steel, no further evaluation of the extreme total stress intensity range is necessary. The low cycle fatigue limits for the containment material are not exceeded for the highly conservative value of stress intensity range considered in this analysis.

2.1.3.4 Buckling

Regulatory Guide 7.6, paragraph C.5, states that buckling of a shipping cask containment vessel must not occur under any circumstances. Precluding large deformations assures that the assumptions of elastic analyses and quasi-linear stress allowances remain valid as stated in paragraph C.6 of the above reference.

Two concentric stainless steel shells, both welded to a large ring at each end, define the primary cask structure. The annulus between the shells is filled with lead. The inner shell is considered to be the only load bearing member, taking no credit for the outer shell or the elastic support of the lead in the analyses. The analyses demonstrate that the inner shell will not buckle for normal transport or hypothetical accident conditions. For reference, the nominal dimensions of the cask shells follow.

Shell	Mean Diameter (D_m)(in)	Thickness (T)(in)	Length (L)(in)	D_m /T**	L/D_m***
Outer Shell	27.58	1.20	181.25*	23.0	6.6
Inner Shell	14.12	0.75	181.25	18.8	12.8

* Assumed shell length, no credit taken for the end forgings.

** Mean diameter divided by thickness.

*** Length divided by mean diameter.

The NAC-LWT cask inner shell is analyzed for structural stability (buckling) using Code Case N-284 (Metal Containment Shell Buckling Design Methods) of the "ASME Boiler and Pressure Vessel Code." The details of these analyses are presented in Section 2.10.6; however, the basic methodology used is as follows:

1. Calculate the theoretical elastic hoop, axial compression, and inplane shear loading using classical methodology.
2. Calculate shell geometry-dependent capacity reduction factors and shell ovality coefficients. These factors and coefficients account for differences between classical and predicted instability stresses for fabricated shells and for geometric variances from perfect cylinders.
3. Calculate plasticity reduction factors, which are used if the calculated buckling stress exceeds a material's proportional limit.
4. Identify the factors of safety (FS) to be used in the buckling evaluation. Article-1400, Code Case N-284, "ASME Boiler and Pressure Vessel Code," defines the factors of safety to be applied to compressive buckling stresses: (1) FS = 2.0 for Design Conditions and Level A and B Service Limits, which correspond to the normal transport conditions of Regulatory Guide 7.6; and (2) FS = 1.34 for Level D Service Limits, which correspond to the hypothetical accident conditions of Regulatory Guide 7.6. These factors of safety are used in the buckling evaluations of the NAC-LWT cask inner shell.
5. Using the appropriate interaction equations and the factors identified in 2, 3 and 4, calculate the worst case applied compressive stresses and in-plane shear stresses.
6. Compare worst case stresses to the classically determined buckling allowables and determine the margins of safety for the critical locations on the inner shell.

Figure 2.1.3-1 Design Fatigue Curve for High Strength Steel Bolting

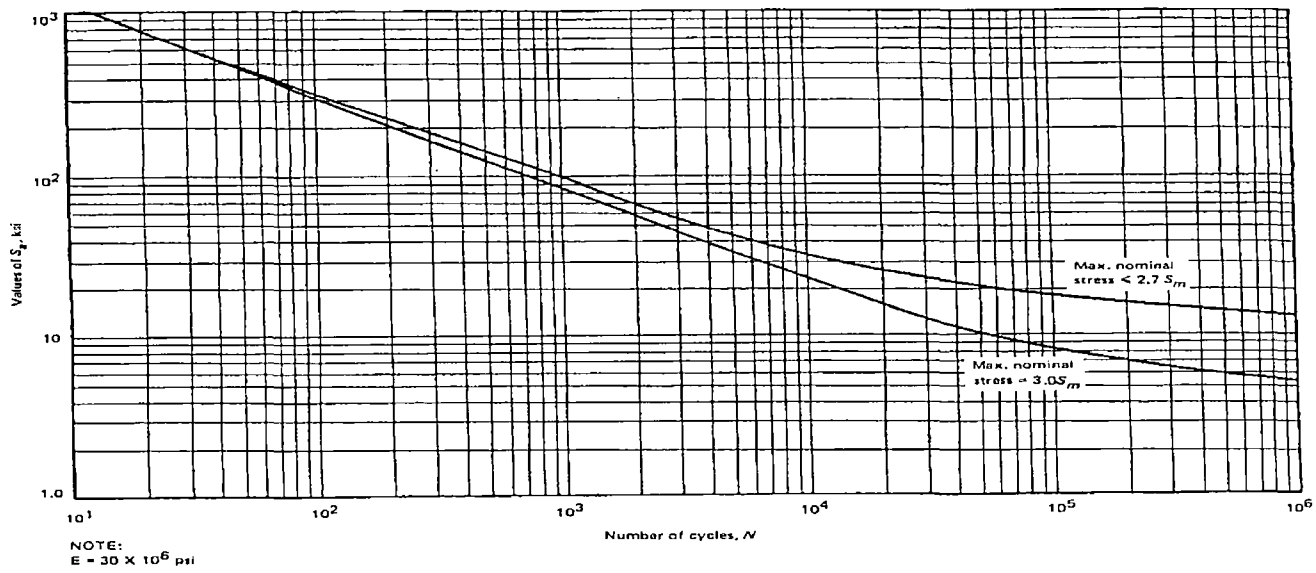

FIG. 1-9.4 DESIGN FATIGUE CURVE FOR HIGH STRENGTH STEEL BOLTING
FOR TEMPERATURES NOT EXCEEDING 700°F
Table 1-9.1 Contains Tabulated Values and a Formula for Accurate
Interpolation of These Curves

Table 2.1.3-1 Extreme Total Stress Intensities

Component	Algebraic Maximum and Minimum Stress Intensities (ksi)	Total Stress Intensity Range (ksi)
Closure Lid (1)	-1310.41[1], 0.0	1310.41[1]
Top Ring (3)	-62.23, 0.0	62.23
Inner Shell (4)	-39.98, 0.0	39.98
Outer Shell (6)	-77.65[1], 0.0	77.65[1]
Bottom (7)	-1311.20[1], 0.0	1311.20
Bottom Cover Plate (8)	-81.86[1], 0.0	81.86[1]

[1] Refer to Section 2.7.1.3 for discussion of these values, which are unrealistic due to finite element model boundary conditions.

2.2 Weights and Centers of Gravity

2.2.1 Major Component Statistics

The weights of the major components of the NAC-LWT cask and their respective centers of gravity are presented in Table 2.2.1-1. The axial location of the center of gravity is measured from the bottom surface of the cask body. The center of gravity is always on the longitudinal centerline of the cask because the cask is essentially axisymmetric about that axis. The center of gravity location of the fuel is representative of typical fuel configurations.

The weights and centers of gravity of the cask package in eight different shipping configurations are presented in

Table 2.2.1-2. In each case, the center of gravity is measured from the bottom surface of the cask body. The term "loaded" refers to the presence of fuel or other radioactive materials in the cask cavity; the term "empty" implies the absence of any fuel or other radioactive materials in the cask cavity. However, the fuel basket does remain in the cask cavity for the "empty" configuration. The weight of a lifting yoke is not included in the tabulated package weights.

All of the values tabulated in Table 2.2.1-1 and Table 2.2.1-2 are calculated to the nearest pound to obtain an accurate cask weight and center of gravity. The cask package weight and center of gravity used in the analyses of this report are the design values - 52,000 pounds and 98.93 inches. A design value of 4,000 pounds is conservatively used for the total weight of the cask contents (including the appropriate basket).

Table 2.2.1-1 Weights of the NAC-LWT Cask Major Components

Component	Weight (pounds)	Axial Center of Gravity Location (inches)
Cask Body	39,906	96.46
Closure Lid and Bolts	941	195.11
Impact Limiters		
Top	1,535	202.98
Bottom	1,320	-3.18
Shield Tank Fluid	3,506	96.26
PWR Fuel Basket and Spacer	874	100.98
PWR High Burnup Rod Payload	1,620	95.33
PWR Fuel Payload (Maximum)	3,126	96.63
BWR Fuel Basket	1,124	97.88
BWR Fuel Payload	1,500	97.88
Metallic Fuel Basket	128	96.40
Metallic Fuel Payload	2,080	96.40
MTR Four Unit Basket	982	96.20
MTR Four Unit Fuel Payload	840[1]	96.20
MTR Four Unit PULSTAR Fuel Payload	2,240[2]	96.20
MTR Five Unit Basket	1,015	96.20
MTR Five Unit Fuel Payload	1,050[1]	96.20
MTR Six Unit Basket	1,002	96.20
MTR Six Unit Fuel Payload	1,260[1]	96.20
GA IFM Basket and Spacer	818	98.06
GA IFM Fuel Payload	148	167.34
TPBAR Basket and Spacer	675	110.40
TPBAR Payload	978[3]	96.00
ANSTO Basket	911	100.95
ANSTO Payload	756	100.95
TPBAR Basket	575	97.43
TPBAR with Rod Transport Canister Payload	1,326[4]	102.26
SLOWPOKE Four Unit Basket	982	96.20
SLOWPOKE Fuel Payload	840[5]	96.20
NRU/NRX Basket & Spacer	845	113.03
NRU/NRX Basket + Spacer + Fuel	1205[6]	116.34

1 For conservatism, a design basis MTR fuel weight of 30 lbs/assy is used in the structural analysis. The maximum MTR element weight is 13.2 lbs for an intact element and 9.7 lbs for the cut elements in the 42-element configuration. The maximum weight for the SLOWPOKE canister is 25 pounds.

2 For conservatism, a bounding weight of 80 pounds is considered for each of the 28 fuel cells for PULSTAR fuel.

3 TPBAR payload represents the combined weight of the TPBAR and consolidation canister. A conservative 1,000 lb weight is applied in the structural analysis.

4 TPBAR with Rod Transport Canister payload represents the combined weight of the 25 TPBARs, the PWR /BWR Rod Transport Canister and the PWR insert.

5 A fuel weight of 30 lbs/assembly is used to compute the weight for this table as compared to the maximum weight for the SLOWPOKE canister of 25 pounds.

6 Each fuel tube in the NRU/NRX basket is limited to 20 pounds of fuel and aluminum caddy.

Table 2.2.1-1 Weights of the NAC-LWT Cask Major Components (cont.)

Component	Weight (pounds)	Axial Center of Gravity Location (inches)
HEUNL Container & Spacer[7]	1,446	104
HEUNL Payload	704	98
SLOWPOKE Fuel Core Basket & Five MTR Baskets	1,160	108
SLOWPOKE Fuel Core Payload	15	164

[7] Includes 4 HEUNL Containers, Container Guide and Container Spacer.

Table 2.2.1-2 Weights and Center of Gravity Locations for the NAC-LWT Cask Shipping Configurations

Component	Weight (pounds)	Axial Center of Gravity Location (inches)
Package -Loaded for Shipment (PWR) Maximum Payload	51,208	98.96
Package – Loaded for Shipment PWR High Burnup Rods	49,702	99.0
Package - Empty for Shipment (PWR)	48,082	99.12
Package - Loaded for Shipment (BWR)	49,832	99.00
Package - Empty for Shipment (BWR)	48,332	99.07
Package - Loaded for Shipment* (Metallic Fuel)	45,910	98.88
Package - Empty for Shipment* (Metallic Fuel)	43,830	99.09
Package - Loaded for Shipment (PULSTAR Fuel, MTR Four Unit Basket)	50,430	99.1
Package - Loaded for Shipment (MTR Fuel, Four Unit Basket)	49,030	99.1
Package - Empty for Shipment (MTR Fuel, Four Unit Basket)	48,190	98.9
Package - Loaded for Shipment (MTR Fuel, Five Unit Basket)	49,273	99.1
Package - Empty for Shipment (MTR Fuel, Five Unit Basket)	48,223	98.9
Package - Loaded for Shipment (MTR Fuel, Six Unit Basket)	49,470	99.1
Package - Empty for Shipment (MTR Fuel, Six Unit Basket)	48,210	98.9
Package - Loaded for Shipment (GA IFM Fuel and Basket)	48,147	99.3
Package - Empty for Shipment (GA IFM Basket)	48,026	99.3
Package – Loaded for Shipment (TPBARs and Basket)	48,861	99.2
Package – Empty for Shipment (TPBAR Basket)	47, 883	99.2
Package - Loaded for Shipment (ANSTO Fuel and Basket)	48,875	99.2
Package - Empty for Shipment (ANSTO Basket)	48,119	99.1

* Neutron Shield Tank is empty.

Table 2.2.1-2 Weights and Center of Gravity Locations for the NAC-LWT Cask Shipping Configurations (cont'd)

Component	Weight (pounds)	Axial Center of Gravity Location (inches)
Package - Loaded for Shipment TPBARs in the PWR/BWR Rod Transport Canister	49,109	99.2
Package - Empty for Shipment (TPBAR Basket for PWR/BWR Rod Transport Canister)	47,783	99.1
Package - Loaded for Shipment (SLOWPOKE Fuel, Four Unit Basket)[1]	49,030	99.1
Package - Empty for Shipment (SLOWOKE Fuel, Four Unit Basket)	48,190	98.9
Package – Loaded for Shipment (NRU/NRX Basket with Fuel Assemblies)	41,111	97.0
Package – Empty for Shipment (NRU/NRX Basket)	40,751	96.8
Package – Empty for Shipment (HEUNL)	48,656	99.2
Package – Loaded for Shipment (HEUNL)	49,360	99.2
Package – Loaded for Shipment (SLOWPOKE Fuel Core, Basket, Five MTR Baskets)[2]	48,400	99.3
Package – Empty for Shipment (SLOWPOKE Fuel Core Basket, Five MTR Baskets)[2]	48,400	99.3
Package - Design for Shipment	52,000	98.93

[1] A fuel weight of 30 lbs/assembly is used to compute the weight for this table as compared to the maximum weight for the SLOWPOKE canister of 25 pounds.

[2] Weight rounded up to nearest 100 pounds.

2.3 Properties of Materials

The NAC-LWT cask body consists of six materials: (1) the inner and outer shells are Type XM-19 stainless steel; (2) the remainder of the cask body, the closure lid and the lifting trunnions are Type 304 stainless steel; (3) the annulus between the cask shells and the cavity in the bottom is filled with chemical copper lead for gamma radiation shielding; (4) the port covers are fabricated from SA-705, Grade 630 (Type 17-4PH) precipitation-hardened stainless steel; (5) the port cover bolts are made from SA-193, Grade B6 (Type 410) stainless steel; and (6) the closure lid bolts are fabricated from SA-453, Grade 660 high alloy steel bolting material.

The PWR and BWR fuel baskets are fabricated from Type 304 stainless steel and 6061-T6 aluminum alloy. The metallic fuel basket is fabricated from 6061-T6 aluminum alloy. The MTR, TRIGA, DIDO and GA IFM fuel baskets are fabricated from Type 304 stainless steel.

2.3.1 Mechanical Properties of Materials

The structural analyses of the NAC-LWT cask for normal operations and accident load conditions utilize the mechanical properties of the component materials. These properties are also used in calculating the allowable stresses for each component under each load condition.

The American Society of Mechanical Engineers is the source for the mechanical properties of Type 304 stainless steel, Type XM-19 stainless steel, SA-705, Grade 630 precipitation-hardened stainless steel, SA-193, Grade B6 (Type 410) stainless steel, and SA-453, Grade 660 high alloy steel bolting material ("ASME Boiler and Pressure Vessel Code," Appendix I). The effects of temperature on the material properties are included. The coefficient of thermal expansion presented in the tables represents the mean value for a temperature range from 70°F to the indicated temperature.

MIL-HDBK-5C is the source for the material properties of the aluminum alloys and for the equations used to evaluate the relationships of their material properties at elevated temperatures.

2.3.1.1 Cask Body Materials

The material of the inner and outer shells is Type XM-19 stainless steel. The remainder of the cask body and the closure lid are Type 304 stainless steel. These materials are selected because they are strong, ductile and highly resistant to corrosion and brittle fracture. The mechanical properties of Type 304 and Type XM-19 stainless steel are listed in Table 2.3.1-1 and Table 2.3.1-2, respectively.

2.3.1.2 Port Cover Materials

The alternate port covers are manufactured from SA-705, 17-4 PH Grade 630 precipitation-hardened stainless steel. The mechanical properties for this material are given in Table 2.3.1-3. The Alternate B port covers are manufactured from SA-479 XM-19 stainless steel. The mechanical properties for this material are given in Table 2.3.1-2.

2.3.1.3 Fuel Basket Materials

The materials used for the fuel basket are 6061-T6 aluminum and Type 304 stainless steel sheet, plate and bar. The mechanical properties of Type 304 stainless steel and 6061-T6 aluminum alloys are listed in Table 2.3.1-1 and Table 2.3.1-4, respectively.

2.3.1.4 Bolting Material

The port cover bolts for the alternate port cover are SA-193, Grade B6 (Type 410) stainless steel as described in Table 2.3.1-5. The bolts for Alternate B port covers are SB-637, Grade N07718, and nickel alloy steel as described in Table 2.3.1-9.

2.3.1.5 Shielding Material (Gamma Radiation)

Chemical copper lead fills the cylindrical region of the cask between the inner and outer cask shells and bottom plates. This lead core provides the required gamma radiation shielding. The presence of copper slightly increases the strength of lead at elevated temperatures. There is no concern that the lead will fail during normal transport conditions because it is completely enclosed inside the cask walls and bottom plates. Its shielding function requires no strength.

The finite element structural analysis program (ANSYS), used in the structural analysis of the cask, requires that the stress versus strain curve for this material be bilinear in the elastic to plastic transition region.

2.3.1.5.1 Static Mechanical Properties of Lead

The static mechanical properties of chemical copper lead are used in the NAC-LWT cask thermal stress analyses. The coefficient of thermal expansion for lead is of particular significance, because it is approximately twice that of stainless steel. The mechanical properties are obtained from testing reports (Tietz, Gallagher, Baumeister, NUREG/CR-0481). The properties are tabulated in Table 2.3.1-7 for the range of temperatures considered in the structural analysis. The bilinearized static stress-strain curve used in the finite element (ANSYS) analysis is shown in Figure 2.3.1-1; it is based on NUREG/CR-0481, Figure 24, and Table 2.3.1-7 of this report.

2.3.1.5.2 Dynamic Mechanical Properties of Lead

The dynamic mechanical properties of chemical copper lead are important for use in the NAC-LWT cask impact analyses. These properties are obtained from the "Cask Designer's Guide" (Shappert), which provides conservative values for dynamic yield strength. This property is used for calculating the shield deformation and for calculation of the maximum deceleration loading. These dynamic mechanical properties are listed in Table 2.3.1-8 for the range of temperatures considered in the structural analysis. The bilinearized dynamic deformation stress-strain curve used in the finite element (ANSYS) structural analysis is shown in Figure 2.3.1-2; it is based on NUREG/CR-0481, Figure 24, and Table 2.3.1-8 of this report.

Figure 2.3.1-1 Static Stress-Strain Curve for Chemical Copper Lead

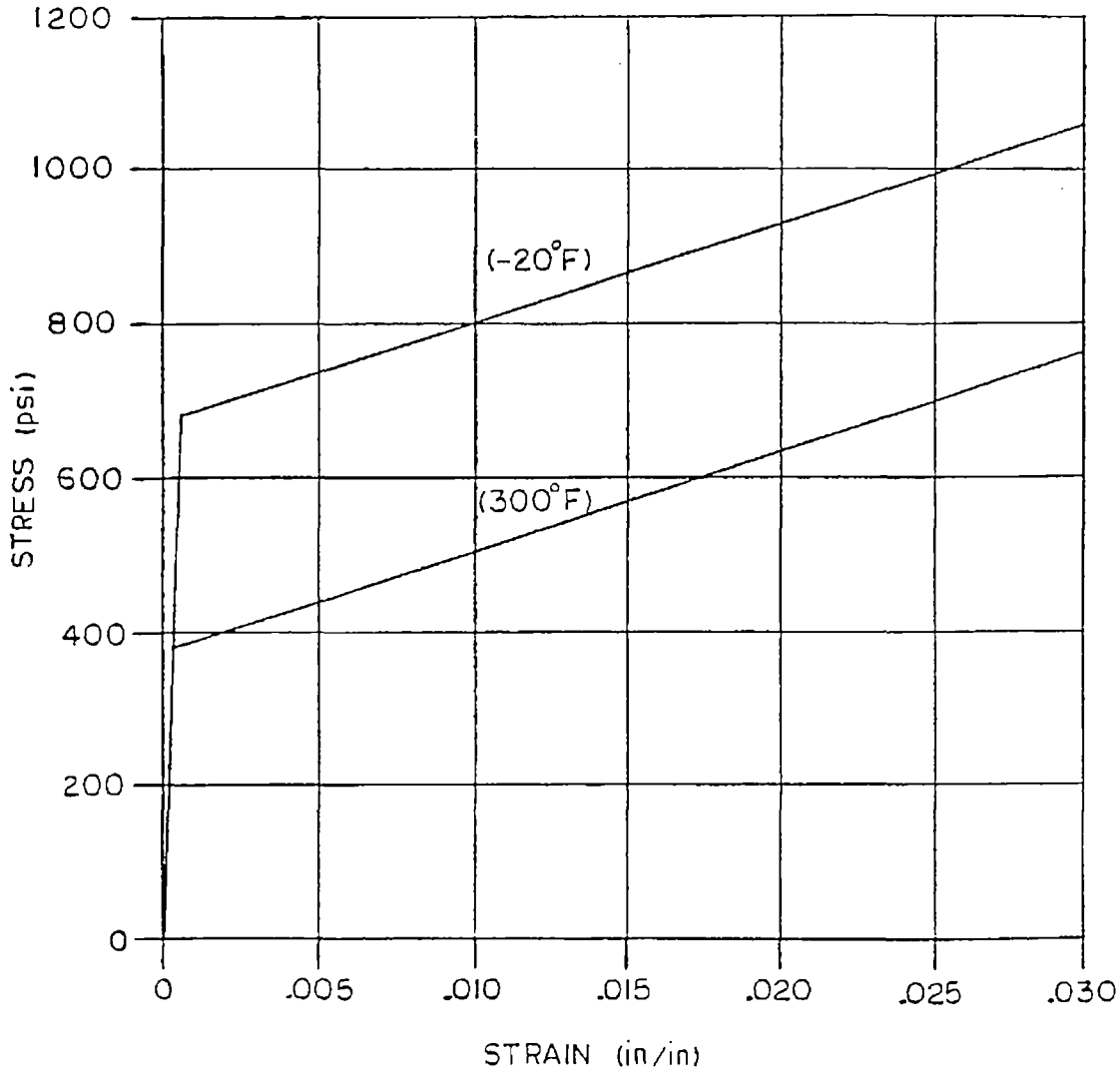

Figure 2.3.1-2 Dynamic Deformation Stress-Strain Curve for Chemical Copper Lead

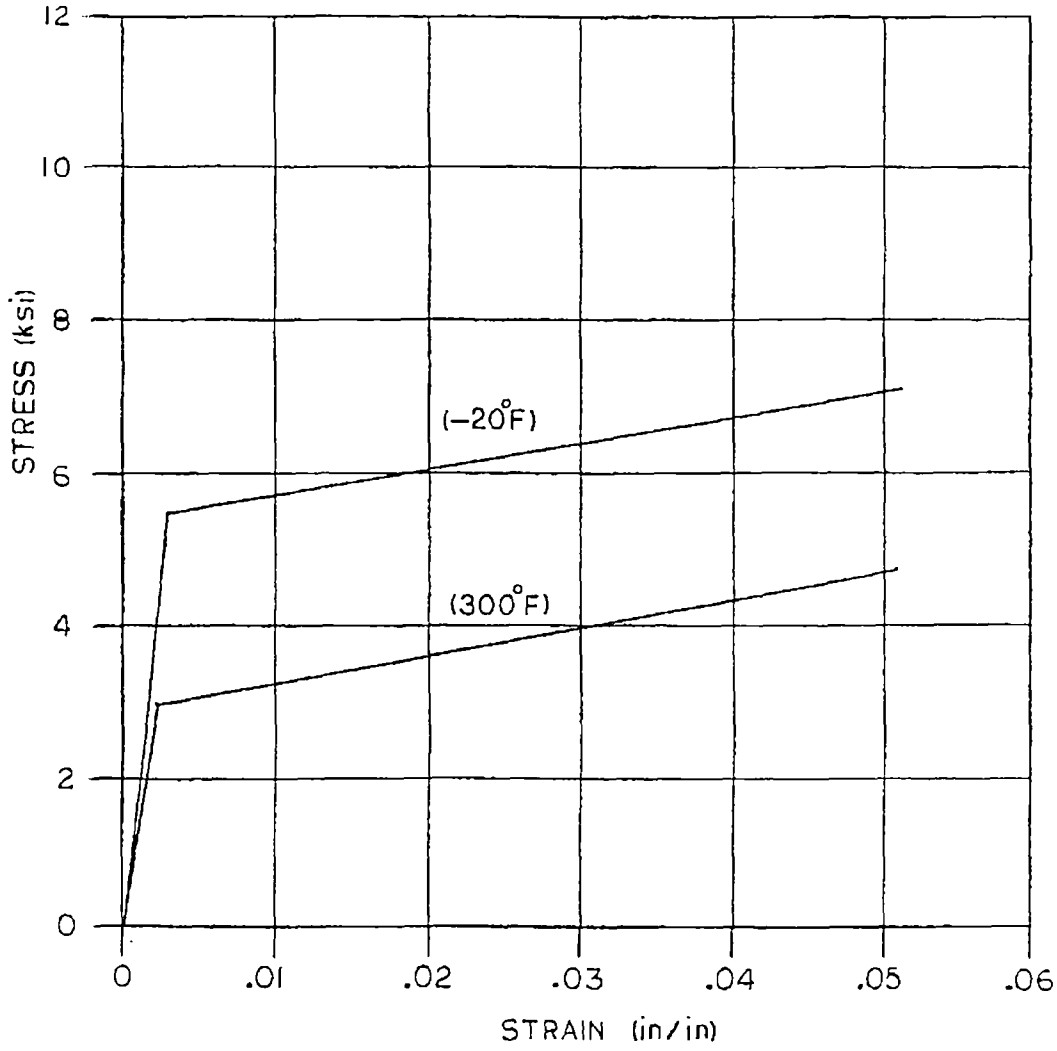

Table 2.3.1-1 Mechanical Properties of Type 304 Stainless Steel

Property (units)/Temperature (°F)	-40	-20	+70	+150	+200	+300	+600	+750
Ultimate Strength (ksi)	79.4	78.8	76.0	73.0	71.0	66.0	63.5	63.1
Yield Strength (ksi)	36.0	35.4	31.4	27.5	25.0	22.5	18.2	17.3
Design Stress Intensity	> 20.0	> 20.0	20.0	20.0	20.0	20.0	16.4	15.6
Modulus of Elasticity (ksi)	28.8E+3	28.7E+3	28.3E+3	27.9E+3	27.6E+3	27.0E+3	25.3E+3	24.4E+3
Alternating Stress @10 Cycles	720.5	718.0	708.0	698.0	690.5	675.5	632.9	610.4
Alternating Stress @10^6 Cycles	28.8	28.7	28.3	27.9	27.6	27.0	25.3	24.4
Strain at Yield (in/in)	0.00125	0.00123	0.00111	0.00099	0.00091	0.00083	0.00072	0.00071
Coefficient of Thermal Expansion (in/in/°F)	8.16E-6	8.23E-6	8.46E-6	8.67E-6	8.79E-6	9.00E-6	9.53E-6	9.76E-6
Poisson's Ratio	0.275							
Density	497 lbm/ft^3 (0.288 lbm/in^3)							

Reference:
ASME Boiler and Pressure Vessel Code, Section III, Division I, Appendix I.

Table 2.3.1-2 Mechanical Properties of Type XM-19 Stainless Steel

Property (units)/Temperature (°F)	-40	-20	+70	+150	+200	+300	+600	+750
Ultimate Strength (ksi)	104.5	103.7	100.0	99.8	99.5	94.3	87.8	85.7
Yield Strength (ksi)	63.0	62.0	55.0	51.0	47.0	43.4	37.3	35.8
Design Stress Intensity (ksi)	> 33.3	> 33.3	33.3	33.2	33.2	31.4	29.2	28.5
Modulus of Elasticity (ksi)	28.8E+3	28.7E+3	28.3E+3	27.9E+3	27.6E+3	27.0E+3	25.3E+3	24.4E+3
Alternating Stress @10 Cycles	720.5	718.0	708.0	698.0	690.5	675.5	632.9	610.4
Alternating Stress @10^6 Cycles	28.8	28.7	28.3	27.9	27.6	27.0	25.3	24.4
Coefficient of Thermal Expansion (in/in/°F)	8.16E-6	8.19E-6	8.27E-6	8.40E-6	8.48E-6	8.65E-6	9.03E-6	9.20E-6
Poisson's Ratio	0.275							
Density	497 lbm/ft^3 (0.288 lbm/in^3)							

Reference:
ASME Boiler and Pressure Vessel Code, Section III, Division I, Appendix I.

Table 2.3.1-3 Mechanical Properties of SA-705, Grade 630, Precipitation-Hardened Stainless Steel

Property (units)/Temperature (°F)	-40	-20	+70	+150	+200	+300	+600	+750
Ultimate Strength (ksi)	> 135.0	> 135.0	135.0	135.0	135.0	135.0	126.7	125.2
Yield Strength (ksi)	> 105.0	> 105.0	105.0	101.1	97.1	93.0	84.7	81.3
Design Stress Intensity	> 45.0	> 45.0	45.0	45.0	45.0	45.0	42.1	41.3
Modulus of Elasticity (ksi)	28.8E+3	28.7E+3	28.3E+3	27.9E+3	27.6E+3	27.0E+3	25.3E+3	24.4E+3
Alternating Stress @10 Cycles	720.5	718.0	708.0	698.0	690.5	675.5	632.9	610.4
Alternating Stress @10^6 Cycles	28.8	28.7	28.3	27.9	27.6	27.0	25.3	24.4
Strain at Yield (in/in)	0.00365	0.00366	0.00371	0.00362	0.00352	0.00344	0.00335	0.00333
Coefficient of Thermal Expansion (in/in/°F)	5.88E-6	5.88E-6	5.89E-6	5.89E-6	5.90E-6	5.90E-6	5.93E-6	5.95E-6
Poisson's Ratio	0.287							
Density	487 lbm/ft^3 (0.282 lbm/in^3)							

References:

1. ASME Boiler and Pressure Vessel Code, Section III, Division I, Appendix I.
2. MIL-HDBK-5C, Section 2.7.4.
3. Baumeister, pages 5 – 6.

Table 2.3.1-4 Mechanical Properties (6061-T6 and T651 per ASTM B-209)

Property (units)/Temperature (°F)	+70	+360[1]	+500[1]
Ultimate Strength (ksi)	42.0	30.2	17.2
Yield Strength (ksi)	35.0	26.6	15.8
Comp. Yield Strength (ksi)	35.0	26.6	15.8
Ultimate Shear Strength (ksi)	27.0	19.4	11.1
Yield Shear Strength (ksi)	20.0	15.2	9.0
Modulus of Elasticity (E), (ksi)	9,900	9,100	8,000
Coefficient of Thermal Expansion (in/in/°F)	12.6×10^{-6}	13.5×10^{-6}	13.9×10^{-6}

1. Strength at elevated temperatures calculated using the following relationships from MIL-HDBK-5A, pages 325, 326, and 328.

   @360°F: $(S_u)_{360} = 0.72(S_u)_{70}$; $(S_y)_{360} = 0.76(S_{70})$; $(E)_{360} = 0.92(E)_{70}$
   @500°F: $(S_u)_{500} = 0.41(S_u)_{70}$; $(S_y)_{500} = 0.45(S_{70})$; $(E)_{500} = 0.81(E)_{70}$

Reference:
MIL-HDBK-5C, pages 3–208 and 3-214.

Property (units)/Temperature (°F)	70	100	200	300	400
Design Stress Intensity[2] (ksi)	10.5	10.5	10.5	8.4	4.4

2. ASME Code, Section II-D, Table 1-B

Table 2.3.1-5 Mechanical Properties of SA-193, Grade B6 High Alloy, Steel Bolting Material

Property (units)/Temperature (°F)	-40	-20	+70	+150	+200	+300	+600	+750
Ultimate Strength (ksi)	> 110.0	> 110.0	110.0	108.2	106.6	104.3	96.8	90.0
Yield Strength (ksi)	> 85.0	> 85.0	85.0	83.5	82.3	80.5	74.8	69.5
Modulus of Elasticity (ksi)	30.3E+3	30.1E+3	29.2E+3	28.8E+3	28.5E+3	27.9E+3	26.1E+3	25.1E+3
Alternating Stress @10^6 Cycles	20.2	20.1	19.8	19.5	19.3	19.0	17.9	17.3
Poisson's Ratio	0.32							
Density	489 lbm/ft^3 (0.283 lbm/in^3)							

References:

1. ASME Boiler and Pressure Vessel Code, Section III, Division I, Appendix I.
2. MIL-HDBK-5C, Section 2.3.1.

Table 2.3.1-6 Mechanical Properties of SA-453, Grade 660 High Alloy, Steel Bolting Material

Property (units)/Temperature (°F)	-40	-20	+70	+150	+200	+300	+600	+750
Ultimate Strength (ksi)	> 130.0	> 130.0	130.0	130.0	130.0	130.0	122.0	120.6
Yield Strength (ksi)	> 85.0	> 85.0	85.0	83.9	82.8	81.9	81.0	80.1
Modulus of Elasticity (ksi)	28.3E+3	28.2E+3	27.8E+3	27.3E+3	27.1E+3	26.7E+3	25.2E+3	23.8E+3
Coefficient of Thermal Expansion (in/in/°F)	7.93E-6	8.00E-6	8.22E-6	8.31E-6	8.39E-6	8.54E-6	8.94E-6	9.11E-6
Poisson's Ratio	0.32							
Density	489 lbm/ft^3 (0.283 lbm/in^3)							

References:

1. ASME Boiler and Pressure Vessel Code, Section III, Division I, Appendix I.
2. MIL-HDBK-5C, Section 2.3.1.

Table 2.3.1-7 Static Mechanical Properties of Chemical Copper Lead

Property (units)/Temperature (°F)	-40	-20	+70	+150	+200	+300	+600
Ultimate Strength (psi)	700	680	640	550	490	380	20
Modulus of Elasticity (ksi)	2.45E+3	2.42E+3	2.28E+3	2.16E+3	2.06E+3	1.94E+3	1.5E+3
Strain at Yield (in/in)	0.000286	0.000281	0.000291	0.000255	0.000238	0.000196	0.000133
Coefficent of Thermal Expansion (in/in/°F)	15.6E-6	15.7E-6	16.1E-6	16.4E-6	16.6E-6	17.2E-6	20.2E-6
Poisson's Ratio	0.40						
Density	708 lbm/ft^3 (0.41 lbm/in^3)						

References:

1. Tietz.
2. Gallagher.
3. NUREG/CR-0481.
4. Baumeister, pages 6-10.

Table 2.3.1-8 Dynamic Mechanical Properties of Chemical Copper Lead

Property (units)/Temperature (°F)	-40	-20	+70	+150	+200	+300	+600
Deformation Yield Strength (psi)	5620	5510	5000	4440	3960	3100	150
Deceleration Loading Yield Strength (ksi)	11,200	11,000	10,320	8870	7800	6100	300
Modulus of Elasticity (ksi)	2.45E+3	2.42E+3	2.28E+3	2.16E+3	2.06E+3	1.94E+3	0.15E+3
Strain at Yield (Deformation) (in/in)	0.00229	0.00228	0.00219	0.00206	0.00192	0.00160	0.00100

References:

1. Shappert.
2. NUREG/CR-0481.

Table 2.3.1-9 Mechanical Properties of SB-637, Grade N07718, Nickel Alloy Steel Bolting Material

Property (units)/Temperature (°F)	-40	-20	+70	+200	+300	+400	+500	+750
Ultimate Strength (ksi)	> 185.0	> 185.0	185.0	177.6	173.5	170.6	168.7	165.0
Yield Strength (ksi)	> 150.0	> 150.0	150.0	144.0	140.7	138.3	136.8	133.8
Modulus of Elasticity (ksi)	29.6E+3	29.5E+3	29.0E+3	28.3E+3	27.8E+3	27.6E+3	27.1E+3	26.1E+3
Coefficient of Thermal Expansion (in/in/°F)			7.05E-6	7.22E-6	7.33E-6	7.45E-6	7.57E-6	7.82E-6
Poisson's Ratio	0.31							
Density	503 lbm/ft^3 (0.291 lbm/in^3)							

Reference:

1. ASME Boiler and Pressure Vessel Code, Section III, Division I.

2.4 General Standards for All Packages

This section demonstrates that general requirements found in 10 CFR 71.43 are addressed in the design and analysis of the NAC-LWT cask, a spent-fuel shipping package. A package is defined as the assembly of components necessary to ensure compliance with 10 CFR 71 for the transportation of radioactive contents. The package includes the radioactive contents.

2.4.1 Minimum Package Size

The minimum transverse dimension of the NAC-LWT package is 44.24 inches (112 cm), and the minimum longitudinal dimension is 199.8 inches (507 cm). Both dimensions are greater than 10 centimeters; therefore, the requirements of 10 CFR 71.43(a) are satisfied.

2.4.2 Tamperproof Feature

One railroad car type seal is looped through a hole near the end of one ball-lock pin, which attaches the impact limiter attachment lugs to the mating cask lugs.

To tamper with the closure lid or port cover bolts, it is necessary to remove the upper impact limiter; thus, a severed seal will indicate purposeful tampering. This satisfies the tamperproof requirement of 10 CFR 71.43(b). This vent port and the drain port are protected by port covers. Both port covers are covered by the upper impact limiter; therefore, they cannot be operated by unauthorized personnel. This satisfies the requirements of 10 CFR 71.43(e).

2.4.3 Positive Closure

Inadvertent opening of the cask closure lid or the port covers from the combined effects of shock, vibration, thermal expansion, internal loads and/or external loads, cannot occur because of the large preload applied to the lid bolts. Loosening of these bolts is resisted by friction from the large clamping forces produced by the applied bolt preload torque. A cask operations procedure is followed, ensuring that each bolt is torqued. It is necessary to deliberately loosen the bolts with a wrench to facilitate inadvertent opening. The cover bolts cannot be loosened/removed while the upper impact limiter is attached with tamper-indicating seals in place. Therefore, the NAC-LWT cask containment system cannot be opened unintentionally and is protected against unauthorized operation; the requirements of 10 CFR 71.43(c) and (e) are satisfied.

2.4.4 Chemical and Galvanic Reactions

The structural materials of this package, which are in direct contact with each other, will not produce significant chemical or galvanic reaction in an electrically conductive environment. An inert stainless steel material is used to separate anodic from cathodic materials. The lead shielding material is completely encapsulated by the stainless steel shells; thereby, being separated from the aluminum basket. The aluminum honeycomb used for impact limiters is sealed inside an aluminum shell. The material of the miscellaneous cask components is stainless steel, which is compatible with all adjacent materials. Therefore, the materials do not have chemical or galvanic reactions in accordance with 10 CFR 71.43(d).

2.4.5 Cask Design

The cask is designed to meet the applicable sections of 10 CFR 71. Criticality, shielding, thermal, radiological and structural requirements of 10 CFR 71 are analytically shown to be satisfied. Conclusions drawn from the structural analyses are supported by quarter scale model drop tests. The NAC-LWT cask is an exclusive use package designed for transport in a 130°F environment such that personnel barrier temperatures do not exceed 180°F; thus, meeting the requirements of 10 CFR 71.43(g).

2.4.6 Continuous Venting

The neutron shield/expansion tank is the only vented system of the NAC-LWT cask. The shield/expansion tank contains a solution of ethylene glycol and water. No venting of the shield/expansion tank occurs during normal operations conditions; thus, meeting the requirements of 10 CFR 71.43(h).

2.5 Lifting and Tiedown Standards

2.5.1 Lifting Devices

The NAC-LWT cask has three types of lifting devices: (1) four lifting trunnions; (2) four lid lifting bolts; and (3) two rotation trunnions. These lifting devices are designed to meet the requirements of NUREG-0612, "Control of Heavy Loads at Nuclear Power Plants."

Lifting of the cask is accomplished by utilizing the lifting trunnions near the top of the cask. Two lifting yokes are used to provide redundancy. Each lifting yoke is attached to two diametrically opposite lifting trunnions. An overhead crane lifts the cask by these yokes. No impact limiter is attached to the cask during lifting and handling. The bottom impact limiter could be attached for protection during handing, but the top impact limiter cannot be used while the lifting yoke is in place.

The lid lifting bolts are used to attach cables for lifting the lid during installation or removal.

The rotation trunnions are used to rotate the cask from the horizontal to the vertical position. The rotation trunnions also support the cask in the transportation cradle.

2.5.1.1 Lifting Trunnion

The NAC-LWT cask is equipped with four lifting trunnions located on the upper ring near the top of the cask and spaced at 90-degree intervals; thus, either a nonredundant, two-arm yoke or a redundant, four-arm yoke system may be used to lift and handle the cask.

2.5.1.1.1 Loads

The lifting trunnions were analyzed for the most severe load, a single, nonredundant load path lift. Using the requirements of 10 CFR 71.45(a), the applied load factor is 3.0 on the yield strength. The yield strength of the material at 200°F is used. Any dynamic load effects are negligible when considered in combination with the large applied load factor.

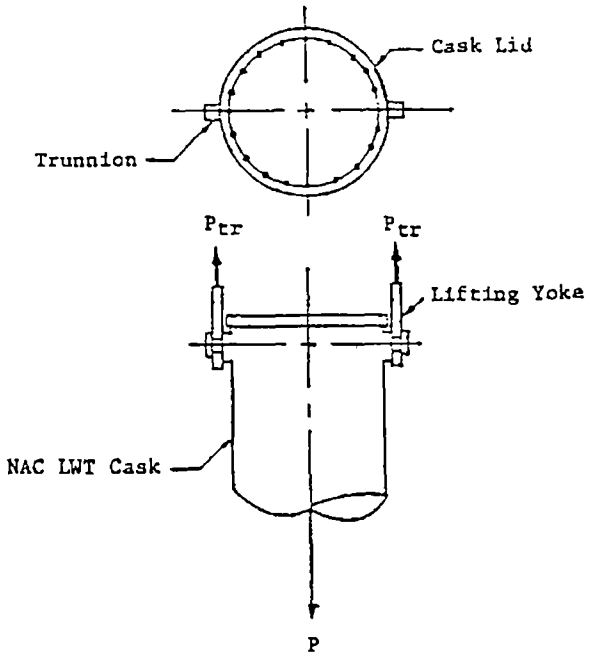

Lifting Trunnion Loads and Reactions

$P = LF \times W$

Fully Loaded Cask Weight (W) = 52,000 lbs

Load Factor on Yield $(LF)_y = 3.0$

$P_y = 3.0\ (52{,}000) = 156{,}000$ lbs

$(P_{tr})_y = 0.5\ (P_y) = 78{,}000$ lbs

2.5.1.1.2 Material Properties at 200°F

Trunnion and Cask Upper Ring (Base Metal)

ASME SA-240, Type 304

$S_y = 25{,}000$ psi

The shear strength is half the tensile strength if the compressive and tensile strengths are equal (Timoshenko, 1976, p. 449), which is conservative for stainless steel.

$$F_{sy} = \frac{S_y}{2} = 12{,}500 \text{ psi}$$

Weld Metal

The weld metal properties exceed those of the base metal, which is a standard welding code practice; therefore, the base metal properties are used for the weld analysis.

2.5.1.1.3 Stress Analysis

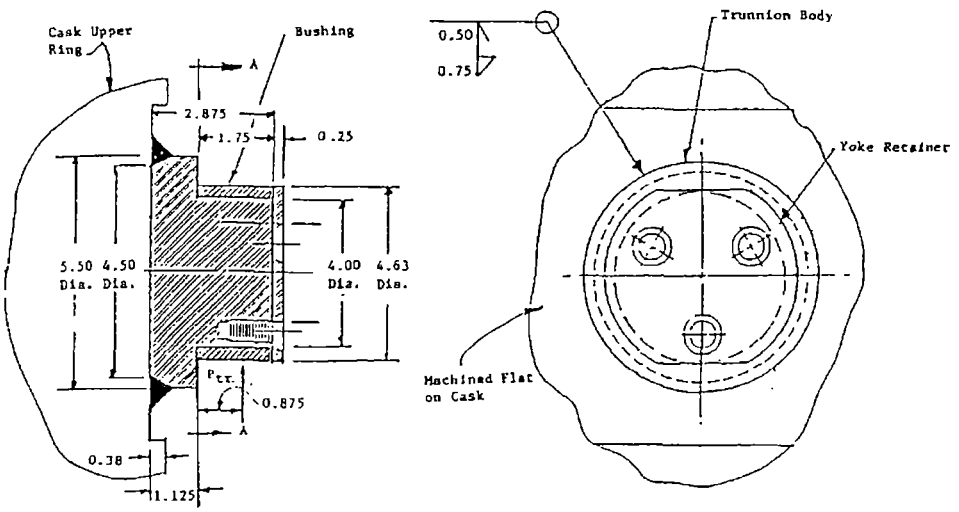

Typical Lifting Trunnion

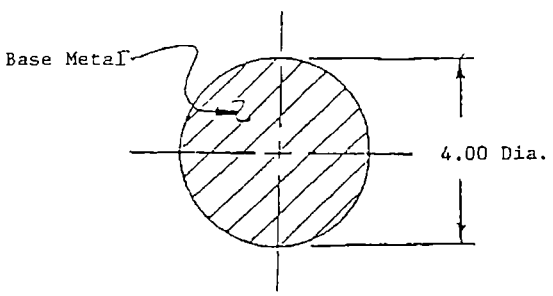

Section A-A

Shear Stress in Base Metal at Section A-A

$$(S_s)_y = \frac{(P_{tr})_y}{A_{aa}} = \frac{78{,}000}{\pi\,(2.00)^2} = 6{,}207 \text{ psi}$$

Margin of Safety at Section A-A

$$(M.S.)_y = \frac{F_{sy}}{(S_s)_y} - 1 = \frac{12{,}500}{6207} - 1 = \underline{+1.01}$$

Critical Weld Section

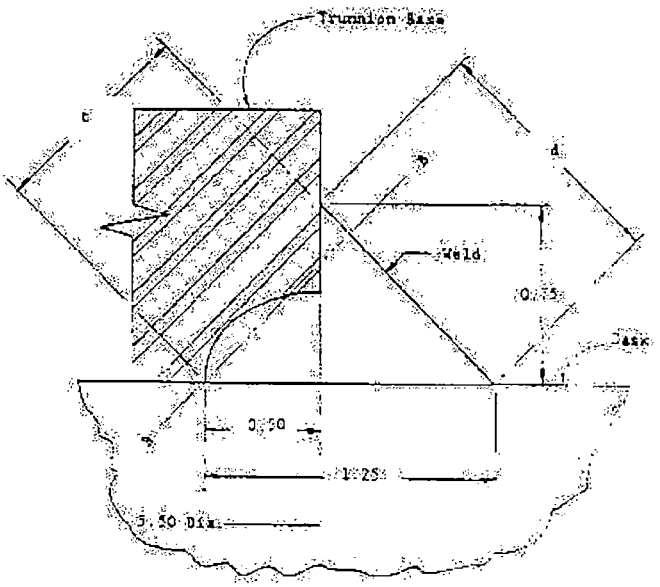

Effective Weld Throat

The most critical section of the weld shown in the above sketch is Section B-B. Its length is:

$$L_{bb} = 0.707\,(1.25) = 0.884 \text{ in}$$

The mean diameter of the center of gravity of Section B-B is:

$$d_{bb} = 5.50 - 2\,(0.50) + 2\,(\frac{1.25}{4}) = 5.125 \text{ inches}$$

Vertical Shear Force/Inch in Welds at Section B-B

$$(f_v)_y = \frac{(P_{tr})_y}{(d)_{bb}} = \frac{78{,}000}{\pi(5.125)} = 4{,}845 \text{ pounds/inch}$$

Horizontal Shear Force/Inch in Welds at Section B-B

$$(f_h)_y = \frac{(M_{bb})_y}{(Z_w)_{bb}} = \frac{78{,}000\ (1.125 + 1.75/2)}{\pi\ (5.125)^2/4} = 7{,}562 \text{ pounds/inch}$$

Combined Shear Force/Inch in Welds at Section B-B

$$(f_r)_y = \sqrt{[(f_v)_y]^2 + [(f_h)_y]^2} = \sqrt{(4845)^2 + (7562)^2}$$

$$= 8{,}981 \text{ pounds/inch}$$

Shear Stress in Weld at Section B-B

$$(f_w)_y = \frac{(f_r)_y}{L_{bb}} = \frac{8981}{0.884} = 10{,}159 \text{ psi}$$

Margin of Safety (MS) in Weld at Section B-B

$$(M.S.)_y = \frac{F_{sy}}{(f_w)_y} - 1 = \frac{12{,}500}{10{,}159} - 1 = \underline{+0.23}$$

2.5.1.1.4 Sequence of Lifting Component Failure

In addition to the load factor requirements in 10 CFR 71.45(a), lifting components must be designed such that, if the component fails under excessive load, the package will continue to meet other 10 CFR 71 requirements. To establish that the package continues to meet other 10 CFR 71 requirements, it is shown below that the trunnions will fail before the containment boundary fails. Trunnion failure enables other cask features (for example, impact limiters, cask body, etc.) to perform their function and bring the cask and contents to rest without breaching containment.

The maximum load carrying capacity of the trunnions, the trunnion welds, and the upper forging are calculated in this section.

Trunnions

The trunnions are manufactured from Type 304 stainless steel. To conservatively evaluate the maximum load carrying capacity of the trunnions, bending is neglected and the trunnion is considered in pure shear failure. The maximum load carrying capacity is calculated by multiplying the ultimate shear strength of Type 304 stainless steel by the cross-sectional area of the trunnion. The ultimate shear strength is calculated by multiplying the ultimate tensile strength (UTS) by 0.50 (Section 2.1.2.2).

$$P_u = (S_{su})(A_t)$$
$$= 446{,}235 \text{ lbs}$$

where:

P_u = maximum load capacity (lb)

S_{su} = (UTS) (0.50), Type 304 stainless steel @ 200°F (psi)

= 35,500 psi

D_t = 4.00 in.

A_t = shear area of trunnion (in^2) = $(\pi/4)(D_t)^2$

= 12.57 in^2

Trunnion Weld Interface

The width of the interface between the trunnion and the weld is $(0.50^2 + 0.75^2)^{0.5} = 0.901$ inch with an effective diameter of 5.0 inches. The ultimate shear capacity of the trunnion at the weld interface is:

$$P_u = (5.0)(\pi\pi(0.901)(35{,}500)$$
$$= 502{,}427 \text{ lbs}$$

Trunnion Weld

Figure 2.5.1-1 shows the lifting component (trunnion and trunnion weld) attached to the upper forging. The applied load, W, acts 2.125 inches from the weld and outer shell. The effects of bending are conservatively ignored because the line of action of the load is less than one diameter from the trunnion weld.

The effective weld area for the fillet/groove weld is the circular ring described by the minimum throat area as described in Section 2.5.1.1.3. The weld area is calculated as:

$$A_w = (L_w)(\pi)(D_m)$$
$$= 14.23 \text{ in}^2$$

where:

A_w = effective weld area (in^2)

L_w = minimum throat length = 0.884 in

D_m = mean diameter = 5.125 inches

The ultimate shear stress, S_{su}, for AWS E308 electrodes, which are used to weld Type 304 stainless steel, is (0.5)(80,000) = 40,000 psi. The maximum load that the trunnion weld can withstand is:

$$P_u = (A_w)(S_{su})$$
$$= 569{,}200 \text{ lbs}$$

Cask Upper Forging

The lifting components are attached to the upper forging of the NAC-LWT cask. Since the upper end casting is a solid piece of Type 304 stainless steel, this calculation considers the 1.25-inch wide ring of parent material beneath the trunnions (shown as a cross-hatched area in Figure 2.5.1-1). The maximum load that the outer shell can withstand is:

$$P_u = (A_p)\,(S_{su})$$
$$= 801{,}590 \text{ lbs}$$

where:

$$A_p = (\pi/4)(D_o^2 - D_i^2)$$
$$= (\pi/4)\,(7.00 - 4.50^2)$$
$$= 22.58 \text{ in}^2$$
$$S_{su} = 35{,}500 \text{ psi}$$

Conclusion

The maximum load carrying capacity of the trunnion, the trunnion/weld interface, the trunnion weld, and the upper forging are summarized in Table 2.5.1-1. The trunnion has a minimum load carrying capacity; its failure under excessive load will not impair the ability of the package to meet the other requirements of 10 CFR 71, Subpart E.

2.5.1.2 Lid Lifting Bolts

The top of the NAC-LWT cask lid is equipped with four 1 - 8 UNC threaded holes on a 9.0-inch square pattern to accommodate bolts to be used to lift the lid. These holes are threaded 1.5 inches deep.

A load factor of 3.0 for yield strength analysis is applied to the load for handling safety. The weight of the lid without attachment bolts is 919 pounds; thus, the tensile force on each bolt is (3.0)(919)/4 = 689 pounds. For conservatism, it is assumed that the bolt and the lid are of the same material, Type 304 stainless steel, which has a yield strength (S_y) equal to 27,500 psi at

150°F. Any dynamic load effects are negligible when considered in combination with the large applied load factors.

The tensile stress area (A_t) for a 1 - 8 UNC bolt, according to Table III.3 of "Screw-Thread Standards for Federal Services," is 0.606 square inches. Therefore, the stress in the bolt is 689/0.606 = 1044 psi and the margin of safety is (27,500/1044) - 1 = +LARGE.

The minimum length of thread engagement (L_e) required to fully develop the tensile strength of the bolt is calculated from "Screw-Thread Standards for Federal Services," Section II, Article 23, which gives the equation:

$$L_e = \frac{2A_t}{\pi n K_{n_{max}} + \left[0.5n + 0.57735\left(E_{s_{min}} - K_{n_{max}}\right)\right]}$$

where ("Screw-Thread Standards for Federal Services," Table III.10):

n = number of threads per inch = 8

$K_{n_{max}}$ = maximum minor diameter of threaded hole = 0.890 in

$E_{s_{min}}$ = minimum pitch diameter of bolt threads = 0.910 in

$$L_e = \frac{2(0.606)}{\pi(8)(0.890)\left[1/2(8) + 0.57735(0.910 - 0.890)\right]} = 0.7318 \text{ in}$$

This length is less than the 1.25-inch actual depth of threads, assuming the first and last threads are inactive; therefore, the internal threads of the tapped hole possess enough strength to cause the bolt to fail before the threads shear.

2.5.1.3 Can Assembly (315-40-98)

The LWT can assembly lifting is accomplish by lifting the assembly at the handle on the can lid. A factor of safety on yield strength of 3 is required for handling safety. The weight lifted by the handle (considering a 10% dynamic load factor) is:

$$W = (350 + 310 + 240 + 75) \times 1.1 = 1{,}072 \text{ lbs}$$

During lifting, the tensile stress at the minimum cross section of the handle is:

$$\sigma_t = \frac{W}{A} = \frac{1{,}072 \text{ lb}}{0.78 \text{ in.}^2} \cong 1{,}374 \text{ psi}$$

where:

$A = (4.25 - 3.0) \times 5/8 = 0.78 \text{ in}^2$

Because the factor of safety, $FS = \frac{17{,}300}{1{,}326} = 13.0 > 3$, the design condition lifting stresses have a factor of safety of 3 on the basis of yield strength is met.

The maximum shear occurs at the center of the handle and is computed as:

$$\tau = \frac{W}{A} = \frac{1{,}072 \text{ lbs}}{(3.23 - 1.5 - 0.23 - 0.88)(0.625) \text{ in.}} \cong 2{,}766 \text{ psi}$$

The factor of safety (FS) is conservatively calculated using a shear allowable of $0.6S_m$ at 750°F.

$$FS = \frac{0.6(17{,}300 \text{ psi})}{2{,}766 \text{psi}} = 3.38 > 3$$

Therefore, the design condition that lifting stresses have a factor of safety of 3 on the basis of yield strength is met.

Figure 2.5.1-1 Trunnion Cross-Section and Forging Shear Area

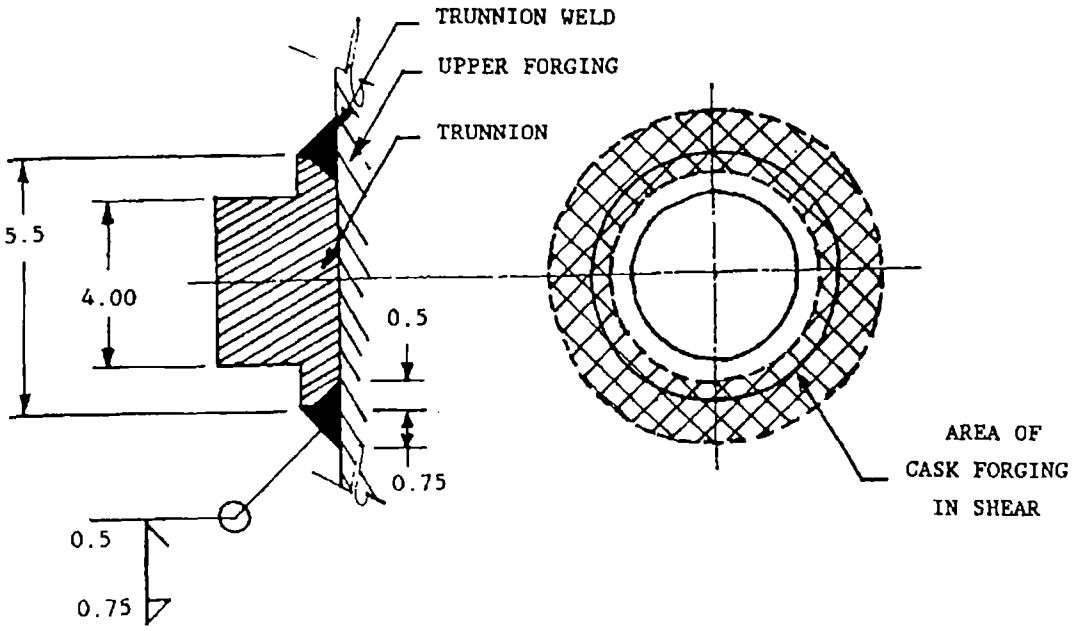

Table 2.5.1-1 Maximum Capacity of the Lifting Components

Lifting Trunnion	446,235 lbs
Trunnion/Weld Interface	502,427 lbs
Trunnion Weld	569,200 lbs
Cask - Upper Forging	801,590 lbs

2.5.2 Tiedown Devices

The NAC-LWT cask is tied down to the shipping skid using the following: (a) rotation trunnions near the bottom at point i (Figure 2.5.2-1); and (b) a 90-degree saddle support, hold-down straps and a shear ring near the top end at point j (Figure 2.5.2-1). Longitudinal force towards the bottom of the cask is resisted by the supports at the rotation trunnions; a shear ring welded to the outer shell resists the longitudinal force towards the top end of the cask. A 0.50-inch gap is provided between the shear ring and the saddle support to accommodate the thermal expansion of the cask.

In accordance with 10 CFR 71.45(b), the tiedown components of the cask are designed for static forces having a vertical component of two times the weight of the package, a longitudinal component of ten times the weight of the package, and a lateral component of five times the weight of the package. The design weight of the NAC-LWT cask with its contents and impact limiters is 52,000 pounds.

2.5.2.1 Discussion and Loads

The resultant force on the shear ring is assumed to act at the centroid of the contact area between the shear ring and the saddle support. Referring to Figure 2.5.2-1, the distance of the centroid from the center of the cask is determined:

$$\bar{y} = (A_o \bar{y}_o - A_i \bar{y}_i)/(A_o - A_i)$$

$$\bar{y} = \left[(2 \sin\theta\, (R_o^3 - R_i^3)\right] / \left[3\theta (R_o^2 - R_i^2)\right]$$

$$= 13.90 \text{ inches}$$

where:

$A = \theta R^2$

$\bar{y} = (2R \sin\theta / 3\theta$

$\theta = 45° = \pi/4$ radians

$R_o = 15.81$ inches

$R_i = 15.06$ inches

There are three loading cases for the tiedown components - vertical, longitudinal, and lateral loads. The reaction forces for each loading case are determined by the equations of equilibrium.

2.5.2.1.1 Vertical Load

Downward Direction Case

$F_y = -2W = -2(52{,}000) = -104{,}000$ lbs

Summing moments M_z about point j:

$\Sigma M_z = -104{,}000(82.22) + 2R_{iy}(165.63) = 0$

$R_{iy} = +25{,}813$ lbs

Summing vertical forces:

$2R_{iy} + R_{jy} - 104{,}000 = 0$

$R_{jy} = 52{,}374$ lbs

Note: $R_{ix} = R_{jx} = 0$ because of the gap provided at the shear ring.

Upward Direction Case

$F_y = +2W = +2(52{,}000) = +104{,}000$ lbs

similarly (Section 2.5.2.1.1),

$R_{iy} = -25{,}813$ lbs

$R_{jy} = -52{,}374$ lbs

Note that the support saddle cannot carry any upward load. Hence, the negative R_{jy} is resisted by tiedown straps.

2.5.2.1.2 Longitudinal Load

Load Toward the Top End of the Cask

$F_x = +10W = +10(52{,}000) = +520{,}000$ lbs

Summing horizontal forces:

$520{,}000 + R_{jx} = 0$

$R_{jx} = -520{,}000$ lbs

Summing moments about j:

$520{,}000(13.90) + 2R_{iy}(165.63) = 0$

$R_{iy} - -21{,}820$ lbs

Summing vertical forces:

R_{jy} - 2(21,820) = 0

R_{jy} - 43,640 lbs

Load Toward the Bottom of the Cask

F_x = -10W = -10(52,000) = -520,000 lbs

Summing horizontal forces:

-520,000 + $2R_{ix}$ = 0

R_{ix} = +260,000 lbs

Summing moments about j:

-520,000(13.90) + 2(260,000)(13.90 + 3) + $2R_{iy}$ (165.63) = 0

R_{iy} = -4,709 lbs

Summing vertical forces:

R_{jy} – 2(4709) = 0

R_{jy} = 9,418 lbs

2.5.2.1.3 Lateral Load

F_z = 5W = 5(52,000) = 260,000 lbs

To find the reactions resisting the above load, it is necessary to find the location of the bearing pressure between the support saddle and the cask surface. The contact surface is one-half of the saddle, as shown in Figure 2.5.2-2. Assume that the horizontal bearing pressure at any point is proportional to the sine function of the angular distance of the point from the lowest point in the saddle.

Referring to Figure 2.5.2-2, take a unit radius:

$dA = \sin\theta[\cos\theta - \cos(\theta + d\theta)]$

$= \sin\theta[\cos\theta - (\cos\theta\cos d\theta - \sin\theta\sin d\theta)]$

For small angle $d\theta$, $\cos d\theta \approx 1$, $\sin d\theta \approx d\theta$

hence,

$dA = \sin^2\theta d\theta$

$$A = \int_0^{\pi/4} \sin^2\theta d\theta$$

$$= \frac{1}{2}\theta - \frac{1}{4}\sin 2\theta$$

$$= (\pi - 2)/8 = 0.1427$$

The first moment of area about the horizontal line through the center is:

$$dM = ydA$$

$$= \cos\theta\sin^2\theta d\theta$$

$$M = \int_0^{\pi/4} \cos\theta os\theta^2 \theta d\theta$$

$$= (\sin^3\theta)/3$$

$$= 0.17785$$

$$\bar{y} = \frac{M}{A} = 0.8259$$

where:

$R = 14.31$ inches

$\bar{y} = 11.82$ inches

Call the location of this centroid: point k.

The horizontal distance from the center of the cask to the support point i is 16.87 inches.

Summing moments about the vertical line through k (Figure 2.5.2-3):

$$260{,}000(82.22) + R'_{iz}(165.63) = 0$$

$$R'_{iz} = -129{,}066 \text{ lbs}$$

Summing forces along the Z-axis:

$$260{,}000 - 129{,}066 + R_{jz} = 0$$

$$R_{jz} = -130{,}934 \text{ lbs}$$

Summing forces along the Y-axis:

$$R_{iy} = -R'_{iy}$$

Summing moments about the longitudinal axis of the cask:

$$130{,}934(11.82) - 129{,}066(3) - R'_{ig}\,(16.87 + 16.87) = 0$$

$$R'_{iy} = 34{,}394 \text{ lbs}$$

$$R_{iy} = -34{,}394 \text{ lbs}$$

(Opposite Lateral Load)

$$F_z = -5W = -5(52{,}000) = -260{,}000 \text{ lbs}$$

The reactions for this case are opposite to the previous case.

2.5.2.1.4 Loads Summary

The results of all the loading cases are summarized in Table 2.5.2-1.

2.5.2.2 Rear Support

The NAC-LWT cask rear tiedown attachment is at the rotation trunnions. There are two rotation trunnions, which are slots located 16 inches above the bottom of the cask and spaced at approximately 180-degree positions in line with two of the lifting trunnions. Each slot is a machined part, which is welded all around to the cask outer shell. The neutron shield tank shell is cut out to provide access to the slots. The geometry details of the shield tank cut-outs and the rotation trunnion slots are shown in Figure 2.5.2-4.

2.5.2.2.1 Loads

The rotation trunnions are analyzed for the cask tiedown load condition defined in 10 CFR 71.45(b). The condition used for this analysis assumes that the cask is supported horizontally on a trailer and is subjected to a 10 g longitudinal shock load simultaneously with a 2 g vertical shock load and a 5 g lateral shock load. The direct lateral load is transferred to the cask through bearing on the large trunnion slot base. Any dynamic load effects are negligible when considered in combination with the large applied load factors. The critical loads on the rotation trunnions are derived in Section 2.5.2.1.

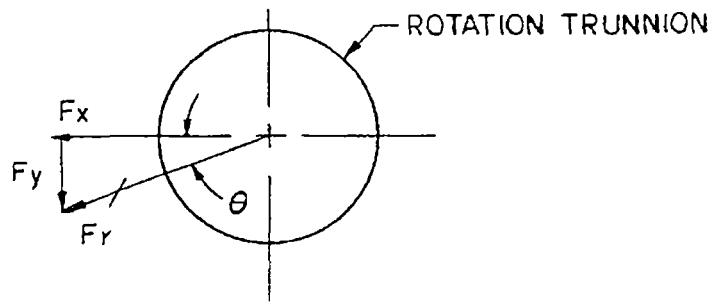

Resultant Load Determination

$$F_r = \sqrt{(F_x)^2 + (F_y)^2}$$

$$= 272{,}632 \text{ lbs}$$

where:

$F_x = 260{,}000$ lbs

$F_y = 82{,}027$ lbs (Table 2.5.2-1; Section 2.5.2.1)

then

$\theta = \arctan(82{,}027/260{,}000)$

$= 17.5$ degrees

2.5.2.2.2 Material Properties at 200°F

The yield strength of each material at 200°F is the allowable stress:

Type 304 stainless steel

$S_y = 25{,}000$ psi

Cask and Trunnion Slot (Base Metal)

The bearing stress ratio is taken from MIL-HDBK-5A where the bearing yield stress for the austenitic stainless steels at ambient temperature is specified as 50,000 psi and the yield strength as 30,000 psi. It is assumed that the ratio of bearing stress to yield stress remains constant up to 200°F:

$S_{bry} = 1.67(25{,}000) = 41{,}750$ psi

The shear strength is (0.6) (yield strength):

$S_{sy} = 0.6S_y = 15{,}000$ psi

Weld Metal

The weld metal properties exceed those of the base metal, based on standard welding code practice; therefore, the base metal properties will be used for the weld analysis:

$(S_{sy})_w = 15{,}000$ psi

2.5.2.2.3 Stress Analysis

Bearing Stress in Trunnion Slot (Figure 2.5.2-4)

$F_y = 272{,}632$ lbs

Length of engagement for 4.00-in diameter pin = 3.25 inches

$A_{br} = 4.00(3.25) = 13.00 \text{ in}^2$

$$S_{br} = \frac{F_r}{A_{br}}$$

$$= 20{,}972 \text{ psi}$$

$$MS = \frac{S_{bry}}{S_{br}} - 1 = \underline{+0.99}$$

Stress in Weld Connecting Trunnion to Cask (Figure 2.5.2-4)

Assume the entire load transferred to the cask outer shell through the weld at the base of the trunnion.

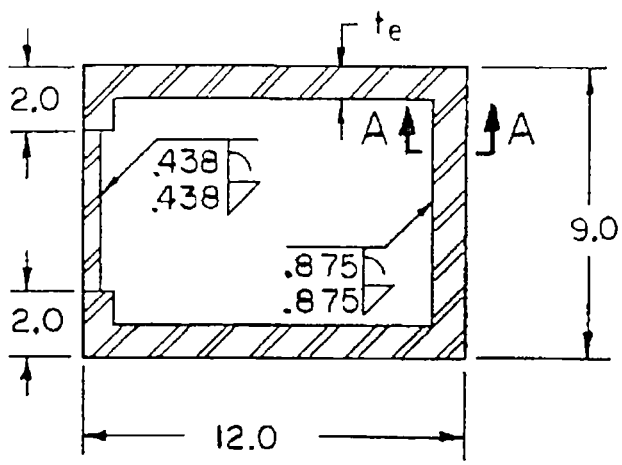

Section Through Weld at Base of Pocket

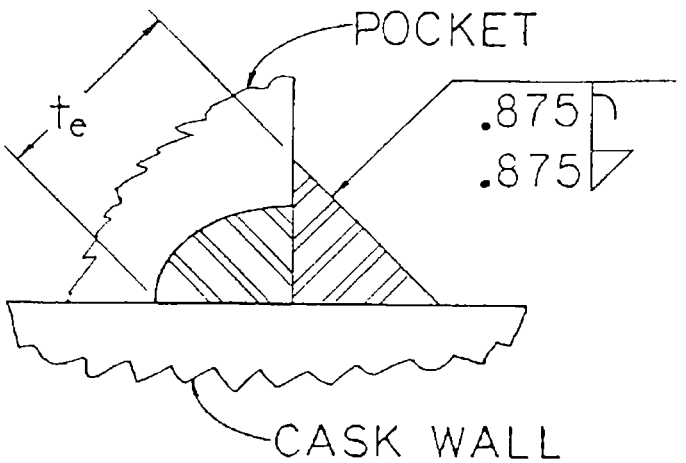

Section A-A

Effective thickness of weld (t_e) = ($\sqrt{2}$) (t_w)

for:

t_w = 0.875 in; t_e = 1.237 in

t_w = 0.438 in; t_e =0.619 in

Section Properties of Weld Group

Area (A_w) = 42.741 in^2

$\bar{y}$ = 4.500 inches

$\bar{x}$ = 6.412 inches

I_{xx} = 501.924 in^4

I_{yy} = 718.398 in^4

J_{xy} = I_{xx} + I_{yy} = 1220.322 in^4

Loads on Weld Group

F_x = 260,000 lbs

F_y = 82,027 lbs

e_x = 6.412 – 4.000 = 2.412 inches

e_z = 19.08 – 14.00 – 3.25/2 = 3.455 inches

$M_x = F_y (e_z) = 82{,}027\ (3.455) = 283{,}403$ in-lbs

$M_y = F_x (e_z) = 260{,}000\ (3.455) = 898{,}300$ in-lbs

$M_z = F_y (e_x) = 82{,}027\ (2.412) = 197{,}849$ in-lbs

Maximum Stresses on Effective Thickness of Weld Group

$$S_X = \frac{F_X}{A_W} + \frac{M_Z C_y}{J_{xy}} = \frac{260{,}000}{42.741} + \frac{(197{,}849)(4.50)}{1220.322}$$
$$= 6813 \text{ psi}$$

$$S_y = \frac{F_y}{A_w} + \frac{M_z C_x}{J_{xy}} = \frac{82{,}027}{42.741} + \frac{(197{,}849)(6.412)}{1220.322}$$
$$= 2959 \text{ psi}$$

$$S_z = \frac{M_x C_y}{I_{xx}} + \frac{M_y C_x}{I_{yy}} = \frac{(283{,}403)(4.5)}{(501.924)} + \frac{(898{,}300)(6.412)}{(718.398)}$$
$$= 10{,}559 \text{ psi}$$

$$S_{smax} = (S_X{}^2 + S_y{}^2 + S_Z{}^2)^{0.5}$$
$$= 12{,}910 \text{ psi}$$

$$M.S. = \frac{(S_{sy})_w}{S_{smax}} - 1 = \underline{+0.16}$$

The positive margins of safety show that the rotation trunnion meets the requirements of 10 CFR 71.45(b).

2.5.2.2.4 Overload – Tiedowns

According to 10 CFR 71.45(b)(3), each tiedown device that is a structural part of a package must be designed so that failure of the device under excessive load would not impair the ability of the package to meet the other requirements of 10 CFR 71. For this reason, the shear capacity of the rotation trunnions, weld and outer shell are compared.

The weld attaching the rotation trunnion to the outer shell and the lower forging is shown in Section 2.5.2.2.3. The shear capacities of the rotation trunnions, weld and outer shell are calculated below (see sketch of Section A-A on page 2.5.2-8 for geometry details).

Rotation Trunnion

The width of the interface between the rotation trunnion base metal and the weld is:

$b_{rt} = \pi(0.875)/2$

$= 1.374$ in

The ultimate shear capacity of the rotation trunnion base metal per inch of length along the weld is:

$F_{rt} = 1.374(0.50\ S_{tu})$

$= 1.374(0.50 \times 71{,}000)$

$= 48{,}777$ lbs/in

Weld

The effective throat of the weld is:

$t_e = 1.414(0.875)$

$= 1.237$ in

The welding electrode used to weld Type 304 stainless steel is AWS E308 with a tensile strength of 80,000 psi. The ultimate shear capacity per inch of length of weld is:

$F_w = 1.237(0.50 \times 80{,}000)$

$= 49{,}480$ lbs/in

Outer Shell

The width of the interface between the weld and the outer shell base metal is:

$b_{os} = 2(0.875)$

$= 1.75$ in

The ultimate shear capacity of the outer shell base metal per inch of length along the weld is:

$F_{os} = 1.75(0.50 \times 71{,}000)$

$= 62{,}125$ lbs/in

The maximum shear capacities per inch of length along the weld interface are summarized as follows:

Rotation trunnion = 48,777 lbs/in

Weld = 49,480 lbs/in

Outer shell= 62,125 lbs/in

Thus, the rotation trunnions and the weld will fail in shear before the outer shell, assuring that failure caused by excessive overload on the rotation trunnions will not impair the ability of the package to meet the other requirements of 10 CFR 71.

2.5.2.3 Front Support

2.5.2.3.1 Discussion

The longitudinal force toward the top end of the cask is resisted by a shear ring welded to the cask outer shell. The shear ring is located at the juncture of the neutron shield shell top plate with the outer shell.

2.5.2.3.2 Shear Ring

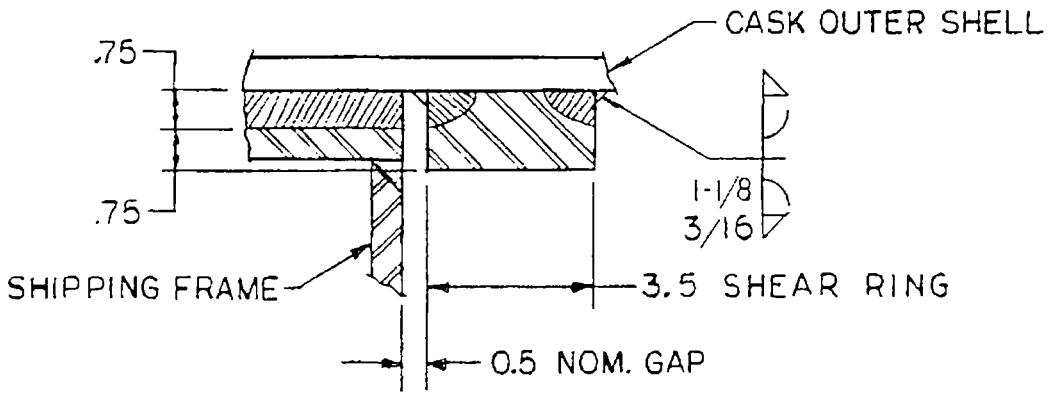

Shear Ring Geometry

The shear ring geometry bears on the shipping frame along a 90-degree arc (Figure 2.5.2-1). The load on the shear ring is:

R_{jx} = 520,000 lbs (Section 2.5.2)

Assuming that 0.75 inch of the ring thickness is in direct bearing against the side of the support frame, the bearing pressure is:

S_{brg} = 520,000/(0.5)(π)(15.06)(0.75)
= 29,309 psi

The allowable bearing on the surface of Type 304 stainless steel is:

$(S_{brg})_{ALL}$ = 41,750 psi at 200°F

The margin of safety for bearing is:

MS = (41,750/29,309) - 1= +0.42

The shear stress across the weld is:

$S_s = (29{,}309)(0.75)/(1.12)(2) = 9{,}813$ psi/in

In addition, the bar is subject to flexure:

$M = (29{,}309)(0.75)(0.75 + 0.375)$

$= 24{,}729$ in-lb/in

The moment of inertia of the welded area is:

$I = (1)(3.5)^3/12 - (1)(1.25)^3/12$

$= 3.410$ in^4

The flexural stress is:

$S_b = (24{,}729)(1.75)/3.410$

$= 12{,}690$ psi

The equivalent stress is:

$$S_{eq} = \left(S_b^{\ 2} + 3S_s^{\ 2}\right)^{0.5}$$

$= 21{,}211$ psi

The margin of safety at 200°F is:

$MS = (25{,}000/21{,}211) - 1 = +0.18$

where:

$S_y = 25{,}000$ psi at 200°F.

Figure 2.5.2-1 Front Support and Tiedown Geometry

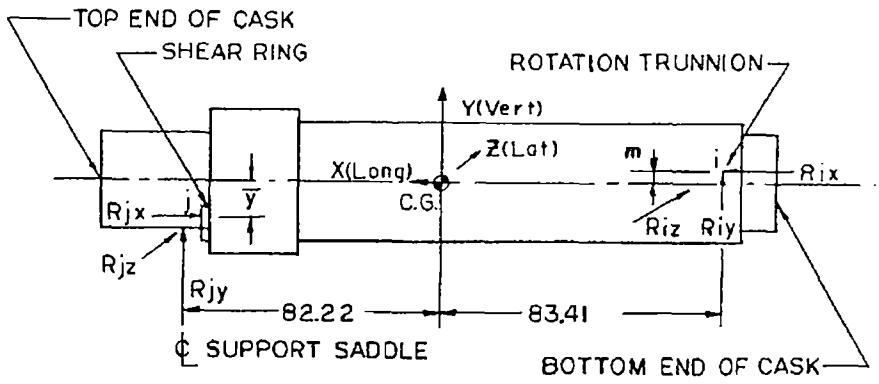

Free Body Diagram

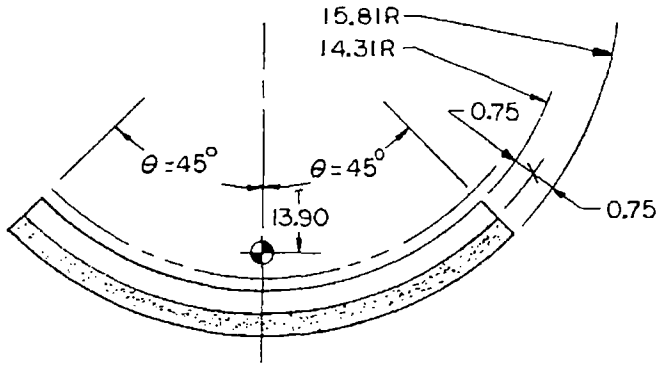

Shear Ring Geometry

Figure 2.5.2-2 Pressure Distribution of Horizontal Bearing Between Cask and Support Saddle

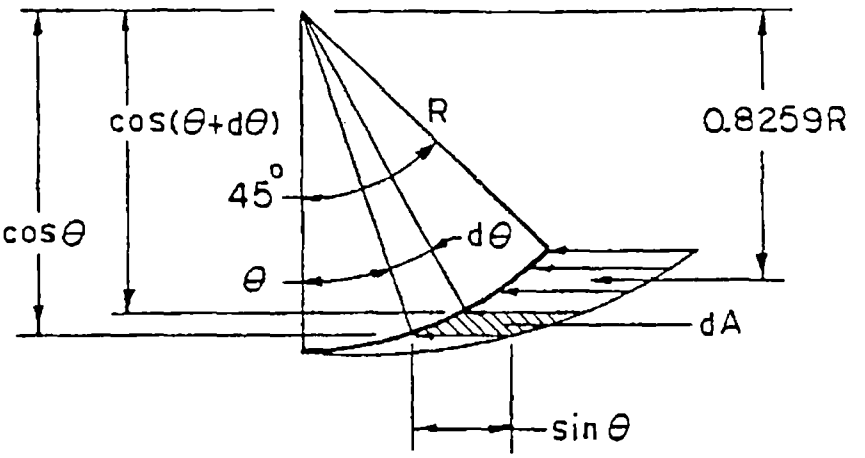

Figure 2.5.2-3 Free Body Diagram of Cask Subjected to Lateral Load

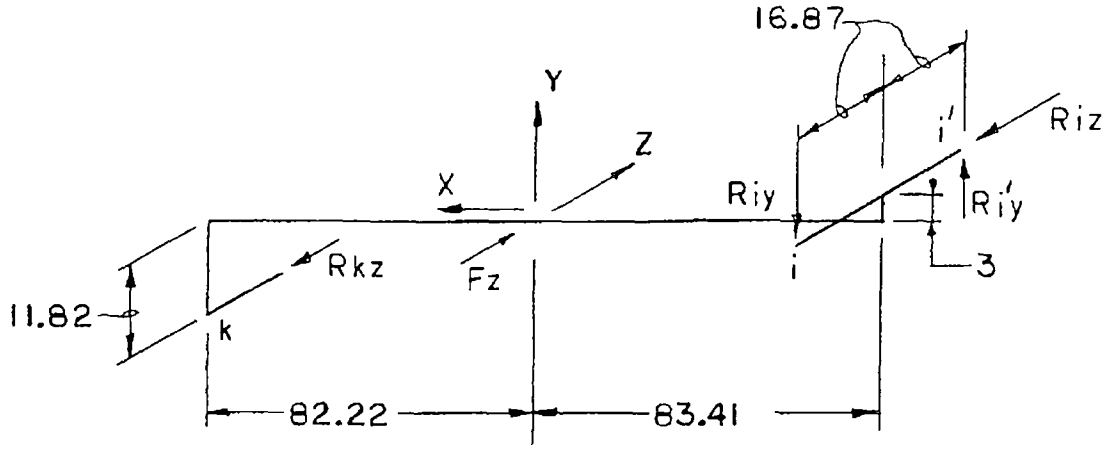

Figure 2.5.2-4 Rotation Trunnion Pocket

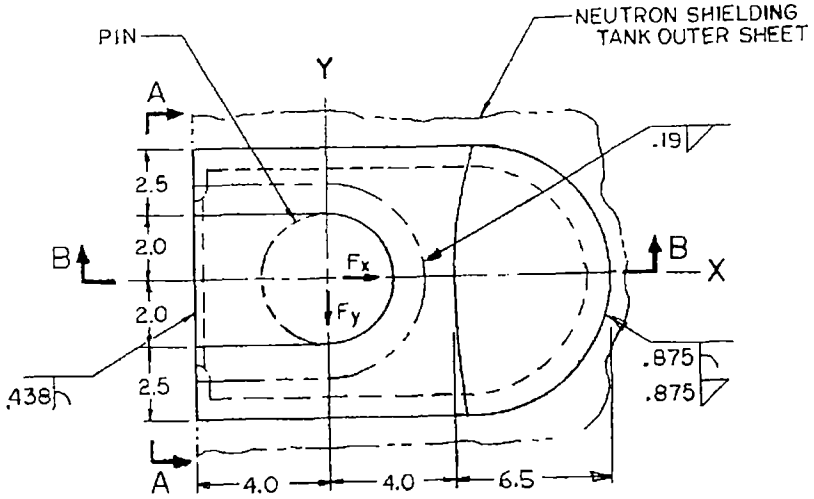

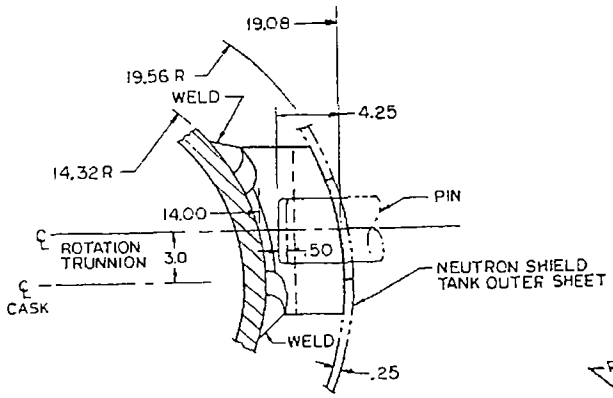

View A-A

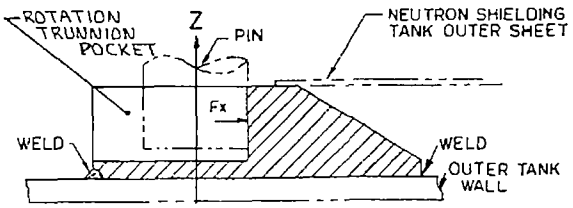

Section B-B

Table 2.5.2-1 Reactions Caused By Tiedown Devices

		Reactions (lb)					
Load Case	Load (lb)	R_{jx}	R_{jy}	R_{jz}	R_{ix}	R_{iy}	R_{iz}
A1	F_y = -104,000	0	52,374	0	0	25,813	0
A2	F_y = 104,000	0	-52,374	0	0	-25,813	0
B1	F_x = 520,000	-520,000	43,640	0	0	-21,820	0
B2	F_x = -520,000	0	9418	0	260,000	-4709	0
C1	F_z = 260,000	0	0	-130,934	0	-34,394	-129,066
C2	F_z = -260,000	0	0	130,934	0	34,394	-129,066
Maximum combined reactions		0	96,014	130,934	260,000	60,207	129,066
(A + B + C)		-520,000	-52,374	-130,934	0	-82,027	0

2.6 Normal Conditions of Transport

2.6.1 Hot Case

2.6.1.1 Discussion

The NAC-LWT cask body and lid are analyzed for structural adequacy in accordance with the requirements of 10 CFR 71.71(l) Heat (normal transport conditions). The cask is assumed to be loaded and ready for shipment in the horizontal position with an ambient temperature of 130°F.

The stress analysis of the cask is performed by the finite element method using the ANSYS computer program (See Sections 2.10.1 and 2.10.2 for model and computer program descriptions).

2.6.1.2 Analysis Description

2.6.1.2.1 Geometry

The finite element model is described in Section 2.10.2. The temperature-dependent material properties presented in Section 2.3 are used in the analysis.

2.6.1.2.2 Loadings

An internal pressure of 50 psig is applied on the cask cavity and lid interior surfaces in the outward normal direction. The pressure loading region includes the lid and upper body forging mating surfaces outward to the inner cask lid seal centerline.

The total cask lid bolt torque, as calculated in Section 2.1.3.2.2, is applied to the bolt, which is modeled as a beam element with a preload force of 39,788.74 pounds/radian (This is equivalent to an initial strain of 0.0021361 in/in-radian).

Cask temperatures as determined in Section 3.4.2 (based on 130°F ambient temperature) are imposed on the model. See Section 2.10.3.1 for the resulting isothermal temperature plot.

Mechanical loads resulting from the total weight of the cask structure and contents are imposed on the model. The total weight of the finite element model is 37,519 pounds, which is less than the design weight of 52,000 pounds (The design weight includes the total weight of the cask and its contents). Therefore, an acceleration of 1.387 g (535.94 in/sec^2) is uniformly applied to the finite element model in the positive global x-direction (The model is defined in the positive x-y plane).

Fabrication stresses are considered negligible as demonstrated in Section 2.6.11.

2.6.1.2.3 Displacement Boundary Conditions

The finite element model is restrained radially at all centerline nodes and longitudinally at the node located on the centerline at the cask model global origin; i.e., at the bottom of the cask model.

2.6.1.3 Detailed Analysis

Stresses throughout the finite element model of the cask body and closure lid are calculated for the combined pressure, bolt preload, thermal and mechanical load conditions as previously described. In accordance with the design criteria presented in Section 2.1.2, the calculated stresses are evaluated as primary membrane (P_m), primary membrane plus primary bending ($P_m + P_b$), S_n and total stress categories. The secondary stresses (thermal) are conservatively included in the primary stress categories and margin of safety calculations; therefore, the 3 S_m limit on the S_n stress intensity range is satisfied because it is enveloped by the 1.0 S_m limit on primary stress intensity.

To satisfy this criteria, procedures have been implemented (as demonstrated in Section 2.10.3) to determine the following:

1. The critical P_m and $P_m + P_b$ section stresses for each cask component.
2. The critical total stress for each cask component.

The most critical sections for each cask component are shown in Figure 2.6.1-1. The maximum P_m and $P_m + P_b$ stresses for each component are reported in Table 2.6.1-1 and Table 2.6.1-2, respectively. Both tables consider the allowable stress for a component with a temperature of 300°F. Additionally, the stresses at representative sections throughout the cask are presented in the tables in Section 2.10.7. These tables document the maximum stress locations tabulated for each component. The critical total stress for each cask component is reported in Table 2.6.1-3. For the fatigue evaluation, refer to Section 2.1.3.2.

The minimum margin of safety is shown to be <u>+0.30</u>, which occurs in component 7 (the Type 304 stainless steel cask bottom) for the condition of $P_m + P_b$ stress. This section is located 5.50 inches axially from the bottom of the cask body at the region where the bottom lead shielding is located.

2.6.1.4 Conclusion

Using conservatively applied loadings and stress categorization, it is demonstrated that the minimum margin of safety for the NAC-LWT cask for the heat condition is +0.30. Therefore, the NAC-LWT cask satisfies the requirements of 10 CFR 71 for consideration of the heat load condition.

Figure 2.6.1-1 NAC-LWT Cask Critical Sections (Hot Case)

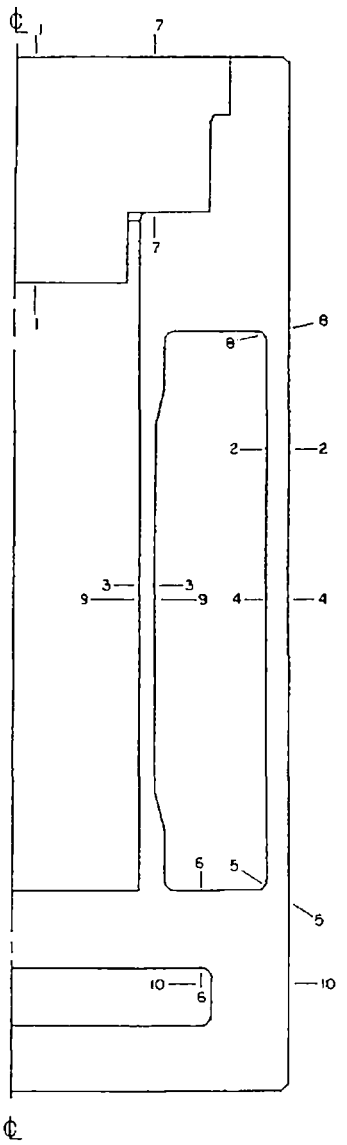

Table 2.6.1-1 Critical Stress Summary (Hot Case) – P_m

		P_m Stresses (ksi)				Principal Stresses					
Comp. No.[1]	Cut Node to Node	S_x	S_y	S_z	S_{xy}	S_1	S_2	S_3	S.I.	Allow. Stress 1.0 S_m	Margin of Safety
	1-1										
1	2302 to 2562	0.67	0.16	-0.44	0.51	0.99	-0.15	-0.44	1.43	20.0	Large
	2-2										
3	1595 to 1598	0.00	10.20	0.27	-0.06	10.20	0.27	0.00	10.20	20.0	+1.0
	3-3										
4	1121 to 1124	-0.03	3.38	0.45	0.00	3.38	0.45	-0.03	3.41	31.4	+8.2
	4-4										
6	1115 to 1118	-0.01	11.18	0.05	0.00	11.18	0.05	-0.01	11.19	31.4	+1.8
	5-5										
7	375 to 300	1.80	6.23	3.47	-4.98	9.46	3.47	-1.43	10.90	20.0	+0.8
	6-6										
8	192 to 342	-5.61	1.21	-0.75	3.56	2.73	-0.75	-7.13	9.85	20.0	+1.0

[1] Refer to Figure 2.10.2-9 for component identification.

Table 2.6.1-2 Critical Stress Summary (Hot Case) – $P_m + P_b$

		$P_m + P_b$ Stresses (ksi)				Principal Stresses					
Comp. No.[1]	Section Cut Node to Node	S_x	S_y	S_z	S_{xy}	S_1	S_2	S_3	S.I.	Allow. Stress 1.5 S_m	Margin of Safety
	7-7										
1	2371 to 2571	-3.06	-0.26	0.10	0.18	0.10	-0.25	-3.08	3.17	30.0	+8.5
	8-8										
3	1852 to 1856	-0.30	13.09	3.90	-0.56	13.11	3.90	-0.32	13.43	30.0	+1.2
	9-9										
4	1101 to 1104	0.00	3.68	0.68	0.00	3.68	0.68	0.00	3.68	47.1	Large
	2-2										
6	1595 to 1598	-0.01	11.59	0.48	-0.06	11.59	0.48	-0.01	11.60	47.1	+3.0
	10-10										
7	168 to 175	-13.48	9.78	1.46	-1.09	9.83	1.46	-13.53	23.36	30.0	+0.3
	6-6										
8	192 to 342	-16.04	1.21	-0.75	3.56	1.91	-0.75	-16.74	18.66	30.0	+0.6

[1] Refer to Figure 2.10.2-9 for component identification.

Table 2.6.1-3 Critical Stress Summary (Hot Case) – Total Range

		Total Stress Range (ksi)				Principal Stresses			Stress Differences		
Comp. No.[1]	Node	S_x	S_y	S_z	S_{xy}	S_1	S_2	S_3	S_1-S_2	S_2-S_3	S_3-S_1
1	2561	1.05	0.01	1.05	-18.80	19.34	1.05	-18.28	18.29	19.33	-37.62
3	1856	-0.30	12.04	3.33	0.18	12.04	3.33	-0.30	8.71	3.63	-12.34
4	1584	0.23	4.07	1.37	0.25	4.09	1.37	0.21	2.72	1.16	-3.88
6	1118	0.00	11.50	0.30	0.00	11.50	0.30	0.00	11.20	0.30	-11.50
7	1	4.81	0.03	4.81	23.99	26.53	4.81	-21.69	21.72	26.50	-48.22
8	192	1.59	-18.05	-7.95	2.20	1.83	-7.95	-18.29	9.78	10.34	-20.12

[1] Refer to Figure 2.10.2-9 for component identification.

2.6.2 Cold Case

2.6.2.1 Discussion

The NAC-LWT cask body and lid are analyzed for structural adequacy in accordance with the requirements of 10 CFR 71.71(c)(2) Cold (normal transport conditions). The cask is assumed to be loaded and ready for shipment in a horizontal position in an ambient steady-state environmental air temperature of -40°F.

The stress analysis of the cask is performed by the finite element method using the ANSYS computer program. See Sections 2.10.1 and 2.10.2 for model and computer program descriptions.

2.6.2.2 Analysis Description

2.6.2.2.1 Geometry

The finite element model is described in Section 2.10.2. The temperature-dependent material properties presented in Section 2.3 are used in this analysis.

2.6.2.2.2 Loadings

An internal pressure of 50 psig is applied on the cask cavity and lid interior surfaces in the outward normal direction. The pressure loading region includes the lid and upper body forging mating surfaces outward to the inner cask lid seal centerline.

The total cask lid bolt torque, as calculated in Section 2.1.3.2.2, is applied to the bolt that is modeled as a beam element with a preload force of 39,788.74 pounds/radian, which is equivalent to an initial strain of 0.0021361 in/in-radian. Cask temperatures as determined in Section 3.4.3 (based on -40°F ambient temperature) are imposed on the model. See Section 2.10.3.2 for the resulting isothermal temperature plot.

Mechanical loads due to the total weight of the cask structure and contents are imposed on the model. Since the total weight of the finite element model is 37,519 pounds, it is less than the design weight (52,000 pounds), which includes the total weight of the cask and its contents. Therefore, an acceleration of 1.387 g (535.94 in/sec^2) is uniformly applied to the finite element model in the positive global x-direction (The model is defined in the positive x-y plane).

Fabrication stresses are considered negligible as demonstrated in Section 2.6.11.

2.6.2.2.3 Displacement Boundary Conditions

The finite element model is restrained radially at all centerline nodes and longitudinally at the node located on the center line at the cask model global origin, i.e., at the bottom of the cask model.

2.6.2.3 Detailed Analysis

Stresses throughout the finite element model of the cask body and closure lid are calculated for the combined pressure, bolt preload, thermal and mechanical load conditions as previously described.

In accordance with the design criteria presented in Section 2.1.2, the calculated stresses are evaluated as P_m, $P_m + P_b$, S_n and total stress categories. The secondary stresses (thermal) are conservatively included in the primary stress categories and margin of safety calculations; therefore, the 3 S_m limit on S_n stress intensity range is satisfied because it is enveloped by the 1.0 S_m limit on primary stress intensity.

To satisfy this criteria, procedures have been implemented (as demonstrated in Section 2.10.3) to determine the following:

1. The critical P_m and $P_m + P_b$ section stresses for each cask component
2. The critical total stress for each cask component.

The most critical sections for each cask component are shown in Figure 2.6.2-1. The maximum P_m and $P_m + P_b$ stresses for each component are reported in Table 2.6.2-1 and Table 2.6.2-2, respectively. Both tables consider the allowable stress for a component with a temperature of 300°F. Additionally, the stresses at representative sections throughout the cask are presented in the tables in Section 2.10.7. These tables document the maximum stress locations tabulated for each component. The critical total stress for each cask component is reported in Table 2.6.2-3. For the fatigue evaluation, refer to Section 2.1.3.2.

The minimum margin of safety is shown to be $\underline{+1.50}$, which occurs in component 7 (the Type 304 stainless steel cask bottom) for the condition of $P_m + P_b$ stress. This section is located 10.50 inches axially from the bottom of the cask body at the intersection of the outer shell with the bottom.

2.6.2.4 Conclusion

Using conservatively applied loadings and stress categorization, it is demonstrated that the minimum margin of safety for the NAC-LWT cask for the cold condition is +1.50. Therefore, the NAC-LWT cask satisfies the requirements of 10 CFR 71 for consideration of the cold load condition.

Figure 2.6.2-1 NAC-LWT Cask Critical Sections (Cold Case)

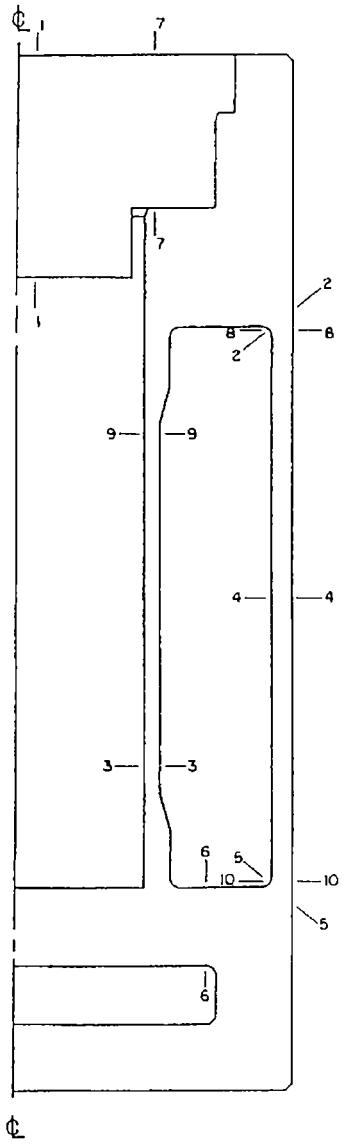

Table 2.6.2-1 Critical Stress Summary (Cold Case) – P_m

		P_m Stresses (ksi)				Principal Stresses					
Comp. No.[1]	Section Cut Node to Node	S_x	S_y	S_z	S_{xy}	S_1	S_2	S_3	S.I.	Allow. Stress 1.0 S_m	Margin of Safety
	1-1										
1	2302 to 2562	0.75	0.07	-0.53	0.51	1.02	-0.20	-0.53	1.55	20.0	Large
	2-2										
3	1835 to 1856	-0.28	6.08	2.12	1.66	6.49	2.12	-0.69	7.18	20.0	+1.8
	3-3										
4	701 to 704	-0.01	-2.59	0.13	-0.01	0.13	-0.01	-2.59	2.72	31.4	Large
	4-4										
6	1115 to 1118	-0.01	7.82	0.06	0.00	7.82	0.06	-0.01	7.83	31.4	+3.0
	5-5										
7	375 to 325	0.24	5.24	3.42	-3.08	6.71	3.42	-1.23	7.93	20.0	+1.5
	6-6										
8	192 to 342	-2.72	-0.74	-0.38	0.82	-0.38	-0.45	-3.01	2.64	20.0	+6.6

[1] Refer to Figure 2.10.2-9 for component identification.

Table 2.6.2-2 Critical Stress Summary (Cold Case) – $P_m + P_b$

		$P_m + P_b$ Stresses (ksi)				Principal Stresses					
Comp. No.[1]	Section Cut Node to Node	S_x	S_y	S_z	S_{xy}	S_1	S_2	S_3	S.I.	Allow. Stress 1.5 S_m	Margin of Safety
	7-7										
1	2371 to 2571	-3.81	-0.39	0.06	0.19	0.06	-0.38	-3.82	3.88	30.0	+6.7
	8-8										
3	1852 to 1856	-0.26	10.30	3.87	-0.19	10.30	3.87	-0.26	10.57	30.0	+1.8
	9-9										
4	1521 to 1524	0.00	-3.08	-0.25	-0.01	0.00	-0.25	-3.08	3.08	47.1	Large
	4-4										
6	1115 to 1118	0.00	8.30	0.48	0.00	8.30	0.48	0.00	8.30	47.1	+4.7
	10-10										
7	346 to 350	-0.23	11.86	5.77	-0.29	11.87	5.77	-0.24	12.10	30.0	+1.5
	6-6										
8	192 to 342	-6.67	-0.74	-0.38	0.82	-0.38	-0.63	-6.78	6.41	30.0	+3.7

[1] Refer to Figure 2.10.2-9 for component identification.

Table 2.6.2-3 Critical Stress Summary (Cold Case) – Total Range

		Total Stress Range (ksi)				Principal Stresses			Stress Differences		
Comp. No.[1]	Node	S_x	S_y	S_z	S_{xy}	S_1	S_2	S_3	S_1-S_2	S_2-S_3	S_3-S_1
1	2561	0.28	0.01	0.27	-18.80	18.95	0.27	-18.66	18.68	18.93	-37.61
3	1856	-0.26	10.18	3.50	-0.01	10.18	3.50	-0.26	6.68	3.76	-10.44
4	1261	0.00	-2.66	-0.39	0.00	0.00	-0.39	-2.66	0.39	2.27	-2.66
6	1278	-0.03	8.16	0.20	0.00	8.16	0.20	-0.03	7.96	0.23	-8.19
7	1	4.64	0.02	4.64	23.99	26.43	4.64	-21.77	21.79	26.41	-48.20
8	192	-0.97	-7.36	-2.70	1.45	-0.66	-2.70	-7.67	2.04	4.97	-7.01

[1] Refer to Figure 2.10.2-9 for component identification.

2.6.3 Reduced External Pressure

The drop in atmospheric pressure to 3.5 psia, as specified in 10 CFR 71.71(c)(3), effectively results in an additional internal pressure in the cask of 11.2 psig. This additional pressure has a negligible effect on the NAC-LWT cask because the cask is conservatively analyzed for a normal operations conditions internal pressure of 50.0 psig in Section 2.6.1.2.

2.6.4 Increased External Pressure

An increased external pressure of 20 psia (5.3 psig external pressure), as specified in 10 CFR 71.71(c)(4), has a negligible effect on the NAC-LWT cask because of the thick outer shell and end closures of the cask. Conservatively, applying a 20-psi external pressure to the expansion tank shell and to the neutron shield tank shell produces hoop stresses of only 1373 psi and 1627 psi, respectively. These stresses are negligible. Additionally, Section 2.6.7 addresses many different loading cases, which exceed these prescribed external pressure requirements.

2.6.5 Vibration

The effect of vibrations normally incident to transportation is considered to be negligible for the NAC-LWT cask. This conclusion is based on the fact that the calculated stresses for vibrations normally incident to transportation are much smaller than the calculated stresses for the normal transport 1-foot side drop event. The following analysis documents this fact.

The normal transport 1-foot side drop, discussed in Section 2.6.7.3, results in an impact deceleration equal to 24.3 g. This impact force produces a 17,420 psi stress intensity in the inner shell and a 23,590 psi stress intensity in the outer shell of the NAC-LWT cask.

As a conservative worst case, it is assumed that the normal transport vibration acceleration is equal to the equivalent acceleration which will produce the normal vertical loading imposed on the tiedown devices by 10 CFR 71.45(b)(1). This regulation specifies a load factor of 2.0 to be applied to the package weight; therefore, it is assumed that the tiedown devices and the cask must resist an imposed 2.0 g vibration acceleration.

The maximum stress intensity range for normal transport vibration is obtained by multiplying the stress from the 1-foot side drop impact by the ratio of acceleration values from vibration to those for the drop impact. Thus the stress intensities in the outer shell (the critical component) are S_{max} = (2/24.3)(23,590) = 1942 psi and S_{min} = -(2/24.3)(23,590) = -1942 psi, and the maximum stress intensity range is S_n = 3884 psi. The allowable alternating stress intensity for austenitic stainless steel is determined as the 10^{11} cycle value from the "ASME Boiler and Pressure Vessel Code," Table I-9.2.2 ratioed for the effect of the 300°F temperature. This value is S_e = 12,975 psi; therefore, the margin of safety for the critical component of the NAC-LWT cask for normal transport vibration is:

MS = (Se /Salt) - 1 = (12,295/1942) - 1 = +Large

where:

Salt = 0.5 Sn

The rotation trunnions serve as the rear tiedown for the NAC-LWT cask during normal transport. The rotation trunnion is the critical tiedown component for all three load axes; the front of the cask is supported in a cradle and restrained vertically by a band attached to the trailer. From Section 2.5.2.2, the critical component on the rotation trunnion is the attachment weld between the trunnion and the cask outer shell, which has an applied shear stress of 11,500 psi. This applied shear stress is produced by the 10.2 g resultant from the combined longitudinal and vertical shock (10.0 g longitudinal and 2 g vertical) tiedown load components.

The same method is used to determine the maximum stress intensity range as is used for the cask, except that the ratio of the normal transport vibration acceleration to the resultant acceleration for the combined longitudinal and vertical shock was used. The allowable alternating stress for the weld is the same as that for the cask. The alternating shear stresses are S_{max} = (2/10.2)(11,500) = 2255 psi and S_{min} = -(2/10.2)(11,500) = -2255 psi, and the maximum stress intensity range is S_n = 4510 psi. The margin of safety for the rotation trunnion as a rear tiedown device for normal transport vibration is:

$$MS = (S_e / S_{alt}) = 1\ (12{,}975/2255) - 1 = +\underline{Large}$$

where:

$$S_{alt} = 0.5\ S_n$$

The NAC-LWT cask satisfies the requirements for normal vibration incident to transportation as required by 10 CFR 71.71(c)(5).

2.6.6 Water Spray

Water causes negligible corrosion of the stainless steel materials used to fabricate the NAC-LWT cask; the cask contents are protected in the sealed cavity. A water spray as specified in 10 CFR 71.71(c)(6) has no adverse effect on this package.

2.6.7 Free Drop (1 Foot)

The free drop scenario outlined by Subpart F of 10 CFR 71 requires the NAC-LWT cask to be structurally adequate for a 1-foot drop (normal transport conditions) onto a flat, essentially unyielding, horizontal surface in the orientation that inflicts the maximum damage to the cask. The following subsections evaluate the cask body; the impact limiters; the closure lid and bolts; the neutron shield shell; the expansion tank shell; and the upper ring components; for the end, side, and corner drop orientations.

2.6.7.1 End Drop (1 Foot)

2.6.7.1.1 Discussion

The NAC-LWT cask is analyzed for the effects of a normal operations end drop impact condition. The event scenario is that the NAC-LWT cask, equipped with an impact limiter, drops 1 foot onto a flat, unyielding, horizontal surface. The cask strikes the surface in a vertical position on either its bottom or its top end.

The 1-foot end drop analysis can be carried out in an identical fashion as was used in the 30-foot accident end drop analysis, Section 2.7.1.1. The general comments, analysis descriptions and the analysis method described in Section 2.7.1.1 also apply to this section.

The only difference between the 30-foot end drop analysis (Section 2.7.1.1) and this 1-foot end drop analysis is the magnitude of the impact force, i.e., impact load, which is expressed in terms of a g factor. The magnitude of the impact force varies with the different drop heights. As calculated in Section 2.6.7-4, the g loads for the 1-foot end drop condition and for the 30-foot end drop condition are 15.8 g and 60 g, respectively. These g loads are conservatively based on a maximum crush strength of 3850 psi for the aluminum honeycomb impact limiters, although the design maximum crush strength is 3675 psi. Also, these analyses conservatively use a 1.12-inch thick outer shell, although the actual outer shell thickness is 1.20 inches. Using the analysis results obtained in Section 2.7.1.1 to represent the structural response of the NAC-LWT cask for the 1-foot end drop condition is conservative and acceptable. Therefore, Tables 2.7-1 through 2.7-15 were used to compose Table 2.6.7-1 through Table 2.6.7-16, for the 1-foot drop analyses. The most critical sections for each component during a particular loading condition are shown in Figure 2.6.7-1 through Figure 2.6.7-5. The critical P_m, $P_m + P_b$, and total stresses for each component are documented in Table 2.6.7-1 through Table 2.6.7-16. The allowable stresses are those defined in Section 2.1.2 for the normal operations conditions based on 300°F. Note that the maximum cask component temperatures are below 300°F for all of the conditions that are considered. Additionally, the stresses at representative sections throughout the cask are

presented in the tables in Section 2.10.7. These tables document the maximum stress locations tabulated for each component.

The secondary stresses (thermal) are conservatively included in the primary stress categories and margin of safety calculations; therefore, the 3 S_m limit on the S_n stress intensity range is satisfied. This is because it is enveloped by the 1.5 S_m limit on $P_m + P_b$ stress intensity.

2.6.7.1.2 Results and Conclusions

Since the margins of safety are positive for all of the cask components, the NAC-LWT cask maintains its containment capability and satisfies the 10 CFR 71 requirements for the 1-foot normal operations end drop condition.

2.6.7.2 Side Drop (1 Foot)

2.6.7.2.1 Discussion

This section presents the evaluation of the structural adequacy of the NAC-LWT cask for the 1-foot side drop impact condition. In this event, the NAC-LWT cask with impact limiters attached over each end experiences a free drop through a distance of 1 foot onto a flat, unyielding surface, and strikes the surface in a horizontal position.

The 1-foot side drop analysis is performed in the same manner as was done for the 30-foot side drop analysis in Section 2.7.1.2. The general comments, analysis descriptions, and the analysis methods described in Section 2.7.1.2 also apply to this section.

The difference between the 30-foot side drop analysis and the 1-foot side drop analysis is the magnitude of the impact force, which varies because of the different drop heights. As determined in Section 2.6.7.4, the g loads for the 1-foot side drop condition and for the 30-foot side drop accident condition are 24.3 g and 49.7 g, respectively.

Analysis of the NAC-LWT cask for the normal operations conditions side drop follows the same methodology as used for the accident side drop analysis. Because all calculations for the accident side drop analysis are performed on a basis of linear elastic behavior, the stress components for the 1-foot side drop condition are calculated by multiplying the 30-foot side drop stress components (resulting from the effects of inertial and impact loads) by the ratio of the 1-foot side drop g load to the 30-foot side drop g load. These stress components are then combined with those induced by the thermal effects, internal pressure, and bolt preload.

2.6.7.2.2 Results and Conclusions

Since the material properties of the cask structure are temperature-dependent, varying environmental temperatures will produce changes in the calculated stresses in the cask for the thermal load cases. Environmental temperatures will not change the calculated stresses in the

cask produced by other types of loads. This is verified by comparing the finite element results for the NAC-LWT cask subjected to a gravity load for different temperature conditions. Also, the stress levels produced by the following thermal loading conditions were evaluated: (1) 100°F ambient temperature with maximum decay heat load, (2) -40°F ambient temperature with maximum decay heat load, and (3) -40°F ambient temperature with no decay heat load. The combination effect of the thermal loads with other load types (e.g., inertial body load) has also been studied. It is determined that the side drop event with 100°F ambient temperature represents the worst case for the normal operations 1-foot side drop condition. Therefore, only the stress results produced by a 1-foot side drop with 100°F ambient temperature are reported.

Stress components and stress intensities are calculated throughout the finite element model for the combined loads due to internal pressure, bolt preload, thermal, inertia, and impact. Table 2.6.7-16 through Table 2.6.7-19 report the P_m stress intensities, the $P_m + P_b$ stress intensities, the S_n stress intensities, and the total stress intensities for each cask component, which are obtained from the finite element side drop analysis. Additionally, the stresses at representative sections throughout the cask are presented in the tables in Section 2.10.7. These tables document the maximum stress locations tabulated for each component.

As mentioned previously, the finite element cask model conservatively ignores the effect of the neutron shield shell on the overall bending of the cask structure.

The margins of safety reported in Table 2.6.7-16 through Table 2.6.7-18 are positive for all cask components. It has been demonstrated that all margins of safety are positive for the normal operations 1-foot side drop condition.

The NAC-LWT cask maintains its containment capability and satisfies the 10 CFR 71 requirements for the normal operations 1-foot side drop condition.

2.6.7.3 Corner Drop (1 Foot)

2.6.7.3.1 Discussion

The analysis of the NAC-LWT cask for a 1-foot corner drop condition uses the same methods as those used for the hypothetical accident oblique drop analyses. The general comments, analysis descriptions, and analysis methods discussed in Section 2.7.1.3 also apply to this section. The difference between the hypothetical accident analysis and the normal operations conditions analysis in this section is the drop height. Refer to Section 2.6.7.4 for the calculation of the g loads induced by a normal operations conditions 1-foot corner drop and by an accident condition 30-foot corner drop. These g loads are conservatively based on a maximum crush strength of 3850 psi for the aluminum honeycomb impact limiters, although the design maximum crush strength is 3675 psi. The stress components for the 1-foot corner drop are calculated by multiplying the accident condition stress components (resulting from the effects of inertial and

impact loads) by the ratio of the 1-foot corner drop g load to the 30-foot corner drop g load. These stress components, then, are combined with those resulting from internal pressure, bolt preload, and thermal effects. These analyses conservatively use a 1.12-inch thick outer shell, although the actual outer shell thickness is 1.20 inches.

2.6.7.3.2 Results and Conclusions

The most critical sections for each component during a particular loading condition are shown in Figure 2.6.7-7 through Figure 2.6.7-9. Table 2.6.7-20 through Table 2.6.7-23 report the maximum P_m stress intensities, the maximum $P_m + P_b$ stress intensities, the maximum S_n stress intensities, and the maximum total stress intensities for each component resulting from the 1-foot top corner drop condition with a 130°F ambient temperature and maximum decay heat load. Similarly, Table 2.6.7-24 through Table 2.6.7-27 report those stress intensities resulting from the 1-foot bottom corner drop condition with a 130°F ambient temperature and maximum decay heat load. Also, Table 2.6.7-28 through Table 2.6.7-31 report the stress intensities for each component resulting from the 1-foot top corner drop condition with a -40°F ambient temperature. Additionally, the stresses at representative sections throughout the cask are presented in the tables in Section 2.10.7. These tables document the maximum stress locations for each component.

It has been demonstrated that all margins of safety are positive for the normal operations 1-foot corner drop condition. The NAC-LWT cask maintains its containment capability and satisfies the 10 CFR 71 requirements for the normal operations 1-foot corner drop condition.

2.6.7.4 Impact Limiters

2.6.7.4.1 Introduction

Removable impact limiters are supplied with the NAC-LWT cask to ensure that the design impact loads on the cask are not exceeded for any of the defined impact conditions. These defined conditions are:

1. The cask falls 1 foot and lands on: (a) its side, impacting both limiters simultaneously; (b) flat on one limiter at either end; or (c) oblique on either corner (the center of gravity is directly above the corner of the impact limiter).
2. The cask, having experienced a normal operating conditions 1-foot drop, is dropped through a distance of 30 feet and lands on its end, its side, or at any oblique angle. The impact limiter analysis considers a 31-foot drop (1 foot + 30 feet). This provides conservative impact loads, which are used in the cask analyses.

2.6.7.4.2 Assumptions

The following assumptions form the basis for the impact limiter analysis:

1. The cask impacts on an unyielding surface.
2. The impact limiter remains in position on the cask during all impact events. (The qualification of the impact limiter attachment is presented in Section 2.6.7.4.7.)

2.6.7.4.3 Load Conditions

The impact limiters described and analyzed in the following paragraphs decelerate the cask by applying a force in the direction opposite the motion of the cask. The deceleration force is generated by crushing the aluminum honeycomb material of the limiter between the cask and the unyielding surface. The energy absorbed during crushing is the net force, the vector sum of the cask weight (downward) and the deceleration force (upward), multiplied by the distance crushed. The amount of energy an impact limiter can absorb is calculated for various cask impact orientations, from vertical (0°) to horizontal (90°).

The specific loading conditions for the impact limiters are defined by 10 CFR 71.71(c)(7), 10 CFR 71.73(c)(1) and Regulatory Guide 7.8, as follows:

1. A 1-foot fall of the cask on one limiter, impacted at any angle from vertical (flat end) to corner (cask center of gravity is directly above the point of impact).
2. A 1-foot fall of the cask horizontally, so that the side surfaces of both limiters impact the unyielding surface simultaneously.
3. Any of the 1-foot falls can be followed by a 30-foot fall at an end, a side, or an oblique orientation.

Based on these loading conditions, the NAC-LWT cask impact limiters are designed for a 31-foot fall. Either of the first two conditions plus the third condition is equivalent to a single drop at the combined heights, as explained in Section 2.6.7.4.5. The maximum impact force and the maximum crush depth for the 1-foot falls are obtained from the computer output for the 31-foot fall analyses at the value of the energy dissipated in a 1-foot fall. This method is explained in Section 2.6.7.4.5.

2.6.7.4.4 Descriptions – Impact Limiters

Figure 2.6.7-10 shows the location on the cask and the primary dimensions of the impact limiters. A different impact limiter is used on the bottom of the cask to reduce weight. The top impact limiter diameter is larger because it is required to clear the cask lifting trunnions and to be of sufficient depth over the trunnions to prevent the limiter from behaving as a solid in the event of a side impact. The larger diameter provides greater distance from the point of impact to the cask body; however, the effective depth of the limiter is maintained at the trunnions and the same corner impact absorption capability is retained. Figure 2.6.7-11 shows a cross-section of the top impact limiter.

The bottom impact limiter does not have the cut-outs for the trunnions. It has a smaller outside diameter and larger bottom depth than the top impact limiter.

Each impact limiter consists of two different layers of aluminum honeycomb, which are enclosed in a thin outer aluminum shell. The layers of aluminum honeycomb are separated by a thin aluminum sheet. The honeycomb material absorbs the impact energy as it is crushed. A typical load versus deflection curve for aluminum honeycomb is presented in Figure 2.6.7-12. The force deflection curves and test data for the NAC-LWT cask impact limiters at the various drop angles are provided in Appendix 2.10.12. The nominal crush strength of the bottom layer of aluminum honeycomb is 250 psi axially, and is negligible radially. The nominal crush strength of the second layer is 3500 psi in both the axial and the radial directions. The tolerance on the crush strength is +5, -10 percent. The bottom, 250-psi crush strength, single-directional layer of honeycomb material absorbs the majority of the energy in a 1-foot flat impact on the end, and limits the impact force to a value acceptable for normal operations. The lower crush strength is necessary because the impact area is considerably greater in a flat bottom impact than in any other orientation. The second, 3500-psi crush strength, multi-directional layer of honeycomb material absorbs the majority of the energy in an impact on the corner of the impact limiter, and all of the energy in an impact on the side of the impact limiter. Both crushable aluminum honeycomb materials behave as a solid when compressed to 30 percent of their original depth.

The outside diameters of the impact limiters are 65.25 inches and 60.25 inches for the top and bottom impact limiters, respectively. The depth of the bottom aluminum honeycomb layer is 1.5 inches on each limiter. The second aluminum honeycomb layer is 14.0 inches deep for the top impact limiter and 14.5 inches for the bottom impact limiter. The top impact limiter has four recesses to provide clearance around the trunnions. This clearance is closed during the impact for a 30-foot side drop. Therefore, the trunnion provides a rigid foundation for the impact limiter in the region near the trunnion.

The impact limiter shells are positioned against the cask lid and bottom surfaces; the impact limiters overlap the cask cylinder by a length of 12 inches. The shells are mechanically attached to the cask as described in Section 2.6.7.4.7.

For each of the impact load conditions considered in this analysis, the impact limiters remain in position on the cask and absorb the energy of the impact; thus, they limit the impact load to the values calculated in this section.

2.6.7.4.5 Method of Analysis

The primary areas of analytical evaluation that are required in an impact limiter analysis are: (1) crush depth; (2) maximum crush force; and (3) attachment to the cask. The crush depth and

maximum crush force are dependent on the crush strength of the crushable material, the area engaged in crushing, the geometry of the impact limiter, and the energy to be dissipated.

Deceleration forces for constant crush strength aluminum honeycomb impact limiters are directly related to the area crushing. The area engaged in crushing can be best explained by examining the experimental results of a top end drop impact test. Figure 2.6.7-13 shows a quarter-scale model impact limiter just before crushing begins. The cask and the unyielding surface are rigid and undeformable compared to the honeycomb material. The 3.9 inches of honeycomb material are trapped in place between the cask and the impacted surface.

The 250-psi crush strength honeycomb is designed to absorb the potential energy of the cask in a 1-foot drop. The area of the 250-psi honeycomb covering the entire bottom of the impact limiter is 208.7 square inches. The higher crush strength honeycomb structurally supports or "backs" the lower crush strength honeycomb, even if just the cask backs the higher crush strength honeycomb. The force necessary to begin crushing the 250 psi crush strength material is 52,168 pounds. The quarter-scale model weighs approximately 800 pounds; therefore, the 52,168 pounds of force is equivalent to 65 g for the model (The normal operation g-load for the full-size cask is calculated to be 16.3 g).

The 3500-psi crush strength honeycomb absorbs the kinetic energy of the cask in a 30-foot drop. The area of the bottom of the scale model cask is 40.7 square inches. The force necessary to crush the 3500-psi crush strength honeycomb trapped between the model cask and the impacted surface is 142,500 pounds, or 178 g, based on the model weight of 800 pounds.

A force imbalance is immediately established between the lower and higher strength honeycombs at the onset of crushing. It requires 52,168 pounds to crush the lower strength honeycomb, which is 2.7 times smaller than the force required to crush the higher strength honeycomb. The lower strength honeycomb of constant crush strength will crush until lock-up occurs. When lock-up occurs, the crush strength of the lower strength honeycomb increases and exceeds that of the higher strength honeycomb. Crushing now begins beneath the cask because the force to crush the 16.3-inch diameter of the locked-up, lower strength honeycomb exceeds the 142,500 pounds necessary to crush the backed-up higher strength honeycomb.

The cask has kinetic energy gained while falling prior to the impact limiter contacting the unyielding surface. (Section 2.10.12 gives a more complete description of the kinetic energy gain.) Some kinetic energy was dissipated in crushing the lower strength honeycomb. The remaining energy will be absorbed by crushing the higher strength honeycomb between the cask and the impacted surface. The cask "backs" the higher crush strength honeycomb; therefore, the maximum force is easily compared with the average maximum force from the quasi-static test as adjusted to reflect the dynamic crush strength of the honeycomb (For an explanation of the term "dynamic" as applied to quasi-static tests, refer to Appendix 2.10.12).

Figure 2.6.7-14 is a photograph of a section of an end impact tested quarter-scale limiter. The average maximum force from the end drop quasi-static crush test is 158,400 pounds. If the backed and unbacked area were to crush, the required force would be 3500 psi x $\pi/4$ $(16.3)^2$ = 730,400 pounds of force. This is a factor of 4.6 times more than the actual measured force and shows that the unbacked area did not contribute to the limiter force. The calculated maximum force using the backed-up area of the limiter is approximately 11 percent lower than the test results. The scale model limiter crush test, therefore, demonstrates that the unbacked area did not crush and generate a force. One reason for the difference is the shearing of the high crush strength honeycomb, which is clearly visible in Figure 2.6.7-14. Shearing acts in a plane, surrounding the shear area. In an end impact crush, the plane is a thin ring with a diameter equal to the diameter of the cask. Since the crush force is proportional to the backed area, which depends on the square of the cask diameter, for the full-scale impact limiters, shearing becomes a much less significant part of the maximum force.

Figure 2.6.7-14 shows the sequence of crushing and the backed area as described above. The lower crush strength honeycomb is crushed to stack height completely to the outer edge of the cask. Higher crush strength honeycomb beneath the cask is crushed, while material on the "other side" of the shear plane is uncrushed.

The combination of the accurate prediction of measured impact limiter crush forces and the visual evidence in the sectioned limiter after the test shows that only the backed-up area crushes for aluminum honeycomb with a 3500-psi, multi-directional, dynamic crush strength.

The cask orientation for a corner impact is defined by the angle from vertical of the cask's longitudinal axis when the cask center of gravity is vertically aligned with the impact point on the limiter. This angle is 15.74 degrees for the top limiter and 14.52 degrees for the bottom limiter.

A proprietary computer program, RBCUBED, is used to analyze an impact limiter for an impact event, to determine the dynamics of the event, to determine the forces generated during that event, and to determine the depth of crush (Section 2.10.1.2).

The computer program, RBCUBED, is run for many combinations of crushable material strength until satisfactory results are obtained. Two runs are made for each impact orientation. One run is made using the maximum value of the aluminum honeycomb crush strength, 105 percent of the nominal crush strength, to determine the maximum force on the cask. A second run, using the minimum value for the aluminum honeycomb crush strength, 90 percent of the nominal crush strength, is also made to find the maximum crush depth of the crushable material.

A single RBCUBED run is necessary to determine the reaction force for a 1-foot fall and a subsequent 30-foot fall. The 1-foot fall crushes the limiter a distance (δ_1), and absorbs

12 inches × 52,000 lbs = 0.624 × 10^6 inch-pounds of energy. Then, the impact limiter must absorb the additional energy of 360 inches × 52,000 lbs = 18.72 × 10^6 inch-pounds by crushing an additional distance (δ_2) from a 30-foot drop. The total displacement is $\delta_1 + \delta_2$ and the total energy is (18.72 + 0.624) × 10^6 = 19.344 × 10^6 inch-pounds. Dividing this energy by the cask weight gives 372 inches (31 feet), which demonstrates that a 1-foot fall followed by a 30-foot fall can be evaluated from data for a 31-foot fall. The maximum impact force and the maximum crush depth for the 1-foot fall can be obtained from the RBCUBED output for the 31-foot fall analysis at the value of the energy dissipated in a 1-foot fall.

2.6.7.4.6 Results

The data in Table 2.6.7-32 and Table 2.6.7-33 give the results of the impact limiter design analyses for a 1-foot fall and a subsequent 30-foot fall, respectively. The calculated g loads for the 30-foot fall side impact are based on the 3675-psi design maximum crush strength of the multidirectional aluminum honeycomb. The calculated g loads for all of the other 1-foot and 30-foot fall impacts are conservatively based on an aluminum honeycomb maximum crush strength of 3850 psi. A design cask weight of 52,000 lbs is used.

The calculated (RBCUBED) and measured (quasi-static, adjusted for dynamic crush strength) force-deflection curves for the NAC-LWT cask impact limiters for all drop orientations are presented in Appendix 2.10.12. To verify the results, the area under the curves is calculated by the trapezoidal method. This area represents the energy dissipated for each of the cases, i.e., E_{max} = 19.344 × 10^6 inch-pounds for the top limiter at maximum strength, and E_{min} = 19.206 × 10^6 inch-pounds for the bottom limiter at minimum strength. The potential energy to be dissipated consists of the cask weight (52,000 lbs) multiplied by the distance the cask falls (372 inches), i.e., E_p = 372 × 52,000 = 19.344 × 10^6 inch-pounds. The calculated and actual values compare within 0.71 percent, which indicates that the proper amount of potential energy is dissipated in the RBCUBED analysis. Another check is to multiply the total crush area (the maximum area backed by the cask) by the crush strength of the impact limiters to determine the reacting force. This hand-calculated value of the reaction force for maximum impact limiter crush strength compares within 0.38 percent of the RBCUBED calculated value for the bottom impact limiter and within 1.88 percent for the top impact limiter. The hand-calculated value of the reaction force for minimum impact limiter crush strength compares within 0.46 percent of the RBCUBED calculated value for the bottom impact limiter and within 1.83 percent for the top impact limiter. These results verify both the energy absorption and the reaction force calculations of RBCUBED for the impact limiters.

A study of a side drop shows that the cask will come to rest at an angle of 0.76 degrees with the horizontal because the radius of the top limiter is 2.5 inches larger than that of the bottom limiter.

The RBCUBED analysis, analyzing the side drop as horizontal, is not affected by this small angle because the horizontal component of the forces is negligible.

With both impact limiters at their minimum allowable crush strength (maximum crush depth case), clearance is maintained between the neutron shield/expansion tank and the unyielding surface for the 1-foot side impact.

An evaluation of the displacements obtained from the RBCUBED runs is as follows:

1. The RBCUBED run for the 31-foot side drop assumes the cask is a rigid element and does not include the trunnions; therefore, the displacement from the 31-foot drop must be analyzed, by referring to Figure 2.6.7-11, as follows:

   The free distance of crushable material between the impact limiter and the trunnion equals 14.995 inches. The aluminum honeycomb compresses to 70 percent of its free height before exhibiting behavior as a solid (10.497 inches). The RBCUBED run for the 31-foot side drop with the crushable material at minimum strength calculates a crush depth of 10.00 inches; thus, 0.497 inch of crushable material remains before solid height occurs. Therefore, an impact directly on a trunnion does not change the energy absorbing characteristics of the impact limiter for this condition.

   The impact from a 31-foot side drop on the bottom impact limiter with the crushable material at minimum strength exhibits solid behavior at a displacement of 10.73 inches, which leaves 0.43 inch displacement before solid height occurs (crush depth = 10.30 inches).

2. The impact from a 31-foot flat end drop onto the top impact limiter with the crushable material at minimum strength exhibits solid behavior at a displacement of 10.85 inches, which leaves 0.61 inch displacement before solid height occurs. Similarly, for the bottom impact limiter, solid behavior occurs at 11.20 inches, which leaves 0.90 inch displacement before solid height occurs.

3. For a 31-foot corner drop on the top impact limiter with the crushable material at minimum crush strength, the crush distance of 12.72 inches is much less than the solid height displacement of 16.86 inches. Similarly, for the bottom impact limiter, the 12.70-inch crush distance is much less than the 15.83-inch solid height displacement.

The cask analysis for these impact conditions is based on the maximum deceleration (g) derived from the RBCUBED results. The critical condition for maximum lateral deceleration from both a 1-foot and a 31-foot drop is the side drop with the crushable material at its maximum strength. The critical condition for maximum longitudinal deceleration from a 1-foot drop is the flat bottom drop with the crushable material at its maximum strength, and from a 31-foot drop is the corner drop. The longitudinal component of the deceleration from the 31-foot corner drop was used as the longitudinal criteria; that is, 60.4 cos 15.74 degrees equals 58.1 g. Nevertheless, a 60.0 g (deceleration) is conservatively used as the maximum longitudinal deceleration. The design g load factors (deceleration values) for the NAC-LWT cask analyses are summarized in Table 2.6.7-34. The design g load for the 31-foot side drop is based on the 3675-psi design

maximum crush strength of the aluminum honeycomb impact limiters. The design g loads for all of the other 1-foot and 31-foot drops are conservatively based on an aluminum honeycomb maximum crush strength of 3850 psi.

2.6.7.4.7 Impact Limiter Attachment Analysis

A three-part design criteria applies to the method of attachment of the impact limiters to the cask body. These three criteria are as follows:

1. The impact limiters must remain attached to the cask body during normal handling and transport. Satisfaction of this criterion ensures that the limiters will be in a proper position to perform their impact limiting function in the event of a free drop (normal or accident).
2. In a free drop (normal or accident), the limiter(s) making initial contact with the unyielding surface must remain in position on the end(s) of the cask for the full duration of the initial impact. Satisfaction of this criterion ensures that the limiter(s) will be able to properly perform their impact limiting function.
3. In a free drop (normal or accident) involving an initial impact on a single impact limiter, the limiter on the opposite end of the cask must remain attached to the cask during the initial impact. Satisfaction of this criterion ensures that the limiter will be in a proper position to perform its impact limiting function in a subsequent secondary impact following the initial impact.

Section 2.6.7.4.7 demonstrates that each of the above criterion are satisfied.

Impact Limiter Attachment During Normal Handling and Transport

Attachment of the impact limiters to the cask body during normal handling and transport is ensured by demonstrating that the attachment hardware (pins, lugs and associated welds) does not yield under normal handling and transport conditions. The worst case loading associated with normal handling and transport is taken to be a 10-g axial loading associated with rail transport [10 CFR 71.45 (b)]. This bounds the 2.0-g load corresponding to the peak shock loading expected as the result of truck transport (per ANSI N14.23 for air ride suspensions). For this normal condition evaluation, it will be assumed that only two of the four attachment points for each limiter are effective. The load, P, per attachment point therefore becomes:

$$P = 10.0(1535)/2$$
$$= 7{,}675 \text{ lbs}$$

where 1,535 lbs is the weight of the heaviest (top) impact limiter.

Analysis of Impact Limiter Lug

The geometry of the impact limiter lug is as shown in Figure 2.6.7-15. As shown, the lug has an outer width of 2.0 inches, a hole diameter of 0.53 inch and an edge distance of 1.7 inches. The

lug is made of 6061-T651 aluminum and is 0.5 inch thick. According to Table 2.3.1-4, the yield strength of the aluminum at 150°F is 32,700 psi. Potential failure modes of tension across the net section and 40-degree shearout are considered as follows:

Tension Across the Net Section

$P = 7{,}675$ lbs

$A = 0.5(2.0 - 0.53)$

$= 0.735\ in^2$

$S_t = 7{,}675/0.735 = 10{,}442$ psi ($S_y = 32{,}700$ psi)

$MS = 32{,}700/10{,}442 - 1$

$= +\underline{2.13}$

40-Degree Shearout

$P = 7{,}675$ lbs

$e = 1.7 - (0.53/2) \cos 40°$

$= 1.497$ inches

$A_s = 2(0.5)(e)$

$= 1.497\ in^2$

$S_s = 7{,}675/1.497$

$= 5{,}127$ psi ($0.6\ S_y = 19{,}620$ psi)

$MS = 19{,}620/5{,}127 - 1$

$= +\underline{2.83}$

An optional impact limiter lug configuration permits the gusset plate impact limiter attachment tab to be an assembly of the tab and gusset plate using a full-penetration weld. The structural strength of the weld using a mock-up test confirms that the minimum weld yield strength is equal to or greater than 10 ksi. The only stress applicable to the weld is the tension across the entire section of the weld. Using the bounding load of 7,675 pounds, the margin of safety for the weld region is:

$MS = 10{,}000/7{,}675 - 1$

$= \underline{+0.30}$

Both the 6061-T651 continuous tab gusset configuration and the optional full-penetration weld assembly configuration are confirmed to maintain the attachment of the impact limiters to the cask body for truck or rail transport.

Analysis of Cask Lug

The geometry of the cask lug is a shown in Figure 2.6.7-16. As shown, the lug actually consists of two, 0.5-inch thick lugs, which are integral to a common base plate (the lugs and base plate are machined from one piece). Each of these two lugs is 2.0 inches wide, has a hole diameter of 0.53 inch and has a minimum edge distance of 0.72 inch. The base plate is 1.6 inches wide and 2.0 inches long. The material used is Type 304 stainless steel, which exhibits a yield strength at 150°F of 27,500 psi. Potential failure modes of 40-degree shearout and failure of the weld (3/8-inch bevel plus 3/8-inch fillet), which attaches the base plate to the cask body, are considered as follows:

40-Degree Shearout

$F = P/2 = 1535/2$

$= 768$ lbs

$e = 0.72 - (0.53/2) \cos 40°$

$= 0.517$ in

$A_s = 2(0.5)(e)$

$= 0.517 \text{ in}^2$

$S_s = 768/0.517$

$= 1485$ psi ($0.6\ S_y = 16{,}500$ psi)

MS = 16,500/1485 - 1 = +Large

Weld Stresses

The analysis of the weld will conservatively ignore the 3/8-inch bevel weld and only consider the 3/8-inch fillet weld around the perimeter of the base plate. Stresses in this weld resulting from the imposed bending moment and the imposed direct shear load will both be treated as shear stresses, combined using a square root sum of squares approach and compared against a shear allowable limit. The stress in the weld due to the applied moment is as follows:

$s_1 = 4.24M/(h[b^2 + 3L(b + h)])$

$= 2006$ psi

where:

$M = 1.78(P) = 2732$ in-lb

$P = 1{,}535$ lbs

$h = 3/8 = 0.375$ in

$b = 2.0$ inches

$L = 1.6$ inches

The stress in the weld due to the applied shear load is:

$s_2 = P/A_s$

$= 804$ psi

where:

$P = 1{,}535$ lbs

$A_s = 2(1.6 + 2.0)(0.707)(0.375)$

$= 1.909$ in^2

The combined stress is therefore:

$s = (s_1^2 + s_2^2)^{0.5}$

$= 2161$ psi ($0.6\ S_y = 16{,}500$ psi)

$MS = 16{,}500/2161 - 1$

$= +$Large

Analysis of Ball-Lock Pin

The 1/2-inch, AVIBANK 57459-1 ball-lock pins have a 36,800-pound capacity in double shear. With an applied load of 1,535 lbs, the margin of safety is very large.

Response of Impact Limiter(s) During Initial Impact of Package with Ground

The second criterion applicable to the impact limiters requires that the limiter(s) making initial contact with the unyielding surface must remain in position on the end(s) of the cask for the full duration of the initial impact. To satisfy this criterion, attachment hardware (pins, lugs and/or associated welds) may fail during an impact event as long as the limiter(s) being crushed remains in position on the end of the cask and does not separate from the cask. The ability of the limiter to remain in position during an impact is demonstrated with reference to a series of dynamic, free drop tests (end, center of gravity over corner, side and oblique), during which some attachment hardware failure occurred, and to several static crush tests, during which the only attachment mechanism was a strip of duct tape. All of the tests were performed using quarter-scale models of the limiters. Analytic evaluations are also presented to further justify that the limiters will remain in position during the impact.

Dynamic Free Drop Test Results

As presented in Appendix 2.10.8, a series of 30-foot free drop tests were performed on a quarter-scale model of the NAC-LWT cask. Drop orientations included an end drop, a center of gravity over struck corner drop, a side drop and an oblique drop with a subsequent secondary impact. A study of the drop test photographs presented in Appendix 2.10.8 indicates that although attachment hardware failed in some of the dynamic free drop tests, the limiters did not physically

separate from the cask body and did completely perform their intended impact limiting function. In fact, the limiters wedged themselves even more securely onto the cask body.

At all times during the testing, the limiters remained in position on the ends of the cask. Notably, rebound from the drop pad due to the whipping action of the restraint cables, did not result in the limiters separating from the cask even though some attachment hardware failure had occurred. This observation demonstrates a tendency for the limiters to become wedged onto the cask body as the result of an impact.

Based on the above test observations, the conclusion reached is that the limiters will remain in position on the cask body during the full duration of the free drop impact event.

Static Crush Test Results

A series of quasi-static crush tests have been performed on quarter-scale models of the bottom impact limiter for the NAC-LWT cask. The limiter orientations tested were end (axial), side and center of gravity over corner (15.7 degrees from axial). The purpose of the quasi-static crush tests was to document the force-deflection and energy absorption characteristics of the honeycomb material used in the impact limiter. Additionally, the tests demonstrated that the limiters need not be mechanically attached to the cask body in order to remain in position to absorb the energy of crushing. No attachment between the model limiter and the test fixture was used for the end (axial) test. A strip of duct tape was adequate to retain the model limiters in position on the side (90-degree) and center of gravity over corner (15.7-degree) fixtures. Once crushing of the limiter is initiated, its cup-shaped geometry causes it to maintain its position on the fixture, which is identical to a quarter-scale model cask body. Thus, attachment of the impact limiter to the cask body is not necessary for maintaining proper position and energy absorption capability.

Analytic Evaluations

Although the results from the above discussed test programs are considered to be the primary proof that the limiters will remain in position during the impact event and properly perform their impact limiting function, analytic studies can also be used to confirm the test observations. Analytic assessments presented in this evaluation indicate that failure of the attachment hardware can be expected to occur for some drop orientations, but subsequent to such failure, the cask tends to wedge into the limiter and separation of the limiter from the cask does not occur. As shown, a significant resistance to the applied separation moment exists due to a combination of crushing of the limiter at the cask interface and due to frictional resistance that exists there. This total resistance is shown to be greater than the applied separation moment and is approximately 7.9 times greater than that provided by the attachment hardware alone.

Additionally, it is noted that the maximum applied separation moment occurs early in the impact when crush depths are small. As crush depths increase, the moment arm and the separation moment decrease to zero. The maximum separation moments occur early in the impact event when the package still possesses a significant downward velocity (87 percent of the initial impact velocity). Additionally, the duration of the impact is very short (approximately 0.04 to 0.06 seconds) and minimal rotation (approximately 1 degree) of the package occurs during the impact. Thus, the cask "drives" into the limiter and physically "traps" the limiter between the cask body and the ground.

The remainder of this section presents a detailed analytic study of the center of gravity over top corner impact event. This near vertical orientation, coupled with the fact that little energy will be converted into rotational energy of the entire package (that is, the center of gravity is over the impacted corner), makes this particular orientation a representative worst case regarding the development of significant separation moments. The available impact limiter analysis program results associated with the corner drop are summarized in Figure 2.6.7-17. The crush depths, crush forces and package velocities presented in the summary figure are directly available from the impact limiter analysis program, RBCUBED, and the separation moment is calculated based on the geometry (that is, the crush footprint) existing at the particular position of interest. Of note, the velocity of the package is still 466.2 inches/second (87 percent of the initial impact velocity) when the maximum separation moment of 7.67×10^6 inch-pounds has developed.

Capability of Attachment Hardware

Figure 2.6.7-18 presents a free body diagram for the top impact limiter during a top down center of gravity over corner impact. With point "A" being the pivot point of the impact limiter on the cask, taking moments about point "A" yields the following:

$$F_i x_i = 14.45\ F_2 + (14.45 + 16.1)\ F_1$$
$$= 14.45\ F_1 + 30.55\ F_1$$
$$= 45.0\ F_1 = \text{separation moment}$$

where:

F_1 = maximum force on a lug

$F_2 = 2(F_1/2) = F_1$

$F_3 = 0.0$ (approximately)

F_i = impact force at limiter to ground interface

x_i = moment arm for force F_i

According to the section titled "Response of Secondary Impact Limiter During Initial Impact of Package," the failure mode for the attachment hardware is tension on the net section of the

impact limiter lug. Failure will occur at a load of 28,445 pounds, which corresponds to a stress equal to the ultimate strength of the aluminum lug. Substitution into the above separation moment equation indicates that a moment of 1.28×10^6 inch-pounds can be expected to fail the attachment hardware. As seen from Figure 2.6.7-17, this moment is exceeded prior to 2 inches of crush occurring for the limiter. Attachments may, therefore, fail in the center of gravity over top corner drop.

Resistance to Separation Following Attachment Hardware Failure

If attachments do fail, the cask tends to wedge itself into the limiter as shown in the free body diagram presented as Figure 2.6.7-19. From that figure:

f_{max} = force required to crush limiter honeycomb

= 28.9 S_c (projected area x crush strength) = 28.9(3850)

= 111,265 lb/in

where:

S_c = crush strength of honeycomb used in limiter

= 3850 psi (conservative upper bound crush strength, which was the case selected for Figure 2.6.7-17; the design upper bound crush strength is 3675 psi)

From moment equilibrium:

$F_i x_i = (6\ f_{max}) = 36\ f_{max}$

$= 4.006 \times 10^6$ in-lb

A significant frictional resistance to separation of the limiter also exists. Selecting a coefficient of friction of approximately 0.5 for aluminum on steel (Baumeister, pages 3-26), the frictional resistance to the separation moment is:

$M_f = F_f\, d$

$= 6.145 \times 10^6$ in-lb

where:

F_f = friction force

$0.5(6\ f_{max}) = 3\ f_{max} = 333{,}795$ lbs

and with the centroid of a 180-degree arc (that is, the arc over which f_{max} acts) being located at 63.7 percent of its radius:

d = 0.637(28.9)

= 18.41 inches

The total resistance to separation, therefore, becomes:

$M_t = 4.006 \times 10^6 + 6.145 \times 10^6$

$= 10.151 \times 10^6$ in-lb

This total resistance to separation exceeds the maximum applied separation moment of 7.67×10^6 inch-pounds (Figure 2.6.7-17). Separation of the limiter from the cask body will not occur. As discussed in the section titled "Dynamic Free Drop Test Results," this particular center of gravity over corner case was tested. Test results are consistent with the preceding analysis in that attachment hardware did fail, that the cask did tend to wedge itself into the impact limiter, and that physical separation did not occur (Appendix 2.10.8, Figures 2.10.8-15 and 2.10.8-16).

Response of Secondary Impact Limiter During Initial Impact of Package

The final criterion to be satisfied is for a free drop (normal or accident) involving an initial impact on a single impact limiter, that the limiter on the opposite end of the cask (secondary limiter) must remain attached to the cask during the initial impact. This ensures that the secondary limiter will be in position to absorb the secondary impact and, as discussed in the section titled "Response of Impact Limiter(s) During Initial Impact of Package with Ground," it remains in position for the full duration of the secondary impact and performs its impact limiting function. Attachment is ensured by demonstrating that the attachment hardware (pins, lugs and associated welds) does not fail during the initial impact while the far end of the transport cask is rotating about the end that is in contact with the ground. For this evaluation, the worst case loading on the secondary impact limiter to separate it from the cask is bounded by the condition that all of the kinetic energy at the time of impact is converted to angular rotation. The angular rotation speed (ω) results in a radial angular acceleration (A_r) of the far end of the cask (a radius of r) that is computed by $r\omega^2$. The angular speed is determined by using conservation of energy,

$$\omega = \sqrt{\frac{2WH}{I}}$$

where:

The moment of inertia of the cask (I) about the point of rotation is computed for a 199.8-in long, 39.23-in diameter, right circular cylinder about the edge in conjunction with the impact limiter (M_L) (see page 34 of "Formulas for Natural Frequency and Mode Shape," Robert D. Blevins, Ph.D, Krieger Publishing Co., Inc., 1984):

$$I = (M) \times \left[\frac{1}{12} \left(3 \times (R)^2 + (L)^2 \right) + (R)^2 \right] + M_L \times L^2$$

$$= (118.2\ \text{lb}\cdot\text{sec}^2/\text{in}) \times \left[\frac{1}{12}\left(3\times\left(\frac{39.23\ \text{in}}{2}\right)^2 + (199.8\ \text{in})^2\right) + \left(\frac{39.23\ \text{in}}{2}\right)^2\right] + 3.97\times 199.8^2$$

$$= 6.09\times 10^5\ \text{lb}\cdot\text{sec}^2\cdot\text{in}$$

where,

M = mass of the empty cask, less the weight of one impact limiter =

$$\frac{45{,}673\ \text{lbs}}{386.4\ \text{in}/\text{sec}^2} = 118.2\ \text{lb}\cdot\text{sec}^2/\text{in}$$

M_L = mass of the impact limiter = $\dfrac{1{,}535\ \text{lbs}}{386.4\ \text{in}/\text{sec}^2} = 3.97\ \text{lb}\cdot\text{sec}^2/\text{in}$

The bounding angular velocity is therefore:

$$\varpi = \sqrt{\frac{2\times W\times H}{I}} = \sqrt{\frac{2\times 47{,}208\ \text{lbs}\times 360\ \text{in}}{6.09\times 10^5\ \text{lb}\cdot\text{sec}^2\cdot\text{in}}} = 7.47\ \text{rad}/\text{sec}$$

The radial acceleration (A_r) (g) using a radius of 200 inches from the bottom to the top end of the cask is:

$$A_r(g) = \frac{200\ \text{in}\times\left(7.47\ \text{rad}/\text{sec}\right)^2}{386.4} = 28.9\ \text{g's}$$

The calculations for the stress conservatively use the maximum acceleration of 30 g's. With four attachment points, the load, P, per attachment point therefore becomes:

P = 30 × 1,535/4
= 11,513 lbs

where 1,535 pounds is the weight of the heaviest (top) impact limiter.

Analysis of Impact Limiter Lug

The impact limiter lug is evaluated using the same approach as was used in the section titled "Analysis of Impact Limiter Lug," but the allowable limit is based on ultimate strength rather than yield strength. As shown in Table 2.3.1-4, the ultimate strength of 6061-T651 aluminum at 150°F is 38,700 psi. Potential failure modes of tension across the net section and 40-degree shearout are considered as follows:

Tension Across the Net Section

$P = 11{,}513$ lbs

$A = 0.5(2.0 - 0.53)$

$= 0.735\ in^2$

$S_t = 11{,}513/0.735$

$= 15{,}664$ psi ($S_u = 38{,}700$ psi)

$MS = 38{,}700/15{,}664 - 1$

$= +1.47$

40-Degree Shearout

$P = 11{,}513$ lbs

$e = 1.7 - (0.53/2) \cos 40°$

$= 1.497$ inches

$A_s = 2(0.5)(e)$

$= 1.497\ in^2$

$S_s = 11{,}513/1.497$

$= 7{,}691$ psi ($0.6\ S_u = 23{,}220$ psi)

$MS = 23{,}220/7{,}691 - 1$

$= +2.02$

An optional impact limiter lug configuration permits the gusset plate impact limiter attachment tab to be an assembly of the tab and gusset plate using a full-penetration weld, as described in Section 8.2.1.1, Impact Limiter Attachment Lug Repairs. Structural strength of the weld using a mock-up test confirms that the minimum weld tensile strength is equal to or greater than 20 ksi. The only stress applicable to the weld is the tension across the entire section of the weld. Using the bounding load of 11,513 pounds, the tensile stress is 11,513 (2×1/2) or 11,513 psi and the margin of safety for the weld region is:

$MS = 20{,}000/11{,}513 - 1$

$= \underline{+0.74}$

Both the 6061-T651 continuous tab gusset configuration and the optional full-penetration weld assembly configuration are confirmed to maintain the attachment of the impact limiters during the bounding condition of the accident side drop condition.

Analysis of Cask Lug

The cask lug is evaluated using the same approach as was used in the section titled "Analysis of Impact Limiter Lug," but the allowable limit is based on ultimate strength rather than yield strength. The ultimate strength of Type 304 stainless steel at 150°F is 73,000 psi. Potential failure modes of 40-degree shearout and failure of the weld (3/8-inch bevel plus 3/8-inch fillet), which attaches the base plate to the cask body, are considered as follows:

40-Degree Shearout

$F = P/2 = 23{,}179/2$

$= 11{,}590$ lbs

$e = 0.72 - (0.53/2) \cos 40°$

$= 0.517$ in

$A_s = 2(0.5)(e)$

$= 0.517 \text{ in}^2$

$S_s = 11{,}590/0.517$

$= 22{,}418$ psi ($0.6\ S_u = 43{,}800$ psi)

$MS = 43{,}800/22{,}418 - 1$

$= +0.95$

Weld Stresses

The analysis will again conservatively ignore the 3/8-inch bevel weld and only consider the 3/8-inch fillet weld around the perimeter of the base plate.

The stress in the weld due to the applied moment is:

$s_1 = 4.24\ M/(h[b^2 + 3\ L(b + h)])$

$= 30{,}292$ psi

where:

$M = 1.78(P) = 41{,}259$ in-lb

$P = 23{,}179$ lbs

$h = 3/8 = 0.375$ in

$b = 2.0$ in

$L = 1.6$ in

The stress in the weld due to the applied shear load is:

$s_2 = P/A_s$

$= 12{,}142$ psi

where:

$P = 23{,}179$ lbs

$A_s = 2(1.6 + 2.0)(0.707)(0.375)$

$= 1.909$ in^2

The combined stress is therefore:

$s = (s_1^2 + s_2^2)^{0.5}$

$= 32{,}635$ psi ($0.6\ S_u = 43{,}800$ psi)

$MS = 43{,}800/32{,}635 - 1$

$= +0.34$

Analysis of Ball-Lock Pin

The 1/2-inch, AVIBANK 57459-1 ball-lock pins have a 36,800-pound capacity in double shear. With an applied load of 23,179 pounds, the margin of safety becomes:

$MS = 36{,}800/23{,}179 - 1$

$= +0.59$

2.6.7.5 Closure Lid

2.6.7.5.1 Discussion

The NAC-LWT cask closure lid is analyzed for structural adequacy in accordance with the requirements of 10 CFR 71.73(c)(1) free drop (hypothetical accident condition). The cask is assumed to be inverted, with the lid downward, when dropped through a distance of 30 feet onto a flat, unyielding, horizontal surface. The structural evaluation is performed by classical elastic analysis methods.

2.6.7.5.2 Analysis Description

Geometry

The closure lid geometry is shown in Figure 2.6.7-20. The lid is bolted in position on the upper end of the cask. The lid material is Type 304 stainless steel. The temperature-dependent material properties for Type 304 stainless steel, which are presented in Section 2.3, are used in this analysis.

Loadings

During impact, the cask cavity contents are considered to apply an internal inertia pressure on the interior surface of the lid in the outward normal direction. The impact limiter applies an external inertia pressure on the exterior lid surface in the inward normal direction; however, this pressure is conservatively ignored in this analysis. Each bolt is torqued to a preload force of 21,000 pounds. The lid is also loaded with an assumed 50-psig internal pressure for the 130°F ambient temperature hot case.

Displacement Boundary Conditions

The closure lid is restrained from vertical and rotational deformation at the 17.875-inch bolt circle diameter by the preloaded lid bolts.

Detailed Analysis

For the loading and boundary conditions described, the structural behavior of the closure lid may be assessed by superposition of maximum stresses from Section 2.6.1, which includes consideration of thermal effects, bolt preload, and internal pressure, with the maximum stresses produced by the inertia loading. The maximum $P_m + P_b$ component stresses from Section 2.6.1 (Table 2.6.1-2) are:

S_x = -3060 psi; S_y = - 260 psi; S_z = 100 psi; S_{xy} = 180 psi

The free body diagram of Figure 2.6.7-21 can be evaluated by applying formulas from Case 6 (Roark, page 217) for a uniformly loaded circular plate.

The total deceleration force of the contents, F_D = 4000 lbf × 60 g deceleration = 240,000 lbf, creates a pressure, W, on the lid interior surface:

$$W = \frac{240,000}{\pi(8.938)^2} = 956 \text{ psi}$$

The maximum radial, tangential, and vertical stresses on the lid are:

$$S_r = \frac{3Wa^2}{4t^2}$$

$$= 895 \text{ psi}$$

$$S_t = \frac{3Wa^2\gamma}{4t^2}$$

$$= 246 \text{ psi}$$

$$S_v = -W$$

$$= -956 \text{ psi}$$

where:

a = 8.938 inches

$\gamma = 0.275$

t = 8.0 inches

Conservatively combining these stresses with $P_m + P_b$ stresses from Section 2.6.1 (Table 2.6.1-2), the total $P_m + P_b$ component stresses on the lid are:

$S_x = -3955$ psi; $S_y = -1216$ psi; $S_z = 346$ psi; $S_{xy} = 180$ psi

For small S_{xy}, the stress intensity becomes S.I. = $S_z - S_x = 4301$ psi. Since the maximum cask lid temperature is less than 300°F for the 130°F ambient temperature hot case (Section 3.4.2), the closure lid allowable $P_m + P_b$ stress is 72,000 psi (3.6 S_m). Therefore, the minimum margin of safety is +Large; thus, containment is maintained.

2.6.7.5.3 Conclusion

It is demonstrated by use of a conservative loading that the minimum margin of safety is +4.23 and containment is maintained. Therefore, the NAC-LWT cask lid satisfies the requirements of 10 CFR 71 for consideration of the closure lid impact in the 30-foot free drop accident.

2.6.7.6 Bolts - Closure Lid (Normal Conditions of Transport)

The NAC-LWT cask closure lid is bolted to the cask body top forging with twelve 1 - 8 UNC bolts fabricated from SA-453, Grade 660 high alloy steel. The threaded portion of the bolt engages the cask body a minimum of 1.875 inches. In accordance with the free drop provisions of the normal conditions of transport, 10 CFR 71.71(c)(7), this bolted closure has been carefully

evaluated for structural adequacy and found to satisfy all regulatory requirements and design criteria. Details of this analytic evaluation follow.

The simultaneous loads that may be imposed upon the cask closure bolts include: pressure loads, thermal differential expansion loads, pre-loads and inertial loads arising from impact responses. For a given set of initial conditions, the pressure loads, thermal loads and pre-loads all remain constant. Inertial impact loads, however, vary with impact orientation and bolt location. Lateral impact loads acting upon the lid are directly related to the mass of the lid and the lateral impact acceleration. Longitudinal impact loads acting on the lid are proportional to the longitudinal impact acceleration, as well as, the mass of the lid and the payload within the containment cavity.

In general, these lid impact loads impose unequal individual forces, or loadings, in the closure bolts. This NAC-LWT cask evaluation conservatively assumes a set of impact forces that induce maximum containment closure separation forces and bolt loadings. With this conservative assumption, the external impact force is presumed to be located at a point where it cannot restrain those forces that tend to separate the cask lid from the cask body. This assumption locates the external impact force at the lower corner of the lid-body interface. With this assumption the lower corner of the lid is assumed to be pinned (by the impact forces), and bolt tension forces are assumed to vary linearly from zero at this pinned lower corner to a maximum value at the opposite, or upper, corner of the lid.

A complete range of impact orientations is evaluated, from an end impact at 0 degrees to a flat side impact at 90 degrees, and at 5-degree increments in between. Loads are derived from the normal impact accelerations summarized within Table 2.6.7-34. Where necessary, impact accelerations have been interpolated at 5-degree increments from those values given in Table 2.6.7-34.

The details of this analytic evaluation are described and performed within Section 2.10.9 for both normal conditions of transport and hypothetical accident conditions. Normal conditions of transport results are summarized in Table 2.6.7-35 and Table 2.6.7-36, corresponding to a "hot" initial condition and a "cold" initial condition, respectively. The hot initial condition bolt temperature is taken at 227°F, as summarized in Table 3.4-2. The cold initial condition bolt temperature is assumed to be -20°F, per regulatory requirements. Physical properties for the SA-453, Grade 660 bolts are conservatively taken at 300°F and at room temperature (70°F) for hot and cold conditions, respectively. As defined within Table 2.1.2-1, the allowable bolt stress is taken as S_y, leading to allowable direct tension stresses of 81.9 and 85.0 ksi, at 300°F and 70°F, respectively. Based on this thorough evaluation, the closure bolts incur a maximum stress intensity of 61,012 psi, which results in a minimum margin of safety of 34 percent. See Table 2.6.7-35 (at 5°):

$$MS = 81.9/61.042 - 1$$
$$= +0.34$$

Bolt engagement may be evaluated by computing shear stresses within the SA-336, Type 304, end forging material. At 300°F, the allowable shear stress is 0.5 S_y, or 11.25 ksi, according to Tables 2.1.2-1 and 2.3.1-1. The maximum tensile load is found as the product of the maximum bolt stress intensity, noted above, and the bolt stress area; that is, (61,042 psi)(0.6051) = 36,937 pounds. The shear area per inch of engagement for a 1 - 8 UNC internal thread is 2.325 in^2/in ("Table Speeds Calculation of Strength of Threads," pp. 41-49). The resultant shear stress and margin of safety within the top body forging is:

$$\tau = P/A = (36{,}937)/[(2.325)(1.875)]$$
$$= 8473 \text{ psi}$$
$$MS = 11.25/8.473 - 1$$
$$= +0.33$$

Using consistently conservative assumptions, the NAC-LWT cask lid bolted closure can be shown to satisfy the performance and structural integrity requirements of 10 CFR 71.71(c)(7) for normal conditions of transport.

2.6.7.7 Neutron Shield Tank

2.6.7.7.1 Introduction

The neutron shield tank is welded to, and concentric with, the NAC-LWT cask outer shell. The tank consists of eight cells. The neutron shield fluid flows freely through holes in the longitudinal stiffeners between these cells. During thermal expansion or contraction, fluid passes through the valve assembly into or out of the expansion tank, which is external to and concentric with, the shield tank. Table 2.6.7-37 summarizes the results of the structural analyses described below. The table shows positive margins of safety, demonstrating that each component of the neutron shield tank satisfies the requirements of the normal operations conditions 1-foot free drop as described in 10 CFR 71.71. Classical analysis techniques are used to demonstrate that each tank component withstands the hydrodynamic loads from a 1-foot side or end drop in combination with internal tank pressure. Similarly, classical analyses show that the shield/expansion tank does not rupture, nor does the check valve sustain damage during the penetration test.

The shield tank wall has a mean diameter of 39.04 inches, is located approximately 23 inches below the top edge of the upper end casting, and extends 164 inches longitudinally. Constructed entirely of Type 304 stainless steel, the tank external shell and eight longitudinal stiffeners are 0.24-inch thick plate. Each end of the tank is a 0.50-inch thick end plate. Equally spaced

between stiffeners are eight 0.24-inch thick gusset plates, which provide additional support to the end plates.

A 56 percent by volume ethylene glycol and water solution provides the neutron shielding. The shield tank fluid volume (excluding stiffeners) is 84,742 cubic inches or approximately 370 gallons (3,280 pounds) of fluid. At the upper end, concentric with the shield tank, is the expansion tank. The expansion tank is 46 inches long and is constructed from 0.32-inch thick stainless steel plate; there are eight cells divided by equally spaced plate stiffeners with holes in them, which enables the fluid to flow from chamber to chamber. The expansion tank empty volume is 13,245 cubic inches. It is filled with 11.5 gallons (103 pounds) of solution initially, leaving an expansion volume of 10,589 cubic inches. At the bottom of the expansion tank is a siphon tube, which goes around the shield tank and exits at its top. Volumetric expansion forces fluid through the siphon tube. During heating, the solution in the shield tank expands into the expansion tank avoiding uncontrolled pressurization of the shield/expansion tank. A pressure relief valve in the shield tank assures that the tank structure is protected against over pressurization. The pressure relief valve is set to begin relieving pressure at 165 psig. Initially, the expansion tank is filled with 11.5 gallons of fluid to assure that the shield tank remains filled at -40°F. A cross section of the upper end of the cask with pertinent dimensions is shown in Figure 2.6.7-22.

2.6.7.7.2 Structural Criteria

The neutron shield tank and expansion tank analyses use 10 CFR 71 and Regulatory Guide 7.8 to determine load/ambient conditions to bound other load conditions. In this way, the shield/expansion tank components are conservatively analyzed for the most severe structural loads at maximum temperatures; thus, the material properties and allowable stresses have minimum values.

The 10 CFR 71 requires that all transport packages weighing more than 30,000 pounds be evaluated to determine the consequences of a free fall through a distance of 1-foot onto a horizontal, unyielding surface for normal operation; cask orientation during the fall shall be such that maximum damage is inflicted upon the cask. End and side drop g loads are the most severe normal operating loads that the cask sustains; analyses of the shield and expansion tanks are based on the end and side drop loads. All other cask drop orientations produce less severe g loads.

Table 2 in Regulatory Guide 7.8 defines three initial ambient states that guide the analyses. The two extreme cases used to envelope analyses are:

1. 100°F ambient temperature, with maximum insolation, decay heat, internal pressure, weight, and minimum external pressure

2. 20°F ambient temperature, with no insolation or decay heat, minimum internal pressure, weight, and external pressure.

These conditions are used to evaluate the shield tank fluid temperatures (Actually, Sections 3.4.2 and 3.4.3 results, which are based on the more limiting ambient temperatures of 130°F and -40°F are used). With the fluid temperatures established, it is then possible to calculate the shield/expansion tank pressures for the extreme cases and the resulting amount of fluid flowing between the shield tank and the expansion tank (for expansion tank sizing). Table 2.6.7-38 summarizes the calculated shield tank fluid temperatures used in analyzing the shield tank structure.

Since the functional and structural adequacy of the neutron shield and expansion tanks depend on linear elastic evaluations, the allowable stress criteria is selected as the material yield strength. All calculated stresses are less than this criteria. From Table 2.6.7-38, the highest average fluid temperature is 227°F; therefore, material properties for 250°F are used in the analyses. The evaluation of the shield/expansion tank and the resulting conclusions are conservative.

2.6.7.7.3 Neutron Shield and Expansion Tank Loads

Structural, hydrostatic/hydraulic pressure and expansion pressure are the three components of shield tank loads. Structural loads result from decelerating the cask structure. Hydrostatic and hydraulic loads (water hammer) result from the shield tank fluid decelerating against the shield tank structure. Expansion pressure loads are generated when the fluid expands during heating. An explanation of how each type of load is calculated follows.

Structural loads are loads imposed on the structure by the weight of the structure itself. The stainless steel materials from which the cask is fabricated all have mass and are acted upon by gravity and the normal operations conditions 1-foot drop deceleration. Shield tank structural components weigh approximately 2,116 pounds. Expansion tank components weigh approximately 610 pounds. These loads are included in the analysis of the tanks.

Hydrostatic pressure is the pressure at a given depth within a fluid caused by the mass of the fluid being accelerated by gravity. Hydraulic pressure is the hydrostatic pressure acted upon by accelerations other than gravity. To determine the hydrostatic pressure of fluid acting on the plate, the following formula is used:

$$p = \rho g h$$

where:

ρ = mass density of fluid (lbm/in^3)
g = acceleration due to gravity (in/sec/sec)
h = height of fluid above point considered (in)

When the cask is vertical, the maximum fluid height in the shield tank is 164 inches, which is equivalent to 6.3 psig under the acceleration of gravity (1 g). When the cask is in the horizontal position, there is a 39-inch maximum fluid height (diameter of shield tank) or 1.56 psig (1 g). The presence of the expansion tank around the shield tank is conservatively neglected, because the fluid pressure acting on the exterior of the shield tank reduces the forces acting on the shield tank components. During a 1-foot end drop (normal operations conditions), the cask undergoes a 15.8 g deceleration (Section 2.6.7.4). This results in a hydraulic pressure of 100 psig (6.3 psig × 15.8 g) at the bottom of the shield tank. Similarly, during the side drop, the pressure at the lowest point on the shield tank is 38 psig (1.56 psig × 24.3 g). The maximum hydrostatic and hydraulic pressures for the end and side drops and the location of the maximum pressure for the shield tank analyses are shown in the following sketches.

1-Foot End Drop (15.8 g)

Maximum Hydrostatic Pressure	Maximum Hydraulic Pressure
6.3 psig	100 psig

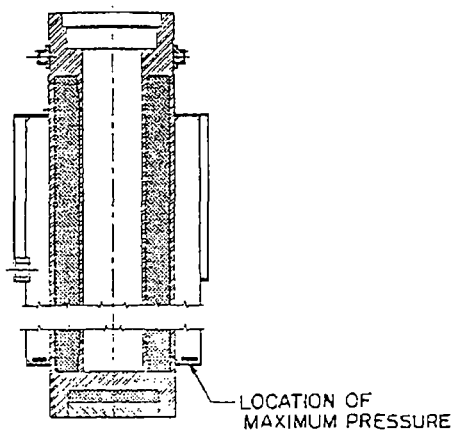

Vertical Orientation

1-Foot Side Drop (24.3 g)

Maximum Hydrostatic Pressure	Maximum Hydraulic Pressure
1.56 psig	38 psig

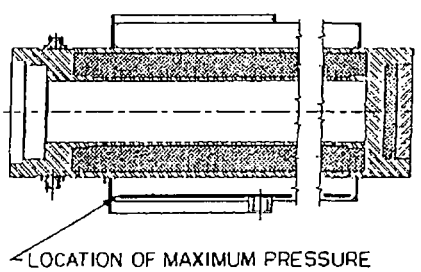

Horizontal Orientation

The g loads for various drop orientations and how they were calculated are explained in Section 2.6.7.4.

Once the shield/expansion tank is filled, it is a sealed compartment, which will not permanently deform under normal transport conditions. The neutron shield tank solution expands or contracts when heated or cooled. During heating the liquid expansion causes fluid to flow into the expansion tank, compressing the air in the expansion tank and causing the pressure to increase. Similarly, as the cask fluid temperatures reach 40°F, there is sufficient fluid in the expansion tank to always keep the neutron shield tank completely filled.

The neutron shield tank is completely filled in the upright configuration, when the fluid and ambient conditions are at 68°F. The 56 percent by volume ethylene glycol and water solution has a density of 67.07 lbs/ft^3 at 68°F. After the neutron shield tank is filled, 11.5 gallons of solution are poured into the expansion tank. Both tanks are then sealed.

The normal transport condition of maximum decay heat load, 100°F ambient temperature and maximum insolation results in an average (natural and forced mixing of fluid is assumed) shield tank fluid temperature of 227°F. The volume of fluid that enters the expansion tank as the temperature increases from 68°F to 227°F is:

$$\Delta V = V_1\left(\frac{\rho_1}{\rho_2} - 1\right) = 5539 \text{ in}^3$$

where:

ρ_1 = 67.07 lb/ft^3 = density of 56 percent ethylene glycol and water solution at 68°F

ρ_2 = 63.07 lb/ft^3 = density of 56 percent ethylene glycol and water solution at 230°F

V_1 = 87,398 lb/in^3 = volume of fluid in the expansion and shield tank at 68°F

ΔV = volume of fluid entering the expansion tank

Then the increased uniform air pressure in the expansion tank at 230°F is:

$$P_2 = P_1\left(\frac{V_1 T_2}{T_1 V_2}\right) = 40.3 \text{ psia } (25.6 \text{ psig})$$

where:

P_1 = 14.7 psia

V_1 = 10,589 in^3 (expansion tank air volume at 68°F)

T_1 = 528°R = 68°F

T_2 = 690°R = 230°F

$V_2 = 10{,}589\ in^3 - 5539\ in^3 - 5050\ in^3$ (expansion tank air volume at 230°F)

The same analysis procedure was used to calculate the pressures at other significant normal operating states; these pressures are presented in Table 2.6.7-39. Properties for the 56 percent by volume ethylene glycol and water solution are presented in Table 3.2-5. Two normal operating conditions are presented in Table 2.6.7-39, and are helpful in understanding how the cask operates, but are all bounded by the pressure relief valve release pressure (PRVR) shown in Table 2.6.7-39. The PRVR pressure is used to establish the structural loads for shield and expansion tank analyses.

Thus, the magnitude of the expansion pressure is determined as discussed previously by the volume of fluid added to the expansion tank during the initial filling. It is assumed that 11.5 gallons of fluid are added to the expansion tank, 0.5 gallons more than specified. This results in a maximum expansion pressure of 26 psig.

In addition to the expansion pressure acting radially outward, 10 CFR 71, Subpart F, requires that the cask be able to sustain a reduced external pressure. The cask is initially filled and pressurized at atmospheric pressure (14.7 psia). When the external pressure is reduced to 3.5 psia, there is a relative increase in internal pressure of 11.5 psig (rounded to 12 psig). The reduced external pressure load has been included in the analysis as an increase in internal pressure.

The calculated pressures for the end drop load condition are as follows:

Reduced external pressure	12 psig
Hydraulic pressure	100 psig
Expansion pressure	26 psig
TOTAL	138 psig

The calculated pressures for the side drop load condition are as follows:

Reduced external pressure	12 psig
Hydraulic pressure	38 psig
Expansion pressure	26 psig
TOTAL	76 psig

These pressures are conservatively assumed to add algebraically and represent the highest pressure expected at a point on the shield/expansion tank structure. All other pressures within the shield/expansion tank are less because the hydraulic pressure is a function of fluid depth.

2.6.7.7.4 Neutron Shield Tank Structural Analyses

To simplify analysis of the shield tank structure, the use of symmetry, superposition and analysis of worst case loads are employed to reduce the number of calculations to be performed. Major shield tank structural components are shown in Figure 2.6.7-23. Analyses performed and resulting conclusions for one location of the shield tank are directly applicable to the same relative location elsewhere on the shield tank structure. For reasons stated earlier, the normal operating conditions 1-foot end drop loads envelope all other normal operations conditions drop orientations, and is the only loading condition that is considered in the following analyses. Moreover, the bottom end drop g load is more severe than the top end drop, and is used in both the top and bottom end drop analyses. The shield tank analysis is performed with the shield tank pressure equal to 180 psig, a pressure 42 psig higher than the calculated 138 psig for the end drop (which envelops the side drop condition).

The bottom end plate, shield tank shell, gussets, top end plate, and welds are the major components of interest in the shield tank evaluation for normal transport conditions.

To ensure a conservative analysis of the neutron shield and expansion tank structure, several simplifying assumptions are made for all analyses performed (other assumptions are stated with each analysis). The allowable stress is taken as the yield strength of Type 304 stainless steel at 250°F, which is 23,750 psi. This is conservative since the maximum calculated shield/expansion tank normal operating temperature is 227°F.

Finally, the edge restraint of the structural components analyzed is considered to be simply supported. The smallest welds are considered in the analyses; a larger weld assures a conservative analysis.

Weld Allowable Stresses

The shield and expansion tanks are constructed primarily from 0.24-inch thick Type 304 stainless steel plate. The plates are welded together using 0.188-inch fillet welds, using Type 308 weld material. From the Metals Handbook, 9th Edition, Volume 3, page 20, the ultimate tensile strength is 75.0 ksi. The allowable strength for shield tank fillet welds is:

$$S_{ALL} = (0.3)(75{,}000)$$
$$= 22{,}500 \text{ psi}$$

or:

$$f_{ALL} = (0.707)(22{,}500)\omega$$
$$= 15{,}900\omega \text{ lb/in}$$

where:

f_{ALL} = fillet allowable (lb/in)

ω = fillet weld size (in)

The only size fillet weld considered in the shield tank analysis is a 0.188-inch fillet. Therefore, the 0.188-inch fillet weld has an allowable strength of:

$$f_{ALL} = (15{,}900)(0.188 \text{ in})$$
$$= 2980 \text{ lb/in}$$

Structural Loads

Shield tank and end plate loads are considered in the neutron shield tank analysis. The weight of a unit depth of the 0.24-inch thick shield tank plate material is considered to be located at the mass centroid of the plate assembly. The mass centroid is 6.13 inches from the outer shell, as shown in the following analysis:

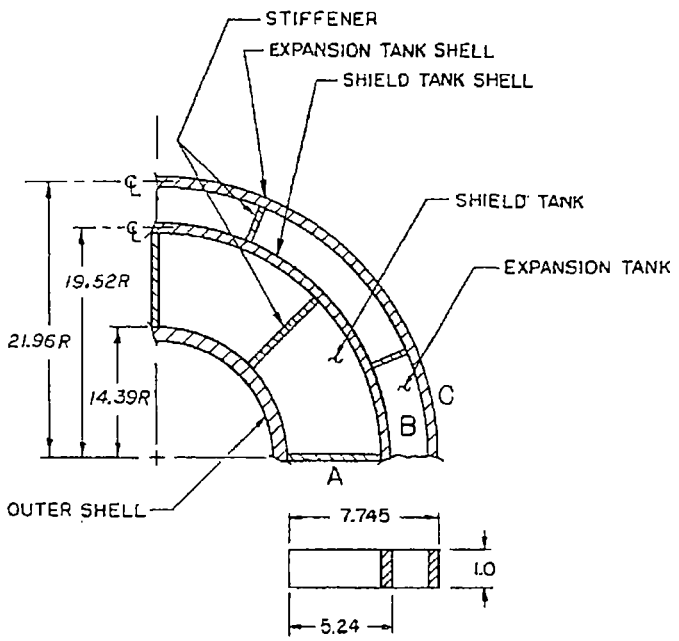

Quarter Section - NAC LWT Cask

Two "A" plates weigh 1.051 pounds with a mass centroid at 3.87 inches from the outer shell.
Two "B" plates weigh 2.005 pounds with a mass centroid at 5.12 inches from the outer shell.
Two "C" plates weigh 3.032 pounds with a mass centroid at 7.59 inches from the outer shell.
The total weight of the plates is 6.09 pounds.

The mass centroid is located at:

$$\bar{x} = \frac{(1.051\ \text{lb})(3.873\ \text{in}) + (2.005\ \text{lb})(5.12\ \text{in}) + (3.032\ \text{lb})(7.59\ \text{in})}{5.643\ \text{lb}}$$

$$= 6.134\ \text{in}$$

The weight of the neutron shield tank structural plates is considered to act at 6.09 inches from the outer shell. The weight of one stiffener and shield/expansion tank shell section is 3.54 pounds.

The shield tank end plates are 0.5-inch thick stainless steel plate. To determine the structural load, the weight of the plate was divided by its area. The resulting structural load is 3 pounds/square inch.

Shield Tank Shell

The shield tank shell is analyzed as a thin-walled tube, taking no credit for the eight radial stiffeners, which run the length of the tank. Using Case 1 (Roark, page 298), the meridional and hoop stresses are calculated:

$$S_1 = \frac{pR}{2t} = 7414\ \text{psi}$$

where:

p = 180 psig

R = 19.44 inches

t = 0.24 in

and

$$S_2 = \frac{pR}{t} = 14{,}827\ \text{psi}$$

Von Mises yield criterion is used to calculate an equivalent stress, S_e, which is compared to the yield strength of stainless steel.

$$S_e = \frac{1}{\sqrt{2}}\left[(S_1 - S_2)^2 + (S_2 - S_3)^2 + (S_3 - S_1)^2\right]^{0.5}$$

$$= 12{,}841\ \text{psi}$$

where:

S_1 = 7414 psi

$S_2 = 14{,}827$ psi

$S_3 = 0$ psi

then

$$M.S. = \frac{S_{ALL}}{S_e} - 1 = \underline{+0.07}$$

where:

$S_{ALL} = (0.577)(23{,}750 \text{ psi})$
$= 13{,}700$ psi

Stiffener

A 1-inch longitudinal section of the neutron shield tank is analyzed. The total pressure load (180 psi) acts equally between stiffeners as shown in Figure 2.6.7-24. No credit is taken for support from the end plates or the expansion tank end plate. The load acting on the stiffener (L = 2772 pounds) is the area of the tank shell 15.4 square inches (15.4 inches × 1 inch) multiplied by the total end drop pressure, 180 psi. The cross sectional area, A_p, of a 1-inch section of the stiffener plate is 0.24 square inches (0.24 inch × 1.0 inch). The tensile stress acting on the stiffener is calculated:

$$S_T = \frac{L}{A_p} = 11{,}746 \text{ psi}$$

then

$$M.S. = \frac{S_{ALL}}{S_T} - 1 = \underline{+0.17}$$

where:

$S_{ALL} = 13{,}700$ psi (Section 2.6.7.7.4)

The stiffeners are the structural members locating the shield tank shell and providing support for the end plates (similar to the gussets) during end drops. This analysis demonstrates that the stiffeners have adequate strength to withstand the maximum pressure in the shield tank. The analysis in Section 2.6.7.7.4 shows that the shield tank shell has adequate strength to withstand the maximum pressure in the shield tank. All other drop orientations offer less severe structural loads on both the stiffeners and tank shell. Lightening holes in each stiffener do not affect the structural integrity of the shield tank and stiffeners. Lightening holes are located away from the ends of the stiffeners where the hydraulic component of the pressure load is less severe.

Stiffener Weld

A unit section (1 inch longitudinal) of stiffener weld is analyzed. Two loads act on the weld attaching the stiffener to the cask outer shell. The drop pressure load acting on the stiffener is L = 2772 pounds (see section titled "Stiffener"). In addition to the pressure load, the structural load (L_s) is calculated concentrating the mass of the tank (stiffeners and shell) unit section (see section titled Structural Loads). The structural pressure loads and welds being examined are shown in Figure 2.6.7-25. Treating the two 1-inch welds as lines and determining the weld loading using methodology found in Design of Welded Structures (Blodgett, Section 7.4):

Tensile Load

$f_t = 2772/2$

$= 1{,}386$ lb/in

where:

$L = 2{,}772$ lbs

Shear Load

$f_s = 55.9/2$

$= 28.0$ lb/in

where:

$L_s = 3.54 \text{ lb} \times 15.8 \text{ g}$

$= 55.9$ lbs

15.8 g = end drop g load (Section 2.6.7.4)

The end drop structural load produces a bending moment on the weld group (Figure 2.6.7-25). The bending moment (M) is 343 inch-pounds (6.13 inches × 55.9 pounds). The section properties of the weld group are calculated from Blodgett, Table 5, page 7.4-7,

$$S_\omega = \frac{d^2}{3}$$

$$= 0.33 \text{ in}^2$$

where:

d = 1 in

Bending Load

$$f_b = \frac{M}{S_\omega}$$

$$= 343/0.33$$

$$= 1038 \text{ lb/in}$$

The resultant load on the weld group is calculated:

$$f_r = \sqrt{f_1^2 + f_2^2}$$

$$= 2424 \text{ lb/in}$$

where:

$f_1 = f_s = 28.0$ lb/in

$f_2 = f_t + f_b$

$= 2{,}424$ lb/in

The allowable weld load is $f_{ALL} = 2{,}980$ lb/in; therefore, the margin of safety is:

$$M.S. = \frac{f_{ALL}}{f_r} - 1 = \underline{+0.23}$$

Gusset Weld

It is assumed that the end drop load on the end plate is shared equally between the stiffeners and gussets (Figure 2.6.7-26). The fillet weld attaching the gusset to the cask outer shell and end plate is 0.188 inch and is on both sides of the gusset. Bending and shear stresses on the weld group A are calculated in the following analyses. Since the gussets and stiffeners share the end drop load, the end plate area, which the gusset must support, is calculated:

$$A = [\pi(R_o^2 - R_i^2) - (16)(T_{PLT})(R_o - R_i)]/16$$

$$= 33.95 \text{ in}^2$$

where:

$R_o = 19.6$ inches

$R_i = 14.3$ inches

$T_{PLT} = 0.25$ in

The distributed load is composed of the end drop pressure load (180 psig) and a structural load (3 psig) equivalent to the end plate weight. The concentrated load (L) is calculated by multiplying the area (A) by the sum of the distributed loads (183 psig): L = 6,213 pounds. Therefore, the moment acting on weld group A is:

$$M = L\left(\frac{5.1}{2}\right)$$

$$= 15{,}843 \text{ in-lb}$$

The section properties of the weld group are calculated from Blodgett, Table 5, page 7.4-7:

$$S_{\omega} = \frac{d^2}{3}$$

$$= 12 \text{ in}^2$$

where:

d = 6 inches

Bending Load

$$f_b = \frac{M}{S_{\omega}}$$

$$= 1320 \text{ lb/in}$$

Shear Load

$$f_s = \frac{L}{W_{LEN}}$$

$$= 518 \text{ lb/in}$$

where:

L = 6,213 lbs

W_{LEN} = 2 × 6 inches

= 12 inches

The resultant load on the weld group is calculated by:

$$f_r = \sqrt{f_1^{\,2} + f_2^{\,2}}$$

$$= 1418 \text{ lb/in}$$

where:

$f_1 = f_s = 518$ lb/in

$f_2 = f_b = 1320$ lb/in

The allowable weld load is f_{ALL} = 2980 lb/in; therefore, the margin of safety is:

$$M.S. = \frac{f_{ALL}}{f_r} - 1 = \underline{+1.10}$$

Bottom End Plate

It is assumed that the portions of the end plate between a gusset and the adjacent stiffener can be modeled by a rectangular plate of the appropriate dimensions. The width (b) of the plate is the difference between radii of the cask outer shell and the shield tank shell as shown in Figure 2.6.7-27. The length (a) of the plate is the average of the inner and outer arc lengths, 6.7 inches ((7.7 inches + 5.6 inches)/2). Using Case 36 (Roark, page 225), the maximum bending stress on the 0.5-inch thick end plate is:

$$S_b = \beta \frac{wb^2}{t^2}$$
$$= 8{,}525 \text{ psi}$$

where:

$\beta = 0.4146$

$w = 183$ psi (see section titled "Gusset Weld")

$b = 5.3$ inches

$t = 0.5$-in thick

The margin of safety is:

$$M.S. = \frac{S_{ALL}}{S_B} - 1 = \underline{+1.79}$$

where:

$S_{ALL} = S_{y_{250\ F}}$

$= 23{,}750$ psi

Gusset Plate Cross-Section

The plate was modeled as a large weld, with the throat in tension during an end drop. The end drop load (L) acting on the gusset is the load acting on the end plate between the gusset and adjacent stiffener. The gusset root cross-section (R) is considered to be in tension (Figure 2.6.7-28). From the section titled "Gusset Weld," the load on the gusset root is L = 6213 pounds. The gusset root cross-sectional area is calculated:

$A_R = 0.707(h)(T_{PLT})$

$= 0.865 \text{ in}^2$

where:

h = 5.1 in (shortest leg)

T_{PLT} = 0.24 in (thickness)

Calculating the tensile load:

$$S_T = \frac{L}{A_R}$$

$$= 7180 \text{ psi}$$

The margin of safety is:

$$M.S. = \frac{S_{ALL}}{S_T} - 1 = \underline{+LARGE}$$

where:

S_{ALL} = 23,750 psi

End Plate Welds

Peripheral weld group B (Figure 2.6.7-29) is considered to be in shear during an end drop. The end plate load is 6213 pounds, from the section titled "Gusset Weld." The area of weld material is:

$$A_W = 0.707\left\{\frac{3}{16}[2(19.6 - 14.3) + 7.7] + \frac{3}{8}(5.6)\right\}$$

$$= 3.9 \text{ in}^2$$

The tensile stress on weld group B is:

$$S_T = \frac{L}{A_W}$$

$$= 1593 \text{ psi}$$

The margin of safety is:

$$M.S. = \frac{S_{ALL}}{S_T} - 1 = \underline{+LARGE}$$

where:

S_{ALL} = 23,750 psi

Top End Plate - Normal Operations Conditions

In the analyses of the section titled "Bottom End Plate" and Section 2.6.7.8.2, the 0.5-inch thick bottom end plates are shown to be structurally adequate. This analysis shows that the top end plate, which is in effect equivalent to both bottom end plates welded together at the shield tank shell, is structurally adequate. Two bounding conditions are considered. The first condition considers the shield tank top end plate loaded with a pressure of 180 psig and the expansion tank top end plate unloaded. Using Case 38 (Roark, page 113), considering a unit strip of top end plate, where the two end points are considered pinned, the maximum bending stress is 10,272 psi, and the margin of safety equals +0.33. The second condition considers both the shield and expansion tank end plates loaded at 180 psig. Again using Case 38, the bending stress equals 11,172 psi, resulting in a margin of safety of +0.23. The maximum normal operations conditions pressure in the expansion tank is 162 psig; therefore, the top end plate is adequate for the normal operations conditions.

2.6.7.8 Expansion Tank

The expansion tank is located at the upper end of the cask and is concentric with the shield tank. As its name implies, the expansion tank provides a location for fluid to expand into during fluid heating; thus, protecting both the neutron shield tank and the expansion tank from over-pressurization during normal operations conditions. A description of the expansion tank, structural criteria, and structural loads is presented in Sections 2.6.7.7.1 through 2.6.7.7.3. Table 2.6.7-40 summarizes the results of the structural analyses described in the following sections. The table shows adequate margins of safety for each component of the expansion tank examined. Therefore, the normal operations conditions requirements of 10 CFR 71 are satisfied.

To simplify analysis of the expansion tank structure, the use of symmetry, superposition, and worst case loads are employed to reduce the number of calculations to be performed and yet provide a thorough analysis. Major expansion tank structural components are shown in Figure 2.6.7-30. Analysis of the expansion tank uses the same format and simplifying assumptions as were used in the neutron shield tank structural analysis.

2.6.7.8.1 Expansion Tank Shell

The expansion tank shell is analyzed as a thin-walled tube, taking no credit for the eight radial stiffeners, which run the length of the tank. Using Case 1 (Roark, page 298), the meridional and hoop stresses are calculated:

$$s_1 = \frac{pR}{2t}$$

$$= 6269 \text{ psi}$$

$$S_2 = \frac{pR}{t}$$

$$= 12,537 \text{ psi}$$

where:

p = 180 psig

R = 21.94 inches

t = 0.32 in

Von Mises yield criterion is used to calculate an equivalent stress (S_e), which is compared to the yield strength of Type 304 stainless steel.

$$S_e = \frac{1}{\sqrt{2}} \left[(S_1 - S_2)^2 + (S_2 - S_3)^2 + (S_3 - S_1)^2\right]^{0.5}$$

$$= 10,857 \text{ psi}$$

where:

S_3 = 0 psi

then

$$M.S. = \frac{S_{ALL}}{S_e} - 1 = \underline{+0.26}$$

where:

S_{ALL} = 0.577 (23,750 psi)

= 13,700 psi

2.6.7.8.2 Bottom End Plate

It is assumed that the sections of end plate between stiffeners can be represented by a rectangular plate of appropriate dimensions. The width (b) of the plate is the difference between radii of the neutron shield tank and expansion tank shells, as shown in Figure 2.6.7-31. The length (a) of the plate is the average of the inner and outer arch lengths, a = 16.4 inches ((17.3 + 15.4)/2). Using Case 36 (Roark, page 225), the maximum bending stress on the 0.5-inch thick end plate is:

$$S_{max} = \beta \frac{wb^2}{t^2}$$

$$= 3375 \text{ psi}$$

where:

β = 0.75

w = 180 psig

b = 2.5 inches

t = 0.5 in

then

$$M.S. = \frac{S_{ALL}}{S_{max}} - 1 = \underline{+LARGE}$$

where:

S_{ALL} = 23,750 psi (S_y at 250°F)

2.6.7.8.3 Stiffener

The drop load is assumed to be distributed over all stiffeners equally. It is further assumed that the stiffener examined is in tension resulting from the drop load, as shown in Figure 2.6.7-32. The analysis shown below is for a 1-inch section (longitudinal) without credit for end plate welds. The drop pressure load is L = 3,114 pounds (17.3 in^2 x 180 psi). Additionally, the stiffener must support itself and the expansion tank shell during a drop, which adds an additional 45 pounds of structural load, bringing the total load (L) on the stiffener to 3,159 pounds. The cross sectional area of the 1-inch section analyzed is 132 in^2.

$$S_T = \frac{L}{A}$$

$$= 10,029 \text{ psi}$$

The margin of safety is:

$$M.S. = \frac{S_{ALL}}{S_T} - 1 = \underline{+0.37}$$

where:

S_{ALL} = 0.577(23,750) psi

= 13,700 psi

2.6.7.8.4 Stiffener Weld

This analysis of a unit section (1-inch longitudinal) of expansion tank shell assumes that the drop load is equally distributed among all stiffeners. The load acting on the weld attaching the stiffener to the adjacent shield tank stiffener equals the load acting on the stiffener, L = 3,114 pounds (Section 2.6.7.8.3). The weld is a 0.188-inch fillet, both sides with a total throat area, A_w = 0.265 in^2. The tensile stress acting on the weld is:

$$S_T = \frac{L}{A_w}$$

$$= 11,750 \text{ psi}$$

The resulting margin of safety is:

$$M.S. = \frac{S_y}{S_T} - 1 = \underline{+0.17}$$

where:

$S_y = 0.577(23,750)$ psi

$= 13,700$ psi

2.6.7.9 Upper Ring/Outer Shell Intersection Analysis

Membrane and bending stresses are induced in the upper ring/outer shell intersection region of the cask body. These stresses are calculated using a detailed finite element model (Figure 2.6.7-33) and the ANSYS PC-Linear computer program.

The upper ring/outer shell intersection region is conservatively analyzed utilizing an axisymmetric model, axisymmetric loading and minimum ring cross section properties. The actual loading occurs only at the two lifting trunnions, and the minimum ring cross section occurs only at four 90-degree locations around the ring circumference. The model is restrained in the longitudinal direction by roller boundary conditions on the inner and outer shells (Figure 2.6.7-34) located 10 inches below the upper ring/outer shell intersection (attenuation length = 2.5 $(Rt)^{0.5}$ = 9.81 inches). A fine mesh grid is used in the model in regions where peak stresses caused by concentration effects are expected. The following assumptions are made in this analysis:

1. The stiffness and support of the lead shell are not included.
2. The support/restraint of the upper ring provided by the closure lid and bolts is not included.
3. A uniform average temperature of 300°F is used in the analysis.
4. ANSYS STIF42 isoparametric quadrilateral elements adequately represent the cask geometry.

The sections analyzed as critical are shown in Figure 2.6.7-35. Section c-c is critical for P_m stress, and section a-a is critical for $P_m + P_b$ stress.

Applied Loads

The normal operations lifting trunnion loads used in this analysis are:

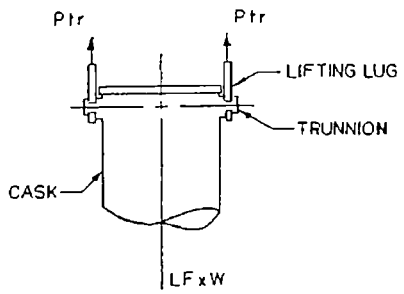

Lifting Load On Trunnions

Load Factor (LF) = 1.15

Cask Weight (W) = 52,000 lbs

P_{tr} = (LF)(W/2) = (1.15)(52,000/2) = 29,900 lbs

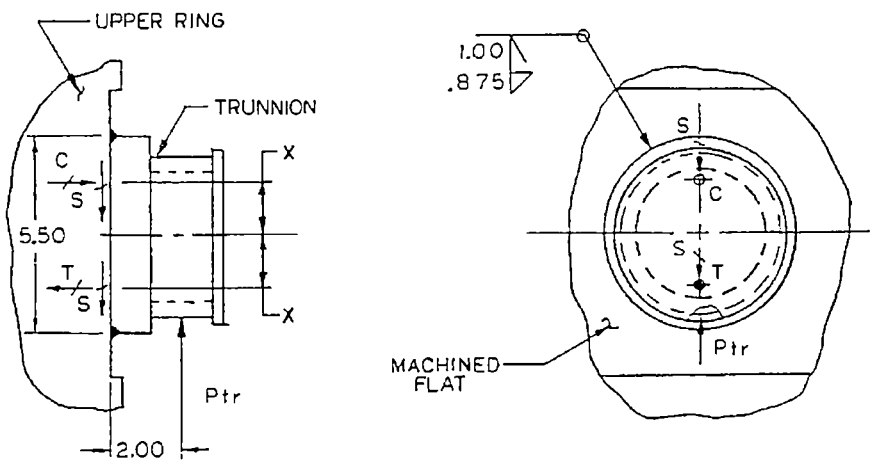

Lifting Trunnion Load Geometry

The concentrated loads were used to represent the distributed loads in the trunnion weld.

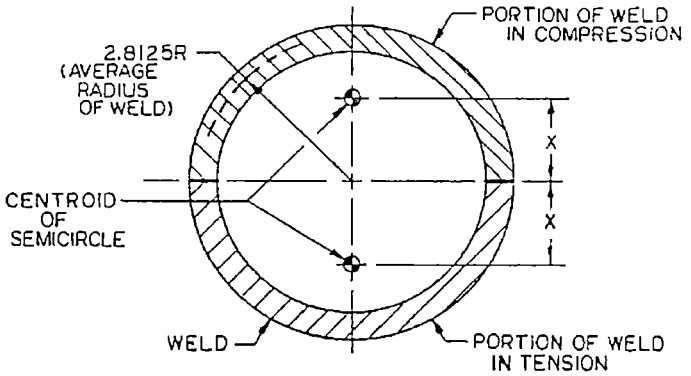

Trunnion Weld Group Centroid

To determine the trunnion weld group centroid:

$x = 0.6366\ R_{avg}$

$= 0.6366\ (2.8125)$

$= 1.790$ inches

$T = C = y\ (P_{tr}/2x)$

$= 2.00\ (29{,}900)\ /\ 2\ (2.8125)$

$= 16{,}704$ lbs

$S = P_{tr}/2$

$= 29{,}900/2$

$= 14{,}950$ lbs

Assume these loads are uniform over the trunnion weld diameter:

$T_u = C_u = 16{,}704/2(2.8125)$

$= 2969.6$ lb/in

$S_u = 14{,}950/2(2.8125)$

$= 2657.8$ lb/in

The ANSYS program requires that the loads for an axisymmetric model be input as load/radian:

Radians enclosed in 1 inch of circumference = 1/radius = 11/13.94 = 0.0717

$T_r = C_r = (2969.6)/0.0717$

= 41,396.22 lb/rad

S = 2657.8/0.0717
= 37,049.73 lb/rad

Calculated Stress Summary - Normal Operations Conditions

As anticipated, the maximum stresses occur at the upper ring/outer shell intersection, in the region of the machined flat and the internal radius of the outer shell. This analysis conservatively considers an outer shell thickness of 1.12 inches (actual shell thickness is 1.20 inches).

Stress peaking is present at the intersection of the outside surface of the outer shell with the upper ring because of stress concentration effects. The three sections through this region were investigated to determine the maximum stress intensity.

Section	Node	ANSYS Output Stress Summary			
		Radial S_x (ksi)	Axial S_y (ksi)	Hoop S_z (ksi)	Shear S_{xy} (ksi)
	66	1.6	7.3	2.9	-0.6
a-a	65	-0.1	4.9	1.9	-0.4
	64	-2.6	-0.4	-0.2	0.8
	66	1.6	7.3	2.9	-0.6
b-b	61	-0.7	5.1	1.6	0.5
	56	1.1	1.8	0.6	0.6
	66	1.6	7.3	2.9	-0.6
c-c	61	-0.7	5.1	1.6	0.5
	56	-0.2	4.5	0.6	0.6

The P_m and the $P_m + P_b$ stress components are determined by linearization of the ANSYS output stress components across sections a-a, b-b, and c-c. The principal stresses are calculated using the classical stress transformation law (Table 2.6.7-41).

The total normal operations lifting condition component stresses, principal stresses, and stress intensities at the critical section are calculated by combining the principal stresses from lifting, section b-b, with the internal pressure hot case (Table 2.6.1-1 and Table 2.6.2-2).

The P_m principal stress summary is:

Load Condition	Principal Stresses (ksi)		
	S_1	S_2	S_3
Lifting	5.5	-0.3	2.0
Internal Pressure	2.9	0.4	-0.4
Total	8.4	0.1	1.6

P_m stress differences are: S_{12} = 8.3 ksi, S_{23} = -1.5 ksi, and S_{31} = -6.8 ksi.
P_m stress intensity is S_i = 8.3 ksi.
Allowable stress intensity is S_a = 1.0 S_m = 20.0 ksi (Table 2.3.1-1).

$$M.S. = \frac{S_a}{S_i} - 1 = \underline{+1.41}$$

The $P_m + P_b$ principal stress summary is:

Load Condition	Principal Stresses (ksi)		
	S_1	S_2	S_3
Lifting	9.1	-2.7	4.0
Internal Pressure	4.2	1.5	0.2
Total	13.3	-1.2	4.2

The $P_m + P_b$ stress differences are: S_{12} = 14.5 ksi, S_{23} = -5.4 ksi, and S_{31} = -9.1 ksi.
The $P_m + P_b$ stress intensity is S_i = 14.5 ksi.
Allowable stress intensity is S_a = 1.5 S_m = 30.0 ksi.

$$M.S. = \frac{S_a}{S_i} - 1 = \underline{+1.07}.$$

The maximum peak stress, S_y = 7.3 ksi, is less than 1.5 S_m; therefore, a fatigue evaluation is not required.

2.6.7.10 PWR/BWR Rod Transport Canister Assembly Analysis

2.6.7.10.1 Discussion

The NAC-LWT PWR/BWR Rod Transport Canister is analyzed for structural adequacy in accordance with the requirements of 10 CFR 71 for a 1-foot drop (normal transport condition). The structural evaluation is performed by classical elastic analysis methods. The components

evaluated include the can weldment, internal spacer, 4 × 4 and 5 × 5 inserts (rod holder), PWR insert, BWR fuel assembly lattice spacer and can weldment spacer. In the 5×5 insert configuration, four of the tubes comprising the insert may be replaced with a single larger tube to accommodate an oversize nonfuel-bearing component (e.g., a single BWR water rod or a CE guide tube). Evaluations are performed for the inserts being comprised of 16 or 25 tubes to accommodate the fuel rods and these evaluations are considered to bound the insert configuration containing a single BWR water rod. The presence of the BWR water rod reduces the inertial loading due to contents, as well as employs a larger cross-section for the BWR water rod as compared to four smaller tubes containing fuel rods.

2.6.7.10.2 Analysis Description

Geometry

The geometry of the can assembly is shown in Drawing 315-40-098. Note that the tube component of the can assembly is fabricated from a 6-in.×6-in.×0.5-in.-thick tube that is machined to the final dimensions of 5.5-in.×5.5-in.×0.25-in.-thick. The can assembly is positioned within the basket during transport of the cask. If the cask is equipped with a PWR basket, the PWR insert is required to provide correct positioning within the basket. The can assembly is constructed of Type 304 stainless steel with the exception of the PWR insert, which is constructed of 6061 Aluminum.

Loadings

The magnitude of the impact force varies according to the drop height and drop orientation. As calculated in Section 2.6.7.4, the g-loads for the 1-foot end and side drops are 15.8 and 24.3g, respectively.

Detailed Analysis

The maximum temperatures of the components are shown below. For the can weldment and components outside the can weldment, the temperatures are significantly below 700°F, which are within the 800°F design limits. For the tubes supporting the fuel pins, the maximum temperatures are determined to be 925°F. The tubes, which are only used with the insert for the high burnup pins, are shown to be acceptable using ASME Code, Section III, Division I, Subsection NH, which specifies allowable stresses above 800°F. The remaining components are shown to be acceptable using the stress allowable in ASME Code, Section III, Subsection NB.

Thermal Stresses

To evaluate effects of the calculated temperatures within the can assembly, the nominal dimensions of the can are used to calculate the resulting thermal expansions. The coefficient of thermal expansion for ASME SA 240 Type 304 stainless steel is 9.0×10^{-6} in./in.-°F. All

components of the can assembly are constructed of Type 304 stainless steel, except for the PWR insert. The PWR insert is made of 6061 Aluminum with a coefficient of thermal expansion of 13.5E-6 in/in-°F. The following temperatures are used in the thermal expansion calculation and material property definitions.

Component Name	Maximum Operating Temperature (°F)	Temperature Used for Calculation (°F)
Aluminum PWR Insert	394	400
Can Weldment	538	575
5 × 5 Insert	885	925

Since the 5 × 5 insert is larger than the 4 × 4 insert, it is bounding for the thermal expansion calculations. The nominal gap between the insert and internal spacer is 3.56 – 3.44 = 0.12 inch. The growth of the insert is 3.44 × 9.0 E-6 in/in-°F × (925-70)°F = 0.027 inch. Since the growth of the insert is less than the nominal gap, no interference will occur.

The nominal gap between the internal spacer and can shell is 5.0 – 4.94 = 0.06 inch. The growth of the internal spacer is 4.94 × 9.0 E-6 in/in-°F × (575-70)°F = 0.023 inch. Since the growth of the internal spacer is less than the nominal gap, no interference will occur.

The nominal gap between the can shell and PWR insert is 5.75 – 5.5 = 0.25 inch. The growth of the can shell is 5.5 × 9.0 E-6 in/in-°F × (575-70)°F = 0.025 inch. Since the growth of the can shell is less than the nominal gap, no interference will occur.

Because the differential thermal expansion causes no interference or binding, no further thermal stress evaluation is required.

Can Weldment

The can weldment is contained within the basket assembly and not subjected to bending stresses in the side-drop case.

For the end drop, the can weldment is loaded by its own weight. The can contents bear against the bottom or top of the can assembly, depending on drop orientation.

LWT Can Body Compressive Stress

Under normal operating conditions the tube is evaluated for a 15.8 g acceleration for the end drop. The compressive load (P) on the tube is the combined weight of the lid and tube times the appropriate g factor.

The compressive stress (S_c) in the tube body is:

$$S_c = \frac{P}{A} = \frac{4{,}898 \text{ lb}}{4.98 \text{ in}^2} \cong 984 \text{ psi}$$

where:

$A = \pi (0.75^2 - 0.5^2) + 4 \times 4.0 \times 0.25 = 4.98 \text{ in}^2$

$P = 310 \times 15.8 = 4{,}898$ lbs (conservatively, the weight of the tube, lid, and bottom plate is used)

The margin of safety (MS) is then:

$$MS = \frac{S_m}{S_c} - 1 = \frac{17{,}300 \text{ psi}}{984 \text{ psi}} - 1 = +16.6.$$

LWT Can Body Bearing Stress

For the bottom end drop, the can base feet are subjected to a bearing stress. The compressive load (P) on the base is the combined weight of the can assembly, fuel and insert, and the internal spacer times the appropriate g factor.

$P = [310 \text{ (can weldment)} + 350 \text{ (fuel)} + 75 \text{ (tube insert)} + 240 \text{ (internal spacer)}] \times 15.8 = 15{,}405$ lbs

The compressive stress (S_c) in the feet is:

$$S_c = \frac{P}{A} = \frac{15{,}405}{2.8} \cong 5{,}502 \text{ psi}$$

where:

$A = 4 \text{ x } 0.5 \text{ x } (2.0 - 0.6) = 2.8 \text{ in}^2$

The margin of safety (MS) for bearing is then:

$$MS = \frac{S_m}{S_c} - 1 = \frac{17{,}300 \text{ psi}}{5{,}502 \text{ psi}} - 1 = +2.14$$

Can Internal Pressure

Can weldment internal pressure is considered insignificant in the end-drop and side-drop cases because it will tend to reduce the compressive loads on the can tube sides.

The effect of internal pressure is evaluated for the bending stress that the pressure imposes on the can weldment sides. Conservatively, a one-inch-wide section of the tube wall, equal in length to the outside dimension of the tube (L = 5.5 in.) is analyzed as a cantilevered beam with a uniform load.

The maximum moment (M) is determined by the following relation:

$$M = \frac{wL^2}{12} = \frac{(85 - 14.7)(5.5^2)}{12} \cong 177.2 \text{ in.-lb}$$

where w is the maximum differential pressure across the can wall due to the maximum normal temperature (assumes that the cask internal pressure is atmospheric). The 85 psia envelopes the pressure reported in Section 3.4.4.2.

The combined stress (σ) in the 0.25-inch thick tube wall is:

$$\sigma = \frac{Mc}{I} + \frac{wL}{t}$$

$$= \frac{(177.2)(0.125)}{0.0013} + \frac{(85 - 14.7)(5.5)}{0.25} \cong 18{,}600 \text{ psi}$$

The margin of safety (MS) is:

$$MS = \frac{1.5 S_m}{\sigma} - 1 = \frac{25.35 \text{ ksi}}{18.6 \text{ ksi}} - 1 = +0.36 \text{ for the normal condition}$$

Can Lid Bolt Analysis

The tensile force (F_p) on each lid bolt due to internal pressure is:

$$F_p = \frac{PA}{n} = \frac{(85 - 14.7)(3.75^2)}{8} \cong 123.6 \text{ lbs}$$

where

P = the pressure differential across the can wall at maximum normal temperature (assumes cask internal pressure is atmospheric)

A = 3.75 in × 3.75 in, the area of the can lid exposed to pressure

n = 8, number of bolts

The total tensile force on each lid bolt is F_p + the initial preload force, F_i = 635 lbs

The lid bolt tensile stress (σ) is:

$$\sigma = \frac{F_p + F_i}{A_t} = \frac{758.6}{0.049} = 15{,}480 \text{ psi}$$

where

A_t = 0.049 in.^{2}, the bolt tensile stress area $\frac{\pi}{4}(0.25^2)$

The margin of safety (MS) for the normal condition is:

$$MS = \frac{S_y}{\sigma} - 1 = \frac{18.8 \text{ ksi}}{15.48 \text{ ksi}} - 1 = +0.21$$

Can Tube Buckling

The tube is evaluated, using the Euler formula, to determine the critical buckling load (P_{cr}):

$$P_{cr} = \frac{K\pi^2 EI}{L^2} = \frac{3.26\pi^2(24.4\times10^6)(24.2)}{(165.5)^2} = 0.698 \times 10^6 \text{ lbs}$$

where:

$E = 24.4 \times 10^6$ psi at 750°F

$$I = \frac{5.5^4 - 5.0^4}{12} = 24.2 \text{ in}^4$$

L = tube body length (165.5 inches)

Because the maximum compressive load (310 × 15.8 = 4,898 lbs) is much less than the critical buckling load (698×10^3 lbs), the tube has adequate resistance to buckling.

Internal Spacer

The internal spacer body is contained within the can assembly and not subjected to bending in the side drop condition.

The compressive stress in the internal spacer rails during the side drop is determined as follows:

$$\sigma_b = \frac{Wg}{A} = \frac{665 \text{ x } 24.3}{123.7} \cong 130.6 \text{ psi}$$

where:

W = total load = 350 (fuel) + 240 (internal spacer) + 75 (4x4 insert) = 665 lbs

g = 24.3 (normal condition side drop)

A = 123.7 in^2 cross-sectional area of spacer rails, 4 × 0.188 × (165.25 – 2 × 0.38)

The resulting margin of safety is large.

Internal Spacer Compressive Stress

For the end drop, the internal spacer shell is loaded by its own weight. The insert rail stiffness is conservatively neglected in the strength.

Under normal operating conditions, the spacer is evaluated for a 15.8 g acceleration. The compressive load (P) on the shell is due to the weight of the internal spacer. The entire weight of the internal spacer times the appropriate g factor will be used to calculate the compressive load.

P = 240 × 15.8 = 3,792 lbs

The compressive stress (S_c) in the internal spacer body is:

$$S_c = \frac{P}{A} = \frac{3{,}792}{1.69} \cong 2{,}244 \text{ psi}$$

where:

$A = (3.936^2 - 3.56^2) - 12 \times 0.5 \times 0.188 = 1.69 \text{ in}^2$

The margin of safety (MS) is then:

$$MS = \frac{S_m}{S_c} - 1 = \frac{17{,}300}{2{,}244} - 1 = +6.71$$

Internal Spacer Buckling

The shell is evaluated, using the Euler formula for an axially distributed load, to determine the critical buckling load (P_{cr}):

$$P_{cr} = \frac{K\pi^2 EI}{L^2} = \frac{3.26\pi^2(24.4\times10^6)(6.615)}{(165.25)^2} = 0.19 \times 10^6 \text{ lbs}$$

where:

$E = 24.4 \times 10^6$ psi at 750°F

$I = \frac{3.936^4 - 3.56^4}{12} = 6.615 \text{ in}^4$

L = spacer body length (165.25 inches)

Because the maximum compressive load (240×15.8 = 3,792 lbs) is much less than the critical buckling load (190×10^3 lbs), the internal spacer has adequate resistance to buckling.

4×4 and 5×5 Inserts

The 4×4 and 5×5 inserts are contained within the internal spacer. The 4×4 inserts are supported by straps on 10-inch spacing. These straps provide a clearance of 0.31 inches and will allow bending of the tubes to occur. The 5×5 insert tubes are evaluated for a diametrically opposed load due to the weight of the adjacent tubes during the side drop.

The 4×4 insert lower tube will be evaluated as a fixed-fixed beam over a 10-inch span. The weight of the 3 tubes above (as well as lower tube self-weight) will be considered in the analysis. The stiffness of the tubes above the lower tube will conservatively be neglected. The combined weight (P) of the fuel pins and insert tubes are considered as a uniformly distributed load over the 10-inch span. In addition, the weights are scaled by the appropriate deceleration factor depending on the drop orientation and condition being evaluated.

The maximum bending stress (f_b) is determined as follows:

$$f_b = \frac{Wlg}{12Z} = \frac{5.8(10.0)24.3}{12x0.0092} \cong 12{,}766 \text{ psi}$$

where:

W = load on 10-inch section = (14 + 9.5) x 4 x 10/163.0 = 5.8 lbs

l = 10 inches (span of tube)

g = 24.3 (normal condition side drop)

Z = $\pi/32\ (0.6875^4\text{-}0.6315^4)\ /\ 0.6875 = 0.0092\ \text{in}^3$ (section modulus of the tube)

The margin of safety (MS) is:

$$MS = \frac{1.5S_m}{\sigma_{max}} - 1 = \frac{1.5(12{,}050)}{12{,}766} - 1 = +0.42$$

The bending moment due to the diametrically opposed line load on the 5×5 insert is calculated by the following:

$$M_b = \frac{WRg}{\pi} = \frac{70/163.0 \text{ x } 0.344 \text{ x } 24.3}{\pi} \cong 1.143 \text{ lb} - \text{in}$$

where:

W = total load = 14 × 4 + 70/5 = 70 lbs

g = 24.3 (normal condition side drop)

R = 0.6875/2 = 0.344 in (radius of insert tube)

The resulting bending stress is:

$$f_b = \frac{6M_b}{t^2} = \frac{6 \text{ x } 1.143}{0.028^2} \cong 8{,}745 \text{ psi}$$

The margin of safety (MS) is:

$$MS = \frac{1.5\ S_m}{\sigma_{max}} - 1 = \frac{1.5(12{,}050)}{8{,}745} - 1 = +1.07$$

<u>4×4 and 5×5 Insert Tube Compressive Stress</u>

Under normal operating conditions, the tube is evaluated for a 15.8 g acceleration. The compressive load (P) on the shell is due to the weight of the tube. The entire weight of the tube is calculated as:

P = $\pi/4\ (0.6875^2\text{-}0.6315^2)$ x 163.0 x 0.288 = 2.72 lbs

The compressive stress (S_c) in the tube body is:

$$S_c = \frac{P}{A} = \frac{2.72 \text{ x}15.8}{0.058} \cong 741 \text{ psi}$$

where:

$A = \pi/4\ (0.6875^2 - 0.6315^2) = 0.058 \text{ in}^2$

The margin of safety (MS) is then:

$$MS = \frac{S_m}{S_c} - 1 = \frac{14{,}100}{741} - 1 = +18.0$$

PWR Insert

The PWR insert contains the can assembly for insertion into the PWR basket. The PWR insert comprises a square box section with smooth sides. Therefore, no bending stresses will be introduced in the side drop condition.

PWR Insert Bearing Stress

The bearing load (P) on the PWR insert is due to the weight of the loaded can assembly. The entire weight of the assembly times the appropriate g factor will conservatively be used to calculate the bearing load.

W = bearing load = [350 (fuel) + 310 (can) + 240 (internal spacer) + 75 (4x4 insert)] x 24.3 = 23,693 lbs

The compressive stress (S_c) in the tube body is:

$$S_c = \frac{P}{A} = \frac{23{,}693}{921.3} \cong 26 \text{psi}$$

where:

$A = 5.5 \times 167.5 = 921.3 \text{ in}^2$

The margin of safety (MS) is then:

$$MS = \frac{S_y}{S_c} - 1 = \frac{23{,}500}{26} - 1 = +\text{Large}$$

PWR Insert Body Compressive Stress

Under normal operating conditions, the tube is evaluated for a 15.8 g acceleration. The compressive load (P) on the body is due to the weight of the PWR insert. The entire weight of the PWR insert, times the appropriate g factor, will conservatively be used to calculate the compressive load.

$P = 650 \text{ lb} \times 15.8 = 10{,}270 \text{ lbs}$

The compressive stress (S_c) in the tube body is:

$$S_c = \frac{P}{A} = \frac{10{,}270}{39.2} \cong 262 \text{ psi}$$

where:

$$A = (8.5^2 - 5.75^2) = 39.2 \text{ in}^2$$

The margin of safety (MS) is then:

$$MS = \frac{S_y}{S_c} - 1 = \frac{23{,}500}{262} - 1 = +\text{Large}$$

PWR Insert Tube Buckling

The tube is evaluated, using the Euler formula, to determine the critical buckling load (P_{cr}):

$$P_{cr} = \frac{K\pi^2 EI}{L^2} = \frac{3.26\pi^2\left(8.8\text{x}10^6\right)\left(343.9\right)}{\left(167.0\right)^2} = 3.86\times10^6 \text{ lbs}$$

where:

$E = 8.8\times10^6$ psi at 400°F

$I = \frac{8.5^4 - 5.75^4}{12} = 343.9 \text{ in}^4$

L = tube body length (167.0 inches)

Because the maximum compressive load (650 x 15.8 = 10,270 lbs) is much less than the critical buckling load (3.86×10^6 lbs), the PWR insert has adequate resistance to buckling.

PWR Insert Assembly Bolts

The PWR insert is comprised of four short and four long aluminum plates joined with ½-13 UNC × 1.5-in. long socket head cap screws to form a hollow box. Each plate is secured to each adjacent plate using three screws.

The screws joining the plates are loaded in shear when the two lift tabs are used to lift the PWR insert and its payload. The controlling load path is through the lift tab attached to the shorter side plate and the three screws connecting the shorter side plate to the adjacent long plate. The distance from the line of load application (centerline of the lift tab) to the centerline of the 3-screw pattern is approximately 3.6 inches. Any internal moment created by this eccentricity is reacted by the strong-direction section modulus of the side plates and is effectively countered by the stiffness inherent in the overall symmetry of the box section. The screw shear stress (τ) in each of the 3 screws is:

$$\tau = \frac{P/2}{A} = \frac{900}{3(0.130)} = 2{,}308 \text{ psi}$$

where:

P = [310 (can weldment)+350 (fuel rods)+240 (internal spacer)+70 (5×5 insert)+650 (PWR insert)]×1.1 = 1,782 lbs, use 1,800 lbs for analysis. (Total lift weight with 10% dynamic load factor.)

A = screw cross-sectional area = $(0.4069^2 \times \pi)/4 = 0.130 \text{ in}^2$ (Thread minor diameter)

The safety factor (FS) is calculated using a shear allowable of $0.6S_m$ at 750°F.

$$FS = \frac{0.6(15{,}600)}{2{,}308} = 4.06 > 3$$

where

S_m = 15,600 psi for commercial austenitic stainless steel.

Therefore the design condition that lifting stresses have a load factor of 3 on the basis of yield strength is met.

Can Weldment Spacer

The can weldment spacer prevents the PWR basket, PWR insert, fuel, and can weldment from shifting during transport. The spacer (Drawing 315-40-125, Item 10) is placed on the top of the can weldment. The spacer is bolted to the bottom side of the lid and the cruciform stiffener functions as the spacer between the lid and can weldment. The maximum load applied to the spacer occurs during the top end drop. To bound both normal and accident conditions, stresses are compared using accident load conditions and are compared to allowable stresses for normal operating conditions. The stress in the spacer is:

$$\sigma = \frac{P \times g}{A} = \frac{1{,}945 \times 60}{8.4} = 13{,}893 \text{ psi}$$

where:

P= Conservative weight of the PWR basket, PWR insert, fuel, and can weldment

= 1,945 lbs

g= Top end drop acceleration (60g)

A= Cross-sectional area of cruciform

$= 2 \times 7 \times 0.63 - 0.63^2 = 8.4 \text{ in}^2$

The margin of safety (MS) is:

$$MS = \frac{1.0 \times S_m}{\sigma} - 1 = \frac{17{,}500 \text{ psi}}{13{,}893 \text{ psi}} - 1 = +0.26$$

where:

S_m = The stress intensity of 304 stainless steel at 500°F

Because the height-to-diameter ratio (4.5/6.0 = 0.75) is less than one, the spacer has adequate resistance to buckling.

Using a bounding weight of 50.0 lbs for the spacer, the maximum shear stress on the 1/8-inch fillet weld corresponds to the hypothetical accident bottom end drop condition of 60g. The shear stress in the weld is computed as:

$$\tau = \frac{60 \times 50}{28.0 \times 0.707 \times 0.125} = 1{,}212 \text{psi}$$

where:

the perimeter of cruciform is 28.0 in [(7-0.625) × 4 + 0.625 × 4]

The margin of safety, based on the normal conditions of transport allowable stress, is:

$$MS = \frac{0.6S_m}{\tau} - 1 = \frac{0.6 \times 17{,}500}{1{,}212} - 1 = +7.66$$

The can weldment spacer is, therefore, determined to be structurally adequate for normal and accident conditions for the NAC-LWT cask.

Fuel Assembly Lattice Spacer

The BWR fuel assembly lattice fits into the PWR insert in place of the can assembly. The fuel assembly lattice holds up to 25 intact BWR fuel rods. To accommodate the fuel assembly lattice, the bottom plate of the PWR insert is removed. This allows the fuel assembly lattice to rest on the bottom of the cask. To prevent the PWR basket from shifting during transport, a spacer (Drawing 315-40-125, Item 12) is placed at the top of the fuel assembly lattice. The spacer is bolted to the bottom side of the lid and eight 1-inch diameter posts function as the spacer between the lid and PWR basket. The maximum load applied to the spacer occurs during the top end drop. To bound both normal and accident conditions, accident stresses are compared to the normal allowable stress. The stress in the spacer is:

$$\sigma = \frac{P \times g}{A \times Np} = \frac{400 \times 60}{0.785 \times 8} = 3{,}822 \text{ psi}$$

where:

P= Conservative weight of the PWR basket

g= Top end drop acceleration (Table 2.6.7-34)

A= Cross-sectional area of a post

Np = Number of posts

The margin of safety is:

$$MS = \frac{1.0 \times S_m}{\sigma} - 1 = \frac{17{,}500 \text{ psi}}{3{,}822 \text{ psi}} - 1 = +3.58$$

where:

S_m = The stress intensity of 304 stainless steel at 500°F

Buckling of the post is evaluated using the Euler formula. The critical buckling load (P_{cr}) is:

$$P_{cr} = \frac{K\pi^2 EI}{L^2} = \frac{0.25\pi^2(25.8 \times 10^6)(0.0491)}{(13.4)^2} = 17{,}407 \text{ lbs}$$

where:

E = Modulus of elasticity = 25.8×10^6 psi at 500°F

I = Moment of inertia $= \frac{\pi \times d^4}{64} = 0.0491 \text{ in}^4$

d = Post diameter = 1 in

L = Post length = 13.38 inches

K = Euler buckling coefficient for fixed-free column = 0.25 (Marks, 9th Ed., p. 5-42)

Because the maximum compressive load (400/8 × 60 = 3,000 lbs) is less than the critical buckling load (17,407 lbs), the spacer has adequate resistance to buckling.

Figure 2.6.7-1 1-Foot Bottom End Drop with 130°F Ambient Temperature and Maximum Decay Heat Load

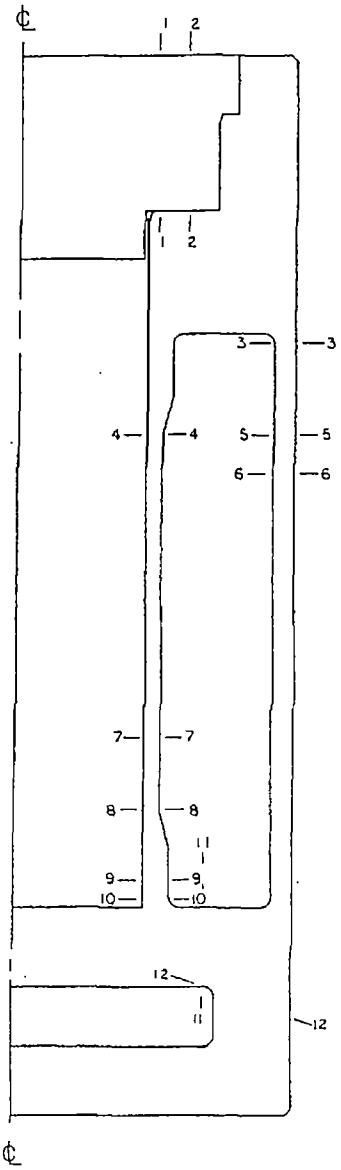

Figure 2.6.7-2 1-Foot Bottom End Drop with -40°F Ambient Temperature and Maximum Decay Heat Load

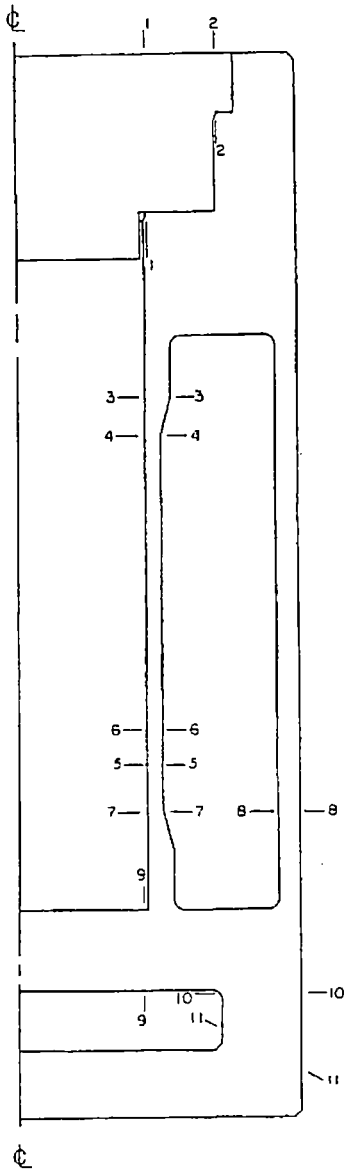

Figure 2.6.7-3 1-Foot Bottom End Drop with -40°F Ambient Temperature and No Decay Heat Load

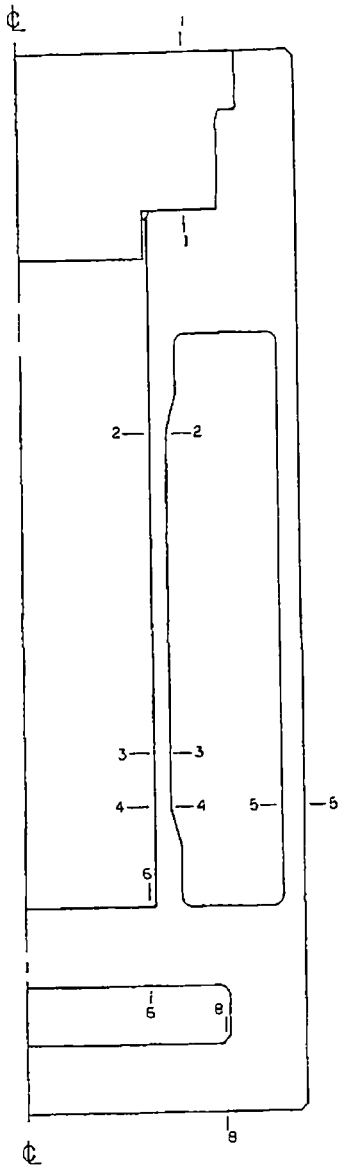

Figure 2.6.7-4 1-Foot Top End Drop with 130°F Ambient Temperature and Maximum Decay Heat Load

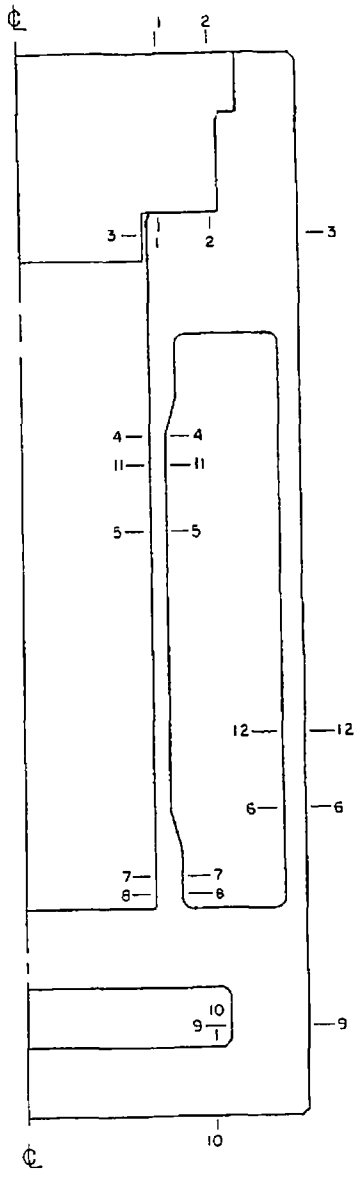

Figure 2.6.7-5 1-Foot Top End Drop with -40°F Ambient Temperature and Maximum Decay Heat Load

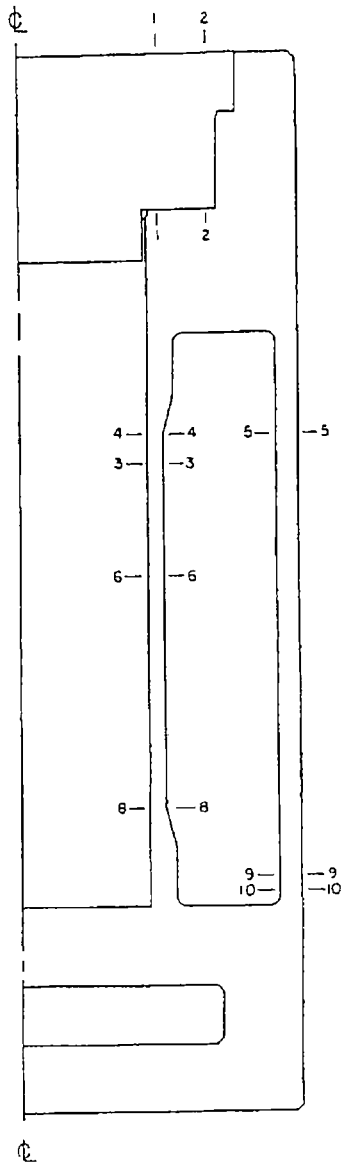

Figure 2.6.7-6 NAC-LWT Cask Critical Sections (1-Foot Side Drop with 100°F Ambient Temperature)

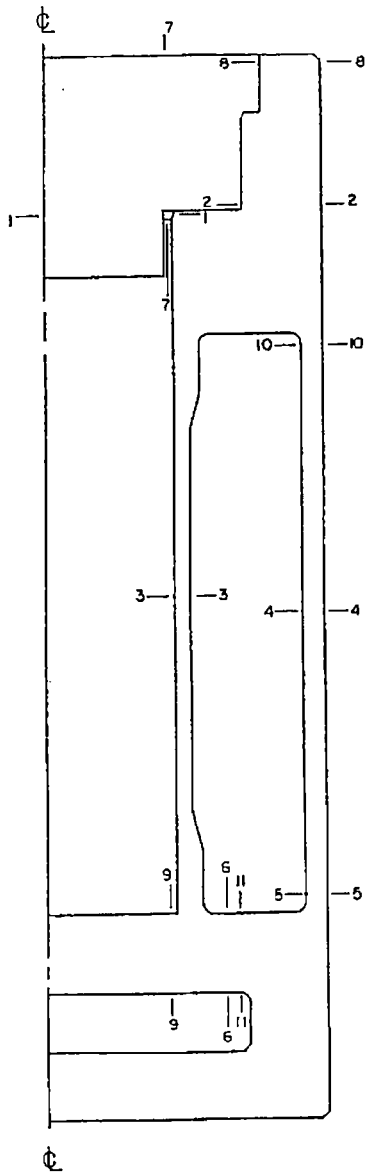

Figure 2.6.7-7 1-Foot Top Corner Drop with 130°F Ambient Temperature and Maximum Decay Heat Load - Drop Orientation = 15.74 Degrees

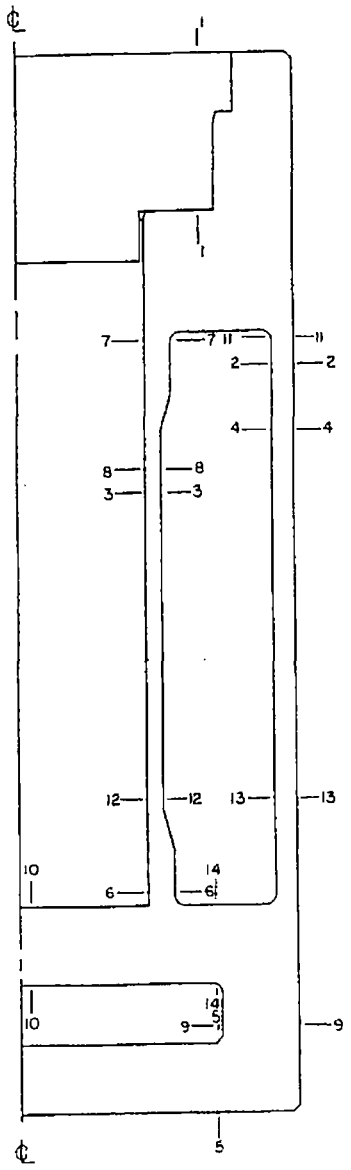

Figure 2.6.7-8 1-Foot Bottom Corner Drop with 130°F Ambient Temperature and Maximum Decay Heat Load - Drop Orientation = 15.74 Degrees

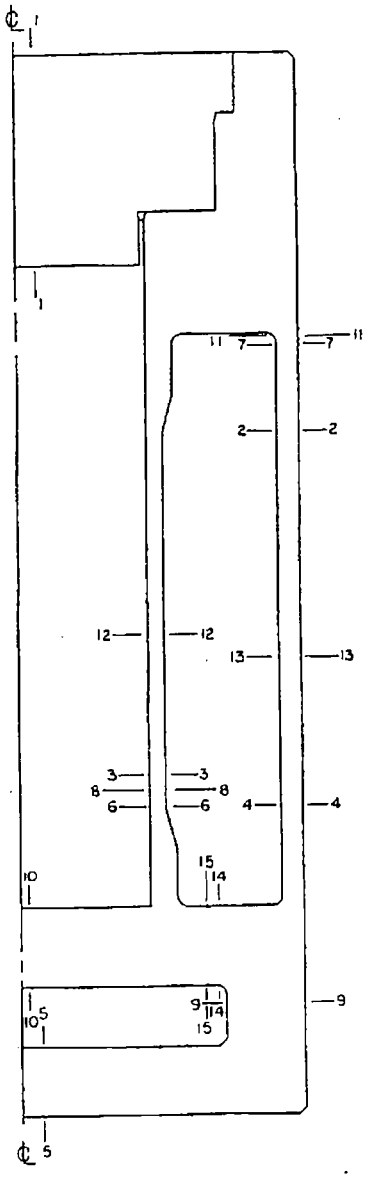

Figure 2.6.7-9 1-Foot Top Corner Drop with -40°F Ambient Temperature and No Decay Heat Load – Drop Orientation = 15.74 Degrees

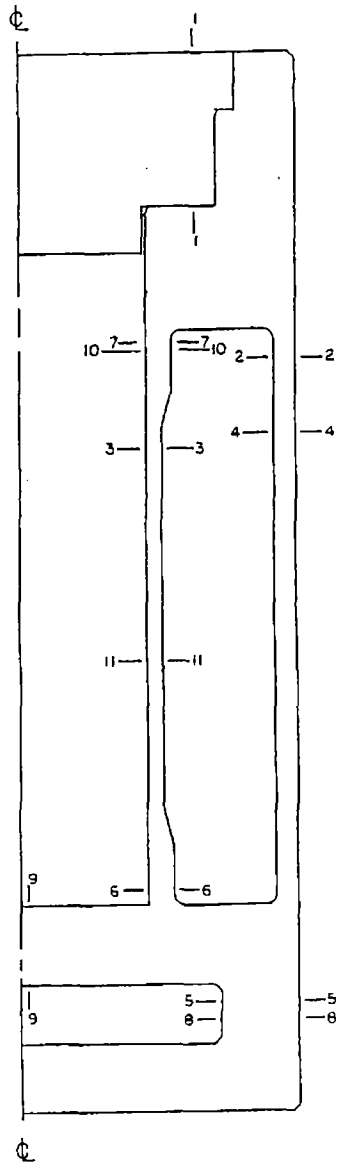

Figure 2.6.7-10 NAC-LWT Cask with Impact Limiters

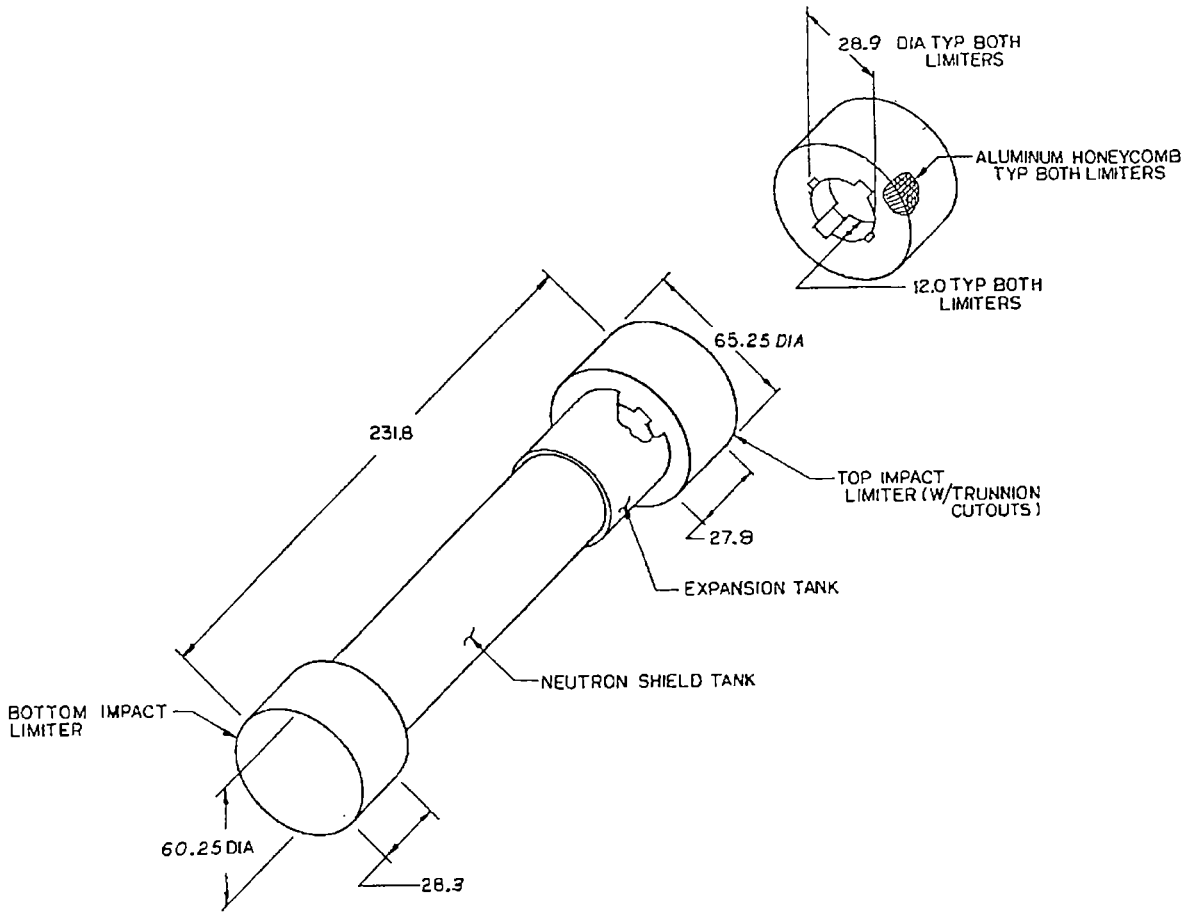

Figure 2.6.7-11 Cross-Section of Top Impact Limiter

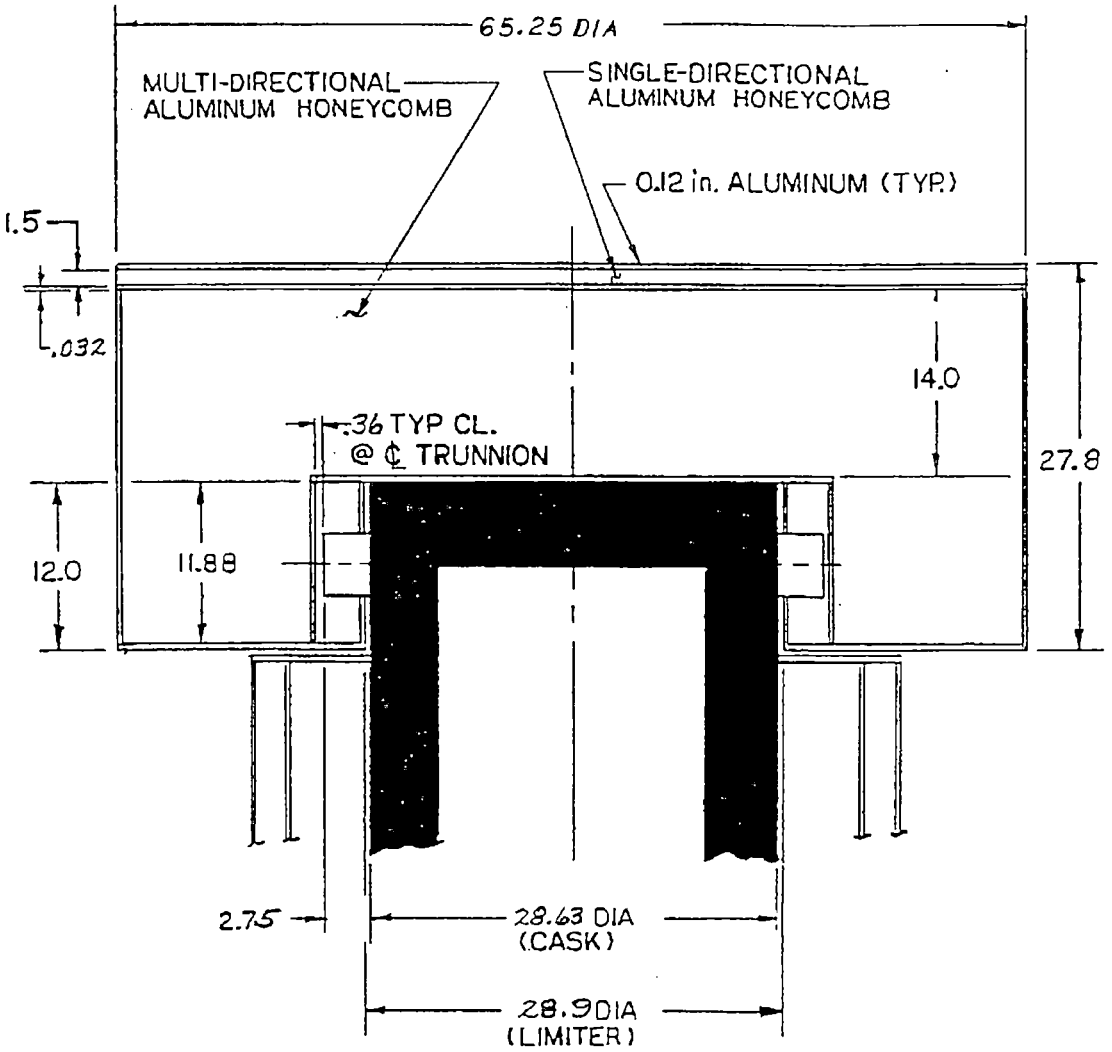

Figure 2.6.7-12 Load Versus Deflection Curve (Typical Aluminum Honeycomb)

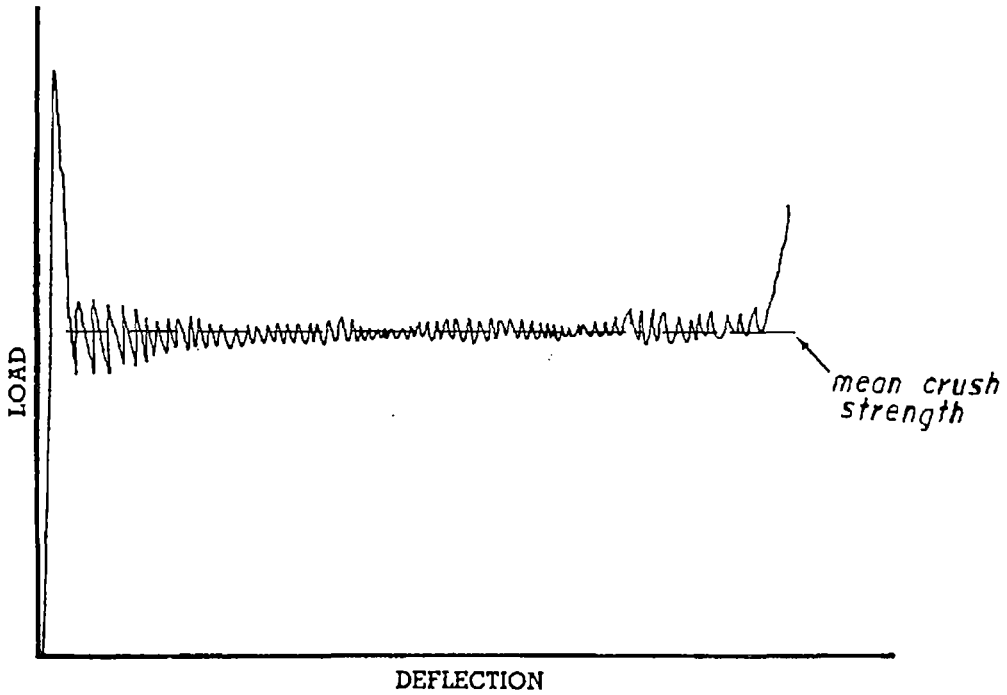

Figure 2.6.7-13 Quarter-Scale Model Limiter End Drop Cross-Section

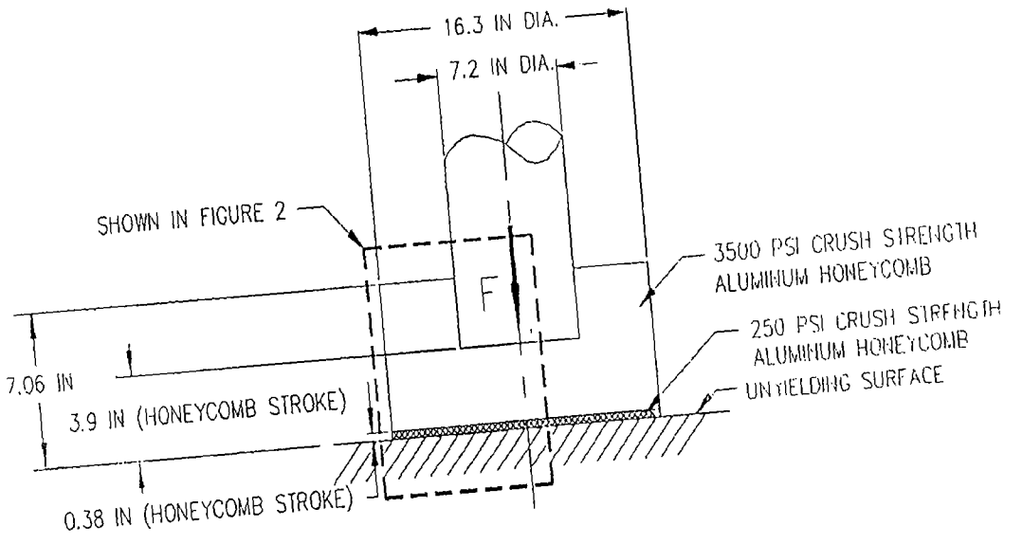

Figure 2.6.7-14 End Drop Impact Limiter Cross-Section

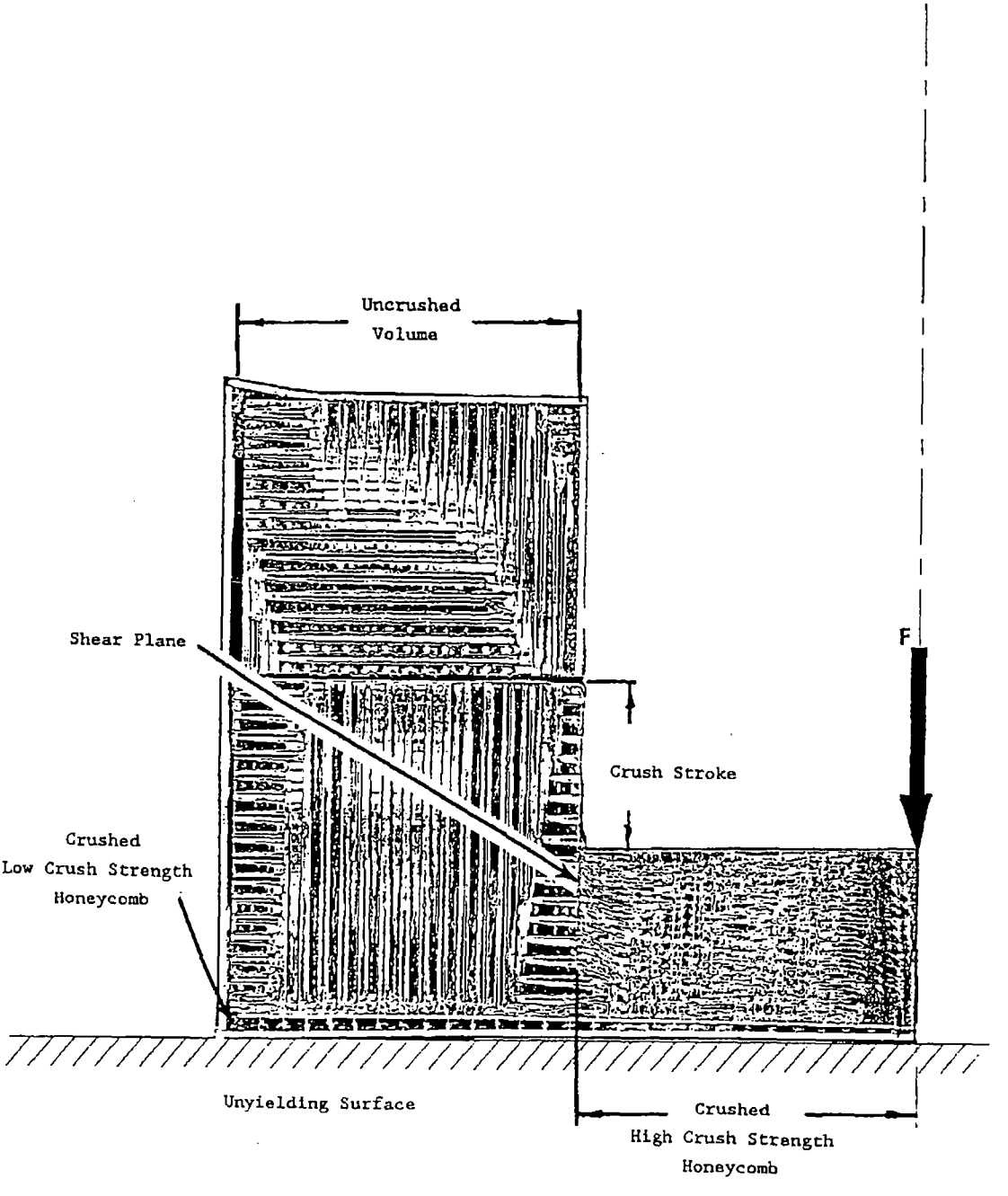

Figure 2.6.7-15 Impact Limiter Lug Detail

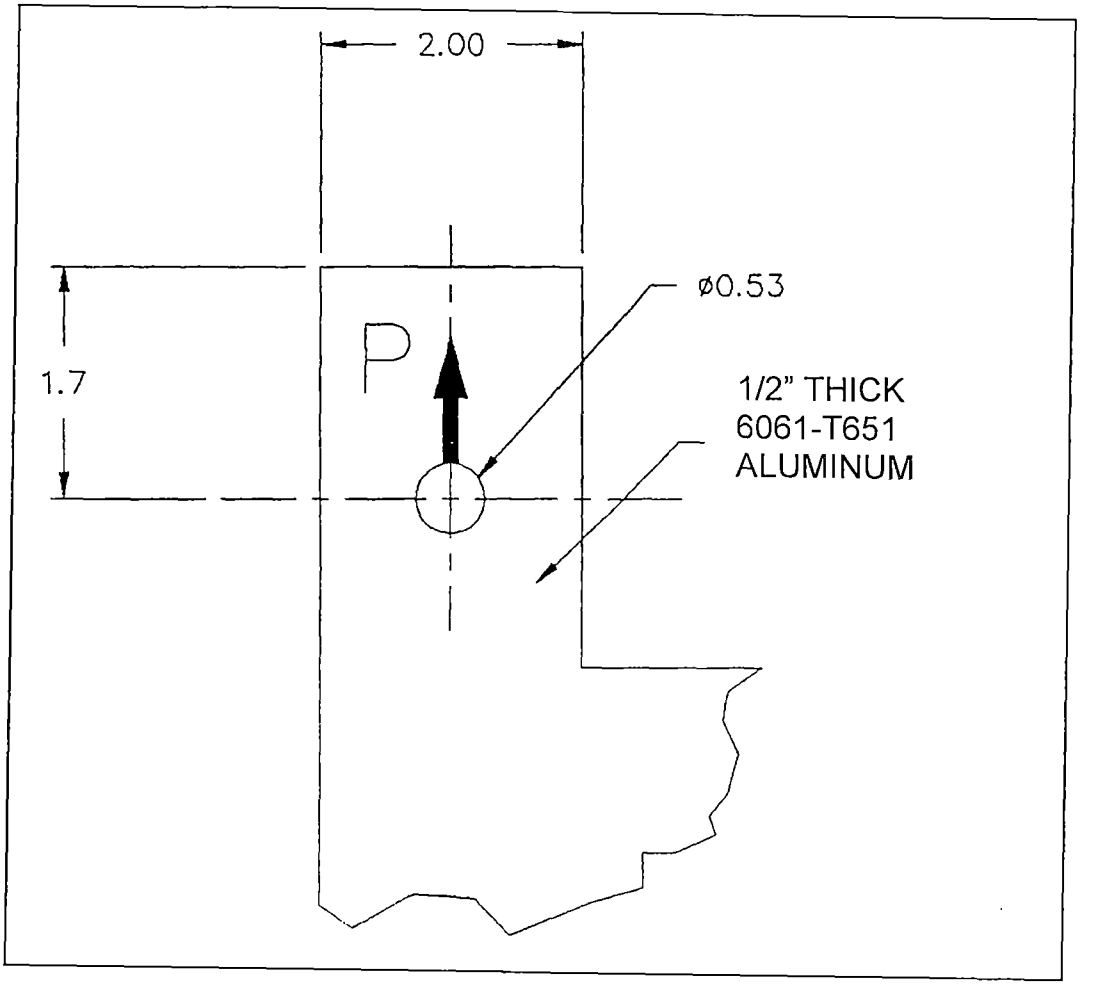

Figure 2.6.7-16 Cask Lug Detail

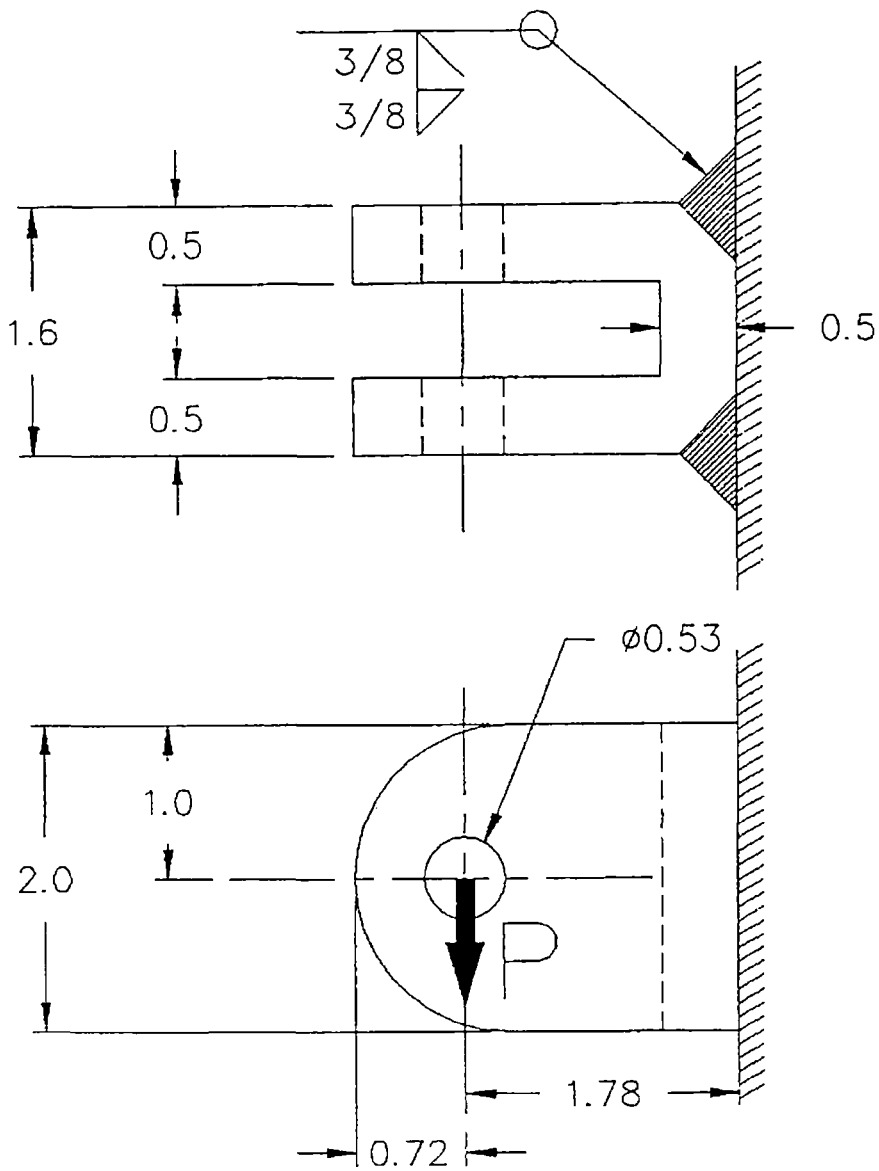

Figure 2.6.7-17 RBCUBED Output Summary – Center of Gravity Over Top Corner

Position	Crush Depth (in)	Crush Force, F_i (lb)	Package Velocity (in/sec)	Approximate Separation Moment (in-lb)
1	2	2.30×10^5	543.4	2.25×10^6
2	4	9.74×10^5	514.8	6.63×10^6
3	6	1.83×10^6	466.2	7.67×10^6
4	8	2.63×10^6	381.2	5.75×10^6

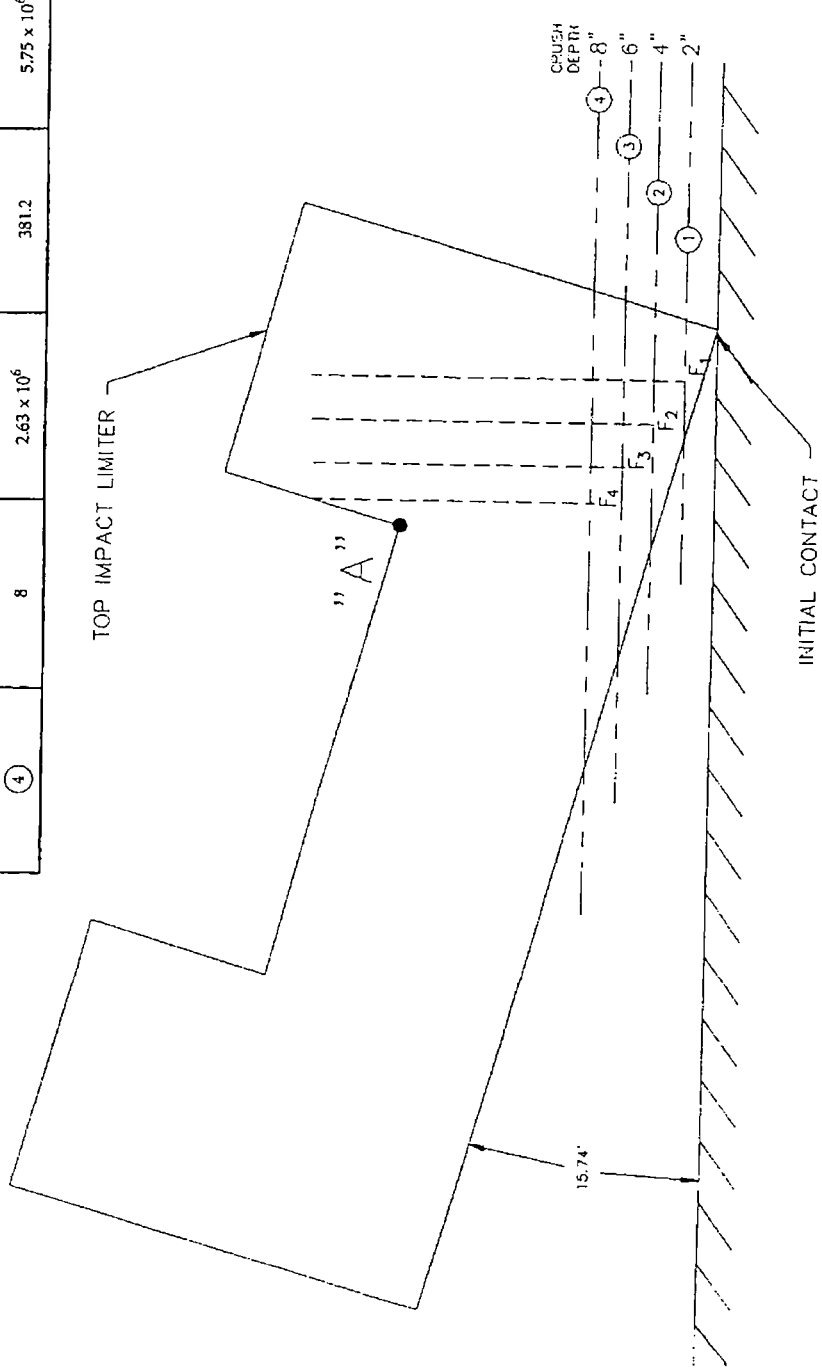

Figure 2.6.7-18 Free Body Diagram – Top Impact Limiter – Center of Gravity Over Corner

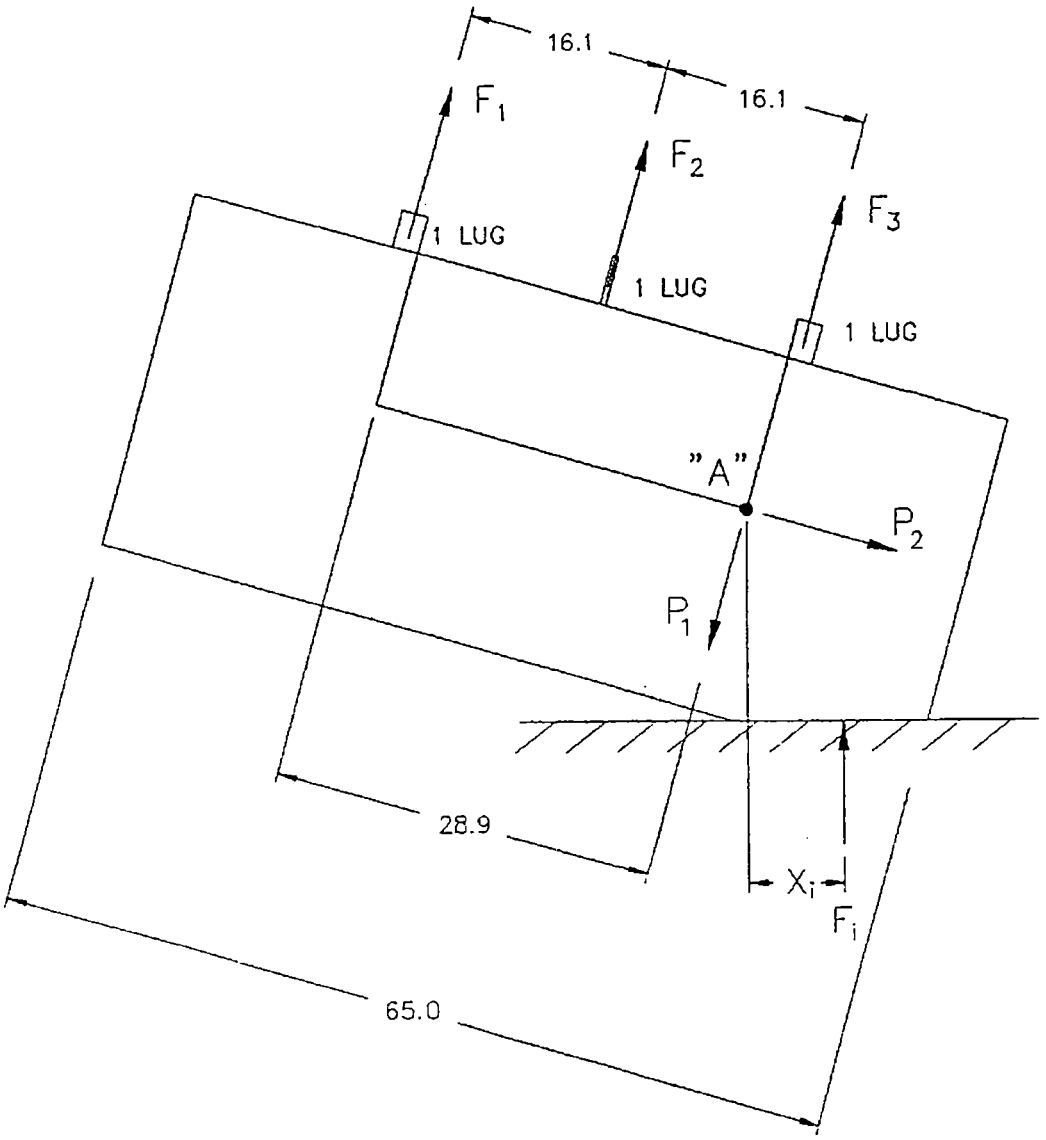

Figure 2.6.7-19 Free Body Diagram – Top Impact Limiter – Cask Wedging Forces

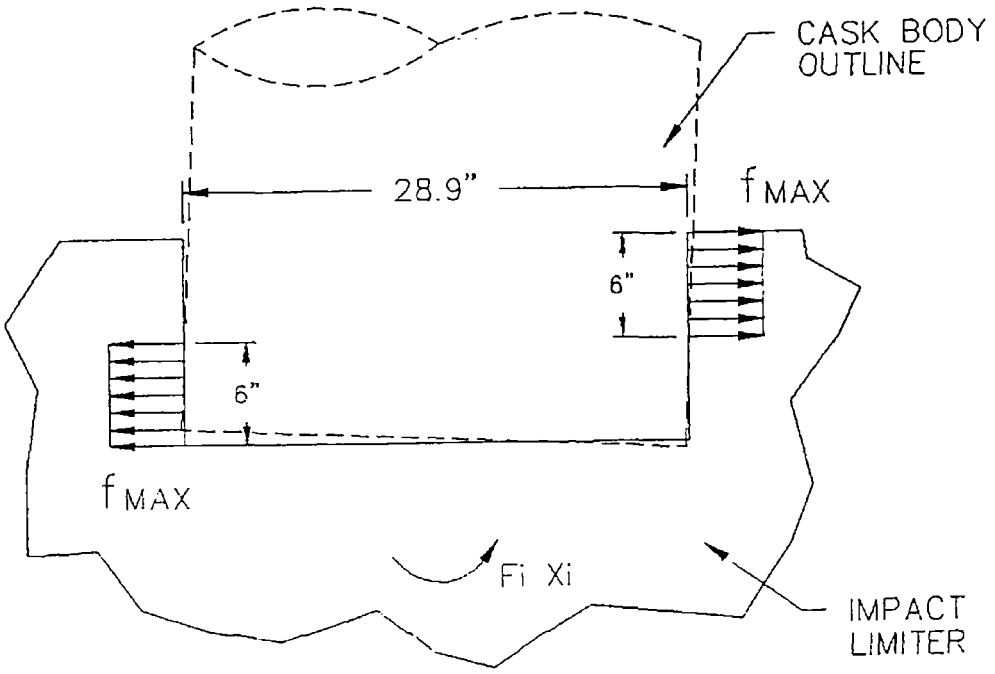

Figure 2.6.7-20 Cask Lid Configuration

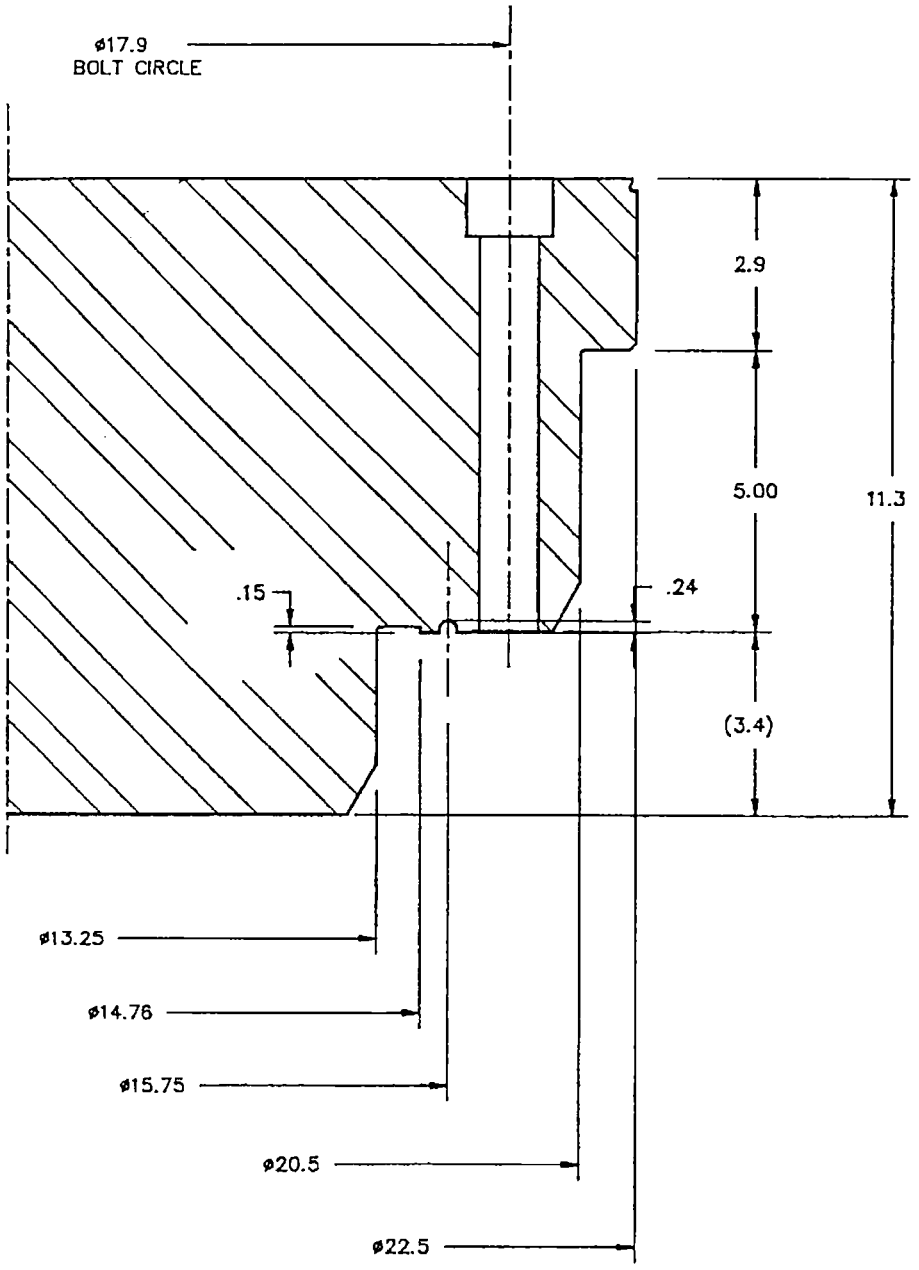

Figure 2.6.7-21 Closure Lid Free Body Diagram

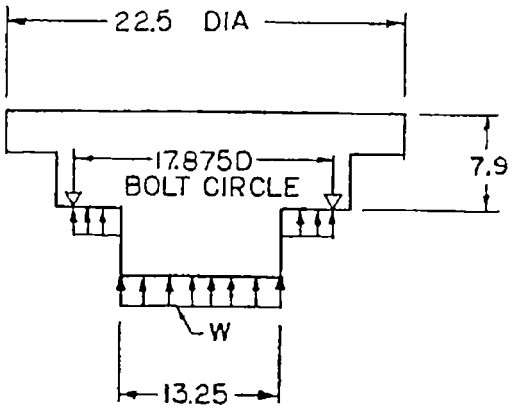

▽= SUPPORT

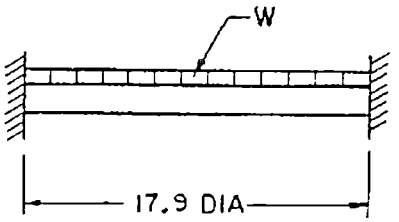

Figure 2.6.7-22 NAC-LWT Cask Cross-Section

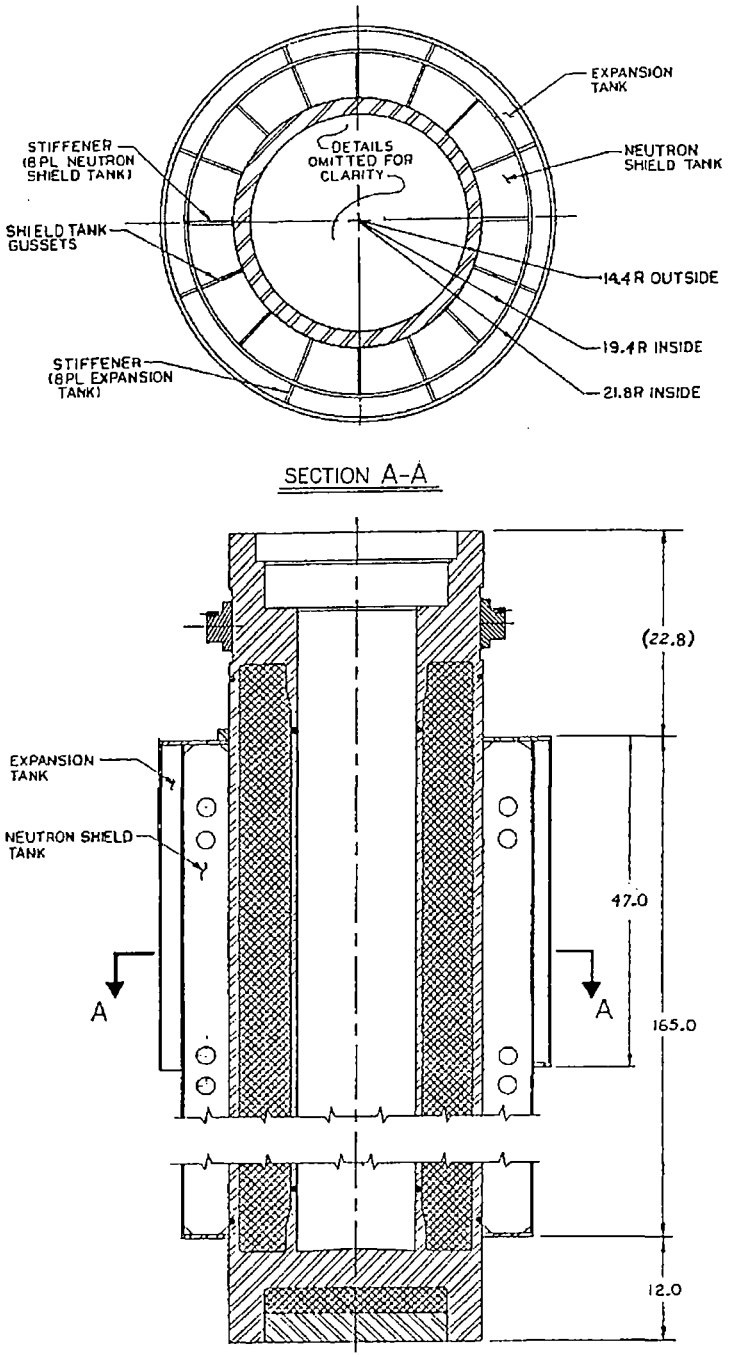

Figure 2.6.7-23 Component Parts of Shield Tank Structure

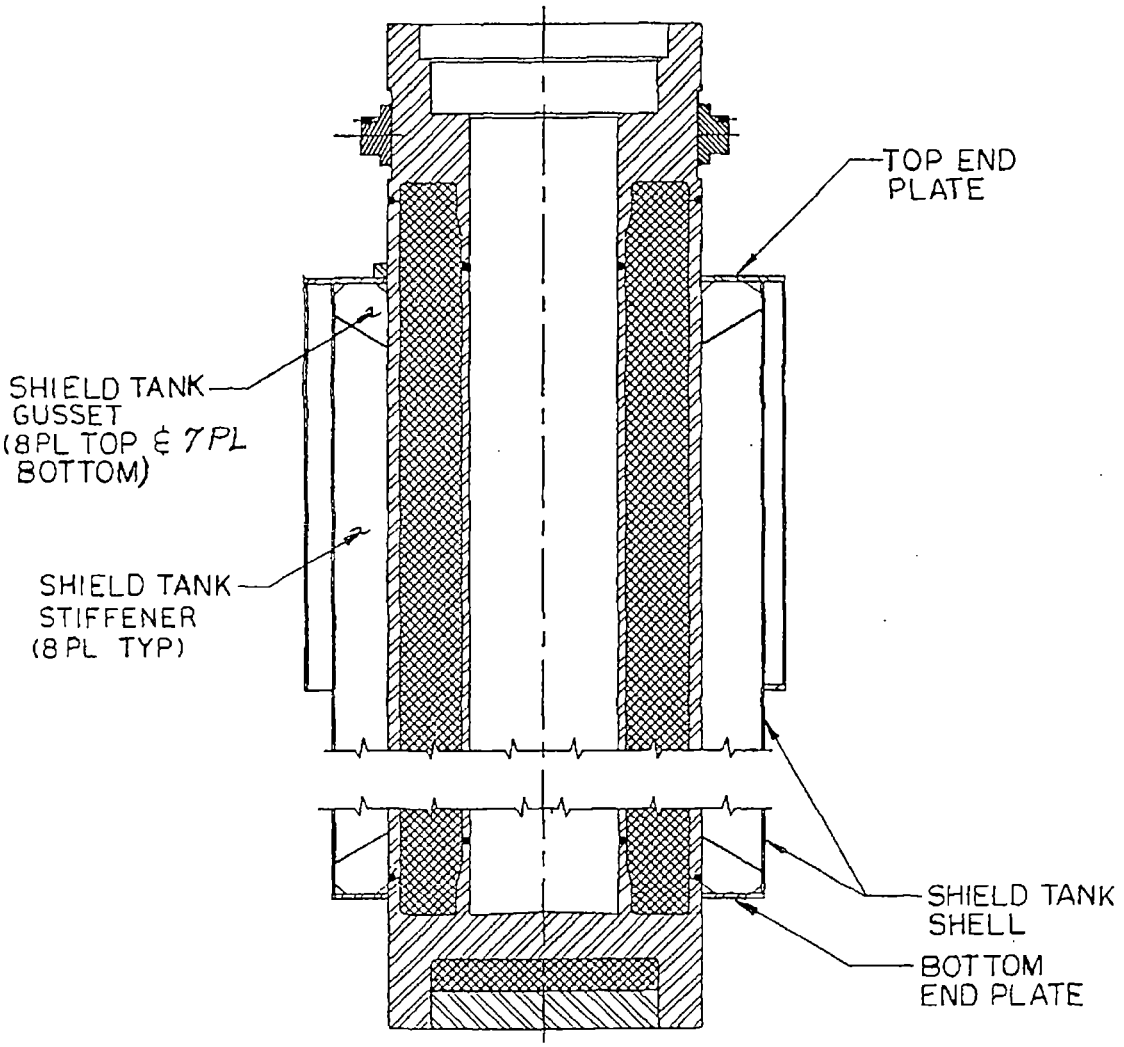

Figure 2.6.7-24 Shield Tank Cross-Section

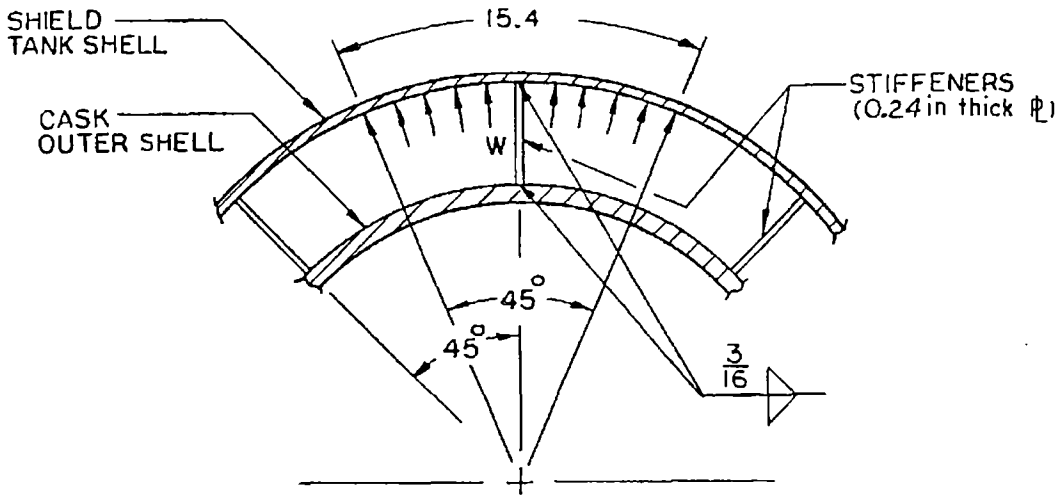

Figure 2.6.7-25 Shield Tank Quarter-Section Geometry

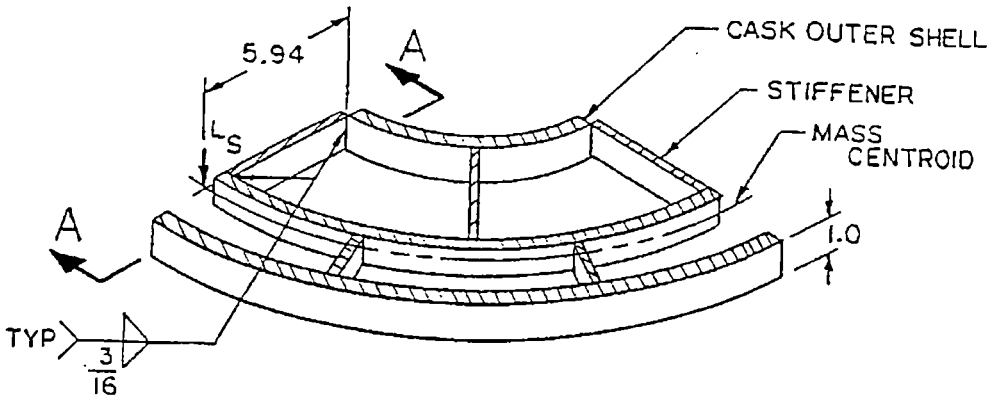

One Quarter of Tank Unit Section

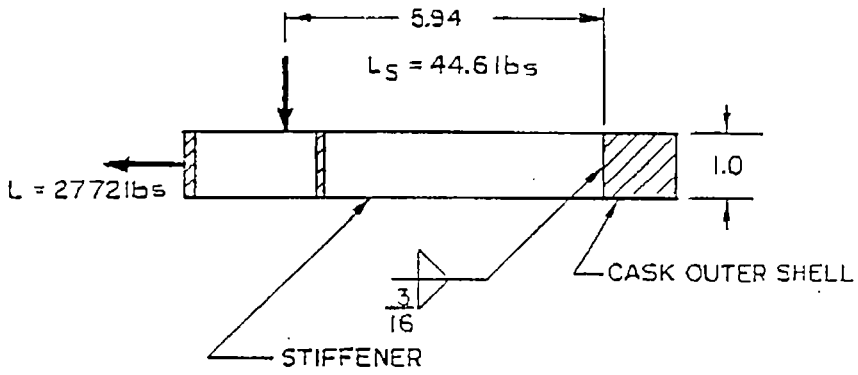

Section A-A

Figure 2.6.7-26 Partial Bottom/Top End Plate Plan and Cross-Section

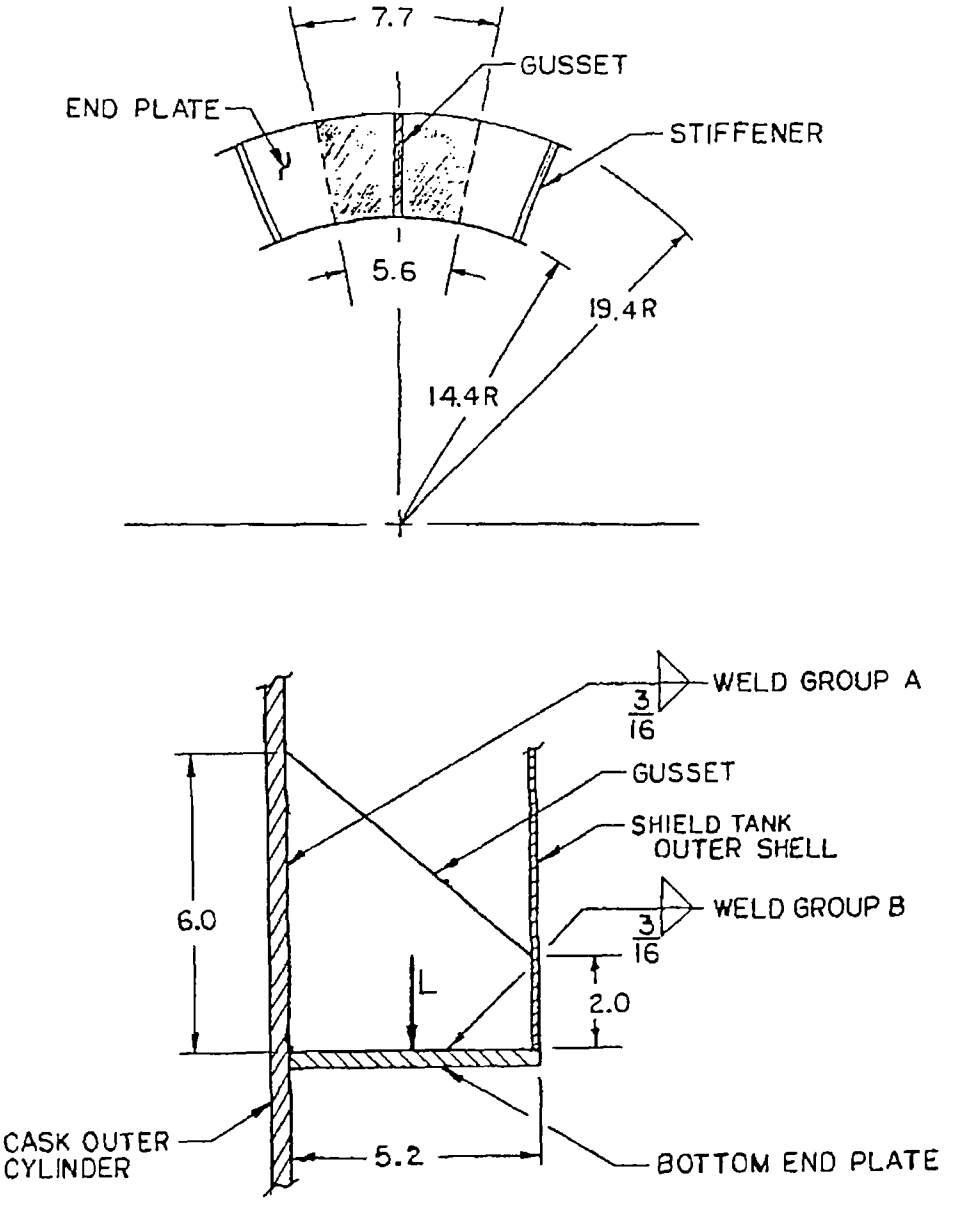

Figure 2.6.7-27 Shield Tank End Plate

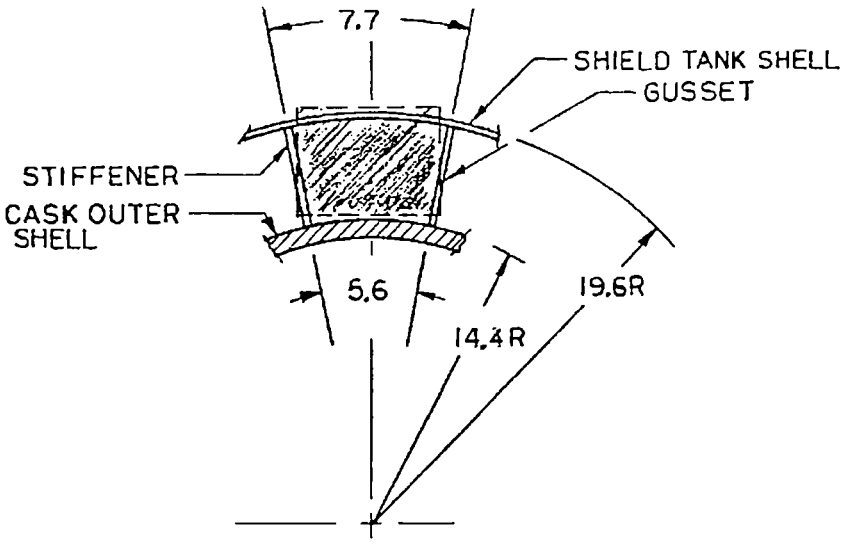

Figure 2.6.7-28 Gusset Profile

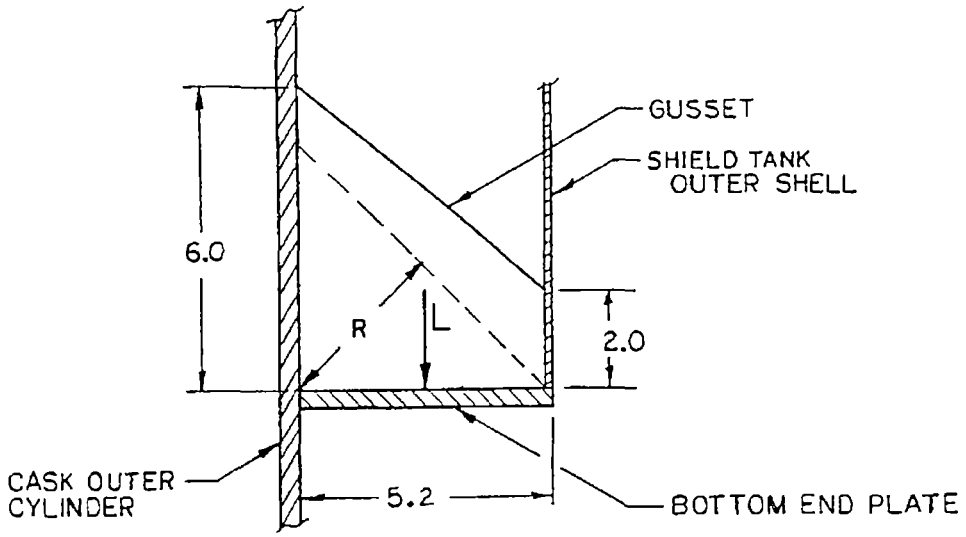

Figure 2.6.7-29 End Plate Welds

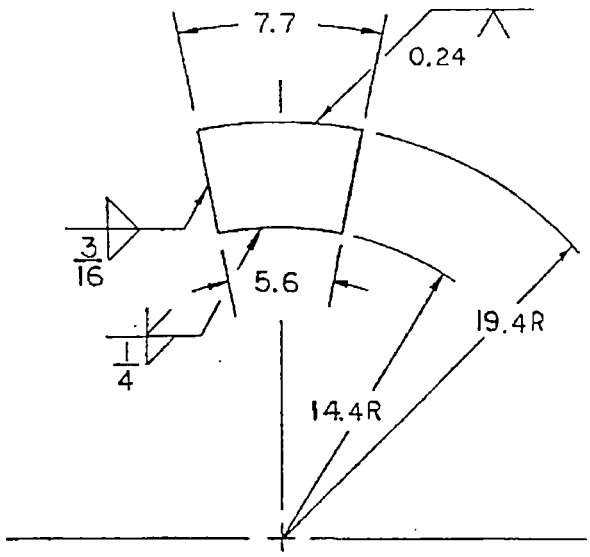

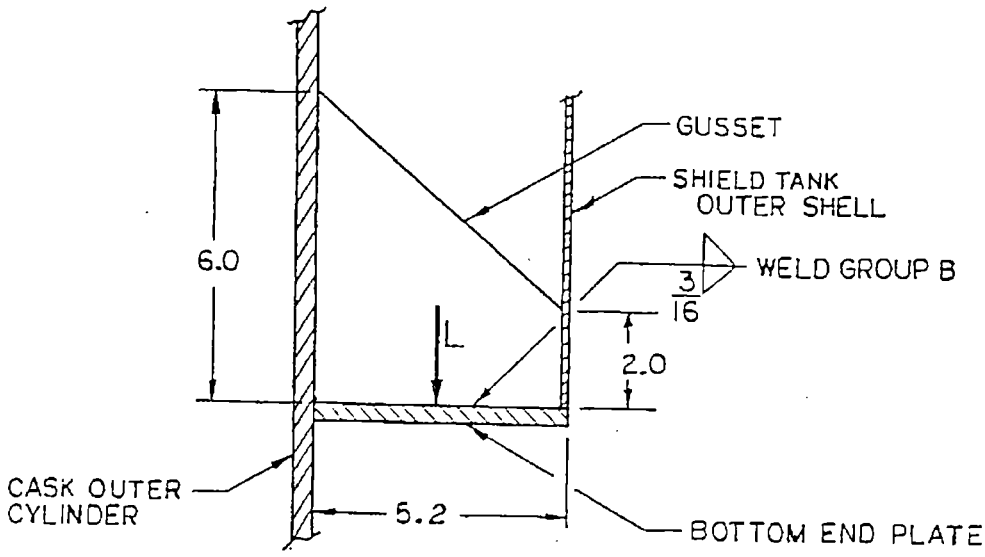

Figure 2.6.7-30 Component Parts of the Expansion Tank Structure

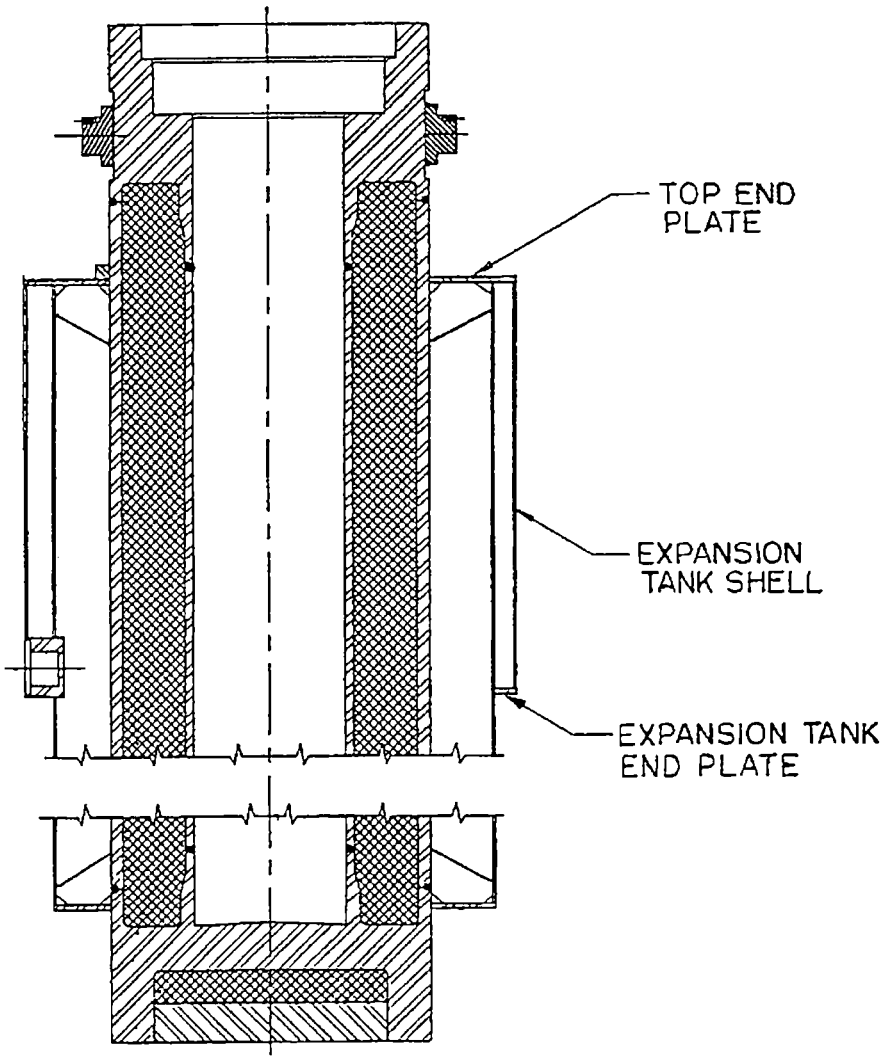

Figure 2.6.7-31 Expansion Tank Top and Bottom End Plate

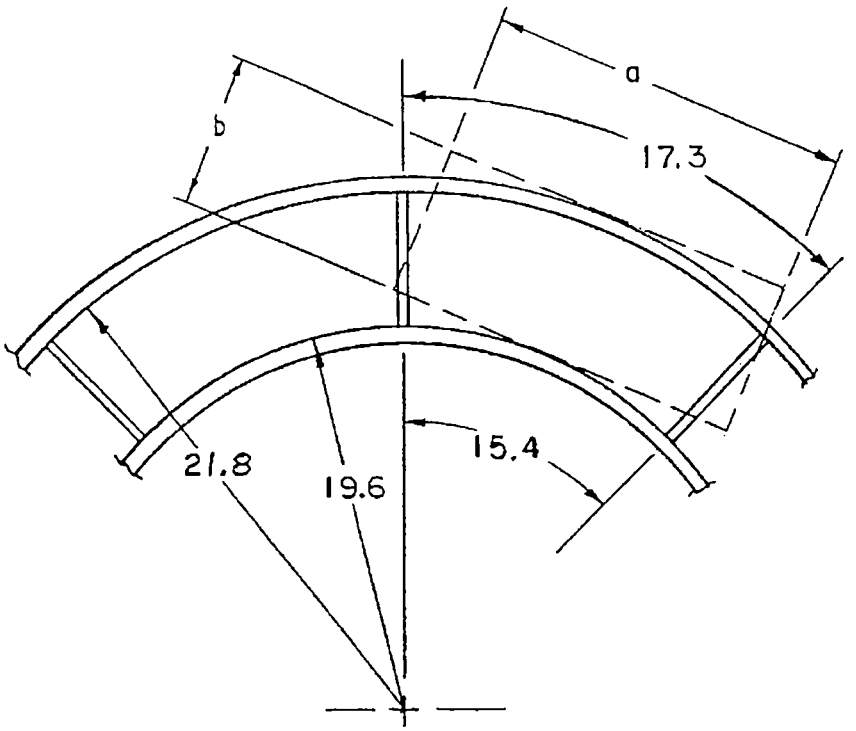

Figure 2.6.7-32 Expansion Tank Stiffener Load Geometry

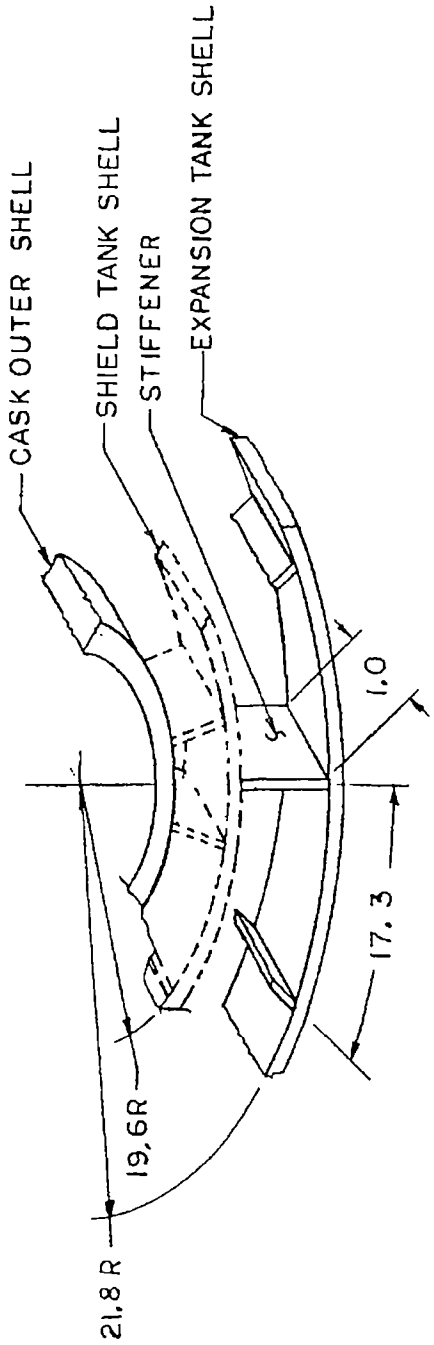

Figure 2.6.7-33 Cask Upper Ring at Trunnion – ANSYS Model

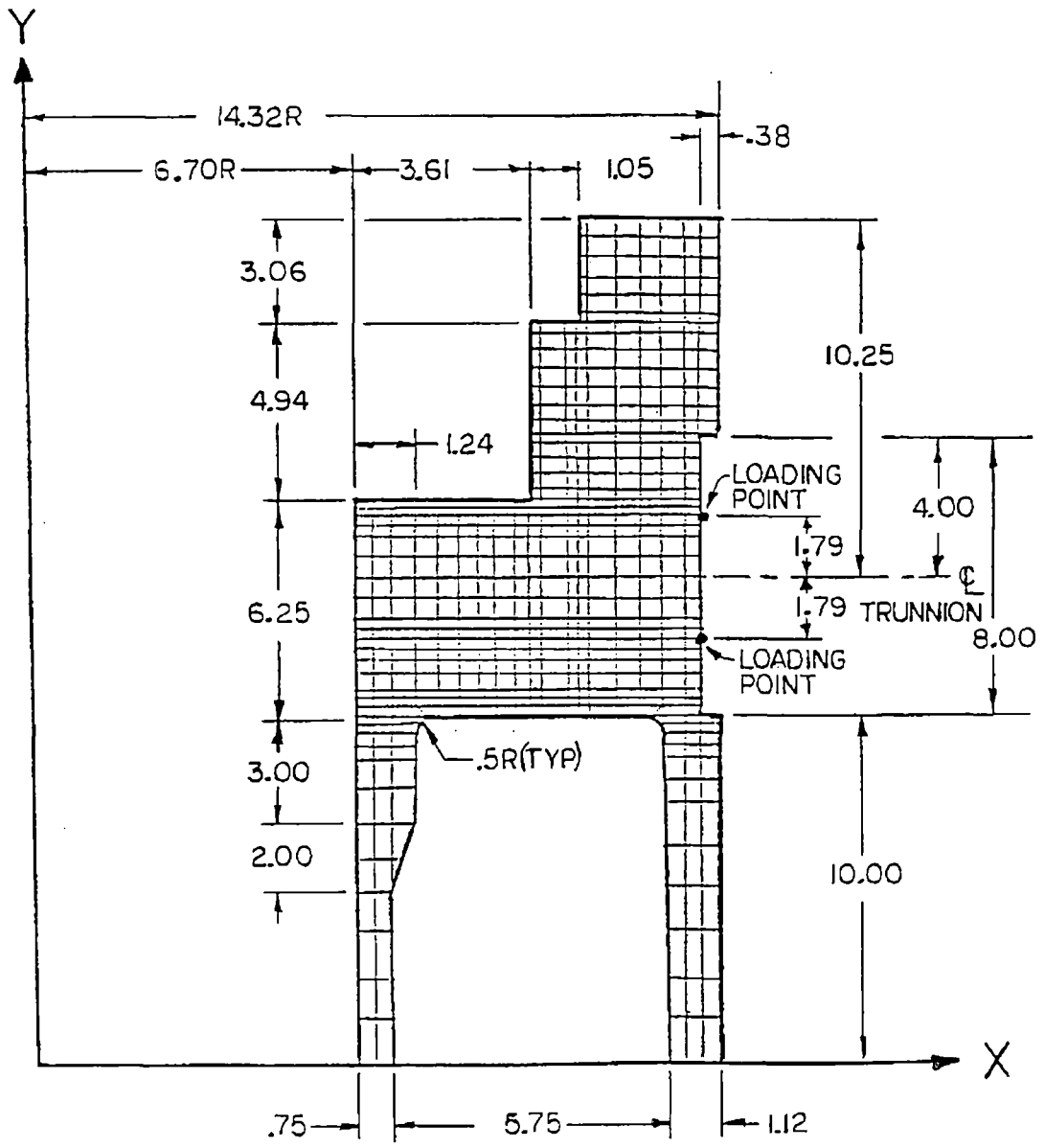

Figure 2.6.7-34 Cask Upper Ring at Trunnion – Model Loads and Boundary Conditions

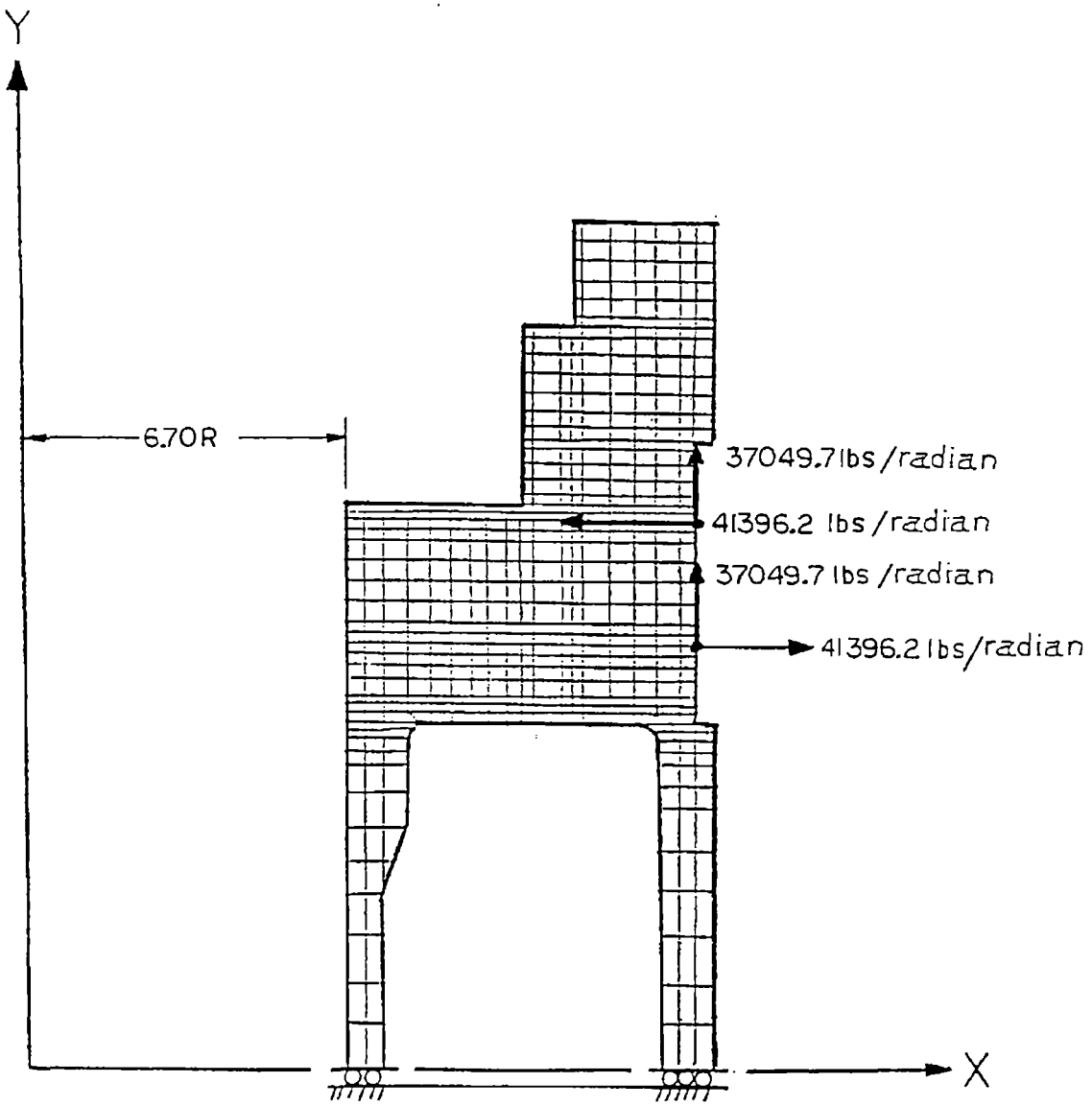

Figure 2.6.7-35 NAC-LWT Cask Upper Ring at Trunnion – Critical Sections

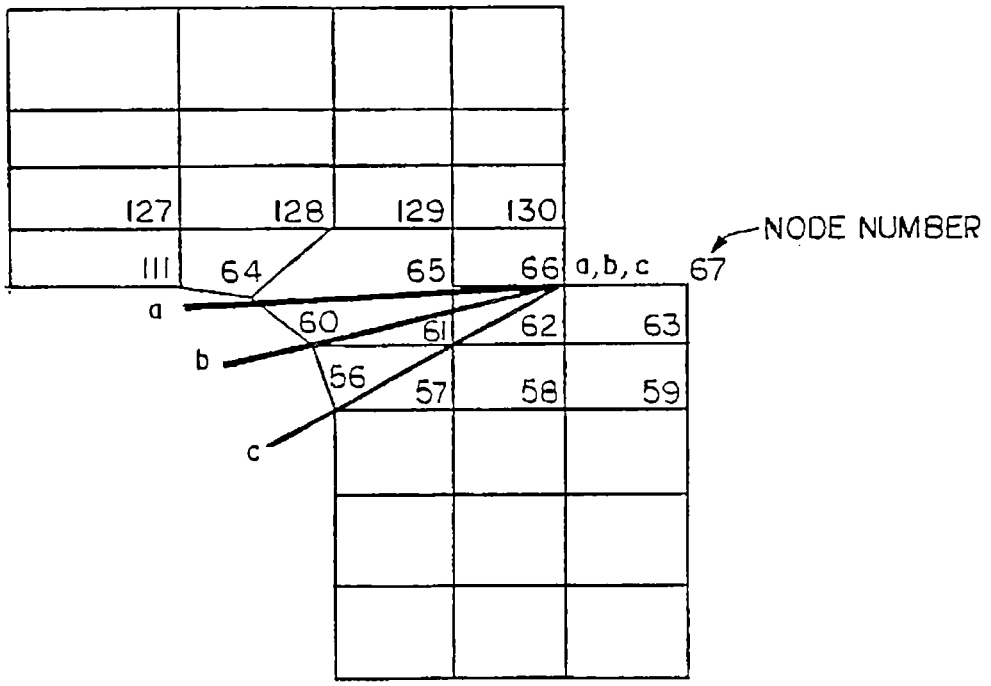

Table 2.6.7-1 Critical Stress Summary (1-Foot Bottom End Drop) – Loading Condition 1 – P_m

Loading Condition 1: 130°F Ambient Temperature and Maximum Decay Heat Load

		P_m Stresses[1] (ksi)				Principal Stresses					
Comp. No.[2]	Section Cut Node to Node	S_x	S_y	S_z	S_{xy}	S_1	S_2	S_3	S.I.	Allow. Stress 1.0 S_m	Margin of Safety
	2-2										
1	2375 to 2575	-0.17	-0.23	0.62	0.40	0.62	0.2	-0.6	1.22	20.0	Large
	4-4										
3	1581 to 1584	-0.1	-4.54	-0.16	-0.14	-0.1	-0.16	-4.55	4.45	20.0	+3.49
	7-7										
4	701 to 704	-0.03	-8.44	0.51	-0.02	0.51	-0.03	-8.44	8.94	31.4	+2.51
	6-6										
6	1515 to 1518	0.00	1.98	-0.16	-0.04	1.98	0.00	-0.16	2.14	31.4	Large
	11-11										
7	192 to 342	-6.50	1.18	1.28	1.69	1.54	1.28	-6.85	8.39	20.0	+1.38
	10-10										
8	361 to 365	0.77	-5.40	3.89	-0.99	3.89	0.92	-5.55	9.44	20.0	+1.19

[1] Conservatively based on a 1.12-inch thick outer shell and on a 3850-psi crush strength aluminum honeycomb impact limiter (Section 2.6.7.1.1).

[2] Refer to Figure 2.10.2-9 for component identification.

Table 2.6.7-2 Critical Stress Summary (1-Foot Bottom End Drop) – Loading Condition 1 - $P_m + P_b$

Loading Condition 1: 130°F Ambient Temperature and Maximum Decay Heat Load

		$P_m + P_b$ Stresses[1] (ksi)				Principal Stresses					
Comp. No.[2]	Section Cut Node to Node	S_x	S_y	S_z	S_{xy}	S_1	S_2	S_3	S.I.	Allow. Stress 1.5 S_m	Margin of Safety
	1-1										
1	2371 to 2571	-3.91	-0.35	0.11	0.00	0.11	-0.35	-3.91	4.01	30.0	+6.48
	3-3										
3	1835 to 1838	-0.1	4.66	2.25	0.29	4.68	2.25	-0.1	4.76	30.0	+5.30
	8-8										
4	621 to 624	0.15	-10.37	-1.16	0.28	0.16	-1.16	-10.38	10.54	47.1	+3.47
	5-5										
6	1595 to 1598	-0.01	3.03	0.57	0.00	3.03	0.57	-0.01	3.04	47.1	Large
	12-12										
7	150 to 193	9.25	-5.21	2.76	0.63	9.27	2.76	-5.24	14.51	30.0	+1.06
	9-9										
8	381 to 385	-0.21	-13.14	2.03	-1.07	2.03	-0.12	-13.23	15.26	30.0	+0.97

[1] Conservatively based on a 1.12-inch thick outer shell and on a 3850-psi crush strength aluminum honeycomb impact limiter (Section 2.6.7.1.1).

[2] Refer to Figure 2.10.2-9 for component identification.

Table 2.6.7-3 Critical Stress Summary (1-Foot Bottom End Drop) – Loading Condition 1 - Total Range

Loading Condition 1: 130°F Ambient Temperature and Maximum Decay Heat Load

		Total Stress Range[1] (ksi)				Principal Stresses			Stress Differences		
Comp. No.[2]	Node	S_x	S_y	S_z	S_{xy}	S_1	S_2	S_3	S_1-S_2	S_2-S_3	S_3-S_1
1	2376	0.80	-4.48	-0.22	-0.31	0.82	-0.22	-4.50	1.04	4.28	-5.32
3	1805	-0.19	-5.27	-2.19	-0.78	-0.07	-2.19	-5.39	2.12	3.20	-5.32
4	604	-0.69	-12.07	-1.65	0.61	-0.66	-1.65	-12.10	0.99	10.45	-11.44
6	1595	-0.02	2.93	0.48	0.00	2.93	0.48	-0.02	2.45	0.50	-2.95
7	192	12.54	-7.35	3.46	-3.90	13.28	3.46	-8.09	9.82	11.55	-21.37
8	361	-0.03	-16.44	0.82	-1.40	0.82	0.09	-16.57	0.73	16.65	-17.38

1 Conservatively based on a 1.12-inch thick outer shell and on a 3850-psi crush strength aluminum honeycomb impact limiter (Section 2.6.7.1.1).

2 Refer to Figure 2.10.2-9 for component identification.

Table 2.6.7-4 Critical Stress Summary (1-Foot Bottom End Drop) – Loading Condition 2 – P_m

Loading Condition 2: -40°F Ambient Temperature and Maximum Decay Heat Load

		P_m Stresses[1] (ksi)				Principal Stresses					
Comp. No.[2]	Section Cut Node to Node	S_x	S_y	S_z	S_{xy}	S_1	S_2	S_3	S.I.	Allow. Stress 1.0 S_m	Margin of Safety
	2-2										
1	2478 to 2578	0.03	-0.11	1.28	0.02	1.28	0.03	-0.11	1.39	20.0	Large
	4-4										
3	1581 to 1584	-0.15	-7.90	-0.93	-0.26	-0.14	-0.93	-7.91	7.77	20.0	+1.57
	6-6										
4	701 to 704	-0.02	-12.08	0.20	-0.03	0.20	-0.02	-12.08	12.28	31.4	+1.56
	8-8										
6	615 to 618	0.00	-2.85	0.80	0.00	0.80	0.00	-2.85	3.65	31.4	+7.60
	11-11										
7	100 to 143	-3.18	-4.19	2.15	2.18	2.15	-1.45	-5.93	8.07	20.0	+1.50
	7-7										
8	601 to 604	-0.23	-11.12	-1.21	0.46	-0.21	-1.21	-11.13	10.93	20.0	+0.83

1 Conservatively based on a 1.12-inch thick outer shell and on a 3850-psi crush strength aluminum honeycomb impact limiter (Section 2.6.7.1.1).

2 Refer to Figure 2.10.2-9 for component identification.

Table 2.6.7-5 Critical Stress Summary (1-Foot Bottom End Drop) – Loading Condition 2 - $P_m + P_b$

Loading Condition 2: -40°F Ambient Temperature and Maximum Decay Heat Load

		$P_m + P_b$ Stresses[1] (ksi)				Principal Stresses					
Comp. No.[2]	Section Cut Node to Node	S_x	S_y	S_z	S_{xy}	S_1	S_2	S_3	S.I.	Allow. Stress 1.5 S_m	Margin of Safety
	1-1										
1	2371 to 2571	-4.10	-0.43	0.14	0.00	0.14	-0.43	-4.10	4.24	30.0	+6.08
	3-3										
3	1701 to 1705	0.04	-8.08	-1.59	-0.34	0.05	-1.59	-8.10	8.15	30.0	+2.68
	5-5										
4	621 to 624	0.18	-13.91	-1.67	0.32	0.19	-1.67	-13.91	14.10	47.1	+2.34
	8-8										
6	615 to 618	0.03	-4.12	0.63	0.00	0.63	0.03	-4.12	4.75	47.1	+8.92
	10-10										
7	193 to 200	3.76	-9.04	1.83	-0.76	3.81	1.83	-9.09	12.89	30.0	+1.32
	9-9										
8	185 to 335	-12.66	-0.38	-0.11	1.93	-0.09	-0.11	-12.96	12.87	30.0	+1.33

1 Conservatively based on a 1.12-inch thick outer shell and on a 3850-psi crush strength aluminum honeycomb impact limiter (Section 2.6.7.1.1).

2 Refer to Figure 2.10.2-9 for component identification.

Table 2.6.7-6 Critical Stress Summary (1-Foot Bottom End Drop) – Loading Condition 2 - Total Range

Loading Condition 2: -40°F Ambient Temperature and Maximum Decay Heat Load

		Total Stress Range[1] (ksi)				Principal Stresses			Stress Differences		
Comp. No.[2]	Node	S_x	S_y	S_z	S_{xy}	S_1	S_2	S_3	S_1-S_2	S_2-S_3	S_3-S_1
1	2376	0.67	-4.03	0.05	-0.35	0.70	0.05	-4.06	0.65	4.11	-4.75
3	1805	-0.32	-9.36	-3.82	-1.34	-0.12	-3.82	-9.56	3.70	5.74	-9.44
4	604	-0.90	-15.99	-2.51	0.80	-0.86	-2.51	-16.03	1.65	13.52	-15.17
6	618	0.03	-4.20	0.57	0.00	0.57	0.03	-4.20	0.54	4.23	-4.77
7	143	-5.58	-14.56	-1.04	0.55	-1.04	-5.55	-14.59	4.51	9.05	-13.55
8	361	0.01	-14.97	-0.81	-1.62	0.18	-0.81	-15.14	0.99	14.33	-15.33

1 Conservatively based on a 1.12-inch thick outer shell and on a 3850-psi crush strength aluminum honeycomb impact limiter (Section 2.6.7.1.1).

2 Refer to Figure 2.10.2-9 for component identification.

Table 2.6.7-7 Critical Stress Summary (1-Foot Bottom End Drop) – Loading Condition 3 – P_m

Loading Condition 3: -40°F Ambient Temperature and No Decay Heat Load

		P_m Stresses[1] (ksi)				Principal Stresses					
Comp. No.[2]	Section Cut Node to Node	S_x	S_y	S_z	S_{xy}	S_1	S_2	S_3	S.I.	Allow. Stress 1.0 S_m	Margin of Safety
	1-1										
1	2375 to 2575	-0.21	0.00	-0.03	0.18	0.1	-0.03	-0.31	0.41	20.0	Large
	2-2										
3	1581 to 1584	-0.22	-3.78	-5.48	-0.28	-0.19	-3.80	-5.48	5.29	20.0	+2.78
	3-3										
4	621 to 624	0.04	-7.76	-1.05	0.24	0.04	-1.05	-7.77	7.81	31.4	+3.02
	5-5										
6	615 to 618	0.00	-6.85	-0.13	0.00	0.00	-0.13	-6.85	6.85	31.4	+3.58
	8-8										
7	18 to 118	-10.02	-0.60	-2.86	2.62	0.08	-2.86	-10.70	10.78	20.0	+0.86
	4-4										
8	601 to 604	-0.16	-7.07	-0.78	0.34	-0.14	-0.78	-7.09	6.95	20.0	+1.88

1 Conservatively based on a 1.12-inch thick outer shell and on a 3850-psi crush strength aluminum honeycomb impact limiter (Section 2.6.7.1.1).

2 Refer to Figure 2.10.2-9 for component identification.

Table 2.6.7-8 Critical Stress Summary (1-Foot Bottom End Drop) – Loading Condition 3 - $P_m + P_b$

Loading Condition 3: -40°F Ambient Temperature and No Decay Heat Load

		$P_m + P_b$ Stresses[1] (ksi)				Principal Stresses					
Comp. No.[2]	Section Cut Node to Node	S_x	S_y	S_z	S_{xy}	S_1	S_2	S_3	S.I.	Allow. Stress 1.5 S_m	Margin of Safety
	1-1										
1	2375 to 2575	-1.99	0.00	-0.03	0.18	0.01	-0.03	-2.01	2.02	30.0	Large
	2-2										
3	1581 to 1584	0.01	-3.30	-5.65	-0.28	0.03	-3.33	-5.65	5.68	30.0	+4.28
	3-3										
4	621 to 624	0.12	-8.99	-1.30	0.24	0.13	-1.30	-9.00	9.13	47.1	+4.16
	5-5										
6	615 to 618	0.00	-7.06	-0.19	0.00	0.00	-0.19	-7.06	7.06	47.1	+5.67
	8-8										
7	18 to 118	-20.14	-0.6	-2.86	2.62	-0.25	-2.86	-20.49	20.23	30.0	+0.48
	6-6										
8	185 to 335	-8.83	1.55	1.16	2.22	2.0	1.16	-9.29	11.29	30.0	+1.66

1 Conservatively based on a 1.12-inch thick outer shell and on a 3850-psi crush strength aluminum honeycomb impact limiter (Section 2.6.7.1.1).

2 Refer to Figure 2.10.2-9 for component identification.

Table 2.6.7-9 Critical Stress Summary (1-Foot Bottom End Drop) – Loading Condition 3 - Total Range

Loading Condition 3: -40°F Ambient Temperature and No Decay Heat Load

		Total Stress Range[1] (ksi)				Principal Stresses			Stress Differences		
Comp. No.[2]	Node	S_x	S_y	S_z	S_{xy}	S_1	S_2	S_3	S_1-S_2	S_2-S_3	S_3-S_1
1	2376	0.96	-3.75	-0.64	-0.11	0.96	-0.64	-3.75	1.60	3.11	-4.71
3	2176	3.74	-17.36	-1.84	-2.41	4.01	-1.84	-17.90	5.85	16.06	-21.91
4	604	-0.58	-10.47	-1.81	0.56	-0.55	-1.81	-10.50	1.26	8.69	-9.95
6	615	0.01	-7.05	-0.19	0.00	0.01	-0.19	-7.05	0.20	6.86	-7.06
7	143	0.08	-23.96	-3.03	-2.73	0.39	-3.03	-24.27	3.42	21.24	-24.66
8	361	-0.02	-10.55	0.26	-1.38	0.26	-0.16	-10.73	0.10	10.89	-10.99

1 Conservatively based on a 1.12-inch thick outer shell and on a 3850-psi crush strength aluminum honeycomb impact limiter (Section 2.6.7.1.1).

2 Refer to Figure 2.10.2-9 for component identification.

Table 2.6.7-10 Critical Stress Summary (1-Foot Top End Drop) – Loading Condition 1 – P_m

Loading Condition 1: 130°F Ambient Temperature and Maximum Decay Heat Load

		P_m Stresses[1] (ksi)				Principal Stresses					
Comp. No.[2]	Section Cut Node to Node	S_x	S_y	S_z	S_{xy}	S_1	S_2	S_3	S.I.	Allow. Stress 1.0 S_m	Margin of Safety
	2-2										
1	2377 to 2577	-7.46	-0.06	0.09	0.15	0.09	-0.05	-7.46	7.55	20.0	+1.65
	4-4										
3	1581 to 1584	-0.20	-7.58	-0.57	-0.33	-0.18	-0.57	-7.60	7.42	20.0	+1.70
	5-5										
4	1481 to 1484	-0.03	-8.19	0.52	0.02	0.52	-0.03	-8.19	8.71	31.4	+2.60
	12-12										
6	695 to 698	0.00	2.39	-0.10	0.04	2.40	0.00	-0.10	2.50	31.4	Large
	10-10										
7	17 to 117	-1.04	1.54	2.36	-2.84	3.37	2.36	-2.87	6.23	20.0	+2.21
	7-7										
8	401 to 405	-0.03	-2.63	1.89	-0.39	1.89	0.03	-2.69	4.58	20.0	+3.37

1 Conservatively based on a 1.12-inch thick outer shell and on a 3850-psi crush strength aluminum honeycomb impact limiter (Section 2.6.7.1.1).

2 Refer to Figure 2.10.2-9 for component identification.

Table 2.6.7-11 Critical Stress Summary (1-Foot Top End Drop) – Loading Condition 1 - $P_m + P_b$

Loading Condition 1: 130°F Ambient Temperature and Maximum Decay Heat Load

		$P_m + P_b$ Stresses[1] (ksi)				Principal Stresses					
Comp. No.[2]	Section Cut Node to Node	S_x	S_y	S_z	S_{xy}	S_1	S_2	S_3	S.I.	Allow. Stress 1.5 S_m	Margin of Safety
	1-1										
1	2371 to 2571	-12.69	-0.13	-0.22	-1.01	-0.05	-0.22	-12.77	12.72	30.0	+1.36
	3-3										
3	1941 to 1956	0.84	-10.28	-3.31	0.03	0.84	-3.31	-10.28	11.12	30.0	+1.70
	11-11										
4	1561 to 1564	0.12	-9.50	-0.89	-0.22	0.13	-0.89	-9.51	9.64	47.1	+3.89
	6-6										
6	615 to 618	-0.02	3.50	0.78	0.00	3.50	0.78	-0.02	3.52	47.1	Large
	9-9										
7	143 to 150	-7.68	6.60	1.37	1.33	6.72	1.37	-7.80	14.52	30.0	+1.07
	8-8										
8	381 to 385	-0.15	-6.77	0.67	-0.49	0.67	-0.12	-6.81	7.47	30.0	+3.02

1 Conservatively based on a 1.12-inch thick outer shell and on a 3850-psi crush strength aluminum honeycomb impact limiter (Section 2.6.7.1.1).

2 Refer to Figure 2.10.2-9 for component identification.

Table 2.6.7-12 Critical Stress Summary (1-Foot Top End Drop) – Loading Condition 1 - Total Range

Loading Condition 1: 130°F Ambient Temperature and Maximum Decay Heat Load

		Total Stress Range[1] (ksi)				Principal Stresses			Stress Differences		
Comp. No.[2]	Node	S_x	S_y	S_z	S_{xy}	S_1	S_2	S_3	S_1-S_2	S_2-S_3	S_3-S_1
1	2371	2.76	-10.30	0.04	3.56	3.67	0.04	-11.21	3.63	11.25	-14.88
3	1962	-1.54	-12.69	-5.46	-1.00	-1.45	-5.46	-12.78	4.01	7.32	-11.33
4	1584	-0.62	-10.96	-1.54	-0.54	-0.59	-1.54	-10.98	0.95	9.44	-10.39
6	615	-0.01	3.43	0.72	-0.01	3.43	0.72	-0.01	2.71	0.73	-3.44
7	143	-7.68	6.79	1.34	2.96	7.37	1.34	-8.26	6.03	9.60	-15.63
8	361	-0.07	-8.76	-0.09	-0.78	0.00	-0.09	-8.83	0.09	8.74	-8.83

1 Conservatively based on a 1.12-inch thick outer shell and on a 3850-psi crush strength aluminum honeycomb impact limiter (Section 2.6.7.1.1).

2 Refer to Figure 2.10.2-9 for component identification.

Table 2.6.7-13 Critical Stress Summary (1-Foot Top End Drop) – Loading Condition 2 – P_m

Loading Condition 2: -40°F Ambient Temperature and Maximum Decay Heat Load

		P_m Stresses[1] (ksi)				Principal Stresses					
Comp. No.[2]	Section Cut Node to Node	S_x	S_y	S_z	S_{xy}	S_1	S_2	S_3	S.I.	Allow. Stress 1.0 S_m	Margin of Safety
	2-2										
1	2377 to 2577	-7.42	-0.08	0.30	0.18	0.30	-0.08	-7.42	7.72	20.0	+1.59
	4-4										
3	1581 to 1584	-0.24	-10.89	-1.33	-0.44	-0.22	-1.33	-10.91	10.69	20.0	+0.87
	6-6										
4	1481 to 1484	-0.02	-11.77	0.24	0.04	0.24	-0.02	-11.77	12.01	31.4	+1.61
	5-5										
6	1595 to 1598	0.01	-2.37	1.0	0.02	1.0	0.01	-2.37	3.37	31.4	+8.32
	10-10										
7	375 to 378	-1.35	1.92	2.97	-0.61	2.97	2.03	-1.45	4.42	20.0	+3.52
	8-8										
8	601 to 604	-0.13	-7.55	-0.80	0.27	-0.12	-0.80	-7.56	7.44	20.0	+1.69

1 Conservatively based on a 1.12-inch thick outer shell and on a 3850-psi crush strength aluminum honeycomb impact limiter (Section 2.6.7.1.1).

2 Refer to Figure 2.10.2-9 for component identification.

Table 2.6.7-14 Critical Stress Summary (1-Foot Top End Drop) – Loading Condition 2 - $P_m + P_b$

Loading Condition 2: -40°F Ambient Temperature and Maximum Decay Heat Load

		$P_m + P_b$ Stresses[1] (ksi)				Principal Stresses					
Comp. No.[2]	Section Cut Node to Node	S_x	S_y	S_z	S_{xy}	S_1	S_2	S_3	S.I.	Allow. Stress 1.5 S_m	Margin of Safety
	1-1										
1	2371 to 2571	-12.88	-0.21	-0.19	-1.02	-0.13	-0.19	-12.96	12.84	30.0	+1.34
	4-4										
3	1581 to 1584	-0.52	-12.05	-1.44	-0.45	-0.51	-1.44	-12.07	11.56	30.0	+1.60
	3-3										
4	1561 to 1564	0.17	-13.22	-1.52	-0.30	0.17	-1.52	-13.23	13.40	47.1	+2.51
	5-5										
6	1595 to 1598	0.04	-3.78	0.86	0.02	0.86	0.04	-3.78	4.64	47.1	+9.15
	9-9										
7	395 to 398	-0.18	7.35	4.97	-0.78	7.42	4.97	-0.26	7.69	30.0	+2.90
	8-8										
8	601 to 604	-0.18	-7.94	-0.67	0.27	-0.18	-0.67	-7.95	7.78	30.0	+2.86

1 Conservatively based on a 1.12-inch thick outer shell and on a 3850-psi crush strength aluminum honeycomb impact limiter (Section 2.6.7.1.1).

2 Refer to Figure 2.10.2-9 for component identification.

Table 2.6.7-15 Critical Stress Summary (1-Foot Top End Drop) – Loading Condition 2 - Total Range

Loading Condition 2: -40°F Ambient Temperature and Maximum Decay Heat Load

		Total Stress Range[1] (ksi)				Principal Stresses			Stress Differences		
Comp. No.[2]	Node	S_x	S_y	S_z	S_{xy}	S_1	S_2	S_3	S_1-S_2	S_2-S_3	S_3-S_1
1	2371	2.56	-10.43	0.01	3.61	3.50	0.01	-11.37	3.49	11.38	-14.87
3	1962	-1.54	-12.88	-5.92	-1.05	-1.44	-5.92	-12.98	4.48	7.06	-11.54
4	1584	-0.85	-15.19	-2.48	-0.76	-0.81	-2.48	-15.23	1.67	12.75	-14.42
6	1598	0.02	-3.94	0.76	0.02	0.76	0.02	-3.94	0.74	3.96	-4.70
7	378	-0.19	7.42	4.95	-0.07	7.42	4.95	-0.19	2.47	5.14	-7.61
8	361	-0.02	-7.21	-1.70	-1.00	0.16	-1.70	-7.38	1.86	5.68	-7.54

1 Conservatively based on a 1.12-inch thick outer shell and on a 3850-psi crush strength aluminum honeycomb impact limiter (Section 2.6.7.1.1).

2 Refer to Figure 2.10.2-9 for component identification.

Table 2.6.7-16 Critical Stress Summary (1-Foot Side Drop) – Loading Condition 1 – P_m

Loading Condition 1: 100°F Ambient Temperature and Maximum Decay Heat Load

		P_m Stresses (ksi)				Principal Stresses					
Comp. No.[1]	Section Cut Node to Node	S_x	S_y	S_z	S_{xy}	S_1	S_2	S_3	S.I.	Allow. Stress 1.0 S_m	Margin of Safety
	1-1										
1	2361 to 2370	-3.39	-0.30	0.06	-0.26	0.06	-0.28	-3.42	3.48	20.0	+4.74
	2-2										
3	1969 to 1976	-10.14	1.89	-4.53	-1.65	2.11	-4.53	-10.37	12.47	20.0	+0.60
	3-3										
4	1141 to 1144	-0.11	15.43	0.25	0.00	15.43	0.25	-0.11	15.54	31.4	+1.02
	4-4										
6	1115 to 1118	-0.05	31.36	1.31	0.00	31.36	1.31	-0.05	31.4	31.4	+0.00
	5-5										
7	395 to 398	-2.17	4.06	-5.51	0.78	4.15	-2.27	-5.51	9.66	20.0	+1.07
	6-6										
8	192 to 342	-5.47	-0.35	-3.06	0.18	-0.35	-3.06	-5.48	5.13	20.0	+2.89

[1] Refer to Figure 2.10.2-9 for component identification.

Table 2.6.7-17 Critical Stress Summary (1-Foot Side Drop) – Loading Condition 1 - $P_m + P_b$

Loading Condition 1: 100°F Ambient Temperature and Maximum Decay Heat Load

		$P_m + P_b$ Stresses (ksi)				Principal Stresses					
Comp. No.[1]	Section Cut Node to Node	S_x	S_y	S_z	S_{xy}	S_1	S_2	S_3	S.I.	Allow. Stress 1.5 S_m	Margin of Safety
	7-7										
1	2301 to 2561	-0.78	0.06	0.82	3.96	3.62	0.82	-4.34	7.96	30.0	+2.77
	8-8										
3	2150 to 2156	-4.40	-0.08	-20.16	0.01	-0.08	-4.40	-20.16	20.08	30.0	+0.49
	3-3										
4	1141 to 1144	-0.07	16.41	0.86	0.00	16.41	0.86	-0.07	16.48	47.1	+1.86
	4-4										
6	1115 to 1118	0.01	33.37	1.50	0.00	33.37	1.50	0.01	33.36	47.1	+0.41
	5-5										
7	395 to 398	-1.11	16.09	-0.89	0.78	16.12	-0.89	-1.14	17.26	30.0	+0.74
	9-9										
8	177 to 327	-8.25	-1.80	0.27	-1.47	0.27	-1.48	-8.58	8.85	30.0	+2.39

[1] Refer to Figure 2.10.2-9 for component identification.

Table 2.6.7-18 Critical Stress Summary (1-Foot Side Drop) – Loading Condition 1 - S_n

Loading Condition 1: 100°F Ambient Temperature and Maximum Decay Heat Load

		S_n Stresses (ksi)				Principal Stresses					
Comp. No.[1]	Section Cut Node to Node	S_x	S_y	S_z	S_{xy}	S_1	S_2	S_3	S.I.	Allow. Stress 3.0 S_m	Margin of Safety
	1-1										
1	2361 to 2370	-9.54	-1.04	-1.24	-0.19	-1.04	-1.24	-9.55	8.51	60.0	+6.05
	10-10										
3	1815 to 1818	-0.09	22.64	2.62	-1.58	22.75	2.62	-0.20	22.95	60.0	+1.61
	3-3										
4	1141 to 1144	-0.07	17.55	0.98	0.00	17.55	0.98	-0.07	17.62	94.2	+4.34
	4-4										
6	1115 to 1118	0.01	38.01	1.65	0.00	38.01	1.65	0.01	38.00	94.2	+1.48
	11-11										
7	395 to 398	-1.10	19.46	0.52	0.51	19.47	0.52	-1.12	20.59	60.0	+1.91
	6-6										
8	177 to 327	-12.34	-1.86	-3.80	-1.48	-1.66	-3.80	-12.55	10.89	60.0	+4.51

[1] Refer to Figure 2.10.2-9 for component identification.

Table 2.6.7-19 Critical Stress Summary (1-Foot Side Drop) – Loading Condition 1 - Total Range

Loading Condition 1: 100°F Ambient Temperature and Maximum Decay Heat Load

		Total Stress Range (ksi)				Principal Stresses			Stress Differences		
Comp. No.[1]	Node	S_x	S_y	S_z	S_{xy}	S_1	S_2	S_3	S_1-S_2	S_2-S_3	S_3-S_1
1	2561	0.06	0.02	1.33	15.24	15.28	1.33	-15.19	13.95	16.52	-30.47
3	1815	1.72	24.87	3.61	7.38	27.05	3.61	-0.46	23.44	4.07	-27.51
4	1144	-0.07	17.55	0.96	0.00	17.55	0.96	-0.07	16.59	1.03	-17.62
6	1118	0.01	37.98	1.61	0.00	37.98	1.61	0.01	36.37	1.60	-37.97
7	395	-1.10	22.68	1.30	1.50	22.78	1.30	-1.20	21.48	2.50	-23.98
8	192	-22.96	-1.15	-9.18	-0.81	-1.10	-9.18	-23.00	8.08	13.82	-21.90

[1] Refer to Figure 2.10.2-9 for component identification.

Table 2.6.7-20 Critical Stress Summary (1-Foot Top Corner Drop) – Loading Condition 1 – P_m – Drop Orientation = 15.74 Degrees

Loading Condition 1: 130°F Ambient Temperature and Maximum Decay Heat Load

		P_m Stresses[1] (ksi)				Principal Stresses					
Comp. No.[2]	Section Cut Node to Node	S_x	S_y	S_z	S_{xy}	S_1	S_2	S_3	S.I.	Allow. Stress 1.0 S_m	Margin of Safety
	1-1										
1	2377 to 2577	-5.07	-0.37	-0.71	-0.29	-0.35	-0.71	-5.09	4.74	20.0	+3.22
	2-2										
3	1775 to 1778	-0.05	-4.39	0.55	0.01	0.55	-0.05	-4.39	4.95	20.0	+3.04
	3-3										
4	1501 to 1504	-0.03	-3.11	0.36	0.01	0.36	-0.03	-3.11	3.47	31.4	+8.05
	4-4										
6	1595 to 1598	-0.01	-3.94	0.52	0.03	0.52	-0.01	-3.94	4.46	31.4	+6.04
	5-5										
7	18 to 118	-1.72	2.83	0.47	-2.50	3.94	0.47	-2.83	6.76	20.0	+1.96
	6-6										
8	381 to 385	-1.83	-2.67	0.82	-0.32	0.82	-1.73	-2.77	3.60	20.0	+4.56

1 Conservatively based on a 1.12-inch thick outer shell and on a 3850-psi crush strength aluminum honeycomb impact limiter (Section 2.6.7.3.1).

2 Refer to Figure 2.10.2-9 for component identification.

Table 2.6.7-21 Critical Stress Summary (1-Foot Top Corner Drop) – Loading Condition 1 - $P_m + P_b$ – Drop Orientation = 15.74 Degrees

Loading Condition 1: 130°F Ambient Temperature and Maximum Decay Heat Load

		$P_m + P_b$ Stresses[1] (ksi)				Principal Stresses					
Comp. No.[2]	Section Cut Node to Node	S_x	S_y	S_z	S_{xy}	S_1	S_2	S_3	S.I.	Allow. Stress 1.5 S_m	Margin of Safety
	1-1										
1	2377 to 2577	-6.69	-0.37	-0.71	-0.29	-0.35	-0.71	-6.70	6.34	30.0	+3.73
	7-7										
3	1821 to 1825	-0.02	-4.40	1.73	0.32	1.73	0.00	-4.43	6.16	30.0	+3.87
	8-8										
4	1561 to 1564	0.06	-4.51	-0.67	-0.13	0.06	-0.67	-4.52	4.58	47.1	+9.28
	4-4										
6	1595 to 1598	0.01	-4.03	0.45	0.03	0.45	0.01	-4.03	4.47	47.1	+9.54
	9-9										
7	143 to 150	-7.82	11.71	1.04	1.55	11.83	1.04	-7.94	19.77	30.0	+0.52
	10-10										
8	176 to 326	-2.87	7.16	0.74	-0.96	0.74	-2.66	-7.37	8.10	30.0	+2.70

1 Conservatively based on a 1.12-inch thick outer shell and on a 3850-psi crush strength aluminum honeycomb impact limiter (Section 2.6.7.3.1).

2 Refer to Figure 2.10.2-9 for component identification.

Table 2.6.7-22 Critical Stress Summary (1-Foot Top Corner Drop) – Loading Condition 1 - S_n – Drop Orientation = 15.74 Degrees

Loading Condition 1: 130°F Ambient Temperature and Maximum Decay Heat Load

		S_n Stresses[1] (ksi)				Principal Stresses					
Comp. No.[2]	Section Cut Node to Node	S_x	S_y	S_z	S_{xy}	S_1	S_2	S_3	S.I.	Allow. Stress 3.0 S_m	Margin of Safety
	1-1										
1	2377 to 2577	-6.82	-0.40	0.32	-0.13	0.32	-0.40	-6.82	7.14	60.0	+7.40
	11-11										
3	1852 to 1856	-0.19	7.89	4.10	-0.42	7.91	4.10	-0.21	8.12	60.0	+6.39
	12-12										
4	601 to 604	0.09	-3.42	-0.54	-0.21	0.11	-0.54	-3.44	3.54	94.2	Large
	13-13										
6	615 to 618	-0.02	15.94	1.30	0.00	15.94	1.30	-0.02	15.95	94.2	+4.90
	14-14										
7	193 to 343	-7.81	12.82	1.50	1.46	12.93	1.50	-7.92	20.84	60.0	+1.88
	6-6										
8	381 to 385	-4.22	-7.18	-0.60	-0.96	-0.60	-3.93	-7.47	6.86	60.0	+7.74

1 Conservatively based on a 1.12-inch thick outer shell and on a 3850-psi crush strength aluminum honeycomb impact limiter (Section 2.6.7.3.1).

2 Refer to Figure 2.10.2-9 for component identification.

Table 2.6.7-23 Critical Stress Summary (1-Foot Top Corner Drop) – Loading Condition 1 - Total Range – Drop Orientation = 15.74 Degrees

Loading Condition 1: 130°F Ambient Temperature and Maximum Decay Heat Load

		Total Stress Range[1] (ksi)				Principal Stresses			Stress Differences		
Comp. No.[2]	Node	S_x	S_y	S_z	S_{xy}	S_1	S_2	S_3	S_1-S_2	S_2-S_3	S_3-S_1
1	2561	1.48	-1.26	0.20	43.95	44.08	0.20	-43.86	43.88	44.06	-87.94
3	1856	-0.19	7.24	3.70	0.08	7.24	3.70	-0.19	3.54	3.89	-7.43
4	1584	-0.13	-2.05	0.02	-0.11	0.02	0.12	-2.06	0.14	1.93	-2.08
6	1595	-0.05	7.09	0.97	0.01	7.09	0.97	-0.05	6.12	1.02	-7.14
7	192	-7.81	14.07	1.73	3.37	14.58	1.73	-8.32	12.85	10.05	-22.90
8	385	-7.64	-8.88	-3.12	-1.02	-3.12	-7.07	-9.46	3.95	2.39	-6.34

1 Conservatively based on a 1.12-inch thick outer shell and on a 3850-psi crush strength aluminum honeycomb impact limiter (Section 2.6.7.3.1).

2 Refer to Figure 2.10.2-9 for component identification.

Table 2.6.7-24 Critical Stress Summary (1-Foot Bottom Corner Drop) – Loading Condition 1 – P_m – Drop Orientation = 15.74 Degrees

Loading Condition 1: 130°F Ambient Temperature and Maximum Decay Heat Load

		P_m Stresses[1] (ksi)				Principal Stresses					
Comp. No.[2]	Section Cut Node to Node	S_x	S_y	S_z	S_{xy}	S_1	S_2	S_3	S.I.	Allow. Stress 1.0 S_m	Margin of Safety
	1-1										
1	2301 to 2561	-1.28	-0.32	0.62	0.30	0.62	-0.24	-1.37	1.99	20.0	Large
	2-2										
3	1595 to 1598	-3.44	-3.78	-1.65	-0.68	-1.65	-2.91	-4.31	2.66	20.0	+6.51
	3-3										
4	661 to 664	-0.04	-2.98	0.28	0.02	0.28	-0.04	-2.98	3.26	31.4	+8.63
	4-4										
6	615 to 618	-0.01	-4.93	0.28	-0.03	0.28	-0.01	-4.93	5.21	31.4	+5.03
	5-5										
7	2 to 102	-5.98	-3.63	-0.03	2.73	-0.03	-1.83	-7.78	7.76	20.0	+1.58
	6-6										
8	601 to 604	-0.10	-2.94	0.09	0.13	0.09	-0.09	-2.95	3.04	20.0	+5.58

1 Conservatively based on a 1.12-inch thick outer shell and on a 3850-psi crush strength aluminum honeycomb impact limiter (Section 2.6.7.3.1).

2 Refer to Figure 2.10.2-9 for component identification.

Table 2.6.7-25 Critical Stress Summary (1-Foot Bottom Corner Drop) – Loading Condition 1 - $P_m + P_b$ – Drop Orientation = 15.74 Degrees

Loading Condition 1: 130°F Ambient Temperature and Maximum Decay Heat Load

		$P_m + P_b$ Stresses[1] (ksi)				Principal Stresses					
Comp. No.[2]	Section Cut Node to Node	S_x	S_y	S_z	S_{xy}	S_1	S_2	S_3	S.I.	Allow. Stress 1.5 S_m	Margin of Safety
	1-1										
1	2301 to 2561	-4.05	-0.32	0.38	1.31	0.38	0.09	-4.46	4.84	30.0	+5.20
	7-7										
3	1815 to 1818	-1.55	4.49	-4.47	0.28	4.51	-1.56	-4.47	8.98	30.0	+2.34
	8-8										
4	621 to 624	0.04	-4.09	-0.52	0.09	0.04	-0.52	-4.10	4.14	47.1	Large
	4-4										
6	615 to 618	-0.02	-5.20	0.30	-0.03	0.30	-0.02	-5.20	5.49	47.1	+7.58
	9-9										
7	168 to 175	9.21	-3.47	-0.15	-0.29	9.22	-0.15	-3.48	12.70	30.0	+1.36
	10-10										
8	176 to 326	-6.65	0.00	-0.82	0.00	0.00	-0.82	-6.65	6.65	30.0	+3.51

1 Conservatively based on a 1.12-inch thick outer shell and on a 3850-psi crush strength aluminum honeycomb impact limiter (Section 2.6.7.3.1).

2 Refer to Figure 2.10.2-9 for component identification.

Table 2.6.7-26 Critical Stress Summary (1-Foot Bottom Corner Drop) – Loading Condition 1 - S_n – Drop Orientation = 15.74 Degrees

Loading Condition 1: 130°F Ambient Temperature and Maximum Decay Heat Load

		S_n Stresses[1] (ksi)				Principal Stresses					
Comp. No.[2]	Section Cut Node to Node	S_x	S_y	S_z	S_{xy}	S_1	S_2	S_3	S.I.	Allow. Stress 3.0 S_m	Margin of Safety
	1-1										
1	2301 to 2561	-6.94	-0.68	-0.30	-0.06	-0.30	-0.68	-6.94	6.64	60.0	+8.04
	11-11										
3	1852 to 1856	-0.13	11.99	3.05	-0.24	12.00	3.05	-0.13	12.13	60.0	+3.95
	12-12										
4	1301 to 1304	0.00	4.74	0.69	0.00	4.74	0.69	0.00	4.74	94.2	Large
	13-13										
6	1275 to 1278	-0.01	12.83	0.30	0.00	12.83	0.30	-0.01	12.84	94.2	+6.34
	14-14										
7	193 to 343	17.94	-0.43	1.20	2.27	18.22	1.20	-0.71	18.93	60.0	+2.17
	15-15										
8	192 to 342	-16.86	-0.12	-1.41	3.03	0.41	-1.41	-17.40	17.81	60.0	+2.37

1 Conservatively based on a 1.12-inch thick outer shell and on a 3850-psi crush strength aluminum honeycomb impact limiter (Section 2.6.7.3.1).

2 Refer to Figure 2.10.2-9 for component identification.

Table 2.6.7-27 Critical Stress Summary (1-Foot Bottom Corner Drop) – Loading Condition 1 - Total Range – Drop Orientation = 15.74 Degrees

Loading Condition 1: 130°F Ambient Temperature and Maximum Decay Heat Load

		Total Stress Range[1] (ksi)				Principal Stresses			Stress Differences		
Comp. No.[2]	Node	S_x	S_y	S_z	S_{xy}	S_1	S_2	S_3	S_1-S_2	S_2-S_3	S_3-S_1
1	2561	0.80	-4.34	0.23	4.73	3.61	0.23	-7.15	3.38	7.38	-10.76
3	1815	0.38	3.10	-0.93	1.68	3.90	-0.42	-0.93	4.32	0.51	-4.83
4	604	-0.19	-2.77	0.11	0.15	0.11	-0.18	-2.78	0.29	2.60	-2.89
6	615	-0.03	5.78	0.94	-0.03	5.78	0.94	-0.03	4.84	0.97	-5.81
7	1	3.73	-1.26	1.97	-43.45	44.76	1.97	-42.29	42.79	44.26	-87.04
8	192	0.11	-18.73	-9.11	2.58	0.46	-9.11	-19.08	9.57	9.97	-19.53

1 Conservatively based on a 1.12-inch thick outer shell and on a 3850-psi crush strength aluminum honeycomb impact limiter (Section 2.6.7.3.1).

2 Refer to Figure 2.10.2-9 for component identification.

Table 2.6.7-28 Critical Stress Summary (1-Foot Top Corner Drop) – Loading Condition 3 – P_m – Drop Orientation = 15.74 Degrees

Loading Condition 3: -40°F Ambient Temperature and No Decay Heat Load

		P_m Stresses[1] (ksi)				Principal Stresses					
Comp. No.[2]	Section Cut Node to Node	S_x	S_y	S_z	S_{xy}	S_1	S_2	S_3	S.I.	Allow. Stress 1.0 S_m	Margin of Safety
	1-1										
1	2377 to 2577	-4.89	-0.34	-0.78	-0.34	-0.32	-0.78	-4.91	4.59	20.0	+3.36
	2-2										
3	1775 to 1778	-0.06	-4.13	0.62	0.01	0.62	-0.06	-4.13	4.75	20.0	+3.21
	3-3										
4	1561 to 1564	0.02	-2.72	-0.33	-0.11	0.03	-0.33	-2.73	2.75	31.4	Large
	4-4										
6	1595 to 1598	-0.01	-3.71	0.53	0.03	0.53	-0.01	-3.71	4.23	31.4	+6.42
	5-5										
7	168 to 175	-2.03	3.20	1.06	-0.33	3.22	1.06	-2.05	5.27	20.0	+2.79
	6-6										
8	381 to 385	-1.93	-7.44	-1.79	0.32	-1.79	-1.91	-7.46	5.67	20.0	+2.53

1 Conservatively based on a 1.12-inch thick outer shell and on a 3850-psi crush strength aluminum honeycomb impact limiter (Section 2.6.7.3.1).

2 Refer to Figure 2.10.2-9 for component identification.

Table 2.6.7-29 Critical Stress Summary (1-Foot Top Corner Drop) – Loading Condition 3 - $P_m + P_b$ – Drop Orientation = 15.74 Degrees

Loading Condition 3: -40°F Ambient Temperature and No Decay Heat Load

		$P_m + P_b$ Stresses[1] (ksi)				Principal Stresses					
Comp. No.[2]	Section Cut Node to Node	S_x	S_y	S_z	S_{xy}	S_1	S_2	S_3	S.I.	Allow. Stress 1.5 S_m	Margin of Safety
	1-1										
1	2377 to 2577	-6.71	-0.34	-0.78	-0.34	-0.33	-0.78	-6.72	6.40	30.0	+3.69
	7-7										
3	1821 to 1825	0.03	-4.61	1.68	0.43	1.68	0.07	-4.65	6.33	30.0	+3.74
	3-3										
4	1561 to 1564	0.06	-3.75	-0.84	-0.11	0.06	-0.84	-3.75	3.81	94.2	Large
	4-4										
6	1595 to 1598	0.01	-3.81	0.45	0.03	0.45	0.01	-3.81	4.26	94.2	Large
	8-8										
7	143 to 150	-0.54	12.44	4.53	-0.50	12.46	4.53	-0.56	13.02	30.0	+1.30
	9-9										
8	176 to 326	-2.90	-8.30	-0.56	-0.22	-0.56	-2.89	-8.31	7.74	30.0	+2.87

1 Conservatively based on a 1.12-inch thick outer shell and on a 3850-psi crush strength aluminum honeycomb impact limiter (Section 2.6.7.3.1).

2 Refer to Figure 2.10.2-9 for component identification.

Table 2.6.7-30 Critical Stress Summary (1-Foot Top Corner Drop) – Loading Condition 3 - S_n – Drop Orientation = 15.74 Degrees

Loading Condition 3: -40°F Ambient Temperature and No Decay Heat Load

		S_n Stresses[1] (ksi)				Principal Stresses					
Comp. No.[2]	Section Cut Node to Node	S_x	S_y	S_z	S_{xy}	S_1	S_2	S_3	S.I.	Allow. Stress 3.0 S_m	Margin of Safety
	1-1										
1	2377 to 2577	-6.95	-0.47	-1.07	-0.53	-0.43	-1.07	-6.99	6.56	60.0	+8.15
	10-10										
3	1801 to 1805	0.47	14.21	7.54	1.89	14.46	7.54	0.22	14.25	60.0	+3.21
	11-11										
4	661 to 664	0.14	-7.03	-1.15	-0.29	0.15	-1.15	-7.04	7.20	94.2	Large
	4-4										
6	1595 to 1598	0.02	-7.43	0.70	0.05	0.70	0.02	-7.43	8.13	94.2	Large
	8-8										
7	143 to 150	-0.54	13.55	4.99	-0.59	13.58	4.99	-0.56	14.14	60.0	+3.24
	6-6										
8	381 to 385	-4.25	-8.32	-1.90	-0.23	-1.90	-4.23	-8.33	6.42	60.0	+8.34

1 Conservatively based on a 1.12-inch thick outer shell and on a 3850-psi crush strength aluminum honeycomb impact limiter (Section 2.6.7.3.1).

2 Refer to Figure 2.10.2-9 for component identification.

Table 2.6.7-31 Critical Stress Summary (1-Foot Top Corner Drop) – Loading Condition 3 - Total Range – Drop Orientation = 15.74 Degrees

Loading Condition 3: -40°F Ambient Temperature and Maximum Decay Heat Load

		Total Stress Range[1] (ksi)				Principal Stresses			Stress Differences		
Comp. No.[2]	Node	S_x	S_y	S_z	S_{xy}	S_1	S_2	S_3	S_1-S_2	S_2-S_3	S_3-S_1
1	2561	0.05	-1.17	-1.15	40.01	39.49	-1.15	-40.61	40.64	39.46	-80.10
3	1805	0.47	16.81	8.08	2.75	17.26	8.08	0.02	9.18	8.06	-17.24
4	1584	-0.04	4.04	-3.61	-0.44	4.09	-0.09	-3.61	4.17	3.52	-7.70
6	1598	-0.02	-7.58	0.65	0.03	0.65	-0.02	-7.58	0.67	7.56	-8.23
7	2	-0.55	14.68	5.23	0.43	14.69	5.23	-0.56	9.46	5.79	-15.25
8	385	-7.60	-7.37	-4.68	-1.24	-4.68	-6.24	-8.73	1.56	2.48	-4.05

1 Conservatively based on a 1.12-inch thick outer shell and on a 3850-psi crush strength aluminum honeycomb impact limiter (Section 2.6.7.3.1).

2 Refer to Figure 2.10.2-9 for component identification.

Table 2.6.7-32 Summary of Results – Impact Limiter Analysis for 1-Foot Free Drop

Analysis Description	Displacement (in)	Force (lb)	Equivalent[1] G Load Factor
Flat End Impact			
Bottom Limiter with Max Crush Strength	0.76	8.22×10^5	15.8
Bottom Limiter with Min Crush Strength	0.94	6.60×10^5	12.7
Top Limiter with Max Crush Strength	0.82	8.22×10^5	15.8
Top Limiter with Min Crush Strength	0.96	6.71×10^5	12.9
Corner Impact			
Bottom Limiter with Max Crush Strength	3.16	6.29×10^5	12.1
Bottom Limiter with Min Crush Strength	3.40	6.29×10^5	12.1
Top Limiter with Max Crush Strength	3.18	6.40×10^5	12.3
Top Limiter with Min Crush Strength	3.42	5.98×10^5	11.5

[1] Equivalent g load factor = Force/52,000.

Table 2.6.7-32 Summary of Results – Impact Limiter Analysis for 1-Foot Free Drop (continued)

Analysis Description	Displacement (in)	Force (lb)	Equivalent[1] G Load Factor
Flat Side Impact			
Bottom Limiter with Max Crush Strength	0.83	1.21×10^6	23.3
Bottom Limiter with Min Crush Strength	0.95	1.03×10^6	19.8
Top Limiter with Max Crush Strength	0.83	1.26×10^6	24.3
Top Limiter with Min Crush Strength	0.94	1.07×10^6	20.6

[1] Equivalent g load factor = Force/52,000.

Table 2.6.7-33 Summary of Results – Impact Limiter Analysis for 30-Foot Free Drop Subsequent to a 1-Foot Fall

Analysis Description	Displacement (in)	Force (lb)	Equivalent[1] G Load Factor
Flat End Impact			
Bottom Limiter with Max Crush Strength	8.50	2.50×10^6	48.1
Bottom Limiter with Min Crush Strength	10.30	2.03×10^6	39.0
Top Limiter with Max Crush Strength	8.47	2.51×10^6	48.3
Top Limiter with Min Crush Strength	10.24	2.04×10^6	39.2
Corner Impact			
Bottom Limiter with Max Crush Strength	11.30	3.08×10^6	59.2
Bottom Limiter with Min Crush Strength	12.70	2.58×10^6	49.6
Top Limiter with Max Crush Strength	11.38	3.14×10^6	60.4
Top Limiter with Min Crush Strength	12.72	2.98×10^6	57.3

[1] Equivalent g load factor = Force/52,000.

Table 2.6.7-33 Summary of Results – Impact Limiter Analysis for 30-Foot Free Drop Subsequent to a 1-Foot Fall (continued)

Analysis Description	Displacement (in)	Force (lb)	Equivalent[1] G Load Factor
Flat Side Impact			
Bottom Limiter with Max Crush Strength	8.60	2.65×10^6	48.7
Bottom Limiter with Min Crush Strength	10.30	2.17×10^6	41.8
Top Limiter with Max Crush Strength	8.42	2.71×10^6	49.7
Top Limiter with Min Crush Strength	10.00	2.22×10^6	42.7

[1] Equivalent g load factor = Force/52,000.

Table 2.6.7-34 Summary of Cask Drop Equivalent G Load Factors

Direction	Equivalent G Load Factor[1]			
	1-Foot Drop	31-Foot Drop		
		Total	Axial[2] Comp.	Lateral[3] Comp.
Lateral (Side)	24.3	49.7	—	49.7
Longitudinal	15.8	60.0	60.0	—
Corner (15.74°)	12.3	60.4	58.2	16.4
Oblique (30°)	—	54.4	47.1	27.2
Oblique (45°)	—	43.8	31.0	31.0
Oblique (60°)	—	44.4	22.2	38.5

[1] Equivalent g load factor = Force/52,000.
[2] Axial Component = total x cosθ where θ = 15.74°, 30°, 45°, or 60°
[3] Lateral Component = total x sinθ where θ = 15.74°, 30°, 45°, or 60°

Table 2.6.7-35 NAC-LWT Cask Hot Bolt Analysis – Normal Conditions

Nominal Diameter (in):	1.00	
Number of Bolts:	12	
Service Stress, Sy (ksi):	81.9	at a 300 degree-F Service Temperature
Bolt Expansion (in/in):	9E-06	
Bolt Modulus (ksi):	26700	
Lid Expansion (in/in):	9E-06	
Lid Modulus (ksi):	27000	
Stress Area (in2):	0.6051	
Grip Length (in):	7.99	
Maximum Pressure (psi):	50	
Seal Diameter (in):	15.750	
Preload Torque (ft-lbs):	260	at RT
Nominal Room Temp, RT:	70	deg-F
Bolt Circle Diameter (in):	17.88	
Lid Diameter (in):	22.50	

(a) Longitudinal Weight (lbs):	4941
(b) Lateral Weight (lbs):	941
Service DT (degrees):	157
[default value =]	230
CALCULATED LOADS & STIFFNESS	
(c) Bolt Thermal Load (lbs):	1423
(d) Bolt Preload (lbs):	34770
(e) Bolt Pressure Load (lbs):	812
(f) Bolt Stiffness (lbs/in):	1.9E+06
(g) Lid Stiffness (lbs/in):	2.1E+07

Angle wrt Vert. (Deg)	Impact Accel. (g)	<**** LOADS (lbs.) ****> Impact Tension	Impact Shear	Bolt Tension Applied	Bolt Tension Net	<**** STRESSES (psi) ****> Direct Tension	Direct Shear	Principal Sig-1	Principal Sig-2	Stress Intens.	Margin of Safety
	(h)		(k)	(l)	(m)	(n)	(o)		(p)	(q)	(r)
0 End	60.00	24705 (i)	0	25517	38292	63282	0	0	63282	63282	0.29
5 (+)	60.13	33641 (j)	411	34453	39027	64497	679	-7	64504	64511	0.27
10 (+)	60.25	33327	820	34138	39001	64454	1356	-29	64483	64511	0.27
15.7 Corner	60.40	32657	1282	33469	38946	64363	2118	-70	64433	64503	0.27
20 (+)	58.60	30924	1572	31736	38804	64128	2597	-105	64233	64338	0.27
25 (+)	56.50	28758	1872	29570	38626	63833	3094	-150	63983	64133	0.28
30 (calc)	54.40	26459	2133	27271	38436	63521	3525	-195	63716	63911	0.28
35 (+)	50.87	23402	2288	24213	38185	63105	3781	-226	63331	63557	0.29
40 (+)	47.33	20364	2386	21176	37935	62692	3943	-247	62939	63186	0.30
45 (calc)	43.80	17394	2429	18206	37691	62289	4014	-258	62546	62804	0.30
50 (+)	44.00	15884	2643	16696	37567	62083	4368	-306	62389	62695	0.31
55 (+)	44.20	14238	2839	15050	37431	61860	4692	-354	62213	62567	0.31
60 (calc)	44.40	12468	3015	13280	37286	61619	4983	-400	62019	62420	0.31
65 (+)	45.68	10843	3247	11655	37152	61398	5366	-465	61863	62329	0.31
70 (+)	46.97	9022	3461	9834	37002	61150	5719	-530	61681	62211	0.32
75 (+)	48.25	7014	3655	7825	36837	60877	6040	-593	61471	62064	0.32
80 (+)	49.53	4831	3825	5643	36657	60581	6322	-653	61233	61886	0.32
85 (+)	50.82	2487	3970	3299	36465	60262	6560	-706	60968	61674	0.33
90 Side	52.10	0	4086	812	36260	59924	6752	-751	60675	61427	0.33

Minimum Margin of Safety: 0.27

Table 2.6.7-36 NAC-LWT Cask Cold Bolt Analysis – Normal Conditions

Nominal Diameter (in):	1.00	
Number of Bolts:	12	
Service Stress, Sy (ksi):	85	at a 70 degree-F Service Temperature
Bolt Expansion (in/in):	8E-06	
Bolt Modulus (ksi):	27800	
Lid Expansion (in/in):	8E-06	
Lid Modulus (ksi):	28300	
Stress Area (in2):	0.6051	
Grip Length (in):	7.99	
Maximum Pressure (psi):	50	
Seal Diameter (in):	15.750	
Preload Torque (ft-lbs):	260	at RT
Nominal Room Temp, RT:	70	deg-F
Bolt Circle Diameter (in):	17.88	
Lid Diameter (in):	22.50	

Longitudinal Weight (lbs):	4941
Lateral Weight (lbs):	941
Service DT (degrees):	-90
[default value =]	0

CALCULATED LOADS & STIFFNESS

Bolt Thermal Load (lbs):	-594
Bolt Preload (lbs):	34770
Bolt Pressure Load (lbs):	812
Bolt Stiffness (lbs/in):	2.0E+06
Lid Stiffness (lbs/in):	2.2E+07

Angle wrt Vert. (Deg)	Impact Accel. (g)	<**** LOADS (lbs.) Impact Tension	Impact Shear	Bolt Tension Applied	Bolt Tension Net ****	<**** STRESSES (psi) Direct Tension	Direct Shear	Principal Sig-1	Principal Sig-2	Stress Intens. ****	Margin of Safety
0 End	60.00	24705	0	25517	36262	59928	0	0	59928	59928	0.42
5 (+)	60.13	33641	411	34453	36993	61135	679	-8	61143	61150	0.39
10 (+)	60.25	33327	820	34138	36967	61093	1356	-30	61123	61153	0.39
15.7 Corner	60.40	32657	1282	33469	36912	61002	2118	-73	61076	61149	0.39
20 (+)	58.60	30924	1572	31736	36771	60768	2597	-111	60879	60990	0.39
25 (+)	56.50	28758	1872	29570	36594	60475	3094	-158	60633	60791	0.40
30 (calc)	54.40	26459	2133	27271	36406	60165	3525	-206	60371	60577	0.40
35 (+)	50.87	23402	2288	24213	36156	59752	3781	-238	59990	60228	0.41
40 (+)	47.33	20364	2386	21176	35908	59341	3943	-261	59602	59863	0.42
45 (calc)	43.80	17394	2429	18206	35665	58940	4014	-272	59212	59484	0.43
50 (+)	44.00	15884	2643	16696	35541	58736	4368	-323	59059	59382	0.43
55 (+)	44.20	14238	2839	15050	35407	58514	4692	-374	58888	59262	0.43
60 (calc)	44.40	12468	3015	13280	35262	58275	4983	-423	58698	59121	0.44
65 (+)	45.68	10843	3247	11655	35129	58055	5366	-492	58547	59039	0.44
70 (+)	46.97	9022	3461	9834	34980	57809	5719	-560	58369	58930	0.44
75 (+)	48.25	7014	3655	7825	34816	57538	6040	-627	58165	58792	0.45
80 (+)	49.53	4831	3825	5643	34638	57243	6322	-690	57933	58622	0.45
85 (+)	50.82	2487	3970	3299	34446	56926	6560	-746	57672	58419	0.46
90 Side	52.10	0	4086	812	34243	56590	6752	-794	57384	58179	0.46

Minimum Margin of Safety: 0.39

Table 2.6.7-37 Summary of Neutron Shield Tank Analysis

Load Condition: 1-Foot End Drop and 1-Foot Side Drop

Description	Stress Magnitude (psi)	Margin of Safety[1]
Tank Shell	12,841	+0.07
Stiffener	11,746	+0.17
Stiffener Weld	2,424 lb/in	+0.23
Gusset Weld	1,418 lb/in	+1.10
Bottom End Plate	8,525	+1.79
Gusset Plate Cross Section	7,180	+LARGE
End Plate Welds	1,593	+LARGE
Top End Plate	11,172	+0.23

This table summarizes the stresses and margins for a design condition of 180 psig (Section 2.6.7.7.4), which envelops both the end drop and side drop conditions.

[1] Based on an allowable stress equal to the yield strength of Type 304 stainless steel at 250°F.

Table 2.6.7-38 Normal Transport Shield Tank Temperatures

Transport Condition	Average Fluid Temperature
100°F/Full Heat Load	227°F
68°F/No Heat Load	68°F
-20°F/Full Heat Load	99°F
-20°F/No Heat Load	-20°F

Table 2.6.7-39 Normal Transport Shield Tank Pressures

Transport Condition	Calculated Tank Pressure
PRVR	165 psig
100°F/Full Heat Load	25.6 psig
68°F/No Heat Load	0 psig

Table 2.6.7-40 Summary of Expansion Tank Analysis

Load Condition: 1-Foot End Drop and 1-Foot Side Drop

Description	Stress Magnitude (psi)	Margin of Safety[1]
Bottom/Top End Plate	3,375	+LARGE
Tank Shell	10,857	+0.26
Tank Stiffener	9,997	+0.37
Shell Weld	11,750	+0.17

This table summarizes the stresses and margins for a design condition of 180 psig (Sections 2.6.7.8 and 2.6.7.7.4), which envelops both the end drop and side drop conditions.

[1] Based on an allowable stress equal to the yield strength of Type 304 stainless steel at 250°F.

Table 2.6.7-41 Upper Ring – Cross-Section Principal Stresses

Section	P_m Stresses							$P_m + P_b$ Stresses						
	Component (ksi)				Principal (ksi)			Component (ksi)				Principal (ksi)		
	S_x	S_y	S_z	S_{xy}	S_1	S_2	S_3	S_x	S_y	S_z	S_{xy}	S_1	S_2	S_3
a-a	-0.8	4.7	1.9	-0.1	4.7	-0.8	1.9	-2.6	9.0	4.0	-1.0	9.1	-2.7	4.0
b-b	0.1	4.9	1.9	-0.2	4.9	0.1	1.9	1.2	8.0	2.9	-1.0	8.1	1.1	2.9
c-c	-0.1	5.5	2.0	0.5	5.5	-0.3	2.0	-0.2	6.5	2.6	1.0	6.6	-0.3	2.6

2.6.8 Corner Drop

According to 10 CFR 71.71(c)(8), this test is not applicable to the NAC-LWT cask because the cask is composed of materials other than fiberboard or wood.

2.6.9 Compression

According to 10 CFR 71.71(c)(9), this test is not applicable to the NAC-LWT cask because the package weight is greater than 5,000 kilograms (11,023 pounds).

2.6.10 Penetration

This condition is defined in 10 CFR 71.71(c)(10) as a 40-inch drop of a 13-pound, 1.25-inch diameter penetration cylinder with a hemispherical end, onto any exposed surface of the cask. The acceptance criteria is that there will be no adverse effects on either the ability of the cask to maintain containment of the contents or to survive a hypothetical accident. The following package components could potentially be damaged by this penetration impact: (1) the impact limiter, (2) the expansion tank, (3) the neutron shield tank, and (4) the port cover. An evaluation of a penetration impact on each of these components follows.

2.6.10.1 Impact Limiter – Penetration

The outer shell of the impact limiter resists puncture of the aluminum honeycomb by the penetration cylinder; however, this resistance is conservatively not considered in the analysis. The 13.0-pound penetration cylinder drops 40.0 inches producing 13.0 x 40.0 = 520 inch-pounds of energy, which is absorbed by the limiter. The minimum crush strength of the limiter is 3150 psi (Section 2.6.7.4.6), and the area of the penetration cylinder is 1.227 square inches. Therefore, using the minimum honeycomb crush strength and the average impact area in the conservation of energy equation, the penetration cylinder will compress the aluminum honeycomb to a depth of 520/[(3150)(1.227)/2] = 0.270 inch. This shallow depression does not adversely affect the performance of the impact limiter.

2.6.10.2 Expansion Tank – Penetration

The expansion tank shell is vulnerable to the penetration cylinder. This analysis documents the expansion tank shell structural adequacy to resist the penetration event.

The expansion tank shell is supported radially every 45 degrees by radial stiffeners. Assume the penetration cylinder impacts the shell at the center of the unsupported region as shown in Figure 2.6.10-1.

Chapter 12-5 of Strength of Materials (Singer) analyzes the problem of a falling object on an elastic member, and derives the following equation for the dynamic impact stress (S_{dyn}) in terms of the static displacement (δ_{st}) and the static stress (S_{st}), where the static values are for the weight (W) resting on the elastic member:

$$S_{dyn} = S_{st}\left[1 + \left(1 + \frac{2h}{\delta_{st}}\right)^{0.5}\right]$$

where:

h = height of drop = 40.0 inches

The static displacement is evaluated by assuming an arched plate with built-in edges (a stiffer plate provides a more conservative analysis), which is centrally loaded by the static weight (W) of the penetration cylinder. The dimensions of the arched plate representing the expansion tank are identified in Figure 2.6.12-2:

t = 0.315 in

r = 22.00 inches

$a = 2\pi r \times 45°/360° = 2\pi(22.0)(0.125) = 17.28$ inches

b = 46.00 inches

Because the aspect ratio is small (2.66:1) the effect of the short edge fixity is considered. The effective width of the plate tangential to the radius is calculated by using Article 36 on page 133 of Formulas for Stress and Strain (Roark). Assume the circular area of the load is half the maximum; therefore, the radius $c = [(0.625)^2/2]^{0.5} = 0.442$ inch, or 0.026(a). The table in the reference does not give a/b values of aspect ratios beyond 2:1; therefore, a/b = 2.0 is assumed.

Interpolation of the table in the reference for c = 0.026(a) yields e/b = 0.59; then, w_e = (0.59)(2)(17.28) = 20.39 inches. The effective width of the plate in the longitudinal direction is the (a) dimension. The amount of load transferred to each edge is calculated by assuming two fixed plates, free on two opposite edges and built-in on the other two, and solving for compatible deflections at the edge common to both plates. The equation for the percent of load taken by each plate is derived as follows:

The terms δ_a and δ_b, P_a and P_b, and k_a and k_b are deflections, loads, and spring constants for plates fixed on the (a) and (b) edges, respectively.

$$\delta_a = \delta_b;\ P_a/k_a = P_b/k_b;\ P_a = P_b(k_a/k_b)$$

$$P_a + P_b = W;\ P_b[(k_a/k_b) + 1] = W$$

$$P_b/W = k_b/(k_a + k_b);\ P_a/W = 1 - P_b/W$$

The spring constant (k_b) for edges fixed at (b) is evaluated as follows:

$k_b = P / \delta_b$

where:

P = any load

δ_b = the deflection due to P

"Charts Simplify Calculations for Moments and Deflections of Circular Arches" (Blake) gives the following equation for the static displacement (δ_b) of the arch with built-in edges:

$$\delta_b = (Pr^3/EI)K_b$$

where:

$$E = 27 \times 10^6 \text{ psi } (300°F)$$

$$r = 22.00 \text{ in}$$

$$I = w_e t^3/12 = (20.39)(0.32)^3/12$$
$$= 0.0531 \text{ in}^3$$

$$K_b = 0.00025 \text{ (Blake, Figure 3, } \beta = 45°)$$

thus

$$\delta_b = \frac{P(0.00025)(22.00)^3}{(27.0 \times 10^6)(0.0531)}$$

$$= P(1.857 \times 10^{-6}) \text{ in}$$

$$k_b = P/\delta_b = 5.385 \times 10^5 \text{ lb/in}$$

The spring constant (k_a) for edges fixed at (a) is evaluated as follows:

$$k_a = P / \delta_a$$

where:

P = any load

δ_a = the deflection due to P

The plate with the edges fixed at (a) is treated as a flat plate with a curvature, which increases the moment of inertia. The equation for the deflection at the center of the plate for a central load (P) is:

$$\delta_a = Pb^3 / 192 EI$$
$$= P(1.379 \times 10^{-5})$$

where:

$I = r^3t\ [a + \sin\alpha \cos\alpha - (2\sin^2\alpha)/\alpha]$ ("Research and Advanced Development Applied Mechanics," page 8)

$= 1.362\ in^4$

$\alpha = \pi/8$ radians

then

$k_a = P/\delta_a = 7.252 \times 10^4$ lb/in

and

$P_b/W = (5.385 \times 10^5)/[(7.252 \times 10^4) + (5.385 \times 10^5)]$

$= 0.881$, or P_b is 88.1 percent of W

$P_a/W = 1 - 0.881 = 0.119$, or P_a is 11.9 percent of W

The static deflection is calculated using the load, P_a, and the spring constant for the curved plate as a longitudinal beam:

$\delta_{st} = 0.881\ W/k_a = 0.881(13.00)/(5.385 \times 10^5)$

$= 2.128 \times 10^{-5}$ in

The static stress is calculated using the formulas from "Charts Simplify Calculations for Moments and Deflections of Circular Arches" (Blake) for an arched plate with a central load (P_a) as follows:

The static bending moment (M_{st}) at the load for the arched plate with built-in edges resulting from the central load P_b is:

$M_{st} = H_b r(\sin\theta - \sin\alpha) - Rr(\cos\alpha - \cos\theta) + M_o$

where:

$M_o = -\ P\ r\ K_m = -0.881\ W\ r\ K_m$

$H_b = P\ K_{hb} = 0.881\ W\ K_{hb}$

$\theta = 90.0°$

$\alpha = 67.5°$

$R = 0.5\ (0.881W) = 0.441W$

$K_m = 0.0225$

$K_{hb} = 2.375$ (Blake, Figure 3, $\beta = 45°$)

then

$H_b = (0.881)(13.0)(2.375) = 27.20$ lbs

$R = 0.441(13.0) = 5.73$ lbs

$M_o/r = -0.881(13.0)(0.0225) = -0.258$ in-lb

$M_{st} = 22.00[27.20(\sin 90.0° - \sin 67.5°) - 5.73 (\cos 67.5° - \cos 90.0°) + (-0.258)]$
$= -8.37$ in-lb

The static stress, determined from the elastic plate formula, is:

$$S_{st} = \frac{6M_{st}}{w_e t^2} + \frac{H_b}{w_e t}$$

$$= 29.06 \text{ psi}$$

Substitution of S_{st} and δ_{st} into the equation for the dynamic impact stress produces:

$$S_{dyn} = 29.06 \left[1 + \left(1 + \frac{(40.0)}{2.128 \times 10^{-5}}\right)^{0.5}\right]$$

$$= 56,374 \text{ psi}$$

This stress exceeds the 22,500 psi yield strength of Type 304 stainless steel at 300°F, but not the 66,000 psi ultimate strength; therefore, it is concluded that an impact by the penetration cylinder would produce a permanent deformation, but it would not rupture the expansion tank shell.

The expansion tank meets the requirements for penetration resistance per 10 CFR 71.71(c)(10).

2.6.10.3 Neutron Shield Tank – Penetration

The neutron shield tank shell is vulnerable to the penetration cylinder. This analysis documents the neutron shield tank shell structural adequacy to resist the penetration event.

The neutron shield tank shell is supported radially every 45 degrees by rigid stiffeners. Assume the penetration cylinder impacts the shell at the center of the unsupported region as shown in Figure 2.6.10-1.

The static displacements and stresses resulting from the impact of a 13-pound penetration cylinder are evaluated by the use of the ANSYS finite element method. The neutron shield tank shell is modeled as a complete circle, represented by 80 two-dimensional elastic beam (STIF3) elements, each spanning a 4.5-degree arc. Each stiffener is represented by four STIF3 elements. One edge of each stiffener is rigidly attached to the outer shell of the cask.

The dimensions of the arched plate representing the shield tank are identified in Figure 2.6.10-2:

$t = 0.24$ in
$r = 19.345$ inches

$a = 2\pi r \times 45°/360°$

$= 2\pi(19.345)(0.125)$

$= 15.12$ inches

$= 164.00$ inches

Because the aspect ratio is large (10.7:1), the effect of the short edge fixity is ignored. The effective width of the plate tangential to the radius is calculated by using Article 36 on page 133 of Formulas for Stress and Strain (Roark). As derived in Section 2.6.10.2, the radius of the load is 0.442 inch, or 0.0292(a). The maximum tabular value in the reference for b/a = 2 is conservatively assumed. Interpolation for c = 0.0292(a) gives e/b = 0.598; then, w_e = (0.598)(2)(15.12) = 18.084 inches.

The properties of the beam elements are as follows:

$E = 27 \times 10^6$ psi at 200°F

$A = 18.084 \times 0.24$

$= 4.268$ in^2

$I = 18.084 \times (0.24)^3/12$

$= 0.0198$ in^4

From the results of the ANSYS finite element analysis, the static deflection and stress at the point of load application are 0.0003451 inch and 116.18 psi, respectively. Substitution of S_{st} and δ_{st} into the equation for the dynamic impact stress (Section 2.6.10.2) produces:

$$S_{dyn} = 116.18 \left[1 + \left(1 + \frac{2(40)}{0.0003451}\right)^{0.5}\right]$$

$$= 56{,}054 \text{ psi}$$

The margin of safety for the noncontainment structure during an accident event is:

$$M.S. = \frac{S_{tu}}{S_{dyn}} - 1 = \frac{66{,}000}{56{,}054} - 1 = \underline{+0.18}$$

Impact by the penetration cylinder may produce a permanent deformation, but it will not rupture the neutron shield tank; therefore, the neutron shield tank meets the requirements for penetration resistance as specified in 10 CFR 71.71(c)(10).

2.6.10.4 Port Cover – Penetration

The port covers are analyzed for impact by the penetration cylinder. This analysis documents the structural adequacy of the port cover to resist the penetration event.

During normal operations, particularly during fuel loading, it is possible that a hand tool could drop onto the NAC-LWT cask. The following analysis is performed to demonstrate that such an occurrence (presumed to be a 13-pound, 1.25-inch diameter projectile dropped through a distance of 40 inches) will not cause loss of the cask containment capability as a result of damage to the port cover. The port cover is shown in Figure 2.6.10-3.

The static displacement and stress is evaluated by assuming the port cover is loaded at the center by the static weight (W) of the penetration cylinder. The port cover is stiffened by the attached cylinder wall and is clamped by the bolts. This geometry requires that the displacement be evaluated in two steps - (1) from the bolt circle to the outside diameter of the cylinder, and (2) from the inside diameter of the cylinder to the center of the plate.

The first step in the calculation is made by using equation (92) from Theory of Plates and Shells (Timoshenko, 1940) and treating the whole plate as being clamped at the bolt circle and finding the displacement at the outside diameter of the cylinder, $a_1 = 1.875$, $r_1 = 1.436$, as follows:

$$\delta_{st} = -\frac{Wr^2}{8\pi D}\ln\frac{r}{a} + \frac{W(a^2 - r^2)}{16\pi D}$$

$$D = \frac{Et^3}{12(1 - \nu^2)}$$

where:

ν = Poisson's ratio = 0.30

$$\delta_{st_1} = -\frac{0.75W(1 - \nu^2)}{\pi Et^3}\left[(a_1^2 - r_1^2) + 2\ln\frac{r_1}{a_1}\right]$$

$$= -9.3505 \times 10^{-8} \text{ in}$$

The second step in the calculation is to treat the portion of the plate from the inside diameter of the cylinder to the center of the plate as clamped, $a_2 = 0.8125$ and $r_2 = 0$, using the same equation, which reduces as follows:

$$\delta_{st_2} = -\frac{0.75Wa_2^2(1 - \nu^2)}{\pi Et^3}$$

$$= -6.7022 \times 10^{-8} \text{ in}$$

The total static displacement of the plate is:

$$\delta_{st} = \delta_{st_1} + \delta_{st_2} = -1.6043 \times 10^{-7} \text{ in}$$

The static stress at the point of impact is calculated using equation (97) from Theory of Plates and Shells (Timoshenko, 1940) using the portion of the plate inside the cylinder as a plate with clamped edges as follows:

$$S_{st} = \frac{W(1 - \nu)}{t^2}\left[0.485 \ln\left(\frac{a_2}{t}\right) + 0.52\right]$$

$$= 3.6974 \text{ psi}$$

Substitution of S_{st} and δ_{st} into the equation for dynamic impact stress referenced in Section 2.6.10.2 produces:

$$S_{dyn} = 3.6974\left[1 + \left(1 + \frac{2(40.0)}{1.6043 \times 10^{-7}}\right)^{0.5}\right]$$

$$= 82,570 \text{ psi}$$

The margin of safety against yield strength of the SA-705, Grade 630, Type H1150 stainless steel port cover at 300°F is:

MS = 93,000/82,570 - 1 = +0.23

The port cover meets the requirements for penetration resistance according to 10 CFR 71.71(c)(10).

2.6.10.5 Alternate Port Cover – Penetration

This analysis documents the adequacy of the alternate port cover design to resist a postulated normal conditions of transport penetration event. Analyses presented evaluate the consequences of the penetration event on the port cover, attachment bolt stresses and inertial loads acting on the port cover to reduce the compressive load on the primary O-ring. A bounding analysis evaluating the consequences of differential thermal expansion on the attachment bolt stresses and the compressive load applied to the port cover primary O-ring is presented in Section 2.7.2.4.3.

The alternate port cover design is shown in Figure 2.6.10-3. The alternate port cover design includes the primary O-ring between the inner face of the port cover barrel and the sealing surface located in the cask top forging. The secondary (test) O-ring is located in a groove on the barrel of the port cover body. Both O-rings are manufactured from Viton®. The alternate port cover body is fabricated from Type 630, 17-4 PH precipitation-hardened stainless steel. The alternate port cover bolts are SA-193 GR B6 (Type 410 stainless steel) socket-head cap screws.

Normal operating condition requirements postulate a penetration event intended to represent a hand tool that inadvertently drops and strikes the port cover installed on the cask. A steel bar of

1-1/4 inch diameter with a hemispherical head and weighing 13 pounds simulates a tool for analysis purposes. The steel bar is assumed to be dropped from a height of 40 inches. This analysis shows that there is no loss of containment capability, even if the tool strikes the alternate port cover in its most vulnerable location.

The bolt preload applies the required compressive force on the face O-ring to maintain a seal between the port cover and the top forging. The O-ring compressive force required to maintain a seal is 120 pounds per linear inch of O-ring, according to the manufacturer. Using the average radius of the O-ring cavity to determine the length of the O-ring, the force to maintain a seal is 861 pounds. The force applied by the bolt preload torque is calculated as:

$$F = T / 0.2\ (d)$$

where:

F = tensile load generated due to bolt torque, pounds

T = installation torque, 100 inch-pounds

d = minimum cross-sectional diameter, 0.281 inch

The calculated force applied by torquing one port cover bolt is 1,780 pounds, approximately twice the compressive load necessary to maintain a seal. There are three bolts for each port cover.

The tensile force applied by the port cover bolts to maintain the load on the O-ring is evaluated. ANSYS is used to model the reaction of the port cover structure to the compressive applied loads. The port cover bolt load acts against the load needed to load the O-ring through the port cover body. Two load cases for normal conditions of transport penetration loading and two load cases for hypothetical accident conditions pin puncture (presented in Section 2.7.2.4.3) are evaluated.

Finite element analysis is used to determine the dynamic impact load resulting from the penetrating loading event. Then the port cover bolt torque preload and pressure loads are evaluated and are combined with the dynamic impact load to determine the total compression load on the inner face O-ring.

A three-dimensional model of the port cover is used to determine the static deflection when a 13-pound load is applied at the center of the port cover exterior. The port cover is a hollow barrel, with a flat thick plate at the outer end of the barrel. The plate and barrel slide into a stepped cylindrical bore in the upper end forging. The only exposed port cover surface is the outer face of the 1-inch thick port cover bolting flange. Deflection of the port cover due to the static load is calculated and used to determine the equivalent dynamic load, resulting from the 40-inch free-fall of the steel bar.

A one-sixth (1/6) section, three-dimensional finite element model of the alternate port cover, shown in Figure 2.6.10-4, was constructed using ANSYS Version 5.5. The model is a 60° wedge section of the port cover body. The body is constructed using SOLID45 3-D structural solid elements, CONTAC52 node-to-node contact elements, and BEAM4 three-dimensional two node beam elements. The node-to-node contact elements are used at the inner end surface, where the O-ring is located, to evaluate the sealing force. An initial strain is specified in the BEAM4 elements to simulate the initial bolt torque preload force. Since the port cover bolt is positioned on a model symmetry plane, the calculated bolt preload force applied to the port cover is half (1/2) of the total preload force. A force of 120 lbs. per linear inch of O-ring is required to maintain a seal. Using the average radius of O-ring cavity, the total required sealing force is calculated to be 861 pounds. Since the model is 1/6 of the actual port cover, this corresponds to a force of 861/6 = 143.5 lbs. required in the model to maintain sealing.

Symmetry boundary conditions are applied to the model at 0° and 60° surfaces. Model nodal coordinate systems have been rotated in the cylindrical coordinate system to facilitate the application of the symmetry boundary conditions. To prevent axial motion of the port cover, the port cover bolt is restrained axially at the bottom. The node-to-node contact elements on the inner end surface, the "ground" node of the contact elements, is fixed in all degrees-of-freedom.

Two simplifying assumptions were made in the ANSYS analysis consistent with accepted engineering practice. First, it is assumed for small deflections that materials behave elastically, and second, nominal dimensions are the basis for the ANSYS model geometry.

The equivalent dynamic loading, from Ugural and Fenster, is calculated using the following relation:

$$P_{dyn} = W\,(1 + (1 + 2h / \delta_{st})^{1/2})$$

where:

P_{dyn} = dynamic load resulting from weight (W) free falling a height (h), lbs

W = weight, 13 lbs

h = drop height, 40 inches

δ_{st} = static deflection resulting from weight (W) on plate, inches

The dynamic penetration load was calculated to be 11,334 pounds, resulting from the 13-pound steel pin dropping a distance of 40 inches on to the port cover. The sealing surface bearing stress is calculated to be 4,027 psi, which results in a margin of safety of +4.9 compared with yield strength of the upper forging. The dynamic load on the port cover is applied as a bearing load, which will pass through the alternate port cover body, to the top forging. Also, the dynamic load

increases the compressive force on the inner end O-ring, trapped in an O-ring groove at the bottom of the port cover body. Thus, the primary seal is not affected.

Bolt preload alone and preload combined with the normal operating pressure are the two load cases evaluated for normal conditions of transport. The normal condition cavity pressure calculated in Section 3.4.4 is 28.3 psia. The allowable bolt stress of 2 S_m or 50,600 psi is conservatively evaluated at 400°F. The normal condition analysis results are:

Load Case	Preload	Preload + Normal Pressure
Evaluation Temperature (°F)	400	400
Calculated Seal Force (lbs)	891	883
Percent O-ring compression (20-30% compression to maintain seal)	25.2[1]	25.2[1]
Bolt Tensile Force (lbs)	1781	1782
Bolt Stress (based on Tensile Stress Area) (psi)	28,720	28,728
Bolt Margin of Safety	0.76	0.76

[1] Maximum compression possible due to metal to metal contact with O-ring fully compressed in O-ring groove.

Figure 2.6.10-1 Impact of Penetration Cylinder on Neutron Shield Tank and Expansion Tank – Points of Impact

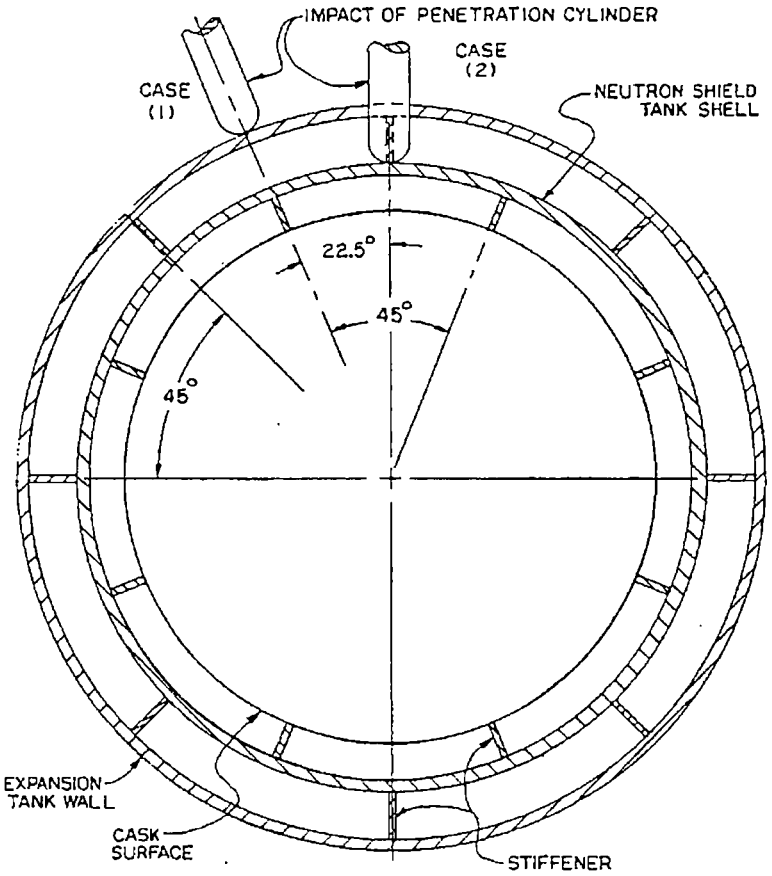

Figure 2.6.10-2 Impact of Penetration Cylinder on Neutron Shield Tank and Expansion Tank – Details for Analysis

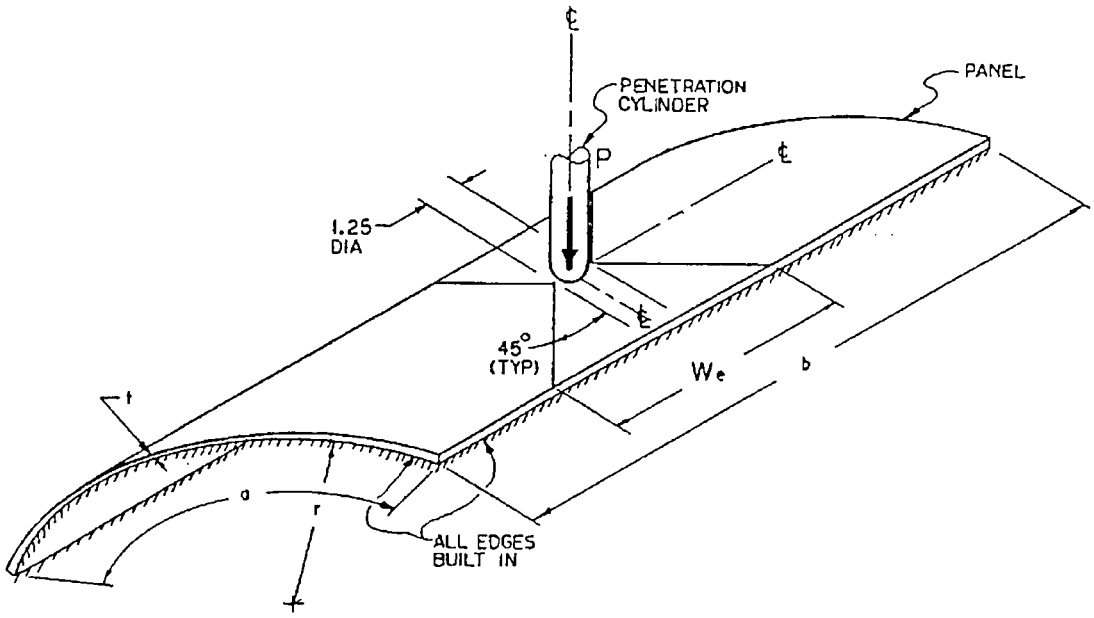

Figure 2.6.10-3 Impact of Penetration Cylinder on Port Cover

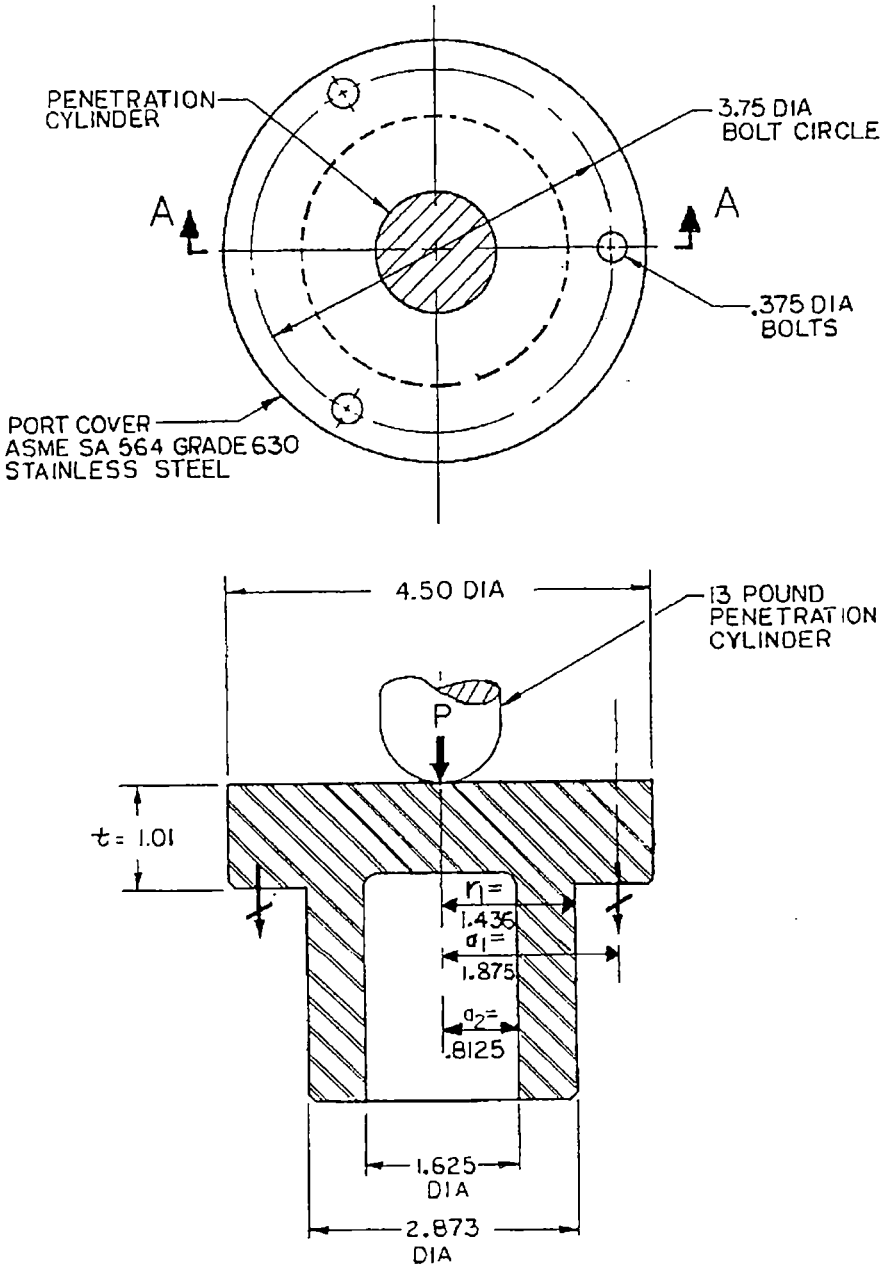

Figure 2.6.10-4 One-Sixth Model of the Alternate Port Cover – 60° Symmetry

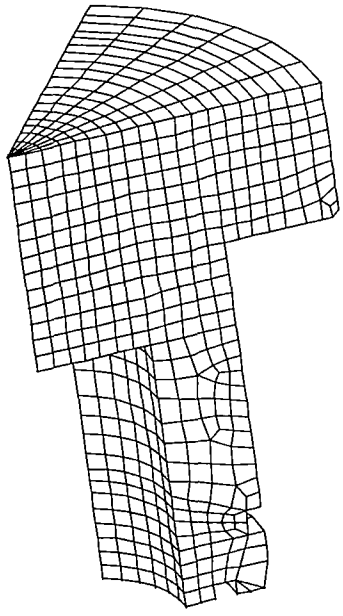

2.6.11 Fabrication Conditions

The process of manufacturing the NAC-LWT cask can introduce thermal stresses in the inner and outer shells as a result of pouring molten lead between them. These thermal stresses are evaluated to provide assurance that the manufacturing process does not adversely affect the normal operation of the cask or its ability to survive an accident. Residual stresses in the containment vessel and the outer shell induced by shrinkage of the lead shielding after the lead pouring operation are relieved early in the life of the cask because of the low yield strength of lead. Any residual stresses in the containment vessel shell due to inelastic strain associated with the secondary local bending stresses, which result from the lead pour thermal gradient, are considered in the total stress range for normal and accident load conditions according to Regulatory Position 7 of Regulatory Guide 7.6.

For the lead pouring process (Appendix 8.3), the temperature of the cask shells is controlled between 550°F (288°C) and 650°F (343°C), and the lead temperature before pouring is between 698°F (370°C) and 790°F (421°C). Heating of the cask is performed using heaters inside the inner shell and heating rings around the outer shell. Heat up is time controlled; consistent with maintaining shell temperatures uniformly. The shell temperatures are measured by thermocouples attached to the shell surfaces. A portable thermometer is also used to measure temperature at any location. Heating is carried out after all the preparations have been completed including melting of the lead in order to minimize the time that the cask is heated.

The lead is poured after the cask reaches the specified temperatures. Prior to lead pouring, the cask flange area is heated with hand-held burners to approximately 572°F (300°C). Pouring is carried out continuously using a filling tube with its open end maintained under the lead surface. The pouring time is kept as short as possible. During pouring, the interior heaters and exterior heating rings are continuously energized.

The cooling process consists of sequentially turning the heating rings and interior heaters off, starting from the lowest point, and of spraying the cask with water from the outside. Molten lead is maintained until the upper surface starts to solidify. This process allows the molten lead to fill the space created by the lead shrinkage as it cools.

2.6.11.1 Lead Pour

2.6.11.1.1 Cask Shell Geometry

At 70°F, the Type XM-19 stainless steel shell geometry is as follows:

Inner Shell

Inside Diameter	d_i	13.375 inches
Outside Diameter	d_o	14.875 inches
Shell Thickness	t_i	0.75 in

Outer Shell

Inside Diameter	D_i	26.375 inches
Outside Diameter	D_o	28.620 inches
Shell Thickness	T_o	1.12 inches

2.6.11.1.2 Stresses Due to Lead Pour

The melting point of lead is 620°F. Assuming that the lead and the inner and outer shells are uniformly at this temperature, the hydrostatic pressure produced by the column of lead is:

$$p = \rho h$$
$$= 72 \text{ psi}$$

where:

$\rho = 0.41$ lb/in^3 (lead density)

$h = 175$ inches (height of lead column)

At 620°F, the shell geometric dimensions are:

$$d'_o = d_o (1 + \alpha\Delta T)$$
$$D'_i = D_i (1 + \alpha\Delta T)$$
$$t' = t (1 + \alpha\Delta T)$$

where:

$$\alpha = 9.05 \times 10^{-6} \text{ in/in/°F at 620°F}$$

$$\Delta T = 620 - 70 = 550°F$$

$$d'_o = 14.875 \left[1 + 9.05 \times 10^{-6}(550)\right] = 14.9490 \text{ in}$$

$$D'_i = 26.375 \left[1 + 9.05 \times 10^{-6}(550)\right] = 26.5063 \text{ in}$$

$$t'_i = 0.75 \left[1 + 9.05 \times 10^{-6}(550)\right] = 0.7537 \text{ in}$$

$$t'_o = 1.12 \left[1 + 9.05 \times 10^{-6}(550)\right] = 1.1256 \text{ in}$$

The inner shell is subjected to an external hydrostatic pressure and the outer shell to an internal hydrostatic pressure, of 72 psi. This causes the inner shell to decrease in diameter and the outer shell to increase in diameter.

The inner shell decreases in size radially (Roark and Young, Case lb, page 448):

$$\Delta r_o = \frac{q(r_o')^2}{Et_i'} = \frac{-72(14.9490/2)^2}{25.2 \times 10^6(0.7537)} = -0.0002 \text{ in}$$

where:

$E = 25.2 \times 10^6$ psi at 620°F.

The outer shell increases in size radially:

$$\Delta R_i = \frac{q(R_i')^2}{Et_o'} = \frac{72(26.5063/2)^2}{25.2 \times 10^6(1.1256)} = 0.0004 \text{ in}$$

The shell geometries at 620°F and 72 psi hydrostatic pressure are:

$d''_o = 14.9490 - 2(0.0002) = 14.9486$

$D''_i = 26.5063 + 2(0.0004) = 26.5055$

The hoop stresses in the inner and outer shells at 620°F are:

$$S_{hi} = \frac{Pd_o''}{2t_i'}$$

$$= \frac{-72(14.9486)}{2(0.7537)} = -714 \text{ psi (inner shell)}$$

$$S_{ho} = \frac{PD_i''}{2t_o'}$$

$$= \frac{72(26.5055)}{2(1.1256)} = 847 \text{ psi (outer shell)}$$

2.6.11.2 Cooldown

2.6.11.2.1 Hoop Stresses

Lead decreases in volume during solidification. As the lower lead region solidifies, the molten lead above fills the shrinkage void between the solidifying lead and the inner and outer shells, thus, maintaining the 72 psi pressure on the shells.

The stress-free inner and outer radii of the solidified lead can be calculated (Roark and Young, Case 1a and 1c, page 504) as:

$$\Delta a = \frac{q}{E}\left[\frac{2ab^2}{a^2 - b^2}\right] - \frac{qa}{E}\left[\frac{a^2 + b^2}{a^2 - b^2} - \nu\right]$$

$$= 0.0004 \text{ in}$$

$$\Delta b = \frac{qb}{E}\left[\frac{a^2 + b^2}{a^2 - b^2} + \nu\right] - \frac{q}{E}\left[\frac{2a^2b}{a^2 - b^2}\right]$$

$$= 0.0002 \text{ in}$$

where:

q = -72 psi pressure
E = 1.47 x 10^6 psi
ν = 0.4 Poisson's ratio
a = 26.5055/2 = 13.2527 inches
b = 14.9486/2 = 7.4743 inches

then

$$R_{o\ell} = 13.2527 + 0.0004 = 13.2531 \text{ in}$$

$$R_{i\ell} = 7.4743 + 0.0002 = 7.4745 \text{ in}$$

When cooled to 70°F, the inside radius of the lead is such that:

$$R'_{i\ell}\ (1 + \alpha\Delta T) = R_{i\ell}$$

where:

$R'_{i\ell}$ = inside radius of the stress-free lead at 70°

α = 20.4 x 10^{-6} in/in/°F

ΔT = 550°F (620-70)

then

$$R'_{i\ell} = 7.3936 \text{ in}$$

likewise

$$R'_{o\ell} = R_{o\ell}/(1 + \alpha\Delta T) = 13.1105 \text{ in}$$

The outside radius of the stress-free inner shell is 14.875/2 = 7.4375 inches, which is larger than the stress-free inner radius of the lead shell. Therefore, there exists an interface pressure between the lead and the inner shell after cooling to 70°F. The interface pressure, when acting on the lead cylinder and inner shell, is such that the inner radius of the lead cylinder is the same as the outer radius of the inner shell (Roark and Young, Case 1a, page 504).

$$R''_{i\ell} = b + \Delta b$$

$$= b + \frac{qb}{E}\left(\frac{a^2 + b^2}{a^2 - b^2} + \nu\right)$$

where:

$R''_{i\ell}$ = inside radius of lead cylinder at 70°F

$\nu = 0.4$

$E = 2.28 \times 10^6$ psi

$a = 13.1105$ inches

$b = 7.3936$ inches

then

$$R''_{i\ell} = 7.3936 + \left(\frac{7.3936q}{2.28 \times 10^6}\right)\left(\frac{13.1105^2 + 7.3936^2}{13.1105^2 - 7.3936^2} + 0.4\right)$$

The outside radius of the inner shell at 70°F under the interface pressure q (Roark and Young, Case 1c, page 504) is:

$$r_o = a_s - \Delta a_s$$

$$= a_s - \frac{qa_s}{E}\left(\frac{a_s^2 + b_s^2}{a_s^2 - b_s^2} - \nu\right)$$

where:

r_o = outside radius of inner shell at 70°F

$a_s = 14.875/2 = 7.4375$ inches

$b_s = 13.375/2 = 6.6875$ inches

$E = 28.3 \times 10^6$ psi

$\nu = 0.275$

then

$$r_o = 7.4375 - \left(\frac{7.4375q}{28.3 \times 10^6}\right)\left(\frac{7.4375^2 + 6.6875^2}{7.4375^2 - 6.6875^2} - 0.275\right)$$

Equating $R''_{i\ell}$ and r_o and solving for q:

q = 4401 psi interface +pressure

The lead shell geometry is:

$$R''_{i\ell} = 7.3936 + \left(\frac{7.3936(4401)}{2.28 \times 10^6}\right)\left(\frac{13.1105^2 + 7.3936^2}{13.1105^2 - 7.3936^2} + 0.4\right)$$

$$= 7.4269 \text{ in}$$

$$R''_{o\ell} = R'_{o\ell} + \frac{q}{E}\left(\frac{2R'_{o\ell}\, R'^{\,2}_{i\ell}}{R'^{\,2}_{o\ell} - R'^{\,2}_{i\ell}}\right)$$

$$= 13.1105 + \left(\frac{4401}{2.28 \times 10^6}\right)\left(\frac{2 \times 13.1105 \times 7.3936^2}{13.1105^2 - 7.3936^2}\right)$$

$$= 13.1341 \text{ in}$$

The corresponding maximum lead shell hoop stress is:

$$S_{hPb} = (4401)\left(\frac{13.1341^2 + 7.4269^2}{13.1341^2 - 7.4269^2}\right)$$

$$= 8538 \text{ psi}$$

Obviously, the lead cannot sustain the above stress. The interference between the lead shell and the inner shell is 0.0439 inches (7.4375 - 7.3936). To fully accommodate this interference, the lead must undergo a strain of 0.0439/7.3936 = 0.0059 or 0.59 percent. From Figure 21 of NUREG/CR-0481, the lead stress for the above strain is 850 psi. The corresponding interface pressure for this stress in the lead shell is:

$$q = (S)\left[\frac{R''^2_{o\ell} - R''^2_{i\ell}}{R''^2_{o\ell} + R''^2_{i\ell}}\right]$$

$$= (850)\left[\frac{13.1341^2 - 7.4269^2}{13.1341^2 + 7.4269^2}\right]$$

$$= 438 \text{ psi interface pressure}$$

The change in geometry of the inner shell for this interface pressure is:

$$\Delta a = \left[\frac{-438}{28.3 \times 10^6}\right]\left[\frac{2(7.4375)(6.6875^2)}{7.4375^2 - 6.6875^2}\right]$$

$$= 0.0010 \text{ in}$$

This can conservatively be neglected in the analysis. The inner shell hoop stress is:

$$S_{his} = (-438)\left[\frac{7.4375^2 + 6.6875^2}{7.4375^2 - 6.6875^2}\right]$$

$$= -4136 \text{ psi}$$

2.6.11.2.2 Axial Stresses

Axial stresses also develop in the lead shell and inner shell during fabrication as a result of the unequal shrinkage of the lead and steel shells. Assume bonding of the lead shell to the inner shell during the cooldown process after completion of lead pouring. The strain in the lead, when cooled to 70°F, is:

$$\epsilon = (\alpha_\ell - \alpha_s)\Delta T$$

$$= 0.0062 \text{ in/in or } 0.62 \text{ percent}$$

where:

$$\alpha_\ell = 20.4 \times 10^{-6} \text{ in/in/°F}$$

$$\alpha_s = 9.05 \times 10^{-6} \text{ in/in/°F}$$

$$\Delta T = 620 - 70 = 550°F$$

Extrapolating from Figure 2.3.1-1, for this strain, an axial stress of approximately 850 psi exists in the lead shell. The total force in the lead caused by assuming non-deformability of the inner shell is:

$$P_{sPb} = p_\ell A_\ell$$

$$= 850\pi(13.1875^2 - 7.4375^2)$$

$$= 316{,}687 \text{ lb tensile force}$$

The corresponding compression stress in the inner shell to maintain equilibrium is:

$$p_{SST} = \frac{P_s}{A_s}$$

$$= \frac{-316{,}687}{\pi[(7.4375)^2 - (6.6875)^2]}$$

$$= -9515 \text{ psi}$$

This is a highly conservative estimate of the compressive stress that can develop in the inner shell for the following reasons:

1. It assumes axial non-deformability of the inner shell and no load development in the outer shell. Any pre-strain in the inner shell reduces the total strain, thus reducing the lead stress and axial force.
2. Creep in the lead is neglected. This also reduces the stress and force in the lead (Section 2.6.11.3).
3. It assumes the strain is uniform through the thickness of the lead shell. A particle away from the inner shell develops less strain, consequently lower stress, than a particle adjacent to the inner shell; this also reduces the total force in the lead shell.

2.6.11.2.3 Effects of Temperature Differential During Cooldown

The preceding analyses assume that the inner and outer shells and the lead are always at the same temperature at any time during the cooldown process. This assumption may not be true under actual conditions. However, because of the high thermal conductivity of the stainless steel and the lead and the time-controlled cooldown process, the temperature differential between any two of the above shells is kept to a minimum. For the effect of temperature differential on the stresses in the shells, a temperature differential of 300°F is conservatively assumed. A temperature differential of this magnitude is very unlikely during the actual lead pour.

When the inner shell is cooler than the lead, the interference between them, as well as the corresponding interface pressure and hoop stresses are less than for the case of equal temperatures. Hence, the preceding analysis is conservative.

When the inner shell is hotter than the lead shell, an analysis is required. Assume the temperature of the inner shell to be 370°F and that of the lead to be 70°F. The inner radius of the stress-free lead shell at 70°F is 7.3936 inches (R'_{it}); the outer radius of the inner shell at 370°F is:

$$R = 7.4375\,[1 + 8.74(10^{-6})(300)]$$
$$= 7.4570 \text{ inches}$$

The interference between the inner shell and the lead is 0.0634 inches. To fully accommodate this interference, the lead has to undergo a strain of 0.0634/7.3936 = 0.0086 inch/inch or 0.86 percent. From Figure 21 of NUREG/CR-0481, the hoop stress in the lead is approximately 900 psi for a 0.0086 inch/inch strain. The interface pressure is:

$$q = (900)\left[\frac{13.1105^2 - 7.3936^2}{13.1105^2 + 7.3936^2}\right]$$

$$= 466 \text{ psi}$$

The hoop stress in the inner shell becomes:

$$S_{his} = (-466)\left[\frac{7.4375^2 + 6.6875^2}{7.4375^2 - 6.6875^2}\right]$$

$$= -4400 \text{ psi}$$

Note that the thermal expansion or contraction of a shell subjected to a constant pressure does not affect the hoop stress; i.e.,

$$S_h = q\left[\frac{(ka)^2 + (kb)^2}{(ka)^2 - (kb)^2}\right] = q\left[\frac{a^2 + b^2}{a^2 - b^2}\right]$$

where:

$$k = 1 + \alpha\Delta T$$

This -4400 psi hoop stress (the inner shell is 300°F hotter than the lead shell) reduces to the previously calculated hoop stress of -4136 psi as both the inner shell and lead reach an ambient temperature of 70°F. This, of course, does not take into account the beneficial effect of the creep properties of the lead.

The axial stress in the inner shell also increases when the inner shell is 300°F hotter than the lead shell. The axial stress of -9515 psi calculated when both the inner shell and lead shell are at 70°F is recalculated for the inner shell temperature of 370°F, $\alpha = 8.74 \times 10^{-6}$:

$$\epsilon_{\ell} = (20.38 - 9.05)(10^{-6})(620 - 70) + (8.74 \times 10^{-6})(370 - 70)$$

$$= 0.0085 \text{ in/in or } 0.85 \text{ percent}$$

Referring to Figure 21 of NUREG/CR-0481, the axial stress in the lead is approximately 900 psi. The corresponding axial stress in the inner shell is -10,300 psi. As before, cooling of the inner shell reduces this stress. The previous assumptions apply in arriving at this inner shell compressive stress.

Temperature differentials between the inner and outer shells are of no consequence, since the axial restraint between them is placed after cooldown when the cask is at a uniform ambient temperature. Welding of the outer shell and the cask bottom to the bottom ring after cooldown is, therefore, a necessary fabrication step.

The question of buckling of the inner shell due to the combined effect of external pressure and fabrication inaccuracies must also be addressed. According to the "ASME Boiler and Pressure Vessel Code," Article NE-4221.1, the difference between the maximum and minimum inside diameters at any cross section shall not exceed 1 percent of the nominal diameter at the cross section under consideration. This amounts to (0.01)(13.375) or 0.13375 inch. The relation between the initial radial deviation, ω_i, and the maximum and minimum diameter (Timoshenko, 1976, Figure 7-10) is:

$$D_{max} = D_{nom} + 2\omega_1$$

$$D_{min} = D_{nom} - 2\omega_1$$

thus

$$D_{max} - D_{min} = 4\omega_1$$

or

$$\Delta D = 4\omega_1$$

Hence, the maximum initial radial deviation allowed is:

$$\omega_{max} = \Delta D/4 = 0.13375/4 = 0.0334 \text{ in}$$

From Timoshenko, 1976, equation (7-16), page 293:

$$S_{cr} = \left[\frac{E_t}{1 - \nu^2}\right]\left[\frac{h}{2R}\right]^2$$

$$= 81,435 \text{ psi}$$

where:

$E_t = 26.7 \times 10^6$ psi at 370°F

$\nu = 0.275$

h = shell thickness = 0.75 in

R = shell radius = 7.0625 inches

This critical buckling stress is well beyond the yield point of the shell material and, thus, cannot exist. Per Timoshenko, 1976, page 294, $S_{cr} = S_{Yp} = 42,000$ psi at 370°F can be used. Then from Timoshenko, 1976, equation (7-12), page 294:

$$q_{cr} = \left[\frac{E}{4(1 - \nu^2)}\right]\left[\frac{h}{R}\right]^3$$

$$= S_{cr}\left[\frac{h}{R}\right]$$

$$= 4460.16 \text{ psi}$$

When the cylinder has fabrication inaccuracies, the external pressure, q_{YP}, required to produce yielding in the extreme fibers can be solved in the following equation (Timoshenko, 1976, equation (e), page 296):

$$q_{YP}^2 - \left[\frac{S_{YP}}{m} + (1 + 6mn)\, q_{cr}\right] q_{YP} + \frac{S_{YP}}{m}\, q_{cr} = 0$$

where:

$S_{YP} = 42,000$ psi at 370°F

$m = R/h = 7.0625/0.75 = 9.4167$

$n = \omega_1/R = \omega_1/7.0625$

then

$$q^2_{YP} - [4460.16 + (1 + 8\omega_1)\, 4460.16]\, q_{YP} + 19,893,211 = 0$$

The value of ω_I can vary from 0.0 inches (perfect cylinder) up to 0.0334 inch maximum allowed according to the "ASME Boiler and Pressure Vessel Code." Solving q_{YP} for varying values of ω_I, gives the following:

Initial Radial Deviation ω_I (in)	Yield Pressure q_{YP} (psi)
0.001	4079
0.01	3365
0.02	2998
0.0334	2675

Thus, the margin of safety against yielding for the inner shell with maximum allowed radial deviation subjected to 466 psi lead pressure (inner shell temperature is 300°F higher than lead temperature) is:

$$M.S. = \frac{2675}{466} - 1 = \underline{+4.74}$$

Since the margin of safety for this conservative load case exceeds zero, the inner shell does not buckle when subjected to the lead pressure produced during the cooling of the cask.

2.6.11.3 Lead Creep

As shown in Sections 2.6.11.2.1 and 2.6.11.2.2, cooling of the lead shell and inner shell introduces a hoop stress of -4136 psi and an axial stress of -9515 psi in the inner shell. However, the high rate of creep of lead at room or elevated temperatures causes the stresses to be relieved early in the life of the cask. From Figure 21 of NUREG/CR-0481, it can be seen that maintaining a constant strain of 0.59 percent at 325°F for only five hours reduces the lead pressure to approximately 200 psi. For this stress in the lead, the corresponding hoop and axial stresses in the inner shell are:

$$\sigma_h = \frac{200}{850}(-4136) = -973 \text{ psi}$$

$$\sigma_a = \frac{200}{850}(-9515) = -2239 \text{ psi}$$

During fabrication following the lead pour, the lead creep relieves the stresses in the lead shell and the stresses in the inner shell to a point that they become negligible.

2.6.12 Fuel Basket / Container Analysis

2.6.12.1 Discussion

To assure that the cask contents are retained in a subcritical and safe configuration, a fuel basket supports the contents both laterally and longitudinally. During normal transport, the cask may sustain a 1-foot free fall to either the side, corner or end drop orientations. Fuel basket designs examined under normal operations conditions are: the PWR basket (Section 2.6.12.2); the BWR basket (Section 2.6.12.4); the metallic fuel basket (Section 2.6.12.5); the MTR basket (Section 2.6.12.6); the TRIGA fuel basket (Section 2.6.12.7); the DIDO fuel basket (Section 2.6.12.8); the GA IFM basket (Section 2.6.12.9); the TPBAR basket and spacer (Section 2.6.12.10); ANSTO fuel basket (Section 2.6.12.11); NRU/NRX fuel basket (Section 2.6.12.14); and the HEUNL containers (Section 2.6.12.15). The transport configuration can also accommodate a combination of an ANSTO top basket module and five DIDO basket modules. Within the top ANSTO module of the ANSTO-DIDO combination basket assembly, a total of up to seven aluminum damaged fuel cans (DFCs) can be placed. The total additional weight of the seven DFCs is less than 35 pounds. The increased weight is bounded by the analysis weight of 1,770 lbs, per Section 2.6.12.11.2, which exceeds the calculated weight of the ANSTO baskets in Table 2.2.1-1 of 1,667 lbs (911 + 756 = 1,667) by 103 pounds. Table 2.2.1-1 confirms that the maximum weight of the four HEUNL containers is bounded by the design basis payload of 4,000 pounds. The analyses demonstrate that each of the basket designs is supported by the inner shell in bearing during a side drop, and that none of the basket designs will buckle during an end drop. The effects of a corner drop are bounded by the side and end drops.

2.6.12.2 PWR Basket Construction

The cylindrical basket body is fabricated from 6061-T6 aluminum alloy extrusions. An open, square, central core extends the length of the basket and provides lateral support for the cask contents. A 13.25-inch outside diameter, 0.125-inch thick aluminum tube that is 4.38 inches long, is bolted to the top of the basket body. This top tube protects the cask inner shell from damage during fuel loading operations and provides lifting points, which are used when the basket is removed from the cask. An aluminum spacer plate assembly is bolted to the bottom of the basket body. The spacer plate assembly supports the fuel basket and contents longitudinally, providing their movement within the cask. Additional spacer fixtures are either bolted to the cask lid or to the base of the fuel basket, if the cask contents do not fill the basket. The maximum spacer loads occur for the 30-foot drop hypothetical accident load conditions. The spacer analysis is presented in Section 2.7.7.8. A groove on the outside of the basket body is

provided for the cask drain tube. The drain tube is connected to a fitting on the cask body, and is used to drain or fill the cask during cask loading or unloading operations.

For the shipment of up to 25 PWR or BWR rods, or up to 16 PWR MOX rods (or mixed MOX and UO_2 rods), a canister with insert will be utilized to position the fuel rod contents within the PWR basket. The canister for the fuel rods will be fabricated from Type 304 stainless steel (minimum thickness 0.12 inch) and will be designed to allow positive handling of the canister during loading and unloading operations. The size, shape, closure design and capacity of the canister will vary depending on the requirements of the shipping and/or receiving facilities. A spacer fabricated from stainless steel will be utilized, as required, to position the PWR/BWR rod canister longitudinally within the NAC-LWT cask cavity. A PWR insert fabricated from 6061-T651 aluminum is used to laterally position the rod canister within the PWR basket. The total weight of the fuel rods, canister and basket insert will be less than the maximum PWR fuel assembly payload weight of 1,650 pounds. Therefore, the up to 25 fuel rods content condition is bounded by the current PWR basket analyses.

2.6.12.3 PWR Basket Analysis

The minimum ambient temperature during normal transport, -40°F, combined with the maximum decay heat load produces an average inner wall temperature of 151°F. The 6061-T6 aluminum alloy expands approximately 1.5 times more per degree Fahrenheit than stainless steel. Assuming that both the cask and basket respond linearly, the maximum as-designed gap between the basket and the cavity, when the basket is centered in the cavity, is 0.094 in. Since aluminum expands faster than stainless steel, any increase in temperature will serve to decrease the basket-cavity gap. Since the gap is small, it is assumed that there is no relative motion between the basket and cask, and that the basket is in contact bearing on the inner shell during a side drop. The basket bearing loads are transmitted to the inner shell and cask structure.

2.6.12.3.1 Bearing Stress Calculation

The bearing stress is calculated using Case 6 (Roark, page 320), which models the cylindrical basket in a circular groove. The maximum compressive stress is calculated using:

$$S_{c_{max}} = 0.798 \left[\frac{\dfrac{P(D_1 - D_2)}{D_1 D_2}}{\dfrac{1 - \nu_1^2}{E_1} + \dfrac{1 - \nu_2^2}{E_2}} \right]^{0.5}$$

$$= 1570 \text{ psi}$$

where the material properties at 250°F are:

Stainless Steel

$D_1 = 13.405$ inches

$E_1 = 27.3 \times 10^6$ psi

$\nu_1 = 0.275$

Aluminum (6061-T6)

$D_2 = 13.25$ inches

$E_2 = 9.4 \times 10^6$ psi

$\nu_2 = 0.334$

contents + basket weight = 4,000 lbs

$P_{1g} = 4{,}000$ lb/178 in = 22.5 lb/in

$P_{24.3g} = (22.5 \text{ lb/in})(24.3 \text{ g}) = 547$ lb/in

(The 24.3 g side drop load is obtained from Table Table 2.6.7-34.)

The allowable compressive stress is selected to be the yield strength $(S_y)_{250\,F}$ of Type 304 stainless steel, 23,800 psi. The margin of safety is calculated as:

$$M.S. = \frac{S_y}{S_{c_{max}}} - 1 = \underline{+Large}$$

2.6.12.3.2 Compressive Stress Calculation

The PWR basket and inner cavity length are designed to ensure that there is very limited longitudinal movement of the basket relative to the cask when the cask is carrying fuel. Additional spacers are attached to the cask or added in the PWR basket, if the fuel contents do not fill the basket cavity. The fuel contents are not attached to the PWR basket, and do not impart any longitudinal structural load on the basket body. However, the PWR basket must support itself during an end drop accident. To determine if the PWR basket is self-supporting, it is analyzed as a column, acted upon by a structural (weight) compressive load.

The PWR basket weighs 840 pounds, which, during a normal operations 1-foot fall, is decelerated at 15.8 g. The g loads are completely described for all cask drop orientations in Section 2.6.7.4. The total compressive load acting over the basket body cross section, 59.2 square inches, is $P_{max} = 840 \times 15.8 = 13{,}272$ pounds. The compressive stress (S_c), conservatively considered to act on the basket body, is 13,272/59.2 = 224 psi.

An Euler column analysis is used to determine the critical buckling stress of the PWR basket body. Assuming that the impacting end is fixed and the other is free, the critical buckling stress (Shigley, page 116) is calculated as:

$$P_{cr} = \frac{n\pi^2 EI}{L^2}$$

$$= 670,700 \text{ psi}$$

where:

$n = 0.25$, end fixity coefficient

$E_{Al_{250\ F}} = 9.4 \times 10^6$ psi

$I_{basket\ body} = 870$ in^4 (Roark, Case 10, page 75)

$L = 178$ inches, inner cavity length

$$M.S. = \frac{P_{cr}}{P_{max}} - 1 = \underline{+Large}$$

2.6.12.4 BWR Basket Construction

The BWR basket is fabricated from 6061-T6 aluminum alloy extrusions. Two open, square cores, located in the center of the basket body, extend the length of the basket, providing lateral support for the cask contents. A 13.25-inch outside diameter, 0.25-inch thick stainless steel tube that is 5.4 inches long is welded to a 0.62-inch thick plate and the top cover assembly is bolted to the basket body. The top cover protects the cask inner shell from damage during fuel loading operations and provides lifting points, which are used when the basket is removed from the cask. A stainless steel spacer plate assembly is bolted to the bottom of the basket body. The spacer plate assembly supports the fuel basket and contents longitudinally, preventing their movement within the cask. Additional spacer fixtures are either bolted to the cask lid or the base of the fuel basket if the cask contents do not fill the basket. A groove on the outside of the basket body is provided for the cask drain tube.

2.6.12.4.1 BWR Basket Analysis

The BWR basket body is fabricated from the same material as the PWR basket body. Moreover, the outer diameter and its tolerance are exactly the same for both basket designs. Therefore, the BWR basket is also considered to be in contact bearing for similar reasons to those stated in Section 2.6.12.3, and all basket bearing loads are transmitted to the cask inner shell.

2.6.12.4.2 Bearing Stress Calculation

The BWR basket and its contents weigh 2,624 pounds. The normal operations conditions 1-foot side drop g load is 24.3, resulting in a total bearing load of 63,760 pounds (2,624 lb x 24.3 g).

The bearing load per unit length ($P_{24.3g}$) is 358 pounds/inch (63,760 lb/178 in). Using Case 6 (Roark, page 320) and the same material properties as described in Section 2.6.12.3.1, the $S_{c_{max}}$ = 1383 psi. The allowable compressive stress is selected to be the yield strength $(S_y)_{250\ F}$ of Type 304 stainless steel, 23,800 psi. The margin of safety is calculated as:

$$M.S. = \frac{S_y}{S_{c_{max}}} - 1 = \underline{+LARGE}$$

2.6.12.4.3 Compressive Stress Calculation

For the same reasons that are stated in Section 2.6.12.3.2, the BWR basket needs only to be self-supporting. The BWR basket weighs 1124 pounds, which during a normal operations 1-foot fall, is decelerated at 15.8 g. The total compressive load acting over the basket body cross-section (72.5 in^2), is P_c = 1124 lb × 15.8 g = 17,759 pounds. The compressive stress (S_c) conservatively considered to act on the basket body is 17,759 lb/72.5 in^2 = 245 psi, which is negligible.

An Euler column analysis is used to determine the critical buckling stress of the BWR basket body. Assuming that the impacting end is fixed and the other end is free, the critical buckling stress (Shigley, page 116) is calculated as:

$$P_{cr} = \frac{n\pi^2 EI}{L^2}$$

$$= 1.0 \times 10^6 \text{ psi}$$

where:

n = 0.25, end fixity coefficient
$E_{Al_{250\ F}} = 9.4 \times 10^6$ psi
$I_{basket\ body}$ = 1,298 in^4 (Roark, Case 10, page 75)
L = 178 in, inner cavity length

$$M.S. = \frac{P_{cr}}{P_c} - 1 = \underline{+LARGE}$$

2.6.12.5 Metallic Fuel Basket Construction

The metallic fuel basket is fabricated from three 5.625-inch outer diameter 6061-T6 aluminum tubes, laterally restrained by five 13.0-inch diameter 0.25-inch thick, 6061-T6 aluminum bulkheads welded along the length of the tubes. Each tube provides lateral support for the cask contents. The uppermost bulkhead has three attachment points, which are lifting points used when the basket is removed from the cask. Welded to the bottom bulkhead is a 9.0-inch outer

diameter, 0.25-inch thick, 6061-T6 aluminum spacer tube, 29.5 inches long, which supports the fuel basket and contents longitudinally, preventing their movement within the cask. A groove on the outside of the basket body is provided for the cask drain tube.

2.6.12.5.1 Metallic Fuel Basket Analysis

The metallic fuel basket body is fabricated from similar material to the PWR basket body. Moreover, the outer diameter of the bulkheads and its tolerance are exactly the same for both basket designs. Therefore, the metallic fuel basket bulkheads are also considered in contact bearing for the same reasons stated in Section 2.6.12.3, and all basket bearing loads are transmitted to the inner shell and cask structure.

2.6.12.5.2 Bearing Stress Calculation

The metallic fuel basket and its contents weigh 2,208 pounds. The normal operations conditions 1-foot side drop g load is 24.3, resulting in a total bearing load of 53,654 pounds (2,208 lb × 24.3 g). It is assumed that the entire bearing load is distributed over the five 0.25-inch thick bulkheads. The bearing load per unit length ($P_{24.3g}$) is 42,924 pounds/inch (53,654 lb/1.25 in). From Case 6 (Roark, page 320) the maximum compressive stress is calculated using:

$$S_{c_{max}} = 0.798 \left[\frac{\dfrac{P(D_1 - D_2)}{D_1 D_2}}{\dfrac{1 - \nu_1^2}{E_1} + \dfrac{1 - \nu_2^2}{E_2}} \right]^{0.5}$$

$$= 36{,}530 \text{ psi}$$

where the material properties at 250°F are:

Stainless Steel

$D_1 = 13.405$ inches
$E_1 = 27.3 \times 10^6$ psi
$\nu_1 = 0.275$

Aluminum (6061-T6)

$D_2 = 13.0$ inches
$E_2 = 9.4 \times 10^6$ psi
$\nu_2 = 0.334$

The allowable compressive stress is selected to be $(1.5)(S_y)_{250\ F}$ of 6061-T6 aluminum, 44,685 psi. The margin of safety is calculated as:

$$M.S. = \frac{S_y}{S_{c_{max}}} - 1 = \underline{+0.22}$$

2.6.12.5.3 Compressive Stress Calculation

For the same reasons that are stated in Section 2.6.12.3.2, the metallic fuel basket needs only to be self-supporting. The metallic fuel basket weighs 128 pounds, which during a normal operating conditions 1-foot fall, is decelerated at 15.8 g. The total compressive load acting over the three fuel tubes is P_F = 2,022 pounds (128 lb × 15.8 g). The total cross sectional area of the three aluminum fuel tubes is 6.48 square inches, resulting in a normal operating conditions compressive stress ($S_{c_{fuel}}$) of 312 psi (2,022 lb/6.48 in^2). The spacer tube must support the basket and its contents during a bottom end drop. The total weight that the spacer tube supports is 2,208 pounds, resulting in a normal operating conditions 1-foot bottom end drop compressive load of P_c = 34,886 pounds. The cross sectional area of the 9.0-inch outer diameter aluminum spacer tube is 6.87 square inches, resulting in a compressive stress ($S_{c_{spacer}}$) of 5078 psi. Assuming that the impacting end is fixed and the other end is free, the critical buckling stresses for each tube column (Shigley, page 116) is calculated:

Fuel Tubes (3)

$$P_{cr} = \frac{n\pi^2 EI}{L^2}$$

$$= 33,550 \text{ psi}$$

where:

n = 0.25, end fixity coefficient
$E_{Al250\ F} = 9 \times 4\ 10^6$ psi
$I_{basket\ body} = 46$ in^4
L = 145.25 in, fuel tube length
MS = $\underline{P_{cr}}$ / P_F - 1 = $\underline{+Large}$

Spacer Tube

$$P_{cr} = \frac{n\pi^2 EI}{L^2}$$

$$= 1,754,000 \text{ psi}$$

n = 0.25, end fixity coefficient
$E_{Al250\ F} = 9.4 \times 10^6$ psi
$I_{spacer\ tube} = 66$ in^4
L = 29.5 in, spacer tube length
MS = $\underline{P_{cr}}$ / P_c - 1 = $\underline{+Large}$

2.6.12.6 MTR Fuel Basket Construction

The MTR modular basket assembly has five configurations. One configuration is for 28 uncut (intact) MTR fuel assemblies (28 MTR – 4 unit basket); the second is for 35 partially cut MTR elements that have had portions of the upper and lower end fittings removed (35 MTR – 5 unit

basket). The third configuration is for 42 MTR fuel assemblies (42 MTR – 6 unit basket) with the upper and lower end fittings removed; and the fourth configuration is for up to 700 PULSTAR fuel elements loaded in the 28 MTR basket. The PULSTAR fuel may be intact fuel assemblies, intact fuel elements (rods) loaded in a fuel rod insert or in fuel cans, or damaged fuel elements, fuel debris, and nonfuel components of fuel assemblies loaded in fuel cans. The fifth configuration is for up to 800 SLOWPOKE intact and/or damaged fuel rods contained in canisters. Each MTR basket configuration consists of one base module, one top module, and two, three or four intermediate modules for the 28, 35 and 42 element configurations, respectively. Each MTR basket module is designed to hold up to seven MTR or PULSTAR fuel assemblies. The modules are not interchangeable between basket configurations. Up to four (4) SLOWPOKE canisters may be loaded in each of the top and the upper intermediate MTR-28 basket modules with the center fuel cells blocked. The lower intermediate and bottom basket modules are installed as axial spacers. The structural analysis is not affected by the specific fuel element design or enrichment as long as the fuel characteristics are in compliance with the fuel characteristics listed in Table 1.2-4 or Table 1.2-14.

Axial fuel and plate spacers may be used to axially position the MTR fuel assemblies in the basket modules. Cell block spacers are used to prevent the loading of fuel assemblies in basket module positions 1, 2 and 3 when LEU MTR fuel elements having >470 g ^{235}U per element (>22 g ^{235}U per plate) are loaded. The presence and/or use of spacers, fuel plate canisters or fuel cans does not affect the structural integrity of the MTR fuel baskets as the total weight of fuel element, spacer and fuel plate canister or fuel can is limited to the evaluated load of 80 pounds/cell. The axial fuel and cell block spacers perform no safety function and are considered dunnage. Plate spacers are used, if required, to ensure that the criticality evaluation required minimum nonfuel hardware is provided.

Each module, fabricated from Type 304 stainless steel, is a weldment made up of two 1/2-inch thick, 13.265-inch diameter, circular plates at each end of the longitudinal divider plates creating seven MTR fuel assembly cavities. The outside wall of the four symmetric outermost fuel compartments is fabricated from 11-gage Type 304 stainless steel sheet. The 1/2-inch thick plate at the top end of the MTR fuel basket module is welded to the exterior surfaces of the fuel tube weldment with a 1/8-inch continuous weld on the under side of the top plate and with a continuous fillet seal weld on the top side. The 1/2-inch thick baseplate is continuously welded to the 1/4-inch thick divider plates and the 5/16-inch thick web plates. The 11-gage sheet metal and the 5/16-inch intermediate webs are discontinued at 1/4 inch from the surface of the baseplate to provide for compartment drainage. The 5/16-inch plate material may be machined to a minimum thickness of 0.28 inch. In addition to the drainage path at the base of each assembly cavity, a 1-inch diameter hole is located at the center of each of the compartments in the module. Each MTR basket base module sits on a 1.5-inch long, 10-inch schedule 80S pipe welded to the 1/2-inch thick baseplate. The 10-inch schedule 80S pipe carries the total weight of the MTR basket assembly and bears directly on the bottom forging of the cask.

The MTR fuel basket base module and intermediate modules have guide pins fixed to the surface of the top support plate. The guide pins fit into holes in the base plate of the top and intermediate modules and provide controlled alignment of the basket assembly. A groove slot on the outside of each basket unit support plate is provided for the clearance of cask drain tube and for circumferential alignment of the MTR basket assembly.

The MTR Plate Canister (canister) is an all-aluminum rectangular canister that is suitable for transport in the NAC-LWT MTR 42 element basket. The canister may be transported in the 28 or 35 element basket if appropriate dunnage is used. The canister is fabricated from ASTM B209 or ASTM B221 6061 aluminum. The canister body comprises two thick walls and two thin walls that are welded together into a rectangular tube to contain up to 23 MTR fuel plates. Each end of the canister body is closed by identical aluminum lids milled from a solid piece to incorporate a lifting bail. The lids are fastened securely to the thick wall plates using aluminum socket head cap screws that are captive in the lid to facilitate closing the canister.

2.6.12.6.1 MTR Fuel Basket Analysis

The MTR basket assembly and the inner shell are both fabricated from Type 304 stainless steel material. The nominal radial gap between the MTR basket assembly and the cask inner shell is 0.055 inch. The nominal radial gap between the basket and the inner shell is 0.0531 inch at the design basis fuel normal operation steady-state temperature. As defined for other NAC-LWT fuel specific basket designs, since the gap between the basket and cask inner shell wall is small, it is assumed that there is no relative motion between the basket and the cask, and that the basket is in contact bearing on the inner shell during a side drop. The basket bearing loads are transmitted to the inner shell and cask structure.

The analysis of the MTR plate canister is presented in Section 2.6.12.6.6.

2.6.12.6.2 MTR Fuel Basket Normal Conditions 1-foot Side Drop

This section evaluates the MTR fuel basket for the normal conditions of transport 1-foot side drop.

Bearing Stress Calculation—Inner Shell (Cask 1-foot Side Drop)

The bearing stress is calculated using Roark's, Table 33, Case 2 (Roark's, 6th Edition), which models the cylindrical basket in a circular groove. The 28 MTR fuel assembly base module is the heaviest module when loaded with 25 PULSTAR fuel elements. The maximum compressive stress, for two elastic bodies with similar elastic modulus, is:

$$\sigma_c = 0.798\sqrt{\frac{\frac{gP(D_1 - D_2)}{D_1 D_2}}{\frac{2(1-\nu^2)}{E}}} = 16{,}679 \text{ psi}$$

where:

g = 1-foot side drop acceleration = 24.3

E = Elastic modulus = 28.3×10^6 psi (conservatively use E @ 70°F)

ν = Poisson's ratio for steel material = 0.275

D_1 = Cask cavity diameter = 13.405 inches

D_2 = Basket diameter = 13.265 inches

t = Thickness of stiffener at mid section of base module (less chamfers)

= $0.5 - 2 \times 0.13 = 0.24$ in

W = Maximum weight of MTR basket with contents (PULSTAR fuel elements)

= 3,222 lbs

W_r = Load supported by 28-assembly basket base module middle ring

= W/9 = 358 lbs

P = W_r/t = 358 lb/0.24 in = 1,491 lb/in

The allowable compressive stress, S_y, of Type 304 stainless steel at a conservative maximum operating temperature envelope of 600°F is 18,200 psi. The margin of safety is calculated as:

$$MS = \frac{S_y}{\sigma_c} - 1 = +0.09$$

Fuel Tube Stresses (Cask 1-foot Side Drop)

The maximum stress in the fuel tubes occurs in the 0.12-inch thick, 11-gage sheet metal tubes which support the entire length of the MTR fuel elements or PULSTAR fuel elements. There are two cases to consider. In the first case, the weight of the fuel assembly is transmitted to the tube through the two aluminum plates at the sides of the fuel assembly. As shown in Figure 2.6.12-1, this load path creates a uniform line load along the length of the tube located about 0.315 inch from the corners. The tube is analyzed as a simple beam, 1-inch wide, 0.12-inch thick, and 3.44-inches long with a concentrated load at 0.315 inch from the ends. The maximum bending moment, M_I, is:

$$M_I = \frac{(8Pa + WL^2) \times g}{8} = 14.0 \text{ in-lb/in}$$

where:

W = Unit tube body weight = $0.288 \times t = 0.0346$ lb/in^2

L = Length = 3.44 inches

P = Bounding fuel load = $P_f / (2 \times L_f) = 1.67$ lb/in

P_f = Fuel weight = 80.0 lbs

L_f = Shortest length over which fuel load is applied = 24 inches

a = Distance from applied load, P to support = 0.315 in

g = 1-foot side drop acceleration = 24.3

In the second case, the weight of the fuel assembly is transmitted to the tube as a uniform load. The load path is shown in Figure 2.6.12-1. The maximum bending moment for this case, M_{II}, is:

$$M_{II} = \frac{(2PL^2 + WL^3) \times g}{8L} = 36.1 \text{ in-lb/in}$$

The maximum bending stress, σ, is:

$$\sigma = \frac{6M_{II}}{t^2} = 15{,}042 \text{ psi}$$

where:

t = Fuel tube thickness = 0.12 in

The stress allowable, $1.5S_m$, is 24,600 psi for Type 304 stainless steel at a conservative temperature of 600°F. The margin of safety is:

$$MS = \frac{24{,}600}{15{,}042} - 1 = +0.64$$

The 11-gage sheet metal tube is continuously welded to the adjacent divider plates with a 1/8-inch fillet weld. This weld resists shear developed in the simple beam analyzed above.

$$V = \frac{(2P + WL) \times g}{L} = 24.4 \text{ lb/in}$$

The shear stress, τ, is:

$$\tau = \frac{V}{t} = 203 \text{ psi}$$

The "throat" thickness of the weld is 0.088 in. The ratio of the plate thickness (0.12 in) to the weld "throat" thickness (0.088 in) is 1.36. The maximum stress of 203 psi calculated above is adjusted by a factor of 1.36 to obtain the maximum stress in the weld for the 1-foot side drop (24.3g). Maximum stress in the weld, S_w, is:

$S_w = 1.36 \times \tau = 276$ psi

The ASME Code, Subsection NG-3352 recommends that the allowable stress be determined for a fillet weld with PT or MT surface examination by implementing a quality factor, n, of 0.4. The stress allowable, S_y, of the base metal, Type 304 stainless steel, is 18,200 psi at a conservative operating temperature envelope of 600°F. The margin of safety for the fillet weld is:

$$MS = \frac{S_y \times n}{S_w} - 1 = \underline{+Large}$$

2.6.12.6.3 MTR Fuel Basket Normal Conditions 1-foot End Drop

This section evaluates the MTR fuel basket for the normal conditions of transport 1-foot end drop.

Bearing Stress Calculation—Bottom Forging (Cask 1-foot End Drop)

When in the vertical position a 0.5-inch thick, 10-inch nominal diameter schedule 80S pipe supports the MTR basket assembly. The 1.5-inch long pipe is welded to the baseplate of the base module. The compressive stress is:

$$\sigma_c = \frac{g \times W}{A} = 3{,}162 \text{ psi}$$

where:

W = Maximum weight of MTR basket with contents (PULSTAR fuel elements) = 3,222 lbs

A = Cross-sectional area of base pipe support = 16.1 in^2

g = 1-foot end drop acceleration = 15.8

The allowable stress, S_y, of Type 304 stainless steel at a conservative maximum operating temperature of 600°F is 18,200 psi. The margin of safety is:

$$MS = \frac{S_y}{\sigma_c} - 1 = +4.76$$

Compressive Stress Calculation—Fuel Tubes (Cask 1-foot End Drop)

The MTR basket assembly and the inner cavity length are designed to ensure that there is minimal longitudinal movement of the basket relative to the cask. The base module of the MTR basket assembly supports itself and the weight of the other basket modules, including fuel content during a 1-foot end drop. The normal operation load compressive stress developed in the basket tube wall is:

$$\sigma_c = \frac{g \times W}{A} = 6{,}208 \text{ psi}$$

where:

W = Maximum weight of MTR basket with contents (PULSTAR fuel elements)
= 3,222 lbs

g = 1-foot end drop acceleration = 15.8

A = Total compartment cross-sectional area at baseplate (Figure 2.6.12-2)
= 8.20 in^2

The allowable compressive stress, S_m, is 16,400 psi conservatively evaluated for Type 304 stainless steel at a conservative maximum operating temperature of 600°F. The margin of safety is:

$$MS = \frac{S_m}{\sigma_c} - 1 = +1.64$$

The Euler elastic buckling load formulation is used to determine the critical buckling load of the MTR basket base module. The base module is treated as simply supported, which results in an effective length that is twice the actual length, thus reducing the critical buckling load by a factor of 4.0. The basket base module buckling load is:

$$P_{cr} = \frac{\pi^2 E I_i}{(L_e)^2} = 1.55 \times 10^6 \text{ lb}$$

The margin of safety is:

$$MS = \frac{P_{cr}}{P_c} - 1 = \underline{+\text{Large}}$$

where:

P_c = Compressive load = 15.8g × 3,222 lbs = 50,908 lbs

I_i = Basket inertia moment = 47.92 in^4

E = Elastic modulus (@ 600°F) = 25.3 × 10^6 psi

L_e = Effective length of 28 assembly basket = 2 × 44.0 inches = 88 inches

Baseplate Stresses (Cask 1-foot End Drop)

The support plate at the top end of the basket modules is continuously welded to the outside periphery of the fuel compartment tubes. The baseplate of a typical basket module is continuously welded to the two 11.57-inch wide, 5/16-inch (min. 0.28-inch considering machining tolerance) thick web plates, and to the two 3.44-inch wide, 1/4-inch thick divider

plates as shown in Figure 2.6.12-2. The ½-inch thick baseplate supports seven MTR or seven DIDO fuel assemblies or 25 PULSTAR fuel elements and is conservatively assumed to be supported by the main longitudinal webs mentioned above during a cask end drop. Two separate load cases are examined. The maximum stress for each case is then combined to obtain the total stress on the baseplate. Figure 2.6.12-2 details the baseplate support.

The first case, Case I, examines a 3.44-inch square plate with two adjacent sides fixed and the other two sides free. The applied pressure over the entire plate is uniform (Roark's, 6th edition, Table 26, Case 11a). The bending stress is:

$$\sigma_I = \frac{-g\beta_I P b^2}{a t^2} = -8{,}947 \text{ psi}$$

where:

P = Fuel weight = 80.0 lbs

g = 1-foot end drop acceleration = 15.8

a = Area of plate = $(3.44 \text{ in})^2 = 11.83 \text{ in}^2$

t = Plate thickness = 0.5 inch

b = Plate width = 3.44 inches

β_I = Boundary condition stress factor = 1.769

The second case, Case II, examines a rectangular plate, 11.57 inches by 3.44 inches, fixed along the long edges, free along the short edges and uniformly loaded (Roark's, 6th edition, Table 26, Case 6a). The bending stress is:

$$\sigma_{II} = \frac{-g\beta_{II} P b^2}{a t^2} = -747 \text{ psi}$$

where:

a = Area of plate = $11.57 \times 3.44 \text{ in} = 39.8 \text{ in}^2$

β_{II} = Boundary condition stress factor = 0.497

The total bending stress is conservatively obtained by adding the individual stresses:

$$\sigma = \sigma_I + \sigma_{II} = -9{,}694 \text{ psi}$$

The allowable stress, 1.5 S_m, is 24,600 psi for Type 304 stainless steel at the conservative maximum temperature envelope of 600°F. The margin of safety is:

$$MS = \frac{24{,}600}{9{,}694} - 1 = +1.54$$

2.6.12.6.4 Fuel Tube Stresses (Cask 1-foot Oblique Drop)

Table 2.6.7-34 summarizes the cask drop g-load factors for six drop orientations: the cask end drop (0 degrees), the cask corner drop (15.74 degrees), the cask oblique drops (30, 45 and, 60 degrees) and the cask side drop (90 degrees). To conservatively envelope the maximum stresses expected for all the 1-foot oblique drops, the calculated stresses of 6,208 psi in Section 2.6.12.6.3 for the end drop and 15,042 psi in Section 2.6.12.6.2 for the side drop are added as absolute values. The maximum stress in the MTR basket that envelops the maximum stresses expected for any 1-foot oblique drop is 21,250 psi. The margin of safety, against stress allowable, 1.5 S_m, of 24,600 psi, at 600°F, is:

$$MS = \frac{24{,}600}{21{,}250} - 1 = +0.16$$

2.6.12.6.5 Fuel Cans in a MTR Basket (Damaged PULSTAR Elements)

PULSTAR Damaged Fuel Can

The PULSTAR can is a modification of the existing damaged fuel can for TRIGA fuel, which has two different design lengths. The PULSTAR fuel can has the same cross-section (can width and wall thickness) as the TRIGA fuel can and is approximately four inches longer than the shorter TRIGA fuel can design. Identical materials of fabrication are used for both TRIGA and PULSTAR fuel cans. As shown in Section 2.6.12.7.6, the TRIGA fuel can is evaluated for a maximum weight of 59.6 lb, which includes a can weight of 20 lbs and a payload of 39.6 lbs. The weights of the PULSTAR fuel can and its maximum payload are approximately 15 lbs and 35 lbs, respectively, for a maximum total weight of 50 lbs. Therefore, the stress evaluation for inertia loads for the PULSTAR can is bounded by the evaluation for the TRIGA can.

The maximum internal pressure for the PULSTAR can is 3.4 atm (gage). The calculation for the TRIGA can in the section titled "Sealed Failed Fuel Can Bolt Evaluation" used a value of 3 atm (gage). In the evaluation of the bolt stresses and loads, the calculation in this section conservatively used a linear load of 700 lb/inch, which bounds the increased internal pressure of 3.4 atm (gage) for the PULSTAR can.

For the e valuation of the failed fuel can tube, the minimum margin of safety is +0.77 (actual stress is 9,241 psi) in the section titled "Sealed Failed Fuel Can Plate Stress Due to Side Drop" for the 1-foot side drop. Considering the damaged fuel can as a thin wall cylinder with a bounding internal pressure of 60 psig, the stresses in circumferential, radial, and longitudinal directions are:

$$\sigma_\theta = \frac{P \times r}{t} = 1{,}500 \text{ psi}$$

$$\sigma_r = -P = -60 \text{psi}$$

$$\sigma_Z = \frac{P \times r}{2 \times t} = 750 \text{ psi}$$

where:

P = 60 psig

r = 3.25/2 in., the radius of the can

t = 0.065 in., the thickness of the can

Combining the stresses caused by can contents (1-ft side drop) and the internal pressure, the bounding stress intensity is:

$$S_{int} = (1{,}500 + 9{,}241) - (-60) = 10{,}801 \text{ psi}$$

The minimum margin of safety for the one-foot side drop and internal pressure is:

$$\text{M.S.} = \frac{1.5\ S_m}{S_{int}} - 1 = +1.28$$

It is concluded that the PULSTAR fuel can is structurally adequate for normal conditions of transport. No additional analysis is required.

PULSTAR Screened Fuel Can

The PULSTAR screened can is a modification of the existing screened fuel can for TRIGA fuel, which has two different design lengths. The PULSTAR screened fuel can has the same cross-section (can width and wall thickness) as the TRIGA screened fuel can and is approximately four inches longer than the shorter TRIGA screened fuel can design. Identical materials of fabrication are used for both TRIGA and PULSTAR fuel cans. As shown in Section 2.6.12.7.5, the TRIGA fuel can is evaluated for a maximum weight of 71 lbs, which includes a maximum can weight of 17 lbs and a payload of 54 lbs. The weights of the PULSTAR screened fuel can and its maximum payload are 12 lbs and 54 lbs, respectively, for a maximum total weight of 66 lbs. Therefore, the evaluation presented in Section 2.6.12.7.5 for the TRIGA screened fuel can bounds the evaluation for the PULSTAR screened fuel can and it may be concluded that the PULSTAR screened fuel can is structurally adequate for normal conditions of transport. No additional analysis is required.

PULSTAR Fuel Rod Insert and Spacer

Intact PULSTAR fuel elements can be placed into the TRIGA fuel rod insert (Dwg. 315-40-096). This insert is identical to the TRIGA fuel rod insert evaluated in Section 2.6.12.7.9. The weight of the individual PULSTAR fuel element is 1.31 lbs, which is bounded by the weight of an

individual TRIGA rod of 1.44 lbs reported in Section 2.6.12.7.9. Therefore no additional evaluation for PULSTAR fuel elements contained in the TRIGA fuel rod insert is required.

For an end drop, the maximum stress is computed using the accelerations for the accident condition, but is compared to the stress allowables for the normal condition. The stress in the aluminum spacer is:

$$\sigma = \frac{Pg}{A} = 0.5 \text{ ksi}$$

where:

P = 65 lbs Bounding load

g = End drop g-load for the 30-foot end drop= 60.0g

A = $\pi r^2 = 8.3 \text{ in}^2$

r = Radius of cylinder = 3.25/2 = 1.625 inches

t = Wall thickness = 0.125 in

The margin of safety is

$$MS = \frac{0.7S_u}{\sigma} - 1 = \frac{0.7 \times 30.2}{0.5} - 1 = \underline{+\text{Large}}$$

Using NUREG / CR-6322, a buckling evaluation of the spacer is performed for the accident condition which corresponds to an acceleration of 60g. The critical buckling stress for the spacer is:

$$\sigma_c = \frac{\pi^2 E}{\left(\frac{KL}{r}\right)^2} = 99.7 \text{ ksi}$$

where:

K = Effective length factor for fixed-free end conditions = 2.0

L = spacer length = 16.5 inches, which bounds 12-inch length

r = Radius of gyration = $\sqrt{I/A}$ =1.1 in

A = Cross-sectional area of spacer = $\pi Dt = 1.28 \text{ in}^2$

I = Moment of inertia = $\frac{\pi D^3 t}{8} = 1.69 \text{ in}^4$

D = Spacer diameter = 3.25 inches

t = Spacer thickness = 0.125 in

E = Modulus of elasticity of aluminum = 9.1×10^6 psi

The margin of safety against buckling is:

$$MS = \frac{\sigma_c}{\sigma} - 1 = \frac{99.7}{0.5} - 1 = \underline{+Large}$$

2.6.12.6.6 MTR Plate Canister Analysis

The MTR Plate Canister (canister) is a handling fixture designed to assist loading MTR fuel plates into the removable modules of the NAC-LWT MTR fuel basket. The fuel basket modules are used to load and unload fuel from the NAC-LWT cask and are the analyzed support structure for the fuel and canister. Therefore, the canister is not a required operational feature for loading or unloading fuel from the cask and serves only as a spacer (dunnage) once inserted into a basket module.

In this section, the canister is evaluated and found to be structurally adequate for all normal conditions of handling and transport. Stresses developed during the normal (one-foot drop) conditions meet all appropriate allowable criteria with positive margins. Classical hand calculations are used to determine the stresses in the canister. Calculated stresses are compared to allowable stresses for non-containment structures shown in Table 2.1.2-2, "Allowable Stress Limits for Noncontainment Structures."

Design deceleration (g) factors used in the canister analysis are shown in Table 2.6.7-34, "Summary of Cask Drop Equivalent G Load Factors." A temperature of 295°F bounds the highest calculated canister temperature and is used for both normal and accident conditions analyses. Stresses for corner and oblique drops are considered to be enveloped by the stresses produced by the end and side drops based on the cask drop acceleration component loads summarized in Table 2.6.7-34.

Maximum Canister Temperature

The maximum heat load allowed in an MTR basket cell is 120 W (409.8 Btu/hr), which is assumed to be transmitted only through one plate of the canister, resulting in a conservative estimate of the ΔT through the thickness of the canister shell. The maximum basket temperature is listed in Table 3.4-6 as 292°F.

The change in temperature through the thickness of the shell is calculated using the following formula:

$$\Delta T = Q\,t / kA = 409.8 \text{ Btu/hr} \times 0.24 \text{ inch} / (6.23 \text{ Btu/hr-in-F} \times 76.26 \text{ in}^2) = 0.21°F$$

where:

$k = 6.77 - 0.0025 \times (292 - 77) = 6.23$ Btu/hr-in-F at 292°F

$A = 25.85(3.2 - 0.125 \times 2) = 76.26$ in^2 is the cross-sectional area of the plate

The peak canister shell temperature is then 292°F + 0.21°F = 292.21°F. A temperature of 295°F is conservatively used for the temperature of the canister.

MTR Plate Canister Weight

The canister component weights are determined by conservatively calculating the volume of each component and multiplying by the density of 6061 aluminum, 0.098 lb/in^3 ("ASME Boiler and Pressure Vessel Code, Section II, Part D – Properties," 1995 with 1995 Addendum).

Can Weldment

$W_{canister} = W_1 + W_2 + W_3 + W_4 = 6.8$ lbs (use 10 lbs for analysis)

where:

Item/Description	Calculation of Weight
1 Plate-A (2)	$W_1 = 25.85 \times 3.20 \times 0.24 \times 0.098 \times 2 = 3.9$ lbs
2 Plate-B (2)	$W_2 = 25.85 \times 2.95 \times 0.125 \times 0.098 \times 2 = 1.9$ lbs
3 Lid (2)	$W_3 = 3.30 \times 3.20 \times 0.25 \times 0.098 \times 2 = 0.5$ lb
4 Bail (2)	$W_4 = [(0.46(4) + 2.94(2)) \times 0.125) + 1.04 \times 0.25] \times 0.098 \times 2 = 0.5$ lb

This weight calculation conservatively neglects holes in the lids.

NAC-LWT MTR Plate Canister Stress Analysis

The canister is evaluated for stresses developed during the normal (one-foot drop) conditions. The empty canister weight is assumed to be 10 pounds and the loaded canister weight is assumed to be 30 lbs throughout the calculations.

Side Drop

The canister is contained within the NAC-LWT MTR 42-element basket assembly in the side-drop case. Because of the support provided by the basket, only the uppermost canister plate is subjected to bending. Bending of the plate is analyzed by considering a 1-inch section as a fixed-fixed beam equal in length to the width of the plate and uniformly loaded by the plate weight times the appropriate acceleration (g).

Normal Operating Condition (1-foot drop)

With the 0.125-in. thick plate uppermost:

The maximum moment (M_{max}) is:

$$M_{max} = \frac{wL^2}{12} = \frac{(0.30)(3.3^2)}{12} = 0.272 \text{ in-lb}$$

$$S_b = \frac{Mc}{I} = \frac{(0.272)(0.0625)}{1.63 \times 10^{-4}} = 104 \text{ psi for the normal operating condition}$$

where:

$$w = 0.125 \times 1.0 \times 1.0 \times 0.098 \times 24.3g = 0.30 \text{ lb/in}$$

$$I = \frac{bh^3}{12} = \frac{(1.0)(0.125^3)}{12} = 1.63\times10^{-4} \text{ in}^4$$

With the 0.24-in. thick plate uppermost:

The maximum moment (M_{max}) is:

$$M_{max} = \frac{wL^2}{12} = \frac{(0.57)(3.3^2)}{12} = 0.517 \text{ in-lb}$$

$$S_b = \frac{Mc}{I} = \frac{(0.517)(0.125)}{1.15\times10^{-3}} = 56 \text{ psi for the normal operating condition}$$

where:

$$w = 0.24 \times 1.0 \times 1.0 \times 0.098 \times 24.3g = 0.57 \text{ lb/in}$$

$$I = \frac{bh^3}{12} = \frac{(1.0)(0.24^3)}{12} = 1.15\times10^{-3} \text{ in}^4$$

The minimum margin of safety (MS) for bending is:

$$MS = \frac{1.5S_m}{S_b} - 1 = \frac{(1.5)(11{,}500)}{104} - 1 = \underline{+\text{Large}}$$

Side Plate Buckling

The 0.125-inch-thick side plates are evaluated as axially loaded compression members. Buckling of the 0.24-inch thick plates is based on this analysis. Considering a 1-inch section of the plate, the slenderness ratio (C_c) is:

$$C_c = \sqrt{\frac{2\pi^2 E}{S_y}} = \sqrt{\frac{2\pi^2 9.6\times10^6}{27{,}900}} = 82.4$$

The radius of gyration (r) is:

$$r = \sqrt{\frac{I}{A}} = 0.036 \text{ in}^4$$

where:

$$I = \frac{bh^3}{12} = \frac{1.0(0.125)^3}{12} = 1.628\times10^{-4} \text{ in}^4$$

$$A = 0.125\times1.0 = 0.125 \text{ in}^2$$

For K = 1,

$$\frac{KL}{r} = \frac{1(3.3)}{0.036} = 91.67$$

For KL/r = 91.67 > C_c = 82.4, the allowable stress (S_a) is:

$$S_a = \frac{12\pi^2 E}{23\left(\frac{KL}{r}\right)^2} = \frac{12\pi^2(9.6\times10^6)}{23(91.67^2)} = 5{,}882 \text{ psi}$$

The allowable load (P_a) is:

$$P_a = S_a \times A = 5{,}882 \text{ psi} \times 0.125 \text{ in}^2 = 735 \text{ lbs}$$

The load (P) imposed upon the 0.125-inch-thick side plate by the 0.24-inch-thick side plate in the normal condition, one-foot side drop is:

$$P = 0.24 \times 1.0 \times 3.3 \times 0.098 \times 24.3g \cong 2 \text{ lbs}$$

This 2-pound load is conservative because the load from the thicker plate is actually shared between the two thinner plates.

The margin of safety (MS) is:

$$MS = \frac{P_a}{P} - 1 = \frac{735}{2} - 1 = +\underline{\text{Large}}$$

<u>End Drop</u>

For the end drop, the can weldment is loaded by its own weight. The canister contents bear against the bottom or top of the canister, depending on drop orientation.

Under normal operating conditions the canister body weldment is evaluated for a 15.8g end drop acceleration. The compressive load (P) on the tube is the combined weight of the lid and body plates times the appropriate g factor.

The compressive stress (S_c) in the canister body weldment is:

$$S_c = \frac{P}{A} = \frac{158 \text{ lb}}{2.24 \text{ in.}^2} \cong 70.5 \text{ psi}$$

where:

$$A = (3.2\times0.24 + 2.82\times0.125)(2) = 2.24 \text{ in}^2$$

P = 10 lb × 15.8g = 158 lb (Conservatively, the entire weight of the canister is used)

The margin of safety (MS) is then:

$$MS = \frac{S_m}{S_c} - 1 = \frac{11{,}500 \text{ psi}}{70.5 \text{ psi}} - 1 = \underline{+\text{Large}}$$

Lifting Bail Compressive Stress

Under normal operating conditions, the lifting bail is evaluated for a 1-foot end drop (15.8g acceleration). The compressive load (P) on the lifting bail is the combined weight of the canister and its contents (30 lbs) times the appropriate g factor.

The compressive stress (S_c) in the canister body weldment is:

$$S_c = \frac{P}{A} = \frac{474 \text{ lb}}{0.965 \text{ in}^2} = 491 \text{ psi}$$

where:

$$A = (0.46 \times 4 + 2.94 \times 2)(0.125) = 0.965 \text{ in}^2$$

$$P = 30 \text{ lb} \times 15.8g = 474 \text{ lbs}$$

The margin of safety (MS) is then:

$$MS = \frac{S_m}{S_c} - 1 = \frac{11{,}500 \text{ psi}}{491 \text{ psi}} - 1 = \underline{+\text{Large}}$$

Canister Body Buckling

The canister body is evaluated for buckling during the end drop by using the Euler formula to determine the critical buckling load (P_{cr}):

$$P_{cr} = \frac{K\pi^2 EI}{L^2} = \frac{0.722\pi^2(9.6 \times 10^6)(2.98)}{(25.85)^2} =$$

305,073 lbs, assuming lower end fixed, upper end free

where:

$E = 9.6 \times 10^6$ psi

$K = 0.722$ (Reference Roark's Table 34, Case 3a)

$$I = \left(\frac{3.3 \text{ x } 3.2^3 - 2.82 \text{ x } 2.95^3}{12}\right) = 2.98^4, \text{ minimum moment of inertia}$$

L = tube body length (25.85 in.)

Because the maximum compressive load (10 lbs × 60g = 600 lbs under the accident condition) is much less than the critical buckling load (305,073 lbs), the canister body has adequate resistance to buckling.

As noted in the first paragraph of this section, the plate canister is only a handling fixture (not a structural component) and only serves as a spacer once inserted into the basket. Thus, retempering of the aluminum plates after welding is not required. The criticality evaluation presented in Section 6.4.3.10 includes the hypothetical separation of the canister fixture.

Figure 2.6.12-1 Cask Side Drop Fuel Tube Loading – MTR Fuel Basket

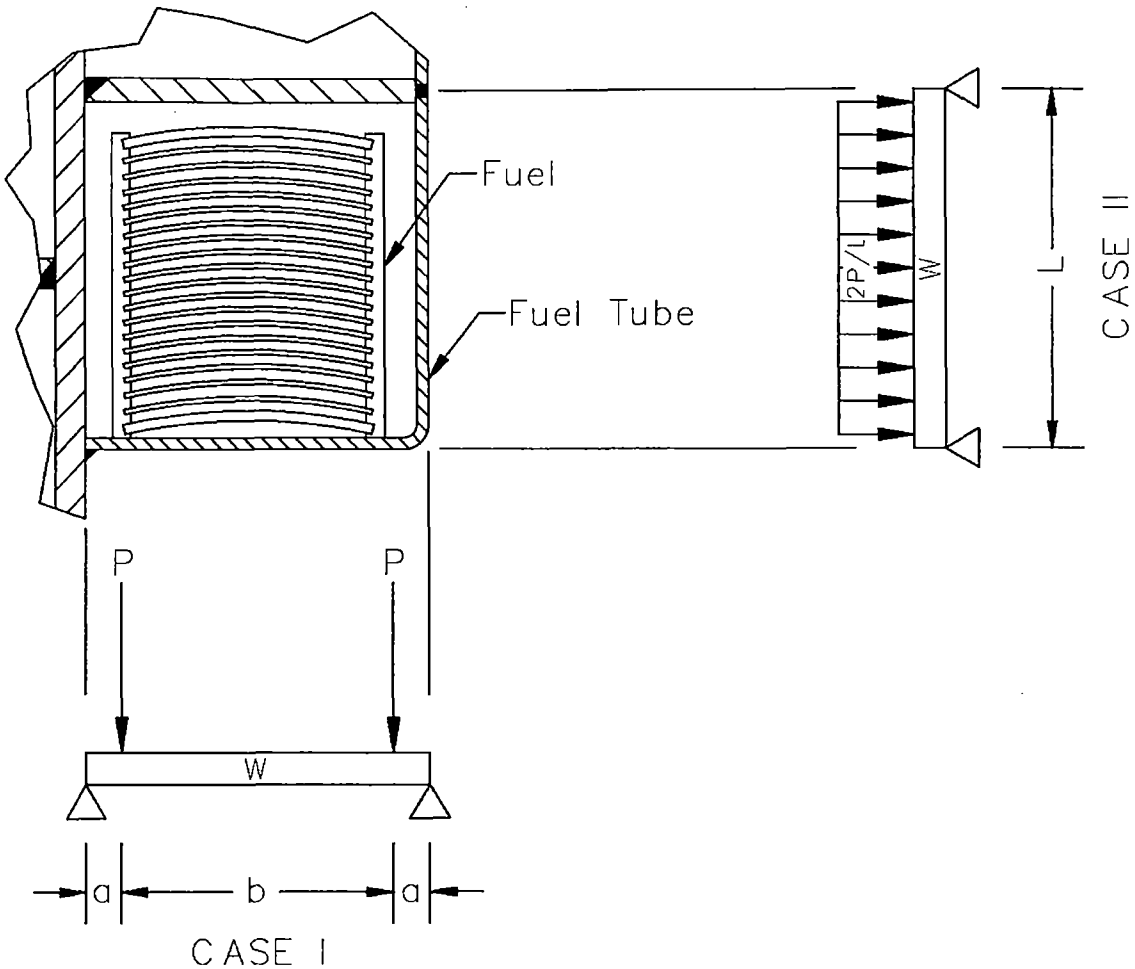

Figure 2.6.12-2 Baseplate Supports for Cask End Drop Loads – MTR Fuel Basket

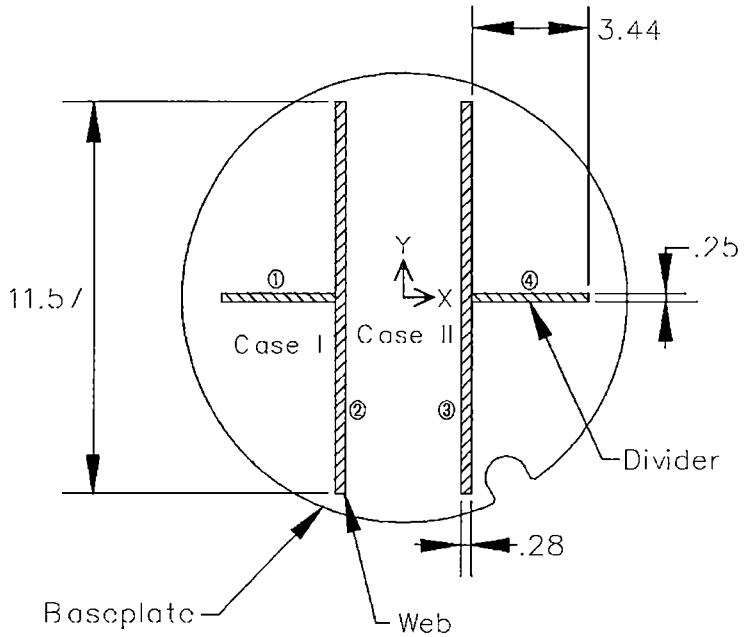

Notes:
Area of shaded portion = 8.20 in²

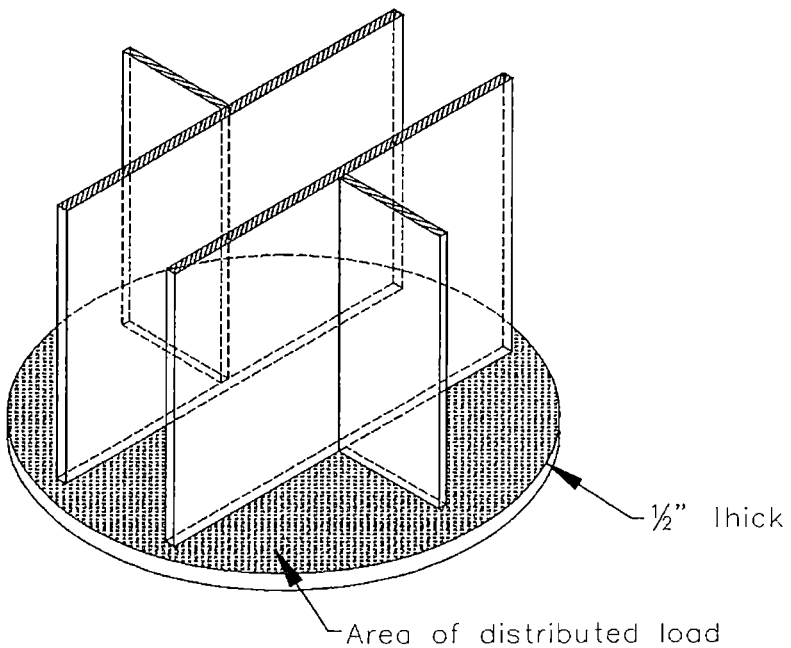

2.6.12.7 TRIGA Fuel Basket One-Foot Drop Evaluation

This section evaluates the stresses in TRIGA fuel baskets as a result of the normal condition one-foot drop. The basket assembly consists of 5 basket modules - a base module, a top module and 3 intermediate modules. During transport all 5 modules must be installed in the cask. The 3 intermediate modules are interchangeable, but the base and top modules are not. The top module is sized to accept TRIGA Fuel Follower elements, which are longer than the typical element. Two basket configurations are available, "nonpoisoned" and "poisoned," where the poisoned basket configuration utilizes borated steel plates for additional criticality control. Each module has up to 7 cells and each open cell holds up to 4 TRIGA fuel elements or up to 16 TRIGA fuel cluster rods. The center cell of each module of the nonpoisoned basket configuration is blocked by a solid 11-gage stainless steel plate that precludes fuel loading in the center cell. The structural evaluation is based on the poisoned TRIGA basket configuration, so that the structural evaluation bounds transportation of the nonpoisoned configuration with the center cell blocked. Intact fuel elements are loaded directly into the module cells, while intact fuel cluster rods are loaded into fuel rod inserts that are placed into the basket cells prior to fuel loading. For the poisoned basket design, an alternative is provided that utilizes one base module and four intermediate modules, along with a spacer to fill the space differential resulting from the use of an additional intermediate module, rather than a top module.

The top and bottom modules are designed to hold up to 4 intact TRIGA fuel elements in screened cans, or failed or damaged TRIGA fuel elements or fuel cluster rods in screened or sealed cans in each of the open cells. Up to four intact fuel elements may be confined within a screened failed fuel can. The screened can is a square tube of 14-gage Type 304 stainless steel, closed on its bottom end with a screen to allow water draining. It is closed with a lid.

Up to two failed TRIGA fuel elements or up to 6 failed TRIGA fuel cluster rods may be transported in a sealed failed fuel can. The sealed can has a circular cross-section and is fabricated from Type 304 stainless steel tubing with a 0.065-inch thick wall. The bottom end includes a check valve and drain plug to facilitate draining. The top end is closed with a metal seal and a lid that is bolted in place.

Each basket module is a Type 304 stainless steel weldment made up of two 1/2-inch thick, 13.27-inch diameter, circular plates at each end of longitudinal divider plates. The divider plates create seven compartments or cells. The outside wall of the four symmetric outermost fuel cells is fabricated from 11- gage Type 304 stainless steel sheet. The 1/2-inch plate at the top end of the module is welded to the exterior surfaces of the divider plates using a continuous 1/8-inch weld on the under side of the top plate and a continuous fillet weld on the top side. The 1/2-inch thick baseplate is continuously welded to the 1/2-inch thick divider plates and the 5/16-inch thick

web plates. The top module has an additional 1-inch thick support plate midway between the top and bottom circular plates that has a continuous fillet weld on the bottom side and a continuous seal weld on the top side. The 11-gage sheet metal, and the 5/16-inch thick (0.28-inches, min) intermediate webs, end 1/2-inch above the top surface of the baseplate to provide for module drainage. In addition, a 1-inch diameter hole is located in the module base plate, at the center of each of the cells. The bottom module sits on a 1.5-inch section of 10-inch diameter, schedule 80S, pipe welded to the baseplate. The pipe carries the total weight of the TRIGA basket assembly, and bears directly on the cask bottom forging. As previously noted, the center cell of each nonpoisoned basket module is blocked with an 11 gage plate welded to the cell walls. This plate prevents loading fuel elements in the center cell. The center cell is open at the bottom to ensure water draining.

Four of the seven cells in each poisoned basket module have a plate of borated stainless steel neutron absorber material on one side to ensure criticality control in transport. The borated plate extends over the active length of the TRIGA fuel assemblies, and covers the width and length of the cell face within the limits of the attachment welds. The configuration of the borated plate is shown in the license drawings in Section 1.4.

The bottom and intermediate modules have guide pins fixed to the surface of the top support plate. The pins fit into holes in the baseplate provided for that purpose to achieve alignment. A cutout in the baseplate and top plate is provided for clearance of the cask drain tube, and for circumferential alignment of the TRIGA basket assembly.

The weights of the TRIGA basket assembly and modules are shown below. The weight includes the heaviest fuel element that could be installed in the module, and failed fuel containers in the top and bottom modules. The calculated weight of each top and bottom module is increased by 70 lbs to account for the poison plates and to conservatively bound the structural analysis. Similarly, the calculated weight of the intermediate module is increased by 140 lbs.

Component	Weight of Fuel (lb) 140 Elements	Weight of Module(s)[1] (lb)	Total Weight (lb)	Length of Module(s) (in)
Bottom Module	247[2]	356	603	34.70
3 Intermediate Modules	741[2]	957	1,698	31.50
Top Module	370[3]	460	830	48.30
Weight of Empty Basket		1,773		
Loaded Weight of Basket			3,131	

Notes:

1. Includes the weight of failed fuel cans plus additional weight added for conservative design evaluation.
2. TRIGA fuel element design-basis weight is 8.82 pounds.
3. TRIGA fuel element design-basis weight is 13.2 pounds for top module.

The weight of TRIGA fuel cluster rods in a basket cell, including the weight of the fuel rod insert, is bounded by that of the TRIGA fuel elements. As reported in Section 1.2.3.1, the design basis weight of a TRIGA fuel element is 8.8 lbs, while the design basis weight of a TRIGA fuel cluster rod is 1.4 lbs and the weight of the insert is 11.2 lbs. Thus, four fuel elements in a cell weigh 35.2 lbs, while 16 fuel cluster rods and an insert in a cell weigh 33.6 lbs. Additionally, the active fuel cluster rod length is slightly longer than the length of the fuel elements, producing a smaller bearing load along the length of the fuel cluster rod and insert.

Therefore, the analyses of TRIGA basket modules and payload presented in the following sections are bounding for both nonpoisoned and poisoned basket configurations, and for all TRIGA fuel types.

2.6.12.7.1 NAC-LWT Inner Shell Bearing Stress Analysis

The nominal radial gap between the TRIGA fuel basket and the cask inner shell is 0.0531 inch at the calculated, steady state, normal conditions fuel temperature. As defined for other NAC-LWT fuel specific basket designs, it is assumed that there is no relative motion between the basket and the cask, and that the basket is in bearing contact with the cask cavity inner shell in the side drop. Bearing loads of the intact fuel, and the screened and sealed failed fuel cans, are thus transmitted directly to the inner shell and cask structure.

Bearing stress is calculated using Case 2C (Young) which models the cylindrical basket in a circular groove. The maximum compressive stress, for two elastic bodies with a similar elastic modulus, is:

$$S_c = 0.798\left\{\frac{\dfrac{gp(D_1 - D_2)}{D_1 D_2}}{\dfrac{2(1-\nu^2)}{E}}\right\}^{1/2} = 15{,}305 \quad \text{psi}$$

where:

g = 24.3, Dynamic load factor for the one-foot side drop

p = 1,256 lb/in., 1 g bearing load

D_1 = 13.405 inches, Cask cavity diameter

D_2 = 13.265 inches, Basket outside diameter.

ν = 0.275, Poisson's ratio for SS 304

E = 28.3 x 10^6 psi, Elastic modulus (conservatively use E at 70°F)

The bounding bearing load, p, is determined using the weight of the bottom module bearing on the inner shell of the cask at the top and bottom circular plates. The bearing surface considers the chamfer at the edge of the circular plates.

The allowable stress S_y = 18,200 psi at 600°F. Therefore:

$$MS = \frac{18{,}200}{15{,}305} - 1 = +0.19$$

2.6.12.7.2 NAC-LWT Bottom Forging Bearing Stress

The TRIGA basket assembly, when in the vertical position, is supported by a 0.5-inch thick, 10-inch nominal diameter schedule 80S pipe. The 1.5-inch long pipe is welded to the baseplate of the base unit. The compressive stress is:

$$S_c = \frac{g \times W}{A} = 3{,}073 \quad \text{psi}$$

where:

g = 15.8 Dynamic load factor for the one-foot end drop

W = 3,131 lbs, Total weight of the basket

A = 16.1 in^2, Area of 10-inch diameter Schedule 80S pipe

The allowable stress, S_y = 18,200 psi at 600 °F.

Therefore:

$$MS = \frac{18{,}200}{3{,}073} - 1 = +\underline{\text{Large}}$$

2.6.12.7.3 TRIGA Basket Compressive Stress Analysis

The TRIGA fuel basket is designed to ensure that the longitudinal movement of the basket relative to the cask inner cavity is limited. The fuel, and screened or sealed can contents are not attached to the basket, and do not impart any longitudinal structural load on the basket body. However, the basket must support itself during an end drop accident. The basket is analyzed as a column, acted upon by a structural (weight) compressive load.

The compressive stress developed in the basket compartment wall is:

$$S_c = \frac{g \times W}{A} = 6{,}033 \quad \text{psi}$$

where:

g = 15.8 Dynamic load factor for the one-foot end drop

W = 3,131 lbs, Total weight of the basket

A = 8.20 in^2, Total compartment cross-section area at base plate.

The allowable stress, S_m = 16,400 psi at 600°F.

Therefore:

$$MS = \frac{16{,}400}{6{,}033} - 1 = +\underline{1.72}$$

The Euler elastic buckling load formulation is used to determine the critical buckling load (P_{cr}) of the 10-inch diameter Schedule 80S pipe and the base module. The pipe and base module are conservatively treated as simply supported, which results in an effective length that is twice the actual length, reducing the critical buckling load by a factor of 4.0. For the 10-inch pipe, the critical buckling load is:

$$P_{cr} = \frac{\pi^2 EI}{L_e^{\ 2}} = 5.88 \times 10^9 \text{ lbs}$$

where:

E = 25.3 x 10^6 psi at 600°F

I = 212 in^4, inertia moment

L_e = 2 x 1.5 = 3.0 in., effective length (2L)

The calculated compressive load is:

P_c = W x g = 3,131 x 15.8 = 49,470 lbs

where:

g = 15.8 Dynamic load factor for the one-foot end drop

W = 3,131 lbs, Total weight of the basket

Therefore:

$$M.S. = \frac{P_{cr}}{P_c} - 1 = \frac{5.88 \times 10^9}{49{,}470} - 1 = +\underline{\text{Large}}$$

The critical buckling load for the base module is calculated using the same equation as above, by applying the moment of inertia of the fuel support structure. The fuel web and divider support structure is shown in the figure in the section titled "Baseplate Stress Due to End Drop."

The moment of inertia for the support structure is:

Item	$(I_o)_{yy}$	A	h	Ah^2	$(I_o)_{xx}$
2-11.57" x 0.28" web plate	0.0	6.48	1.86	22.42	72.28
2-3.44" x 0.25" divider plate	1.7	1.72	3.72	23.80	0.0
Total	1.7			46.22	72.28

$(I_o)_{yy} = I_o + \Sigma\, Ah^2 = 1.7 + 46.22 = 47.92\ in^4$

$(I_o)_{xx} = \Sigma\, I_o = 72.28\ in^4$

Choosing the smaller moment of inertia, $(I_o)_{yy}$, as I:

$I = 47.92\ in^4$

$$P_{cr} = \frac{\pi^2 EI}{L_e^{\ 2}} = \frac{\pi^2 \times 25.3 \times 10^6 \times 47.92}{(2 \times 33.2)^2} = 2.11 \times 10^6 \text{ lbs}$$

where:

$L_e = 2 \times 33.2$ inches

$P_c = W \times g = 3{,}131 \times 15.8 = 49{,}470$ lbs

where:

g = 15.8, Dynamic load factor for 1 foot end drop

W = 3,131 lbs, Total weight of the basket

$$M.S. = \frac{P_{cr}}{P_c} - 1 = \frac{2.11 \times 10^6}{49{,}470} - 1 = +\underline{\text{Large}}$$

2.6.12.7.4 TRIGA Basket Lateral Stress Analysis

The base plate at the end of a typical TRIGA basket module supports the weight of up to 28 TRIGA fuel elements, or the loaded screened or sealed failed fuel cans, when the cask is in the vertical orientation (0 degree drop). With the cask in the horizontal orientation (90 degree drop), the fuel cell divider plates support the entire length of the TRIGA fuel. The base plate and the divider plates share in the support of the TRIGA fuel at drop orientations between 0 and 90 degrees.

Baseplate Stress Due to End Drop

The support plate at the top end of the modules is continuously welded to the outside periphery of the plates, including the support plates that form the fuel cells. The baseplate of the basket module is continuously welded to the two 11.57-inches wide, 5/16-inch thick (0.28-inch min)

web plates, and to the two 3.44-inches wide, 1/4-inch thick divider plates as shown in the following sketch.

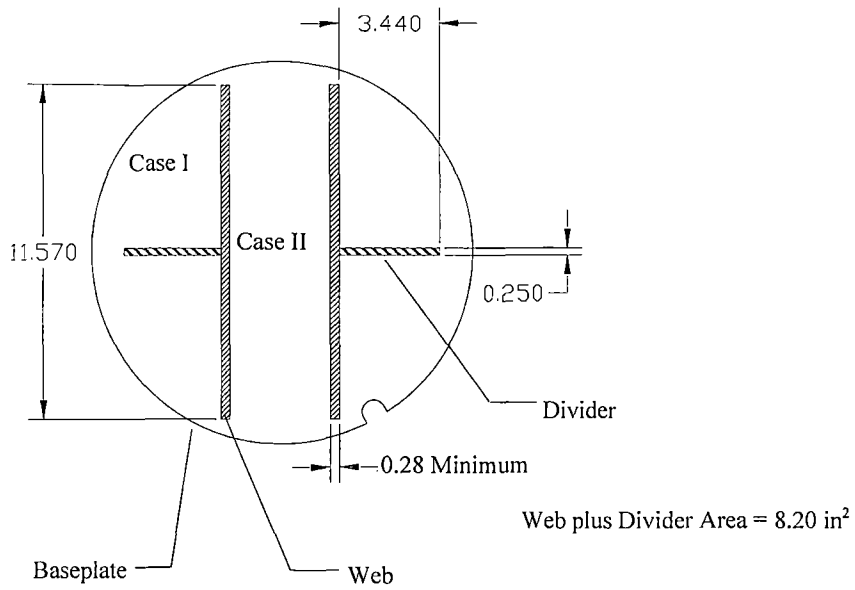

The baseplate supports 28 TRIGA fuel elements and is conservatively assumed to be supported by the main longitudinal support plates during a cask end drop. Two separate load cases are evaluated. The maximum stress for each case is combined to obtain the total stress on the baseplate.

The first case (Case I), evaluates a 3.44-inches square plate with adjacent sides fixed and the other sides free. The applied pressure over the entire plate is uniform (Young, page 471, case 11). The second case, Case II, examines a rectangular plate, 11.57 inches by 3.44 inches, fixed along the long edges, free along the short edges and uniform pressure (Young, page 462, case 6).

For Case I, the 3.44-inches square plate is analyzed as a cantilevered plate supported at two adjacent sides with the other two sides free. Load is assumed uniform over the area of the plate. The bounding fuel weight is applied. The maximum stress is expressed as (Young, page 471, case 11):

$$S_1 = \frac{-g \times B_1 \times P \times b^2}{A \times t^2} = -8{,}944 \text{ psi}$$

where:

g = 15.8, Dynamic load factor for the one-foot end drop

B_1 = 1.769, Boundary condition stress factor

P = 80 lbs, Bounding module fuel weight

b = 3.44 inches, Width of plate

A = $(3.44)^2$ sq. in., Plate area

t = 0.5 in, Plate thickness

Case II, evaluates a plate 3.44-inches by 3.44-inches (width x length), fixed on two opposite sides, with the other two sides free. The maximum stress is expressed as (Young, page 462, case 6):

$$S_{II} = \frac{-g \times B_{II} \times P \times b^2}{A \times t^2} = -2{,}528 \text{ psi}$$

where:

g = 15.8, Dynamic load factor for the one-foot end drop

B_{II} = 0.5, Boundary condition stress factor

P = 80 lbs, Bounding module fuel weight

b = 3.44 inches, Width of plate

A = $(3.44)^2$ sq. in., Plate area

t = 0.5 in., Plate thickness

The total bending stress from Case I and Case II is:

$$S_{total} = S_I + S_{II} = -11{,}472 \text{ psi} < 1.5\ S_m = 24{,}600 \text{ psi}$$

Therefore:

$$MS = \frac{24{,}600}{11{,}472} - 1 = \underline{+1.14}$$

Support Plate Stress Due to Side Drop With Intact Fuel or the Screened Failed Fuel Can

The maximum stress in the support plates that form the fuel cells occurs in the 0.12-inch thick 11 gage sheet metal tubes which support the entire length of the TRIGA fuel elements, or the length of the loaded screened failed fuel can. The weight of the TRIGA fuel element is transmitted through the can walls to the support plates that form the fuel cell. This load path creates a uniform pressure load over the entire area as shown in the following sketch.

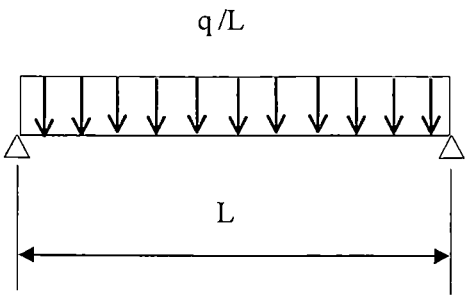

As stated in Section 2.6.12.7, the loading of TRIGA fuel cluster rods is bounded by the TRIGA fuel elements. The fuel weight per unit length for the bounding TRIGA fuel elements is:

Fuel Type	Max. Weight, W (lb)	Max. Length, L (in)	W/L (lb/in)
Aluminum Clad	6.4	28.53"	0.22
Stainless Steel Clad	8.82	29.88"	0.30
Fuel Follower Control Element	13.2	45"	0.29

The intact fuel bounding load, q_i, along the length of the tube is:

$$q_i = \frac{W_i}{L_s} = 1.850 \text{ lb / in}$$

The uniform pressure load for the shorter (L_S) failed fuel in the screened can is:

$$q_f = \frac{W_f}{L_s} = 1.950 \text{ lb/in}$$

The uniform pressure load of the longer (L_L) failed fuel in the screened can is:

$$q_f = \frac{W_f}{L_L} = 1.778 \text{ lb/in}$$

where:

L_S = 29.88 inches, length of short fuel element

L_L = 45 inches, length of long fuel element

Weight of long failed fuel can = 17 lbs

Weight of short failed fuel can = 13 lbs

Added weight for fuel can calculation = 10 lbs

The weight calculation below includes 4 fuel elements, added weight, plus fuel can.

W_f = 58.28 lbs for fuel can with fuel elements having a length of 29.88 inches (L_s)

W_f= 80 lbs for fuel can with fuel elements having a length of 45 inches (L_L)

W_i = 55.28 lbs for fuel can with intact fuel

The bounding load for TRIGA fuel is 1.950 lb/in.

The maximum bending moment is:

$$M_{max} = \frac{(q_f + w) \times gL}{8} = 21.6 \text{ in-lb}$$

where:

q_f = 1.950 lb/in

g = 24.3, dynamic load factor for one foot side drop

t = 0.12-inches (11 gage)

L = 3.44 = width of side support plate (11 gage)

w = 0.288 x 3.44 x t = 0.1185 lb/in, steel beam weight

$$S = \frac{6 \times M_{max}}{t^2} = 9{,}065 \text{ psi}$$

Therefore,

$$MS = \frac{24{,}600}{9{,}065} - 1 = +\underline{1.71}$$

The 11 gage sheet metal is continuously welded to the adjacent divider plates with a 1/8-inch fillet weld. This weld resists the shear developed in the simple beam analysis above.

$$V = \frac{(W_f + wL_s) \times g}{2 \text{ x } L_s} = 25.14 \text{ lbs}$$

where:

W_f = 58.28 lbs

L_s = 29.88 inches

$$S_v = \frac{V}{t \times l} = 210 \text{ psi}$$

The throat thickness of 1/8-inch fillet weld is 0.707 x 0.125 = 0.088-inches. The square of the ratio of the plate thickness (0.12-inch) to the weld throat thickness (0.088-inches) is 1.86. ASME Code Subsection NG-3352 recommends that the calculated stress in a fillet weld be increased by a factor of 1/0.35 = 2.86. The maximum weld stress is:

$S_w = S_v\ (1.86)\ (2.86) = 1{,}117$ psi

The allowable stress is $0.6S_m = 9{,}840$ psi at 600°F.

Therefore:

$$MS = \frac{9{,}840}{1{,}117} - 1 = +\underline{\text{Large}}$$

Support Plate Stress Due To Side Drop For the Sealed Failed Fuel Can

The total bounding weight of the long sealed can is 59.6 lbs, which includes 20 lbs for the can and a bounding weight of 39.6 lbs for the follower control elements.

The maximum stress in the support plates occurs in the 0.12-inch thick (11 gage) sheet metal tubes which supports the entire length of the sealed can. Since the sealed can is cylindrical, its weight is transmitted as a line load over the length to the supporting plate. For a unit cross-section of the supporting plate, the line load is treated as a concentrated load over the supporting plate as shown in the following loading diagram.

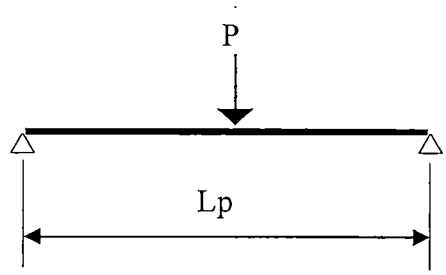

The load of the sealed can and its contents is represented by a uniformly distributed line load along the basket length that is in contact with the sealed can. For a unit length, the concentrated load due to the longer can is:

$$P = \frac{W_f \times g}{L} = 37.71\ \text{lb/in}$$

where:

W_f = 59.6 lbs, weight of the long sealed can (20 lbs) and the follower control elements (39.6 lbs)

g = 24.3, dynamic load factor for one-foot side drop

L = 38.41 inches, length of the longer body sealed can tube

For the shorter can:

$$P = \frac{W_f \times g}{L} = 45.24 \text{ lb/in.}$$

where:

W_f = 43.4 lbs, weight of the shorter sealed can (17 lbs) and bounding fuel element (26.4 lbs)

g = 24.3, dynamic load factor for one-foot side drop

L = 23.31 inches, length of the shorter body sealed can tube

The concentrated load from the shorter can, P = 45.24 lb/in., enveloping both the longer can and short can, is used to calculate the maximum bending moment. The unit length of the basket support plate with the 45.24 lbs concentrated force in the middle is treated as a simply supported beam. The maximum bending moment is:

$$M_{max} = \frac{P \times L_p}{4} = 38.91 \text{ in-lb}$$

where:

P = 45.24 lbs, concentrated load

L_p = 3.44 inches, width of the 11 gage support plate

The maximum bending stress is:

$$S = \frac{6 \times M_{max}}{t^2} = 16{,}321 \text{ psi}$$

where:

M_{max} = 38.91 in-lb, maximum bending moment

t= 0.12 in., thickness of the 11-gage support plate

The margin of safety is:

$$M.S. = \frac{1.5S_m}{S} - 1 = \frac{24{,}600}{16{,}321} - 1 = \underline{+0.51}$$

The 11 gage sheet metal is continuously welded to the adjacent divider plates with a 1/8-inch fillet weld. This weld resists shear developed in the simple beam analyzed above.

$$S_v = \frac{P}{t \times l} = 378 \text{ psi}$$

where:

P = 45.24 lbs, load of unit length

t = 0.12 in, thickness of the 11 gage support plate

The throat thickness of 1/8-inch fillet weld is 0.707 × 0.125 = 0.088 in. The square of the ratio of the plate thickness (0.12 in) to the weld throat thickness (0.088 in) is 1.86. ASME Code Subsection NG-3352 recommends that the calculated stress in a fillet weld be increased by a factor of 1/0.35 = 2.86.

Maximum weld stress is the calculated stress in the material times the above factors.

$S_w = S_v\ (1.86)\ (2.86) = 378 \times 1.86 \times 2.86 = 2{,}011$ psi

The allowable stress is:

$0.6S_m = 9{,}840$ psi @ 600°F,

The margin of safety is:

$$MS = \frac{9{,}840}{2{,}011} - 1 = +\underline{3.9}$$

Maximum Basket Stress Due To Oblique Drop

As shown in the previous sections, the sealed can imposes the largest stress in the basket support plate due to its cylindrical cross-section. Therefore, the maximum stress in the basket is bounded by the stress induced by the sealed failed fuel can.

The maximum stress in the basket during oblique drop is found by combining the absolute value of the maximum stresses found in the basket during side drop and end drop determined in the previous sections. Although the stresses in the two different drop configurations do not occur in the same location, the stress combination method conservatively envelopes the maximum possible stress states during the oblique drop.

The maximum calculated stresses for the 1-foot end drop and the 1-foot side drop are:

Maximum stress = 6,033 psi for end drop
Maximum stress = 16,321 psi for side drop

Adding the two stress values to obtain the total oblique drop stress = 6,033 + 16,321 = 22,354 psi.

Allowable stress = 1.5 S_m = 1.5 x 16,400 = 24,600 psi @ 600°F,

$$MS = \frac{24{,}600}{22{,}354} - 1 = +\underline{0.10}$$

2.6.12.7.5 Screened Failed Fuel Can

This section evaluates the stresses in the screened failed fuel can as a result of the normal condition one-foot drop. The screened failed fuel can is described in Section 2.6.12.7. The screened failed fuel can is analyzed for side and end drops during transportation.

Screened Failed Fuel Can Compressive Stress Analysis

The fuel contents are not attached to the screened can and do not impart any longitudinal structural load on the can. The screened can must support itself during an end drop accident. The can is analyzed as a column acted upon by a structural (weight) compressive load consisting of the weight of the can and its contents. The screened can for fuel follower control rods is used since it is heavier, carries a heavier load and has the same properties as the screened can for the fuel rods.

The compressive stress developed in the screened can wall is:

$S_c = Wg/A = 1{,}145$ psi

where:

W = 71 lbs, weight of screened can and contents

g = 15.8, dynamic load factor for one foot end drop (normal condition)

A = 0.98 in^2, cross-section area of screened can

The allowable stress,

S_m=16,400 psi at 600°F.

Therefore:

MS = (16,400/1,145) - 1 = +Large

Buckling of the screened failed fuel can is evaluated using hypothetical accident loading conditions in Section 2.7.7.9.4. The loading conditions presented in that section bound normal condition loads.

Screened Failed Fuel Can Plate Stress Due to Side Drop

The plate making up the sides of the screened failed fuel can is analyzed for bending as a result of loads applied during a side drop. To bound the analysis, the weight of the longer failed fuel can is used and this load is distributed over the length of the shorter fuel can to determine the load acting on a one-inch wide strip (along the axial length of the can) of the fuel can cross section. This total load on a one-inch strip is conservatively applied to the area between fuel elements (1.5 inches), resting inside of the can. This is the longest span of plate subject to

bending from a side drop and the 1.5-inch long plate section (which is one-inch wide) is considered to be simply supported.

The bending moment in the plate due to a uniform load is:

$M = gPL/8 = 10.3$ in-lb

where:

$g = 24.3$, dynamic load factor for one foot side drop

$P = 2.26$ lbs., Total load on one inch wide strip

$L = 1.5$inches, spacing between fuel elements

The section modulus, s, of the cross-section resisting the bending moment is:

$s = t^2/6 = 0.00093$ in.^{3}

where:

$t = 0.0747$ in, thickness of plate making up the screened failed fuel can

The bending stress is:

$S_b = M/s = 11{,}075$ psi

The allowable stress is: $1.5S_m = 24{,}600$ psi

Therefore:

$MS = (24{,}600/11{,}075) - 1 = +\underline{1.22}$

2.6.12.7.6 Sealed Failed Fuel Can

This section evaluates the stresses in the sealed failed fuel can as a result of the normal condition one-foot side and end drops. The sealed can is described in Section 2.6.12.7.

Sealed Failed Fuel Can Compressive Stress Analyses Due to End Drop

This section analyzes the compressive stress and buckling load in the fuel tube, bottom tube and lifting lugs. The bounding weight of the sealed can used in this analysis is 59.6 lbs, which includes 20 lbs for the can and conservatively 39.6 lbs for the follower control elements. Actual operational capacity is controlled to the weight of two fuel elements.

Fuel Tube

The fuel elements are not attached to the round tube that forms the wall of the can. However, it is conservatively assumed that the shell of the sealed can carries the entire weight of the can and contents. The compressive stress is:

$$\sigma_C = \frac{W \times g}{A} = 1{,}448 \text{ psi}$$

where:

W = 59.6 lbs, conservative weight of the can and contents

g = 15.8, dynamic load factor for one foot end drop

A = $\pi(1.625^2 - 1.56^2) = 0.6504$ in.^{2} cross section area of the can

The margin of safety is:

$$MS = \frac{S_m}{\sigma_C} - 1 = \frac{16{,}400}{1{,}448} - 1 = +\underline{\text{Large}}$$

Bottom Tube

The compressive stress for the bottom tube is:

$$\sigma_C = \frac{W \times g}{A} = 1{,}010 \text{ psi}$$

where:

W = 59.6 lbs, conservative weight of the can and contents

g = 15.8, dynamic load factor for one foot end drop

A = $\pi(1.25^2 - 1.125^2) = 0.9327$ in.^{2} cross section area of bottom tube

The margin of safety is:

$$MS = \frac{S_m}{\sigma_C} - 1 = \frac{16{,}400}{1{,}010} - 1 = +\underline{\text{Large}}$$

Lifting Lug

The sealed can lifting lugs may be subject to compressive or buckling loads in drop accident events. The load is considered evenly distributed to both lugs.

The compressive stress for two lift lugs is:

$$\sigma_C = \frac{W \times g}{A} = 3{,}657 \text{ psi}$$

where:

W = 59.6 lbs, conservative weight of the can and contents

g = 15.8, dynamic load factor for one foot end drop

A = 2 x 0.515 x 0.25 = 0.2575 in.^{2} smallest cross section area of the two lift lugs

The margin of safety is:

$$MS = \frac{S_m}{\sigma_C} - 1 = \frac{16{,}400}{3{,}657} - 1 = +\underline{3.48}$$

Considering the lifting lug as a cantilever beam with a fixed end, the load is carried by an equivalent moment, M:

$$M = (P/2) \times d \times g = 114.2 \text{ in-lbs}$$

where:

g = 15.8, g load factor for the one foot end drop

P = 59.6 lbs, conservative weight of can and contents

d = 0.2425 in, the length of moment arm, measured from the center of the section to the point of load application (.5 - .515/2)

The total stress acting on the neck section is:

$$\sigma = \frac{(M \times c)}{I} + \sigma_C = 13{,}975 \text{ psi}$$

where:

σ_c = compressive stress, 3,657 psi

W = 114.2 in-lbs, equivalent moment

c = 0.515/2 inches, distance from center of neck section to the edge

I = $0.25 \times (0.515)^3/12 = 2.85 \times 10^{-3}$ in^4, moment of inertia of the cross section

The margin of safety is:

$$MS = \frac{1.5S_m}{\sigma_c} - 1 = \frac{24{,}600}{13{,}975} - 1 = +\underline{0.76}$$

Buckling of the Sealed Failed Fuel Can

Buckling of the sealed failed fuel can, the bottom tube and the lifting lug is evaluated in Section 2.7.7.9.5. The loading conditions presented in that section bound the normal condition loads.

Sealed Failed Fuel Can Plate Stress Due to Side Drop

In the one-foot side drop, the sealed can supports the load applied by its contents.

The load applied to the can is considered as a linearly distributed load over the bottom 120° arc. The radial pressure w_x varies linearly from 0 at the beginning, to w at the bottom point of the can, as shown in the following sketch.

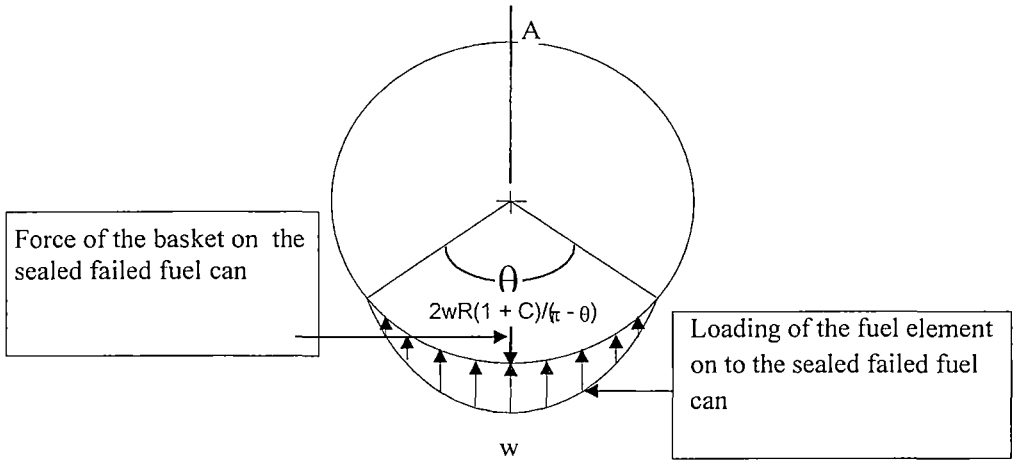

The load is uniformly distributed along the length of the can. For a unit length it is calculated as:

For the longer can:

$$p = \frac{W_f \times g}{L} = 25.05 \text{ lb / in.}$$

where:

W_f = 39.6 lbs, conservative fuel weight of three fuel follower control elements

g = 24.3, dynamic load factor for a one-foot side drop

L = 38.41 inches, length of the longer tube body

For the shorter can:

$$p = \frac{W_f \times g}{L} = 27.52 \text{ lb / in.}$$

where:

W_f = 24.4 lbs, conservative fuel weight of three fuel elements

g = 24.3, dynamic load factor for a one-foot side drop

L = 23.31 inches, length of the shorter tube body

To bound both the longer can and short can, p = 27.52 lb/in. is used to calculate the maximum distributed load.

Since (Young, 6th Edition, Table 17, Case 13):

$$p = 2wR(1 + C) / (\pi - \theta)$$

$$w = \frac{p \times (\pi - \theta)}{2R \times (1 + C)} = 17.73 \text{ lb/in}$$

where:

p = 27.52 lbs, load on this unit length of the can tube

θ = 120° = 2π/3, angle

C = cos (θ) = -0.5

R = 3.25/2, radius of the can

The bending moment occurring at location A and C are respectively (Young, 6th Edition, Table 17, Case 13):

$$M_A = \frac{-wR^2}{\pi(\pi - \theta)} \left\{ 2 + 2C - s(\pi - \theta) + k_2 \left[1 + C - \frac{(\pi - \theta)^2}{2} \right] \right\} = -1.273 \text{ in-lb}$$

$$M_C = \frac{-wR^2}{\pi(\pi - \theta)} \left\{ \pi(\pi - \theta) - 2 - 2C - s\theta + k_2 \left[1 + C - \frac{(\pi - \theta)^2}{2} \right] \right\} = -6.507 \text{ in-lb}$$

where:

w = 17.73 lb/in, maximum distributed load

R = 3.25/2 - 0.625/2, curvature

θ = 120° = 2π/3, angle

C = cos (θ) = -0.5

s = sin(θ) = 0.866

$k_2 = 1 - \alpha = 1$ and $\alpha = \frac{I}{AR^2} = \frac{2.289e-5}{0.6504 \times 1.593^2} = 1.388 \times 10^{-5}$

$I = \frac{1 \times 0.065^3}{12} = 2.289 \times 10^{-5}$ in^4, moment of inertia of ring cross section

$A = \pi(1.625^2 - 1.56^2) = 0.6504$ in^2

The bending stress at location C, for unit length, is:

$$\sigma_c = \frac{M_C}{t^2/6} = 9{,}241 \text{ psi}$$

where:

M_C = 6.507 lb-in., bending moment at location C

t= 0.065 in., thickness of the can

Margin of safety is:

$$MS = \frac{S_m}{\sigma_C} - 1 = \frac{16{,}400}{9{,}241} - 1 = +\underline{0.77}$$

Sealed Failed Fuel Can Bolt Evaluation

The sealed failed fuel can bolts are evaluated using the worst case loading conditions. For analysis purposes, the maximum differential thermal expansion (from accident conditions), lifting loads, and bolt preload are combined to calculate the maximum bolt stresses.

Bolt Thread Stress

The shear stress caused by lifting is:

$$\tau_L = \frac{1.1 \times W}{A_S} = 170 \text{ psi}$$

where:

1.1 = dynamic load factor for lifting

W = total weight of the canister and contents, 59.6 lbs

A_S = shear area of the external thread, 0.3859 in.^{2}

The load caused by pre-load on each bolt is:

$F_T = (\pi \times D \times P)/4 = 1{,}721$ lbs

where:

P = 700 lb/in., conservative linear load required to crush the seal

D = 3.131 inches, diameter of the seal

The linear load, P, considers both the load to seat the metal seal as well as the internal pressure of the gas in the failed fuel canister. The contribution of the pressure to the linear load is:

$$\frac{P_{gas} D}{4} = \frac{(3\,\text{atm})(14.7\,\text{psi / atm})(3.131\,\text{in.})}{4} = 34.5 \text{ lb / in.}$$

Three (3) atm is conservatively used for the internal gas pressure during the fire. The linear load to seat the metal seal is 514 lbs. Combining the linear loads due to the pressure and seal gives a total value of 548.5 lb/inch. For analysis purposes, a conservative value of 700 lb/in. is used.

The shear stress caused by pre-loads in the bolts is:

$$\tau_t = \frac{F_t}{A_s} = 4{,}460 \text{ psi}$$

where:

F_t = 1,721 lbs, bolt pre-load

A_s = shear area for 3/8 -16 UNC 2A thread = 0.3859 sq. inch

Total shear caused by lifting and pre-load is obtained by conservatively adding the shear stresses:

$$\tau = \tau_L + \tau_t = 4{,}630 \text{ psi}$$

The margin of safety is:

$$MS = \frac{0.6S_m}{\tau} - 1 = \frac{0.6 \times 45{,}200}{4{,}630} - 1 = +\underline{4.86}$$

The average tensile stress due to pre-load in the bolts is:

$$S_t = \frac{F_t}{A_t} = 23{,}039 \text{ psi}$$

where:

F_t = 1,721 lbs, bolt pre-load

A_t = tensile stress area for 3/8-14 UNC 2A thread = 0.0747 in^2

The tensile stress due to the differential expansion of the bolt and the top plate is:

$$S_{dt} = \Delta T(\alpha_L - \alpha_{637})E_{637} = 26{,}912 \text{ psi}$$

where:

ΔT = (600 - 70)°F = 530°F (The actual maximum temperature of the can during the fire accident is 551°F.)

α_L = 9.53 x 10^{-6} (in/in/°F), coefficient of thermal expansion of top plate (S.S.304) at 600°F

α_{637} = 7.67 x 10^{-6} (in/in/°F), coefficient of thermal expansion of bolt (SB - 637) at 600°F

E_{637} = 27.3 x 10^6 psi at 600°F, bolt material elastic modulus at 600°F

The total stress due to pre-load and differential expansion of the bolt and the top plate is:

$$S = S_{dt} + S_t = 49{,}951 \text{ psi}$$

The margin of safety is:

$$M.S = \frac{2S_m}{S} - 1 = \frac{2 \times 45{,}200}{49{,}951} - 1 = +\underline{0.81}$$

The relation between the torque value and tensile force is:

$$T = \left[\left(\frac{d_m}{2d}\right)\left(\frac{\tan\lambda + \mu\sec\alpha}{1 - \mu\tan\lambda\sec\alpha}\right) + 0.625\mu\right](F_T)(d) \qquad \text{(Machinery's)}$$

$$T = (0.2096) \times F_T \times d = 135 \text{ in-lb}$$

where:

T = applied torque in inch-pounds

F_T = pre-load force in pounds

d = 3/8 in, bolt diameter

$\tan\lambda = L/(\pi d_m)$

L = 1/16 in

d_m = 0.3911 in, mean diameter of threads

α = 30°, one-half the thread angle

μ = 0.15, coefficient of friction

The torque required to engage the bolt is 135 in-lb. However, the maximum torque is 160 in-lb. The torsional stress due to this torque value is:

$$\tau_t = \frac{T \times r}{J} = \frac{160 \times 0.1875}{1.94 \times 10^{-3}} \text{ psi} = 15{,}464 \text{ psi}$$

where:

T = 160 in-lb, the torque on a bolt

r = (3/8)/2 = 0.1875 in, radius of bolt

J = $(\pi r^4)/2 = (\pi \times 0.1875^4)/2 = 1.94 \times 10^{-3}$ in^4, polar moment of inertia

The margin of safety is:

$$MS = \frac{0.8S_m}{\tau_t} - 1 = \frac{0.8 \times 45{,}200}{15{,}464} - 1 = +\underline{1.34}$$

Top Plate Thread Stress

The effect of Heli-Coil is conservatively ignored. The shear stress consists of two parts; one is caused by the lifting load; the other is caused by the combination of pre-load P (700 lbs/in.) and differential thermal expansion. The shear stress due to the lifting load is:

$$t_L = \frac{1.1 \times W}{A_n} = 118 \text{ psi}$$

where:

1.1 = the dynamic load factor for lifting

W = 59.6 lbs, total weight of the canister and contents

A_n = 0.5548 in^2, shear area of the inner thread

The shear stress due to pre-load and differential thermal expansion in the top plate is:

$$S = \frac{F_t}{A_n} = 6{,}725 \text{ psi}$$

where:

F_t = 1,721+26,912 x 0.0747 = 3,731 lbs, bolt pre-load

A_n = 0.5548 in^2, shear area for 3/8 -16 UNC 2A thread

Total shear caused by lifting, pre-load and differential expansion is obtained by conservatively adding the separate shear stresses:

$$\tau = \tau_L + S = 6{,}843 \text{ psi}$$

The margin of safety is:

$$MS = \frac{0.6S_m}{\tau} - 1 = \frac{0.6 \times 16{,}400}{6843} - 1 = \underline{+0.44}$$

Top Plate Bearing Stress

Top plate bearing stress is developed from the combination of pre-load and the differential thermal expansion of the bolt and the top plate. The pre-load is 1,721 lbs on one bolt and thermal load is 2,010 lbs (0.0747 in^2 × 26,912 psi). The total bearing is 3,731 lbs. Then, the bearing stress on the top plate is:

$$S_b = \frac{P_b}{A_b} = \frac{3731}{0.2311} = 16{,}145 \text{ psi}$$

where:

P_b = 3,731 lbs, total bearing force

$A_b = \pi(0.68^2-0.41^2)/4 = 0.2311$ in^2, bearing area

The margin of safety for top plate is:

$$MS = \frac{1.0S_y}{S_b} - 1 = \frac{18{,}200}{16{,}145} - 1 = +\underline{0.13}$$

2.6.12.7.7 Borated Stainless Steel Plate Weld Stress

The borated stainless steel plate utilized in the poisoned TRIGA baskets is assumed to be welded on two sides to the divider plates using a 1/16-inch fillet weld. This assumption is conservative since the borated plate is welded completely around its periphery. For the end drop condition, the only load applied on the weld is the self weight of the plate, which results in a shear stress. For side drop, the load applied on the weld is the self weight of plate, which also results in shear stress. The plate also carries the weight of the fuel, which results in compressive stress.

The welded area for one stainless steel plate is:

Parameter	Base Module	Intermediate Module	Top Module
Weight of Plate (lb)*	14.44	13.64	21.61
Length of Plate (in)	30.45	28.75	45.55
Cross Section Area (in^2)	99.27	93.73	148.49
Weld Area (in^2)	3.81	3.59	5.69

Using the smallest area, 3.59 in^2 and largest weight, 21.61 lbs, the end drop shear stress is:

$$S_{se} = \frac{g \times W}{A} = \frac{15.8 \times 21.61}{3.59} = 95.11 \text{ psi}$$

where:

g = 15.8 one-foot end drop load factor

W = 21.61 lbs bounding poison plate weight

A = 3.59 in^2 bounding weld area

The allowable shear stress for normal condition is 0.6 S_m = 9840 psi. The margin of safety is:

$$\text{Margin of Safety} = \frac{0.6S_m}{S_{se}} - 1 = \frac{9840}{95.11} - 1 = +\underline{\text{Large}}$$

Using the smallest area, 3.59 in^2 and largest weight, 21.61 lbs, the side drop shear stress is:

$$S_{ss} = \frac{g \times W}{A} = \frac{24.3 \times 21.61}{3.59} = 146.27 \text{ psi}$$

where:

g = 24.3 one-foot side drop load factor

W =21.61 lbs bounding poison plate weight

A = 3.59 in^2 bounding weld area

The allowable shear stress for normal condition is 0.6 S_m = 9840 psi. The margin of safety is:

$$\text{Margin of Safety} = \frac{0.6S_m}{S_{ss}} - 1 = \frac{9840}{146.27} - 1 = +\underline{\text{Large}}$$

The compressive stress is evaluated using a bounding fuel cell weight of 80 lbs. The minimum cross section area is 93.73 in^2.

$$S_c = \frac{g \times W}{A} = \frac{24.3 \times 80}{93.73} = 20.74 \text{ psi}$$

where:

g = 24.3 one-foot side drop load factor

W = 80 lbs bounding fuel cell weight

A = 93.73 in^2 bounding cross section area

The allowable stress is 1.0S_m = 16,400 psi. The margin of safety is:

$$\text{Margin of Safety} = \frac{1.0S_m}{S_c} - 1 = \frac{16{,}400}{20.74} - 1 = +\underline{\text{Large}}$$

This evaluation shows that the weld has large margins of safety for the stresses that could occur in normal conditions.

2.6.12.7.8 TRIGA Fuel Spacer Evaluation

A spacer fabricated from Type 304 stainless steel is used in poisoned TRIGA basket Configuration 2 (base module and 4 intermediate modules). The spacer consists of 8-inch diameter pipe with a 1-inch thick plate welded to the bottom, and a 0.5-inch thick plate welded to the top. The top plate is attached to the underside of the NAC-LWT cask lid using four 1/2-inch diameter SA-193, Grade B6, bolts. It has a calculated weight of 85 lbs.

The spacer and bolts are analyzed for the effects of a normal condition 1-foot side and end drop. The material temperatures and properties are the same as those imposed on the fuel baskets. The compression load is calculated as 50,813 lbs, which results in a calculated stress of 6,049 psi

(Margin of Safety = +1.71). The stress on the bolts in combined shear and tension is 11,881 psi. All margins of safety are positive with a minimum Margin of Safety of +0.21 for the bolts in shear and tension as a result of the side drop condition.

2.6.12.7.9 TRIGA Fuel Cluster Rods Basket One Foot Drop Evaluation

The fuel cluster rod is restrained from motion by the aluminum tube, which has a 0.75-inch outer diameter and a 0.62-inch inner diameter. An array of four by four is inserted into an aluminum shell of 0.125-inch thickness, which is loaded into the stainless steel basket.

The bearing stress between the aluminum tubes is required to be less than the yield stress of the 6061-T6 aluminum. The yield stress is evaluated at the maximum aluminum temperature of 300°F, corresponding to a yield stress of 27.5 ksi. The maximum bearing load would occur between the aluminum tube and the 0.125 aluminum shell (Point 2 in the following sketch), but the maximum bearing stress would occur between two adjacent cylinders (Point 1 in the following sketch).

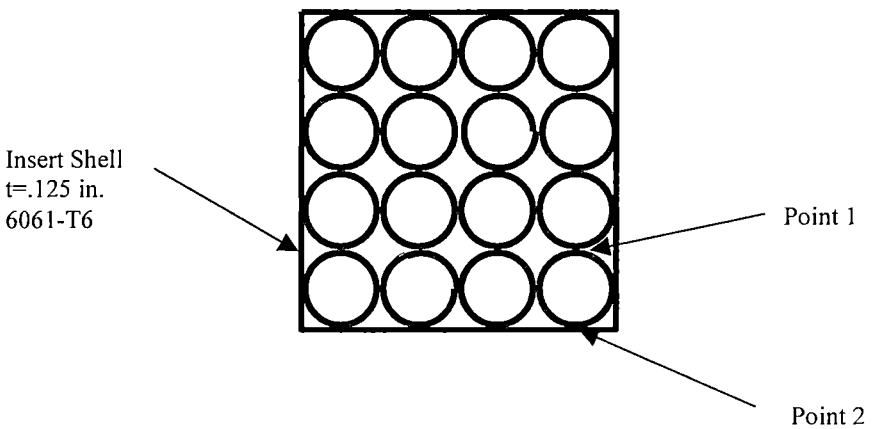

Using Roark, 6th edition, Table 33, Case 2a, which is the bearing stress between two adjacent cylinders, the bearing stress (S_{brg}) is:

$$S_{brg} = .789 \times \sqrt{\frac{P}{K_D C_E}}$$

$$P = \text{the line load} = (3 \text{ tubes}) \left(\frac{1.44}{27.5} + \frac{\pi}{4}(0.75^2 - 0.62^2)(0.098) \right)$$

$$P = 0.198 \text{ lbs/in (for dead weight only)}$$

where:

TRIGA fuel cluster rod weight	=	1.44 lbs
rod length	=	27.5 inches

aluminum density	=	0.098 lb/in^3
aluminum tube OD	=	0.75 in
aluminum tube ID	=	0.62 in

$$C_E = \frac{1-\upsilon_1^2}{E_1} + \frac{1-\upsilon_2^2}{E_2} = 1.937e-7$$

where for 6061-T6 Aluminum at 300°F:

E = 9.2 x 10^6 psi

V = 0.33 and the subscripts 1 and 2 refer to each of the cylinders

where:

$$K_D = \frac{D_1 D_2}{D_1 + D_2} = .375$$

where D is the outer diameter of the tube, .75 in (the subscripts 1 and 2 refer to the individual tubes). The bearing stress corresponding to 24.3 g is:

$$S_{brg} = .798 \times \sqrt{\frac{24.3 \times 0.198}{0.375 \times 1.937e-7}} = 6495 \text{ psi}$$

$$MS = \frac{27400}{6495} - 1 = +\underline{3.21}$$

The bending stress in the aluminum insert tube is evaluated as a curved beam using the diametrical point forces, as contained in Roark's, 6th Edition, Table 17, Case 1.

Conservatively using 400°F to evaluate the aluminum properties, and the weight of four tubes (which results in a line load of 1.33 × 0.198 = 0.263 lbs/in), the maximum bending stress in the aluminum tube is:

$$S_b = \frac{6M}{bt^2}$$

Where b = 1.0 in, which is the axial length for the purpose of the calculation.

$$M = 0.3183 \cdot P \cdot R \cdot k_2$$

$$k_2 = 1 - \alpha$$

$$\alpha = \frac{I}{AR^2}$$

$$t_{ring} = \frac{.75 - .62}{2} = 0.065\text{in} \qquad I = \frac{0.065^3 \times 1}{12} = 2.29\text{e-}5\ \text{in}^4 \qquad A = .065 \times 1 = 0.065\ \text{in}^2$$

$$R = \frac{0.62}{2} + \frac{0.065}{2} = 0.343\text{in} \qquad \alpha = \frac{2.29\text{e-}5}{0.065 \times 0.343^2} = 0.003 \qquad k_2 = 1 - 0.003 = 0.997$$

$$M = 0.3183 \times (4 \times 0.263) \times 0.343 \times 0.997 = 0.115\ \text{in-lb/in}$$

$$S_b = \frac{6 \times 0.115 \times 24.3}{1 \times 0.065^2} = 3969\ \text{psi}$$

$$MS = \frac{1.5S_m}{S_b} - 1 = \frac{8250}{3969} - 1 = +\underline{1.07}$$

Where 24.3 g corresponds to the side drop accelerations.

This verifies that the aluminum insert tube is acceptable for the normal operational conditions.

2.6.12.8 DIDO Fuel Basket Construction

The DIDO modular basket assembly consists of a top module, four intermediate modules, and a base module. The top module is 29.8 inches long and the intermediate modules are each 29.3 inches long and all have an outer diameter of 13.27 inches. The base module has a length of 29.8 inches and an outer diameter of 13.27 inches. Each module is capable of holding seven DIDO fuel assemblies. Each module is a weldment made up of a 13.27 inch diameter 1/2-inch thick base plate and two 13.27 inch diameter 1/2-inch thick support plates scalloped on the inner diameter to fit around six peripheral fuel tubes. The weldment structure, fuel tubes and base and support plates are fabricated from Type 304 stainless steel. Each fuel tube has an inner diameter of 4.01 inches and a wall thickness of 0.12 inches. The bottom of each fuel tube is welded to the 1/2-inch thick base plate. At the bottom of each fuel tube, where it is welded to the base plate, there is a 0.3-inch slot to permit water to drain from the tube. The base plate supports the fuel in the end drop orientation. The base module sits on a 0.5-inch long, 10-inch diameter schedule 80S pipe that is welded to the base plate. The total weight of the DIDO basket assembly bears directly on the bottom forging of the cask through the schedule 80S pipe. The two scalloped 1/2-inch thick support plates and the base plate of each basket module provide lateral support and maintain the fuel configuration in the side drop orientation.

Heat rejection from the DIDO fuel and basket structure is augmented by six aluminum shunts and two heat transfer shells. Each shunt is mechanically attached to the center stainless steel fuel

tube. The heat transfer shell wraps around the 6 outer fuel tubes and is mechanically attached to the drain tube guide bars. The heat shunts are machined to match the outer diameter of the center fuel tube and are held in place by two shunt posts and shunt retainers. The shunt post at the bottom of each basket module is assembled with a tight fit between the shunt post, shunt retainer and base plate to provide a good conductive heat transfer path. The shunt post at the top of the basket is assembled with a slotted hole in the shunt to permit unrestricted differential thermal expansion between the fuel tube and thermal shunt. The aluminum sheet heat transfer shell is held in place against the outside fuel tubes by bolting the edge of the aluminum sheet to the drain tube guide bars. The heat shunts and heat transfer shell are not structural components and are not included in the structural analysis as load carrying components. The mass of the heat shunts and heat transfer shell have been included as loads in the structural analysis.

2.6.12.8.1 DIDO Fuel Basket Cask Interface Analysis

Structural analysis of the DIDO modular fuel basket and the MTR modular fuel basket are similar. DIDO fuel baskets and MTR fuel baskets are made from the same type of stainless steel. The contact points between the basket structure and the cask inner shell and between the basket structure and the cask bottom forging are similar. DIDO fuel baskets have an additional lateral support ring, reducing the side drop bearing stresses. A loaded DIDO fuel basket base module weighs approximately 250 lbs, assuming each DIDO assembly weighs 15 lbs. Loaded top and intermediate modules weigh approximately 247.4 lbs each. A full cask load of six DIDO basket modules represents a total contents weight of 1,487 lbs. The weight of a loaded 28-element MTR basket module is 289 lbs, which bounds the loaded weight of the loaded base DIDO basket module. Therefore, the bearing stress between the basket and the cask inner shell created by the DIDO basket module is bounded by the 28-element MTR fuel basket interface analysis.

The cask contents weight for the loaded 42-element MTR basket is 2,262 lbs, which bounds the cask contents weight of 1,487 lbs for the loaded DIDO basket. Therefore, the bearing stresses between the basket and cask bottom forging and between the basket and the cask lid created by the DIDO fuel baskets, are bounded by the 42-element MTR fuel basket interface analysis.

2.6.12.8.2 DIDO Fuel Basket Structural Analysis

Structural analyses of the DIDO fuel basket for the 1-foot end drop and the 1-foot side drop are performed using a finite element model of one basket module, as shown in Figure 2.6.12-1 and Figure 2.6.12-2, and the ANSYS general purpose computer program. Eight node brick elements (SOLID45) are used to construct the model. Each solid element has the material properties of stainless steel. In each basket module, the elements representing the seven 4.01-inch inner diameter tubes are joined to the base plate and to the two support plates at locations where the

welds are specified to connect the tubes to the plates. By design, the center tube is not connected to any of the six outer tubes. In this evaluation, the center tube is not considered to have any interaction with the outer six tubes, which is conservative, particularly in the side drop orientation where the tube is cantilevered from the base plate.

DIDO Fuel Basket 1-Foot Side Drop Orientation Analysis

The 1-foot side drop analysis of the DIDO fuel basket considers the weight of the center tube and fuel to be transferred to the circular base plate. A bounding fuel assembly weight of 15 pounds is used in the side drop analysis. To model the interaction of the two support plates and the base plate with the 13.375-inch cask inner shell diameter, CONTAC52 elements are used. The CONTACT52 element consists of two nodes, which corresponds to a 3D-line element, limiting transmitted loads to compression. One node of the CONTACT52 element is located on a circular plate, while the second node represents the inner shell, and is constrained in all three degrees of freedom. This boundary condition is considered to be conservative, since it models the inner shell as a rigid surface and minimizes the angle of contact between a circular plate and the cask inner shell, resulting in a more concentrated load at the point of contact. The aluminum heat shunts and aluminum heat transfer shell are not considered to be structural components. The shunts and shells are represented as lumped masses using the MASS21 element. These lumped masses are distributed along the outside of the center tube to represent the distributed weight of the heat shunt. The heat transfer shell is represented with lumped masses distributed along the outer six fuel tubes at the points of contact with the heat transfer shell.

The 1-foot side drop normal condition event is analyzed using an acceleration of 24.3g applied in each of three orientations: 0°, -60°, and -90° with respect to the model's X-axis. Maximum primary membrane stresses for each of the side drop orientations are shown in Table 2.6.12-1. The minimum margin of safety is calculated to be +2.5 for the 0° and 60° orientations. The maximum primary membrane plus bending stresses for each of the side drop orientations are shown in Table 2.6.12-2. The minimum margin of safety is calculated to be + 0.003 for the 60° orientation. Figure 2.6.12-3 presents the location of the maximum primary membrane and the primary membrane plus bending stresses for the side drop load.

DIDO Fuel Basket 1-Foot End Drop Analysis

For the end drop analysis, the finite element model load orientation and boundary conditions are specified to represent axial loading and consideration of the base basket module supporting five stacked modules above it. Equivalent pressure was applied to the area inside of the fuel tube at the top surface of the base plate to represent the fuel in each of the fuel tube locations in each basket module. The weight of the five loaded fuel basket modules, which rest on the base fuel basket module, multiplied by the equivalent acceleration, is applied as an equivalent pressure to

the top edges of the fuel tubes in the base module. A bounding DIDO fuel assembly weight of 15 pounds is used in the end drop analysis. The bounding assembly weight accounts for the fuel assembly and the tube spacer and variations in the weight of either. The total weight resting on the top of the base module is approximately 1,237 pounds. This load was applied as a pressure load on the ends of the fuel tubes.

Total end area of tubes = $7 \times \pi/4 \times (4.25^2 - 4.01^2) = 10.9$ in^2
Equivalent pressure = 1237 lbs/10.9 in^2 = 113.5 psi

The end drop finite element model reflects the base basket design shown on the drawings provided in Section 1.0. The height of the base skirt below the bottom support is 0.5 inch. Four full height drain slots are cut into the base skirt.

For the 1-foot end drop condition, the equivalent pressure load is increased to represent the maximum acceleration of 15.8 g. The maximum primary membrane stress for the end drop orientation is 11.4 ksi (shown in Table 2.6.12-1) resulting in a minimum margin of safety of +0.75. The maximum primary membrane plus bending stress is 13.2 ksi (shown in Table 2.6.12-2) resulting in a minimum margin of safety of + 1.27. Figure 2.6.12-6 presents the location of the maximum primary membrane and the primary membrane plus bending stresses for the end drop load.

Based on these results, it is concluded that the DIDO fuel basket is structurally adequate for normal transport conditions.

2.6.12.8.3 Fuel Assembly Spacer Structural Evaluation

During a top end drop, the spacer would be loaded by the weight of the fuel and the tube spacer. A bounding analysis of the DIDO fuel spacer post and top disk, based on hypothetical accident condition g-loads, is performed. The DIDO fuel assembly weight of 15 lbs is considered to include the weight of the tube spacer. The post is analyzed by determining the membrane stress due to the weight of the fuel assembly and tube spacer acting concentrically on the post. The top disk of the spacer is analyzed as a circular plate with a uniform load acting over the entire surface of the disk. The results, showing the spacer design is adequate to sustain the hypothetical accident top end drop analysis, are:

Component	Primary Membrane Stress (psi)	Allowable Stress (psi) @ Temp.	Margin of Safety	Primary Membrane + Bending (psi)	Allowable Stress (psi) @ Temp.	Margin of Safety
Pin	1,140	46,200	Large	5,082	66,000	12.0
Disk	N/A	46,200	N/A	10,980	66,000	5.0

Figure 2.6.12-3 DIDO Fuel Basket Module Structural Model – Top View

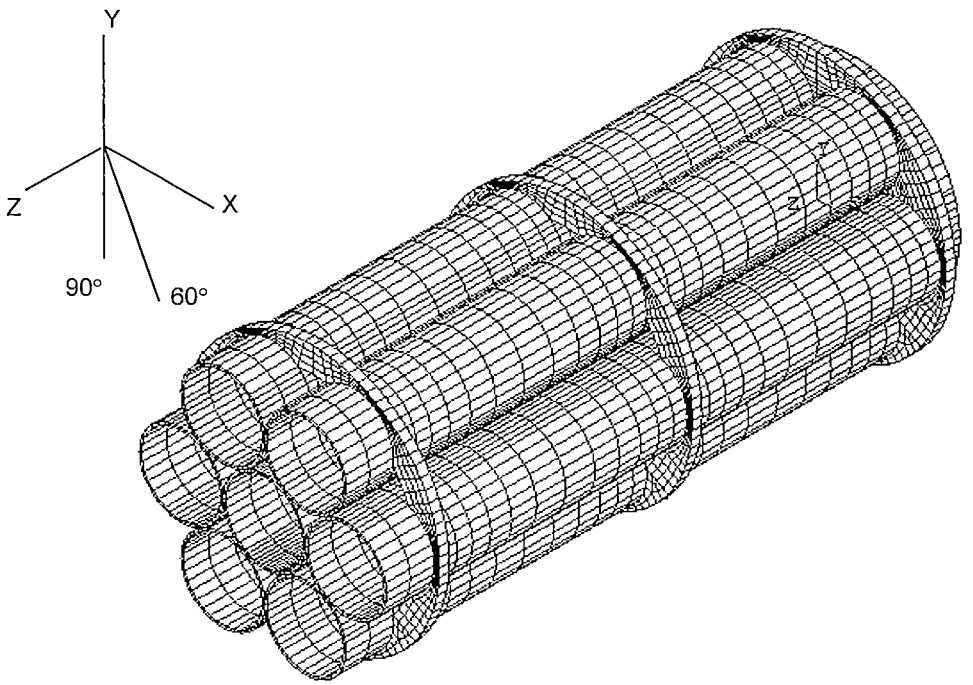

Figure 2.6.12-4 DIDO Fuel Basket Module Structural Model – Bottom View

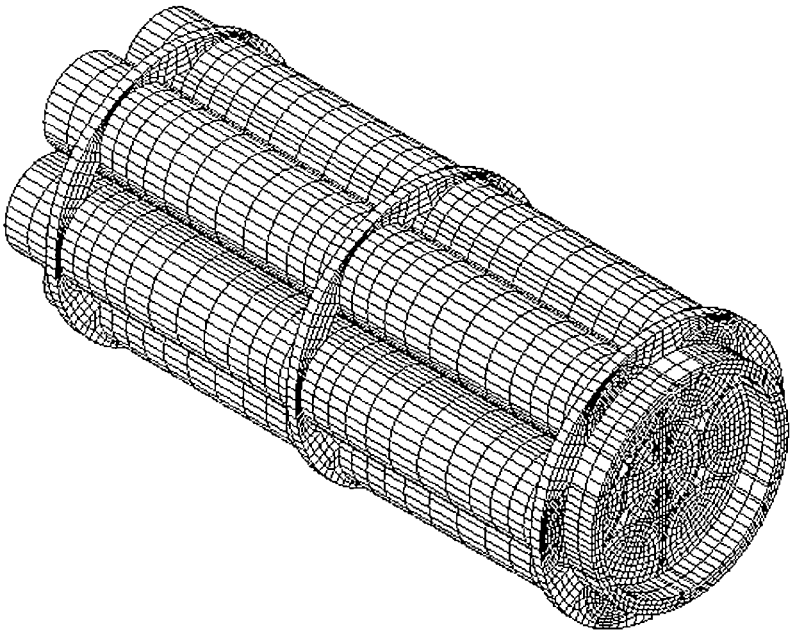

Figure 2.6.12-5 DIDO Fuel Basket Module Maximum Stress Locations for the Side Drop Orientation

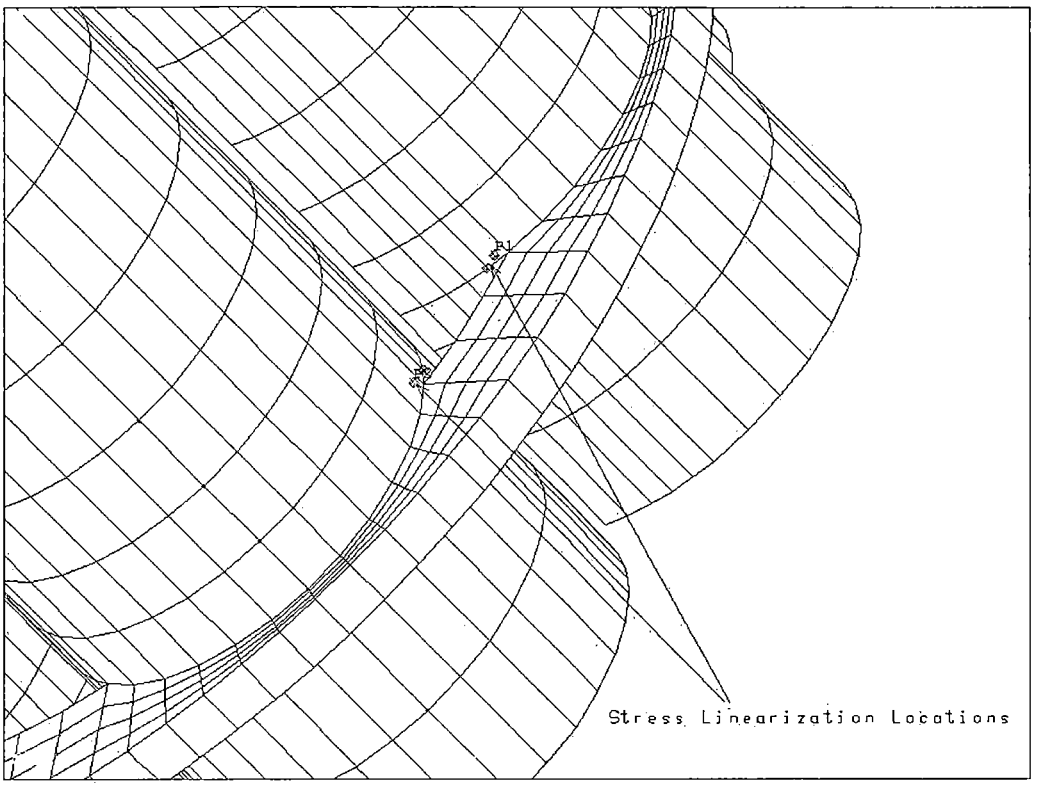

Figure 2.6.12-6 DIDO Fuel Basket Module Maximum Stress Locations for the End Drop Orientation

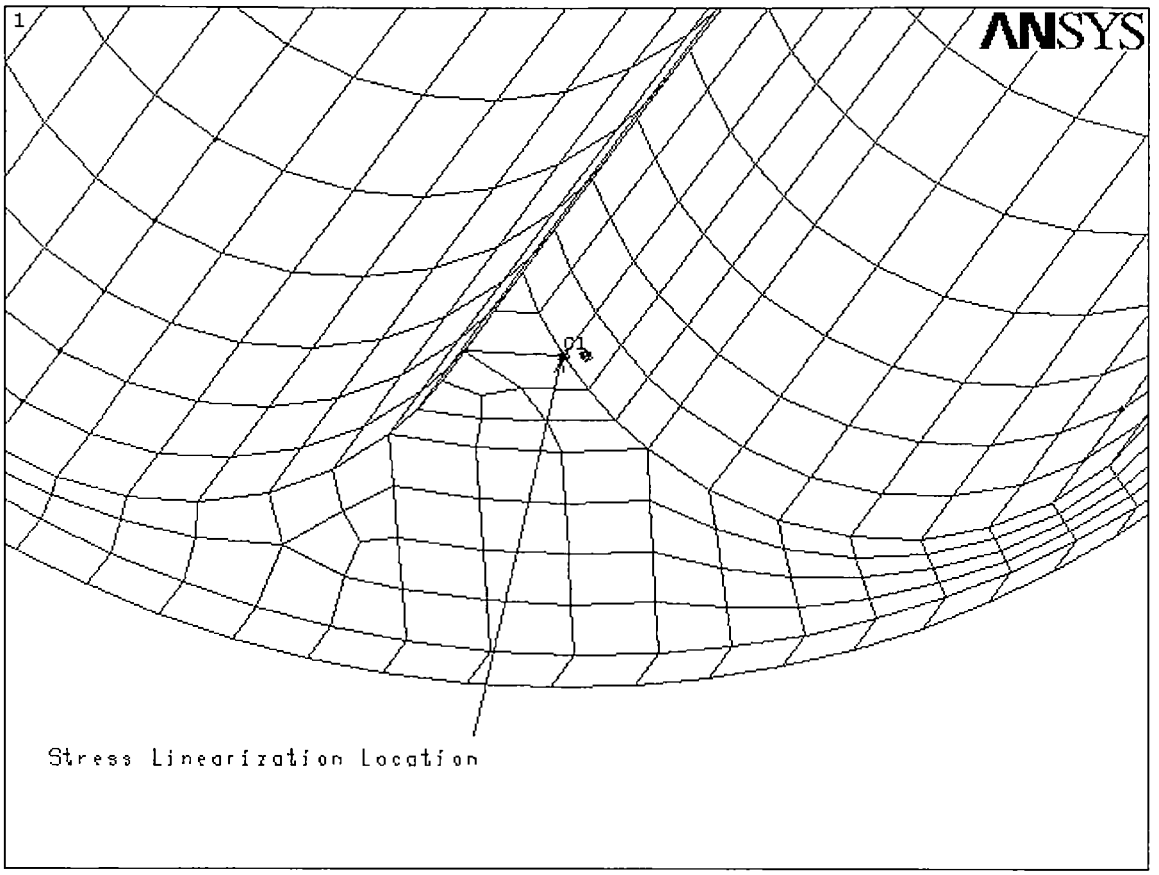

Table 2.6.12-1 Maximum Primary Membrane Stress for the 1-Foot Drop (DIDO Basket)

Location	Load Case 1-ft drop	Membrane (ksi)	Allowable (ksi) [1]	Margin of Safety [2]
Fuel Tube Wall	Side @ 0 Deg[3]	5.7	20.0	2.5
Fuel Tube Wall	Side @ 60 Deg[3]	5.7	20.0	2.5
Fuel Tube Wall	Side @ 90 Deg[3]	5.2	20.0	2.8
Fuel Tube Wall	End drop	11.4[4]	20.0	0.75

Table 2.6.12-2 Maximum Primary Membrane Plus Bending Stress for the 1-Foot Drop (DIDO Basket)

Location	Load Case 1-ft drop	Membrane + Bending (ksi)	Allowable (ksi) [5]	Margin of Safety [2]
Fuel Tube Wall	Side @ 0 Deg[3]	29.6[6]	30.0	0.01
Fuel Tube Wall	Side @ 60 Deg[3]	29.9[6]	30.0	0.003
Fuel Tube Wall	Side @ 90 Deg[3]	24.4[6]	30.0	0.23
Fuel Tube Wall	End drop	13.2[4]	30.0	1.27

1 $P_m \leq S_m$.
2 Margin of safety = (Allowable-Stress/Actual Stress) – 1.
3 Angle orientation shown on Figure 2.6.12-1.
4 The linearized stresses for the end drop case are scaled by the ratio of 360/178.65, which is the full arc-to-arc length of the tube welded to the base plate.
5 $P_m + P_b \leq 1.5S_m$.
6 These stresses are maximum local tube wall stresses and may be considered secondary stresses. They are conservatively considered primary membrane plus bending stresses and are located as shown in Figure 2.6.12-3.

2.6.12.9 General Atomics IFM Basket Construction

The General Atomics Irradiated Fuel Material (IFM) basket consists of a top module assembly designed to carry two IFM Fuel Handling Units (FHUs). Each IFM FHU is associated with RERTR or HTGR fuel materials. A spacer assembly is used to permit the top module assembly to be positioned next to the transport cask lid.

The top module is 43.7 inches long and is made up of two fuel tubes and three support plates. All components are made from ASME SA240 Type 304 stainless steel. The fuel tubes have a 6.0-inch outer diameter and a 0.25-inch wall thickness. Two of the support plates are 0.50-inch thick and the third, center plate, is 1.0-inch thick. The support plates are welded to the fuel tubes with 1/8-inch bevel welds.

Two types of IFM FHU are carried by the top module. One FHU carries irradiated HTGR fuel material and is 5.25 inches in diameter (0.12-inch thick wall) and 39.0 inches long. The other FHU contains irradiated RERTR fuel material, is 4.75 inches in diameter (0.12-inch thick wall), and is 37.25 inches long.

Each end of the FHU is comprised of a 0.25-inch thick plate welded to the container shell. The weld connecting the end plate to the container shell is labeled as a full-penetration butt weld. The dimensions of the end plate and the container shell provide a minimal gap (2 mils when considering maximum tolerances) to permit the end plate to be inserted into the container end. The close tolerances ensure that the two components are effectively in contact along the 0.5-inch common interface length of the end plate and the container. Once the end plate is inserted, a fusion weld procedure is employed to weld the lip of the end plate to the wall of the container. The depth of the weld along the interface between the end plate and the container is equal to approximately 70% of the thickness of the end plate lip or the container lip.

Due to the location of the weld for the end plate, the weld does not transfer any load for the drop conditions. Additionally, since the heat loads are insignificant (13w) and the backfill for the FHU and the cask cavity are limited to atmospheric pressure, the pressure differential across the welded plates is insignificant. Each of these FHUs also has an additional smaller container, which holds the fuel. In these evaluations, the inner container is neglected.

The spacer assembly is 133.0 inches in length, excluding guide pins. The assembly is comprised of one spacer tube and five support plates. The spacer tube consists of a Type 304 stainless steel 8-inch Schedule 80S pipe. The tube has an outside diameter of 8.63 inches and a wall thickness of 0.50 inch. The spacer plates are 1.0-inch thick and are welded to the tube with 1/8-inch bevel welds. Two guide pins are located at the top of the spacer assembly to facilitate alignment with the top module.

2.6.12.9.1 General Atomics IFM Basket Interface Analysis

The structural evaluation of the top module assembly is performed using classical hand calculations. The weight of the top module is bounded by 200 lbs, and the maximum weight of one FHU and its fuel contents is 76 lbs. Therefore, the total weight of a loaded top module system is 200 + 2(76) or 352 lbs. The weight of the spacer assembly is 760 lbs. The total loaded system weight is 1,112 lbs, and this weight is bounded by the design basis contents weight for the LWT system. Therefore, no analysis of the LWT cask body is required.

2.6.12.9.2 General Atomics Top Module Structural Analysis

Structural analyses for the top module for the 1-foot end drop and 1-foot side drop are performed using classical hand calculations.

General Atomics 1-Foot Side Drop Analysis

Top Module:

During a 1-foot side drop, the distributed load on one fuel tube is:

$$W = \frac{\left(76 + 0.291 \times \frac{\pi\left(6.0^2 - 5.5^2\right)}{4} \times 43.7\right)}{43.7} = 3.1 \text{ lb/in}$$

where:

weight of fuel = 76 lbs

length of tube = 43.7 inches

outer diameter = 6.0 inches

inner diameter = 5.5 inches

The maximum bending moment in tube is:

$$M = \frac{3.1 \times 20.35^2}{8} = 160 \text{ in - lbs}$$

The maximum bending stress in the fuel tube for 1g loading is:

$$I = \frac{\pi\left(6.0^4 - 5.5^4\right)}{64} = 18.7 \text{ in}^4$$

$$S_b = \frac{160 \times 3}{18.7} = 26 \text{ psi}$$

The margin of safety for tube bending for a 1-foot side drop (25g) is:

$$MS = \frac{1.5S_m}{S_b} - 1 = \frac{1.5 \times 19350}{25 \times 26} - 1 = + \underline{\text{Large}}$$

During a 1-foot side drop, the support plates bear up against the inner shell of the LWT cask. The center plate will carry the maximum weight. The bearing load on the center plate is:

$$W = \frac{10 \times \frac{[(2 \times 76) + 200]}{40.7} \times 20.35}{8} = 220 \text{ lbs}$$ (Page 2-299, #12, Manual of Steel Construction)

The bearing stress is maximum for the center disk.

The bearing stress is (Item 2c, Table 33, Young):

LWT cask cavity diameter, D1 = 13.375 inches

Support plate diameter, D2 = 13.265 inches

$$K_D = \frac{D_1 D_2}{D_1 - D_2} = 1{,}613$$

$$C_E = \frac{1 - 0.31^2}{26.75e6} + \frac{1 - 0.31^2}{8.29e6} = 1.42e-7$$

$$S_c = 0.798\sqrt{\frac{p}{K_D C_E}} = 0.798\sqrt{\frac{220}{1613 \times 1.42e\text{-}7}} = 782 \text{ psi, 1g loading}$$

where:

p = 220/(1.0) = 220 lbs/in

E = 26.75e6 psi @ 350°F

Effective 'E' of LWT shells with lead:

$$E = \frac{0.75 \times 26.75e6 + 1.25 \times 26.75e6 + 5.75 \times 1.87e6}{7.75} = 8.29e6 \text{ psi}$$

The margin of safety for bearing for a 1-foot side drop (25g) is:

$$MS = \frac{S_y}{25 \times S_c} = \frac{21600}{25 \times 782} - 1 = +0.10$$

During a side drop, the top and bottom support plate welds are in shear. The load on the weld due to 1g is:

$$W = \frac{3 \times \frac{[(2 \times 76) + 200]}{40.7} \times 20.35}{8} = 66 \text{ lbs}$$ (Page 2-299, #12, Manual of Steel Construction)

The weld length is:

$$L = 2(\pi d_{tube} - r_{tube}\theta)$$
$$= 2(\pi \times 6.0 - 3.0 \times 1.57) = 28.3 \text{ inches}$$
$$\theta = \text{non welded arc length} = 90 \text{ deg} = 1.57 \text{ radians}$$

The support disk/ tube weld is a 1/8-inch bevel weld. The stress in the weld for 1g is:

$$S = \frac{66}{(28.3 \times 0.125 \times 0.7071)} = 26.4 \text{ psi, 1g loading}$$

For visual inspection, the weld factor is 0.25 per ASME Section III, Subsection NG-3352. The margin of safety for shear is:

$$MS = \frac{0.25 \times 0.6S_m}{25S} - 1 = \frac{0.25 \times 0.6 \times 19350}{25 \times 26.4} - 1 = +3.4$$

<u>Spacer Assembly:</u>

During a 1-foot side drop, the distributed load on the tube is:

$$W = \frac{760}{129.5} = 5.9 \text{ lb/in, use } 6.0 \text{ lb/in}$$

The maximum bending moment in tube, conservatively assuming a simply supported beam, is:

$$M = \frac{6 \times 32.0^2}{8} = 768 \text{ in - lbs}$$

The bending stress in tube for a 1g loading is:

$$I = \frac{\pi(8.63^4 - 7.63^4)}{64} = 106 \text{ in}^4$$

$$S_b = \frac{768 \times (8.63/2)}{106} = 31 \text{ psi}$$

The margin of safety for bending in the 1-foot side drop (25g) is:

$$MS = \frac{1.5S_m}{S_b} - 1 = \frac{1.5 \times 19350}{25 \times 31} - 1 = + \underline{\text{Large}}$$

During a 1-foot side drop, the support plates bear up against the inner shell of the LWT cask. The maximum load on a support plate during a side drop is:

$$W = 1.143 \times \frac{760}{128.0} \times 32.0 = 217 \text{ lbs}$$ (Page 2-309, #39, Manual of Steel Construction)

The bearing stress is (Item 2c, Table 33, Young):

LWT cask cavity diameter $D_1 = 13.375$ inches

Support plate diameter $D_2 = 13.265$ inches

$$K_D = \frac{D_1 D_2}{D_1 - D_2} = 1{,}613$$

$$C_E = \frac{1-0.31^2}{26.75e6} + \frac{1-0.31^2}{8.29e6} = 1.42e-7$$

$$S_c = 0.798\sqrt{\frac{p}{K_D C_E}} = 0.798\sqrt{\frac{217}{1613 \times 1.42e\text{-}7}} = 777 \text{ psi}$$

where:

$p = 217 / 1.0 = 217$ lb/in

$E = 26.75e6$ psi @ 350°F

Effective 'E' of LWT shells with lead:

$$E = \frac{0.75 \times 26.75e6 + 1.25 \times 26.75e6 + 5.75 \times 1.87e6}{7.75} = 8.29e6 \text{ psi}$$

The margin of safety for bearing is:

$$MS = \frac{S_y}{25 \times S_c} = \frac{21600}{25 \times 777} - 1 = +0.11$$

During a side drop, the top and support plate weld is in shear. The load on the weld is:

$$W = 0.393 \times \frac{760}{128.0} 32.0 = 75 \text{ lbs}$$ (Page 2-309, #39, Manual of Steel Construction)

The weld length is:

$$L = \pi \times 8.63 = 27.1 \text{ inches}$$

The weld between the support disk and tube is a 1/8-inch bevel weld. The stress in the weld for 1g is:

$$S = \frac{75}{(27.1 \times 0.125 \times 0.7071)} = 31 \text{ psi, 1g loading}$$

For visual inspection, the weld factor is 0.25 per ASME Section III, Subsection NG-3352. The margin of safety for shear is:

$$MS = \frac{0.25 \times 0.6S_m}{25S} - 1 = \frac{0.25 \times 0.6 \times 19350}{25 \times 31} - 1 = 2.7$$

Fuel Handling Units (FHU)

The FHUs are analyzed in accordance with ASME Section III, Subsection NG. The bounding weight of a loaded fuel container is 76 lbs.

The side drop is analyzed assuming a circular ring under an external compressive load using Roarks Table 17, Item 1 (Young). The stress in the container shell is:

$$\alpha = \frac{I}{AR^2} = \frac{\pi(2.125^3) \times (0.12)}{\pi\left(2.125^2 - 2.0^2\right) \times 2.125^2} = 0.49$$

$$k_2 = 1 - \alpha = 1 - 0.49 = 0.51$$

$$M = (0.5 - 0.3183k_2)WR = [0.5 - 0.3183(0.51)]\frac{76}{35.5}2.125 = 1.5 \text{ in - lb}$$

$$S = \frac{6(1.5)}{0.12^2} = 0.63 \text{ ksi}$$

The margin of safety is:

$$MS = \frac{1.5S_m}{25S} - 1 = \frac{1.5 \times 19.35}{25 \times 0.63} - 1 = +0.84$$

General Atomics 1-Foot End Drop Analysis

Top Module:

During an end drop, the stress in the fuel tubes is calculated as follows.

The cross-sectional area of a tube is:

$$A = \frac{\pi\left(6.0^2 - 5.5^2\right)}{4} = 4.52 \text{ in}^2$$

Using a top module weight of 200 lbs, fuel weight not included, the stress in the two fuel tubes is:

$$S = \frac{200}{2 \times 4.52} = 22 \text{ psi}$$

The margin of safety is:

$$MS = \frac{S_m}{20S} - 1 = \frac{19350}{20 \times 22} - 1 = +\underline{\text{Large}}$$

Since the axial compression stress in the tubes is minimal, no buckling evaluation is required.

The top end drop is the bounding end drop because the top end has significantly less bearing area than the bottom end, and the weight of the spacer is included.

The bearing area for the top end is assumed to be the two fuel tubes, conservatively neglecting the lifting components. The cross-sectional area is:

$$A = 2\left[\frac{\pi\left(6.0^2 - 5.5^2\right)}{4} - 3.22 \times 0.25\right] = 7.42 \text{ in}^2$$

where:

outer diameter = 6.0 inches

inner diameter = 5.5 inches

cut out arc length = 3.22 inches

$$S = r\theta = 2.875 \times 1.12 = 3.22 \text{ inches}$$

$$\theta = 2 \times \tan^{-1}\left(\frac{1.72}{2.75}\right) = 64.05^\circ = 1.12 \text{ radians}$$

The bearing stress, fuel weight not included, in the module for a 1g loading is:

$$S_{brg} = \frac{200 + 760}{7.42} = 129 \text{ psi}$$

The margin of safety is:

$$S_{brg} = 20 \times 129 = 2.58 \text{ ksi}$$

$$MS = \frac{S_y}{S_{brg}} - 1 = \frac{21.6}{2.58} - 1 = +7.37$$

During an end drop, the self-weight of the center support plate has to be carried by the welds. The weight of the center support plate is:

$$W = 0.291\left\{1.0\left[\frac{\pi \times 13.265^2}{4} - 2\left(\frac{\pi \times 6.0^2}{4}\right)\right]\right\} = 24 \text{ lbs (use 30 lbs)}$$

where:

0.291 lbs/in^3 is the density of 304 stainless steel

1.0 inch is the disk thickness

13.265 inches is the disk diameter

6.0 inches is the cutout diameter

The weld length is:

$$L = 2(\pi d_{tube} - r_{tube}\theta)$$
$$= 2(\pi \times 6.0 - 3.0 \times 1.57) = 28.3 \text{ in.}$$
$$\theta = \text{nonwelded arc length} = 90 \text{ deg} = 1.57 \text{ radians}$$

The welds are 1/8-inch bevel welds on both sides of the disk. The stress in the weld for 1g is:

$$S = \frac{30}{2(28.3 \times 0.125 \times 0.7071)} = 6.0 \text{ psi}$$

For visual inspection, the weld factor is 0.25 per ASME Section III, Subsection NG-3352. The margin of safety for normal conditions is:

$$MS = \frac{0.25 \times 0.6S_m}{20S} - 1 = \frac{0.25 \times 0.6 \times 19350}{20 \times 6} - 1 = +\underline{\text{Large}}$$

Spacer Assembly:

During an end drop, the stress in the tube is calculated as follows.

The cross-sectional area of a tube is:

$$A = \frac{\pi(8.63^2 - 7.63^2)}{4} = 12.77 \text{ in}^2$$

The stress in the tube is:

$$S = \frac{760 + 200 + 2 \times 76}{12.77} = 87 \text{ psi}$$

The margin of safety is:

$$MS = \frac{S_m}{20S} - 1 = \frac{19350}{20 \times 87} - 1 = +\underline{\text{Large}}$$

Since the axial stress in the tube is minimal, no buckling evaluation is required.

For a top and bottom end drop, the bearing stresses for 1g are:

$$A_{top} = 2(9.9 \times 0.3125) = 6.19 \text{ in}^2$$

$$S_{brg} = \frac{760}{6.19} = 123 \text{ psi}$$

$$A_{bot} = \frac{\pi(8.63^2 - 7.63^2)}{4} - (4 \times 1.0 \times 0.5) = 10.77 \text{ in}^2$$

$$S_{brg} = \frac{760 + 200 + 2 \times 76}{10.77} = 103 \text{ psi}$$

The margin of safety is:

$$S_{brg} = 20 \times 123 = 2.46 \text{ ksi}$$

$$MS = \frac{S_y}{S_{brg}} - 1 = \frac{21.6}{2.46} - 1 = +7.78$$

During an end drop, the weight of a support plate has to be carried by the welds to the tube.

The weight of the support plate is:

$$W = 0.291\left(\frac{\pi\left(13.265^2 - 8.63^2\right)}{4} \times 1.0\right) \approx 25 \text{ lbs}$$

The weld length is:

$$L = \pi \times 8.63 = 27.1 \text{ inches}$$

$$S = \frac{25}{2(27.1 \times 0.125 \times 0.7071)} = 5.2 \text{ psi}$$

Since the weld stress is less than the weld stress in the support disks in the top module, no additional analysis is required.

Fuel Handling Unit:

The maximum bearing stress occurs in the top end drop orientation. The bearing area for the handle supports is:

$$A = 2 \times 0.5^2 = 0.5 \text{ in}^2$$

The bearing stress is:

$$S_{brg} = \frac{76}{0.5} = 152 \text{ psi}$$

The margin of safety is

$$S_{brg} = 20 \times 152 = 3.0 \text{ ksi}$$

$$MS = \frac{S_y}{S_{brg}} - 1 = \frac{21.6}{3.0} - 1 = +6.2$$

The top lid and bottom plates sit on a lip in the container shell. The cross-sectional area of the lip is:

$$A = \frac{\pi\left(4.124^2 - 4.0^2\right)}{4} = 0.79 \text{ in}^2$$

Since the area is greater than the handle support area above, no additional analysis is required.

The cross-sectional area of the tube is:

$$A = \frac{\pi\left(4.25^2 - 4.0^2\right)}{4} = 1.62\ \text{in}^2$$

For a 20g end drop, normal conditions, the stress in the tube is:

$$S = \frac{20 \times 76}{1.62} = 0.94\ \text{ksi}$$

$$MS = \frac{S_m}{S} - 1 = \frac{19.35}{0.94} - 1 = +\underline{\text{Large}}$$

Since the axial compression stresses in the tube are minimal, no buckling evaluation is required.

2.6.12.10 TPBAR Basket Analysis

The TPBAR basket is a modified NAC-LWT PWR basket with increased free volume that is fabricated from 6061-T651 aluminum alloy. Figure 2.6.12-7 shows the cross-section of the TPBAR basket. A 13.25-inch outside diameter, 8.25-inch long stainless steel alternate upper fitting is bolted to the top of the basket body. This fitting provides lifting points for removing the basket from the cask. Additionally, this alternate upper fitting prevents the basket from applying load to the TPBAR contents during the top-end drop. A stainless steel lower fitting is bolted to the bottom of the basket body. The lower fitting assembly supports the fuel basket and contents longitudinally. An additional spacer assembly is bolted to the cask lid to prevent the TPBAR contents from shifting axially and rotationally within the basket. A groove on the periphery of the basket body provides for the cask drain tube. The drain tube is connected to a fitting on the cask body for draining or filling the cask during wet cask loading or unloading operations.

The TPBAR basket accommodates two TPBAR content configurations. The first TPBAR content configuration is the shipment of up to 300 production TPBARs (of which two can be prefailed) contained in an open consolidation canister with optional top insert. The consolidation canister body is fabricated from Type 304 stainless steel and the bail is fabricated from Type 7-4 precipitation hardened stainless steel. The consolidation canister is used to load and unload the TPBARs into and from the NAC-LWT cask configured with a TPBAR basket assembly.

The second TPBAR content configuration is the shipment of up to 55 segmented TPBARs, following post-irradiation examinations (PIE), contained in a welded sealed waste container. The waste container is welded to an extension weldment to provide the identical length as the consolidation canister to assure fit-up in the TPBAR basket assembly. The waste container and extension are fabricated from Type 316L stainless steel.

Following placement of the consolidation canister or the waste container with extension in the TPBAR basket, and installation and bolting of the lid, the TPBAR basket and contents are evaluated without consideration of the strength of the consolidation canister or waste container. The TPBAR basket provides a boundary for support on all sides of the consolidation canister and TPBARs for the full length of the canister. The cylindrical TPBAR waste container (external diameter 8.6 inches) is sized to fit within the square cross-section (8.8 inches) of the TPBAR basket. The TPBAR upper end-fitting spacer guides do not permit the consolidation canister to be loaded by the TPBAR basket in any drop orientation. The TPBAR spacer assembly attached to the bottom of the cask lid restricts the movement of the TPBARs in the axial direction and prevents rotation of the TPBAR waste container. Therefore, no additional evaluations are required for the TPBAR consolidation canister or TPBAR waste container and extension weldment.

2.6.12.10.1 TPBAR Basket Body

Structural analyses of the TPBAR basket for 1-foot side and end drops are performed using classical hand calculations. The analyzed weight of the loaded TPBAR consolidation canister is 1,000 lbs, which bounds the loaded weight of the TPBAR waste container and extension of 700 lbs. Therefore, the analyses provided for the consolidation canister are bounding.

TPBAR Basket Body 1-Foot Side Drop Analysis

The TPBAR basket body is constructed of four machined segments held together with aluminum bands at five locations along the axial length of the basket; as well as the top and bottom fittings, which are bolted to the aluminum basket. During a side drop, the TPBAR basket is subjected to bending and bearing stresses. The maximum bending stress occurs at Location 'A' as shown in the following sketch and is due to the content weight. The maximum bending stress is calculated using a cantilevered beam. This is conservative, since it neglects any support of the load due to the edges of the basket being supported by the cask inner shell. The maximum bending stress is:

$$S_b = \frac{6M}{t^2} = \frac{6 \times 152}{0.5^2} = 3.6\,\text{ksi}$$

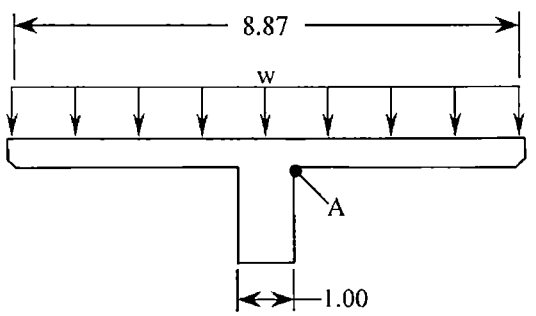

where:

$$w = \frac{W_c \times g}{L \times b} = \frac{1000 \times 25}{144 \times 8.87} = 19.6\,\text{psi}$$

(distributed load of the TPBAR consolidation canister)

W_c = 1,000 lbs, bounding TPBAR canister weight (with TPBARs)

L = 144 inches, length of consolidation canister

b = 8.87 inches, TPBAR basket opening width

g = 25g, bounding side drop acceleration

$$M = w \times \left(\frac{b}{2} - \frac{1}{2}\right) \times \frac{1}{2}\left(\frac{b}{2} - \frac{1}{2}\right)$$

$$= 19.6 \times \left(\frac{8.87}{2} - \frac{1}{2}\right) \times \frac{1}{2}\left(\frac{8.87}{2} - \frac{1}{2}\right) = 152 \text{ in-lb/in, the maximum bending moment}$$

t = 0.5 in, thickness of the flange

The margin of safety is:

$$MS = \frac{1.5S_m}{S_b} - 1 = \frac{1.5 \times 8.4}{3.6} - 1 = +2.5$$

where:

S_m = 8.4 ksi, stress intensity of 6061-T651 aluminum @300°F

The bearing stress in the basket is:

$$S_{brg} = \frac{P}{A} = \frac{47{,}500}{1.00 \times 161.5} = 294 \text{ psi} \approx 0.3 \text{ ksi}$$

where:

P = g × (W_c + W_b) = 25 × (1,000 lbs + 900 lbs) = 47,500 lbs, total side drop load

W_b = 900 lbs, the bounding weight of the TPBAR basket

A = is the minimum bearing area of the basket

The margin of safety is:

$$MS = \frac{S_y}{S_{brg}} = \frac{26.9}{0.3} - 1 = +\underline{\text{Large}}$$

where:

S_y = 26.9 ksi, yield strength of 6061-T651 aluminum @300°F

<u>TPBAR Basket 1-Foot End-Drop Analysis</u>

During an end drop, the maximum compressive stress on the minimum cross-section of the basket body is:

$$S_{comp} = \frac{g \times W_b}{A} = \frac{20 \times 900}{32.26} = 558 \text{ psi} \approx 0.6 \text{ ksi}$$

where:

$A = 9.87^2 - 8.87^2 + 4(1.00 \times (13.25 - 9.87)) = 32.26\ \text{in}^2$, the minimum cross-sectional area of the basket (see Figure 2.6.12-7)

g = 20g, bounding end drop acceleration

W_b = 900 lbs, bounding weight of the TPBAR basket

The margin of safety is:

$$MS = \frac{S_y}{S_{comp}} - 1 = \frac{26.9}{0.6} - 1 = +\underline{\text{Large}}$$

where:

S_y = 26.9 ksi, yield strength of 6061-T651 aluminum @300°F

2.6.12.10.2 TPBAR Basket Upper Fitting

The upper fitting prevents the basket from loading the consolidation canister and TPBARs during a top-end drop. Four (4) spacer guides of the upper fitting are provided for this purpose. The spacer guides have a length of 7.63 inches, a width of 2.0 inches, and a thickness of 1.00 inch with a 45° × 0.25-inch chamfer. A bounding weight of 900 lbs is used for the TPBAR basket analysis. The temperature of the lid and upper region of the NAC-LWT cask body during TPBAR shipment is conservatively assumed to be 300°F. From Chapter 3, a temperature of 300°F bounds the maximum temperature of the upper LWT region for a maximum heat load of 1.05 kW. Since the maximum heat load for the TPBAR shipment is less than 1.0 kW, using 300°F for the analysis of the TPBAR upper fitting is conservative.

TPBAR Basket Upper Fitting 1-Foot Side Drop

During a side drop, the welds that hold the spacer guides to the top fitting are in shear and bending. The shear load on the welds is:

$$P = (b \times t \times L) \times \rho \times g = (2.0 \times 1.0 \times 7.63) \times 0.288 \times 25 = 110\ \text{lbs}$$

where:

b = 2.0 inches, spacer guide width

t = 1.0 in, spacer guide thickness

L = 7.63 inches, spacer guide length

ρ = 0.288 lb/in^3, density of Type 304 stainless steel

g = 25g, side drop acceleration

The welds for the spacer are ⅛-inch fillet welds on three sides. The shear stress in the welds is:

$$\tau = \frac{P}{A} = \frac{110}{0.354} = 311\,\text{psi} = 0.3\ \text{ksi}$$

where:

$A = 0.125 \times 0.707 \times (2.0 + 2 \times 1.0) = 0.354\ \text{in}^2$, weld area

The bending moment is:

$$M = \frac{wL^2}{2} = \frac{(b \times t \times \rho \times g) \times L^2}{2} = \frac{(2 \times 1 \times 0.288 \times 25) \times 7.63^2}{2} = 419\ \text{in-lb}$$

The stress in the weld due to bending is:

$$S = \frac{M}{t \times S_w} = \frac{419}{(0.125 \times 0.707) \times 0.56} = 8.5\ \text{ksi}$$

where:

$S_w = \frac{d^2(2b + d^2)}{3(b + d)} = \frac{1^2(2 \times 2 + 1^2)}{3(2 + 1)} = 0.56\ \text{in}^2$, section modulus of weld (Blodgett)

The maximum shear stress, τ_{max}, in the weld which, is equivalent to the stress intensity divided by two is:

$$\tau_{max} = \frac{\sqrt{S^2 + 4\tau^2}}{2} = \frac{\sqrt{8.5^2 + 4 \times 0.3^2}}{2} = 4.26\ \text{ksi}$$

The margin of safety is:

$$MS = \frac{0.6S_y}{\tau_{max}} - 1 = \frac{0.6 \times 22.5}{4.26} - 1 = +2.17$$

where:

S_y = 22.5 ksi, yield strength of Type 304 stainless steel @300°F

TPBAR Basket Upper Fitting 1-Foot Top-End Drop

For a top-end drop the weight of the TPBAR basket will load the four spacer guides. The membrane stress in the spacer guide is:

$$S = \frac{W_b \times g}{A} = \frac{900 \times 20}{(2.0 \times 1.0) \times 4} = 2.3\ \text{ksi}$$

where:

W_b = 900 lbs, bounding TPBAR basket weight

$A = (2.0 \times 1.0) \times 4 = 8\ \text{in}^2$, cross sectional area of the spacer guide

g = 20g, bounding end drop acceleration

The margin of safety is:

$$MS = \frac{S_y}{S} - 1 = \frac{22.5}{2.3} - 1 = +8.8$$

where:

S_y = 22.5 ksi, yield strength of Type 304 stainless steel @300°F

The bearing stress is:

$$S = \frac{W_b \times g}{A} = \frac{900 \times 20}{6} = 3.0 \text{ ksi}$$

where:

A = (2.0 × 0.75) × 4 = 6 in^2, bearing area of the spacer guide

The margin of safety is:

$$MS = \frac{S_y}{S} - 1 = \frac{22.5}{3.0} - 1 = +6.5$$

The critical buckling load for the spacer is determined by using Euler's buckling equation. The critical buckling load is:

$$W_{cr} = K_c \frac{EI}{L^2} = 2.47 \frac{27 \times 10^6 (0.1667)}{7.63^2} \approx 190.9 \text{ kip}$$

where:

E = 27×10^6 psi, modulus of elasticity of Type 304 stainless steel @ 300°F

K_c = 2.47, buckling constant (Blake, Table 10.3)

$I = \frac{bt^3}{12} = 0.1667$ in^4, minimum moment of inertia for cross section

b = 2.0 inches, spacer guide width

t = 1.0 in, spacer guide thickness

L = 7.63 inches, length of spacer guide

The margin of safety against buckling of the four spacer guides is:

$$MS = \frac{190{,}900}{20 \times 900/4} - 1 = + \underline{\text{Large}}$$

2.6.12.10.3 TPBAR Basket Lower Fitting

The TPBAR basket lower fitting is identical to the lower fitting of the PWR basket. The weight of the loaded TPBAR basket is less than the weight of the loaded PWR basket. Therefore, no further analysis is required.

2.6.12.10.4 TPBAR Spacer

The TPBAR Spacer is designed to limit the movement of the TPBAR contents during transport and to prevent the consolidation canister from loading the TPBARs during a top-end drop. The spacer is constructed of a circular base plate, two triangular spacer bases, two tubes, and two triangular top plates. The circular base plate forms the attachment of the spacer to the lower surface of the NAC-LWT cask closure lid. The circular base plate is attached with Type 304 stainless steel bolts. The two triangular spacer bases are bolted to the circular base plate. The tubes, constructed of 3-inch schedule 80 pipes, are welded to the spacer base and the triangular top plates that provide the interface with the TPBAR contents. The triangular top plates are arranged to form a square with a gap that fits over the consolidation canister or waste container bail and above the consolidation canister contents or the welded top of the waste container. Figure 2.6.12-8 shows the top view of the triangular top plate and tube. The calculated weight of the spacer assembly is 115 lbs. The analyzed loaded weight of the consolidation canister is 1,000 lbs, which bounds the loaded weight of the waste container (700 lbs). During the top-end drop condition, the weight of the consolidation canister is supported by the bail and directly transmitted into the NAC-LWT cask lid. Therefore, only the weight of the TPBARs is supported by the spacer for top-end drop conditions. The temperature of the lid and upper region of the NAC-LWT cask body during TPBAR transport is conservatively assumed to be 300°F. From Chapter 3, a temperature of 300°F bounds the maximum temperature of the upper LWT region for a maximum heat load of 1.05 kW. Since the maximum heat load for the transport of the TPBAR consolidation canister shipment is less than 0.7 kW, using 300°F for the analysis of the TPBAR spacer is conservative. The heat load of the TPBAR waste container is 0.127 kW and, therefore, the evaluated temperatures for the consolidation canister are bounding.

TPBAR Spacer 1-Foot Side Drop

Bolts

During 1-foot side-drop conditions, the weight of the spacer applies a shearing and tensile load to the bolts. The tensile load is due to the moment generated by the cantilever action of the spacer.

The shear stress is:

$$\tau = \frac{P}{A_t} = \frac{719}{0.1419} = 5.1\,\text{ksi}$$

where:

$$P = \frac{W \times g}{4} = \frac{115 \times 25}{4} = 719 \text{ lbs}$$

W = 115 lb, spacer assembly weight abbreviations

g = 25g, side-drop acceleration

$$A_t = 0.7854\left(D - \frac{0.9743}{n}\right)^2 = 0.7854\left(0.5 - \frac{0.9743}{13}\right)^2 = 0.1419 \text{ in}^2$$, tensile area of screw thread with ultimate strength up to 100 ksi

For ½-13UNC bolts (Machinery's Handbook)

n = 13, number of threads per inch

D = 0.50 in, bolt diameter

Kn_{max} = 0.434 in, maximum minor diameter of internal thread

Es_{min} = 0.4435 in, minimum major diameter of external thread

En_{max} =0.4565 in, maximum pitch diameter of internal thread

Ds_{min} =0.4876 in, minimum major diameter of external thread

L_e = 1.0 in, Thread engagement

$$P = \frac{M}{d} = \frac{16{,}891}{2 \times 4.95} = 1{,}706 \text{ lbs}$$, the tensile load

d = 9.9 in, maximum distance between bolts

$$M = \frac{wL^2}{2} \times g = \frac{\left(\frac{115}{11.75}\right)\left(11.75^2\right)}{2} \times 25 = 16{,}891 \text{ in - lb}$$, the prying moment generated by the cantilever action of the spacer

The bolt tensile stress due to the moment, M, is:

$$S = \frac{P}{A_t} = \frac{1706}{0.1419} = 12.0 \text{ ksi}$$

The membrane stress intensity on the fastener is:

$$SI = \sqrt{S^2 + 4\tau^2} = \sqrt{12.0^2 + 4 \times 5.1^2} = 15.7 \text{ ksi}$$

The margin of safety is:

$$MS = \frac{S_y}{SI} - 1 = \frac{22.5}{15.7} - 1 = +0.43$$

where:

S_y = 22.5 ksi, yield strength of Type 304 stainless steel @300°F

The shear stress on the external threads is:

$$\tau = \frac{P}{A_S} = \frac{1706}{0.7789} = 2.2 \text{ ksi}$$

where:

$$A_S = 3.1416 n L_e Kn_{max}\left[\frac{1}{2n} + 0.57735(Es_{min} - Kn_{max})\right]$$

$$= 3.1416(13)(1.00)(0.434)\left[\frac{1}{2(13)} + 0.57735(0.4435 - 0.434)\right]$$

$$= 0.7789 \text{ in}^2\text{, shear area of the bolt threads}$$

The margin of safety is:

$$MS = \frac{0.6S_y}{\tau} - 1 = \frac{0.6 \times 22.5}{2.2} - 1 = +6.14$$

Spacer Welds

Using a bounding weight (W) of 25 pounds for the tube and triangular plates, the shear load on the welds is:

$$P = W \times g = 25 \times 25 = 625 \text{ lbs}$$

where:

g = 25 g, side-drop acceleration

The welds for the spacer are ¼-inch fillet weld. The shear stress in the weld is:

$$\tau = \frac{P}{t_w 0.707 \pi d} = \frac{625}{0.25 \times 0.707 \times (\pi \times 3.5)} = 322 \text{ psi}$$

where:

t_W = 0.25 in, weld size

d = 3.5 inches, outside diameter of 3-inch schedule-80 pipe

The stress in the weld due to bending is:

$$S = \frac{M}{t \times S_w} = \frac{5{,}263}{(0.25 \times 0.707)9.62} = 3.1 \text{ ksi}$$

where:

$M = wL = 25 \times 25 \times 8.42 = 5{,}263 \text{ in - lb}$, the bending moment

$S_w = \frac{\pi d^2}{4} = \frac{\pi \times 3.5^2}{4} = 9.62 \text{ in}^2$, section modulus of the weld (Blodgett)

The maximum shear stress (τ_{max}) in the weld, which is equivalent to the stress intensity divided by two, is:

$$\tau_{max} = \frac{\sqrt{S^2 + 4\tau^2}}{2} = \frac{\sqrt{3.1^2 + 4 \times 0.3^2}}{2} = 1.6 \text{ ksi}$$

The margin of safety is:

$$MS = \frac{0.6S_y}{\tau_{max}} - 1 = \frac{0.6 \times 22.5}{1.6} - 1 = +7.4$$

where:

S_y = 22.5 ksi, yield strength of Type 304 stainless steel @300°F

TPBAR Spacer 1-Foot Top-End Drop

When loaded in the consolidation canister, the TPBARs (held in the shape of a square) load the spacer tubes via the triangular top plates during top-end drop conditions. The compressive load applied to the tubes during the top-end drop is the weight of the TPBARs, 795 lbs (300 TPBARs at a bounding weight of 2.65 lbs per TPBAR), times the bounding acceleration of 20g (actual 15.8 g). For this analysis, W=1,000 lbs, is conservatively used.

Tube

The compressive stress in the tubes is:

$$S = \frac{W \times g}{A} = \frac{1000 \times 20}{2 \times \left(\frac{\pi}{4}\left(3.5^2 - 2.9^2\right)\right)} = 3.3 \text{ ksi}$$

where:

A = the cross sectional area of a 3-inch schedule-80 pipe with an outer diameter of 3.5 inches and a thickness of 0.3 inch

The margin of safety is:

$$MS = \frac{S_y}{S} - 1 = \frac{22.5}{3.3} - 1 = +5.8$$

where:

S_y = 22.5 ksi, yield strength of Type 304 stainless steel @300°F

Triangular Top Plate

Referring to the dimensions provided in Figure 2.6.12-8, the pressure applied to a triangular plate is

$$P_{TP} = \frac{1}{2} \times \frac{1000}{0.5 \times 7.43 \times 7.43} \times 20 = 362 \text{ psi}$$

The bending moment in the top plate is (see Line A in Figure 2.6.12-6)

$$M = 362 \times \left(0.5 \times 4.18^2\right) \times \left(\frac{1}{3} \times 4.18\right) = 4406 \text{ in-lb}$$

The bending stress in the plate is:

$$S = \frac{6M}{bt^2} = \frac{6 \times 4{,}406}{4.18 \times 0.75^2} = 11.2 \text{ ksi}$$

The margin of safety is:

$$MS = \frac{1.5S_m}{S} - 1 = \frac{1.5 \times 20.0}{11.2} - 1 = +1.68$$

where:

S_m = 20.0 ksi, stress intensity of Type 304 stainless steel @300°F

TPBAR Spacer 1-Foot Bottom-End Drop

During the one-foot bottom-end drop, the inertial load of the spacer is applied to the bolts that affix the spacer to the NAC-LWT cask lid and the welds used to fabricate the spacer assembly. The maximum bottom-end drop acceleration is 20g.

Bolts

Four bolts (½-13UNC, Type 304 stainless steel) hold the spacer assembly to the bottom of the NAC-LWT cask lid and six bolts hold the spacer base to the circular base plate. For this evaluation, only the four spacer assembly bolts are considered since the individual bolt load is higher and the thread engagement length is shorter. The Internal lid thread evaluation is not required since high strength Helicoil inserts are utilized. Using the spacer assembly weight of 115 lbs and an acceleration of 20g, the critical bolt load is:

$$P = \frac{115 \times 20}{4} = 575 \text{ lbs}$$

The tensile stress is:

$$S = \frac{P}{A_t} = \frac{575}{0.1419} = 4.1 \text{ ksi}$$

The margin of safety is:

$$MS = \frac{S_y}{S} - 1 = \frac{22.5}{4.1} - 1 = +4.49$$

where:

S_y = 22.5 ksi, yield strength of Type 304 stainless steel @300°F

The shear stress in the bolt thread is:

$$\tau = \frac{P}{A_s} = \frac{575}{0.7789} = 0.74 \text{ ksi}$$

The margin of safety is:

$$MS = \frac{0.6S_y}{\tau} - 1 = \frac{0.6(22.5)}{0.74} - 1 = +\underline{\text{Large}}$$

Spacer Welds

During a 1-foot bottom-end drop (20g), the spacer weld is loaded by the inertial load of the spacer tube and the triangular top plate (25 lbs bounding). The weld is a ¼-inch fillet weld. The weld stress is:

$$S_w = \frac{W \times g}{t(0.707)(\pi d)} = \frac{25 \times 20}{0.25 \times 0.707 \times (\pi \times 3.5)} = 257 \text{ psi} = 0.3 \text{ ksi}$$

where:

d = 3.5 in, outside diameter of 3-inch schedule 80 pipe
t = 0.25 in, weld size

The margin of safety is:

$$MS = \frac{0.6S_y}{S_w} - 1 = \frac{0.6(22.5)}{0.3} - 1 = +\underline{\text{Large}}$$

where:

S_y = 22.5 ksi, yield strength of Type 304 stainless steel @300°F

Figure 2.6.12-7 Cross-Section of TPBAR Basket

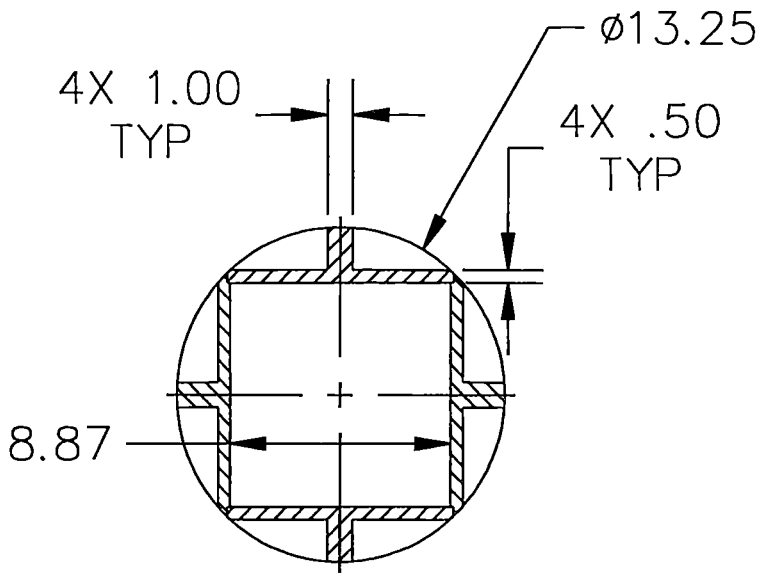

(Unit = inches)

Figure 2.6.12-8 TPBAR Spacer Schematic Triangular Top Plate and Tube

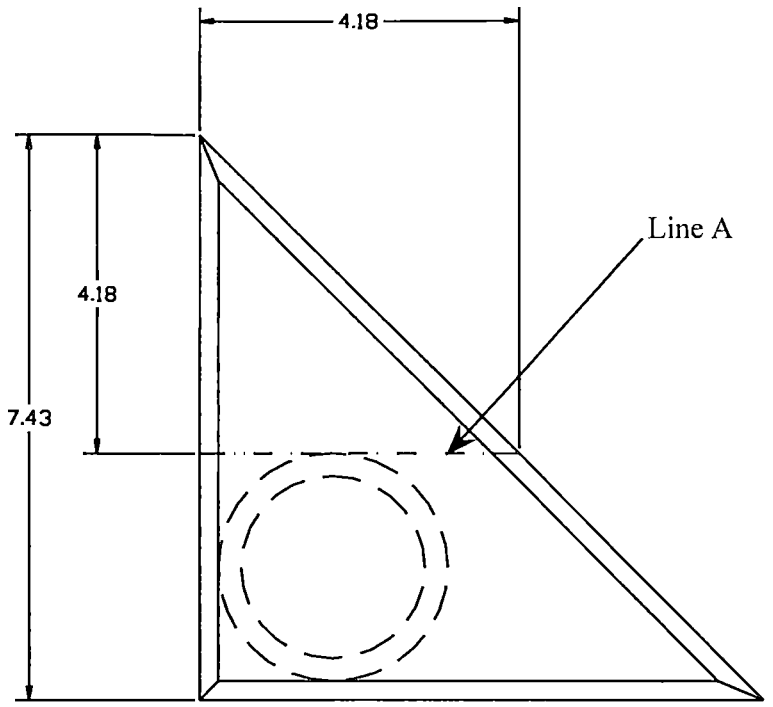

(Unit = inches)

2.6.12.11 ANSTO Basket Analysis

The ANSTO modular basket assembly consists of a top module, four intermediate modules, and a base module. The top and base modules are each 29.8 inches long; each of the four intermediate modules is 29.3 inches long (not including guide pins); and all six modules have an outer diameter of 13.27 inches. Each module is capable of holding up to seven spiral fuel assemblies or MOATA plate bundles. Each module is a weldment made up of a 13.27-inch-diameter, 1/2-inch-thick base plate and six 13.27-inch-diameter, 1/2-inch-thick support plates scalloped on the inner diameter to fit around six peripheral fuel tubes. The weldment structure, fuel tubes, and base and support plates are fabricated from Type 304 stainless steel. Each of the seven fuel tubes in each module has an outer diameter of 4.375 inches and a wall thickness of 0.125 inch. The bottom of each fuel tube is welded to the 1/2-inch-thick base plate. At the bottom of each fuel tube, where it is welded to the base plate, there is a 0.3-inch slot to permit water to drain from the tube. The base plate supports the fuel assembly/bundle in the end drop orientation. The base module sits on a 0.5-inch-high, 10-inch-diameter ring that is welded in segments to the base plate. The total weight of the ANSTO basket assembly bears directly on the bottom forging of the cask through the ring. The six scalloped 1/2-inch-thick support plates and the base plate of each basket module provide lateral support and maintain the fuel configuration in the side drop orientation.

2.6.12.11.1 ANSTO Basket Body 1-Foot Side Drop Analysis

Structural analyses of the ANSTO basket for 1-foot side and end drops are performed using classical hand calculations.

The inertia load of the LWT cask for a 1-foot side drop is 25g. A conservative loading condition of a diametrically loaded ring (Table 17, Case 1, Roark) is considered, which neglects any load distribution. Also, it is conservative to assume that there are three loaded fuel tubes acting on the top of a fuel tube since, in reality, there are only two of them. The stresses in the circumferential direction and in the longitudinal direction are added without regard to their signs. Since the circumferential direction and the longitudinal direction also correspond to the direction of the principal stresses, the addition of the two magnitudes reflects the possibility of the principal stresses being of opposite signs.

The maximum applied load to a fuel tube for the circumferential bending stress is:

$$P_s = (3W_{FT} + 3W) \times 25 = 2{,}415 \text{ lbs}$$

where:

W_{FT} = 14.2 lbs, maximum fuel tube weight

W = 18.0 lbs, maximum average fuel assembly weight

The bending moment in the fuel tube is:

$$M = \frac{wRk_2}{\pi} = \frac{84 \times 2.13 \times 1.00}{\pi} = 57 \text{ in-lb/in}$$ (Table 17, Case 1, Roark)

where:

$$w = \frac{P_s}{L_t} = 84 \text{ lb/in}$$

L_t = 28.81 inches, shortest fuel tube length

R = 2.13 inches, mean radius of fuel tube

k_2 = $1-\alpha = 1.00$

$$\alpha = \frac{I}{A \times R^2} = \frac{bt^3/12}{b \times t \times R^2} = 2.87 \times 10^{-4}$$

b = 1.0 in, unit length

t= 0.125 in, tube wall thickness

The circumferential bending stress in the fuel tube is:

$$\sigma c = \frac{6M}{bt^2} = \frac{6 \times 57}{1 \times 0.125^2} = 21.9 \text{ ksi}$$

The stress in the fuel tube in the longitudinal direction is calculated assuming the fuel tube acts like a beam. The maximum bending moment occurs at the top of the basket where the fuel tube acts like a cantilever beam. (The maximum moment for a cantilevered beam with a uniform loading of w (lb/in) and length (l) is $wl^2/2$, as compared to the maximum moment $wl^2/8$ for a simply supported beam.) The bending moment in the tube is:

$$M = \frac{wl^2}{2} = \frac{84 \times 4.0^2}{2} = 672 \text{ in-lb}$$

where:

l = 4.0 inches, the length of the tube extending beyond the support plates

The bending stress is:

$$\sigma_I = F\frac{Mc}{I} = \frac{672 \times 2.19}{3.77} \approx 1.1 \text{ ksi}$$

where:

c = 2.19 inches, distance to extreme outer fiber of tube from centroid of tube

I = 3.77 in^4, tube moment of inertia

F = 2.725, factor to account for the effect of the small diameter-to-length ratio on bending for a cantilevered tube. This is obtained for a uniformly loaded beam in Article 7.10 in Roark.

The maximum stress in the tube is:

$$\sigma_b = 21.9 + 1.1 = 23.0 \text{ ksi}$$

The margin of safety is:

$$MS = \frac{1.5S_m}{\sigma_b} - 1 = +0.26$$

where:

S_m = 19.4 ksi, design stress intensity, Type 304 stainless steel, 350°F

The bearing stress on the support plate is calculated using Table 33, Case 2c from Roark.

The maximum weight of a loaded module is the weight of the base module, W_{BM} = 280 lbs. The weight of the loaded basket is supported by the six support plates and the base plate (i.e., total of seven). The bearing stress on a support plate is:

$$\sigma_{brg} = 0.591\sqrt{\frac{pE}{K_D}} = 3.6 \text{ ksi}$$

where:

$$p = \frac{W}{7t_d}g = \frac{280}{7 \times 0.5} \times 25 = 2{,}000 \text{ lb/in, bearing load for 25g side drop}$$

t_d = 0.5 in, support disk thickness

g = 25g, side drop inertia load

$$K_D = \frac{D_1 D_2}{D_1 - D_2} = 1{,}366.81$$

D_1 = 13.395 inches, LWT cask inner diameter

D_2 = 13.265 inches, support disk diameter

E = 25.7×10^6 psi, modulus of elasticity, Type 304 stainless steel, 350°F

The margin of safety is:

$$MS = \frac{S_y}{\sigma_{brg}} - 1 = +5.06$$

where:

S_y = 21.8 ksi, yield strength, Type 304 stainless steel, 350°F

2.6.12.11.2 ANSTO 1-Foot End Drop Evaluation

The inertia load for the LWT for a 1-foot end drop is 20g. The applied load to the ANSTO basket is:

$$P = W_{total} \times 20 = 35{,}400 \text{ lbs}$$

where:

W_{total} = 1,770 lbs, total weight of loaded basket, which bounds the calculated weight of 1,667 lbs

The minimum cross-sectional area is at the base of the fuel tubes where the cutouts for water drainage are located. The cross-sectional area is:

$$A = \frac{\left[\frac{\pi}{4}\left(D_o^2 - D_i^2\right) \times 6\right]}{2} + \left[\frac{\pi}{4}\left(D_o^2 - D_i^2\right) - 6 \times l_c \times t_t\right] = 5.93 \text{ in}^2$$

where:

D_o = 4.375 inches, tube outer diameter

D_i = 4.125 inches, tube inner diameter

l_c = 1.00 in, cutout length in center tube

t_t = 0.125 in, tube wall thickness

The membrane stress in the basket is:

$$\sigma = \frac{P}{A} = \frac{35{,}400}{5.93} = 5.97 \text{ ksi}$$

The margin of safety is:

$$MS = \frac{S_m}{\sigma} - 1 = +2.2$$

where:

S_m = 19.4 ksi, design stress intensity, Type 304 stainless steel, 350°F

The support plates are welded to the fuel tube with 1/16-inch bevel welds on both sides of the plate. The area of the weld is:

$$A_W = \frac{6(\pi D_o)}{2} \times 2t_w = 5.15 \text{ in}^2$$

where:

D_o = 4.375 inches, outer diameter of tube

t_w = 1/16 in, weld thickness

The bounding weight of the support plates is 20.1 lbs; and the bounding g-load factor is 60. A weld quality factor of 0.25 for a surface visual examination is divided into the calculated stress. This factor corresponds to the largest stress reduction factor in Table NG-3352-1 of the ASME Code. Therefore, the stress in the weld is:

$$\sigma_W = \frac{20.1 \times 60}{A_w\,(0.25)} = 936 \text{ psi}$$

The margin of safety using normal conditions allowable is:

$$MS = \frac{0.6S_m}{\sigma_w} - 1 = +\underline{\text{Large}}$$

where:

S_m = 19.4 ksi, design stress intensity, Type 304 stainless steel, 350°F

2.6.12.11.3 ANSTO Thermal Stress Evaluation

Thermal stress caused by a temperature gradient in the basket is calculated in this section. The thermal stress is minimal since the basket is free to expand. The thermal stress occurs as the hotter tubes expand radially against the basket support plates, which are at a lower temperature.

The maximum thermal stress of the fuel tube is back-calculated from the displacement computed using equations for circular rings from Table 17, Case 1, Roark.

The diametrical displacements caused by the thermal expansions for the center tube (Δ_1) and the tube adjacent to it (Δ_2) are calculated as:

$$\Delta_1 = \alpha \times \Delta T \times R_t = 4.58 \times 10^{-3} \text{ in}$$

where:

$\alpha = 9.1 \times 10^{-6}$ /°F, coefficient of thermal expansion, Type 304 stainless steel, 350°F

ΔT= 230°F (300-70), T_{max} of the basket is conservatively considered to be 300°F

70°F is room temperature

R_t = 2.19 inches (4.375/2), radius of the fuel tube outer surface

$$\Delta_2 = \alpha \times \Delta T \times D_t = 9.17 \times 10^{-3} \text{ in}$$

where,

$\alpha = 9.1 \times 10^{-6}$ /°F, coefficient of thermal expansion, Type 304 stainless steel, 350°F

ΔT= 230°F (300-70), T_{max} of the basket is conservatively considered to be 300°F

70°F is room temperature

D_t = 4.375, diameter of the fuel tube

The displacement caused by the thermal expansions for the outer surface of the support plate (Δ_s) is calculated as:

$$\Delta_S = \alpha \times \Delta T \times R_S = 8.58 \times 10^{-3} \text{ in}$$

where,

$\alpha = 9.1 \times 10^{-6}$ /°F, coefficient of thermal expansion, Type 304 stainless steel, 350°F

ΔT= 144°F (214-70), T_{max} of the inner shell

70°F is room temperature

R_S = 6.55 inches (13.1/2), radius of the support plate

Note: 214°F is conservatively used to result in a minimum Δ_S in order to maximize the thermal stress.

The deformation that results in thermal stress is -5.17×10^{-3} inch ($\Delta s - \Delta_1 - \Delta_2$). Therefore, the fuel tube will experience a reduction in diameter due to the differential thermal expansion of the fuel tubes and support plates. It is conservative to assume that all deformation occurs at the center tube. Using Case 1 in Table 17 of Roark, the change in the diameter of the circular ring, D_V, and the moment, M_A, are given by:

$$D_V = 0.1488\times\frac{WR^3}{EI} \quad \text{and} \quad M_A = \frac{WR\times k_2}{\pi}$$

therefore:

$$M_A = \frac{D_V\times EI}{0.1488\times R^2}\times\frac{k_2}{\pi}$$

where:

W is the load due to differential thermal expansion

$D_V = 5.17\times10^{-3}$ inch, change in the diameter due to thermal stress

R = 2.13 inches, mean radius of fuel tube

$E = 25.7\times10^6$ psi, modulus of elasticity, Type 304 stainless steel, 350°F

$I = bt^3/12$, inertial of the cross-section

b = 1.0 in, unit length

t = 0.125 in, tube wall thickness

$k_2 = 1-\alpha = 1.00$

$$\alpha = \frac{I}{A\times R^2} = \frac{bt^3/12}{b\times t\times R^2} = 2.87\times10^{-4}$$

The thermal stress is:

$$\sigma = \frac{6M_A}{bt^2} = \frac{D_V E t k_2}{0.2976\pi R^2} = \frac{5.17\times10^{-3}\times25.7\times10^6\times0.125\times1.0}{0.2976\times\pi\times2.13^2} = 3{,}916 \text{ psi}$$

The maximum P+Q stress in the basket is conservatively calculated by combining the bending stress and thermal stress in the basket. The P+Q stress is:

$$\sigma_{pq} = \sigma_b + \sigma_{th} = 23.0 + 3.9 = 26.9 \text{ ksi}$$

The margin of safety is:

$$MS = \frac{3S_m}{\sigma_{pq}} - 1 = +1.16$$

where:

S_m = 19.4 ksi, design stress intensity, Type 304 stainless steel, 350°F

2.6.12.12 TPBAR Basket with the PWR/BWR Rod Transport Canister

This section provides the structural analysis for the shipment of up to 25 individual TPBARs in the PWR/BWR Rod Transport Canister, the PWR insert and the TPBAR basket. Section 2.6.12.10 provides the structural evaluation of the TPBAR basket, with 300 TPBARs, considering a slightly lower contents weight (1800 lbs) than the TPBARs in the PWR/BWR Rod Transport Canister configuration (1901 lbs). The effects of the increased weight loading for the TPBAR basket are addressed in this section. The structural evaluation of the PWR/BWR Rod Transport Canister and the PWR insert is performed in Section 2.6.7.10.

TPBAR Basket Body 1-Foot Side Drop Analysis – Normal Condition

The TPBAR basket body is constructed of four machined segments that are held together with aluminum bands at five locations along the axial length of the basket, as well as the top and bottom fittings, which are bolted to the aluminum basket. During a side drop, the TPBAR basket is subjected to bending and bearing stresses. The maximum bending stress occurs at Location 'A' in the following figure and is due to the content weight. The maximum bending stress is calculated using a cantilevered beam. This is conservative since it neglects any support of the load due to the edges of the basket being supported by the cask inner shell. The maximum bending stress is:

$$S_b = \frac{6M}{t^2} = \frac{6 \times 226}{0.5^2} = 5.42 \text{ ksi}$$

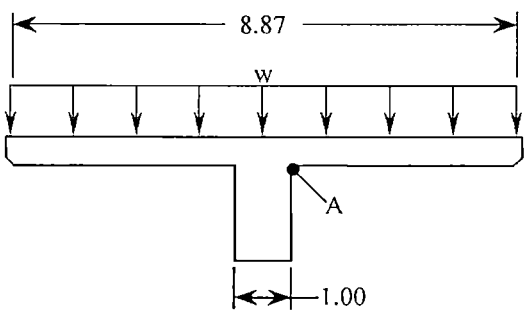

where:

$$w = \frac{W_c \times g}{L \times b} = \frac{1{,}650 \times 25}{159.5 \times 8.87} = 29.2 \text{ psi},$$

the distributed load transfer by the PWR insert on the TPBAR basket

W_c = 1,650 lb, bounding TPBAR contents weight (with TPBARs, PWR/BWR Rod Transport Canister and the PWR insert)

L = 159.5 in, loadable length of the TPBAR basket

b = 8.87 in, TPBAR basket opening width

g = 25g, bounding side drop acceleration

$$M = w \times \left(\frac{b}{2} - \frac{1}{2}\right) \times \frac{1}{2}\left(\frac{b}{2} - \frac{1}{2}\right)$$

$$= 29.2 \times \left(\frac{8.87}{2} - \frac{1}{2}\right) \times \frac{1}{2}\left(\frac{8.87}{2} - \frac{1}{2}\right) = 226 \text{ in-lb/in, the maximum bending moment}$$

t = 0.5 in, thickness of the flange

The margin of safety is

$$MS = \frac{1.5S_m}{S_b} - 1 = \frac{1.5 \times 8.4}{5.42} - 1 = +1.32$$

where:

S_m = 8.4 ksi, stress intensity of 6061-T6 aluminum @ 300°F

The bearing stress in the basket is

$$S_{brg} = \frac{P}{A} = \frac{63{,}750}{1.00 \times 161.5} = 395 \text{ psi} = 0.4 \text{ ksi}$$

where:

P = g × (W_c + W_b) = 25 × (1,650 lb + 900 lb) = 63,750 lb, total side drop load

W_b = 900 lb, the bounding weight of the TPBAR basket

A = is the minimum bearing area of the basket

The margin of safety is

$$MS = \frac{S_y}{S_{brg}} = \frac{26.9}{0.4} - 1 = +\text{large}$$

where:

S_y = 26.6 ksi, yield strength of 6061-T6 aluminum @ 300°F

TPBAR Basket – End Drop

In an end drop scenario, the basket is only loaded by its own weight. The TPBAR basket weight is bounded by what was considered for the end drop analysis of the TPBAR basket in Section 2.6.12.10. Additionally, the assumed component temperatures remain conservative. Therefore, the results of section 2.6.12.10 are bounding and no further analysis is required.

TPBAR Basket Upper Fitting

The TPBAR basket upper fitting is identical to what was analyzed for the TPBAR basket in Section 2.6.12.10. The TPBAR basket weight and component temperatures considered in Section 2.6.12.10 are conservative. Therefore, the results of the Section 2.6.12.10 are bounding and no further analysis is required.

TPBAR Basket Lower Fitting

The TPBAR basket lower fitting is identical to the lower fitting of the PWR basket. The weight of the loaded TPBAR basket is less than the weight of the loaded PWR basket. Therefore, no further analysis is required.

PWR Insert

The PWR insert contains the PWR/BWR Rod Transport Canister assembly for insertion into the TPBAR basket. The PWR insert is not a structural component and, therefore, an analysis of its performance under normal conditions is not required.

PWR/BWR Rod Transport Canister Assembly Analysis

The PWR/BWR Rod Transport Canister is identical to the configuration analyzed in Section 2.6.7.10. The fuel weight considered in the Section 2.6.7.10 analysis for the PWR/BWR fuel (350 lbs) bounds the fuel weight of 25 TPBARs in the PWR/BWR Rod Transport Canister (66 lbs). Therefore, no further analysis is required for the canister.

Internal Spacer

The internal spacer for the PWR/BWR Rod Transport Canister is identical to what was analyzed in Section 2.6.7.10. The fuel weight considered in the Section 2.7.1.7 analysis for the PWR/BWR fuel (350 lbs) bounds the fuel weight of 25 TPBARs in the PWR/BWR Rod Transport Canister (66 lbs). Therefore, no further analysis is required for the internal spacer.

4×4 and 5×5 Inserts

The 4×4 and 5×5 inserts for the PWR/BWR Rod Transport Canister are identical to what was analyzed in Section 2.6.7.10. The fuel weight considered in the Section 2.7.1.7 analysis for the PWR/BWR fuel (350 lbs) bounds the fuel weight of 25 TPBARs in the PWR/BWR Rod

Transport Canister (66 lbs). Therefore, no further analysis is required for the 4×4 and 5×5 inserts.

2.6.12.13 SLOWPOKE Fuel Canister Assembly

Evaluation of the SLOWPOKE fuel canister assembly components for normal conditions of transport includes longitudinal (end) and lateral (side) 1-foot drop evaluations. The 'g' loads of 20 g's and 25 g's (Table 2.6.7-34) are conservatively assumed for a 1-foot end drop and a 1-foot side drop, respectively. Evaluation of all the assembly components for the normal condition of transport is given below. Table 2.6.12-3 gives the summary of weights and other dimensions of the SLOWPOKE fuel canister assembly components.

Table 2.6.12-3 Summary of SLOWPOKE Fuel Canister Assembly Component Dimensions and other Inputs

Component	Canister Weldment	Canister Insert	Fuel
Weight, W, lbs (6)	12.3+1.6=13.9(1)	7.6(4)	3.5(5)
Length, L, in	39.81	9.25×4=37(2)	8.66×4=34.64(2)
Outer Dimension/Diameter, D, in	3.3	0.50	0.206
Inner Dimension/Diameter, d, in	2.8	0.402	0.166
Number of Component, n	1	25	25
Area of Each Tube, A, in^2	2.8(3)	6.943×10^{-2}	1.169×10^{-2}
Stiffness K= (EA/L), lbs/in	670,987	447,517	80,464
Material	6061-T6 Aluminum	6061-T6 Aluminum	6061-T6 Aluminum
Elastic Modulus, $\times10^6$ psi (7)	9.54	9.54	9.54

Note:
1) The weight of the canister weldment is conservatively assumed as12.3 lbs instead of the estimated drawing weight of 11 lbs.
2) Total length of four sets arranged in the canister assembly.
3) Maximum canister weldment cross sectional area.
4) Weight of four 5×5 inserts.
5) Weight of 100 fuel rods and each fuel rod weighs 15.659 grams is 3.445 which is conservatively rounded up to 3.5.
6) The total weight of the SLOWPOKE fuel canister assembly is 25.0 lbs (13.9+7.6+3.5).
7) Elastic modulus is taken at 200°F.

Canister Weldment

The canister weldment is a square tube made of four quarter inch aluminum plates welded along their lengths. The canister weldment is evaluated for longitudinal (end) and lateral (side) drops for normal conditions of transport. For stress analysis, the area of the canister weldment is calculated near the lid where the cross sectional area is smallest. The detailed analysis of the canister weldment is given below.

Evaluation of the canister weldment for the 1-foot end drop:

The compressive stress on the canister weldment is calculated as:

$$\sigma_c = \frac{WG_{E1}}{2(A1+A2)} = \frac{12.3 \times 20}{2(0.5225+0.4975)} = 120.5\,psi$$

where:

W = 12.3 lbs, Weight of the canister weldment

G_{E1} = 20 g, 1-foot end drop 'g' load

A1 = (2.8-0.71) ×0.25=0.5225 in^2, Cross sectional area of Side wall-A

A2 = (2.8-0.81) ×0.25=0.4975 in^2, Cross sectional area of Side wall-B

Margin of safety is:

$$MS = \frac{Membrane\ Allowable}{Compressive\ Stress} - 1 = \frac{10500}{120.5} - 1 = +Large$$

Buckling analysis of canister weldment:

Column slenderness ratio separating elastic and inelastic buckling:

$$C_C = \sqrt{\frac{2\pi^2 E}{F_y}} = \sqrt{\frac{2\pi^2 \times 9.54 \times 10^6}{3.12 \times 10^4}} = 77.65$$

Slenderness ratio Kl/r:

$$kl/r = \frac{1.0 \times l}{\sqrt{I/A}} = \frac{1.0 \times 39.44}{\sqrt{3.66/2.04}} = 29.42$$

where:

E = 9.54×10^6 psi, Elastic modulus of aluminum at 200°F

F_y = 3.12×10^4 psi, Yield strength of aluminum at 200°F

l = 39.44 in, Length of canister weldment wall

I = $2 \times \left(\frac{2.8 \times 0.25^3}{12} + 2.8 \times 0.25 \times \left(2.8/2\right)^2 \right) + 2 \times \left(\frac{0.25 \times 2.8^3}{12} \right) = 3.66\ in^4$, Moment of inertia

A = $2 \times (0.523 + 0.498) = 2.04\ in^2$, Cross sectional area of weldment

If Kl/r < Cc, then

Allowable compressive stress on the tube:

$$F_a = \frac{\left[1 - \frac{(kl/r)^2}{2C_C^2}\right]F_y}{\frac{5}{3} + \frac{3(kl/r)}{8C_C} - \frac{(kl/r)^3}{8C_C^3}} = \frac{\left[1 - \frac{(29.42)^2}{2 \times 77.65^2}\right]3.12 \times 10^4}{\frac{5}{3} + \frac{3(29.42)}{8 \times 77.65} - \frac{(29.42)^3}{8 \times 77.65^3}} = 16{,}089$$

Margin of safety is:

$$MS = \frac{Allowable\,Comp\,Stress}{Maximum\,Comp\,Stress} - 1 = \frac{16089}{120.5} - 1 = +Large$$

For the 1-foot side drop, the weldment wall is assumed to be fixed at all the corners.

The bending stress on the canister weldment wall is calculated as (Roark's, 7th Edition, Table 11.4):

$$\sigma_b = \frac{-\beta_1 q b^2}{t^2} = \frac{-(0.5 \times 0.696 \times 2.8^2)}{0.25^2} = -43.65\ psi$$

where:

β_1 = 0.5, Parameter for a/b = ∞

q = $\frac{W}{4} \times G_{S1} \times \frac{1}{A} = \frac{12.3}{4} \times 25 \times \frac{1}{39.44 \times 2.8} = 0.696\ psi$, Uniformly distributed load

W = 12.3 lbs, Weight of the canister weldment

G_{S1} = 25 g, 1-foot side drop 'g' load

A = 39.44×2.8 = 110.43in^2, Area of the weldment wall

Margin of safety:

$$MS = \frac{Bending\,Allowable}{Compressive\,Stress} - 1 = \frac{15750}{43.65} - 1 = +\text{Large}$$

Canister Lid

The canister lid is a one-inch aluminum plate which covers the top end of the canister weldment. The lid assembly includes the lid plate, handle, housing, latch, and handle cap screw. For the normal conditions of transport analysis, the lid is assumed to be simply supported at the outer edges and the total weight (inertial load) is assumed to act at the central rectangular area. The total weight of the SLOWPOKE fuel canister assembly with fuel is 25.0 pounds.

For the 1-foot end drop:

The bending stress on the canister lid is calculated by assuming the inertial load acts at the center of the lid and is simply supported at all edges (Roark's, 7th Edition, Table 11.4).

$$\sigma_{b-Lid} = \frac{\beta W}{t^2} = \frac{1.28 \times W_t \times G_{E1}}{t^2} = \frac{1.28 \times 25.0 \times 20}{1.0^2} = 640\,psi$$

where:

β = 1.28, Parameter for $a_1/b = a/b_1 = 0.2$
W_t = 25.0 lbs, Weight of the canister weldment assembly with fuel
G_{E1} = 20 g, 1-foot end drop 'g' load
t = 1.0 in^2, Thickness of the lid

Margin of safety is:

$$MS = \frac{Bending\ Allowable}{Bending\ Stress} - 1 = \frac{15750}{640} - 1 = +Large$$

During the 1-foot end drop, the lid handle can shear or puncture the canister lid. The shear stress on the lid due to the handle is:

$$\tau_{l-h} = \frac{W_t G_{E1}}{A_1} = \frac{W_t G_{E1}}{2(w_1 + t_1) \times 2} = \frac{25.0 \times 20}{2(1.0 + 0.65) \times 2} = 75.76\,psi$$

where:

w_1 = 1.0 in, Width of the handle
t_1 = 0.65 in, Thickness of the handle

Margin of safety is:

$$MS = \frac{Shear\ Allowable}{Shear\ Stress} - 1 = \frac{15615}{75.76} - 1 = +Large$$

During the 1-foot end drop, the canister weldment can shear the lid. The shear stress on the lid due to canister weldment is:

$$\tau_{l-w} = \frac{W_t G_{E1}}{A_2} = \frac{W_t G_{E1}}{4 w_2 t_2} = \frac{25.0 \times 20}{(4 \times 2.75 \times (1 - 0.38))} = 73.31\,psi$$

where:

w_2 = 2.75 in, Width of the lid at the canister weldment seating
t_2 = 1-0.38=0.62 in, Thickness of the lid at the canister weldment seating

Margin of safety is:

$$MS = \frac{Shear\ Allowable}{Shear\ Stress} - 1 = \frac{15615}{73.31} - 1 = +Large$$

Lid Handle

The aluminum lid handle is 0.65" thick and 2.5" tall and is fastened to the lid plate using two socket head cap screws. For the end drop, the entire end drop load is transferred through the lid handle.

For 1-foot end drop:

The membrane or compressive stress on the lid handle is calculated as:

$$\sigma_{mh} = \frac{W_t G_{E1}}{A_3} = \frac{W_t G_{E1}}{2 \times w_3 t_3} = \frac{25.0 \times 20}{2 \times 1.0 \times 0.65} = 384.6\, psi$$

where:

W_t = 25.0 lbs, Weight of the canister weldment assembly with fuel
G_{E1} = 20 g, 1-foot end drop 'g' load
w_3 = 1.0 in, Width of the lid handle
t_3 = 0.65 in, Thickness of the lid handle

Margin of safety is:

$$MS = \frac{Membrane\,Allowable}{Membrane\,Stress} - 1 = \frac{10500}{384.6} - 1 = +Large$$

The bearing stress on the lid handle during end drop is calculated as:

$$\sigma_{bH} = \frac{W_t G_{E1}}{A_4} = \frac{W_t G_{E1}}{L_h \times t_3} = \frac{25.0 \times 20}{3.75 \times 0.65} = 205.1\, psi$$

where:

L_h = 3.75 in, Length of the lid handle
t_3 = 0.65 in, Thickness of the lid handle

Margin of safety is:

$$MS = \frac{Bearing\,Allowable}{Bearing\,Stress} - 1 = \frac{31230}{205.1} - 1 = +Large$$

Housing

The housing supports the latch and the spring mechanism; these three components maintain the position of the lid. Figure 2.6.12-9 shows the housing with dimensions and critical locations for evaluation. On the housing, compressive or membrane stresses are evaluated at Location MN, bearing stresses are evaluated at Location RS, bending stresses are evaluated at Location A and shear stresses are evaluated at Location A.

For the end drop, the canister insert along with fuel contacts the housing at Location RS (Figure 2.6.12-9). The weight of the insert and the fuel transferred to the housing is 11.1 pounds.

The membrane stress on the housing Location MN (Figure 2.6.12-9) is calculated as:

$$\sigma_{mHo} = \frac{W_t G_{E1}}{A_5} = \frac{W_t G_{E1}}{2(w_5 - d)t_5} = \frac{(7.6+3.5)\times 20}{2(0.75-0.38)0.75} = 400\,psi$$

where:

W_t = 7.6+3.5 = 11.1 lbs, Weight of the canister insert and fuel

G_{E1} = 20 g, 1-foot end drop 'g' load

W_5-d = (0.75-0.38) = 0.37 in, Width of the housing at Location MN

t_5 = 0.75 in, Thickness of the housing at Location MN

Margin of safety is:

$$MS = \frac{Membrane\ Allowable}{Membrane\ Stress} - 1 = \frac{10500}{400} - 1 = +Large$$

The bearing stress on the housing Location RS (Figure 2.6.12-9) is calculated as:

$$\sigma_{bHo} = \frac{W_t \times G_{E1}}{A_6} = \frac{W_t \times G_{E1}}{2 \times w_5 \times t_5} = \frac{(7.6+3.5)\times 20}{2\times 0.75\times 0.75} = 197.3\,psi$$

where:

W_5 = 0.75 in, Width of the housing at Location RS

t_5 = 0.75 in, Thickness of the housing at Location RS

Margin of safety is:

$$MS = \frac{Bearing\ Allowable}{Bearing\ Stress} - 1 = \frac{31230}{197.3} - 1 = +Large$$

The shearing stress on the housing Location A (Figure 2.6.12-9) is:

$$\tau_A = \frac{W_t G_{E1}(R)}{A_7} = \frac{W_t G_{E1}(R)}{2h_1 \times 2t} = \frac{(7.6+3.5)\times 20 \times \left(0.38/0.75\right)}{2\times 0.25\times 2\times 0.75} = 150\,psi$$

where:

R = Ratio of load on the curved section

$$= \frac{\text{Thickness of curved section (Length AA)}}{\text{Thickness of housing (Length RS)}} = \frac{0.38}{0.75} = 0.51$$

(Note: R = 0.51, Half of the load on the housing is conservatively applied on the curved section of the housing)

h_1 = 0.25 in, Height of the housing at Location A

t = 0.75 in, Thickness of the housing at Location A

Margin of safety is:

$$MS = \frac{Shear\ Allowable}{Shear\ Stress} - 1 = \frac{15615}{150} - 1 = +Large$$

The bending stress on the housing Location A is (assumed as beam fixed at two ends):

$$\sigma_A = M\frac{Y}{I} = \frac{W_a L^2}{12}\frac{Y}{I} = \frac{W_t G_{E1} R}{L}\frac{L^2}{12}\frac{Y}{I}$$

$$= \frac{(7.6+3.5)\times 20\left(0.38/0.75\right)}{0.38}\frac{0.38^2}{12}\frac{0.25/2}{9.77\times 10^{-4}} = 455.7\ psi$$

where:

I = $(bh_1^3/12) = (0.75\times 0.25^3/12) = 9.77\times 10^{-4}\ in^4$, Moment of inertia at Location A

Y = 0.25/2 in, Height of the housing from mid point at Location A

L = 0.38 in, Length of the housing (Length AA)

The stress intensity on the housing Location A is:

$$\sigma_S = \sqrt{\sigma_A^2 + 4\tau_A^2} = \sqrt{455.7^2 + 4\times 150^2} = 546\ psi$$

Margin of safety is:

$$MS = \frac{Bending\ Allowable}{Stress\ Intensity} - 1 = \frac{15750}{546} - 1 = +Large$$

Location B:

The shearing stress on housing Location B is:

$$\tau_B = \frac{W_t G_{E1}(R)}{A_B} = \frac{W_t G_{E1}(R)}{2(h_2 \times t)} = \frac{(7.6+3.5)\times 20\times\left(0.38/0.75\right)}{2(0.06\times 0.75)} = 1{,}250\ psi$$

where:

h_2 = 0.06 in, Height of the housing at Location B (Figure 2.6.12-9)

t = 0.75 in, Thickness of the housing at Location B (Figure 2.6.12-9)

Margin of safety is:

$$MS = \frac{Shearing\ Allowable}{Shearing\ Stress} - 1 = \frac{15615}{1250} - 1 = +Large$$

Figure 2.6.12-9 SLOWPOKE Fuel Canister Assembly Housing

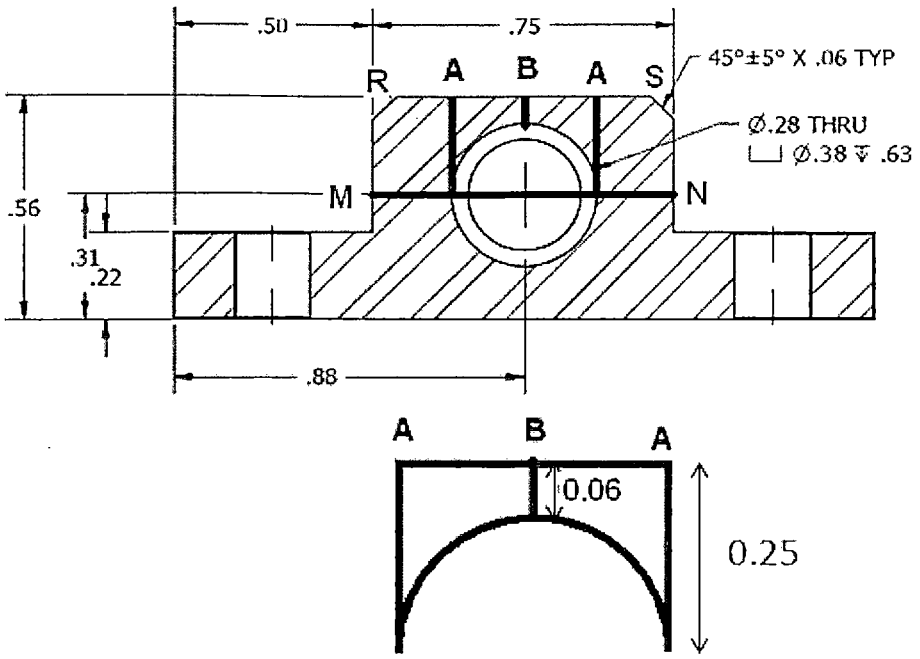

Canister Insert

The fuel tubes are placed inside the aluminum canister insert (four inserts per canister) during transportation. The canister insert tubes are arranged in a 4×4 or 5×5 matrix on a base plate. The canister insert is evaluated for normal conditions of transport only. Conservatively for analysis purposes, the fuel weight is added to the canister insert weight. Both the 4×4 and 5×5 matrix insert tubes have the same thickness (0.1"), but the 5×5matrix insert tube is smaller than the 4×4 matrix insert tube. Therefore, only 5×5 matrix insert is evaluated because the 5×5 matrix insert has a lower moment of inertia and area, and weighs more than the 4×4 matrix insert.

For the 1-foot end drop:

The compressive or membrane stress on the canister insert is calculated as:

$$\sigma_{ci} = \frac{W_{if} G_{E1}}{25 \times A} = \frac{W_{if} \times G_{E1}}{25 \times \pi (D^4 - d^4)/4} = \frac{(7.6 + 3.5) \times 20}{25 \times \pi (0.5^2 - 0.402^2)/4} = 128\, psi$$

where:

W_{if} = 7.6+3.5 = 11.1 lbs, Weight of the canister insert and fuel
G_{E1} = 20 g, 1-foot end drop 'g' load
D = 0.5 in, Outer diameter of the 5×5 insert tube
d = 0.402 in, Inner diameter of the 5×5 insert tube

Margin of safety is:

$$MS = \frac{Membrane\ Allowable}{Compressive\ Stress} - 1 = \frac{10500}{128} - 1 = +Large$$

Buckling Analysis of canister weldment:

Column slenderness ratio separating elastic and inelastic buckling:

$$C_C = \sqrt{\frac{2\pi^2 E}{F_y}} = \sqrt{\frac{2\pi^2 \times 9.54 \times 10^6}{3.12 \times 10^4}} = 77.65$$

Slenderness ratio Kl/r:

$$kl/r = \frac{1.0 \times l}{\sqrt{I/A}} = \frac{1.0 \times 9.25}{\sqrt{\dfrac{\pi(0.5^4 - 0.402^4)/64}{\pi(0.5^2 - 0.402^2)/4}}} = 57.67$$

where:

E = 9.54×10^6 psi, Elastic modulus of aluminum at 200°F
F_y = 3.12×10^4 psi, Yield strength of aluminum at 200°F

l = 9.25 in, Length of canister insert tube

I = $\pi(0.5^4 - 0.402^4)/64 = 1.79\times10^{-3}$ in^{-3}, Moment of inertia of insert tube

A = $\pi(0.5^2 - 0.402^2)/4 = 0.069$ in^2, Cross sectional area of the insert tube

If Kl/r < Cc, then

Allowable compressive stress on the tube:

$$F_a = \frac{\left[1-\frac{(kl/r)^2}{2C_C^2}\right]F_y}{\frac{5}{3}+\frac{3(kl/r)}{8C_C}-\frac{(kl/r)^3}{8C_C^3}} = \frac{\left[1-\frac{(57.67)^2}{2\times77.65^2}\right]3.12\times10^4}{\frac{5}{3}+\frac{3(57.67)}{8\times77.65}-\frac{(57.67)^3}{8\times77.65^3}} = 11{,}942$$

Margin of safety is:

$$MS = \frac{Allowable\,Comp\,Stress}{Maximum\,Comp\,Stress} - 1 = \frac{11{,}942}{128} - 1 = +Large$$

For the 1-foot side drop, the insert is assumed to be simply supported at the ends and the weight is acting along the length of the insert.

The bending stress on the insert is calculated as (Roark's, 7th Edition, Table 8.1):

$$\sigma_{bi} = M\frac{y}{I} = \frac{W_a l^2}{8}\frac{D/2}{I} = \frac{W_{if}G_{S1}}{25\times l}\frac{l^2}{8}\frac{D/2}{I} = \frac{(7.6+3.5)\times25}{25\times9.25}\frac{9.25^2}{8}\frac{0.5/2}{1.79\times10^{-3}} = 1{,}793\ psi$$

where:

G_{S1} = 25 g, 1-foot side drop 'g' load

Margin of safety is:

$$MS = \frac{Bending\,Allowable}{Bending\,Stress} - 1 = \frac{15750}{1793} - 1 = 7.78$$

Lid Latch and Plunger

For the 1-foot top end drop, the load path through the lid, does not contain the lid latches or the plungers.

For the 1-foot side drop analysis of latch and plunger, the accident condition loads (60 g's) are used with normal condition allowables. This bounds both the normal and accident conditions of transport.

During the side drop, the latch experience 60 g's and the maximum shear stress occur at Location SA.

The shear stress on the latch at Location SA (Figure 2.6.12-10) is:

$$\tau_{SA} = \frac{W_P G_{S1}}{A_{SA}} = \frac{0.05 \times 60}{0.5 \times (0.76 - 2 \times 0.3) \times \tan(30)} = 65\ psi$$

where:

W_P = Weight of the latch = Volume ×Density of Aluminum
~ 0.5×0.5× (1.13+0.31) ×0.1 = 0.036 ~ 0.05 lbs

G_{S1} = 60 g, 30-foot side drop 'g' load

A_{SA} = 0.5× (0.76-2×0.3) × tan (30) = 0.046 in^2, Area of the latch at Location SA

Margin of safety is:

$$MS = \frac{Shear\ Allowable}{Shear\ Stress} - 1 = \frac{15615}{65} - 1 = +\text{Large}$$

Shear stress on the steel plunger is:

$$\tau_{PL} = \frac{W_P G_{S1}}{A_P} = \frac{W_P G_{S1}}{\pi/4 \times d^2} = \frac{0.05 \times 60}{\pi/4 \times 0.16^2} = 149\ psi$$

where:

d = 0.16 in, Diameter of the plunger nose

Margin of safety is:

$$MS = \frac{Shear\ Allowable}{Shear\ Stress} - 1 = \frac{6250}{149} - 1 = +Large$$

Figure 2.6.12-10 SLOWPOKE Fuel Canister Assembly Latch and the Free Body Diagram

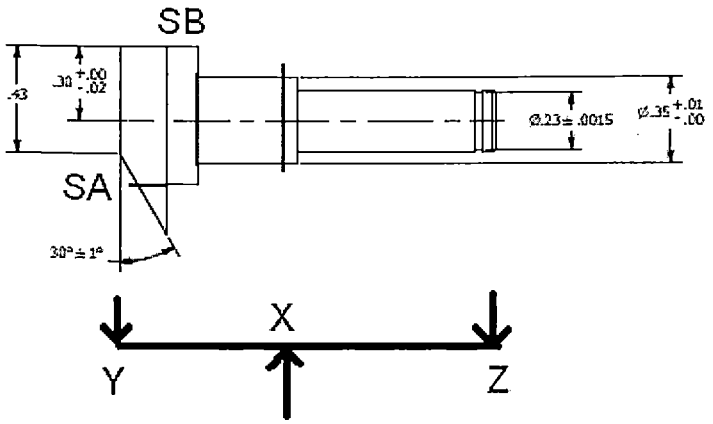

2.6.12.14 NRU/NRX Fuel Basket

The NRU/NRX fuel basket assembly consists of a top basket weldment, lid assembly and a basket spacer assembly. The basket weldment is 122.25 inches long and consists of 18 fuel tubes with a 2.5-inch outside diameter with a 0.12-inch wall thickness. Each fuel tube is capable of holding a single NRU/NRX fuel assembly or equivalent fuel rod quantity. NRU/NRX fuel assemblies/rods may be placed inside of an aluminum caddy. NRX fuel assemblies/rods shall be placed into a caddy. The total weight inside each fuel tube is limited to 20 pounds, which includes the weight of the aluminum caddy and NRU/NRX fuel assembly/rods. The 6 center tubes are supported by a center tube assembly which consists of 1.5-inch Schedule 80 pipe with 6 equally spaced scalloped center locators. The lower end of the center tube assembly is welded to the bottom support disk and the top end is bolted to the lid assembly. The 12 outer tubes are supported by 7 scalloped, circular support disks. There is a top support disk, 5 center support disks and a bottom support disk. These support disks have an outer diameter of 13.27 inches and are ½ inch thick. The 12 outer tubes are welded to these support disks on the outside of the tubes.

The spacer assembly is 51.8 inches long and consists of a center tube with an outside diameter of 8.0 inches and a wall thickness of 0.12 inches. This center tube is welded to 3 circular support disks. The spacer assembly rests on a base tube that consists of a 10-inch Schedule 80 pipe. The base tube is welded to the base disk. The total weight of the NRU/NRX basket assembly plus the spacer assembly bears directly on the bottom forging of the cask through the base tube.

The basket assembly, basket spacer assembly and lid assembly are fabricated from SA 240, Type 304 stainless steel. The lid assembly attachment bolts are made from SA564, Type 630 (17-4PH).

2.6.12.14.1 NRU/NRX End Drop Analysis for Normal Conditions of Transport

This section includes the evaluation of the NRU/NRX basket and spacer assembly components for lateral (side) and longitudinal (end) 1-foot drops. The acceleration load of 25 g's is conservatively assumed for end and side drops for normal conditions of transport.

Basket/Lid Assembly

Basket assembly consists of 18 cylindrical tube assemblies with a center tube assembly and 7 outer support disks. The center tube assembly is not attached to the 6 tubes in the middle of the basket but the outer 12 tubes are welded to the outer support disks. All 18 tube assemblies are welded to the bottom support disk. The basket lid assembly is attached to the top support disk and the center tube assembly with 7 lid bolts with a 3/8-16 UNC thread. One bolt attaches the lid to the center tube assembly and 6 bolts attach the lid to the top support disk. The bottom support disk is attached to the center tube assembly by two 1/4 inch fillet welds around the entire circumference and the outer tubes by a 1/16 inch fillet weld spanning 60 degrees.

2.6.12.14.1.1 Top End Drop

The acceleration for a 1 foot top end drop is 25 g.

Fuel Tube Assembly

The compressive stress on the fuel tube assembly is calculated as:

$\sigma_c = Wg/18(A_{tube}) = 1.86$ ksi for 25 g

where; W = Weight of (basket assembly + 18 fuel assemblies + spacer assembly)
= 695 lbs + 30 + 18(20lbs) + 115 lbs = 1,200 lbs

Note: This is conservative since the weight of the top disk (5 lbs) is not carried by the fuel tubes in a top end drop.

and

$A_{tube} = \pi/4(OD^2-ID^2) = 0.897$ in^2

OD = 2.5 in
ID = 2.26 in

Margin of safety:

$MS = (1.0S_m/\sigma_c)-1 = 9.0$

where $S_m = 18.6$ ksi for SA240, Type 304 at 400 °F

Fuel tube buckling analysis

The column length to radius ratio is;

$L/r_m = 20.5/1.19 = 17.2$

where;

L= distance between disks = 20.5 in
r_m = mean radius of fuel tube = ¼(OD+ID) = 1.19 in

This means that the tube will not buckle as a classical Euler column, instead the buckling mode would be localized buckling (bellows or diamond pattern). For this mode of buckling, the critical compressive stress is given by Blake;

$$S_{cr} = E\frac{0.605 - m^2 x10^{-7}}{m(1+0.004\phi)} = 264.1 \text{ ksi}$$

where;

$E = 26.5x10^6$ psi for SA240, Type 304 at 400 °F
$S_y = 20.7$ ksi for SA240, Type 304 at 400 °F
$\phi = E/S_y = 1280$
$m = r_m/t = 9.92$
$r_m = 1/2(OD/2+ID/2) = 1.19$ in
$t = 1/2(OD-ID) = 0.12$ in

Margin of safety:

$MS = (S_{cr}/\sigma_c)-1 = \text{large}$

Note: All margins of safety greater than 10 are reported as large.

Support Disk to Tube Welds

The welds for the middle 5 support disks only carry the disk self-weight in a top end drop. The middle support disks are attached to the outer 12 tubes with a 1/16-inch fillet weld on each side of the support disk. Due to lack of access, these welds only extend 60 degrees in the circumferential direction around each tube.

The primary stress in these attachment welds is shear.

$\tau = Wg/A_{eff} = 0.09$ ksi for 25 g

where;

W = middle disk weight = 5 lbs
$A_{eff} = 12[2(60/360)(\pi D_{tube})(t_{eff})] = 1.39 \text{ in}^2$
$D_{tube} = 2.5$ inch
$t_{eff} = 0.7071(1/16) = 0.0442$ in

Margin of safety:

$MS = (0.6S_m/\tau)-1 = \text{large}$

where S_m = 18.6 ksi for SA240, Type 304 at 400 °F

Center Tube to Bottom Disk Weld

The fuel tube assembly consists of a cylindrical tube attached to a tube cap on the bottom of the fuel tube. This cap is then welded to the bottom disk to form part of the center tube assembly. This attachment weld is a full circumference double sided 1/8-inch fillet weld. This weld does not support the full weight of the center tube assembly since the center tube assembly is also bolted to the basket lid assembly at the top of the basket. For the weld calculation, it is conservatively assumed that this weld will carry the full weight of the center tube assembly.

The primary stress in these attachment welds is shear.

$$\tau = Wg/A_{eff} = 1.32 \text{ ksi for } 25 \text{ g}$$

where;

W = center tube assembly weight = 56 lbs
$A_{eff} = 2(\pi D_{center\ tube})(t_{eff}) = 1.06 \text{ in}^2$
$D_{tube} = 1.9$ inch
$t_{eff} = 0.7071(1/8) = 0.0884$ in

Margin of safety:

$$MS = (0.35 \times 0.6S_m/\tau)-1 = 1.96$$

where S_m = 18.6 ksi for SA240, Type 304 at 400 °F

0.35 = weld quality factor for visual inspection, ASME Section III Subsection NG, Table 3352-1.

Basket Tube End Cap to Bottom Disk Weld

The basket tube end cap is welded to the base disk with a 1/4-inch fillet weld around the circumference. However, the end cap fits inside of a hole in the base disk so this weld would not be loaded significantly by the top end drop. The reaction load for the top end drop would be carried primarily by bearing between the end cap and the base disk.

Bearing stress between the fuel tube end cap and the base disk

$\sigma_b = Wg/18A_{end\ cap} = 0.479$ ksi for 25 g

where;

W = Weight of (basket+lid+18 fuel assemblies-base disk)
= 695 lbs + 30 lbs + 18(20 lbs) – 20 lbs = 1,065 lbs

$A_{end\ cap} = \pi/4[(OD_{end\ cap})^2 - (ID_{bottom\ disk\ opening})^2] = 3.09\ in^2$

$OD_{end\ cap} = 2.5$ in
$ID_{bottom\ disk\ opening} = 1.52$ in

Margin of safety:

$MS = (1.0S_y/\sigma_b)-1 = large$

where $S_y = 20.7$ ksi for SA240, Type 304 at 400 °F

Basket Lid Assembly

The basket lid assembly is a 1/2-inch stainless steel plate which covers the top end of the basket assembly. The lid assembly includes the lid plate, lid collar, collar cover plate, and lifting lugs. For the analysis, the lid is assumed to be simply supported at the location of the lid collar tube and the total weight (impact load) is assumed to act on the bottom face of the lid. The total weight of the NRU/NRX basket assembly, spacer assembly plus 18 fuel assemblies is 1,170 lbs.

Since the basket lid plate is not a solid disk, due to the presence of several holes in the lid plate, the bending stress on the canister lid is calculated with a finite element analysis model (FEA). A quarter symmetry model of the lid plate was constructed. The following depicts the FEA Model.

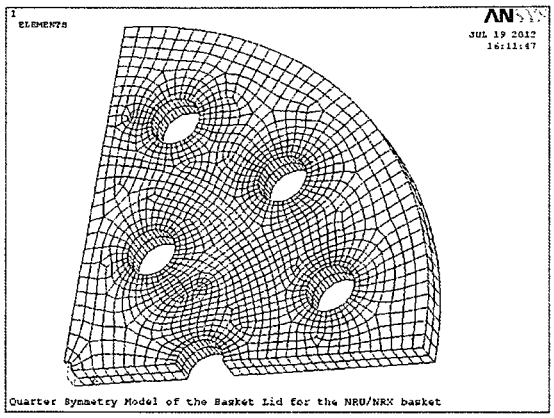

The linearized membrane stress and membrane plus bending stress for a 1 g load are 281 psi and 676 psi, respectively. Since this is a linear model, these stresses can be scaled. Therefore, for a 25 g load;

$P_m = 7.03$ ksi

$P_m + P_b = 16.9$ ksi

Margin of safety:

$MS_m = (1.0S_m/P_m) - 1 = 1.65$

$MS_{m+b} = (1.5S_m/P_m + P_b) - 1 = 0.65$

where $S_m = 18.6$ ksi for SA240, Type 304 at 400 °F

Lid Collar Tube

The lid collar tube is attached to the top of the basket lid. The lid collar tube is also subjected to compressive stress in the top end drop:

$\sigma_c = Wg/A_{collar\ tube} = 10.1$ ksi for 25 g

where;

W = Weight of (basket assembly + basket lid assembly + 18 fuel assemblies + spacer assembly)
= 695 lbs + 30 lbs + 18(20 lbs) + 115 lbs = 1,200 lbs

$A_{collar\ tube} = \pi/4(OD^2 - ID^2) = 2.97\ in^2$

for

OD = 8.0 in
ID = 7.76 in

Margin of safety:

$MS = (1.0S_m/\sigma_c) - 1 = 0.84$

where S_m = 18.6 ksi for SA240, Type 304 at 400 °F

Bearing Stress between the Basket Lid Assembly and the LWT Cask Lid

$\sigma_b = Wg/A_{collar+cover\ plate} = 0.781$ ksi for 25 g

where;

W = 1,200 lbs

$A_{collar+cover\ plate} = \pi/4(OD^2) - A^2 = 38.43\ in^2$

OD = 8.0 in
A = Width of opening in collar cover plate = 3.44 in

Margin of safety:

$MS = (1.0S_y/\sigma_b) - 1 =$ large

where S_y = 20.7 ksi for SA240, Type 304 at 400 °F

Bottom Support Disk

This disk will only support the weight of the spacer assembly (115 lbs) for the top end drop whereas it will support the total weight of the basket assembly, the basket lid assembly and the 18 fuel assemblies (1,085 lbs) in the bottom end drop case. Therefore, the bottom end drop will be controlling for the bottom support disk.

Spacer Assembly

For the top end drop, the spacer assembly is only subjected to its own weight. However, in the bottom end drop the spacer assembly will have to carry the weight of the basket assembly and the fuel assemblies. Therefore, the bottom end drop will be controlling for the spacer assembly.

Fuel Caddy

The fuel assembly/rods may be contained in an aluminum caddy. The caddy consists of a cylinder with an end cap on the bottom. The cylinder has a 2.0-inch outer diameter and a 0.065-inch wall thickness and is constructed from 6061-T6 aluminum.

The only loading that the caddy will experience is its own weight of 5 lbs during the top end drop.

The compressive stress on the fuel caddy is calculated as:

$\sigma_c = Wg/A_{net} = 0.374$ ksi for 25 g

where; W = Weight of fuel caddy = 5 lbs

$A_{net} = \pi/4(OD^2-ID^2)[360-2\theta)/360] = 0.334\ in^2$

OD = 2.0 in
ID = 2.0-2(0.065) = 1.87 in

and

$\Theta = 2\ Sin^{-1}\ (L/2r) = 53.5°$

where; L= 0.9 in (lateral width of cut-out in caddy wall) and r = OD/2

Margin of safety:

$$MS = (1.0S_m/\sigma_c)-1 = \text{large}$$

where S_m = 5.6 ksi for 6061-T6 aluminum at 400 °F

2.6.12.14.1.2 Bottom End Drop

The acceleration for a 1-foot top end drop is 25 g.

Fuel Tube Assembly

The compressive stress on the fuel tube assembly is less than the top end drop since only the weight of the basket assembly and the basket lid assembly is supported in this case.

W = Weight of basket assembly + Weight of basket lid assembly = 695 lbs + 30 lbs = 725 lbs

Since this is less than the weight of 1,200 lbs supported by the tubes in the top end drop, the top end drop is controlling.

Support Disk to Basket Tube End Cap Welds

The load on these welds is the same for the bottom end drop as the top end drop; therefore, the shear stress would be the same.

Center Tube to Bottom Disk Weld

The fuel tube assembly consists of a cylindrical tube attached to a tube cap on the bottom of the fuel tube. This attachment weld is a full circumference 3/16-inch fillet weld. This weld would not support the full weight of the center tube assembly since the reaction load would be through the basket lid assembly. For the weld calculation, it is conservatively assumed that this weld will carry the full weight of the basket plus the lid and fuel assemblies.

The primary stress in these attachment welds is shear.

$$\tau = Wg/18A_{eff} = 2.35 \text{ ksi for 25 g}$$

where;

W = basket + lid + fuel assemblies – bottom disk
= 695 lbs + 30 lbs +18(20 lbs) – 15 lbs = 1,070 lbs

$A_{eff} = (\pi D_{bottom\ disk\ opening})(t_{eff}) = 0.633\ in^2$

$D_{bottom\ disk\ opening} = 1.52$ inch

$t_{eff} = 0.7071(3/16) = 0.1326$ in

Margin of safety:

$$MS = (0.35 \times 0.6S_m/\tau) - 1 = 3.75$$

where S_m = 18.6 ksi for SA240, Type 304 at 400 °F

0.35 = weld quality factor for visual inspection, ASME Section III Subsection NG, Table 3352-1.

Basket Lid Assembly

The basket lid assembly will not experience any significant loading in the bottom end drop.

Bottom Support Disk

The bottom support disk is a 1/2-inch stainless steel plate which covers the bottom end of the basket assembly. The bottom support disk is part of the center tube assembly which includes the center tube center locators and the center bolt insert. For the analysis, the bottom disk is assumed to be simply supported at the location of the lid collar tube from the spacer assembly below the basket assembly and the total weight (impact load) is assumed to act on the top face of the bottom support disk.

Since the bottom support disk plate is not a solid disk due to the presence of several holes in the lid plate, the bending stress on the canister lid is calculated with a finite element analysis model (FEA). A quarter symmetry model of the lid plate was constructed.

The FEA model of the basket lid plate is shown as follows:

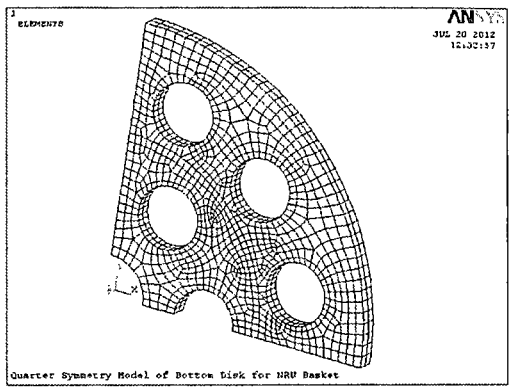

The linearized membrane stress and membrane plus bending stress for a 1 g load are 351 psi and 960 psi, respectively. Since this is a linear model, these stresses can be scaled. Therefore, for a 25 g load:

$P_m = 8.78$ ksi

$P_m + P_b = 24.03$ ksi

Margin of safety:

$MS_m = (1.0S_m/P_m) - 1 = 1.11$

$MS_{m+b} = (1.5S_m/P_m + P_b) - 1 = 0.16$

where $S_m = 18.6$ ksi for SA240, Type 304 at 400 °F

Spacer Assembly

The spacer assembly will be subjected to its own weight plus the weight of the basket, lid and fuel assemblies.

Spacer Tube

The spacer tube will experience a compressive stress due to the bottom end drop. The compressive stress is given by;

$\sigma_c = Wg/A_{spacer\ tube} = 9.93$ ksi for 25 g

where;

W = Weight of (basket assembly + basket lid assembly + 18 fuel assemblies + spacer assembly- base disk)

= 395 lbs + 30 lbs + 18(20 lbs) + 115 lbs – 20 lbs = 1,180 lbs

$A_{spacer\ tube} = \pi/4(OD^2\text{-}ID^2) = 2.97\ in^2$

for

OD = 8.0 in
ID = 7.76 in

Margin of safety:

$MS = (1.0S_m/\ \sigma_c) = 2.0$

where S_m = 18.6 ksi for SA240, Type 304 at 400 °F

Spacer tube buckling analysis

The column length to radius ratio is:

$L/r_m = 23.5/3.94 = 5.96$

where;

L= distance between disks = 23.5 in
r_m = mean radius of spacer tube = ¼(OD+ID) = 3.94

This means that the tube will not buckle as a classical Euler column, instead the buckling mode would be localized buckling (bellows or diamond pattern). For this mode of buckling, the critical compressive stress is given in Blake:

$$S_{cr} = E\frac{0.605 - m^2 x10^{-7}}{m(1+0.004\phi)} = 79.8\ ksi$$

where;

$E = 26.5\times10^6$ psi for SA240, Type 304 at 400 °F
$S_y = 20.7$ ksi for SA240, Type 304 at 200 °F
$\varnothing = E/S_y = 1280$
$m = r_m/t = 32.83$
$r_m = 1/2(OD/2+ID/2) = 3.94$ in
$t = 1/2(OD-ID) = 0.12$ in

Margin of safety:

$MS = (S_{cr}/\sigma_c) - 1 = 7.04$

Base disk

Since there is only a small offset between the spacer tube OD and the ID [1/2(9.56-8.0) = 0.78] of the base ring below the base disk, there will not be any significant bending of the base disk in the spacer assembly.

Spacer base

The spacer base is a cylindrical tube beneath the base disk of the spacer assembly. This tube will be subjected to a compressive stress due to the total weight of the basket, lid, fuel and spacer assemblies.

$\sigma_c = Wg/A_{spacer\ base} = 2.05$ ksi for 25 g

where;

W = Weight of (basket assembly + basket lid assembly + 18 fuel assemblies + spacer assembly)
= 695 lbs + 30 lbs + 18(20 lbs) = 115 lbs = 1,200 lbs

$A_{spacer\ base} = \pi/4(OD^2-ID^2)-2(\text{slot width})(\text{tube thickness}) = 14.6\ in^2$

OD = 10.75 in
ID = 9.75 in
Slot width = 0.75 in
Tube thickness = ½(OD-ID) = 0.5 in

Margin of safety:

$$MS = (1.0S_m/\sigma_c) - 1 = 8.07$$

where S_m = 18.6 ksi for SA240, Type 304 at 400 °F

Fuel caddy

The fuel caddy will only experience the self-weight of the aluminum cylinder for the bottom end drop. This weight is less than the total weight of the cylinder plus the bottom plate. Therefore, the top end drop is controlling for this component.

2.6.12.14.1.3 Side Drop

The acceleration for the 1 foot side drop is 25 g. For the side drop, the reaction loads will be carried by the support disks. The fuel tubes will be subjected to bending between the support disks.

Fuel Tube Assembly

The fuel tube assemblies are supported by five middle support disks plus a top disk and a bottom disk. The fuel tubes are unsupported between the support disks. To calculate the bending stress, the fuel tube section between the support disks will be assumed to be a simply supported beam. This is a conservative approach since the presence of the support disk and the continuity of the tube will add stiffness at the point where the fuel tube passes through the support disk.

$M_{max} = wl^2/8 = 23.74$ in-lbs

where;

$w = (W_{tube} + W_{fuel})/L = 0.452$ lbs/in
$W_{tube} = 32$ lbs
$W_{fuel} = 20$ lbs
L = length of fuel = 9'7" = 115 in
l = disk spacing = 20.5 in

Then the bending stress is given by;

$$\sigma_b = Mc/I = 1.17 \text{ ksi for 25 g}$$

where;

$c = OD_{tube}/2 = 1.25$ in
$I = \pi/64(OD^4-ID^4) = 0.636$ in^4
$OD_{tube} = 2.5$ in
$ID_{tube} = 2.26$ in

Margin of safety:

$MS = (1.5S_m/\sigma_c) - 1 = \text{large}$

where; $S_m = 18.6$ ksi for SA240, Type 304 at 400 °F

Support Disk Bearing Stress

From Roark, Table 33, Case 2c

$\sigma_c^{Max} = 0.591(pE/K_D)^{1/2} = 6.52$ ksi for 25 g

where;

$K_D = D_1D_2/(D_1-D_2) = 1690$

D_1 = ID of LWT Cask = 13.375 in
D_2 = OD of Support Disk = 13.27 in
$p = gW/L$
W = (basket lid assembly + weight of fuel assemblies) = 725 lbs + 18(20 lbs) = 1,085 lbs
L = total thickness of support disks = 7(1/2) = 3.5 in

Margin of safety:

$MS = (1.0S_y/\sigma_c) - 1 = 2.17$

where; $S_y = 20.7$ ksi for SA240, Type 304 at 400 °F

Center Tube Assembly

The fuel tube assemblies are supported by five center locators plus a top support disk and a bottom support disk. The center tube is unsupported between the center locators. To calculate the bending stress, the fuel tube section between the support disks will be assumed to be a simply supported beam. This is a conservative approach since the presence of the support disk and the continuity of the tube will add stiffness at the point where the fuel tube passes through the support disk.

$M_{max} = g(wl^2/8) = 407.5$ in-lbs for 25 g

where;

$w = \rho A = 0.3103$ lbs/in
$\rho = 0.29$ lbs/in^3
$A = \pi/4(OD^2-ID^2) = 1.07$
$OD_{tube} = 1.90$ in
$ID_{tube} = 1.50$ in
l = length of between center locators = 20.5 in

Then the bending stress in the center tube assembly is given by;

$\sigma_b = Mc/I = 0.99$ ksi for 25 g

where;

$c = OD_{tube}/2 = 0.95$ in
$I = \pi/64(OD^4-ID^4) = 0.391$ in^4

Margin of safety:

$MS = (1.5S_m/\sigma_c) - 1$ = large

where; $S_m = 18.6$ ksi for SA240, Type 304 at 400 °F

2.6.12.14.1.4 Thermal Stress

The thermal stress in the basket assembly is determined from a finite element model and the temperature distribution from a corresponding thermal model. A complete description of the thermal model is given in Chapter 3. The structural model for thermal stress evaluation was derived from the thermal model by deleting the elements associated with modeling of the gas conduction and radiation effects. Then, the remaining thermal conduction elements were converted to the corresponding structural elements. The temperature distribution was applied to the structural model by reading the temperature from the thermal results. The structural FEA model is shown below.

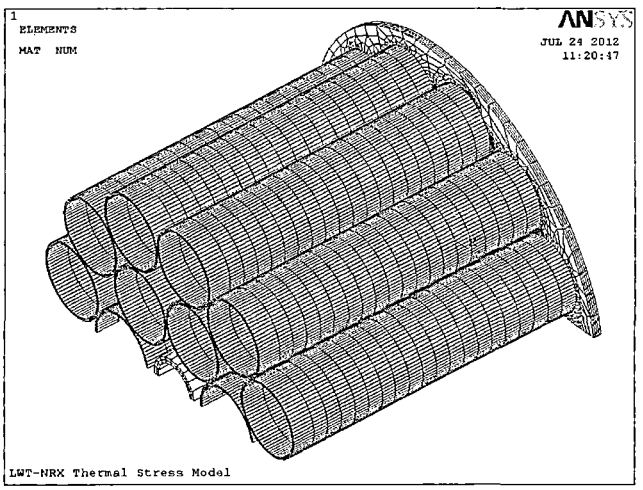

Structural Model Used to Evaluate Thermal Stresses

Standard symmetry boundary conditions were applied to the two cut planes (XY plane and XZ plane) and all of the nodes at the cut end of the fuel tubes were coupled in the UZ degree of freedom. To prevent rigid body motion, all nodes on the YZ plane were constrained in the UX direction. A plot of the calculated thermal stresses is shown as follows.

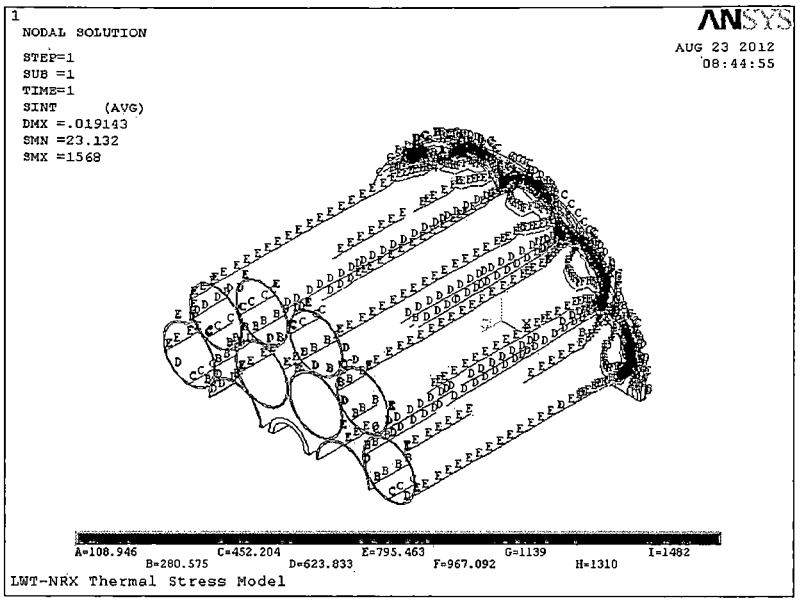

Thermal Stresses

The maximum peak thermal stress in the model is 1.6 ksi as shown in the stress plot. These stresses are conservatively combined with the maximum calculated stress from the drop cases for normal conditions of transport and compared to the primary plus secondary allowable of $3.0S_m$.

$$P_{m+b} + Q_{max} = 24.95 \text{ ksi} + 1.5 \text{ ksi} = 26.45 \text{ ksi}$$

Margin of Safety

$$MS = [3.0S_m / (P_{m+b} + Q_{max})] - 1 = 1.11$$

where; S_m = 18.6 ksi for SA240, Type 304 at 400 °F

2.6.12.15 HEUNL Container

[redacted]

There will be a total of 4 HEUNL containers in the LWT cask. A support spacer will be located at the bottom of the LWT cask between the bottom container and the bottom forging of the LWT cask. The HEUNL containers and the support ring are structurally evaluated with a combination of standard handbook formulas and finite element models.

The weight of each container is 350 lbs and the weight of the HEUNL fluid was calculated to be 176 lbs which gives a total of 526 lbs. A partially filled container would weigh less but it is conservative to use the weight of a fully filled container.

2.6.12.15.1 Finite Element Models

HEUNL Container FEA Model

The finite element model (FEA) was constructed of ANSYS SOLID45 3D elements and CONTAC52 gap elements. Both the HEUNL container and contained fluid were modeled. There

are CONTAC52 elements between the outside surface of the fluid region and the inner surface of the container to model the compression only loading by the liquid. For the side drop case, CONTAC52 elements were added to the outer surface of the guide rails to determine the load distribution between the HEUNL container and the inner surface of the LWT cask. The HEUNL container FEA model is shown in the Figure 2.6.12-11 through Figure 2.6.12-13.

Figure 2.6.12-11 HEUNL Container – Outside View

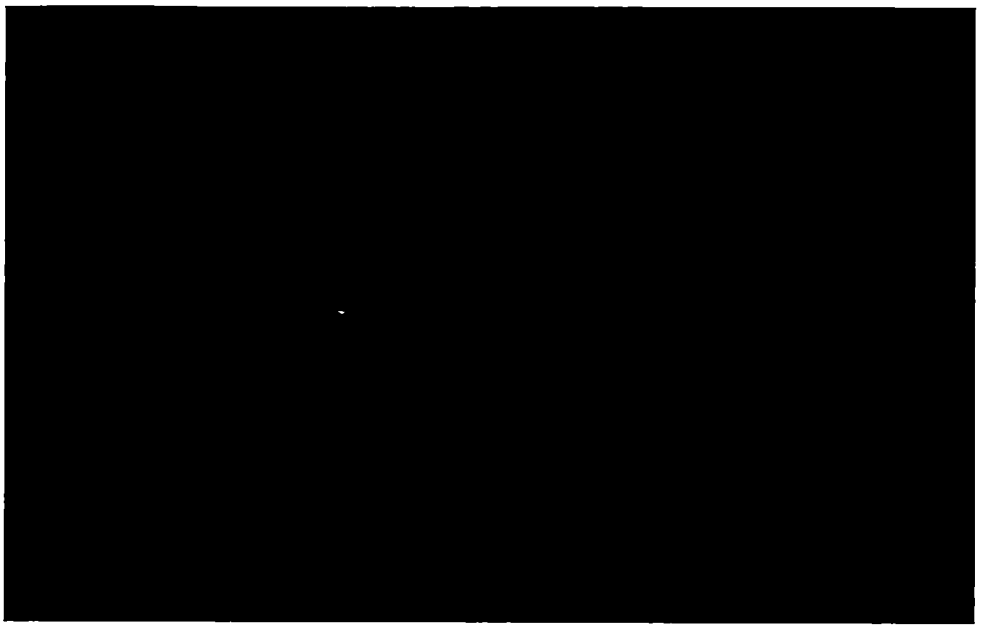

Figure 2.6.12-12 HEUNL Container – Inside View

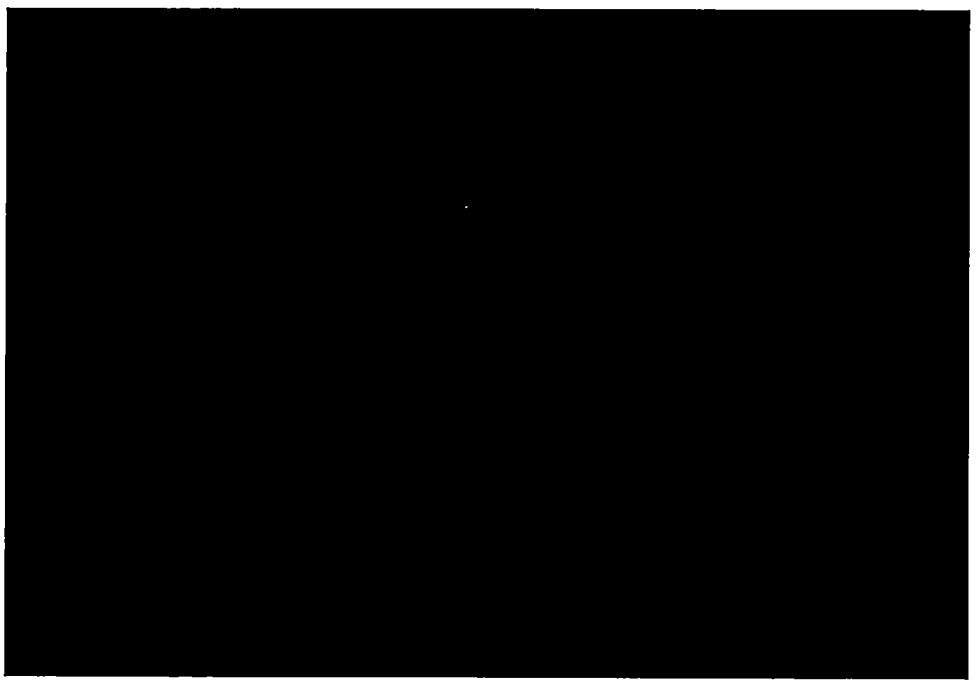

Figure 2.6.12-13 HEUNL Container – Gap Elements Shown

Support Ring Model

The support ring is a flat annular, machined ring. The support ring is constructed from SA-240, Type 304. An axisymmetric FEA model of the support ring was constructed for the bottom drop structural evaluation. Gap elements were placed at the bottom edge of the ring to account for possible lift-off of one edge. The support ring is not loaded significantly by the side drop or the top end drop. The FEA Model is shown in Figure 2.6.12-14. Vertical constraints were applied to the lower end of the gap elements and a pressure load was applied to the model top surface for the inertial load of the containers.

Figure 2.6.12-14 HEUNL Container Support Ring – Axisymmetric Model

[redacted]

Closure Assembly Model

The closure lid is a circular flat plate which is attached to the container head with six ½ inch-13 UNC cap screws. There are two O-rings under the closure lid for sealing purposes. A quarter symmetry model is used for the closure assembly. The closure lid, the O-rings, a portion of the container head and the liquid region are modeled with ANSYS SOLID45, 3D solid elements. The bolts are modeled with ANSYS BEAM4, 3D beam elements. The beam elements representing the bolts are connected to the 3D solid elements with a spider array of rigid, massless beam elements. The FEA model is shown in Figure 2.6.12-15 and 2.6.12-16.

Figure 2.6.12-15 Closure Assembly Model

[redacted]

Figure 2.6.12-16 Bolt Modeling

[redacted]

Fill/Drain Port FEA Model

The fill/drain port model is shown in Figure 2.6.12.17. The geometry was imported into the ANSYS software from AutoCAD and meshed with SOLID186, 3D solid elements. Due to the complexity of the geometry, tetrahedral elements are used. This is an acceptable approach since the elements have mid-side nodes. Note that the fluid region is included in the model for evaluation of freezing of the HEUNL fluid due to cold conditions. In the model, the fluid region extends up to the bottom edge of the counter-bore which neglects the presence of the quick disconnect. This is a conservative approach since it produces more expansion in this region.

Also note that a mesh sensitivity study was conducted to arrive at the mesh density shown below.

Figure 2.6.12-17 Fill/Drain Port Model

[redacted]

2.6.12.15.2 HEUNL Container 1-Foot Drop Cases and Pressure Cases

The HEUNL container is evaluated for both end drops (top and bottom drops) and a side drop. An equivalent acceleration of 25 g is used to evaluate the 1-foot drops.

For each drop case the FEA model is utilized. The linearized stresses are checked at 14 section locations. These sections used are shown in Figure 2.6.12-18 and Figure 2.6.12-19.

Figure 2.6.12-18 HEUNL Container – Section Locations

[redacted]

Figure 2.6.12-19 HEUNL Container – Section Locations

[redacted]

Sections P6, P7 and P13 are not shown in the figures but are located at the center of the container shell half way between the bottom end cap and the top end cap.

The allowable stress S_m for SA-240, Type 304 at 200 °F is 20 ksi.

Design Pressure Case

As identified in Section 8.1.4.4 the canister is to be hydrostatically tested to 140 +10/-0 psig. This condition is treated as a normal condition, which bounds the maximum pressure expected during normal operational conditions identified in Section 4.5.6. A pressure case of 150 psig was evaluated. For this case a 30° sector of the 180° model was used and the liquid region of material was eliminated.

The maximum membrane stress intensity from the 14 section cuts was 3.24 ksi and the maximum membrane plus bending stress intensity was 4.83 ksi. For the Normal Conditions of Transport, the margin of safety is 4.67 for the membrane stress and 5.21 for the membrane plus bending stress.

1 Foot Side Drop

For the side drop each container rests against the inner shell of the LWT cask. The gap elements on the outside surface of the guide bars have two nodes. The outermost nodes are constrained in the radial, tangential and axial direction. This boundary condition represents the inner surface of the LWT cask as rigid, which is a conservative approach since this produces higher loads on the container guide rails.

For the side drop case an acceleration of 25 g is applied in the lateral (X) direction.

The maximum membrane stress intensity from the 14 section cuts was 2.58 ksi and the maximum membrane plus bending stress intensity was 4.77 ksi. For the Normal Conditions of Transport, the margin of safety is 6.75 for the membrane stress and 5.29 for the membrane plus bending stress. For additional details refer to item 1 in Section 2.6.12.15.5.

The bearing stress between the guide rail and the inner surface of the LWT cask was also computed. Assuming that the entire weight of the filled container is supported by one guide rail, the bearing stress is 0.322 ksi. This gives a margin of safety greater than 10. For additional details refer to item 1 in Section 2.6.12.15.5.

1 Foot Bottom End Drop

For the bottom end drop case an acceleration of 25 g is applied in the vertical (Z) direction. The lowest container rests on the spacer ring, which rests on the bottom forging of the LWT cask. The vertical acceleration accounts for the weight of the lowest container; however, the remaining 3 containers are stacked on the top of the lowest container. To account for the weight of the other

three containers an equivalent pressure load is applied to the top of the FEA model for the bottom container.

The maximum membrane stress intensity from the 14 section cuts was 4.44 ksi and the maximum membrane plus bending stress intensity was 6.52 ksi. Comparing this to the allowable stress gives a margin of safety of 3.50 for the membrane stress and 3.60 for the membrane plus bending stress. For additional details refer to item 1 in Section 2.6.12.15.5.

The bearing stress between the lowest container and the top surface of the support spacer was computed. The bearing stress is 5.82 ksi. This gives a margin of safety against the yield strength of 3.30. The bearing stress between the bottom of the support ring and the bottom of the LWT cask was also checked. This bearing stress is 2.0 ksi, which gives a margin of safety of greater than 10. For additional details refer to item 1 in Section 2.6.12.15.5.

The container wall was also evaluated for potential buckling with a standard closed form solution. The calculated critical buckling stress calculated was 131 ksi. Compared to the calculated compressive stress in the container wall of 5.96 ksi, the margin of safety is greater than 10. For additional details refer to item 1 in Section 2.6.12.15.5.

The revised support ring FEA model was utilized to evaluate this case. The maximum membrane stress intensity calculated was 6.70 ksi and the maximum membrane plus bending stress intensity was 17.54 ksi. Comparing this to the allowable stress gives a margin of safety of 1.99 for the membrane stress and 0.71 for the membrane plus bending stress. For additional details refer to item 1 in Section 2.6.12.15.5.

1 Foot Top End Drop

For the top end drop case an acceleration of 25 g is applied in the vertical (-Z) direction. The topmost container rests on the closure lid of the LWT cask. The vertical acceleration accounts for the weight of the lowest container; however, the remaining 3 containers are stacked on the top of the lowest container. To account for the weight of the other three containers, an equivalent pressure load is applied to the bottom of the FEA model of the top container.

The maximum membrane stress intensity from the 14 section cuts is 5.01 ksi and the maximum membrane plus bending stress intensity is 5.96 ksi. Comparing this to the allowable stress gives a margin of safety of 2.99 for the membrane stress and 4.03 for the membrane plus bending stress. For additional details refer to item 1 in Section 2.6.12.15.5.

The bearing stress between the topmost container and the bottom surface of the LWT cask closure lid was also checked. The bearing stress is 1.76 ksi, which gives a margin of safety greater than 10. For additional details refer to item 1 in Section 2.6.12.15.5.

The container wall was evaluated for potential buckling with a standard closed form solution. The calculated critical buckling stress calculated was 131 ksi. The calculated compressive stress in the container wall is 5.96 ksi; therefore, the margin of safety is greater than 10. For additional details refer to item 1 in Section 2.6.12.15.5.

Pressure Case Combined with Drop Cases

The maximum stress intensities for the pressure case are added absolutely to the maximum stress intensities for the drop cases to get the combined stress intensity. The maximum combined membrane stress intensity is 7.13 ksi and the maximum combined membrane plus bending stress intensity is 9.74 ksi. Comparing this to the allowable stress gives a margin of safety of 1.81 for the membrane stress and 2.08 for the membrane plus bending stress. For additional details refer to item 1 in Section 2.6.12.15.5.

Liquid Sloshing

[redacted]

Thermal Stresses

Since the heat load for each HEUNL container is less than 5 Watts, there will not be any significant thermally induced stresses for the Normal Condition of Transport.

Extreme Cold Ambient Conditions (-40 °F)

[redacted]

2.6.12.15.3 Closure Assembly Model

The closure assembly model is evaluated for the conditions of bolt preload, normal pressure loading and cold conditions. The bolt preload requirement was determined by the maximum load required to resist the blow-off load for maximum pressure or the maximum load required to compress the O-rings to the point of metal-to-metal contact between the closure lid and the top of the container. The compression load required to compress the seals was larger than that required to resist the blow-off load. The bolt preload requirement was determined to be 18,000 lbs or 3,000 lbs per bolt.

The bolt preload for the FEA model was achieved by specifying as an initial strain for the beam elements representing the bolts.

Normal Condition Pressure Case

The stresses are linearized through the closure lid at two locations; 1) the center of the lid and 2) at the location of the maximum stress which is from the bottom of the counter-bore to the bottom of the lid. These paths are shown in Figure 2.6.12-20.

Figure 2.6.12-20 Stress Linearization Paths in Closure Lid

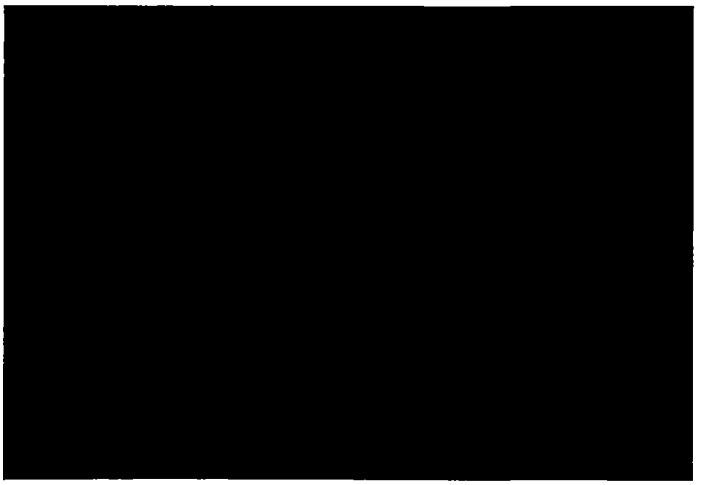

The normal condition pressure of 100 psi was applied to the lower surface of the closure lid from the center out to the inner diameter of the inner O-ring. The maximum stress occurs at the counter-bore for the cap screws in the lid. The linearized stresses at the two locations were checked. The maximum membrane stress was 12.2 ksi and the maximum membrane plus bending stress was 18.46 ksi. Comparing these stresses to the allowable stress gives a margin of safety of 0.64 for membrane stress and 0.63 for membrane plus bending.

The contact pressure on the inner seal is checked to ensure that full contact between the closure lid and the inner seal is maintained. This validates the assumption that the pressure load only extends to the inner radius of the inner seal.

The maximum axial bolt load calculated for the 100 psi case was 3,162 lbs. Using the thread tensile area, the bolt tensile stress calculated was 22.98 ksi. The maximum bolt moment calculated was 133.6 in-lbs. This produces a bending stress of 18.52 ksi. The combined axial plus bending stress is 41.5 ksi.

Bolt Stresses

Using an allowable stress of $(S_m)_{BM}$ = 36.85 ksi for SA 705, Type 630 (17-4 PH) at 150°F gives a margin of safety of 2.21 for the axial stress and 1.66 for axial plus bending stress.

Thread shear stress

The shear stress for the internal threads in the container is limiting since the bolt is SA 705, Type 630 and the container is SA 240, Type 304. The internal thread shear stress for a bolt load of 3,162 lbs is 3.48 ksi. Using the allowable for shear stress gives a margin of safety of 2.45.

For additional details refer to item 1 in Section 2.6.12.15.5.

Cold Conditions

[redacted]

Since the pressure in the container for cold conditions is 38.2 psig (52.9 psia), it is assumed that this pressure exists underneath the closure lid also. The 100 psig normal condition pressure load is applied from the center of the lid out to the inner radius of the inner seal.

The maximum stress occurs at the counter-bore for the cap screws in the lid. The linearized stresses at the two locations were checked. The maximum membrane plus bending stress was 28.86 ksi. Since this is a displacement controlled load, the allowable stress for membrane plus bending is $3S_m$. For SA 240, Type 304 at -40 °F, S_m is 20 ksi. Therefore the margin of safety is 1.08 based on the linearized membrane plus bending stress.

The contact pressure on the inner seal is checked to ensure that full contact between the closure lid and the inner seal is maintained. This validates the assumption that the pressure load only extends to the inner radius of the inner seal.

The maximum axial bolt load calculated for the cold condition case was 5,921 lbs. Using the thread tensile area, the bolt tensile stress calculated was 43.03 ksi. The maximum bolt moment calculated was 470.9 in-lbs. This produces a bending stress of 65.27 ksi. The combined axial plus bending stress is 108.3 ksi.

Bolt Stresses

Using an allowable stress of $(S_m)_{BM}$ = 38.3 ksi for SA 705, Type 630 (17-4 PH) for less than 100°F gives a margin of safety of 0.78 for the axial stress and 0.06 for axial plus bending stress.

Thread shear stress

The shear stress for the internal threads in the container is limiting since the bolt is SA 705, Type 630 and the container is SA 240, Type 304. The internal thread shear stress for the bolt load of 5,921 lbs is 6.52 ksi. Using the allowable for shear stress gives a margin of safety of 0.84.

For additional details refer to item 1 in Section 2.6.12.15.5.

2.6.12.15.4 Fill/Drain Port Model

[redacted]

To evaluate the stresses due to cold conditions, two paths are defined along the inner radius of the port passage. These paths are shown in Figure 2.6.12-21.

Figure 2.6.12-21 Stress Linearization Paths in Fill/Drain Ports

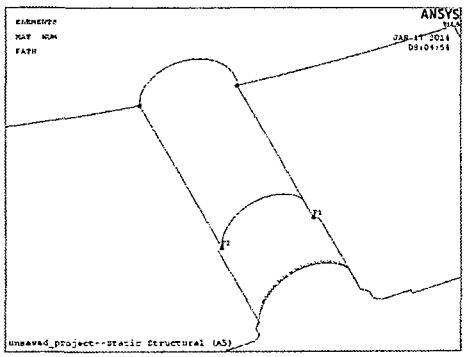

The maximum linearized stresses at these two locations are 16.78 ksi for membrane stress and 20.16 ksi for membrane plus bending stress. Since this is a displacement controlled load, the allowable stress for membrane plus bending is $3S_m$. For SA 240, Type 304 at -40 °F, S_m is 20 ksi. Therefore the margin of safety for the membrane plus bending stress is 1.98.

For additional details refer to item 1 in Section 2.6.12.15.5.

2.6.12.15.5 HEUNL Structural Calculations

1. 65008500-2010 "Canister Structural Evaluations for HEUNL in the NAC-LWT"

2.6.12.16 SLOWPOKE Fuel Core Basket

The SLOWPOKE fuel core basket assembly consists of the basket weldment, lid assembly weldment and an internal spacer assembly weldment. The basket weldment is 26.05 inches in length and consists of a circular cylinder which has an outer diameter of 10.75 inches with a 0.5-inch wall thickness. A base plate is welded to the bottom end of the cylinder and an annular ring with a 13.27-inch outer diameter and 0.75-inch thickness is welded to the top of the cylinder. A second annular ring with a 13.27-inch outer diameter and 0.5-inch thickness is welded near the midpoint of the cylinder. The lid assembly weldment is bolted to the top annular ring with six cone head bolts. The internal spacer assembly weldment fits inside of the basket and is bolted to the lid assembly with six socket head screws. The spacer assembly is 15.75 inches long and consists of a cylinder with two end plates attached. The outer diameter of the spacer cylinder is 8.0 inches and has a wall thickness of 0.38 inches. A shield plate, which has an outer diameter of 9.5 inches and is 1.5 inches thick, is welded to the lower end of the spacer cylinder and a base plate, with an outer diameter of 9.5 inches and 2.5 inches thick, is welded to the top end of the spacer cylinder.

The axial stack up of the basket, lid assembly and spacer leaves an axial gap of 9.8 inches between the end of the spacer assembly and the top of the basket base plate for the SLOWPOKE fuel core assembly. This space is sufficient to contain the SLOWPOKE fuel core assembly.

Due to the relatively small length of the SLOWPOKE basket as compared to the internal length of the LWT cask, five empty MTR basket assemblies are used as spacers between the lower end of the SLOWPOKE basket and the bottom forging of the cask. There are four intermediate MTR basket assemblies and one MTR base basket assembly between the SLOWPOKE basket and the bottom of the LWT cask.

The basket assembly, lid assembly and spacer assembly are fabricated from either SA-240/SA-269, Type 304 stainless steel or SA-269, Type 304 stainless steel. The cone head bolts are fabricated of SA-240, Type XM-19 stainless steel and the socket head screws are fabricated from SA-193, Grade B8S stainless steel.

2.6.12.16.1 SLOWPOKE Drop Analysis for the Normal Conditions of Transport

This section includes the evaluation of the SLOWPOKE basket, lid and spacer assemblies for longitudinal (end) and lateral (side) drop cases. The accelerations for the 1-foot drop cases are: an acceleration of 20 g for the end drop cases and 25 g for the side drop case.

The structural evaluation of the SLOWPOKE basket utilizes classic hand calculations.

Top End Drop

The acceleration used for the 1-foot top end drop is 20 g. The components which resist the load in a top end drop are; the lid assembly which is subjected to the weight of the loaded SLOWPOKE basket plus the 5 MTR spacers. For conservatism a bounding weight of 350 pounds is used for the loaded SLOWPOKE basket weight. The MTR basket assemblies have a bounding weight of 200 pounds each. The actual weights of these components are less.

A summary of the calculated stresses and margins of safety for the top end drop case are given in Table 2.6.12-4. Details of the calculations are given in Item 1 of Section 2.6.12.16-2.

Table 2.6.12-4 Stress Summary for Top End Drop Case

Assembly	Component	Stress Category	Calculated Stress (ksi)	Margin of Safety
Basket	Base Plate	Bearing	1.08	19.0
	Shell	Compression	1.49	11.9
Lid	Collar	Compression	9.09	1.12
	Collar cover plate	Bearing	0.87	23.8
Spacer	Shell	Compression	0.22	86.7
	Spacer/lid(1)	Bearing	0.034	633
	Spacer/lid(1)	Shear	0.16	70.9

Note:
(1) The spacer assembly bears against the base plate of the lid assembly for the top end drop case.

Bottom End Drop

The top end drop is the limiting case for the SLOWPOKE basket assembly since the basket components are only subjected to the weight of the loaded basket and will not be subjected to the weight of the empty MTR basket assemblies used as spacers below the SLOWPOKE basket. There is an increase in the bottom end drop bolts loads for the bolts attaching the basket lid spacer to the lid. However the bolt loads for the basket lid spacer are bounded by the side drop case.

Side Drop

The acceleration used for the 1 foot side drop is 25 g. The components which resist the load in a side drop are; the basket base plate and annular rings. In addition the spacer assembly is cantilevered from the lid assembly in the side drop case which produces bending and shear stresses in the spacer shell. This load case also results in bounding bolt loads for both the socket head screws and the cone head bolts.

A summary of the calculated stresses and margins of safety for the side drop case are given in Table 2.6.12-5. Details of the calculations are given in in Item 1 of Section 2.6.12.16-2.

Table 2.6.12-5 Stress Summary for Side Drop Case

Assembly	Component	Stress Category	Calculated Stress (ksi)	Margin of Safety
Basket	Shell	Bending	1.42	19.4
		Shear	0.212	20.8
	Base plate/rings	Bearing	5.25	3.14
Spacer	Shell	Bending	0.9	31.2
		Shear	0.2	56.6
Lid	Socket head screws	Tensile	6.11	2.42
		Thread shear	0.93	5.74
Lid	Cone head bolts	Tensile(2)	14.21	1.17
		Thread shear(1)	8.48	2.05

Notes:
(1) Bounding thread shear stress for external/internal shear
(2) For the reduced section of the cone head bolt

2.6.12.16.2 SLOWPOKE Structural Calculation

1. NAC Calculation 50026-2001, "Structural Evaluation of the SLOWPOKE Fuel Core Basket."

2.6.12.17 Conclusion

Loads generated during normal operations conditions for each basket assembly design result in total equivalent stresses, which each basket body can adequately sustain. Analyses show that all basket-bearing stresses during a side drop are much less than the material yield strength. Column analyses demonstrate that each basket assembly is self-supporting during an end drop. The minimum Margin of Safety, for all basket designs, is +0.10 as reported in Section 2.6.12.7.4 for the TRIGA basket; +0.003 as shown in Table 2.6.12-2 for the DIDO basket; +0.10 as reported in Section 2.6.12.9.2 for the GA fuel basket; +0.26 as reported in Section 2.6.12.11.1 for the ANSTO basket, +7.78 as reported in Section 2.6.12.13 for the SLOWPOKE fuel canister assembly; and +1.12 as reported in Section 2.6.12.14 for the NRU/NRX basket and 1.12 as reported in Section 2.6.12.16 for the SLOWPOKE fuel core. The HEUNL container has a minimum margin of safety of +0.06 as reported in Section 2.6.12.15.3. Therefore, it can be concluded that all basket designs have sufficient structural integrity for adequate service during normal conditions of transport.

2.7 Hypothetical Accident Conditions

The 10 CFR 71.73 requires the NAC-LWT cask to be structurally adequate for the free drop, puncture, fire and water immersion hypothetical accident scenario. In the free drop analyses, the cask impact orientation evaluated is that which inflicts the maximum damage to the cask. The 10 CFR 71.73 also requires the cask accident assessment to be at the most unfavorable ambient temperature in the range from –20°F to 100°F. The NAC-LWT cask is evaluated for structural integrity for the hypothetical accident conditions in this section.

2.7.1 Free Drop (30 Feet)

The NAC-LWT cask is required by 10 CFR 71.73(c)(1) to demonstrate structural adequacy for a free drop through a distance of 30 feet onto a flat, unyielding, horizontal surface. The cask strikes the surface in an orientation that inflicts maximum damage. In determining which orientation produces the maximum damage, the NAC-LWT cask is evaluated for impact orientations in which the cask strikes the impact surface on its top end, top end oblique, side, bottom end, and bottom end oblique. The impact limiters and the impact limiter attachments are evaluated in Section 2.6.7.4 for all loading conditions.

Impacts with the maximum and minimum weights of contents are considered. The environmental temperature for the drop is between -20°F and 100°F. Internal heat generation from the contents and insolation are also considered. Regarding internal pressure, the maximum or minimum normal operations pressure is applied to produce the critical stress condition in conjunction with the other loads previously discussed. Closure lid bolt preload and fabrication stresses are also considered. The analyses for the end and oblique drop accidents are conservatively based on a cask outer shell thickness of 1.12 inches. The side drop analyses are based on the cask outer shell thickness of 1.20 inches.

The following method and assumptions are adopted in all of the drop analyses:

1. The finite element method is utilized to do the impact analyses. The analyses are performed by the ANSYS computer program.
2. The analyses assume linearly elastic behavior of the cask.
3. The impact loads calculated in Section 2.6.7.4 are statically applied to the impact surface of the cask. The dynamic wave propagation produced by the impact is assumed to spread throughout the cask body simultaneously.
4. The finite element model of the NAC-LWT cask includes only the major structural components of the cask body; thus, the weight of the modeled cask body, 37,519 lbs, does not include the weight of the neutron shield material, the neutron shield shell nor the contents. However, the applied loads on the cask model are based on a cask design weight of 52,000 lbs.
5. To account for the lead slump during the drops and the differential thermal expansion between the cask stainless steel shells and lead shell, gap elements are used in the finite element model.
6. Although the 10 CFR 71.73 only requires the cask accident drop assessment to be at the most unfavorable ambient temperature in the range from –20°F to 100°F, the NAC-LWT cask is conservatively evaluated in all cases except the side drop for the ambient temperature in the range from -40°F to 130°F. The side drop evaluation uses an ambient temperature range of –40°F to 100°F.

Four accident conditions were identified for a detailed finite element stress presentation:

1. A 30-foot top end drop (drop orientation = ϕ = 0°, where ϕ is defined as the impact orientation; that is, the angle between the impact direction and the cask centerline), 130°F ambient temperature, maximum decay heat load.
2. A 30-foot top corner drop (drop orientation ϕ = 15.74°), 130°F ambient temperature, maximum decay heat load.
3. A 30-foot top oblique drop (drop orientation = ϕ = 60°), 130°F ambient temperature, maximum decay heat load.
4. A 30-foot side drop (drop orientation = ϕ = 90°), 100°F ambient temperature, maximum decay heat load.

The top end (ϕ = 0°), top corner (ϕ = 15.74°), top oblique (ϕ = 60°) and side (ϕ = 90°) drops envelope all of the drop orientations.

The types of loading involved in the four accident conditions include: (1) thermal, (2) internal pressure, (3) closure lid bolt preload, and (4) impact and inertial loads resulting from the impact event. These loadings and the boundary conditions, used in the finite element analyses, are discussed in Sections 2.7.1.1.2 through 2.7.1.3.2. Appendix 2.10.10 gives a thorough look at the procedures, analysis and stress results for the 30-foot drop accident conditions. The stress results, calculated for each individual loading at the 123 nodal points on the cask, are tabulated in Tables 2.10.10-6 through 2.10.10-15. Both the stress components and the principal stresses are included.

Note that the fabrication stresses are considered negligible as explained in Section 2.6.11. The puncture analysis is performed using classical hand calculations, as shown in Section 2.7.2.

2.7.1.1 End Drop

2.7.1.1.1 Discussion

The NAC-LWT cask is evaluated for the hypothetical accident end drop conditions to demonstrate its structural adequacy in accordance with the requirements of 10 CFR 71.73. The event scenario is that the NAC-LWT cask, equipped with impact limiters, falls through a distance of 30 feet onto a flat, unyielding, horizontal surface. The cask strikes the surface in a vertical position and, consequently, an end impact on the bottom or the top of the cask occurs. The types of loading involved in an end drop accident include (1) closure lid bolt preload, (2) internal pressure, (3) thermal, (4) inertial body load, and (5) impact load due to the end drop. There are six credible end impact conditions to be considered, according to Regulatory Guide 7.8:

1. Bottom end drop with 130°F ambient temperature and maximum decay heat load
2. Bottom end drop with -40°F ambient temperature and maximum decay heat load
3. Bottom end drop with -40°F ambient temperature and no decay heat load
4. Top end drop with 130°F ambient temperature and maximum decay heat load
5. Top end drop with -40°F ambient temperature and maximum decay heat load
6. Top end drop with -40°F ambient temperature and no decay heat load

The finite element analysis method is utilized to perform the end drop stress evaluation for the NAC-LWT cask.

2.7.1.1.2 Analysis Description

The detailed geometry and finite element model of the NAC-LWT cask are thoroughly described in Section 2.10.2. The cask is modeled as an axisymmetric structure assembly of ANSYS STIF42 isoparametric elements.

The dynamic wave propagation produced by the impact is assumed to spread throughout the cask body simultaneously. In addition, the equivalent static method is adopted to do the impact evaluations. The analyses assume linearly elastic behavior of the cask and that the fabrication stresses are negligible.

Based on the previous assumptions and discussions, the applied loads on the finite element model are as follows:

1. Closure lid bolt preload

   The required total preload of 250,000 lbs, as calculated in Section 2.6.7.6, is converted to an initial strain of 0.0021361 inch/inch/radians and is applied to the bolt, which is modeled as a vertical beam element.

2. Internal pressure

   The cask internal pressure is temperature dependent and is evaluated in Section 3.4.4. Pressures of 50 psig and 12 psig are applied on the interior surfaces of the cask cavity for the hot ambient and cold ambient cases, respectively.

3. Thermal

   There are three thermal conditions.

   A. The heat transfer analysis performed in Section 3.4.2 determined the cask temperatures for the hot environment (130°F temperature) with maximum insolation and maximum decay heat load. See Section 2.10.3.1 for the resulting isothermal temperature plot.

B. Similarly, the heat transfer analysis performed in Section 3.4.3 calculated the cask temperatures for the cold environment (-40°F ambient) with maximum decay heat load and no insolation. See Section 2.10.3.2 for the resulting isothermal temperature plot.

C. The third thermal condition evaluates the cask subjected to an ambient temperature of -40°F with no decay heat load and no insolation.

4. Inertial body load

   Applying D'Alembert's principle, the inertial effects created by an impact can be represented by equivalent static forces. In the analyses, a 76.8 g inertial load is vertically applied on the mass of the cask modeled. The 76.8 g value is derived from the multiplication of 60 g (shown in Table 2.6.7-34) and the factor of $\frac{48{,}000}{37{,}519}$, where 48,000 lbs is the cask body design weight and 37,519 lbs is the finite element model weight (The 60-g value is conservatively based on a 3,850-psi maximum crush strength of aluminum honeycomb, although the design maximum crush strength is only 3,675 psi).

   The inertial load resulting from the 4,000-pound contents weight is simulated as an equivalent static pressure load (1,708 psi) uniformly applied on the interior surface of the cask impact end.

5. Impact load

   The impact load is assumed to be uniformly applied over the impact surface of the cask. A uniform pressure of 4,852 psi is applied on the model. This pressure is obtained by dividing the total impact load ($60 \times 52{,}000$ lb $= 3.12 \times 10^6$ lb) by the impact area, 643 in^2 which is the bottom (or top end) surface area of the cask (Refer to note in 4).

Boundary conditions that are imposed on the model of the cask to restrain rigid body motion include: (1) the nodes located on the vertical centerline are restrained from moving radially, and (2) vertical restraints are imposed on the edge nodes located on the free surface; that is, the nonimpact end.

2.7.1.1.3 Results and Conclusions

The stresses throughout the finite element model are calculated for the combined load conditions. Based on the design criteria presented in Section 2.1.2 and Regulatory Guide 7.6, the calculated stresses are categorized into P_m , $P_m + P_b$, and total stress categories. The secondary stresses (thermal) are conservatively included in the primary stress categories and the margin of safety calculations.

As demonstrated in Section 2.10.3.3, procedures have been implemented to determine the critical Pm, Pm + Pb, and total stresses for each cask component. The calculated stresses are conservatively based on an outer shell thickness of 1.12 inches, although the design outer shell thickness is 1.20 inches. The most critical sections for each component during a particular loading condition are shown in Figure 2.7.1-1 through Figure 2.7.1-5. The critical Pm, Pm + Pb, and total stresses for each component are documented in Table 2.7.1-1 through Table 2.7.1-15. Additionally, the stresses at representative sections throughout the cask are presented in the tables in Section 2.10.7. These tables document the maximum stress locations tabulated for each component. Appendix 2.10.10 presents tabulated detailed stresses for the individual load conditions for the stress points at each section selected for analysis. Tabulations are also presented for the various combinations of the individual load cases.

The allowable stresses for the cask components are determined based on 300°F. Note that the maximum cask temperature is below 300°F for all of the conditions considered and the allowable stresses are, therefore, conservative.

Comparing the analyses results from loading condition 2, as documented in Table 2.7.1-4 through Table 2.7.1-6 and in Table 2.7.1-10 through Table 2.7.1-12, it is evident that the most critical Pm, Pm + Pb, and total stresses are comparable for the bottom and the top end drops. Furthermore, the margins of safety are very large. It is, therefore, expected that the top end drop under loading condition 3 will produce results similar to those for the bottom end drop under loading condition 3. Thus, analyzing the top end drop under loading condition 3 is considered to be unnecessary and is not performed.

The analyses demonstrate that all margins of safety are positive for all of the end drop accident conditions.

The documentation of the NAC-LWT cask adequacy in satisfying the buckling criteria for the stresses of the end drop conditions is presented in Section 2.10.6. The NAC-LWT cask maintains its containment capability and satisfies the 10 CFR 71 requirements for the end drop accident condition.

2.7.1.2 Side Drop

2.7.1.2.1 Discussion

This section presents the evaluation of the structural adequacy of the NAC-LWT cask for the hypothetical accident, 30-foot drop, side impact condition. The event scenario is that the NAC-LWT cask, with an impact limiter attached over each end, experiences a free drop through a distance of 30 feet onto a flat, unyielding surface and strikes the surface in the horizontal position. The types of loading involved in a side drop accident are similar to those discussed in

Section 2.7.1.1 for the end drop accident condition. However, for the side drop accident condition, both the inertial load and the side impact load are nonaxisymmetric and require special consideration for them to be applied on an axisymmetric model using the ANSYS harmonic elements.

There are three credible side impact conditions to be evaluated and discussed: (1) side drop with 100°F ambient temperature and maximum decay heat load, (2) side drop with -40°F ambient temperature and maximum decay heat load, and (3) side drop with -40°F ambient temperature and no decay heat load. Finite element analyses were performed for these side impact evaluations.

2.7.1.2.2 Analysis Description

The NAC-LWT cask is modeled as an axisymmetric structure utilizing the ANSYS STIF25 elements. The finite element mesh is illustrated in Section 2.10.2.

The analyses utilize linearly elastic structural behavior of the cask and the fabrication stresses are negligible.

There are five loads applied on the finite element model - closure lid bolt preload, internal pressure, thermal, inertial body load and impact load. The first three loads are the same as those described in Section 2.7.1.1. The inertial body load and the side impact load are nonaxisymmetric and require further discussion.

The 63.56-g inertial load is transversely applied on the mass of the cask model. The 63.56 g is determined from the side impact acceleration 49.7 g (determined in Section 2.6.7.4) multiplied by the weight factor of 48,000 / 37,519, where 48,000 lbs is the cask body design weight and 37,519 lbs is the cask finite element model weight.

The inertial load produced by the contents is applied as an equivalent static pressure (177.1 psi) on the interior surface of the cask; to be specific, the pressure is uniformly distributed along the cavity length with a circumferential variation. The method used to calculate the pressure of the contents is identical to that for the determination of the impact load pressure.

The impact load applied on the finite element model is nonaxisymmetric and localized. Consequently, it requires special consideration. The cask body (excluding the neutron shield shell) is conservatively assumed to resist the entire impact load due to the side drop accident. This impact load is calculated as $49.7 \times 52{,}000 = 2.58 \times 10^6$ pounds, where the factor 49.7 g was previously explained. The impact load is applied to the finite element model as a distributed pressure over the impact surface of the cask. The distribution of impact pressure is assumed to be uniform, in the longitudinal direction, but sinusoidally varied in the circumferential direction. A cosine-shaped pressure distribution is selected, which is peaked at the center and spread over a

90-degree arc in the circumferential direction as shown in Figure 2.7.1-6. The region of the applied pressure (a 90° arc) is defined based on the "crush" geometry of an impact limiter designed to limit the impact force for a 30-foot drop. The assumption of a "peaked" pressure distribution is a conservative, classical, stress analysis procedure. Variations in the shape and/or magnitude of the applied pressure distribution are expected to produce a localized stress variation in the pressure-applied region. Since the cask body is massive in this region, the variation in stress level is negligible.

Based on the previous discussion, a cosine-shaped pressure distribution, p(θ), in the circumferential direction (Figure 2.7.1-6) is selected as:

$$p(\theta) = \begin{cases} \bar{p} \cos 2\theta, & \text{for } -45° \le \theta \le 45° \\ 0 \quad , & \text{for } 315° > \theta > 45° \end{cases} \tag{1}$$

where $\bar{p}$ represents the peaked value at the 0-degree orientation and is determined from the following equation,

$$P = \left[\int_0^{2\pi} p(\theta) \cos\theta \; r \, d\theta\right] \ell$$

$$= 0.5 \; (2.58 \times 10^6) = 1.29 \times 10^6 \text{ lb} \tag{2}$$

where:

r = outside radius of outer shell = 14.3075 in

ℓ = interface lengths between the cask and the impact limiters, 11.88 inches are actually engaged with both the bottom and the top impact limiters. In the calculation, 11.25 inches is conservatively used for the bottom engagement and 11.00 inches is conservatively used for the top.

P = side drop impact force at each end of the cask

Thus, the impact pressures, $\bar{p}$, applied on the finite element model are 8,498 psi near the bottom end and 8,691 psi near the top end. These pressures are uniformly distributed element pressures along the longitudinal direction.

In order to use an axisymmetric finite element model to analyze a nonaxisymmetric loading, it is necessary to use the ANSYS harmonic element and harmonic function capability. This is

achieved by defining the pressure distribution, as shown in equation (1), in terms of a Fourier series of harmonic functions, as:

$$p(\theta) = A_o + A_1\cos\theta + A_2\cos 2\theta + A_3\cos 3\theta + A_4\cos 4\theta + A_5\cos 5\theta \qquad (3)$$

Note that, since the impact load is centered at the 0-degree orientation, all loading terms are of the form cos iθ. Each term of the series represents an individual axisymmetric load mode and is defined by the load coefficient (A_i), the number of harmonic waves in the mode shape, and the symmetry condition (cos iθ). The analytical results for the defined nonaxisymmetric loading are the summation of the results of each of the individual axisymmetric load term analyses. The load coefficients, A_i, are determined by the ANSYS PREP6 routine, and equation (3) becomes

$$p(\theta) = \bar{p}\,[0.1590 + 0.2999\cos\theta + 0.2498\cos 2\theta + 0.1799\cos 3\theta + 0.1059\cos 4\theta + 0.0427\cos 5\theta] \qquad (4)$$

Equations (1) and (4) are illustrated in Figure 2.7.1-7. The figures indicate that the Fourier series function contains six terms. The combination of these six terms adequately represents the desired impact pressure distribution. Consequently, six loading mode analyses are required to evaluate the effect on the cask body resulting solely from the impact load during the side impact event.

In summary, the finite element analysis of the side drop condition considers the combined loads resulting from internal pressure, bolt preload, thermal, inertia and impact. Nine loading mode analyses are developed such that their combination evaluates the effects previously mentioned. Table 2.7.1-16 summarizes the load analyses and their descriptions.

To combine the stress results produced by the nine loading mode analyses; the following steps are performed:

1. Utilize the Fourier series coefficients, as reported in equation (4), to multiply the results obtained from load mode analyses 4 through 9. This provides the stresses that result from the impact load.
2. Combine the results obtained from Step 1 and load mode analyses 1 and 3. This provides the stresses caused by the combined effects of internal pressure, bolt preload, inertial, and impact. The resulting stresses are used to calculate the P_m stress intensities and the $P_m + P_b$ stress intensities.
3. Combine the results from Step 1 and load mode analyses 2 and 3. This provides the results to be used to calculate the total stress intensities.

The boundary conditions imposed upon the model of the cask to restrain rigid body motions are defined as follows:

1. The top node located on the vertical centerline is restrained from moving radially.
2. The bottom node located on the vertical centerline is fixed completely.
3. A displacement constrained condition is imposed on the interface surface at the bolt location between the lid and the upper ring. This constrained condition is only imposed for the analysis of the impact load case and the inertial body load case.

2.7.1.2.3 Results and Conclusions

To balance the demands of analytical accuracy and computational efficiency, it is conservatively assumed that the sliding coefficient is zero between the lead/steel interface in the finite element analysis. This significantly minimizes the total number of iterations required for the analysis to converge; yet, it provides conservative analysis results because the horizontal shear resistance at the lead/steel interface is ignored, making the cask structure more flexible under bending. The stresses calculated by the finite element analysis are compared with the hand-calculated stress results. The finite element method indicates that the maximum bending stress, 1,373 psi, occurs at the midpoint of the cask outer shell due to a 1 g inertial load. The hand calculation considers the cask structure as a hollow, circular cross section beam, simply supported at each end, which gives 1,353 psi at the midpoint of the cask outer shell for a 1 g inertial load. The finite element and hand-calculated results agree extremely well. The hand-calculated results are presented in Table 2.10.11-2.

Since the material properties of the cask structure are temperature-dependent, varying environmental temperatures will produce changes in the calculated stresses in the cask for the thermal load cases; but they will not change the calculated stresses in the cask produced by the other types of loads. This is verified by comparing the finite element results for the NAC-LWT cask subjected to a gravity load for different temperature conditions. Also, the stress levels produced by the following different thermal conditions were evaluated: (1) 100°F ambient temperature with maximum decay heat load, (2) -40°F ambient temperature with maximum decay heat load, and (3) -40°F ambient temperature with no decay heat load. The combination effect of the thermal loads with other load types (e.g., inertial body load) has also been studied. It is determined that the side drop event with 100°F ambient temperature represents the worst case for the 30-foot side drop accident condition. Therefore, only the stress results produced by a 30-foot side drop with 100°F ambient temperature are reported.

Stress components and stress intensities are calculated throughout the finite element model for the combined loads due to internal pressure, bolt preload, thermal, inertial, and impact.

The critical sections for each cask component are shown in Figure 2.7.1-8. Table 2.7.1-17 through Table 2.7.1-19 report the P_m stress intensities, the $P_m + P_b$ stress intensities, and the total stress intensities for each cask component, which are obtained from the finite element side drop

analysis. The total P_m and $P_m + P_b$ stresses at representative sections throughout the cask are presented in the tables in Appendix 2.10.7. These tables document the maximum stress locations tabulated for each component. Appendix 2.10.10 presents tabulated detailed stresses for the individual load conditions for the stress points at each section selected for analysis. Tabulations are also presented for the various combinations of the individual load cases.

As mentioned previously, the finite element cask model conservatively ignores the effect of the neutron shield shell on the overall bending of the cask structure.

The margins of safety in Table 2.7.1-17 and Table 2.7.1-18 are positive for all cask components.

The documentation of the NAC-LWT cask adequacy in meeting the buckling criteria for the stresses of the side drop is presented in Section 2.10.6.

It has been demonstrated that all margins of safety are positive for the 30-foot side drop conditions. The NAC-LWT cask maintains its containment capability and satisfies the 10 CFR 71 requirements for the 30-foot side drop accident condition.

2.7.1.3 Oblique Drops

2.7.1.3.1 Discussion

This section presents the structural evaluation of the NAC-LWT cask for the hypothetical accident 30-foot oblique drops. In this event, the NAC-LWT cask, equipped with an impact limiter over each end, falls through a distance of 30 feet onto a flat, unyielding surface. According to NRC Regulatory Guide 7.8, "The center of gravity is usually considered to be directly above the impact area; however, evaluations of other oblique drop orientations are requested 'when appropriate'." An impact at an orientation angle of 15.74 degrees is defined as a corner impact, i.e., the center of gravity of the cask is vertically above the impacting edge of the cask. The NAC-LWT cask is evaluated for four oblique drop orientations (15.74, 30, 45, and 60 degrees) under varying ambient conditions. The types of loading involved in an oblique drop accident are similar to those described in Sections 2.7.1.1 and 2.7.1.2; the inertial loading and the impact loading are nonaxisymmetric and must be applied to the axisymmetric finite element model using the ANSYS harmonic elements. This method is similar to that used for the side drop analyses.

Four credible oblique impact orientations (15.74, 30, 45, and 60 degrees) are considered. For each oblique impact orientation, four combinations of ambient temperature, decay heat load, and cask end loading are evaluated:

1. Top end oblique drop, 130°F ambient temperature, maximum decay heat load.
2. Top end oblique drop, -40°F ambient temperature, maximum decay heat load.

3. Top end oblique drop, -40°F ambient temperature, no decay heat load.
4. Bottom end oblique drop, 130°F ambient temperature, maximum decay heat load.

The finite element analysis method is used for the oblique impact evaluations.

The hypothetical accident oblique drop initial impacts are followed by a secondary impact or "slapdown" of the cask on the end opposite the initially impacted end. The secondary impact is addressed in Section 2.10.4; the energy dissipation requirements for slapdown are shown to be well within the energy absorption capabilities of the NAC-LWT cask impact limiters. Thus, slapdown is not a limiting case for the cask and is not considered any further.

2.7.1.3.2 Analysis Description

Similar to the side impact analysis, the ANSYS STIF25 element is utilized to model the NAC-LWT cask. The finite element model is illustrated in Section 2.10.2.

The oblique drop analyses assume that the cask exhibits linear elastic behavior and that the fabrication stresses are negligible. There are five loads applied on the finite element model – closure lid bolt preload, internal pressure, thermal, inertial body load and impact load. The first three loads are the same as those described in Section 2.7.1.1. The inertial body load and the oblique impact load are nonaxisymmetric and require further discussion.

The inertial body load is the same as that discussed in Section 2.7.1.2, with an additional consideration in the oblique impact analysis. Both lateral and longitudinal inertial loads are applied on the cask. Unique g loads are applied on the mass of the cask model. Table 2.7.1-20 summarizes the applied g loads and their components (lateral and axial) for the different drop orientations. Refer to Section 2.6.7.4 for the detailed calculations of the g loads for the different oblique drop orientations. The g loads are conservatively based on a 3,850-psi maximum crush strength of aluminum honeycomb, although the design maximum crush strength is only 3,675 psi.

The cavity contents force components are applied to the inside of the cask body finite element model. The lateral component of the inertial load produced by the contents is applied to the cask model similarly to the side impact analysis, i.e., uniformly along the cavity length with a cosine-shaped distribution over a 2θ arc (the same sector of the cask on which the lateral impact load is applied) in the circumferential direction. The axial component of the inertial load due to the contents is applied on the end of the cavity of the cask model with the same cosine-shaped distribution over a 2θ arc as that described previously, and with a uniform distribution in the radial direction from the inside diameter of the cask cavity to its axial centerline. Table 2.7.1-21 summarizes the applied contents pressures used in the analyses.

The impact load condition is applied to the cask model similarly to the inertial body load. The lateral component of the impact load is applied to the side of the cask model at the impacting end, uniformly over the 11.25-inch long impact limiter region with a cosine-shaped distribution in the circumferential direction along a 2θ arc. The axial component of the impact load is applied to the impacting end of the cask model with a cosine-shaped distribution in the circumferential direction along an arc of 2θ (the same sector of the cask on which the lateral impact load component is applied) and with a uniform distribution in the radial direction from the outside diameter of the end of the cask to its axial centerline. Table 2.7.1-21 summarizes the pressures produced by the impact loads, which are calculated using the same method as presented in Section 2.7.1.2.

These load distributions of the impact force components and the cavity contents force components on the cask model are selected as being realistic, yet conservative, representations of the actual loadings on the cask for an oblique impact. Variations from actual load distributions are expected to be negligible. In addition, at locations on the cask away from the loading region, the stress results are not affected by the shape of the load distributions.

As shown in the side drop analysis (Section 2.7.1.2), six loading mode analyses are adequate to evaluate the effect on the cask body of the impact load during the oblique impact event. The modal coefficients for the oblique impact are determined by the ANSYS PREP6 routine and reported in Table 2.7.1-22.

In summary, the finite element analyses of the oblique drop conditions consider the combined loads due to internal pressure, bolt preload, thermal, inertia, and impact. Sixteen loading analyses are developed such that the various combinations of the defined load conditions are all considered. The sixteen loading combinations are summarized in Table 2.7.1-23.

To combine the analysis results produced by the sixteen loading mode analyses, the following steps are performed:

1. Utilize the Fourier series coefficients, as reported in Table 2.7.1-22, to multiply the results obtained from load analyses 5 through 16. This provides the stress results due to the oblique impact load.
2. Combine the results obtained from step 1 and load mode analyses 1, 3, and 4. This provides the stresses due to the effects of internal pressure, bolt preload, inertia, and impact. The resulting stresses are used to calculate the P_m stress intensities and the $P_m + P_b$ stress intensities.
3. Combine the results from step 1 and load mode analyses 2, 3, and 4. This gives the results which are used to calculate the total stress intensities.

The boundary conditions that are imposed upon the model of the cask to restrain rigid body motions are defined as follows:

1. On the vertical centerline of the cask, the node on the end opposite the impact is completely fixed.
2. On the vertical centerline of the cask, the node on the end near the impact is restrained from moving radially.
3. On the outside radius of the model, the node on the end opposite the impact is fixed in the radial direction to prevent rigid body rotation, but it is free to move axially.
4. A displacement constrained condition is imposed on the interface surface at the bolt location between the lid and the upper ring. This constrained condition is only imposed for the analyses of the impact load case and the inertial body load case.

2.7.1.3.3 Results and Conclusions

Similar to the discussion presented in Section 2.7.1.2.3, the friction coefficient at the interface between the lead and the stainless steel shells is conservatively assumed to be zero. The stress results produced by the following three oblique impact conditions are reported:

1. Top end oblique drop, 130°F ambient temperature, maximum decay heat load.
2. Top end oblique drop, -40°F ambient temperature, no decay heat load.
3. Bottom end oblique drop, 130°F ambient temperature, maximum decay heat load.

These three oblique drop conditions represent the bounding cases for all of the 30-foot oblique drop accident conditions. Four oblique orientations of the cask (15.74, 30, 45, and 60 degrees) are analyzed for each of the ambient temperature/heat load bounding conditions.

The stresses throughout the cask body are calculated for the combined load conditions. Based on the design criteria presented in Section 2.1.2 and Regulatory Guide 7.6, the calculated stresses are categorized into P_m, $P_m + P_b$, and total stress categories.

As demonstrated in Section 2.10.3.3, procedures have been implemented to determine the critical P_m, $P_m + P_b$, and total stresses for each cask component. The most critical sections for each component during a particular loading condition are shown in Figure 2.7.1-10 through Figure 2.7.1-21. The critical P_m, $P_m + P_b$, and total stresses for each component are documented in Table 2.7.1-24 through Table 2.7.1-59, with the following additional considerations: (1) the boundary effect on the finite element analysis results; and (2) the boundary effect on stress results. The calculated stresses are conservatively based on an outer shell thickness of 1.12 inches, although the design outer shell thickness is 1.20 inches. Additionally, the stresses at representative sections throughout the cask are presented in the tables in Section 2.10.7. These tables document the maximum stress locations tabulated for each component. Appendix 2.10.10 presents tabulated detailed stresses for the individual load conditions for the stress points at each section selected for analysis. Tabulations are also presented for the various combinations of the individual load cases.

Boundary Effect on Finite Element Analyses Results

As discussed previously, the oblique drop condition induces an eccentric (angular) momentum, which causes a rigid body rotation of the cask and a slapdown onto the unyielding surface. To eliminate this rigid body rotation in the oblique drop evaluation, certain displacement restraints are imposed on the finite element model. These restraints cause localized peak stresses in the immediate vicinity of boundary conditions. This boundary effect attenuates very rapidly at locations slightly away from the boundary region. Component 7 (bottom closure plate) exhibits this boundary effect; refer to P_m and $P_m + P_b$ stress intensities reported in Table 2.7.1-51, Table 2.7.1-52, Table 2.7.1-54, Table 2.7.1-55, Table 2.7.1-57 and Table 2.7.1-58. The case reported in Table 2.7.1-58 is selected to illustrate the attenuation of the boundary effect, because the stresses produced by the 60 degree oblique drop condition are most critical. Figure 2.7.1-22 shows the plot of the sectional stresses versus radial location with respect to the axial centerline of the cask. It is obvious that the structural behavior of the bottom cover plate is disturbed in the region from node 1 to node 3, because the calculated $P_m + P_b$ stress intensity is less than the P_m stress intensity. Consequently, these stresses are considered to be unrealistic and are disregarded.

This decision is justified by observing the stress plots shown in Figure 2.7.1-23 and Figure 2.7.1-24. In Figure 2.7.1-23, three curves are shown for the cask bottom (refer to Figure 2.7.1-25 for the location) for the 30-foot bottom oblique drop condition:

1. Curve 1 represents the P_m stress intensities versus the radial location, which are produced by the total loading, i.e., the combined result from load analyses 1 and 3 through 16. (See Table 2.7.1-23 for load analyses identification.)
2. Curve 2 is similar to curve 1, but is produced by a partial loading, i.e., the combined result from load analyses 3, 4, 5, 6, 11, and 12 only.
3. Curve 3 is identical to curve 2, except that the boundary restraint is moved to node 3; it was at node 1 for curves 1 and 2.

The close agreement between curves 1 and 2 indicates that the partial loading case is adequate to simulate the structural behavior of the cask produced by the total loading case. Comparing the stress values represented by curves 2 and 3, the curves clearly indicate that the stresses are greatly reduced in the vicinity of the boundary by changing the location of the displacement restraint from node 1 to node 3. This documents the statement that the stresses in the vicinity of the boundary restraint are unrealistic and are disregarded. Similarly, the plot of $P_m + P_b$ stress intensity (Figure 2.7.1-24) indicates the stress reduction, which results from shifting the location of the boundary restraint. Consequently, the stress results (excluding the boundary effect region; i.e., from section cut d through the rest of component 7; Figure 2.7.1-25) obtained from the finite element analyses are evaluated and reported. This criterion is applicable to all of the other drop orientation cases.

Figure 2.7.1-26 and Figure 2.7.1-27 show the same boundary effect on the stress results for the 30-degree and 45-degree impact orientations (in the vicinity of the boundary in the bottom closure plate of the cask) as is indicated in Figure 2.7.1-25. Thus, the criterion developed for the 60 degree orientation is applicable.

The following tables report the stress results excluding the boundary effect: Table 2.7.1-51, Table 2.7.1-52, Table 2.7.1-54, Table 2.7.1-55, Table 2.7.1-57 and Table 2.7.1-58.

Boundary Effect on Stress Results

The stresses reported in Table 2.7.1-49 indicate that the maximum $P_m + P_b$ stress intensity of component 1 is 69.74 ksi. Again, this is as a result of the boundary effect at this section cut (node 2561). This value of 69.74 ksi is unrealistically high. The next highest $P_m + P_b$ stress intensity for component 1 is 6.79 ksi, located at the section next to the section containing the boundary restraint. (Note that the stress value is one order of magnitude lower).

The method described in Section 2.7.1.3.2 to determine the stresses in the vicinity of the free end of the NAC-LWT cask for the oblique drops is conservative. Inertia loads on the cask, which are responsible for dynamic equilibrium during an oblique drop impact, consist of translational deceleration, the angular deceleration and the centrifugal deceleration. The crushing force generated by the limiter and the translational decelerations are determined from RBCUBED (Section 2.10.1.2) for the particular drop of interest. Results from RBCUBED are used to determine the input into ANSYS for the deceleration of the cask body and the pressure load for the contents. The remaining inertia forces representing the angular deceleration and the centrifugal deceleration are established by the imposed displacement boundary conditions at node 1 (at the center line of the model at the bottom end) and node 2561 (at the center line at the top end). While the actual physical loading is distributed over the body, the analysis procedures cause the boundary restraint to behave as a point load. This produces a concentration of the load in the free end of the cask and results in unrealistically large stresses in this region.

The stresses in the end region can also be determined by using the analysis results from the end drop and the side drop. In each case the effect of the geometrical discontinuities are present since the physical boundaries coincide. The manner in which the forces are developed in an oblique drop can be expressed as a combination of the end drop and side drop. The end drop represents the loads generated by the axial translational deceleration. The load path of the axial load in the end drop is the same as for the oblique drop. In the side drop, the loads generated by the cask body and contents must be reacted by the impact limiter crush forces. In the oblique drop, however, the lateral angular deceleration balances the translational deceleration. This represents some conservatism since the limiter load is concentrated in the end region (for the side drop), while the angular deceleration is not (for the oblique drop).

The actual superposition of the side drop results and end drop results is accomplished by applying a separate factor to the component stresses for each load case prior to the algebraic combination.

The factor for the end drop results is the ratio of the axial translational decelerations which is the only nonhomogeneous boundary condition applied to the model. This factor is expressed as:

$$K1 = \frac{Aao}{Aae} \qquad (1)$$

where:

Aao = axial deceleration component for the oblique drop

Aae = axial deceleration for the end drop

The factor for the side drop results is the ratio of the lateral translational decelerations, which again is the only nonhomogeneous boundary condition applied to the model. This factor is:

$$K2 = \frac{Alo}{Als} \qquad (2)$$

where:

Alo = lateral deceleration component for the oblique drop

Als = lateral deceleration for the side drop

Since superposition requires the stress components to be added, the stress intensity (maximum principal stress difference) must be recomputed once the component stresses have been determined for the combined case. Thus for each "superimposed" stress component,

$$Sij = K1(S'ij) + K2(S''ij) \qquad (3)$$

where:

S'ij the stress component for the end drop (i = x, y, z, xy)

S"ij the stress component for the side drop (i = x, y, z, xy)

The stresses are to be evaluated for the end region and for portions of the cask shell itself. The factors for the different angles are specified below.

Angle of Drop(degrees)	K1	K2
15.74 (corner)	0.970	0.330
30	0.785	0.547
45	0.517	0.624
60	0.370	0.775

These factors are applied to the $P_m + P_b$ stresses, the S_n stresses, and stress ranges on a stress component level. This implies that the factors are applied to thermal stresses in the stress summaries. Since Kl + K2 is greater than unity for any angle, this method will provide some conservatism. All principal stresses and stress intensities are based on the revised stress components. For the critical stress summaries, the maximum stress components listed for the side drop (for the affected cask components only) are combined with the maximum stress components listed for the end drop. This ensures that the maximum stress for the oblique drops is truly the maximum for the component listed in the critical stress summary.

A measure of how far the combined stress methodology should extend axially along the cask shell is given by a fraction of the shell wave length. The formula used is:

$$L' = 2.4\,(rt)^{0.5} \qquad (4)$$

where:

r = mean radius

t = thickness

The value of r for the NAC-LWT cask is taken to be 14.5 inches. The outer shell comprises approximately 80 percent of the effective cross-sectional bending rigidity (See Section 2.10.11 for this computation). For computational purposes the thickness for the outer shell, which is 1.2 inches, is used. The estimated distance along the shell is determined to be 10 inches. This corresponds to a position between section cut "J" and section cut "L" of the cask shell in Figure 2.10.7-1 for the top end drop. For the bottom drop, this places the boundary of the re-evaluated stresses near section cut "T" for the top. It should be noted that the section cuts identifiers start with A at the center line of the bottom end and progresses to Z at the center line at the top end. The node numbers begin with "1" at the center line of the cask at the bottom and monotonically increase to 2561 at the center line at the top center line. This nodal numbering pattern allows the region of affected stresses to be identified by a node number. The location of the stresses to be revised by the superposition method for the top end drops and the bottom end drops are identified on the following page.

Impact End	Section Cuts[1]	Node Numbers[2]
Top	A through J	1 through 698
Bottom	S through Z	1481 through 2561

[1] The section cuts are identified in Figure 2.10.7-1 and their coordinates are listed in Table 2.10.7-1.

[2] The node numbers versus nodal coordinates are specified in Table 2.10.2-1.

Conclusion

The documentation of the NAC-LWT cask adequacy in meeting the buckling criteria for the stresses of the oblique drop is presented in Section 2.10.6.

It has been demonstrated that all margins of safety are positive for the 30-foot oblique drop conditions. The NAC-LWT cask maintains its containment capability and satisfies 10 CFR 71 requirements for the 30-foot oblique drop accident condition.

2.7.1.4 Shielding for Lead Slump Accident

Following the 30-foot free drop, the lead region may experience slumping resulting in a reduction in the shielding capabilities of the cask. The shielding evaluation of the lead slump accident was performed in a series of steps. Initially, QAD-CG was used to model the cask without any lead to see if this simple model would give a reasonable dose rate. It was determined that a more detailed analysis was required. This included calculating the lead gap that was formed because of contraction following the lead pour. The HEATING5 computer program (Turner) is used to calculate the temperatures throughout the cask assuming no gap. The resulting maximum temperature of the lead was 245°F. The gap was calculated based on this temperature. This gap value is then used to find the amount that the lead slumps at either the top or the bottom, depending on the cask drop orientation. The calculation is performed as follows:

$$V_1 = \pi[(r_o - s)^2 - r_i^2]h_1$$

$$V_2 = \pi[r_o^2 - r_i^2]h_2$$

Setting $V_1 = V_2$ and solving for h_2:

$$h_2 = \frac{[(r_o - s)^2 - r_i^2]h_1}{r_o^2 - r_i^2}$$

$$= \frac{[(13.19 - .0417)^2 - (7.45)^2](175.0)}{(13.19)^2 - (7.45)^2}$$

$$= 173.37 \text{ in}$$

therefore:

$$\Delta h = h_1 - h_2 = 175.0 - 173.37 = 1.63 \text{ inches}$$

where:

V_1 = volume of the lead after contraction (in^3)

V_2 = volume of the lead following the pour (in^3)

r_o = outside radius of lead region (in)

r_i = inside radius of lead region (in)

h = height of lead region (in)

s = gap (in) (Section 3.2)

The lead slump calculated using this method (1.63 inches) is much larger than the lead slump determined in the finite element analysis (Section 2.10.5), which makes the resulting dose rates conservative. At this point, another model is created using QAD-CC to determine the final dose rates 1 meter from the surface of the cask through this "window" in the lead shielding (Details of the models are found in Figures 5.3.3-3 through 5.3.3-5). This process is followed for both the top and bottom end-fittings of a PWR assembly and the bottom end-fitting of a BWR assembly. The BWR bottom end-fitting is analyzed since it is larger and has a higher Co 60 source than the PWR bottom end-fitting. The analysis is not performed for the BWR top end-fitting because it is smaller and, therefore, has a lower source strength than the PWR top end-fitting.

The resulting dose rates are less than the 49 CFR 73 limits, and can be found in Table 5.1.1-6. The analysis shows that the loss of lead shielding resulting from a lead slump accident will not result in a substantial loss in shielding effectiveness and that the dose rates from this accident are small when compared to the loss of neutron shield accident evaluated in Section 2.7.2.5.

2.7.1.5 Bolts – Closure Lid (Hypothetical Accident – Free Drop)

Section 2.6.7.6 provides a general description of the analysis approaches employed to demonstrate structural integrity of the NAC-LWT cask closure system for both normal conditions of transport and hypothetical accident conditions.

A complete range of impact orientations is evaluated, from an end impact at 0 degrees to a flat side impact at 90 degrees, and at 5-degree increments in between. Loads are derived from the hypothetical accident impact accelerations summarized within Table 2.6.7-34 and Table 2.7.1-20. Where necessary, impact accelerations have been interpolated at 5-degree increments from those values given in Table 2.6.7-34.

The details of this analytic evaluation are described and performed within Section 2.10.9 for both normal conditions of transport and hypothetical accident conditions. Hypothetical accident condition results are summarized in Table 2.7.1-60 and Table 2.7.1-61, corresponding to a "hot"

initial condition and a "cold" initial condition, respectively. The hot initial condition bolt temperature is taken at 227°F, as summarized in Table 3.4-2. The cold initial condition bolt temperature is assumed to be -20°F, per regulatory requirements. Physical properties for the SA-453, Grade 660 bolts are conservatively taken at 300°F and room temperature (70°F) for hot and cold conditions, respectively. As defined within Table 2.1.2-1, allowable bolt stress is taken as S_y, leading to an allowable direct tension stress of 81.9 ksi and 85.0 ksi, at 300°F and 70°F respectively. Based on this thorough evaluation, the closure bolts incur a maximum stress intensity of 64,511 psi, which result in a minimum margin of safety of 27 percent. See Table 2.7.1-60 (at 5°):

$$MS = 81.9/64.511 - 1$$
$$= +\underline{0.27}$$

Bolt engagement may be evaluated by computing shear stresses within the SA-336, Type 304, and forging material. At 300°F, the allowable shear stress is 0.5 S_U, or 33 ksi, according to Tables 2.1.2-1 and 2.3.1-1. The maximum tensile load is found as the product of the maximum bolt stress intensity, noted above, and the bolt stress area, or (64,511 psi) (0.6051) = 39,036 lbs. The shear area per inch of engagement for a 1 - 8 UNC internal thread is 2.325 in^2/in ("Table Speeds Calculation of Strength of Threads"). The resultant shear stress and margin of safety within the top body forging is:

$$\tau = P/A = (39{,}036) / [(2.325)(1.875)]$$
$$= 8{,}954 \text{ psi}$$
$$MS = 33.0/8.954 - 1$$
$$= +\underline{2.69}$$

Using consistently conservative assumptions, the NAC-LWT cask lid bolted closure is shown to satisfy the performance and structural integrity requirements of 10 CFR 71.73(c)(1) for hypothetical accident conditions.

2.7.1.6 Crush

The dynamic crush test required by 10 CFR 71.73 (c) (2) does not apply to the NAC-LWT cask. The mass of the NAC-LWT exceeds 500 kg and the overall package density is greater than 1,000 kg/m^3.

2.7.1.7 Rod Shipment Can Assembly Analysis

2.7.1.7.1 Discussion

The NAC-LWT rod shipment can assembly is analyzed for structural adequacy in accordance with the requirements of 10 CFR 73 for a 30-foot drop (hypothetical accident condition). The structural evaluation is performed by classical elastic analysis methods. The components evaluated include the can weldment, internal spacer, 4×4 and 5×5 inserts, and the PWR insert. The analysis follows the same methodology as that used for the normal conditions analysis contained in Section 2.6.7.10.

2.7.1.7.2 Analysis Description

Geometry

The geometry of the can assembly is shown in Drawing 315-40-098. Note that the tube component of the can assembly is fabricated from a 6-in. × 6-in. × 0.5-in.-thick tube that is machined to the final dimensions of 5.5-in. × 5.5-in. × 0.25-in.-thick. The can assembly is positioned within the basket during transport of the cask. If the cask is equipped with a PWR basket, the PWR insert is required to provide correct positioning within the basket. The can assembly is constructed of Type 304 stainless steel with the exception of the PWR insert, which is constructed of 6061 Aluminum.

Loadings

The magnitude of the impact force varies according to the drop height and drop orientation. As calculated in Section 2.6.7.4, the g-loads for the 30-foot end and side drops are 60 and 49.7 g, respectively.

Detailed Analysis

Can Weldment

The can body is contained within the basket assembly and is not subjected to bending stresses in the side-drop case.

For the end drop, the can weldment is loaded by its own weight. The can contents bear against the bottom or top of the can assembly, depending on drop orientation.

LWT Can Weldment Compressive Stress

Under hypothetical accident conditions, the tube is evaluated for a 60 g acceleration for the end drop. The compressive load (P) on the tube is the combined weight of the lid and tube body times the 60 g factor.

The compressive load (P) is:

$$P = 310 \times 60 = 18{,}600 \text{ lbs}$$

The compressive stress (S_c) in the tube body is:

$$S_c = \frac{P}{A} = \frac{18{,}600}{4.98} \cong 3{,}735 \text{ psi}$$

The margin of safety (MS) is then:

$$MS = \frac{0.7S_u}{S_c} - 1 = \frac{0.7(63{,}100)}{3{,}735} - 1 = +10.8$$

LWT Can Weldment Bolt Stresses

During the top end drop, the can assembly impacts on the lid handle. The insert and fuel rods strike the lid and the internal spacer strikes the flange. The resulting lid and flange deformations could result in prying forces on the lid bolts. To compute the force in the lid bolts due to a 30-foot top end drop, a 3-D finite element model of the lid, lid handle, flange, and can tube is constructed. The lid, lid handle, flange, and can tube are modeled using solid elements (SOLID45). The bolts are included in the model using beam elements (BEAM4) originating at the top of the lid and terminating at the top of the flange. The interface between the lid and flange uses contact element (COMBIN40) to model the interaction at this joint. The model represents 1/4 of the can assembly cross section. A uniform pressure load is applied to the inner lid surface to represent the weight of the fuel rods (350 lbs) and insert (75 lbs) multiplied by the 60g-accident acceleration loading. Nodal forces applied to the edge of the flange represent the weight of the internal spacer (240 lbs) multiplied by the 60g-accident acceleration. A plot of the model along with the applied loads follows.

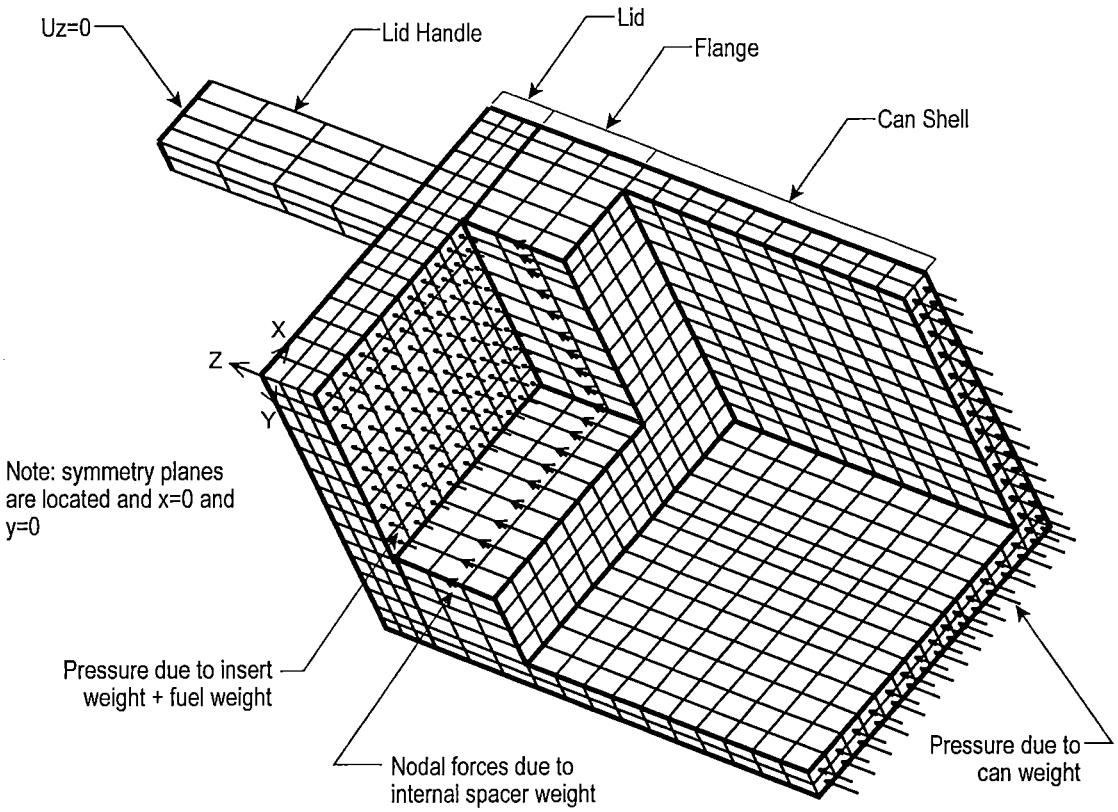

Since the entire can is not modeled, the weight of the can (310 lbs) multiplied by the 60g-accident acceleration is applied using a uniform pressure applied to the "cut surface" on the can shell. Because internal pressure opposes the impact force, thus reducing the bolt tensile load, its effect is not included in the analysis. Symmetry boundary conditions are applied at x = 0 and y = 0 positions on the model. The axial load is reacted at the top of the handle by restraining the Uz degree of freedom at this surface.

An initial strain is applied to the bolt beam elements to simulate the bolt preload. The bolt tension due to the bolt preload is calculated from the following relation. Each lid bolt is initially installed with a torque of 35 ± 5 in.-lb. The tensile force (P_B) in the bolt due to the maximum installation torque (T = 40 in.-lbs) is:

$$P_B = \frac{T}{\left(\frac{l}{2\pi} + \frac{d_2\mu_1}{2\cos\alpha} + \frac{(d + b\mu_2)}{4}\right)} = 635 \text{ lbs} \quad \text{(Machinery's Handbook, equation 22)}$$

where:

l = 0.0556 in, thread lead = 1/n

d_2 = 0.2732 in, pitch diameter

d = 0.3125 in, nominal bolt diameter

b = 0.5 in, nominal diameter of bolt head contact surface

α = 30°, 1/2 thread angle

$\mu_1 = \mu_2 = 0.15$, friction coefficient

From the finite element analysis, the maximum bolt tensile load (F), including preload and impact load, is 904 lbs. The maximum bolt stress is:

$$S = F / A = 904/((\pi/4)\ (0.25)^2) = 18.42 \text{ ksi}$$

Where F is the resulting bolt tensile force and A is the bolt cross-sectional area. The allowable bolt stress for pressure containing structures is S_y.

At 575°F, the yield stress for 316 stainless steel SA-479 is 19.1 ksi and the ultimate stress is 71.8 ksi. Therefore, the allowable stress is19.1 ksi. The resulting margin of safety is:

$$MS = \frac{S_y}{S} - 1 = \frac{19.1}{18.42} - 1 = +0.03$$

Therefore, the lid bolts maintain structural integrity during the end drop.

During the end impact, puncture of the can ends is possible by the fuel rods, an insert tube, or the lid handle. Since the lid is half the thickness of the can bottom plate, only puncture of the lid will be considered. Conservatively considering that the fuel rod weight and insert weight impacts the lid, the resulting shear stress is calculated as:

$$S = \frac{F}{A} = \frac{(350 + 75)x60}{\pi(0.6875)(0.5)} = 23.6 \text{ ksi}$$

where F is the weight of the fuel (350 lbs) and insert (75 lbs) and A is the shear area of the insert tube. The allowable for a pure shear loading during accident drop conditions is 0.5 S_u or 0.5 (63.7 ksi) = 31.85 ksi at 575°F for the 304 SS lid. The resulting margin of safety is:

$$MS = \frac{0.5S_u}{S} - 1 = \frac{31.85}{23.6} - 1 = +0.35$$

Considering puncture due to the lid handle,

$$S = \frac{F}{A} = \frac{(350 + 75 + 310)\ x\ 60}{2(1.25x2 + 2x0.625)(0.5)} = 11.76\text{ksi}$$

where F is the weight of the fuel (350 lbs), insert (75 lbs), and can (310 lbs) and A is the shear area of handle at the lid intersection. The resulting margin of safety is:

$$MS = \frac{0.5S_u}{S} - 1 = \frac{31.85}{11.76} - 1 = +1.71$$

Can Internal Pressure

Can weldment internal pressure is considered insignificant in the end-drop and side-drop cases because it will tend to reduce the compressive loads on the can tube sides.

The effect of internal pressure is evaluated for the bending stress that the pressure imposes on the can weldment sides. Conservatively, a one-inch-wide section of the tube wall, equal in length to the outside dimension of the tube (L = 5.5 in) is analyzed as a simply supported beam with a uniform load.

The maximum moment (M) is determined by the following relation:

$$M = \frac{wL^2}{8} = \frac{(140-14.7)(5.5^2)}{8} \cong 474 \text{ in.-lb}$$

where w is the maximum differential pressure across the can wall due to the fire accident temperature (assumes that the cask internal pressure is atmospheric).

The bending stress (σ) in the tube wall is:

$$\sigma = \frac{Mc}{I} = \frac{(474 \text{ in.-lb})(0.125 \text{ in})}{0.0013 \text{ in.}^4} \cong 45.58 \text{ ksi}$$

The margin of safety (MS) is:

$$MS = \frac{3.6S_m}{\sigma} - 1 = \frac{56.16 \text{ ksi}}{45.58 \text{ ksi}} - 1 = +0.23$$

Can Lid Bolt Analysis

The tensile force (F_p) on each lid bolt due to internal pressure is:

$$F_p = \frac{PA}{n} = \frac{(140-14.7)(3.75^2)}{8} \cong 220.3 \text{ lbs}$$

where:

P = the pressure differential across the can wall (100% rod failure with fire temperature and assuming atmospheric pressure in the cask)

A = 3.75 inches × 3.75 inches, the area of the can lid exposed to pressure

n = 8, number of bolts

The total tensile force on each lid bolt is F_p + the initial preload force, F_i = 635 lbs

The lid bolt tensile stress (σ) is:

$$\sigma = \frac{F_p + F_i}{A_t} = \frac{855.3}{0.049} = 17.46 \text{ ksi}$$

where:

At = 0.049 in^2, the bolt tensile stress area $\frac{\pi}{4}\left(0.25^2\right)$

The margin of safety (MS) for the hypothetical accident condition is:

$$MS = \frac{S_y}{\sigma} - 1 = \frac{19.1}{17.46} - 1 = +0.09$$

Can Tube Buckling

The critical buckling load was calculated (see Section 2.6.7.10) as 698 × 10^3 pounds. Since the actual compressive load of 310 × 60 = 18,600 lbs is much less than the critical buckling load, the tube has adequate resistance to buckling.

Internal Spacer

The internal spacer is contained within the can assembly and is not subjected to bending in the side drop condition.

The compressive stress in the internal spacer rails during the side drop is determined as follows:

$$\sigma_b = \frac{Wg}{A} = \frac{665 \text{ x } 49.7}{123.7} \cong 267.2 \text{ psi}$$

where:

W = total load = 350 (fuel) + 240 (internal spacer) + 75 (4x4 insert) = 665 lbs

g = 49.7 (hypothetical accident condition side drop)

A = 123.7 in^2 cross-sectional area of spacer rails, 4 × 0.188 × (165.25 – 2 x 0.38)

The resulting margin of safety is Large.

Internal Spacer Compressive Stress

For the end drop, the internal spacer shell is loaded by its own weight. The insert rail stiffness is conservatively neglected in the strength.

Under hypothetical accident conditions, the spacer is evaluated for a 60 g acceleration. The compressive load (P) on the shell is due to the weight of the internal spacer. The entire weight of the internal spacer times the 60 g factor is used to calculate the compressive load.

The compressive load (P) is:

$$P = 240 \times 60 = 14{,}400 \text{ lbs}$$

The compressive stress (S_c) in the spacer body is:

$$S_c = \frac{P}{A} = \frac{14{,}400}{1.69} \cong 8{,}521 \text{ psi}$$

The margin of safety (MS) is then:

$$MS = \frac{0.7S_u}{S_c} - 1 = \frac{0.7(63{,}100)}{8{,}521} - 1 = +4.18$$

Internal Spacer Buckling

The critical buckling load was calculated (see Section 2.6.7.10) as 190×10^3 pounds. Since the actual compressive load ($240 \times 60 = 14{,}400$ lbs) is much less than the critical buckling load, the tube has adequate resistance to buckling.

4×4 and 5×5 Inserts

The 4×4 and 5×5 inserts are contained within the internal spacer. The 4×4 inserts are supported by straps on 10-inch spacing. These straps provide a clearance of 0.31 inches and will allow bending of the tubes to occur. The 5×5 insert tubes are evaluated for a diametrically opposed load due to the weight of the adjacent tubes during the side drop.

The 4×4 insert lower tube will be evaluated as a fixed-fixed beam over a 10-inch span. The weight of the 3 tubes above (as well as lower tube self-weight) will be considered in the analysis. The stiffness of the tubes above the lower tube will conservatively be neglected. The combined weight (P) of the fuel pins and insert tubes are considered as a uniformly distributed load over the 10-inch span. In addition, the weights are scaled by the 60 g deceleration factor.

The maximum bending stress (f_b) is determined as follows:

$$f_b = \frac{Wlg}{12\,Z} = \frac{5.8(10.0)49.7}{12x0.0092} \cong 26{,}111 \text{ psi}$$

where:

W = load on 10-inch section = $(14 + 9.5) \times 4 \times 10/163.0 = 5.8$ lbs

l = 10 inch (span of tube)

g = 49.7 (accident condition side drop)

Z = $\pi/32\ (0.6875^4 - 0.6315^4) / 0.6875 = 0.0092\ in^3$ (section modulus of the tube)

The margin of safety (MS) is:

$$MS = \frac{1.0\ S_u}{\sigma_{max}} - 1 = \frac{1.0(48{,}160)}{26{,}111} - 1 = +0.84$$

The bending moment due to the diametrically opposed line load on the 5x5 insert is calculated by the following:

$$M_b = \frac{WRg}{\pi} = \frac{70/163.0 \text{ x } 0.344 \text{ x } 49.7}{\pi} \cong 2.34 \text{ lb} - \text{in}$$

where:

W = total load = 14 x 4 (fuel) + 70/5 (tube) = 70 lbs

g = 49.7 (hypothetical accident condition side drop)

R = 0.6875/2 = 0.344 in (radius of insert tube)

The resulting bending stress is:

$$f_b = \frac{6M_b}{t^2} = \frac{6 \text{ x } 2.34}{0.028^2} \cong 17{,}908 \text{ psi}$$

The margin of safety (MS) is:

$$MS = \frac{1.0\ S_u}{\sigma_{max}} - 1 = \frac{1.0(48{,}160)}{17{,}908} - 1 = +1.69$$

<u>4×4 and 5×5 Insert Tube Compressive Stress</u>

Under hypothetical accident conditions, the tube is evaluated for a 60 g acceleration. The compressive load (P) on the shell is due to the weight of the tube. The entire weight of the tube is calculated as:

The compressive load (P) is:

P = 2.72 x 60 = 163.2 lbs

The compressive stress (S_c) in the tube body is:

$$S_c = \frac{P}{A} = \frac{163.2}{0.058} \cong 2{,}814 \text{ psi}$$

where:

$A = \pi/4\ (0.6875^2 - 0.6315^2) = 0.058\ in^2$

The margin of safety (MS) is then:

$$MS = \frac{0.7S_u}{S_c} - 1 = \frac{0.7(48{,}160)}{2{,}814} - 1 = +11.0$$

PWR Insert

The PWR insert contains the can assembly for insertion into the PWR basket. The PWR insert comprises a square box section with smooth sides. Therefore, no bending stresses will be introduced in the side drop condition.

PWR Insert Body Compressive Stress

Under accident conditions, the tube is evaluated for a 60 g acceleration. The compressive load (P) on the body is due to the weight of the PWR insert. The entire weight of the PWR insert times the 60 g factor will conservatively be used to calculate the compressive load.

The compressive load (P) is:

$P = 650 \times 60 = 39{,}000$ lbs

The compressive stress (S_c) in the tube body is:

$$S_c = \frac{P}{A} = \frac{39{,}000}{39.2} \cong 995\text{psi}$$

where:

$A = (8.5^2 - 5.75^2) = 39.2\ in^2$

The margin of safety (MS) is then:

$$MS = \frac{0.7S_u}{S_c} - 1 = \frac{0.7(25{,}800)}{995} - 1 = +17.2$$

PWR Insert Tube Buckling

The critical buckling load was calculated (see Section 2.6.7.10) as 3.86×10^6 pounds. Since the maximum compressive load (650 x 60 = 39,000 lbs) is much less than the critical buckling load (3.86×10^6 lb), the PWR insert has adequate resistance to buckling.

Figure 2.7.1-1 30-Foot Bottom End Drop with 130°F Ambient Temperature and Maximum Decay Heat Load

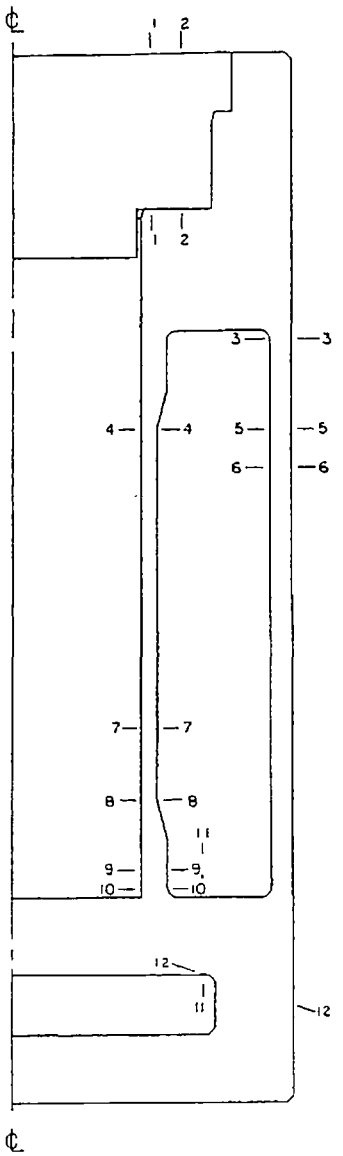

Figure 2.7.1-2 30-Foot Bottom End Drop with -40°F Ambient Temperature and Maximum Decay Heat Load

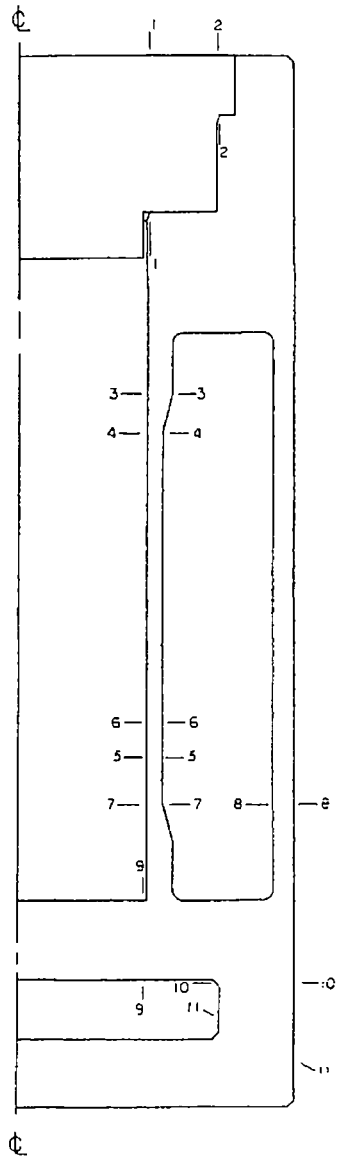

Figure 2.7.1-3 30-Foot Bottom End Drop with -40°F Ambient Temperature and No Decay Heat Load

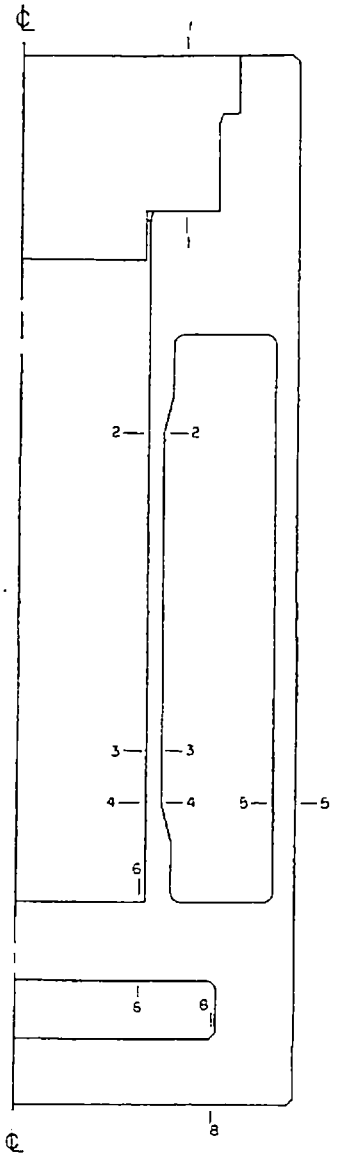

Figure 2.7.1-4 30-Foot Top End Drop with 130°F Ambient Temperature and Maximum Decay Heat Load

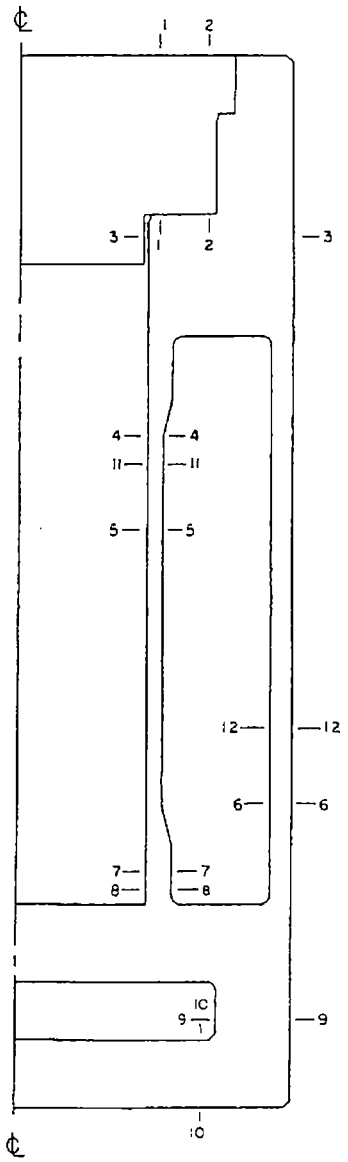

Figure 2.7.1-5 30-Foot Top End Drop with -40°F Ambient Temperature and Maximum Decay Heat Load

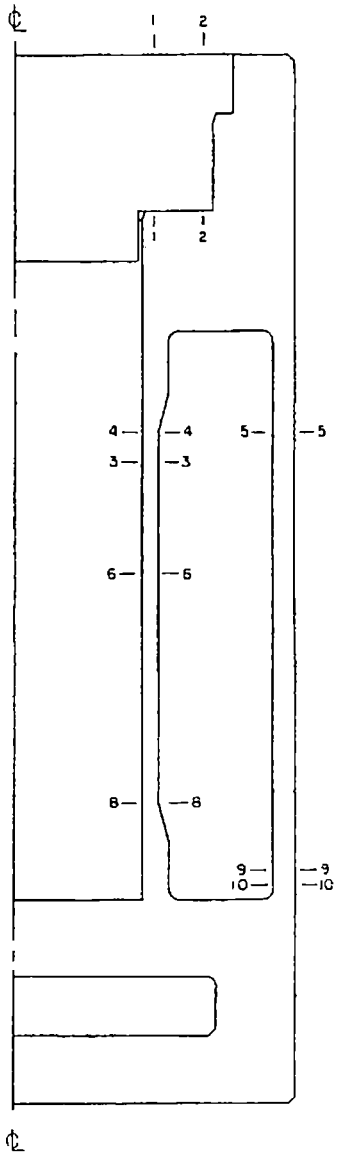

Figure 2.7.1-6 Circumferential Load Distribution for Cask Side Drop Impact

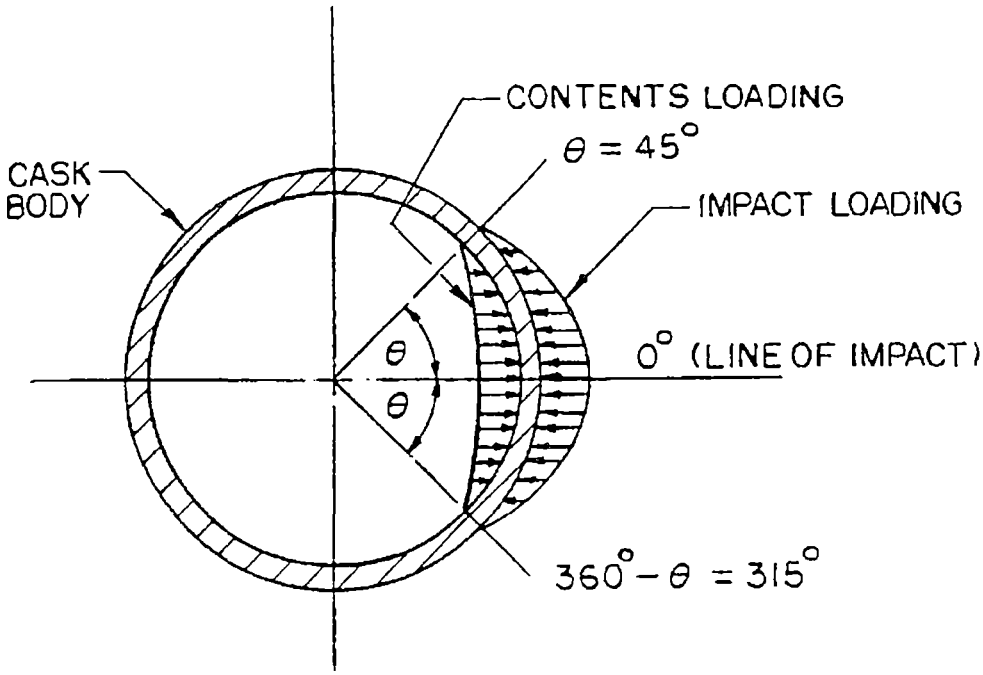

Figure 2.7.1-7 Six Term Fourier Series Representation of Circumferential Load Distribution for Cask Side Drop Impact

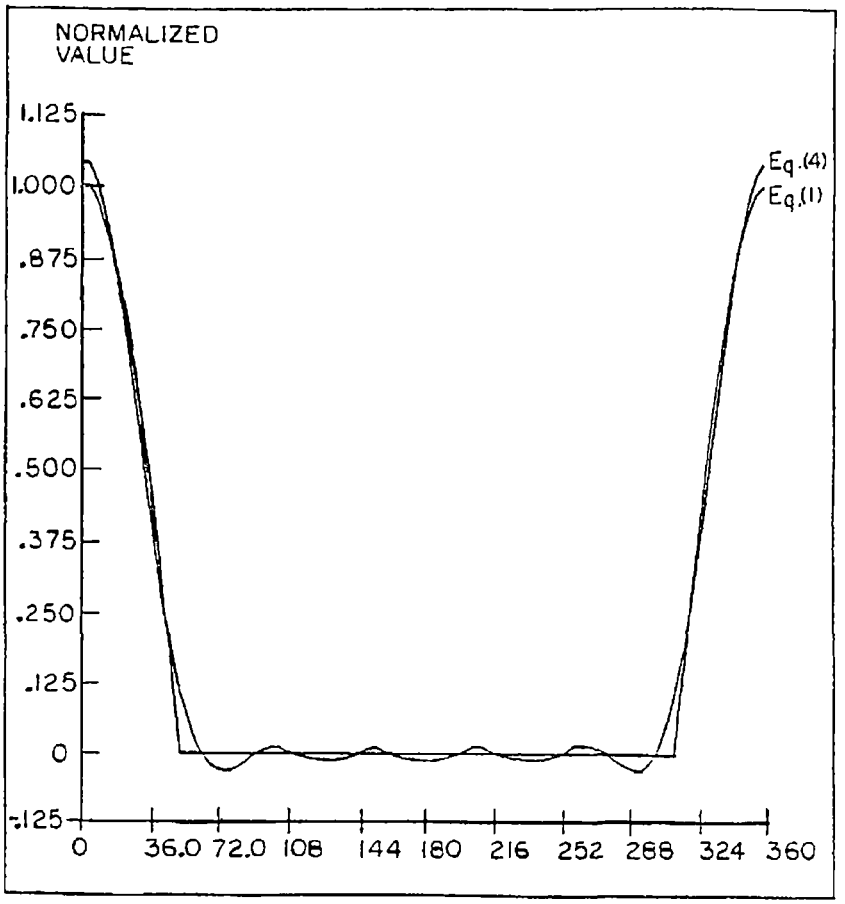

Figure 2.7.1-8 NAC-LWT Cask Critical Sections (30-Foot Side Drop with 100°F Ambient Temperature)

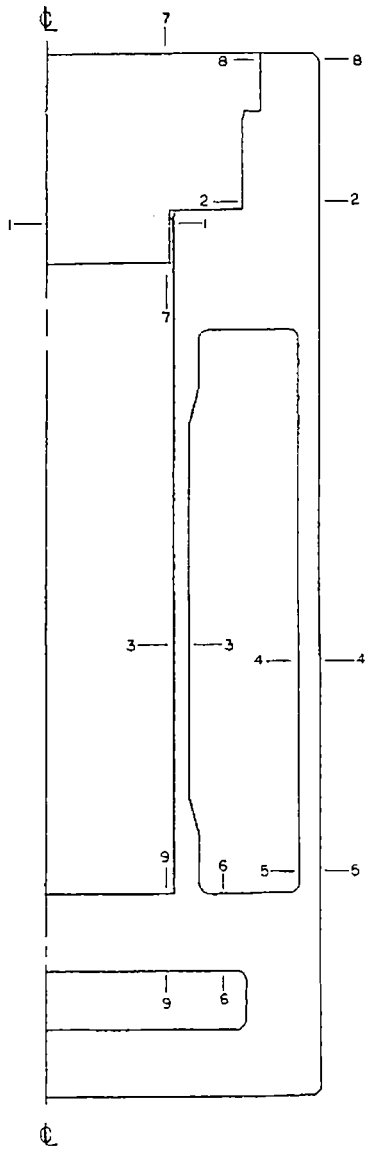

Figure 2.7.1-9 Circumferential Load Distribution for Cask Oblique Drop Impact

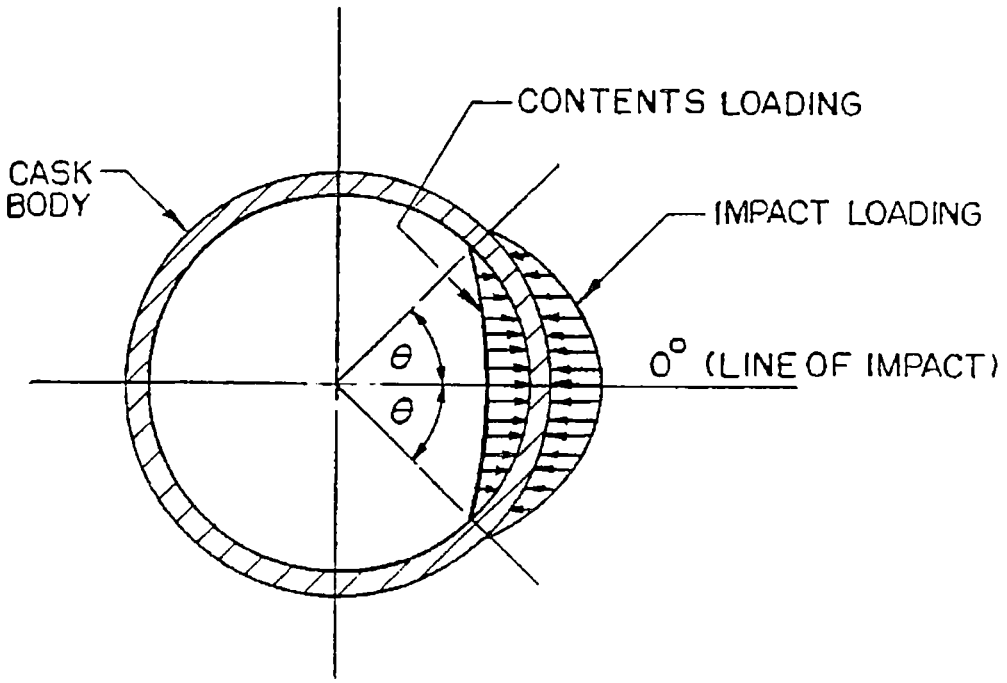

Figure 2.7.1-10 30-Foot Top Corner Drop with 130°F Ambient Temperature – Drop Orientation = 15.74 Degrees

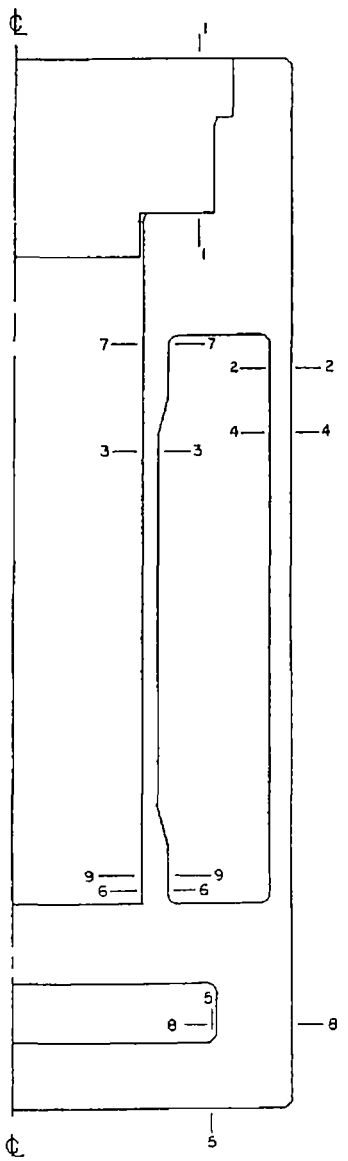

Figure 2.7.1-11 30-Foot Top Oblique Drop with 130°F Ambient Temperature – Drop Orientation = 30 Degrees

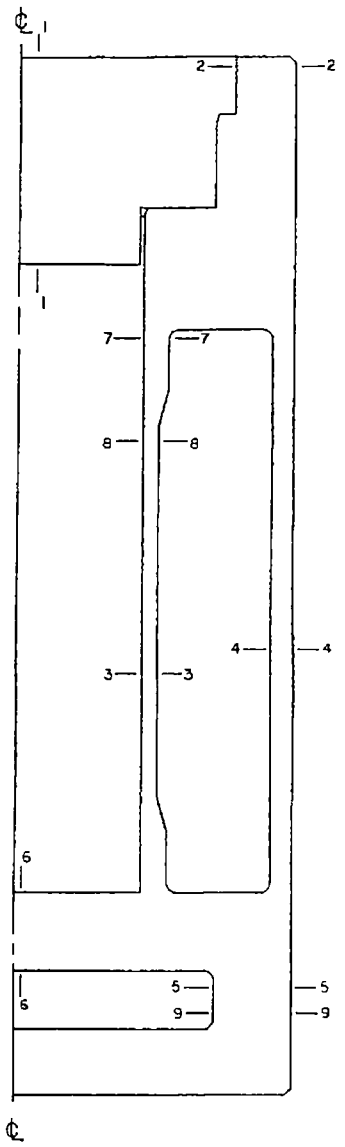

Figure 2.7.1-12 30-Foot Top Oblique Drop with 130°F Ambient Temperature – Drop Orientation = 45 Degrees

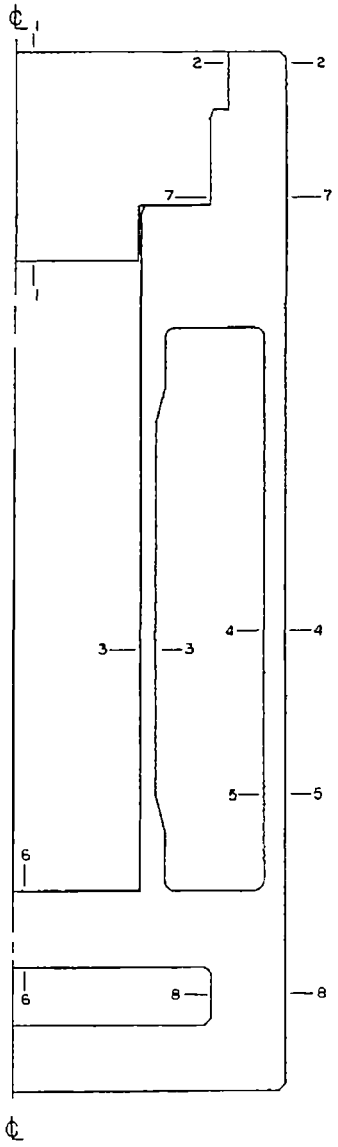

Figure 2.7.1-13 30-Foot Oblique Drop with 130°F Ambient Temperature – Drop Orientation = 60 Degrees

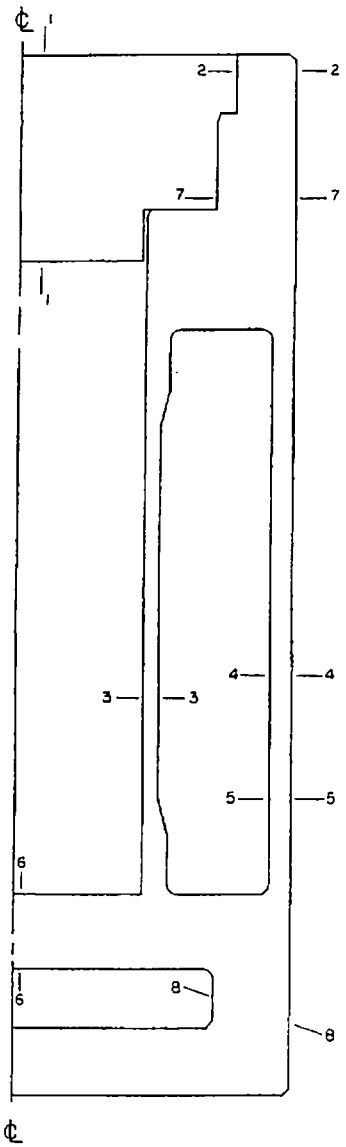

Figure 2.7.1-14 30-Foot Top Corner Drop with -40°F Ambient Temperature – Drop Orientation = 15.74 Degrees

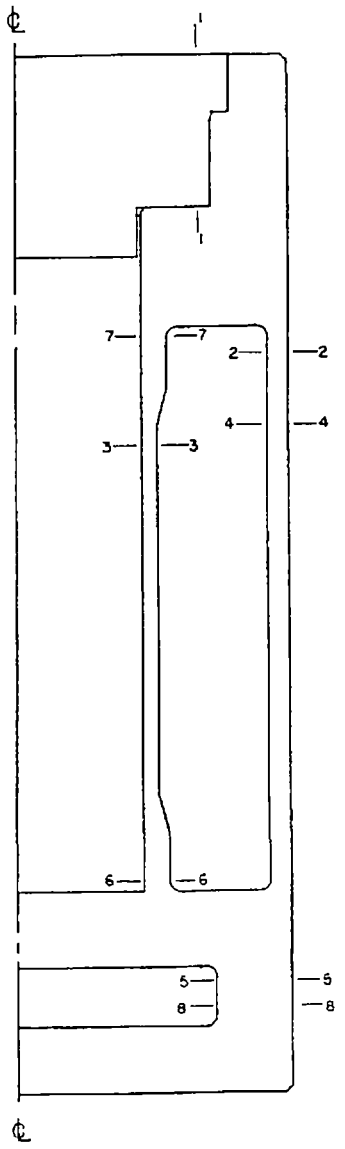

Figure 2.7.1-15 30-Foot Top Oblique Drop with -40°F Ambient Temperature – Drop Orientation = 30 Degrees

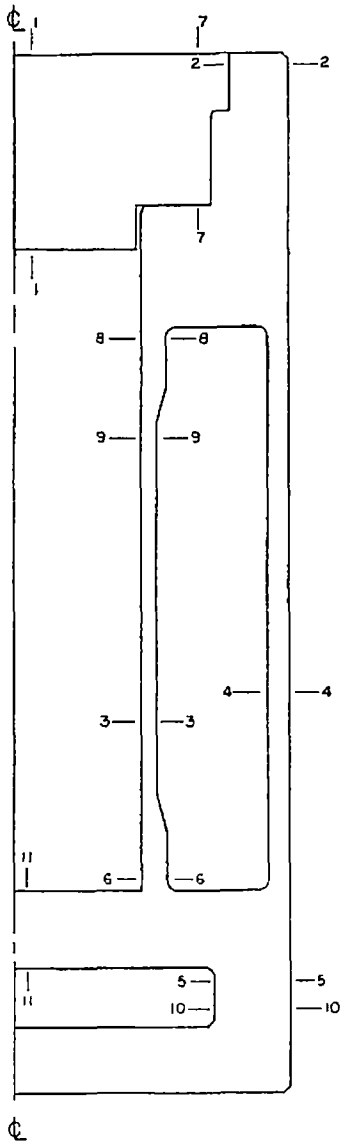

Figure 2.7.1-16 30-Foot Top Oblique Drop with -40°F Ambient Temperature – Drop Orientation = 45 Degrees

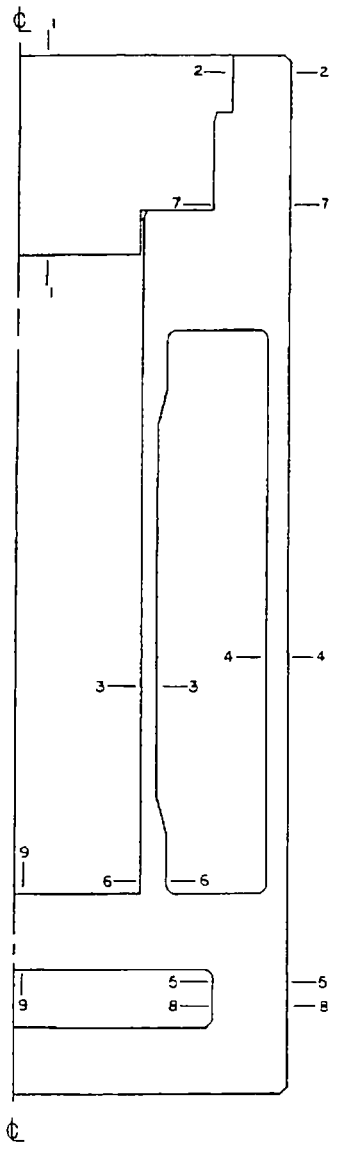

Figure 2.7.1-17 30-Foot Top Oblique Drop with -40°F Ambient Temperature – Drop Orientation = 60 Degrees

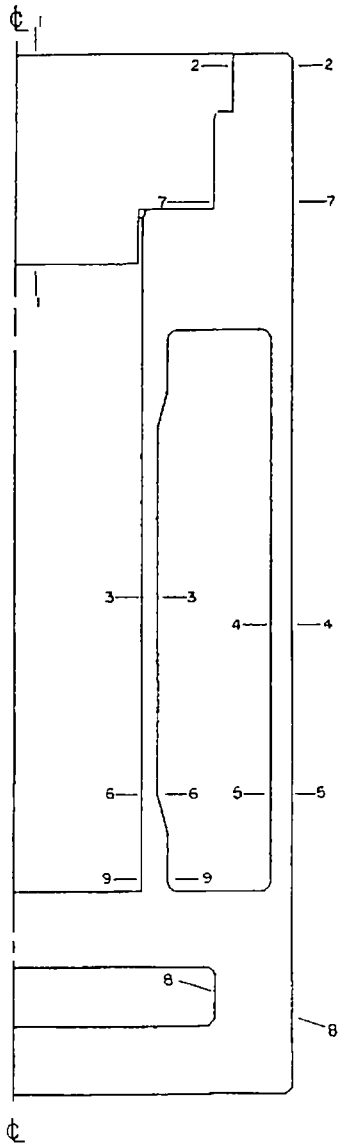

Figure 2.7.1-18 30-Foot Bottom Oblique Drop with 130°F Ambient Temperature – Drop Orientation = 15.74 Degrees

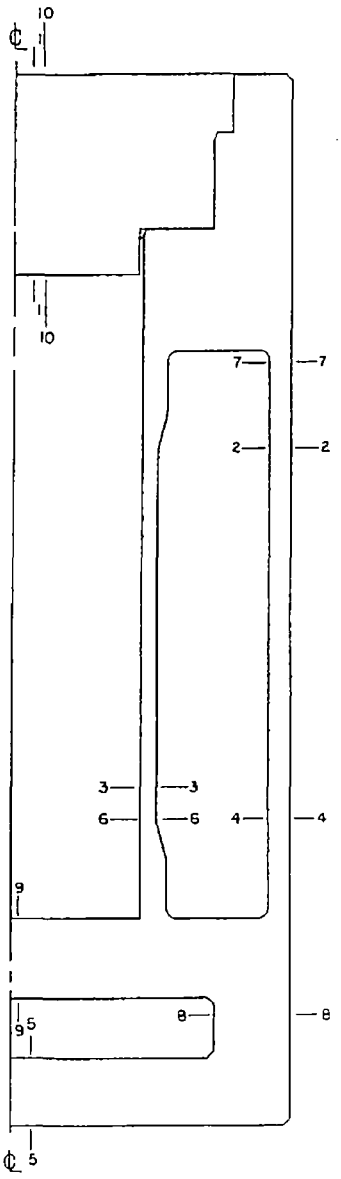

Figure 2.7.1-19 30-Foot Bottom Oblique Drop with 130°F Ambient Temperature – Drop Orientation = 30 Degrees

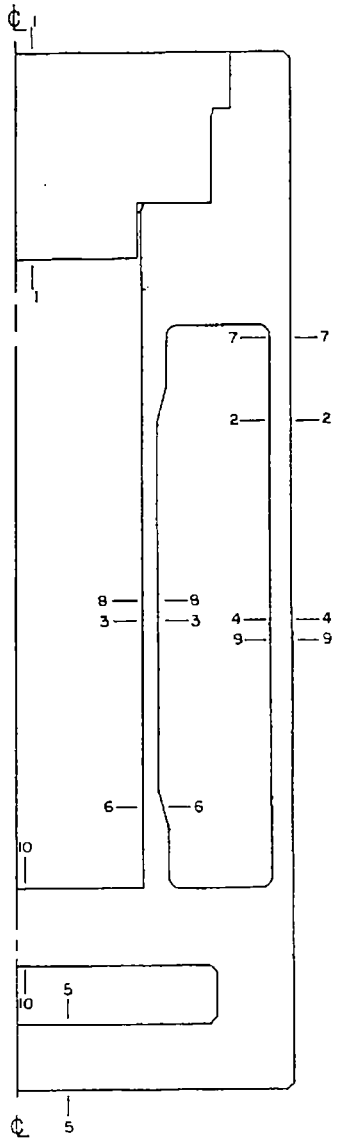

Figure 2.7.1-20 30-Foot Bottom Oblique Drop with 130°F Ambient Temperature – Drop Orientation = 45 Degrees

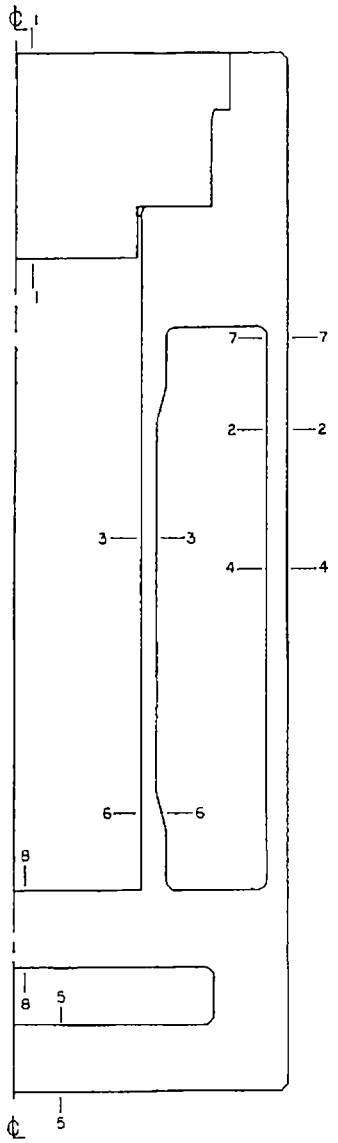

Figure 2.7.1-21 30-Foot Bottom Oblique Drop with 130°F Ambient Temperature – Drop Orientation = 60 Degrees

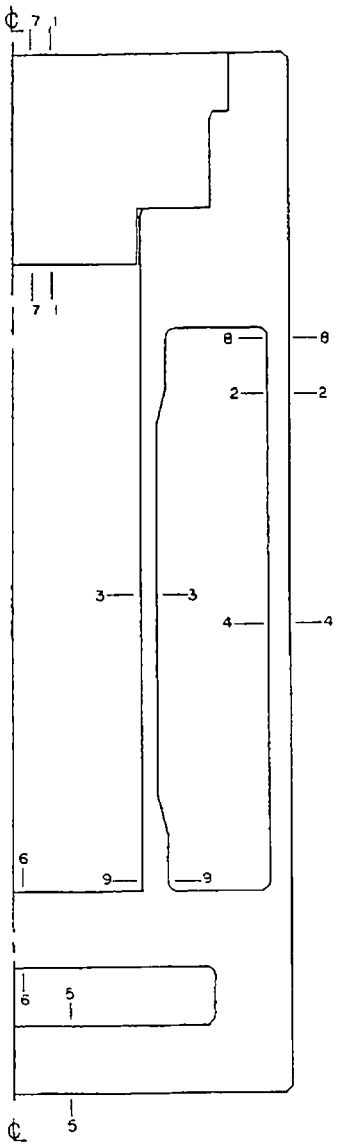

Figure 2.7.1-22 Sectional Stress Plot – 30-Foot Bottom Oblique Drop with 130°F Ambient Temperature – Drop Orientation = 60 Degrees

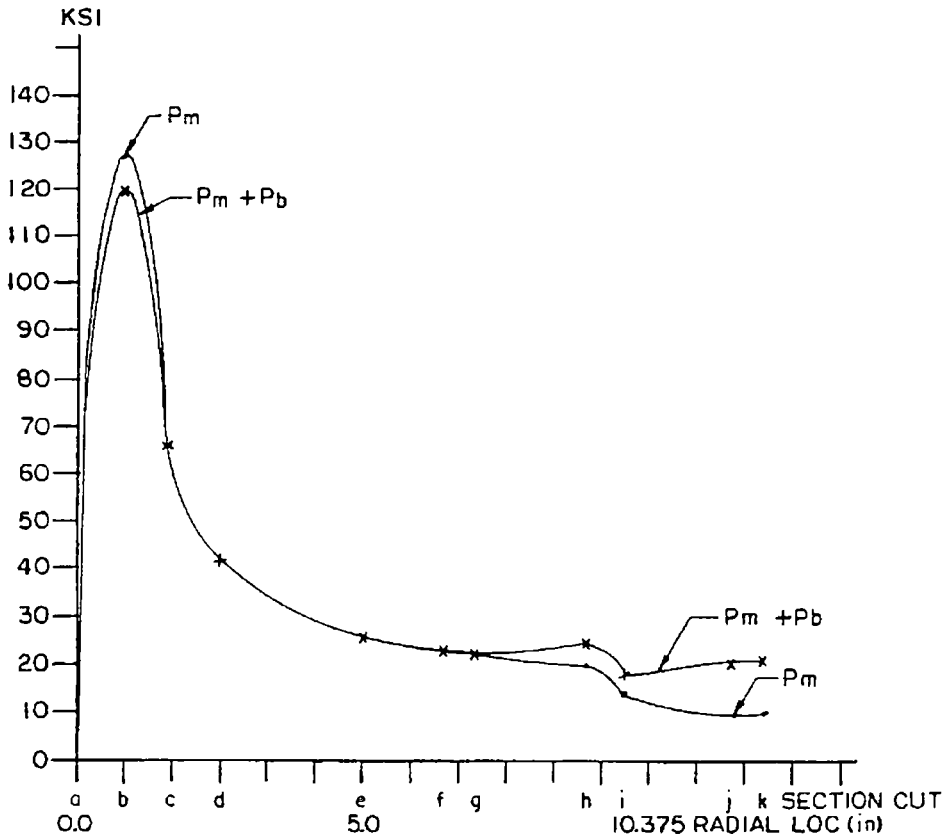

Note: Refer to Figure 2.7.1-25 for identification of the section cut.

Figure 2.7.1-23 Sectional Stress Plot (P_m) – 30-Foot Bottom Oblique Drop with 130°F Ambient Temperature – Drop Orientation = 60 Degrees

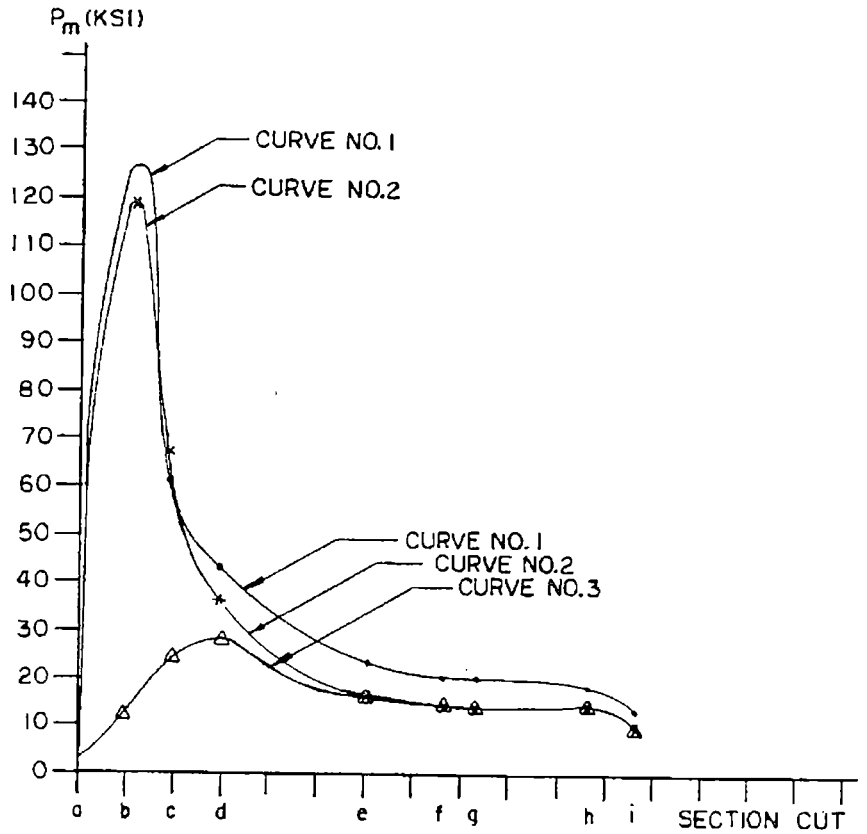

Note: Refer to Figure 2.7.1-25 for identification of the section cut.

Figure 2.7.1-24 Sectional Stress Plot ($P_m + P_b$) – 30-Foot Bottom Oblique Drop with 130°F Ambient Temperature – Drop Orientation = 60 Degrees

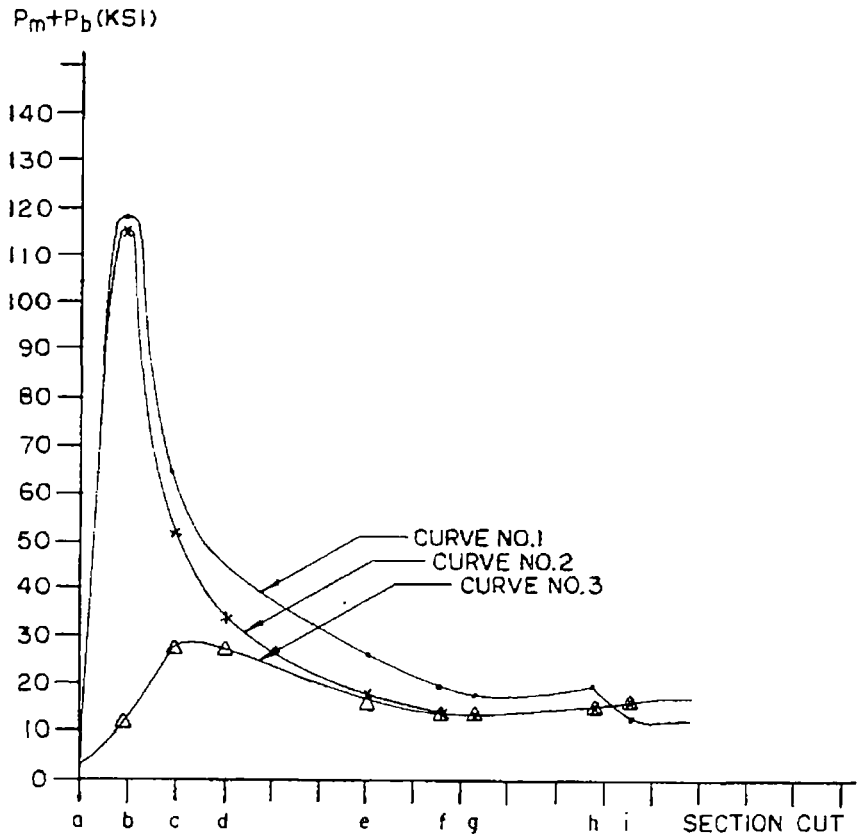

Note: Refer to Figure 2.7.1-25 for identification of the section cut.

Figure 2.7.1-25 Bottom Closure Plate – Section Cut Identification

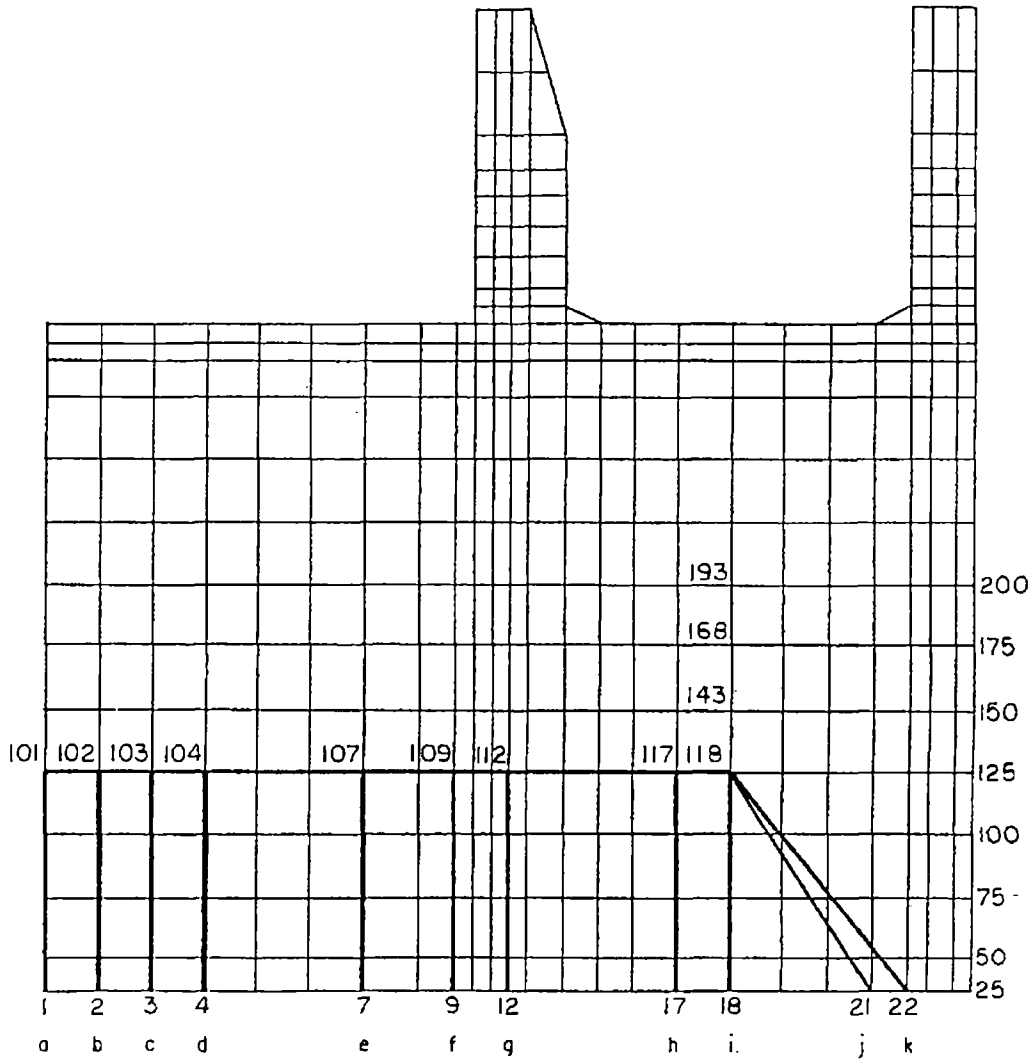

Figure 2.7.1-26 Sectional Stress Plot – 30-Foot Bottom Oblique Drop with 130°F Ambient Temperature – Drop Orientation = 45 Degrees

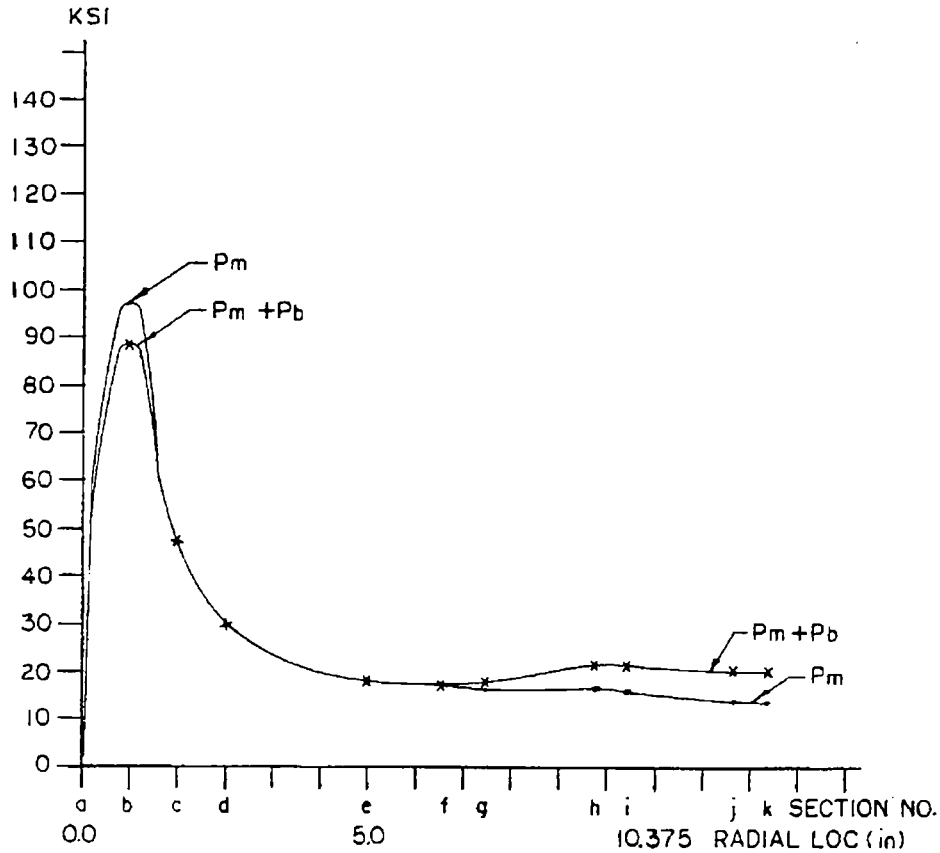

Note: Refer to Figure 2.7.1-25 for identification of the section cut.

Figure 2.7.1-27 Sectional Stress Plot – 30-Foot Bottom Oblique Drop with 130°F Ambient Temperature – Drop Orientation = 30 Degrees

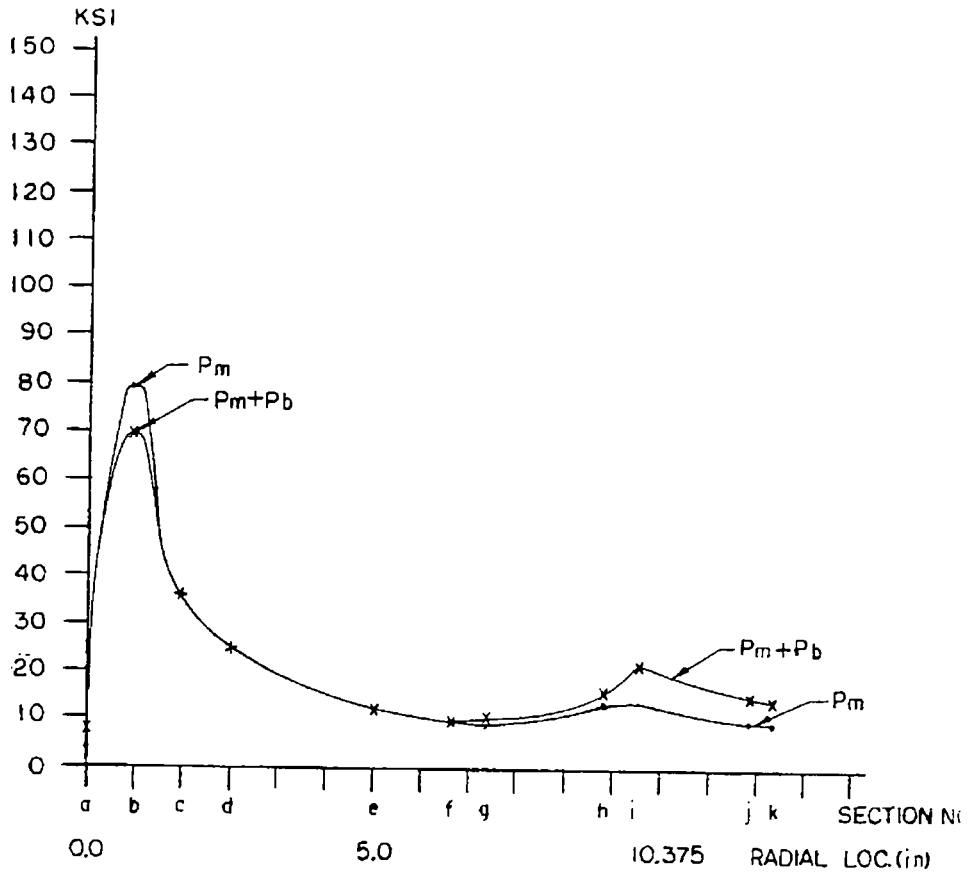

Note: Refer to Figure 2.7.1-25 for identification of the section cut.

Table 2.7.1-1 Critical Stress Summary (30-Foot Bottom End Drop) – Loading Condition 1 – P_m

Loading Condition 1: 130°F Ambient Temperature and Maximum Decay Heat Load

		P_m Stresses** (ksi)				Principal Stresses					
Comp. No.*	Section Cut Node to Node	S_x	S_y	S_z	S_{xy}	S_1	S_2	S_3	S.I.	Allow. Stress 0.7 S_u	Margin of Safety
	2-2										
1	2375 to 2575	-0.17	-0.23	0.62	0.40	0.62	0.2	-0.6	1.22	46.2	Large
	4-4										
3	1581 to 1584	-0.1	-4.54	-0.16	-0.14	-0.1	-0.16	-4.55	4.45	46.2	+9.38
	7-7										
4	701 to 704	-0.03	-8.44	0.51	-0.02	0.51	-0.03	-8.44	8.94	66.0	+6.38
	6-6										
6	1515 to 1518	0.00	1.98	-0.16	-0.04	1.98	0.00	-0.16	2.14	66.0	Large
	11-11										
7	192 to 342	-6.50	1.18	1.28	1.69	1.54	1.28	-6.85	8.39	46.2	+4.51
	10-10										
8	361 to 365	0.77	-5.40	3.89	-0.99	3.89	0.92	-5.55	9.44	46.2	+3.89

* Refer to Figure 2.10.2-9 for component identification.

** Conservatively based on a 1.12-inch thick outer shell and on a 3,850-psi crush strength aluminum honeycomb impact limiter (Section 2.7.1.1).

Table 2.7.1-2 Critical Stress Summary (30-Foot Bottom End Drop) – Loading Condition 1 – $P_m + P_b$

Loading Condition 1: 130°F Ambient Temperature and Maximum Decay Heat Load

		$P_m + P_b$ Stresses** (ksi)				Principal Stresses					
Comp. No.*	Section Cut Node to Node	S_x	S_y	S_z	S_{xy}	S_1	S_2	S_3	S.I.	Allow. Stress 1.0 S_u	Margin of Safety
	1-1										
1	2371 to 2571	-3.91	-0.35	0.11	0.00	0.11	-0.35	-3.91	4.01	66	Large
	3-3										
3	1835 to 1838	-0.1	4.66	2.25	0.29	4.68	2.25	-0.1	4.76	66	Large
	8-8										
4	621 to 624	0.15	-10.37	-1.16	0.28	0.16	-1.16	-10.38	10.54	94.3	+8.94
	5-5										
6	1595 to 1598	-0.01	3.03	0.57	0.00	3.03	0.57	-0.01	3.04	94.3	Large
	12-12										
7	150 to 193	9.25	-5.21	2.76	0.63	9.27	2.76	-5.24	14.51	66	+3.54
	9-9										
8	381 to 385	-0.21	-13.14	2.03	-1.07	2.03	-0.12	-13.23	15.26	66	+3.33

* Refer to Figure 2.10.2-9 for component identification.

** Conservatively based on a 1.12-inch thick outer shell and on a 3,850-psi crush strength aluminum honeycomb impact limiter (Section 2.7.1.1).

Table 2.7.1-3 Critical Stress Summary (30-Foot Bottom End Drop) – Loading Condition 1 – Total Range

Loading Condition 1: 130°F Ambient Temperature and Maximum Decay Heat Load

		Total Stress Range** (ksi)				Principal Stresses			Stress Differences		
Comp. No.*	Node	S_x	S_y	S_z	S_{xy}	S_1	S_2	S_3	S_1-S_2	S_2-S_3	S_3-S_1
1	2376	0.80	-4.48	-0.22	-0.31	0.82	-0.22	-4.50	1.04	4.28	-5.32
3	1805	-0.19	-5.27	-2.19	-0.78	-0.07	-2.19	-5.39	2.12	3.20	-5.32
4	604	-0.69	-12.07	-1.65	0.61	-0.66	-1.65	-12.10	0.99	10.45	-11.44
6	1595	-0.02	2.93	0.48	0.00	2.93	0.48	-0.02	2.45	0.50	-2.95
7	192	12.54	-7.35	3.46	-3.90	13.28	3.46	-8.09	9.82	11.55	-21.37
8	361	-0.03	-16.44	0.82	-1.4	0.82	0.09	-16.56	0.73	16.65	-17.38

* Refer to Figure 2.10.2-9 for component identification.

** Conservatively based on a 1.12-inch thick outer shell and on a 3,850-psi crush strength aluminum honeycomb impact limiter (Section 2.7.1.1).

Table 2.7.1-4 Critical Stress Summary (30-Foot Bottom End Drop) – Loading Condition 2 – P_m

Loading Condition 2: -40°F Ambient Temperature and Maximum Decay Heat Load

		P_m Stresses** (ksi)				Principal Stresses					
Comp. No.*	Section Cut Node to Node	S_x	S_y	S_z	S_{xy}	S_1	S_2	S_3	S.I.	Allow. Stress 0.7 S_u	Margin of Safety
	2-2										
1	2478 to 2578	0.03	-0.11	1.28	0.02	1.28	0.03	-0.11	1.39	46.2	Large
	4-4										
3	1581 to 1584	-0.15	-7.90	-0.93	-0.26	-0.14	-0.93	-7.91	7.77	46.2	Large
	6-6										
4	701 to 704	-0.02	-12.08	0.20	-0.03	0.20	-0.02	-12.08	12.28	66.0	+4.37
	8-8										
6	615 to 618	0.00	-2.85	0.80	0.00	0.80	0.00	-2.85	3.65	66.0	Large
	11-11										
7	100 to 143	-3.18	-4.19	2.15	2.18	2.15	-1.45	-5.93	8.07	46.2	Large
	7-7										
8	601 to 604	-0.23	-11.12	-1.21	0.46	-0.21	-1.21	-11.13	10.93	46.2	Large

* Refer to Figure 2.10.2-9 for component identification.

** Conservatively based on a 1.12-inch thick outer shell and on a 3,850-psi crush strength aluminum honeycomb impact limiter (Section 2.7.1.1).

Table 2.7.1-5 Critical Stress Summary (30-Foot Bottom End Drop) – Loading Condition 2 – $P_m + P_b$

Loading Condition 2: -40°F Ambient Temperature and Maximum Decay Heat Load

		$P_m + P_b$ Stresses** (ksi)				Principal Stresses					
Comp. No.*	Section Cut Node to Node	S_x	S_y	S_z	S_{xy}	S_1	S_2	S_3	S.I.	Allow. Stress 1.0 S_u	Margin of Safety
	1-1										
1	2371 to 2571	-4.10	-0.43	0.14	0.00	0.14	-0.43	-4.10	4.24	66	Large
	3-3										
3	1701 to 1705	0.04	-8.08	-1.59	-0.34	0.05	-1.59	-8.10	8.15	66	+7.10
	5-5										
4	621 to 624	0.18	-13.91	-1.67	0.32	0.19	-1.67	-13.91	14.10	94.3	+5.68
	8-8										
6	615 to 618	0.03	-4.12	0.63	0.00	0.63	0.03	-4.12	4.75	94.3	Large
	10-10										
7	193 to 200	3.76	-9.04	1.83	-0.76	3.81	1.83	-9.09	12.89	66	+4.12
	9-9										
8	185 to 335	-12.66	-0.38	-0.11	1.93	-0.09	-0.11	-12.96	12.87	66	+4.13

* Refer to Figure 2.10.2-9 for component identification.

** Conservatively based on a 1.12-inch thick outer shell and on a 3,850-psi crush strength aluminum honeycomb impact limiter (Section 2.7.1.1).

Table 2.7.1-6 Critical Stress Summary (30-Foot Bottom End Drop) – Loading Condition 2 – Total Range

Loading Condition 2: -40°F Ambient Temperature and Maximum Decay Heat Load

		Total Stress Range** (ksi)				Principal Stresses			Stress Differences		
Comp. No.*	Node	S_x	S_y	S_z	S_{xy}	S_1	S_2	S_3	S_1-S_2	S_2-S_3	S_3-S_1
1	2376	0.67	-4.03	0.05	-0.35	0.7	0.05	-4.06	0.65	4.11	-4.75
3	1805	-0.32	-9.36	-3.82	-1.34	-0.12	-3.82	-9.56	3.70	5.74	-9.44
4	604	-0.90	-15.99	-2.51	0.80	-0.86	-2.51	-16.03	1.65	13.52	-15.17
6	618	0.03	-4.2	0.57	0.00	0.57	0.03	-4.20	0.54	4.23	-4.77
7	143	-5.58	-14.56	-1.04	0.55	-1.04	-5.55	-14.59	4.51	9.05	-13.55
8	361	0.01	-14.97	-0.81	-1.62	0.18	-0.81	-15.14	0.99	14.33	-15.33

* Refer to Figure 2.10.2-9 for component identification.

** Conservatively based on a 1.12-inch thick outer shell and on a 3,850-psi crush strength aluminum honeycomb impact limiter (Section 2.7.1.1).

Table 2.7.1-7 Critical Stress Summary (30-Foot Bottom End Drop) – Loading Condition 3 – P_m

Loading Condition 3: -40°F Ambient Temperature and No Decay Heat Load

		P_m Stresses** (ksi)				Principal Stresses					
Comp. No.*	Section Cut Node to Node	S_x	S_y	S_z	S_{xy}	S_1	S_2	S_3	S.I.	Allow. Stress 0.7 S_u	Margin of Safety
	1-1										
1	2375 to 2575	-0.21	0.00	-0.03	0.18	0.1	-0.03	-0.31	0.41	46.2	Large
	2-2										
3	1581 to 1584	-0.22	-3.78	-5.48	-0.28	-0.19	-3.80	-5.48	5.29	46.2	+7.73
	3-3										
4	621 to 624	0.04	-7.76	-1.05	0.24	0.04	-1.05	-7.77	7.81	66.0	+7.45
	5-5										
6	615 to 618	0.00	-6.85	-0.13	0.00	0.00	-0.13	-6.85	6.85	66.0	Large
	8-8										
7	18 to 118	-10.02	-0.60	-2.86	2.62	0.08	-2.86	-10.70	10.78	46.2	+3.29
	4-4										
8	601 to 604	-0.16	-7.07	-0.78	0.34	-0.14	-0.78	-7.09	6.95	46.2	+5.65

* Refer to Figure 2.10.2-9 for component identification.

** Conservatively based on a 1.12-inch thick outer shell and on a 3,850-psi crush strength aluminum honeycomb impact limiter (Section 2.7.1.1).

Table 2.7.1-8 Critical Stress Summary (30-Foot Bottom End Drop) – Loading Condition 3 – $P_m + P_b$

Loading Condition 3: -40°F Ambient Temperature and No Decay Heat Load

		$P_m + P_b$ Stresses** (ksi)				Principal Stresses					
Comp. No.*	Section Cut Node to Node	S_x	S_y	S_z	S_{xy}	S_1	S_2	S_3	S.I.	Allow. Stress 1.0 S_u	Margin of Safety
	1-1										
1	2375 to 2575	-1.99	0.00	-0.03	0.18	0.01	-0.03	-2.01	2.02	66	Large
	2-2										
3	1581 to 1584	0.01	-3.30	-5.65	-0.28	0.03	-3.33	-5.65	5.68	66	Large
	3-3										
4	621 to 624	0.12	-8.99	-1.30	0.24	0.13	-1.30	-9.00	9.13	94.3	+9.32
	5-5										
6	615 to 618	0.00	-7.06	-0.19	0.00	0.00	-0.19	-7.06	7.06	94.3	Large
	8-8										
7	18 to 118	-20.14	-0.6	-2.86	2.62	-0.25	-2.86	-20.49	20.23	66	+2.26
	6-6										
8	185 to 335	-8.83	1.55	1.16	2.22	2.0	1.16	-9.29	11.29	66	+4.85

* Refer to Figure 2.10.2-9 for component identification.

** Conservatively based on a 1.12-inch thick outer shell and on a 3,850-psi crush strength aluminum honeycomb impact limiter (Section 2.7.1.1).

Table 2.7.1-9 Critical Stress Summary (30-Foot Bottom End Drop) – Loading Condition 3 – Total Range

Loading Condition 3: -40°F Ambient Temperature and No Decay Heat Load

		Total Stress Range** (ksi)				Principal Stresses			Stress Differences		
Comp. No.*	Node	S_x	S_y	S_z	S_{xy}	S_1	S_2	S_3	S_1-S_2	S_2-S_3	S_3-S_1
1	2376	0.96	-3.75	-0.64	-0.11	0.96	-0.64	-3.75	1.60	3.11	-4.71
3	2176	3.74	-17.36	-1.84	-2.41	4.01	-1.84	-17.63	5.85	15.79	-21.64
4	604	-0.58	-10.47	-1.81	0.56	-0.55	-1.81	-10.50	1.26	8.69	-9.95
6	615	0.00	-7.05	-0.19	0.00	0.00	-0.19	-7.05	0.19	6.86	-7.05
7	143	0.08	-23.96	-3.03	-2.73	0.39	-3.03	-24.27	3.42	21.24	-24.65
8	361	-0.02	-10.55	0.26	-1.38	0.26	0.16	-10.73	0.10	10.89	-10.99

* Refer to Figure 2.10.2-9 for component identification.

** Conservatively based on a 1.12-inch thick outer shell and on a 3,850-psi crush strength aluminum honeycomb impact limiter (Section 2.7.1.1).

Table 2.7.1-10 Critical Stress Summary (30-Foot Top End Drop) – Loading Condition 1 – P_m

Loading Condition 1: 130°F Ambient Temperature and Maximum Decay Heat Load

		P_m Stresses** (ksi)				Principal Stresses					
Comp. No.*	Section Cut Node to Node	S_x	S_y	S_z	S_{xy}	S_1	S_2	S_3	S.I.	Allow. Stress 0.7 S_u	Margin of Safety
	2-2										
1	2377 to 2577	-7.46	-0.06	0.09	0.15	0.09	-0.05	-7.46	7.55	46.2	+5.12
	4-4										
3	1581 to 1584	-0.20	-7.58	-0.57	-0.33	-0.18	-0.57	-7.60	7.42	46.2	+5.29
	5-5										
4	1481 to 1484	-0.03	-8.19	0.52	0.02	0.52	-0.03	-8.19	8.71	46.2	+6.57
	12-12										
6	695 to 698	0.00	2.39	-0.10	0.04	2.40	0.00	-0.10	2.50	46.2	Large
	10-10										
7	17 to 117	-1.04	1.54	2.36	-2.84	3.37	2.36	-2.87	6.23	46.2	+6.42
	7-7										
8	401 to 405	-0.03	-2.63	1.89	-0.39	1.89	0.03	-2.69	4.58	46.2	+9.09

* Refer to Figure 2.10.2-9 for component identification.

** Conservatively based on a 1.12-inch thick outer shell and on a 3,850-psi crush strength aluminum honeycomb impact limiter (Section 2.7.1.1).

Table 2.7.1-11 Critical Stress Summary (30-Foot Top End Drop) – Loading Condition 1 – $P_m + P_b$

Loading Condition 1: 130°F Ambient Temperature and Maximum Decay Heat Load

		$P_m + P_b$ Stresses** (ksi)				Principal Stresses					
Comp. No.*	Section Cut Node to Node	S_x	S_y	S_z	S_{xy}	S_1	S_2	S_3	S.I.	Allow. Stress 1.0 S_u	Margin of Safety
	1-1										
1	2371 to 2571	-12.69	-0.13	-0.22	-1.01	-0.05	-0.22	-12.77	12.72	66.0	+4.19
	3-3										
3	1941 to 1956	0.84	-10.28	-3.31	0.03	0.84	-3.31	-10.28	11.12	66.0	+4.94
	11-11										
4	1561 to 1564	0.12	-9.50	-0.89	-0.22	0.13	-0.89	-9.51	9.64	94.3	+8.78
	6-6										
6	615 to 618	-0.02	3.50	0.78	0.00	3.50	0.78	-0.02	3.52	94.3	Large
	9-9										
7	143 to 150	-7.68	6.60	1.37	1.33	6.72	1.37	-7.80	14.52	66.0	+3.55
	8-8										
8	381 to 385	-0.15	-6.77	0.67	-0.49	0.67	-0.12	-6.81	7.47	66.0	+7.84

* Refer to Figure 2.10.2-9 for component identification.

** Conservatively based on a 1.12-inch thick outer shell and on a 3,850-psi crush strength aluminum honeycomb impact limiter (Section 2.7.1.1).

Table 2.7.1-12 Critical Stress Summary (30-Foot Top End Drop) – Loading Condition 1 – Total Range

Loading Condition 1: 130°F Ambient Temperature and Maximum Decay Heat Load

		Total Stress Range** (ksi)				Principal Stresses			Stress Differences		
Comp. No.*	Node	S_x	S_y	S_z	S_{xy}	S_1	S_2	S_3	S_1-S_2	S_2-S_3	S_3-S_1
1	2371	2.76	-10.30	0.04	3.56	3.67	0.04	-11.21	3.63	11.25	-14.88
3	1962	-1.54	-12.69	-5.46	-1.00	-1.45	-5.46	-13.05	4.01	7.59	-11.60
4	1584	-0.62	-10.96	-1.54	-0.54	-0.59	-1.54	-10.99	0.95	9.45	-10.40
6	615	-0.01	3.43	0.72	-0.01	3.43	0.72	-0.01	2.71	0.73	-3.44
7	143	-7.68	6.79	1.34	2.96	7.37	1.34	-8.26	6.03	9.60	-15.63
8	361	-0.07	-8.76	-0.09	-0.78	0.00	-0.09	-8.83	0.09	8.74	-8.83

* Refer to Figure 2.10.2-9 for component identification.

** Conservatively based on a 1.12-inch thick outer shell and on a 3,850-psi crush strength aluminum honeycomb impact limiter (Section 2.7.1.1).

Table 2.7.1-13 Critical Stress Summary (30-Foot Top End Drop) – Loading Condition 2 – P_m

Loading Condition 2: -40°F Ambient Temperature and Maximum Decay Heat Load

		P_m Stresses** (ksi)				Principal Stresses					
Comp. No.*	Section Cut Node to Node	S_x	S_y	S_z	S_{xy}	S_1	S_2	S_3	S.I.	Allow. Stress 0.7 S_u	Margin of Safety
	2-2										
1	2377 to 2577	-7.42	-0.08	0.30	0.18	0.30	-0.08	-7.42	7.72	46.2	+4.98
	4-4										
3	1581 to 1584	-0.24	-10.89	-1.33	-0.44	-0.22	-1.33	-10.91	10.69	46.2	+3.32
	6-6										
4	1481 to 1484	-0.02	-11.17	0.24	0.04	0.24	-0.02	-11.77	12.01	66.0	+4.59
	5-5										
6	1595 to 1598	0.01	-2.37	1.0	0.02	1.0	0.01	-2.37	3.37	66.0	Large
	10-10										
7	375 to 378	-1.35	1.92	2.97	-0.61	2.97	2.03	-1.45	4.42	46.2	+9.45
	8-8										
8	601 to 604	-0.13	-7.55	-0.80	0.27	-0.12	-0.80	-7.56	7.44	46.2	+5.21

* Refer to Figure 2.10.2-9 for component identification.

** Conservatively based on a 1.12-inch thick outer shell and on a 3,850-psi crush strength aluminum honeycomb impact limiter (Section 2.7.1.1).

Table 2.7.1-14 Critical Stress Summary (30-Foot Top End Drop) – Loading Condition 2 – $P_m + P_b$

Loading Condition 2: -40°F Ambient Temperature and Maximum Decay Heat Load

		$P_m + P_b$ Stresses** (ksi)				Principal Stresses					
Comp. No.*	Section Cut Node to Node	S_x	S_y	S_z	S_{xy}	S_1	S_2	S_3	S.I.	Allow. Stress 1.0 S_u	Margin of Safety
	1-1										
1	2371 to 2571	-12.88	-0.21	-0.19	-1.02	-0.13	-0.19	-12.96	12.84	66.0	+4.14
	4-4										
3	1581 to 1584	-0.52	-12.05	-1.44	-0.45	-0.51	-1.44	-12.07	11.56	66.0	+4.71
	3-3										
4	1561 to 1564	0.17	-13.22	-1.52	-0.30	0.17	-1.52	-13.23	13.40	94.3	+6.03
	5-5										
6	1595 to 1598	0.04	-3.78	0.86	0.02	0.86	0.04	-3.78	4.64	94.3	Large
	9-9										
7	395 to 398	-0.18	7.35	4.97	-0.78	7.42	4.97	-0.26	7.69	66.0	+7.58
	8-8										
8	601 to 604	-0.18	-7.94	-0.67	0.27	-0.18	-0.67	-7.95	7.78	66.0	+7.48

* Refer to Figure 2.10.2-9 for component identification.

** Conservatively based on a 1.12-inch thick outer shell and on a 3,850-psi crush strength aluminum honeycomb impact limiter (Section 2.7.1.1).

Table 2.7.1-15 Critical Stress Summary (30-Foot Top End Drop) – Loading Condition 2 – Total Range

Loading Condition 2: -40°F Ambient Temperature and Maximum Decay Heat Load

		Total Stress Range** (ksi)				Principal Stresses			Stress Differences		
Comp. No.*	Node	S_x	S_y	S_z	S_{xy}	S_1	S_2	S_3	S_1-S_2	S_2-S_3	S_3-S_1
1	2371	2.56	-10.43	0.01	3.61	3.50	0.01	-11.37	3.49	11.38	-14.87
3	1962	-1.54	-12.88	-5.92	-1.05	-1.44	-5.92	-12.98	4.48	7.06	-11.54
4	1584	-0.85	-15.19	-2.48	-0.76	-0.81	-2.48	-15.23	1.67	12.75	-14.42
6	1598	0.02	-3.94	0.76	0.02	0.76	0.02	-3.94	0.74	3.96	-4.70
7	378	-0.19	7.42	4.95	-0.07	7.42	4.95	-0.19	2.47	5.14	-7.61
8	361	-0.02	-7.21	-1.7	-1.0	0.16	-1.70	-7.38	1.86	5.68	-7.54

* Refer to Figure 2.10.2-9 for component identification.

** Conservatively based on a 1.12-inch thick outer shell and on a 3,850-psi crush strength aluminum honeycomb impact limiter (Section 2.7.1.1).

Table 2.7.1-16 Side Drop Load Analysis Description

Load Analysis No.	Description	ANSYS Mode No.**
1	Bolt Preload + Internal Pressure	0
2	Thermal + Bolt Preload + Internal Pressure	0
3	Inertial Body Load (excluding content load)	1
4	Impact Load + Content Load*	0
5	Impact Load + Content Load*	1
6	Impact Load + Content Load*	2
7	Impact Load + Content Load*	3
8	Impact Load + Content Load*	4
9	Impact Load + Content Load*	5

* The same circumferential distribution arc is applied to both the impact load and content load.

** ANSYS Mode No. "0" indicates loading type is axisymmetric, while other positive numbers indicate loading types are nonaxisymmetric.

Table 2.7.1-17 Critical Stress Summary (30-Foot Side Drop) – Loading Condition 1 – P_m

Loading Condition 1: 100°F Ambient Temperature and Maximum Decay Heat Load

		P_m Stresses (ksi)				Principal Stresses					
Comp. No.*	Section Cut Node to Node	S_x	S_y	S_z	S_{xy}	S_1	S_2	S_3	S.I.	Allow. Stress 0.7 S_u	Margin of Safety
	1-1										
1	2361 to 2370	-6.94	-0.61	0.13	-0.53	0.13	-0.57	-6.99	7.12	46.2	+5.49
	2-2										
3	1969 to 1976	-20.74	3.86	-9.26	-3.37	4.32	-9.26	-21.20	25.51	46.2	+0.81
	3-3										
4	1141 to 1144	-0.22	31.55	0.52	0.00	31.55	0.52	-0.22	31.77	66.0	+1.08
	4-4										
6	1115 to 1118	-0.10	65.09	2.67	0.00	65.09	2.67	-0.10	65.19	66.0	+0.01
	5-5										
7	395 to 398	-4.44	8.30	-11.27	1.59	8.49	-4.64	-11.27	19.76	46.2	+1.34
	6-6										
8	192 to 342	-11.19	-0.72	-6.26	0.36	-0.71	-6.26	-11.20	10.50	46.2	+3.40

* Refer to Figure 2.10.2-9 for component identification.

Table 2.7.1-18 Critical Stress Summary (30-Foot Side Drop) – Loading Condition 1 – $P_m + P_b$

Loading Condition 1: 100°F Ambient Temperature and Maximum Decay Heat Load

		$P_m + P_b$ Stresses (ksi)				Principal Stresses					
Comp. No.*	Section Cut Node to Node	S_x	S_y	S_z	S_{xy}	S_1	S_2	S_3	S.I.	Allow. Stress 1.0 S_u	Margin of Safety
	7-7										
1	2301 to 2561	-1.60	0.12	1.68	8.10	7.40	1.68	-8.88	16.29	66.0	+3.05
	8-8										
3	2150 to 2156	-8.99	-0.17	-41.23	0.03	-0.17	-8.99	-41.23	41.06	66.0	+0.61
	3-3										
4	1141 to 1144	-0.15	33.56	1.75	0.00	33.56	1.75	-0.15	33.71	94.3	+1.80
	4-4										
6	1115 to 1118	0.02	68.25	3.06	0.00	68.25	3.06	0.02	68.23	94.3	+0.38
	5-5										
7	395 to 398	-2.27	32.90	-1.83	1.59	32.97	-1.83	-2.34	35.31	66.0	+0.87
	9-9										
8	177 to 327	-16.88	-3.68	0.56	-3.01	0.56	-3.03	-17.54	18.10	66.0	+2.65

* Refer to Figure 2.10.2-9 for component identification.

Table 2.7.1-19 Critical Stress Summary (30-Foot Side Drop) – Loading Condition 1 – Total Range

Loading Condition 1: 100°F Ambient Temperature and Maximum Decay Heat Load

		Total Stress Range** (ksi)				Principal Stresses			Stress Differences		
Comp. No.*	Node	S_x	S_y	S_z	S_{xy}	S_1	S_2	S_3	S_1-S_2	S_2-S_3	S_3-S_1
1	2561	0.13	0.04	2.72	31.16	31.25	2.72	-31.07	28.53	33.79	-62.32
3	1815	3.52	50.86	7.38	15.09	55.33	7.38	-0.94	47.95	8.32	-56.27
4	1144	-0.15	35.89	1.96	0.00	35.89	1.96	-0.15	33.93	2.11	-56.27
6	1118	0.02	77.67	3.29	0.00	77.67	3.29	0.02	74.38	3.27	-77.65
7	395	-2.26	46.39	2.66	3.07	46.59	2.66	-2.46	43.93	5.12	-49.05
8	177	-46.95	-2.35	-18.78	-1.66	-2.25	-18.78	-47.05	16.53	28.27	-44.80

* Refer to Figure 2.10.2-9 for component identification.

Table 2.7.1-20 G Loads – Oblique Drop

Drop Orientation	G Load*	Adjusted G Load**	Lateral Component	Axial Component
15.74°	60.4	77.27	20.96	74.37
30.0°	54.4	69.59	34.80	60.27
45.0°	43.8	56.03	39.62	39.62
60.0°	44.4	56.80	49.19	28.40

* Refer to Section 2.6.7.4 for g load calculations. The g loads are conservatively based on a maximum crush strength of 3850 psi for the aluminum honeycomb impact limiters, although the design maximum crush strength is 3675 psi.

** Adjusted g load = (g load)(cask body weight/model weight)
= (g load)(48,000/37,519)

Table 2.7.1-21 Impact and Contents Pressures – Oblique Drop

Impact Location	Drop Orientation	θ Angle*	Impact Pressure* (psi)		Content Pressure* (psi)	
			Lateral	Axial	Lateral	Axial
Top	15.74°	90.00°	3370	14768	35	5298.8
Top	30.0°	83.34°	5834	12925	60.6	4637.5
Top	45.0°	65.32°	7812	10840	81.2	3889.4
Top	60.0°	52.88°	11470	9599	119.3	3444.1
Bottom	15.74°	90.00°	3292	14768	34.9	5199.8
Bottom	30.0°	87.59°	5549	12294	58.8	4328.7
Bottom	45.0°	68.35°	7389	10359	78.3	3647.4
Bottom	60.0°	55.22°	10820	9191	114.7	3236.2

* The angle 2θ determines the pressure distribution arc in the circumferential direction (Figure 2.7.1-9). The same arc is chosen for both impact pressure and content pressure to be applied.

Table 2.7.1-22 Fourier Series Modal Coefficients – Oblique Drop

		Fourier Series Coefficents for Each Loading Mode					
Impact Location	Drop Orientation	Mode 0	Mode 1	Mode 2	Mode 3	Mode 4	Mode 5
Top	15.74°	0.318334	0.500064	0.212287	0.000064	-0.042393	0.000064
Top	30.0°	0.294779	0.479776	0.236186	0.030107	-0.041325	-0.015759
Top	45.0°	0.230640	0.407149	0.271864	0.119183	0.009851	-0.031607
Top	60.0°	0.186891	0.344502	0.266534	0.165172	0.070325	0.004581
Bottom	15.74°	0.318334	0.500064	0.212287	0.000064	-0.042393	0.000064
Bottom	30.0°	0.309638	0.493021	0.221703	0.010632	-0.043160	-0.005739
Bottom	45.0°	0.241699	0.421390	0.269221	0.104574	-0.003428	-0.034201
Bottom	60.0°	0.195189	0.357110	0.239495	0.158298	0.058632	-0.005100

Table 2.7.1-23 Oblique Drop Load Analysis Description

Load Analysis No.	Description	ANSYS Mode No.*
1	Bolt Preload + Internal Pressure	0
2	Thermal + Bolt Preload + Internal Pressure	0
3	Inertial Body Load (Lateral Direction)	1
4	Inertial Body Load (Axial Direction)	0
5	Impact Load + Content Load (Lateral)	0
6	Impact Load + Content Load (Lateral)	1
7	Impact Load + Content Load (Lateral)	2
8	Impact Load + Content Load (Lateral)	3
9	Impact Load + Content Load (Lateral)	4
10	Impact Load + Content Load (Lateral)	5
11	Impact Load + Content Load (Axial)	0
12	Impact Load + Content Load (Axial)	1
13	Impact Load + Content Load (Axial)	2
14	Impact Load + Content Load (Axial)	3
15	Impact Load + Content Load (Axial)	4
16	Impact Load + Content Load (Axial)	5

* ANSYS Mode No. "0" indicates loading type is axisymmetric, while other positive numbers indicate loading types are nonaxisymmetric.

Table 2.7.1-24 Critical Stress Summary (30-Foot Top Corner Drop) – Loading Condition 1 – P_m – Drop Orientation = 15.74 Degrees

Loading Condition 1: 130°F Ambient Temperature and Maximum Decay Heat Load

		P_m Stresses (ksi)**				Principal Stresses					
Comp. No.*	Section Cut Node to Node	S_x	S_y	S_z	S_{xy}	S_1	S_2	S_3	S.I.	Allow. Stress 0.7 S_u	Margin of Safety
	1-1										
1	2377 to 2577	-24.38	-1.69	-3.35	-0.98	-1.65	-3.35	-24.42	22.78	46.2	+1.03
	2-2										
3	1775 to 1778	-0.26	-21.63	2.63	0.06	2.63	-0.26	-21.63	24.26	46.2	+0.90
	3-3										
4	1561 to 1564	0.12	-17.16	-2.01	-0.63	0.14	-2.01	-17.18	17.32	66.0	+2.81
	4-4										
6	1595 to 1598	-0.03	-19.40	2.58	0.13	2.58	-0.03	-19.40	21.98	66.0	+2.00
	5-5										
7	18 to 118	-2.47	4.23	-1.43	-2.23	4.91	-1.43	-3.15	8.05	46.2	+4.74
	6-6										
8	361 to 365	-3.72	-2.79	-0.23	-0.26	-0.23	-2.72	-3.79	3.56	46.2	Large

* Refer to Figure 2.10.2-9 for component identification.

** Conservatively based on a 1.12-inch thick outer shell and on a 3,850-psi maximum crush strength aluminum honeycomb impact limiter (Section 2.7.1.3).

Table 2.7.1-25 Critical Stress Summary (30-Foot Top Corner Drop) – Loading Condition 1 – $P_m + P_b$ – Drop Orientation = 15.74 Degrees

Loading Condition 1: 130°F Ambient Temperature and Maximum Decay Heat Load

		$P_m + P_b$ Stresses (ksi)**				Principal Stresses					
Comp. No.*	Section Cut Node to Node	S_x	S_y	S_z	S_{xy}	S_1	S_2	S_3	S.I.	Allow. Stress 1.0 S_u	Margin of Safety
	1-1										
1	2377 to 2577	-27.51	-1.69	-3.35	-0.98	-1.65	-3.35	-27.55	25.90	66.0	+1.55
	2-2										
3	1775 to 1778	0.08	-20.95	7.55	1.47	7.55	0.18	-21.05	28.60	66.0	+1.31
	3-3										
4	1561 to 1564	0.33	-22.71	-4.58	-0.63	0.35	-4.58	-22.72	23.07	94.3	+3.09
	4-4										
6	1595 to 1598	0.04	-19.76	2.23	0.13	2.23	0.04	-19.77	22.00	94.3	+3.29
	8-8										
7	143 to 150	-8.20	17.26	0.73	1.81	17.39	0.73	-8.33	25.72	66.0	+1.57
	9-9										
8	381 to 385	-5.72	-7.78	0.83	-1.47	0.83	-4.95	-8.54	9.38	66.0	+6.04

* Refer to Figure 2.10.2-9 for component identification.

** Conservatively based on a 1.12-inch thick outer shell and on a 3,850-psi maximum crush strength aluminum honeycomb impact limiter (Section 2.7.1.3).

Table 2.7.1-26 Critical Stress Summary (30-Foot Top Corner Drop) – Loading Condition 1 – Total Range – Drop Orientation = 15.74 Degrees

Loading Condition 1: 130°F Ambient Temperature and Maximum Decay Heat Load

		Total Stress Range** (ksi)				Principal Stresses			Stress Differences		
Comp. No.*	Node	S_x	S_y	S_z	S_{xy}	S_1	S_2	S_3	S_1-S_2	S_2-S_3	S_3-S_1
1	2561***	2.74	-6.25	-3.49	215.9	214.19	-3.49	-217.70	217.68	214.21	-431.89
3	1815	-1.46	-18.25	2.52	0.59	2.52	-1.44	-18.27	3.96	16.83	-20.79
4	1584	-1.38	-23.60	-4.79	-1.37	-1.30	-4.79	-23.68	3.49	18.89	-22.39
6	1595	-0.06	-7.75	3.43	2.38	3.43	0.62	-8.43	2.81	9.04	-11.86
7	2	-8.20	21.90	2.18	3.88	22.39	2.18	-8.69	20.21	10.87	-31.08
8	361	-15.56	-9.27	-6.28	-1.30	-6.28	-9.01	-15.82	2.73	6.81	-9.54

* Refer to Figure 2.10.2-9 for component identification.

** Conservatively based on a 1.12-inch thick outer shell and on a 3,850-psi maximum crush strength aluminum honeycomb impact limiter (Section 2.7.1.3).

*** Stresses at node 2561 are unrealistic, resulting from the boundary effect. See Section 2.7.1.3.3 for the discussion of the boundary effect on the stress results.

Table 2.7.1-27 Critical Stress Summary (30-Foot Top Oblique Drop) – Loading Condition 1 – P_m – Drop Orientation = 30 Degrees

Loading Condition 1: 130°F Ambient Temperature and Maximum Decay Heat Load

		P_m Stresses (ksi)**				Principal Stresses					
Comp. No.*	Section Cut Node to Node	S_x	S_y	S_z	S_{xy}	S_1	S_2	S_3	S.I.	Allow. Stress 0.7 S_u	Margin of Safety
	1-1										
1	2302 to 2562	-18.88	-13.60	2.04	-10.79	2.04	-5.13	-27.35	29.39	46.2	+0.57
	2-2										
3	2150 to 2156	-3.01	-12.69	-26.09	0.09	-3.01	-12.69	-26.09	23.07	46.2	+1.00
	3-3										
4	941 to 944	-0.07	14.41	0.82	0.00	14.41	0.82	-0.07	14.48	66.0	+3.56
	4-4										
6	1035 to 1038	-0.05	30.01	1.60	0.00	30.01	1.60	-0.05	30.06	66.0	+1.20
	5-5										
7	168 to 175	-3.25	5.75	-4.31	-1.36	5.95	-3.45	-4.31	10.26	46.2	+3.50
	6-6										
8	176 to 326	-6.14	-2.46	-1.94	-0.11	-1.94	-2.46	-6.15	4.21	46.2	+9.98

* Refer to Figure 2.10.2-9 for component identification.

** Conservatively based on a 1.12-inch thick outer shell and on a 3,850-psi maximum crush strength aluminum honeycomb impact limiter (Section 2.7.1.3).

Table 2.7.1-28 Critical Stress Summary (30-Foot Top Oblique Drop) – Loading Condition 1 – $P_m + P_b$ – Drop Orientation = 30 Degrees

Loading Condition 1: 130°F Ambient Temperature and Maximum Decay Heat Load

		$P_m + P_b$ Stresses (ksi)**				Principal Stresses					
Comp. No.*	Section Cut Node to Node	S_x	S_y	S_z	S_{xy}	S_1	S_2	S_3	S.I.	Allow. Stress 1.0 S_u	Margin of Safety
	1-1										
1	2302 to 2562	2.72	-13.60	2.04	-10.79	8.09	2.04	-18.97	27.06	66.0	+1.44
	7-7										
3	1821 to 1825	0.06	-20.55	7.79	1.54	7.79	0.17	-20.66	28.46	66.0	+1.32
	8-8										
4	1561 to 1564	0.29	-18.93	-3.81	-0.57	0.30	-3.81	-18.95	19.25	94.3	+3.90
	4-4										
6	1035 to 1038	0.01	31.34	1.65	0.00	31.34	1.65	0.01	31.33	94.3	+2.00
	9-9										
7	143 to 150	-7.27	23.18	0.07	1.91	23.80	0.07	-7.39	30.69	66.0	+1.15
	6-6										
8	176 to 326	-9.35	-7.33	0.83	-2.03	0.83	-6.07	-10.61	11.44	66.0	+4.77

* Refer to Figure 2.10.2-9 for component identification.

** Conservatively based on a 1.12-inch thick outer shell and on a 3,850-psi maximum crush strength aluminum honeycomb impact limiter (Section 2.7.1.3).

Table 2.7.1-29 Critical Stress Summary (30-Foot Top Oblique Drop) – Loading Condition 1 – Total Range – Drop Orientation = 30 Degrees

Loading Condition 1: 130°F Ambient Temperature and Maximum Decay Heat Load

		Total Stress Range** (ksi)				Principal Stresses			Stress Differences		
Comp. No.*	Node	S_x	S_y	S_z	S_{xy}	S_1	S_2	S_3	S_1-S_2	S_2-S_3	S_3-S_1
1	2561***	2.57	-5.32	-2.66	423.0	421.64	-2.66	-424.39	424.30	421.73	-846.04
3	1856	0.38	-7.44	3.51	-0.14	3.51	0.38	-7.44	3.13	7.83	-10.95
4	1584	-1.14	-19.57	-3.72	-1.19	-1.06	-3.72	-19.65	2.66	15.93	-18.58
6	1038	0.01	41.20	1.89	0.00	41.20	1.89	0.01	39.31	1.88	-41.19
7	25	-7.27	30.71	2.51	4.00	31.12	2.51	-7.68	28.62	10.19	-38.81
8	177	-25.74	-8.16	-10.34	-1.52	-8.03	-10.34	-25.87	2.31	15.52	-17.84

* Refer to Figure 2.10.2-9 for component identification.

** Conservatively based on a 1.12-inch thick outer shell and on a 3,850-psi maximum crush strength aluminum honeycomb impact limiter (Section 2.7.1.3).

*** Stresses at node 2561 are unrealistic, resulting from the boundary effect. See Section 2.7.1.3.3 for the discussion of the boundary effect on the stress results.

Table 2.7.1-30 Critical Stress Summary (30-Foot Top Oblique Drop) – Loading Condition 1 – P_m – Drop Orientation = 45 Degrees

Loading Condition 1: 130°F Ambient Temperature and Maximum Decay Heat Load

		P_m Stresses (ksi)**				Principal Stresses					
Comp. No.*	Section Cut Node to Node	S_x	S_y	S_z	S_{xy}	S_1	S_2	S_3	S.I.	Allow. Stress 0.7 S_u	Margin of Safety
	1-1										
1	2302 to 2562	-20.53	-16.65	3.19	-13.28	3.19	-5.17	-32.01	35.21	46.2	+0.31
	2-2										
3	2150 to 2156	-3.91	-10.88	-30.14	0.10	-3.91	-10.88	-30.14	26.23	46.2	+0.76
	3-3										
4	961 to 964	-0.09	17.88	0.84	0.01	17.88	0.84	-0.09	17.97	66.0	+2.67
	4-4										
6	1055 to 1058	-0.06	37.32	1.84	0.00	37.32	1.84	-0.06	37.38	66.0	+0.77
	5-5										
7	615 to 618	-3.31	5.98	-5.81	-0.48	6.00	-3.33	-5.81	11.81	46.2	+2.91
	6-6										
8	176 to 326	-7.00	-1.81	-2.93	0.02	-1.81	-2.93	-7.00	5.19	46.2	+7.90

* Refer to Figure 2.10.2-9 for component identification.

** Conservatively based on a 1.12-inch thick outer shell and on a 3,850-psi maximum crush strength aluminum honeycomb impact limiter (Section 2.7.1.3).

Table 2.7.1-31 Critical Stress Summary (30-Foot Top Oblique Drop) – Loading Condition 1 – $P_m + P_b$ – Drop Orientation = 45 Degrees

Loading Condition 1: 130°F Ambient Temperature and Maximum Decay Heat Load

		$P_m + P_b$ Stresses (ksi)**				Principal Stresses					
Comp. No.*	Section Cut Node to Node	S_x	S_y	S_z	S_{xy}	S_1	S_2	S_3	S.I.	Allow. Stress 1.0 S_u	Margin of Safety
	1-1										
1	2302 to 2562	7.92	-16.65	3.19	-13.28	13.73	3.19	-22.45	36.18	66.0	+0.82
	7-7										
3	1969 to 1996	-44.85	-17.81	-11.30	0.12	-11.30	-17.81	-44.85	33.55	66.0	+0.97
	3-3										
4	961 to 964	-0.03	19.01	1.30	0.01	19.01	1.30	-0.03	19.05	94.3	+3.95
	4-4										
6	1055 to 1058	0.01	39.00	1.96	0.00	39.00	1.96	0.01	38.99	94.3	+1.41
	8-8										
7	143 to 150	-5.39	23.94	-0.43	1.68	24.04	-0.43	-5.48	29.52	66.0	+1.24
	6-6										
8	176 to 326	-10.61	-5.80	0.70	-2.13	0.70	-4.99	-11.42	12.11	66.0	+4.45

* Refer to Figure 2.10.2-9 for component identification.

** Conservatively based on a 1.12-inch thick outer shell and on a 3,850-psi maximum crush strength aluminum honeycomb impact limiter (Section 2.7.1.3).

Table 2.7.1-32 Critical Stress Summary (30-Foot Top Oblique Drop) – Loading Condition 1 – Total Range – Drop Orientation = 45 Degrees

Loading Condition 1: 130°F Ambient Temperature and Maximum Decay Heat Load

		Total Stress Range** (ksi)				Principal Stresses			Stress Differences		
Comp. No.*	Node	S_x	S_y	S_z	S_{xy}	S_1	S_2	S_3	S_1-S_2	S_2-S_3	S_3-S_1
1	2561***	2.31	-3.96	-1.76	508.3	507.48	-1.76	-509.13	509.24	507.37	-1016.62
3	1969	-47.18	-32.83	-18.27	5.25	-18.27	-30.95	-49.06	12.68	18.11	-30.79
4	964	-0.02	21.80	1.65	0.02	21.80	1.65	-0.02	20.15	1.67	-21.82
6	1058	0.01	48.86	2.21	0.00	48.86	2.21	0.01	46.65	2.20	-48.85
7	25	-5.38	32.46	2.35	3.45	32.77	2.35	-5.69	30.42	8.04	-38.46
8	177	-29.33	-6.00	-11.77	-1.44	-5.91	-11.77	-29.42	5.86	17.66	-23.51

* Refer to Figure 2.10.2-9 for component identification.

** Conservatively based on a 1.12-inch thick outer shell and on a 3,850-psi maximum crush strength aluminum honeycomb impact limiter (Section 2.7.1.3).

*** Stresses at node 2561 are unrealistic, resulting from the boundary effect. See Section 2.7.1.3.3 for the discussion of the boundary effect on the stress results.

Table 2.7.1-33 Critical Stress Summary (30-Foot Top Oblique Drop) – Loading Condition 1 – P_m – Drop Orientation = 60 Degrees

Loading Condition 1: 130°F Ambient Temperature and Maximum Decay Heat Load

		P_m Stresses (ksi)**				Principal Stresses					
Comp. No.*	Section Cut Node to Node	S_x	S_y	S_z	S_{xy}	S_1	S_2	S_3	S.I.	Allow. Stress 0.7 S_u	Margin of Safety
	1-1										
1	2302 to 2562	-24.77	-21.65	4.65	-17.41	4.65	-5.72	-40.69	45.35	46.2	+0.02
	2-2										
3	2150 to 2156	-5.64	-9.89	-36.97	0.13	-5.63	-9.90	-36.97	31.34	46.2	+0.47
	3-3										
4	981 to 984	-0.15	23.48	0.65	0.03	23.48	0.65	-0.15	23.63	66.0	+1.79
	4-4										
6	1075 to 1078	-0.08	49.11	2.30	0.00	49.11	2.30	-0.08	49.19	66.0	+0.34
	5-5										
7	615 to 618	-3.83	7.00	-7.86	0.18	7.01	-3.83	-7.86	14.87	46.2	+2.11
	6-6										
8	176 to 326	-8.68	-1.53	-4.15	0.13	-1.53	-4.15	-8.69	7.16	46.2	+5.45

* Refer to Figure 2.10.2-9 for component identification.

** Conservatively based on a 1.12-inch thick outer shell and on a 3,850-psi maximum crush strength aluminum honeycomb impact limiter (Section 2.7.1.3).

Table 2.7.1-34 Critical Stress Summary (30-Foot Top Oblique Drop) – Loading Condition 1 – $P_m + P_b$ – Drop Orientation = 60 Degrees

Loading Condition 1: 130°F Ambient Temperature and Maximum Decay Heat Load

		$P_m + P_b$ Stresses (ksi)**				Principal Stresses					
Comp. No.*	Section Cut Node to Node	S_x	S_y	S_z	S_{xy}	S_1	S_2	S_3	S.I.	Allow. Stress 1.0 S_u	Margin of Safety
	1-1										
1	2302 to 2562	14.65	-21.65	4.65	-17.41	21.66	4.65	-28.65	50.31	66.0	+0.31
	7-7										
3	1969 to 2016	-62.10	-19.16	-9.36	2.21	-9.36	-19.05	-62.22	52.86	66.0	+0.25
	3-3										
4	981 to 984	-0.09	24.96	1.44	0.03	24.96	1.44	-0.09	25.06	94.3	+2.76
	4-4										
6	1075 to 1078	0.01	51.35	2.56	0.00	51.35	2.56	0.01	51.33	94.3	+0.84
	8-8										
7	125 to 168	-4.60	27.94	-0.91	1.72	28.03	-0.91	-4.69	32.72	66.0	+1.02
	6-6										
8	176 to 326	-13.14	-5.36	0.68	-2.51	0.68	-4.62	-13.88	14.56	66.0	+3.53

* Refer to Figure 2.10.2-9 for component identification.

** Conservatively based on a 1.12-inch thick outer shell and on a 3,850-psi maximum crush strength aluminum honeycomb impact limiter (Section 2.7.1.3).

Table 2.7.1-35 Critical Stress Summary (30-Foot Top Oblique Drop) – Loading Condition 1 – Total Range – Drop Orientation = 60 Degrees

Loading Condition 1: 130°F Ambient Temperature and Maximum Decay Heat Load

		Total Stress Range** (ksi)				Principal Stresses			Stress Differences		
Comp. No.*	Node	S_x	S_y	S_z	S_{xy}	S_1	S_2	S_3	S_1-S_2	S_2-S_3	S_3-S_1
1	2561***	1.60	-3.05	-0.43	655.2	654.48	-0.43	-655.93	654.91	655.50	-1310.41
3	1969	-67.53	-43.53	-23.94	-1.29	-23.94	-43.46	-67.60	19.52	24.14	-43.66
4	984	-0.08	27.75	1.78	0.03	27.75	1.78	-0.08	25.97	1.86	-27.83
6	1078	0.02	61.20	2.81	0.00	61.20	2.81	0.02	58.39	2.79	-61.18
7	25	-4.59	38.46	2.56	3.47	38.74	2.56	-4.87	36.19	7.43	-43.61
8	177	-36.41	-5.06	-14.59	-1.58	-4.98	-14.59	-36.49	9.60	21.90	-31.51

* Refer to Figure 2.10.2-9 for component identification.

** Conservatively based on a 1.12-inch thick outer shell and on a 3,850-psi maximum crush strength aluminum honeycomb impact limiter (Section 2.7.1.3).

*** Stresses at node 2561 are unrealistic, resulting from the boundary effect. See Section 2.7.1.3.3 for the discussion of the boundary effect on the stress results.

Table 2.7.1-36 Critical Stress Summary (30-Foot Top Corner Drop) – Loading Condition 3 – P_m – Drop Orientation = 15.74 Degrees

Loading Condition 3: -40°F Ambient Temperature and No Decay Heat Load

		P_m Stresses (ksi)**				Principal Stresses					
Comp. No.*	Section Cut Node to Node	S_x	S_y	S_z	S_{xy}	S_1	S_2	S_3	S.I.	Allow. Stress 0.7 S_u	Margin of Safety
	1-1										
1	2377 to 2577	-23.41	-1.57	-3.70	-1.18	-1.50	-3.70	-23.48	21.97	46.2	+1.1
	2-2										
3	1775 to 1778	-0.30	-20.30	3.03	0.08	3.03	-0.30	-20.30	23.33	46.2	+1.0
	3-3										
4	1561 to 1564	0.14	-13.57	-2.03	-0.54	0.16	-2.03	-13.59	13.75	66.0	+3.80
	4-4										
6	1595 to 1598	-0.03	-18.20	2.61	0.15	2.61	-0.03	-18.20	20.82	66.0	+2.17
	5-5										
7	168 to 175	-2.77	4.60	-0.84	-0.07	4.60	-0.84	-2.78	7.38	46.2	+5.26
	6-6										
8	381 to 385	-3.82	-7.56	-2.84	0.38	-2.84	-3.78	-7.60	4.76	46.2	+8.71

* Refer to Figure 2.10.2-9 for component identification.

** Conservatively based on a 1.12-inch thick outer shell and on a 3,850-psi maximum crush strength aluminum honeycomb impact limiter (Section 2.7.1.3).

Table 2.7.1-37 Critical Stress Summary (30-Foot Top Corner Drop) – Loading Condition 3 – $P_m + P_b$ – Drop Orientation = 15.74 Degrees

Loading Condition 3: -40°F Ambient Temperature and No Decay Heat Load

		$P_m + P_b$ Stresses (ksi)**				Principal Stresses					
Comp. No.*	Section Cut Node to Node	S_x	S_y	S_z	S_{xy}	S_1	S_2	S_3	S.I.	Allow. Stress 1.0 S_u	Margin of Safety
	1-1										
1	2377 to 2577	-27.21	-1.57	-3.70	-1.18	-1.51	-3.70	-27.27	25.75	66.0	+1.56
	7-7										
3	1821 to 1825	0.20	-21.52	7.75	1.92	7.75	0.37	-21.69	29.45	66.0	+1.24
	3-3										
4	1561 to 1564	0.29	-18.60	-4.46	-0.54	0.30	-4.46	-18.61	18.92	94.3	+3.98
	4-4										
6	1595 to 1598	0.04	-18.68	2.26	0.15	2.26	0.04	-18.68	20.94	94.3	+3.50
	8-8										
7	143 to 150	-0.92	17.99	4.22	-0.23	17.99	4.22	-0.93	18.92	66.0	+2.49
	6-6										
8	381 to 385	-5.74	-8.92	-0.47	-0.73	-0.47	-5.58	-9.08	8.61	66.0	+6.66

* Refer to Figure 2.10.2-9 for component identification.

** Conservatively based on a 1.12-inch thick outer shell and on a 3,850-psi maximum crush strength aluminum honeycomb impact limiter (Section 2.7.1.3).

Table 2.7.1-38 Critical Stress Summary (30-Foot Top Corner Drop) – Loading Condition 3 – Total Range – Drop Orientation = 15.74 Degrees

Loading Condition 3: -40°F Ambient Temperature and No Decay Heat Load

		Total Stress Range** (ksi)				Principal Stresses			Stress Differences		
Comp. No.*	Node	S_x	S_y	S_z	S_{xy}	S_1	S_2	S_3	S_1-S_2	S_2-S_3	S_3-S_1
1	2561***	0.53	-5.77	-5.37	196.6	194.01	-5.37	-199.25	199.38	193.88	-393.25
3	1815	-1.78	-34.09	-0.31	1.13	-0.31	-1.74	-34.13	1.43	32.39	-33.82
4	1584	-1.07	-13.54	-7.81	-1.49	-0.89	-7.81	-13.72	6.92	5.91	-12.82
6	1598	-0.07	-22.77	2.35	0.07	2.35	-0.07	-22.77	4.42	22.70	-25.12
7	2	-0.93	22.51	5.68	0.95	22.54	5.68	-0.97	16.86	6.65	-23.51
8	385	-15.51	-7.77	-7.85	-1.52	-7.48	-7.85	-15.80	0.36	7.95	-8.32

* Refer to Figure 2.10.2-9 for component identification.

** Conservatively based on a 1.12-inch thick outer shell and on a 3,850-psi maximum crush strength aluminum honeycomb impact limiter (Section 2.7.1.3).

*** Stresses at node 2561 are unrealistic, resulting from the boundary effect. See Section 2.7.1.3.3 for the discussion of the boundary effect on the stress results.

Table 2.7.1-39 Critical Stress Summary (30-Foot Top Oblique Drop) – Loading Condition 3 – P_m – Drop Orientation = 30 Degrees

Loading Condition 3: -40°F Ambient Temperature and No Decay Heat Load

		P_m Stresses (ksi)**				Principal Stresses					
Comp. No.*	Section Cut Node to Node	S_x	S_y	S_z	S_{xy}	S_1	S_2	S_3	S.I.	Allow. Stress 0.7 S_u	Margin of Safety
	1-1										
1	2302 to 2562	-16.20	-12.40	1.94	-9.53	1.94	-4.59	-24.02	25.96	46.2	+0.78
	2-2										
3	2150 to 2156	-2.78	-11.71	-24.46	0.10	-2.78	-11.71	-24.46	21.68	46.2	+1.13
	3-3										
4	941 to 944	-0.01	11.94	0.15	0.00	11.94	0.15	-0.01	11.95	66.0	+4.52
	4-4										
6	1035 to 1038	-0.04	27.17	1.33	0.00	27.17	1.33	-0.04	27.21	66.0	+1.49
	5-5										
7	168 to 175	-3.49	6.05	-3.83	0.39	6.06	-3.50	-3.83	9.90	46.2	+3.67
	6-6										
8	381 to 385	-6.22	-6.32	-4.05	0.41	-4.05	-5.86	-6.68	2.63	46.2	+16.56

* Refer to Figure 2.10.2-9 for component identification.

** Conservatively based on a 1.12-inch thick outer shell and on a 3,850-psi maximum crush strength aluminum honeycomb impact limiter (Section 2.7.1.3).

Table 2.7.1-40 Critical Stress Summary (30-Foot Top Oblique Drop) – Loading Condition 3 – $P_m + P_b$ – Drop Orientation = 30 Degrees

Loading Condition 3: -40°F Ambient Temperature and No Decay Heat Load

		$P_m + P_b$ Stresses (ksi)**				Principal Stresses					
Comp. No.*	Section Cut Node to Node	S_x	S_y	S_z	S_{xy}	S_1	S_2	S_3	S.I.	Allow. Stress 1.0 S_u	Margin of Safety
	1-1										
1	2377 to 2577	-27.70	-2.51	-3.18	-2.00	-2.35	-3.18	-27.86	25.51	66.0	+1.59
	8-8										
3	1821 to 1825	0.23	-21.21	8.11	2.18	8.11	0.45	-21.43	29.54	66.0	+1.23
	9-9										
4	1561 to 1564	0.23	-13.23	-3.71	-0.43	0.24	-3.71	-13.25	13.49	94.3	+5.99
	4-4										
6	1035 to 1038	0.01	28.33	1.36	0.00	28.33	1.36	0.01	28.32	94.3	+2.33
	10-10										
7	143 to 150	-1.38	23.77	2.90	0.26	23.77	2.90	-1.39	25.15	66.0	+1.62
	11-11										
8	176 to 326	-9.37	-8.25	-0.22	-1.43	-0.22	-7.27	-10.35	10.13	66.0	+5.51

* Refer to Figure 2.10.2-9 for component identification.

** Conservatively based on a 1.12-inch thick outer shell and on a 3,850-psi maximum crush strength aluminum honeycomb impact limiter (Section 2.7.1.3).

Table 2.7.1-41 Critical Stress Summary (30-Foot Top Oblique Drop) – Loading Condition 3 – Total Range – Drop Orientation = 30 Degrees

Loading Condition 3: -40°F Ambient Temperature and No Decay Heat Load

		Total Stress Range** (ksi)				Principal Stresses			Stress Differences		
Comp. No.*	Node	S_x	S_y	S_z	S_{xy}	S_1	S_2	S_3	S_1-S_2	S_2-S_3	S_3-S_1
1	2561***	0.55	-4.91	-4.43	388.2	286.03	-4.43	-390.39	390.36	386.06	-776.42
3	1821	0.41	-23.19	9.86	0.65	9.86	0.43	-23.21	9.43	23.64	-33.07
4	1584	-0.72	-7.54	-6.57	-1.20	-0.52	-6.57	-7.74	6.05	1.17	-7.23
6	1038	0.01	24.74	1.37	0.00	24.74	1.37	0.01	23.37	1.36	-24.73
7	25	-1.39	31.20	5.34	1.62	31.28	5.34	-1.47	25.94	6.81	-32.75
8	385	-25.70	-6.95	-11.61	-1.69	-6.79	-11.61	-25.85	4.81	14.24	-19.06

* Refer to Figure 2.10.2-9 for component identification.

** Conservatively based on a 1.12-inch thick outer shell and on a 3,850-psi maximum crush strength aluminum honeycomb impact limiter (Section 2.7.1.3).

*** Stresses at node 2561 are unrealistic, resulting from the boundary effect. See Section 2.7.1.3.3 for the discussion of the boundary effect on the stress results.

Table 2.7.1-42 Critical Stress Summary (30-Foot Top Oblique Drop) – Loading Condition 3 – P_m – Drop Orientation = 45 Degrees

Loading Condition 3: -40°F Ambient Temperature and No Decay Heat Load

		P_m Stresses (ksi)**				Principal Stresses					
Comp. No.*	Section Cut Node to Node	S_x	S_y	S_z	S_{xy}	S_1	S_2	S_3	S.I.	Allow. Stress 0.7 S_u	Margin of Safety
	1-1										
1	2302 to 2562	-18.06	-15.24	2.98	-11.92	2.98	-4.65	-28.65	31.63	46.2	+0.46
	2-2										
3	2150 to 2156	-3.61	-10.04	-28.16	0.10	-3.61	-10.04	-28.16	24.55	46.2	+0.88
	3-3										
4	981 to 984	-0.01	14.90	0.16	0.00	14.90	0.16	-0.01	14.91	66.0	+3.43
	4-4										
6	1055 to 1058	-0.05	33.61	1.52	0.00	33.61	1.52	-0.05	33.66	66.0	+0.96
	5-5										
7	168 to 175	-3.47	6.17	-5.50	0.68	6.22	-3.52	-5.50	11.72	46.2	+2.94
	6-6										
8	381 to 385	-7.05	-4.35	-4.32	0.36	-4.30	-4.32	-7.10	2.79	46.2	+15.54

* Refer to Figure 2.10.2-9 for component identification.

** Conservatively based on a 1.12-inch thick outer shell and on a 3,850-psi maximum crush strength aluminum honeycomb impact limiter (Section 2.7.1.3).

Table 2.7.1-43 Critical Stress Summary (30-Foot Top Oblique Drop) – Loading Condition 3 – $P_m + P_b$ – Drop Orientation = 45 Degrees

Loading Condition 3: -40°F Ambient Temperature and No Decay Heat Load

		$P_m + P_b$ Stresses (ksi)**				Principal Stresses					
Comp. No.*	Section Cut Node to Node	S_x	S_y	S_z	S_{xy}	S_1	S_2	S_3	S.I.	Allow. Stress 1.0 S_u	Margin of Safety
	1-1										
1	2302 to 2562	7.23	-15.24	2.98	-11.92	12.38	2.98	-20.38	32.76	66.0	+1.01
	7-7										
3	1969 to 1996	-41.18	-16.23	-10.45	0.25	-10.45	-16.23	-41.19	30.74	66.0	+1.15
	3-3										
4	981 to 984	0.00	15.70	0.16	0.00	15.70	0.16	0.00	15.70	94.3	+5.01
	4-4										
6	1055 to 1058	0.01	35.09	1.62	0.00	35.09	1.62	0.01	35.08	94.3	+1.69
	8-8										
7	143 to 150	-1.51	24.33	1.43	0.59	24.34	1.43	-1.52	25.87	66.0	+1.55
	9-9										
8	176 to 326	-10.63	-6.40	0.00	-1.74	0.00	-5.78	-11.25	11.25	66.0	+4.87

* Refer to Figure 2.10.2-9 for component identification.

** Conservatively based on a 1.12-inch thick outer shell and on a 3,850-psi maximum crush strength aluminum honeycomb impact limiter (Section 2.7.1.3).

Table 2.7.1-44 Critical Stress Summary (30-Foot Top Oblique Drop) – Loading Condition 3 – Total Range – Drop Orientation = 45 Degrees

Loading Condition 3: -40°F Ambient Temperature and No Decay Heat Load

		Total Stress Range** (ksi)				Principal Stresses			Stress Differences		
Comp. No.*	Node	S_x	S_y	S_z	S_{xy}	S_1	S_2	S_3	S_1-S_2	S_2-S_3	S_3-S_1
1	2561***	0.57	-3.66	-3.33	467.6	466.1	-3.33	-469.2	469.4	465.82	-935.21
3	1969	-43.14	-27.23	-17.08	2.69	-17.08	-26.79	-43.58	9.71	16.80	-26.50
4	984	-0.93	6.36	-8.61	0.00	6.36	-0.93	-8.61	7.29	7.68	-14.97
6	1058	0.01	31.49	1.62	0.00	31.49	1.62	0.01	29.87	1.61	-31.48
7	25	-1.51	32.78	4.22	1.88	32.89	4.22	-1.61	28.67	5.83	-34.50
8	385	-29.31	-5.19	-12.60	-1.55	-5.09	-12.60	-29.41	7.50	16.81	-24.31

* Refer to Figure 2.10.2-9 for component identification.

** Conservatively based on a 1.12-inch thick outer shell and on a 3,850-psi maximum crush strength aluminum honeycomb impact limiter (Section 2.7.1.3).

*** Stresses at node 2561 are unrealistic, resulting from the boundary effect. See Section 2.7.1.3.3 for the discussion of the boundary effect on the stress results.

Table 2.7.1-45 Critical Stress Summary (30-Foot Top Oblique Drop) – Loading Condition 3 – P_m – Drop Orientation = 60 Degrees

Loading Condition 3: -40°F Ambient Temperature and No Decay Heat Load

		P_m Stresses (ksi)**				Principal Stresses					
Comp. No.*	Section Cut Node to Node	S_x	S_y	S_z	S_{xy}	S_1	S_2	S_3	S.I.	Allow. Stress 0.7 S_u	Margin of Safety
	1-1										
1	2302 to 2562	-22.17	-19.88	4.31	-15.80	4.31	-5.18	-36.87	41.18	46.2	+0.12
	2-2										
3	2150 to 2156	-5.21	-9.13	-34.47	0.13	-5.20	-9.13	-34.47	29.27	46.2	+0.58
	3-3										
4	1021 to 1024	-0.01	19.85	0.18	0.00	19.85	0.18	-0.01	19.86	66.0	+2.32
	4-4										
6	1075 to 1078	-0.06	44.14	1.89	0.00	44.14	1.89	-0.06	44.20	66.0	+0.49
	5-5										
7	615 to 618	-3.94	7.14	-7.64	1.01	7.23	-4.03	-7.64	14.87	46.2	+2.11
	6-6										
8	601 to 604	-8.72	-3.35	-5.15	0.38	-3.32	-5.15	-8.75	-5.42	46.2	+7.52

* Refer to Figure 2.10.2-9 for component identification.

** Conservatively based on a 1.12-inch thick outer shell and on a 3,850-psi maximum crush strength aluminum honeycomb impact limiter (Section 2.7.1.3).

Table 2.7.1-46 Critical Stress Summary (30-Foot Top Oblique Drop) – Loading Condition 3 – $P_m + P_b$ – Drop Orientation = 60 Degrees

Loading Condition 3: -40°F Ambient Temperature and No Decay Heat Load

		$P_m + P_b$ Stresses (ksi)**				Principal Stresses					
Comp. No.*	Section Cut Node to Node	S_x	S_y	S_z	S_{xy}	S_1	S_2	S_3	S.I.	Allow. Stress 1.0 S_u	Margin of Safety
	1-1										
1	2302 to 2562	13.46	-19.88	4.31	-15.80	19.76	4.31	-26.18	45.94	66.0	+0.44
	7-7										
3	1969 to 2016	-56.85	-17.63	-8.69	2.13	-8.69	-17.51	-56.97	48.28	66.0	+0.37
	3-3										
4	1021 to 1024	0.00	20.91	0.18	0.00	20.91	0.18	0.00	20.92	94.3	+3.51
	4-4										
6	1075 to 1078	0.01	46.11	2.12	0.00	46.11	2.12	0.01	46.10	94.3	+1.05
	8-8										
7	125 to 168	-1.83	28.22	0.42	0.94	28.25	0.42	-1.86	30.10	66.0	+1.19
	9-9										
8	381 to 385	-13.15	-5.79	0.19	-2.23	0.19	-5.17	-13.77	13.96	66.0	+3.73

* Refer to Figure 2.10.2-9 for component identification.

** Conservatively based on a 1.12-inch thick outer shell and on a 3,850-psi maximum crush strength aluminum honeycomb impact limiter (Section 2.7.1.3).

Table 2.7.1-47 Critical Stress Summary (30-Foot Top Oblique Drop) – Loading Condition 3 – Total Range – Drop Orientation = 60 Degrees

Loading Condition 3: -40°F Ambient Temperature and No Decay Heat Load

		Total Stress Range** (ksi)				Principal Stresses			Stress Differences		
Comp. No.*	Node	S_x	S_y	S_z	S_{xy}	S_1	S_2	S_3	S_1-S_2	S_2-S_3	S_3-S_1
1	2561***	0.06	-2.82	-1.96	603.5	602.12	-1.96	-604.88	604.08	602.92	-1207.00
3	1969	-62.00	-37.03	-22.36	1.03	-22.36	-36.99	-62.04	14.63	25.05	-39.68
4	1024	-0.93	11.58	-8.59	0.00	11.58	-0.93	-8.59	12.51	7.66	-20.17
6	1078	0.01	42.52	2.12	0.00	42.52	2.12	0.01	40.40	2.11	-42.51
7	25	-1.82	38.70	3.89	2.35	38.83	3.89	-1.96	34.94	5.85	-40.79
8	177	-36.39	-4.49	-15.18	-1.66	-4.40	-15.18	-36.48	10.78	21.30	-32.08

* Refer to Figure 2.10.2-9 for component identification.

** Conservatively based on a 1.12-inch thick outer shell and on a 3,850-psi maximum crush strength aluminum honeycomb impact limiter (Section 2.7.1.3).

*** Stresses at node 2561 are unrealistic, resulting from the boundary effect. See Section 2.7.1.3.3 for the discussion of the boundary effect on the stress results.

Table 2.7.1-48 Critical Stress Summary (30-Foot Bottom Oblique Drop) – Loading Condition 1 – P_m – Drop Orientation = 15.74 Degrees

Loading Condition 1: 130°F Ambient Temperature and Maximum Decay Heat Load

		P_m Stresses (ksi)**				Principal Stresses					
Comp. No.*	Section Cut Node to Node	S_x	S_y	S_z	S_{xy}	S_1	S_2	S_3	S.I.	Allow. Stress 0.7 S_u	Margin of Safety
	1-1										
1	2301 to 2561	-2.46	-0.42	-0.64	0.21	0.64	-0.40	-2.48	3.12	46.2	+13.80
	2-2										
3	1595 to 1598	-6.94	-3.13	-3.21	-1.25	-2.76	-3.21	-7.31	4.56	46.2	+9.14
	3-3										
4	621 to 624	0.07	-16.15	-1.45	0.48	0.09	-1.45	-16.17	16.26	66.0	+3.05
	4-4										
6	615 to 618	-0.05	-24.26	1.38	-0.17	1.38	-0.05	-24.26	25.64	66.0	+1.57
	5-5										
7	2 to 102	-29.38	-17.87	-0.14	13.44	-0.14	-9.01	-38.25	38.11	46.2	+0.21
	6-6										
8	601 to 604	-0.37	-14.99	-0.87	0.68	-0.34	-0.87	-15.02	14.68	46.2	+2.15

* Refer to Figure 2.10.2-9 for component identification.

** Conservatively based on a 1.12-inch thick outer shell and on a 3,850-psi maximum crush strength aluminum honeycomb impact limiter (Section 2.7.1.3).

Table 2.7.1-49 Critical Stress Summary (30-Foot Bottom Oblique Drop) – Loading Condition 1 – $P_m + P_b$ – Drop Orientation = 15.74 Degrees

Loading Condition 1: 130°F Ambient Temperature and Maximum Decay Heat Load

		$P_m + P_b$ Stresses (ksi)**				Principal Stresses					
Comp. No.*	Section Cut Node to Node	S_x	S_y	S_z	S_{xy}	S_1	S_2	S_3	S.I.	Allow. Stress 1.0 S_u	Margin of Safety
	1-1										
1	2301 to 2561	-4.32	-0.30	0.66	2.67	1.03	0.66	-5.65	6.69	66.0	+8.87
	7-7										
3	1815 to 1818	-3.06	4.46	-11.42	0.29	4.48	-3.07	-11.42	15.90	66.0	+3.15
	3-3										
4	621 to 624	0.27	-20.83	-3.90	0.48	0.28	-3.90	-20.84	21.12	94.3	+3.46
	4-4										
6	615 to 618	-0.11	-25.58	1.47	-0.17	1.47	-0.11	-25.58	27.05	94.3	+2.48
	8-8										
7	168 to 175	45.23	-16.97	-0.74	-1.45	45.26	-0.74	-17.01	62.27	66.0	+0.06
	9-9										
8	176 to 326	-32.63	0.00	-4.06	0.00	0.00	-4.06	-32.63	32.63	66.0	+1.02

* Refer to Figure 2.10.2-9 for component identification.

** Conservatively based on a 1.12-inch thick outer shell and on a 3,850-psi maximum crush strength aluminum honeycomb impact limiter (Section 2.7.1.3).

Table 2.7.1-50 Critical Stress Summary (30-Foot Bottom Oblique Drop) – Loading Condition 1 – Total Range – Drop Orientation = 15.74 Degrees

Loading Condition 1: 130°F Ambient Temperature and Maximum Decay Heat Load

		Total Stress Range** (ksi)				Principal Stresses			Stress Differences		
Comp. No.*	Node	S_x	S_y	S_z	S_{xy}	S_1	S_2	S_3	S_1-S_2	S_2-S_3	S_3-S_1
1	2561	0.82	-4.33	0.68	9.98	8.55	0.68	-12.07	7.87	12.75	-20.62
3	1815	0.98	11.67	0.31	4.22	13.14	0.31	-0.49	12.83	0.80	-13.63
4	604	-1.35	-22.40	-4.09	1.23	-1.28	-4.09	-22.47	2.81	18.38	-21.19
6	615	-0.03	-14.25	2.26	-0.28	2.26	-0.02	-14.26	2.28	14.23	-16.52
7	1***	-0.49	-6.30	-9.12	-213.50	210.12	-9.12	-216.91	219.24	207.79	-427.04
8	361	0.02	-28.18	2.01	-2.18	2.01	0.19	-28.35	1.82	28.54	-30.36

* Refer to Figure 2.10.2-9 for component identification.

** Conservatively based on a 1.12-inch thick outer shell and on a 3,850-psi maximum crush strength aluminum honeycomb impact limiter (Section 2.7.1.3).

*** Stresses at node 1 are unrealistic, resulting from the boundary effect. See Section 2.7.1.3.3 for the discussion of the boundary effect on the stress results.

Table 2.7.1-51 Critical Stress Summary (30-Foot Bottom Oblique Drop) – Loading Condition 1 – P_m – Drop Orientation = 30 Degrees

Loading Condition 1: 130°F Ambient Temperature and Maximum Decay Heat Load

		P_m Stresses (ksi)**				Principal Stresses					
Comp. No.*	Section Cut Node to Node	S_x	S_y	S_z	S_{xy}	S_1	S_2	S_3	S.I.	Allow. Stress 0.7 S_u	Margin of Safety
	1-1										
1	2301 to 2561	-3.93	-0.51	0.56	0.02	0.56	-0.51	-3.93	4.49	46.2	+9.30
	2-2										
3	1595 to 1598	-11.42	-1.45	-5.19	-1.95	-1.08	-5.19	-11.79	10.71	46.2	+3.31
	3-3										
4	1261 to 1264	-0.06	16.36	0.81	0.00	16.36	0.81	-0.06	16.42	66.0	+3.02
	4-4										
6	1195 to 1198	-0.05	29.57	1.48	0.00	29.57	1.48	-0.05	29.62	66.0	+1.22
7	2 to 102	-48.76	-30.81	5.29	31.95	5.29	-6.60	-72.97	78.26***	46.2	***
	6-6										
8	501 to 505	-0.06	-11.36	0.85	0.81	0.85	0.00	-11.42	12.27	46.2	+2.77

* Refer to Figure 2.10.2-9 for component identification.

** Conservatively based on a 1.12-inch thick outer shell and on a 3,850-psi maximum crush strength aluminum honeycomb impact limiter (Section 2.7.1.3).

*** This stress is unrealistic and is disregarded. See Section 2.7.1.3.3 for the discussion of the boundary effect on the stress results. The critical section and its stresses for component 7 are:

Section Cut Node to Node	S_x	S_y	S_z	S_{xy}	S_1	S_2	S_3	S.I.	0.7 S_u	MS
5-5 4 to 104	-11.36	-24.02	-2.05	4.49	-2.05	-9.93	-25.45	23.40	46.2	+0.97

Table 2.7.1-52 Critical Stress Summary (30-Foot Bottom Oblique Drop) – Loading Condition 1 – $P_m + P_b$ – Drop Orientation = 30 Degrees

Loading Condition 1: 130°F Ambient Temperature and Maximum Decay Heat Load

		$P_m + P_b$ Stresses (ksi)**				Principal Stresses					
Comp. No.*	Section Cut Node to Node	S_x	S_y	S_z	S_{xy}	S_1	S_2	S_3	S.I.	Allow. Stress 1.0 S_u	Margin of Safety
	1-1										
1	2301 to 2561	-3.94	-0.21	1.01	4.43	2.73	1.01	-6.89	9.62	66.0	+5.86
	7-7										
3	1815 to 1818	-5.00	3.57	-20.79	0.24	3.57	-5.00	-20.79	24.36	66.0	+1.71
	8-8										
4	1241 to 1244	-0.02	17.27	1.03	0.00	17.27	1.03	-0.02	17.29	94.3	+4.45
	9-9										
6	1175 to 1178	0.00	30.88	1.52	0.00	30.88	1.52	0.00	30.88	94.3	+2.04
7	2 to 102	-1.21	-30.81	5.29	31.95	19.20	5.29	-51.22	70.43***	66.0	***
	10-10										
8	176 to 326	-26.38	0.00	-3.46	0.00	0.00	-3.46	-26.38	26.38	66.0	+1.50

* Refer to Figure 2.10.2-9 for component identification.

** Conservatively based on a 1.12-inch thick outer shell and on a 3,850-psi maximum crush strength aluminum honeycomb impact limiter (Section 2.7.1.3).

*** This stress is unrealistic and is disregarded. See Section 2.7.1.3.3 for the discussion of the boundary effect on the stress results. The critical section and its stresses for component 7 are:

Section Cut Node to Node	S_x	S_y	S_z	S_{xy}	S_1	S_2	S_3	S.I.	1.0 S_u	MS
5-5 4 to 104	-13.71	-24.02	-2.05	4.49	-2.05	-12.03	-25.70	23.65	66.0	+1.79

Table 2.7.1-53 Critical Stress Summary (30-Foot Bottom Oblique Drop) – Loading Condition 1 – Total Range – Drop Orientation = 30 Degrees

Loading Condition 1: 130°F Ambient Temperature and Maximum Decay Heat Load

		Total Stress Range** (ksi)				Principal Stresses			Stress Differences		
Comp. No.*	Node	S_x	S_y	S_z	S_{xy}	S_1	S_2	S_3	S_1-S_2	S_2-S_3	S_3-S_1
1	2561	0.70	-3.49	1.32	16.80	15.53	1.32	-18.33	14.22	19.64	-33.86
3	1815	1.78	23.68	2.32	7.64	26.09	2.32	-0.63	23.77	2.94	-26.71
4	604	-1.10	-18.18	-3.00	1.02	-1.04	-3.00	-18.24	1.96	15.24	-17.20
6	1178	0.01	40.71	1.75	0.00	40.71	1.75	0.01	38.96	1.74	-40.70
7	1***	-1.03	-5.20	-6.73	-423.50	420.39	-6.73	-426.62	427.12	419.89	-847.01
8	177	-39.92	-4.9	-27.40	-3.15	-4.62	-27.40	-40.20	22.78	12.80	-35.58

* Refer to Figure 2.10.2-9 for component identification.

** Conservatively based on a 1.12-inch thick outer shell and on a 3,850-psi maximum crush strength aluminum honeycomb impact limiter (Section 2.7.1.3).

*** Stresses at node 1 are unrealistic, resulting from the boundary effect. See Section 2.7.1.3.3 for the discussion of the boundary effect on the stress results.

Table 2.7.1-54 Critical Stress Summary (30-Foot Bottom Oblique Drop) – Loading Condition 1 – P_m – Drop Orientation = 45 Degrees

Loading Condition 1: 130°F Ambient Temperature and Maximum Decay Heat Load

		P_m Stresses (ksi)**				Principal Stresses					
Comp. No.*	Section Cut Node to Node	S_x	S_y	S_z	S_{xy}	S_1	S_2	S_3	S.I.	Allow. Stress 0.7 S_u	Margin of Safety
	1-1										
1	2301 to 2561	-4.42	-0.50	0.40	-0.12	0.40	-0.50	-4.42	4.82	46.2	+8.58
	2-2										
3	1595 to 1598	-12.99	0.06	-5.86	-2.18	0.41	-5.86	-13.35	13.76	46.2	+2.36
	3-3										
4	1241 to 1244	-0.09	19.42	0.87	0.00	19.42	0.87	-0.09	19.51	66.0	+2.38
	4-4										
6	1175 to 1178	-0.06	36.99	1.79	0.00	36.99	1.79	-0.06	37.04	66.0	+0.78
7	2 to 102	-55.62	-36.07	9.42	40.01	9.42	-4.65	-87.03	96.45***	46.2	***
	6-6										
8	501 to 505	-0.06	-8.84	1.04	0.67	1.04	-0.01	-8.89	9.93	46.2	+3.65

* Refer to Figure 2.10.2-9 for component identification.

** Conservatively based on a 1.12-inch thick outer shell and on a 3,850-psi maximum crush strength aluminum honeycomb impact limiter (Section 2.7.1.3).

*** This stress is unrealistic and is disregarded. See Section 2.7.1.3.3 for the discussion of the boundary effect on the stress results. The critical section and its stresses for component 7 are:

Section Cut Node to Node	S_x	S_y	S_z	S_{xy}	S_1	S_2	S_3	S.I.	0.7 S_u	MS
5-5										
4 to 104	-10.17	-27.98	0.97	6.07	0.97	-8.3	-29.85	30.82	46.2	+0.50

Table 2.7.1-55 Critical Stress Summary (30-Foot Bottom Oblique Drop) – Loading Condition 1 – $P_m + P_b$ – Drop Orientation = 45 Degrees

Loading Condition 1: 130°F Ambient Temperature and Maximum Decay Heat Load

		$P_m + P_b$ Stresses (ksi)**				Principal Stresses					
Comp. No.*	Section Cut Node to Node	S_x	S_y	S_z	S_{xy}	S_1	S_2	S_3	S.I.	Allow. Stress 1.0 S_u	Margin of Safety
	1-1										
1	2301 to 2561	-3.02	-0.11	1.11	5.05	3.70	1.11	-6.82	10.52	66.0	+5.27
	7-7										
3	1815 to 1818	-5.66	2.30	-24.56	0.17	2.31	-5.67	-24.56	26.87	66.0	+1.46
	3-3										
4	1241 to 1244	-0.03	20.58	1.32	0.00	20.58	1.32	-0.03	20.62	94.3	+3.57
	4-4										
6	1175 to 1178	0.00	38.64	1.74	0.00	38.64	1.74	0.00	38.64	94.3	+1.44
7	2 to 102	3.28	-36.07	9.42	40.01	28.20	9.42	-60.98	89.18***	66.0	***
	8-8										
8	176 to 326	-17.26	0.00	-1.15	0.00	0.00	-1.15	-17.26	17.26	66.0	+2.82

* Refer to Figure 2.10.2-9 for component identification.

** Conservatively based on a 1.12-inch thick outer shell and on a 3,850-psi maximum crush strength aluminum honeycomb impact limiter (Section 2.7.1.3).

*** This stress is unrealistic and is disregarded. See Section 2.7.1.3.3 for the discussion of the boundary effect on the stress results. The critical section and its stresses for component 7 are:

Section Cut Node to Node	S_x	S_y	S_z	S_{xy}	S_1	S_2	S_3	S.I.	1.0 S_u	MS
5-5										
4 to 104	-12.31	-27.98	0.97	6.07	0.97	-10.23	-30.06	31.03	66.0	+1.13

Table 2.7.1-56 Critical Stress Summary (30-Foot Bottom Oblique Drop) – Loading Condition 1 – Total Range – Drop Orientation = 45 Degrees

Loading Condition 1: 130°F Ambient Temperature and Maximum Decay Heat Load

		Total Stress Range** (ksi)				Principal Stresses			Stress Differences		
Comp. No.*	Node	S_x	S_y	S_z	S_{xy}	S_1	S_2	S_3	S_1-S_2	S_2-S_3	S_3-S_1
1	2561	0.49	-2.29	1.58	19.28	18.44	1.58	-20.23	16.85	21.82	-38.67
3	1815	2.10	29.01	3.47	9.01	31.75	3.47	-0.64	28.28	4.11	-32.39
4	1244	-0.03	23.31	1.61	0.00	23.31	1.61	-0.03	21.70	1.64	-23.34
6	1178	0.01	48.47	1.97	0.00	48.47	1.97	0.01	46.50	1.96	-48.46
7	1***	0.06	-3.93	-3.64	-509.70	507.77	-3.64	-511.64	511.41	508.00	-1019.41
8	177	-40.74	-4.08	-23.25	-2.37	-3.88	-23.25	-40.94	19.37	17.69	-37.06

* Refer to Figure 2.10.2-9 for component identification.

** Conservatively based on a 1.12-inch thick outer shell and on a 3,850-psi maximum crush strength aluminum honeycomb impact limiter (Section 2.7.1.3).

*** Stresses at node 1 are unrealistic, resulting from the boundary effect. See Section 2.7.1.3.3 for the discussion of the boundary effect on the stress results.

Table 2.7.1-57 Critical Stress Summary (30-Foot Bottom Oblique Drop) – Loading Condition 1 – P_m – Drop Orientation = 60 Degrees

Loading Condition 1: 130°F Ambient Temperature and Maximum Decay Heat Load

		P_m Stresses (ksi)**				Principal Stresses					
Comp. No.*	Section Cut Node to Node	S_x	S_y	S_z	S_{xy}	S_1	S_2	S_3	S.I.	Allow. Stress 0.7 S_u	Margin of Safety
	1-1										
1	2302 to 2562	-5.44	-0.56	0.33	-0.26	0.33	-0.54	-5.46	5.79	46.2	+6.99
	2-2										
3	1595 to 1598	-16.11	1.31	-7.24	-2.66	1.71	-7.24	-16.51	18.22	46.2	+1.54
	3-3										
4	1221 to 1224	-0.12	24.94	0.91	-0.02	24.94	0.91	-0.12	25.06	66.0	+1.63
	4-4										
6	1155 to 1158	-0.07	48.97	2.27	0.00	48.97	2.27	-0.07	49.04	66.0	+0.34
7	2 to 102	-69.10	-45.77	14.35	52.94	14.35	-3.22	-111.6	126.00***	46.2	***
	6-6										
8	177 to 327	-3.61	-11.52	1.18	0.46	1.18	-3.58	-11.55	12.73	46.2	+2.63

* Refer to Figure 2.10.2-9 for component identification.

** Conservatively based on a 1.12-inch thick outer shell and on a 3,850-psi maximum crush strength aluminum honeycomb impact limiter (Section 2.7.1.3).

*** This stress is unrealistic and is disregarded. See Section 2.7.1.3.3 for the discussion of the boundary effect on the stress results. The critical section and its stresses for component 7 are:

Section Cut Node to Node	S_x	S_y	S_z	S_{xy}	S_1	S_2	S_3	S.I.	0.7 S_u	MS
5-5										
4 to 104	-10.12	-35.55	3.96	8.66	3.96	-7.45	-38.22	42.18	46.2	+0.10

Table 2.7.1-58 Critical Stress Summary (30-Foot Bottom Oblique Drop) – Loading Condition 1 – $P_m + P_b$ – Drop Orientation = 60 Degrees

Loading Condition 1: 130°F Ambient Temperature and Maximum Decay Heat Load

		$P_m + P_b$ Stresses (ksi)**				Principal Stresses					
Comp. No.*	Section Cut Node to Node	S_x	S_y	S_z	S_{xy}	S_1	S_2	S_3	S.I.	Allow. Stress 1.0 S_u	Margin of Safety
	7-7										
1	2301 to 2561	-2.69	-0.04	1.34	6.28	5.05	1.34	-7.78	12.83	66.0	+4.14
	8-8										
3	1815 to 1818	-7.00	1.59	-31.12	0.13	1.59	-7.01	-31.12	32.72	66.0	+1.02
	3-3										
4	1221 to 1224	-0.06	26.49	1.66	-0.02	26.49	1.66	-0.06	26.55	94.3	+2.55
	4-4										
6	1155 to 1158	0.01	51.14	2.18	0.00	51.14	2.18	0.01	51.13	94.3	+0.84
7	2 to 102	8.63	-45.77	14.35	52.94	40.94	14.35	-78.09	119.00***	66.0	***
	9-9										
8	381 to 385	-0.82	-14.41	-3.80	0.98	-0.75	-3.80	-14.48	13.74	66.0	+3.80

* Refer to Figure 2.10.2-9 for component identification.

** Conservatively based on a 1.12-inch thick outer shell and on a 3,850-psi maximum crush strength aluminum honeycomb impact limiter (Section 2.7.1.3).

*** This stress is unrealistic and is disregarded. See Section 2.7.1.3.3 for the discussion of the boundary effect on the stress results. The critical section and its stresses for component 7 are:

Section Cut Node to Node	S_x	S_y	S_z	S_{xy}	S_1	S_2	S_3	S.I.	1.0 S_u	MS
5-5										
4 to 104	-12.00	-35.55	3.96	8.66	3.96	-9.16	-38.40	42.4	66.0	+0.56

Table 2.7.1-59 Critical Stress Summary (30-Foot Bottom Oblique Drop) – Loading Condition 1 – Total Range – Drop Orientation = 60 Degrees

Loading Condition 1: 130°F Ambient Temperature and Maximum Decay Heat Load

		Total Stress Range** (ksi)				Principal Stresses			Stress Differences		
Comp. No.*	Node	S_x	S_y	S_z	S_{xy}	S_1	S_2	S_3	S_1-S_2	S_2-S_3	S_3-S_1
1	2561	0.40	-1.63	2.03	24.03	23.44	2.03	-24.67	21.41	26.70	-48.11
3	1815	2.66	37.47	4.91	11.41	40.87	4.91	-0.75	35.96	5.66	-41.62
4	1224	-0.05	29.24	1.96	-0.02	29.24	1.96	-0.05	27.28	2.01	-29.29
6	1158	0.01	60.98	2.42	0.00	60.98	2.42	0.01	58.56	2.41	-60.97
7	1***	-0.88	-3.07	-0.83	-655.60	653.63	-0.83	-657.58	654.46	656.75	-1311.20
8	177	-46.34	-4.01	-22.03	-2.06	-3.91	-22.03	-46.46	18.39	24.16	-42.55

* Refer to Figure 2.10.2-9 for component identification.

** Conservatively based on a 1.12-inch thick outer shell and on a 3,850-psi maximum crush strength aluminum honeycomb impact limiter (Section 2.7.1.3).

*** Stresses at node 1 are unrealistic, resulting from the boundary effect. See Section 2.7.1.3.3 for the discussion of the boundary effect on the stress results.

Table 2.7.1-60 NAC-LWT Cask Hot Bolt Analysis Hypothetical Accident Conditions

Nominal Diameter (in):	1.00	
Number of Bolts:	12	
Service Stress, Sy (ksi):	81.9	at a 300 degree-F Service Temperature
Bolt Expansion (in/in):	9E-06	
Bolt Modulus (ksi):	26700	
Lid Expansion (in/in):	9E-06	
Lid Modulus (ksi):	27000	
Stress Area (in2):	0.6051	
Grip Length (in):	7.99	
Maximum Pressure (psi):	50	
Seal Diameter (in):	15.750	
Preload Torque (ft-lbs):	260	at RT
Nominal Room Temp, RT:	70	deg-F
Bolt Circle Diameter (in):	17.88	
Lid Diameter (in):	22.50	

Longitudinal Weight (lbs):	4941
Lateral Weight (lbs):	941
Service DT (degrees):	157
[default value =]	230

CALCULATED LOADS & STIFFNESS

Bolt Thermal Load (lbs):	1423
Bolt Preload (lbs):	34770
Bolt Pressure Load (lbs):	812
Bolt Stiffness (lbs/in):	1.9E+06
Lid Stiffness (lbs/in):	2.1E+07

Angle wrt Vert. (Deg)	Impact Accel. (g)	<**** LOADS (lbs.) **** Impact Tension	Impact Shear	Bolt Tension Applied	Bolt Tension Net ****	<**** STRESSES (psi) **** Direct Tension	Direct Shear	Principal Sig-1	Principal Sig-2	Stress Intens. ****	Margin of Safety
0 End	15.80	6506	0	7317	36795	60808	0	0	60808	60808	0.35
5 (+)	14.69	8216	100	9028	36936	61041	166	0	61041	61042	0.34
10 (+)	13.57	7506	185	8318	36877	60944	305	-2	60946	60947	0.34
15.7 Corner	12.30	6650	261	7462	36807	60828	431	-3	60831	60834	0.35
20 (+)	12.99	6858	349	7670	36824	60856	576	-5	60862	60867	0.35
25 (+)	13.80	7025	457	7837	36838	60879	756	-9	60888	60898	0.34
30 (+)	14.61	7106	573	7918	36845	60890	947	-15	60905	60919	0.34
35 (+)	15.42	7093	693	7905	36843	60888	1146	-22	60910	60931	0.34
40 (+)	16.22	6980	818	7792	36834	60873	1352	-30	60903	60933	0.34
45 (+)	17.03	6764	944	7576	36816	60844	1561	-40	60884	60924	0.34
50 (+)	17.84	6440	1072	7252	36790	60800	1771	-52	60851	60903	0.34
55 (+)	18.65	6007	1198	6819	36754	60741	1980	-64	60805	60870	0.35
60 (+)	19.45	5463	1321	6275	36709	60667	2183	-78	60745	60824	0.35
65 (+)	20.26	4809	1440	5621	36656	60578	2380	-93	60671	60765	0.35
70 (+)	21.07	4047	1553	4859	36593	60474	2566	-109	60583	60692	0.35
75 (+)	21.88	3180	1657	3992	36522	60356	2739	-124	60480	60604	0.35
80 (+)	22.68	2212	1752	3024	36442	60225	2895	-139	60364	60503	0.35
85 (+)	23.49	1150	1835	1962	36355	60080	3033	-153	60233	60386	0.36
90 Side	24.30	0	1906	812	36260	59924	3149	-165	60089	60254	0.36

Minimum Margin of Safety: 0.34

Table 2.7.1-61 NAC-LWT Cask Cold Bolt Analysis Hypothetical Accident Conditions

Nominal Diameter (in):	1.00	
Number of Bolts:	12	
Service Stress, Sy (ksi):	85	at a 70 degree-F Service Temperature
Bolt Expansion (in/in):	8E-06	
Bolt Modulus (ksi):	27800	
Lid Expansion (in/in):	8E-06	
Lid Modulus (ksi):	28300	
Stress Area (in2):	0.6051	
Grip Length (in):	7.99	
Maximum Pressure (psi):	50	
Seal Diameter (in):	15.750	
Preload Torque (ft-lbs):	260	at RT
Nominal Room Temp, RT:	70	deg-F
Bolt Circle Diameter (in):	17.88	
Lid Diameter (in):	22.50	

Longitudinal Weight (lbs):	4941
Lateral Weight (lbs):	941
Service DT (degrees):	-90
[default value = 1	0

CALCULATED LOADS & STIFFNESS

Bolt Thermal Load (lbs):	-594
Bolt Preload (lbs):	34770
Bolt Pressure Load (lbs):	812
Bolt Stiffness (lbs/in):	2.0E+06
Lid Stiffness (lbs/in):	2.2E+07

Angle wrt Vert. (Deg)	Impact Accel. (g)	<**** LOADS (lbs.) **** Impact Tension	Impact Shear	Bolt Tension Applied	Bolt Tension Net	<**** STRESSES (psi) **** Direct Tension	Direct Shear	Principal Sig-1	Principal Sig-2	Stress Intens.	Margin of Safety
0 End	15.80	6506	0	7317	34775	57469	0	0	57469	57469	0.48
5 (+)	14.69	8216	100	9028	34914	57700	166	0	57701	57701	0.47
10 (+)	13.57	7506	185	8318	34856	57604	305	-2	57606	57607	0.48
15.7 Corner	12.30	6650	261	7462	34786	57489	431	-3	57492	57495	0.48
20 (+)	12.99	6858	349	7670	34803	57517	576	-6	57522	57528	0.48
25 (+)	13.80	7025	457	7837	34817	57539	756	-10	57549	57559	0.48
30 (+)	14.61	7106	573	7918	34824	57550	947	-16	57566	57581	0.48
35 (+)	15.42	7093	693	7905	34823	57548	1146	-23	57571	57594	0.48
40 (+)	16.22	6980	818	7792	34813	57533	1352	-32	57565	57597	0.48
45 (+)	17.03	6764	944	7576	34796	57504	1561	-42	57546	57589	0.48
50 (+)	17.84	6440	1072	7252	34769	57460	1771	-55	57515	57569	0.48
55 (+)	18.65	6007	1198	6819	34734	57402	1980	-68	57470	57538	0.48
60 (+)	19.45	5463	1321	6275	34689	57328	2183	-83	57411	57494	0.48
65 (+)	20.26	4809	1440	5621	34636	57240	2380	-99	57339	57437	0.48
70 (+)	21.07	4047	1553	4859	34574	57137	2566	-115	57252	57367	0.48
75 (+)	21.88	3180	1657	3992	34503	57020	2739	-131	57151	57282	0.48
80 (+)	22.68	2212	1752	3024	34424	56889	2895	-147	57036	57183	0.49
85 (+)	23.49	1150	1835	1962	34337	56745	3033	-162	56907	57069	0.49
90 Side	24.30	0	1906	812	34243	56590	3149	-175	56765	56939	0.49

Minimum Margin of Safety: 0.47

2.7.2 Puncture

The puncture accident outlined in 10 CFR 71 Subpart F requires that the NAC-LWT cask suffer no loss of containment as a result of a 40-inch free fall onto an upright 6-inch diameter mild steel bar (puncture pin), which is supported on an unyielding surface. The impact orientation of the cask is required to be such that maximum damage is inflicted upon the cask.

Locations of cask impact with the puncture pin, which will cause maximum cask damage, are direct impact on the (1) cask side - midpoint, (2) center of the cask lid, (3) center of the cask bottom, and (4) cask port covers. Since an impact at any other location is less severe, the NAC-LWT cask is analyzed for the required puncture accident at these four locations.

2.7.2.1 Puncture – Cask Side Midpoint

2.7.2.1.1 Discussion

The NAC-LWT cask is analyzed for structural adequacy in accordance with the requirements of 10 CFR 71.73(c)(2), puncture (hypothetical accident condition). The cask is assumed to be in a horizontal position and dropped through a distance of 40 inches onto a 6-inch diameter, mild steel bar oriented vertically on an unyielding surface. The static structural evaluation of the cask is performed by classical analysis and the use of relations derived from destructive testing.

2.7.2.1.2 Analysis Description

Figure 2.7.2-1 illustrates the local cask midpoint section that has been evaluated for this analysis. It is composed of the initial 1.12-inch design thickness, Type XM-19 stainless steel outer shell, a 5.75-inch thick chemical copper lead middle shell, and a 0.75-inch thick, Type XM-19, stainless steel inner shell. The final design outer shell thickness is 1.20 inches. The additional thickness will only serve to enhance the ability of the NAC-LWT cask to resist the puncture event at the cask side midpoint.

During impact, the puncture pin is considered to apply a force (due to its assumed 47,000 psi dynamic flow stress) of 1.329×10^6 lbs to the cask outer shell midpoint in the inward normal direction. The neutron shield tank is conservatively not considered.

2.7.2.1.3 Detailed Analysis

For an impact occurring on the cask side, the required local cask outer shell thickness (t_r) for puncture integrity is calculated according to the Nelms equation (Shappert) as:

$$t_r = \left[\frac{W}{S_u} \right]^{0.71} = 0.655 \text{ in}$$

where:

W = cask design weight = 52,000 lbs

S_u = cask outer shell ultimate tensile strength at 300°F

= 94,300 psi

From the free body diagram in the sketch that follows, it can be determined that:

$$\text{Deceleration} = \frac{\text{Applied Load}}{\text{Cask Design Weight}} = \frac{1.329 \times 10^6}{52{,}000} = 25.57 \text{ g}$$

letting $W_B = W_L$

W_B = (weight of bottom assembly and limiter) × 25.57 g

= 94,865 lbs

W_L = (weight of cask lid and upper limiter) × 25.57 g

= 94,865 lbs

P = distributed linear load (lb/in)

$$= \frac{(52{,}000)(25.57) - (2)(94{,}865)}{199.75}$$

= 5706.7 lb/in

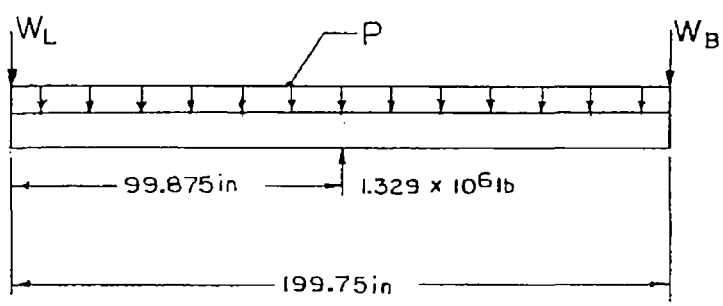

Cask Side Midpoint Puncture - Free Body Diagram